Bond Strength of Concrete Patch Repairs

An Evaluation of Test methods
and
the Influence of Workmanship and Environment

by

Youguang Pan

A Doctoral Thesis

submitted in partial fulfilment of the requirements

for the award of

Doctor of Philosophy of the Loughborough University of Technology

July, 1995

Abstract

Experiments were carried out to study the effect of workmanship and environmental conditions on bond strength for concrete patch repairs. Four repair materials, sand/cement mortar, acrylic modified cementitious mortar, SBR modified cementitious mortar, and flowing concrete, were tested with mainly three test methods (core pull-off test, patch compressive test, and patch flexural test). At the beginning of this project, slant shear tests were also carried out. In the study of the effect of workmanship, the following parameters were included: surface roughness, surface cleanliness, surface soundness, moisture condition, application method, bond coat mistiming, repair material mistiming, and curing methods. In the study of the effect of environmental conditions, four parameters were considered: high temperature curing followed by drying shrinkage, high temperature curing followed by thermal cycling, low temperature curing, and low temperature curing followed by freeze/thaw cycling. A rougher surface produces a higher bond strength, but the increase depends on individual repair material. Sand/cement mortar favours a rough surface, but polymer modified mortars are not very sensitive to surface roughness. Environmental conditions affect the bond strength development, but the effect varies with each repair material. Test results suggest that low temperature curing should be avoided for polymer modified cementitious mortars. In addition to the experimental study, theoretical analyses were carried out to evaluate the available bond test methods. The evaluation was concentrated on answering the following questions: (1) What kind of factors will influence conducting a bond test ? (2) What are the response of each factor involved to a specific test method ? (3) What kind of influences are crucial in ensuring the full development of the bond strength ? (4) Which factors are important to achieve a durable repair ? and (5) What kind of a test can be used to monitor the quality of these crucial factors ? In total, about 800 tests were conducted (500 core pull-off tests, 90 patch compressive tests, 100 patch flexural tests, and 80 slant shear tests).

Key words: concrete repair, bond strength, bond tests, core pull-off test, slant shear test, patch tests, workmanship, environmental conditions

Acknowledgement

I want first and foremost to express my gratitude to Dr Simon Austin and Dr Peter Robins for their supervision, guidance, and encouragement throughout the research programme.

I also want to thank the Science and Engineering Research Council (SERC) for financing the work.

The technical assistance of Mr David Spendlove and Mr Mark Harrod from the laboratory of the Department made the testing more enjoyable and successful.

I also want to thank the Department of Civil and Building Engineering and its staff for their coopeartion, advice and expertise.

CONTENTS

List of Tables

List of Figures

Notations

b gross width of a patch compressive /flexural specimen
c width of the net cross section of an unrepaired patch compressive /flexural specimen
e the distance between the central axes of substrate concrete and repair mortar
f_c cylinder compressive strength of concrete
f_{ct} tensile splitting strength of concrete
f_{cu} cube compressive strength of concrete
f_{ft} flexural tensile strength of concrete
h height of cross section
m_c bending moment acting on the substrate concrete
m_m bending moment acting on the repair mortar
t thickness of the prism or time
t_c the age of the substrate concrete at the time when shrinkage starts
t_m the age of a repair mortar at the time when shrinkage starts
u_c the total displacement in the longitudinal direction in concrete
u_{co} the total displacement in the longitudinal direction at the central axes in the substrate concrete
u_m the total displacement in the longitudinal direction in a repair mortar
u_{mo} the total displacement in the longitudinal direction at the central axes in the repair mortar
w_c the deflection in the substrate concrete
w_c' the differentiation of w_c with respect to x
w_m the deflection in the repair mortar
w_m' the differentiation of w_m with respect to x
z_m the distance of one layer cross section to the centre of the cross section

A_c the area of cross section of the substrate concrete
A_m the area of cross section of a repair mortar
E_c modulus of concrete
E_m modulus of repair material
K_n normal stiffness of the joint per unit length
K_s shear stiffness of the joint per unit length
M bending moment
M_o bending moment applied to a patch flexural specimen
N_c axial load acting on the substrate concrete
N_m axial load acting on the repair mortar
P axial load
P_o axial load applied to a patch compressive specimen

α	the bond angle between the bond interface and longitudinal direction of a specimen
α_a	area ratio ($\alpha_a = A_m/A_c$)
β	ratio of shear bond strength to tensile bond strength
β_t	modulus ratio of a repair mortar to the substrate concrete
ε	longitudinal strain
ε_{cc}	creep strain in concrete
ε_{cm}	creep strain in a repair mortar
ε_{ec}	elastic strain in concrete
ε_{em}	elastic strain in a repair mortar
ε_o	longitudinal strain at the centre of the cross section
ε_{shc}	unrestrained shrinkage strain in concrete
ε_{shm}^*	the ultimate unrestrained shrinkage strain in concrete
ε_{shm}	unrestrained shrinkage strain in a repair mortar
ε_{shc}^*	the ultimate unrestrained shrinkage strain in a repair mortar
ϕ	curvature of an element under bending moment
ϕ_c	creep coefficient of the substrate concrete
ϕ_c^*	the ultimate creep coefficient of the substrate concrete
ϕ_m	creep coefficient of a repair mortar
ϕ_m^*	the ultimate creep coefficient of a repair mortar
μ	coefficient of friction of a bond interface
ν	Poisson's ratio
ν_c	Poisson's ratio of substrate concrete
ν_m	Poisson's ratio of repair mortar
σ_c	longitudinal stress in concrete
σ_m	longitudinal stress in a repair mortar
σ_n	normal stress component acting on a bond interface
σ_o	external stress applied on a specimen
σ_t	tensile bond strength
τ	shear stress developed between the substrate concrete and the repair mortar
τ_n	shear stress component acting on a bond interface
τ_o	shear bond strength

Chapter 1

INTRODUCTION

Chapter 1 Introduction to the study

1.1 Introduction

In many instances, concrete has functioned acceptably in a variety of environments. However, the quality of the finished product is largely dependent on the prevailing job conditions and is controlled by a number of factors. These include weather, knowledge of the behaviour of various materials, and their compatibility in concrete, as well as construction practice. In addition, the serviceability of a concrete structure may be reduced by the disintegrating effects of in-service conditions such as weathering and mechanical action involving cyclic load, wear, and abrasion.

The last two decades have seen the widespread incidence of failures of concrete structures due to durability problems. Estimates of economic losses resulting from failures give dollar figures ranging in the billions. Various estimates indicate the size and form of the repair and refurbishment market to be large and there has been an increasing emphasis on concrete repair and renovation over demolition and new construction. Repair and maintenance, therefore, is a growth market, and has risen over the last ten years from about 25% of construction activity to about 50% [1]. In Hong Kong, the authorities spend about US$13m annually on patch repairs to spalled and delaminated concrete, totaling 65,000m^2 per annum [2]. In the United States, there are about 600,000 highway bridges, and nearly 40% are deficient by current standards and require repair and rehabilitation [3]. It is estimated that about $400 billion will be spent in the United States on the replacement or rehabilitation of highway pavements before the end of the century [4]. In the United Kingdom, the total amount of money used in concrete repair is about £500m annually [5], which accounts for about 25% of the UK construction output [6].

Such a substantial proportion of construction expenditure must be expected to influence the market for repair materials, specialised techniques, and services. This is indeed evidenced by the flood of new materials and expert services to address the specific requirements of the repair market. However, this phenomenal explosion of proprietary products has increased the complexity of material selection and heightened the potential for problems to occur. Evaluation by testing and research has not kept pace with the development of new products. Thus, products are being used before the design professional can be assured that they do indeed fulfil the desired requirements.

1.2 Mechanism and causes of failure

Structural members damaged as a result of reinforcement corrosion or the effects of fire or impact are often reinstated by applying patch repair materials. However, this is usually successful in the long term only if the cause or causes of the original damage has been eliminated, and appropriate materials have been selected and properly applied. This principle may seem self-evident but it is surprising how often it is disregarded, with the result that further repairs have to be carried out within a short time. Sometimes the cause is obvious as, for example, in many cases of accidental damages but, more often than not, careful investigation is required.

Detailed investigations of deteriorated reinforced concrete structures have indicated that probably over 90% of deterioration is due to either design errors, errors in construction, misconceptions in specifications and building codes, or bad workmanship[6, 7].

The next step must be to consider the objectives of the repair, which will be generally to restore or enhance one or more of the following: durability, structural strength, function, and appearance [8]. Of these four requirements, restoration of durability is by far the most common one in repair. The deterioration manifests itself in the cracking of

concrete, usually caused by corrosion of the reinforcement which is associated with a change in volume. This exerts expansive tensile pressure on the concrete cover causing it to crack and ultimately fall off. In ideal conditions, steel reinforcement in concrete is protected from corrosion by the 'passivating effect' of the highly alkaline concrete cover and remains volume stable for many years except in the presence of environmental attack [7, 9, 10].

There are two main reasons why concrete cover fails to protect steel from rusting: the failure of the alkali passivating effect --- carbonation, and the chloride ion induced corrosion.

Absence of the alkaline protective layer around the reinforcement due to neutralisation of the alkali by acids from external sources, mainly carbondioxide, causes carbonation of the concrete cover. This can also occur from direct contact of small areas of reinforcement with the atmosphere resulting from cracking of the cover due to a number of factors including curing shrinkage, plastic settlement or partial tensile failure. Apart from direct contact with the atmosphere through cracks, loss of alkalinity at the concrete/reinforcement interface is generally associated with the following: inadequate depth of concrete cover particularly on links or stirrups which are just as prone to corrosion as the main reinforcement; and permeable cover, which could be caused by the following reasons: too high a water/cement ratio, inadequate cement content in the concrete mix, or inadequate curing in the first few days after placing.

It is now well established that even in good quality, highly alkaline concrete, the presence of chlorides, even at relatively low concentrations can induce serious corrosion of steel reinforcement generally leading to subsequent spalling, and in some cases, especially with dense high strength concrete, it is possible for the complete loss of sections of reinforcing bars to occur without any evidence of concrete spalling. This is because under conditions where availability of oxygen is limited, the black iron

oxide corrosion products are far less expansive than the red oxide which is produced when the concrete cover carbonates and no longer passivates the reinforcement. Under these conditions cracking of the concrete cover does not always occur. The main sources of chloride ions contamination are: de-icing salts (especially on highway structures), structures in a marine environment, chloride ions introduced into the concrete mix during construction (generally from inadequately washed sea dredged aggregates, or the use of calcium chloride accelerating admixtures).

Where the chloride ions have entered the concrete during service, it is considered that there is a significant risk of chloride induced corrosion of the reinforcement where the chloride level is above 0.4% of cement. Chlorides from external sources can only penetrate the concrete cover as a solution in water. Hence the rate of corrosion of steel reinforcement in chloride contaminated concrete will be very much influenced by the permeability of the concrete to moisture and oxygen.

Other kinds of concrete damage could be caused by chemical or physical attack[9]. Chemical attack on the concrete is likely to occur from one or more of the following causes:

(1) Aggressive compounds in solution in the sub-soil and/or ground water.

(2) Aggressive chemicals in the air surrounding the structure.

(3) Aggressive chemicals or liquid stored in, or in contact with, the structure.

(4) Chemical reaction between the constituents of the concrete, such as alkali-aggregate reaction.

Physical aggression (wear and damage) to concrete can arise from a number of causes, the principal ones being:

(1) Freezing and thawing on the outside of structures located in very exposed positions in the areas with severe climate.

(2) Thermal shock caused by a sudden and severe drop in the temperature of the concrete, such as spillage of liquefied gases.

(3) Abrasion to concrete, such as that caused to floors in industrial buildings by steel wheeled trolleys. Similar damage can be caused to the inside of silos, bins and hoppers containing coarse granular materials.

(4) Damage from high velocity water. This damage can be subdivided into three types: cavitation; abrasion from water containing grit; and impact from a high velocity jet.

(5) Abrasion in marine structures caused by sand and shingle thrown against the structure by heavy seas and gale force winds.

Thus before any concrete repairs can be undertaken, it is imperative to establish the root causes of the concrete deterioration. The following methods of establishing the causes can be used for corrosion related problems[10, 11].

(1) the depth of cover;

(2) the depth of carbonation;

(3) the presence and amount of chlorides; and

(4) half-cell potential.

Other in-situ test and inspection techniques were reported by Baker [12], such as crack mapping, hammer testing, and thermography.

1.3 Factors affecting the success of a repair

2.1.1

After establishing the causes of concrete deterioration, evaluation and selection of existing repair materials are crucial steps in repair and rehabilitation.

The selection of a repair material is a predictive effort to maximise future performance or durability. Therefore, selection must be based on the knowledge of the physical and

chemical properties, the function the designer plans to impose on them, and the nature of the environment in which they will be placed. Also, in choosing a material, the designer must be aware that it possesses properties other than those required for basic function. Frequently, these have a greater influence on its durability in service than the properties that dictated its choice. Consequently, all properties of a material must be considered in the light of both function and the effect of each constituents reacting with the environment.

Most specifications for repair stipulate that all damaged or deteriorated concrete should be removed. However, it is not always possible to determine when all such material has been removed because the zones of damaged or deteriorated concrete can not be well defined. On the other hand, whenever concrete is removed using impact tools, there is the potential for superficial damage to the concrete left in place. So in all cases in which concrete has been removed from a structure by vigorous methods, such as impacting or spalling, the remaining concrete should be further prepared using a secondary method to remove any damaged surface material.

It should be born in mind that surface preparation is one of the most critical factors in the performance of a repair system. The repair will only be as good as the effort expended in surface preparation regardless of the nature or quality of the repair material. Surface preparation includes all the steps taken after the removal of large volumes of deteriorated concrete, as well as steps taken to prepare surfaces when little or no concrete is removed. The objective of surface preparation is to provide a dry, even level surface, free of dirt, dust, oil, and grease. However, the desired condition of the concrete surface depends somewhat on the type of repair being undertaken and the conditions of substrate. Surface preparation not only removes extraneous loose material from the substrate surface, but also removes reaction products like laitence that covers the surface.

Proper compaction of repair material is another important issue in concrete repair that has to be addressed. Bond strength depends very much on close contact between the repair material and substrate. Entrapped air voids at the bond interface might be the cause of premature failure because of stress concentration. Proper compaction could be a problem when a repair material has been mixed and left in air for some time, especially in a hot climate, because the workability can be significantly reduced.

Curing after the execution of repair is the last but not the least step to achieve a satisfying repair. Inadequate curing may result in high permeability, lower strength, surface cracking, or other problems relating to durability. The complete repair procedure is summarised as shown in Fig. 1.1.

It is also important to know how long a repair will last because if failure of a repair does occur, question will be raised about the causes. Similar failures need to be avoided, and where possible, service life extended.

1.4 Description of the research carried out in this study

Data obtained from a questionnaire and interviews with engineers and contractors[6] have indicated that failure of a repair work can be divided into short-term failures and medium-to-long term failures. The short term failure is mainly caused by poor workmanship. The medium-to-long term failures can be caused by many factors, such as mismatch of basic physical properties, inappropriate initial selection of materials based on erroneous information, and in-service environmental conditions, particularly extremes of temperature, etc.

Most of the time, failure occurs in the form of an inadequate bond between the repair material and the concrete substrate. There is no doubt that the bond strength is a very important characteristic in concrete repairs because all other discussions on the

performance of repaired systems require that the repair material sticks firmly to the substrate, to protect further corrosion of reinforcement, to reinstate the structural integrity of the damaged structure, or to prevent invasion of harmful ingredients from external sources. Bond strength varies depending on the stress-state imposed on the bond interface. So, there is a need for performance tests and performance criteria for screening and selecting materials for overlays and patching repair materials. There are existing BSI and ASTM test methods and specifications for the determination of bond strength with epoxy-resin bonding systems and latex bonding agents and for the determination of material properties, but test methods and specifications are behind the demand for the determination of bond strength for other types of repair materials. Evaluation of bond test methods has been conducted by several researchers. For example, Knab and Spring [13] judged test methods mainly based on the relative precision of the test results and suggested that a test method should be selected with geometry, loading conditions, and stress state, which are anticipated for in-service repair material. Ohama, et al [14] focused on the performance similarities demonstrated by different methods. Austin and Robins[15, 16] developed a patch test which puts repair into a more realistic stress state. The patch test was used to judge against other test methods. All these were based on experimental studies and have contributed significantly to the understanding of bond performance. But the author felt that a more systematic and, especially, a theoretical study was needed to have a thorough understanding of the different test methods and the relationships between them. For this reason, evaluation of bond test methods will be discussed in this thesis considering current available methods and their response to different conditions.

A successful repair system can only be achieved when both short-term and long-term performances are guaranteed. This requires taking both the workmanship and the environmental conditions into consideration in all aspects of the research, design, and application of repairs. Workmanship includes surface preparation, moisture conditioning of the substrate, and the application of repair material. Discussions on

workmanship have been done by Knab and Spring[13], Austin and Robins[15], Silfwerbrand[17], Cleland, et al[18,19], and Hindo[20] with the main attention paid to surface preparation.

Because of the multi-factors involved in the workmanship, the effect of each factor should be studied under different stress states. The detrimental effect of one factor could well be mitigated under another stress state. Of course, a good quality of repair is always required by emphasising the importance of workmanship, but at the same time one should be careful to avoid unnecessary strict specifications and over-inspection, causing both extra work and extra cost[21]. Obviously there is a need for a systematic study of the workmanship effect. The author used both experimental and theoretical methods in this study and found out that the effect of one factor could be masked by another one, and the dominating factor could be replaced by another one under other situations. The study on the workmanship formed the second part in this research.

Durability of repair requires the study of the effect of service environmental conditions which cover many aspects, such as high and low temperature, thermal cycling, and freeze/thaw cycling. Little research has been carried out on concrete repairs, although much research has been carried out concerning the effect on the properties of repair materials[22-33]. A thorough understanding of the effect of service environmental conditions requires the study on all related aspects -- the effects on the properties of substrate concrete, on the properties of repair materials, and on the bond strength. It is not possible to cover every aspect in this thesis. Preliminary tests were carried out to see the effects of some environmental conditions on the performance of repair systems. In this study, the focus was on the bond strength.

1.5 Layout of the thesis

So far, issues relating to the evaluation of repair systems have been briefly mentioned, and are summarised below:

(1) discussions about which test method/s should be used to select repair materials, to measure bond strength, and to evaluate the quality of repair works;

(2) using the appropriate test method/s to study the effect of workmanship so that satisfying short-term performance can be obtained; and

(3) using the appropriate test method/s to study the effect of service environmental conditions so that the long-term performance can be guaranteed.

These three issues relating to concrete repairs formed the main research subjects in this thesis and were tackled with both experimental and theoretical methods. The thesis is divided into the following chapters.

Chapter 1. Introduction

Chapter 2. Literature Review of Concrete Patch Repairs

Chapter 3. Materials and Test Programme

Chapter 4. Experimental and Analytical Methods

Chapter 5. Evaluation of Bond Test Methods

Chapter 6. Effects of Workmanship on Bond Strength

Chapter 7. Effects of Environmental Conditions on Bond Strength

Chapter 8. Conclusions and Suggestions for Further Research

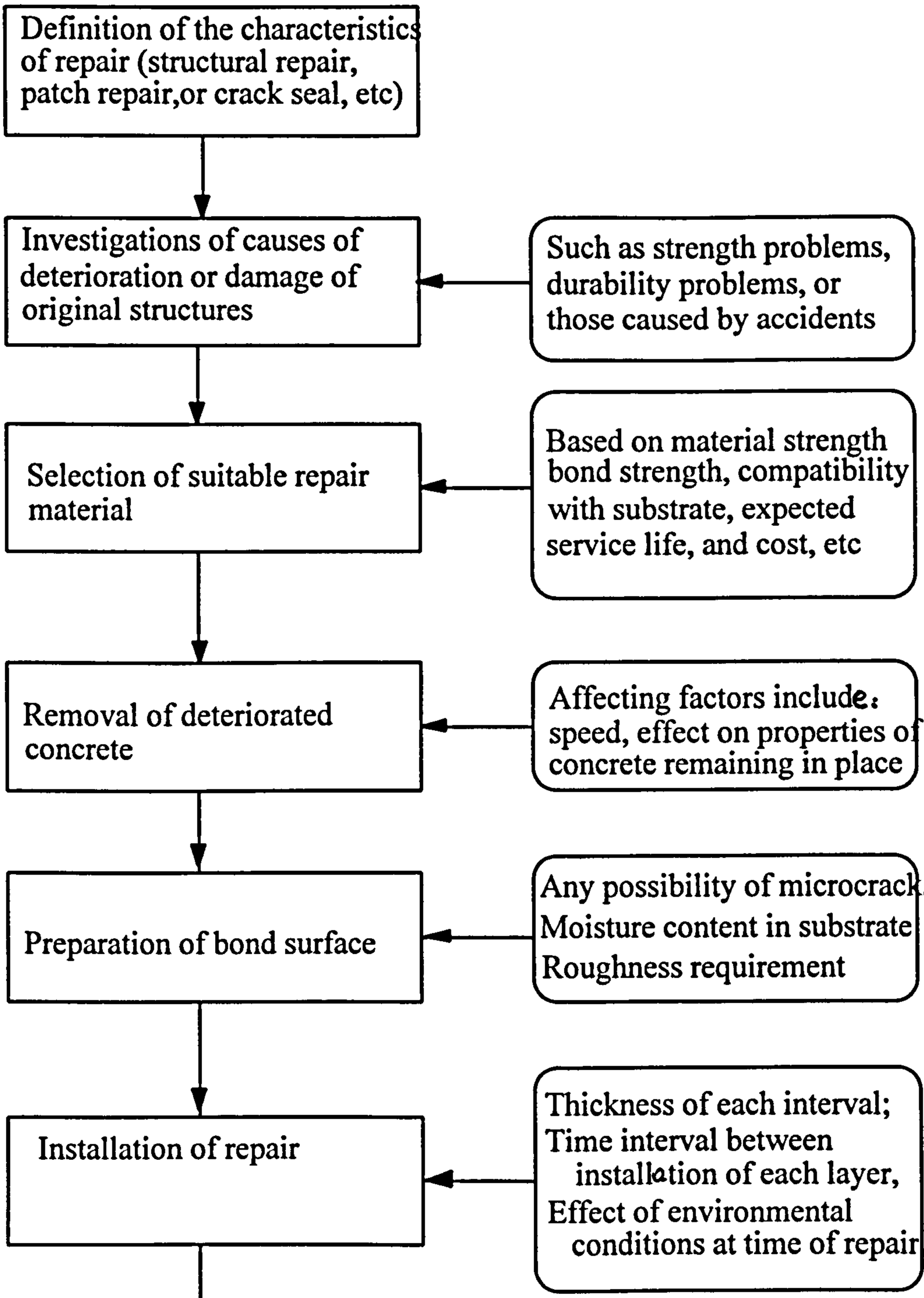

Figure 1.1 General repair procedure and influencing factors

Chapter 2

LITERATURE REVIEW

OF CONCRETE PATCH REPAIRS

Chapter 2 Literature review of concrete repairs

2.1. Introduction

Patch repairs refer to the restoration of relatively small areas of damage to the profile of the surrounding concrete. In repairing such surface damage, it is important to identify the causes of the damage because more than one factor may be involved. Identification of the causes provides the objective of the repair, viz., restoration of durability, structural strength, functionality, or appearance.

From the relationships of workmanship and environmental influences on construction materials and procedures, criteria for selection of materials and techniques can be developed to give a repair that will have a reasonable probability of success. This can be done on the basis of performance specifications and testing to obtain information on physical criteria that are important and crucial in a specific instance.

There are many well established standards for evaluating a single material's properties, but not for bond strength and repair systems. This is evidenced by many different tests methods, different results, and different conclusions. It is not uncommon to find conflicting results. This review will focus on research related to the objectives set out in the Chapter 1:

(1) evaluation of bond test methods;

(2) effects of workmanship on bond strength; and

(3) effect of environmental conditions on bond strength.

2.2 Bond Strength Test Methods

2.2.1 General

An important property of a repair material is the ability to adhere to the substrate. The question of how to measure the bond strength has been the subject of many studies [2, 5, 13, 14, 16-18, 20, 34-76]. Lack of standard tests has resulted in many different results even though the same kind of stress state is imposed on the bond interface.

Some requirements have been put forward for designing a bond test method[5, 13, 15, 20, 37, 38, 40, 42, 43, 48]. Putting these together, they include the following:-

(1) ability to simulate site conditions;

(2) ability to expose only the bond to environmental conditions;

(3) ability to reflect stress state of fairly typical service conditions;

(4) high sensitivity to variation of bond strength;

(5) ability to evaluate in-situ bond strength; and

(6) reproducibility of test results.

No single test method can satisfy all these requirements. The selection is thus heavily dependent on the understanding and the degree of importance given to each requirement under a specific situation.

The test methods that have been used to measure bond strength can be divided into the following categories:-

(1) tensile bond tests;

(2) shear bond tests;

(3) slant shear tests; and

(4) patch repair tests.

2.2.2 Tensile bond tests

2.2.2.1 Direct tensile bond tests

Direct tensile bond tests include the core pull-off test [17, 18, 20, 69, 77], pipe nipple grip uniaxial tensile bond test [13, 37], friction grip tensile bond test[13], dog-bone test [14, 40, 48, 78], and other direct tensile bond tests [14, 48], etc. The basic requirement of a tensile bond test is the application of a uniformly distributed tensile stress over the bond interface.

Core pull-off tests are based on a number of partially destructive in-situ strength tests which have been developed to measure concrete strength by loading the concrete at or near the surface. Examples of some test equipment are the Elcometer Instruments Ltd Model 106 using 20mm diameter dollies; the Limpet pull-off test using a 55mm diameter cores and 50mm diameter dollies; and the Bond-test core case Lok-test L-10 using 75mm diameter cores. (Full description can be found in CIRIA Report[69]).

Although there are variations in the equipment and methods of carrying out pull-off tests, the general test set-up can be referred to as shown in Fig. 2.1 and the general test procedure can be summarised as follows [69].

(1) Prepare a substrate for covering with mortar. Preparation can include scabbling, needle gunning, grit blasting, and splitting, etc.

(2) Apply the mortar to the substrate in a defined manner, or as recommended by the manufacturer.

(3) In many cases tests are carried out on actual structures where steps(1) and (2) have been completed as part of normal site operations.

(4) Stick a steel or aluminium dolly onto the surface of the mortar. The dolly is generally circular with a diameter of between 20 and 75mm, although square plates are also used.

(5) Core around the dolly to provide a defined area to be tested. In some cases a core is drilled prior to bonding on the dolly.

(6) Attach a loading frame to the dolly such that a load can be applied at the right angle to the surface. A frame around the test area provides the reaction force to the load.

(7) Increase the load until a specified level is reached or the specimen fails.

(8) Record the failure stress and the mode of failure (see Fig. 2.2).

The main reasons for choosing a core pull-off test given by different researchers can be summarised as following:-

(1) Representative of actual site conditions [20, 77];

(2) Being able to evaluate in-situ bond strength [15, 20, 77];

(3) Having the advantage of not only providing a quantitative measure of tensile strength but also identifying the location and nature of failure [15, 20, 77]; and

(4) Being only semi-destructive for in-situ repair because the core holes left by the test can be filled with a non-shrink concrete mortar[20].

The accuracy and reproducibility of the core pull-off test results are influenced by factors involved during test preparation. These factors include: coring depth into the substrate, verticality of the drilled cores, the level and evenness of the surface for placing a loading frame, and eccentricities induced by dollies not axially positioned.

Coring into the substrate affects the stress uniformity over the bond interface, but hasn't received much attention. Only a few reports mention the coring depth. Coring

depth was 5mm in [42, 54], 20mm in [73], or just beyond the bond interface [62]. In the author's work[79], the coring was controlled to about 15mm, which agrees with the newly proposed European Standard[60], in which the suggested coring depth is 15 ± 5mm.

Bungey et al's research[80] on surface concrete strength using partial coring method revealed that both the stiffness of the metal dollies and the coring depth affect the uniformity of stress distribution. A higher stiffness dolly produces more uniform stress distribution. But its effect is less marked with the increase in the coring depth.

The pipe nipple grip tensile bond test and friction grip tensile bond test are basically the same except the shear force transfer mechanism is different. A specimen for both cases consists of a 76mm diameter by approximately 76mm long cylinder of repair material bonded to a 76mm diameter by an approximately 76mm long cylinder of substrate concrete [13].

For the pipe nipple grip test, the lateral circumference of the base concrete cylinder with a sawn surface is bonded with epoxy resin inside a nominal 76mm inside diameter by 76mm long black steel pipe nipple. After the epoxy has cured, the specimen is inverted and an empty same size steel pipe is mounted on top of the base concrete, with a rubber 'O'-ring being placed in between the pipes. The rubber 'O'-ring provides about 4.8mm spacing between the pipes at the bond interface. The repair material is then poured into the empty steel pipe nipple. After curing, the repair material has bonded to the sawn surface of the base concrete and to the inside of the pipe nipple into which it has been poured. In order to attach the specimen to a testing machine, pipe caps with special attachments, including universal ball and socket connections, are screwed onto the pipes at both ends.

For the friction grip test, the required friction around the lateral surface area of the bond strength specimen to transfer external load to the bond interface is developed by closing together the sides of the steel pipe which has been split parallel to its longitudinal axis. Two identical split pipe pieces(friction grip) are used, one to grip the repair material and the other to grip the base concrete. Fig. 2.3 shows the two set-ups. Because only the bond area is exposed while much of the base concrete and repair material are sealed by steel pipes, it was claimed by Kuhlmann [37] that this was an important characteristic because it is capable of exposing just the bond plane to different environmental conditions.

It might be assumed that these two methods would produce similar results because they use the same size steel pipes, same surface preparation, same repair materials, and same test procedures, except for the difference in friction transfer. But tests carried out by Knab and Spring [13] showed that the pipe nipple grip test produced much higher failure stress than the friction-grip test. They thought the higher average failure stress was caused , at least in part, by less eccentricity introduced in the pipe nipple test method as compared to the friction grip test method.

BS6319: Part 7[78] describes another test, the so-called dog-bone test, for determination of tensile bond strength. The test specimen is cast in a dog-bone shaped mould giving a cross-sectional area at the waist of 645 mm^2. The geometry is such that during testing the specimen can be held at each end using specially shaped jaws and under tension will break across the narrowest-width.

Judge, et al[40] carried out both dog-bone, and core pull-off test, but the limited test results showed that failure stresses from the dog-bone test were much higher than that from the pull-off test. The difference in failure stresses could be partly caused by difference in surface preparation. The surfaces for pull-off test were acid etched, well

washed and when dry, wire brushed, whilst the others were of broken surfaces. Fig. 2.4 shows the BS6319: Part 7 (dog-bone) mould and tested specimen.

A similar dog-bone test was used by Ohama, et al[14] to investigate the influence of polymer addition on bond strength together with other test methods. If it is compared with another direct tensile test in the same paper (Fig. 2.5), higher failure stresses were obtained using the dog-bone test.

Other direct tensile bond tests have been used to measure the bond strength between cement paste and aggregate by Su, et al [50], and Pye, et al [81].

2.2.2.2 Indirect tensile bond tests

A few indirect tensile bond tests have been tried but only on a very small scale. Those include flexural tests [14, 39, 48] (Fig. 2.6) and tensile split tests [39, 48, 82] (Fig. 2.7).

In [39], flexural tests (Fig. 2.6c and d) and the tensile split test (Fig. 2.7a) were used to compare the sensitivity of test methods to variation in bond strength (also included was the slant shear test). Although a reduction in bond strength was observed using PVA bonding agent compared with the normal sand/cement mortar, the relative decrease in bond strength detected by all these indirect tensile tests was not as sensitive as the slant shear test. In order of sensitivity, the bond strength reduction rate as compared to solid control specimens, from high to low are the following:-

(1) the slant shear test (72-22%);

(2) the flexural-60º test (85%-37%);

(3) the flexural-45º test (90%-46%); and

(4) the split test (96%-78%).

2.2.3 Shear Bond Tests

Shear bond tests can be carried out by applying either a shear force or a torque over the bond interface. In the former case, a more uniform shear stress distribution is set up over the bond interface, while in the latter case, high shear stress gradient can be expected.

In the adhesive industry there are numerous types of test methods for assessing the bond strength between an adhesive and an adherand [83]. Examples include the shear test methods used in [84] (Fig. 2.8) and in [70] (Fig. 2.9). But in terms of concrete patch repair, only a few tests have been reported using shear test methods.

In [14], two direct shear bond tests were conducted (Fig. 2.10). Test results showed that circular cross-section specimens produced higher shear failure stress than square specimens. Because the loading positions were not given, it is not clear whether the difference in failure stress was caused by secondary bending effect or a shape effect of the bond area.

Tayabji [85] reported shear bond test on a bridge deck. Cores of about 94mm in diameter were cut from test sections of the repaired bridge deck. A direct shear test equipment was used. It is interesting to note that with the increase in scarification depth achieved using hydrojetting, which is equal to the repair thickness, shear bond strength decreased dramatically. It might be assumed that for this real repair, deeper scarification by hydrojetting would produce stronger, at least not weaker, bond because a sounder substrate was produced. No explanation was given.

Lavelle [86] carried out shear bond tests, but no information on test configuration can be found.

Researchers in Belfast have devised a 'twist-off' shear test, and have used this method to study the effect of curing conditions on bond strength [18, 41, 87]. The test procedures are basically the same as the core pull-off test except a torque is applied instead of a tensile force (Fig. 2.11). In their first paper[18], the twist-off test was used together with the core pull-off test to study the surface preparation effect. The surfaces were prepared in the following two ways: saw cut and split/chisel hammered. It should be pointed out that while results from the core pull-off test showed a dramatic decrease in bond strength on a split/chisel hammered surface, the twist-off test showed hardly any difference, which renders it unsuitable for detecting surface defects such as microcracks. In another paper [87], the twist-off and pull-off tests were used extensively with different curing conditions and different repair materials. Good correlation and similar trends were recorded.

2.2.4 Slant Shear Tests

The first test of this nature was the 'Arizona Slant Shear Test' which was reported by Kreigh[44]. With this method the strength of repaired 6"x12" concrete cylinders were compared with control specimens. Kreigh claimed that this test represents a condition closer to the actual use and failure mode of concrete. This test suffers from difficulties in making the specimens and is only of practical use for testing large volume concrete repair materials and bonding agents. As a result, a simplified version of this test was developed by Tabor[45]. This used rectangular prism test pieces, prepared in such a way as to remove many of the problems associated with the Arizona test. This test method has been adopted as a part of British Standard Test Methods for Testing Concrete Repair Materials (BS6319 :Part 4)[47].

The basic test procedure can be summarised as follows:

(1) Prepare substrate concrete, split, or saw cut in two halves to produce different surface conditions.

(2) Apply repair mortar onto the substrate to produce a 150x150x55 mm plaque.

(3) Saw cut the central area of the repaired plaque into the size of about 150x55x55mm after curing. One test specimen is produced from each plaque.

(4) Test under a compressive load at the desired age.

(5) Record the failure stress (the nominal axial stress at failure) and the failure mode.

Fig. 2.12 shows the procedures to prepare a specimen.

Rizzo and Sobelman[35], Wall and Shrive[38, 39], Dixon and Sunley[43], Frank[59], Climaco and Regan[63], Hranilovic[84], Godart and Lafuente [88] prefer the slant shear test because they claim that it represents the real stress conditions. Knab and Spring [13], Ohama, et al [14], Austin and Robins[15], Kudlapur, et al[34], Judge, et al[40], Long, et al[41, 77], Alexander, et al[48], and Al-Mandil, et al[89] included the slant shear test in their research to compare with other test methods.

Knab and Spring's results [13] on saw cut and sand papered surface showed that the slant shear test produced very consistent results (three groups of test, and eight specimens in each group). The coefficient of variation of measured bond strengths were 4.8, 11.2, and 4.7 percent, respectively. Because of the significant difference in the absolute values of bond strength and failure modes obtained using different test methods, they emphasised the importance of selecting test methods with geometry, loading conditions and stress state which are anticipated for the in-service material. They concluded that the slant shear test and the pipe nipple tensile test were promising methods for screening and selecting repair materials.

Climaco and Regan[63]'s results from their series 1 tests showed undue mechanical interlock effect. The specimens were repaired with repair mortar applied onto a split and wax coated surface. The measured failure load was about 55 percent of the control solid specimens. Similar effects were observed by Austin and Robins[15]. In order to avoid undue mechanical interlock, in their series 2 tests, Climaco and Regan chose the needlegunning method to prepare the substrate surfaces. The specimen size was increased to 1000mm in height and 150x150mm in cross section. More bond failures were observed as compared with the standard slant shear test, in which the split surface was used.

Recently, some doubts have been raised to question the credibility of the slant shear test. In [14], the bond performance of polymer modified materials was measured using different test methods. By varying the polymer/cement ratio (p/c ratio), the bond strength measured from each method can be plotted against the polymer/cement ratio. All test methods except the slant shear test showed increased bond strengths with increase in p/c ratio up to 20 percent. The slant shear test showed decreased bond strength with increased p/c ratio after 5 percent.

In Long, et al's work[41, 77], conflicting results were also observed between core pull-off and slant shear tests, and between twist-off and slant shear tests. They reported that the slant shear test gave less consistent results. The conflicting results made them question the reliability of this standard test.

In [15], Austin and Robins concluded that the standard slant shear test does not give a true indication of patch repair performance. The test is heavily dependent on the mechanical interlock at the bond plane and the failure stress was found to be merely a function of the compressive strength of the weaker material.

In the case of a bond failure, the Coulomb failure criterion can be used to describe the ultimate strength[48, 59, 63], i.e., a bond failure will occur if the following equation is satisfied.

$$\tau = c + \mu \cdot \sigma \qquad (2.1)$$

or

$$\tau = c + \tan(\phi) \cdot \sigma \qquad (2.2)$$

where τ is the shear stress acting on the bond plane;

σ is the normal stress acting on the bond plane;

c is the adhesion strength;

μ is the coefficient of friction, and

ϕ is the internal friction angle, $\phi = \tan^{-1}(\mu)$.

This suggests a direct relationship between the ultimate strength and the two parameters involved: c and μ (or c and ϕ).

The coefficient of friction, μ, is governed by the roughness of the substrate[59, 63]. Results from [63] showed that the coefficient of friction affects the determination of the critical bond direction which corresponds to the minimum failure load. This obviously casts doubt on the single bond direction (α=30°) suggested in BS6319 : Part 4.

Regan[63] proposed μ=1.4 for rough surfaces with exposed aggregates. ACI 318-83[90] stipulates μ=1.0 for concrete placed against hardened concrete with the surface roughened to a full amplitude of about 6mm. Frank [59] gave μ=0.7 for surfaces sandblasted after removal from moulds. Robins and Austin's results[68] suggested μ=0.8 for smooth surfaces and 1.1 for rough surfaces.

The adhesion strength , c, is assumed to represent shear strength when the normal stress, σ, is zero. But shear strengths obtained from the shear bond test, e.g., the twist-off test, are generally much lower than that predicted using the Coulomb criterion. The general procedure in determining the value of c is to conduct two series of tests with different bond directions. The intersection with the vertical axis is used for manipulating the Coulomb criterion.

Finite element analysis has also been carried out on the slant shear test by Wall and Shrive[38]. Loading was simulated in the finite element models by applying a vertical displacement to the nodes along the top edge of the prism. Materials were assumed to be linear elastic. Results from the finite element analysis showed that bond materials with a modulus of elasticity higher than the substrate cause higher compressive stresses at the bond line and lower tensile stresses in the adjacent concrete than bond materials with a lower modulus of elasticity than the substrate. They concluded that a bond material with a modulus of elasticity that is similar to the adjacent concrete is desirable. Similar results were also obtained by Robins and Austin [68] using the finite element analysis.

2.2.5 Patch Repair Tests

The major shortfall with all test methods mentioned in the previous sections is that they measure the bond strength by direct application of load on the repair material and the substrate. However, in practice, much of the loading of the repair will be induced by changes in strain in the substrate and the loads on the repair will be transmitted from the substrate through the bond interface. This has a direct relationship with property mismatch, such as modulus mismatch and the difference in the coefficients of thermal expansion.

The idea to devise a new test to study bond performance in a more realistic way has led to the design of patch repaired beams and columns.

Burley, et al[62] used the flexural test to study the performance of different repair materials. A series of reinforced concrete beams (2500x205x104mm) were cast. Apart from the controls, the beams were cast with three types of performed faults. The faults were thought to simulate the range caused by corrosion, fire, or impact damage (Fig. 2.13). Because the same reinforcement was used for all beams, it was perhaps not surprising to find that all the measured ultimate loads (including the unrepaired ones) were nearly the same. Similar tests were conducted by Kudlapur, et al [34], Cairns [91], and Mays [92]. Again, because the repair materials were put in the tensile region, no difference in the ultimate bending capacity between repaired and unrepaired specimens was found.

Ramirez, et al[93] carried out repairs of concrete columns with localised partial loss of corners or cover. The research focused on recuperating column strengths. Repaired columns showed increased strength, and failure was caused due to the debond of the repair material.

Emberson and Mays [94] studied the effect of property mismatch using axially loaded patch repair systems. The study was divided into three stages: direct transferring of stress, indirect transferring of stresses in a plain concrete substrate, and indirect transferring of stresses in a reinforced concrete substrate (Fig. 2.14). Finite element analyses were carried out. The results showed that the modulus value of the repair mortar, which determines the stresses transferred to the repair material is of paramount importance in reinforced patch repairs. The effect of Poisson's ratio on stress distribution decreases as the stress is transferred from directly to indirectly. Its effect also decreases from unreinforced to reinforced substrates.

Austin and Robins [16, 68] developed a patch test specially to study the behaviour of shallow concrete patch repairs. A patch test specimen can be loaded in compression, flexure, or directly in tension (by preloading in compression before repair and unloading after repair having been carried out) (Fig. 2.15). In the compression test the specimen exhibited both composite and debonding failure modes. The debonding loads were sensitive to the type of repair material, the roughness of the substrate, and the moisture conditions at the time of repair. In the flexure test the same configuration of cut-out as with the compression tests was used, but only composite failures were recorded. Finite element analysis was also carried out to see the modulus effect on stress distribution. With decreasing modulus, stresses transferred to the repair material were also decreased.

Clearly, the stress state along the bond interface varies in a patch test depending on many factors, such as the geometry of the cut-out, the loading conditions, etc.. A direct comparison between straightforward bond test methods and the patch tests cannot be established unless the stress state has been worked out and bond strength criterion developed. So far, the Coulomb theory has been used to describe the performance under a combined stress state of compression and shear. A complete bond strength criterion is definitely needed.

2.3 Effects of Workmanship on Bond Strength

2.3.1 General

Concrete work for repair requires even more attention to good practice than is necessary for new construction. Therefore, the success of a repair project will depend upon the degree to which the work is executed in compliance with design and specifications.

Data obtained from questionnaires and interviews with engineers and contractors with extensive experience have indicated that poor workmanship is the prime cause of short term failures [6]. But workmanship covers many aspects, such as the removal of deteriorated concrete, surface preparation, application of bond coat and compactness. A careful study of each factor involved will increase the possibility of success.

2.3.2 Surface preparation

2.3.2.1 General

On construction sites, deteriorated concrete has to be removed before any further surface preparation can be done. But in laboratories, a substrate surface is usually produced from a simulated specimen. In order to use results obtained from laboratory studies to guide practical repairs, both practical and laboratory methods should be reviewed. The removal methods are included in this section.

2.3.2.2 Concrete removal techniques

The effectiveness of various removal techniques may vary for deteriorated and sound concrete -- some techniques may be more effective on sound concrete, whilst others may work better on deteriorated concrete. The same removal technique may not be suited for all of the section of a given structure, and the most appropriate technique for each area of the structure should be selected.

Various removal techniques are currently used, and these are categorised by the way in which the process acts on the concrete. These categories are blasting, cutting, impacting, and spalling.

(1) Blasting methods

Blasting methods involve the use of a vigorous expanding gas confined inside a series of boreholes to produce controlled fracture, and microcracks might be caused to concrete left in place.

(2) Cutting methods

Cutting methods generally employ mechanical diamond saw cutting, intense heat from powder torch thermal lance, electric arc equipment, and high pressure water jets to cut around the perimeter of a concrete section to allow their removal.

(3) Impacting methods

The equipment used includes machines that produce a repeated striking at the concrete surface causing fracturing and spalling of the concrete, e.g., jackhammers. High cyclic impact energy delivered to the structure generates vibrations that may damage the remaining concrete, and thus affect the integrity of the structure.

(4) Presplitting methods

Presplitting methods include hydraulic splitters, water pulse devices, and expansive agents. Wedge devices, water pressure pulses, or expansive chemicals are placed in boreholes made at intervals along a predetermined line to induce a crack plane to allow for concrete removal. The pattern, spacing, and depth of the borehole affect the direction and extent of the crack plane and the propagation.

(5) Spalling methods

Spalling methods are chiefly used as secondary means for the removal of concrete. The method employs mechanical devices that generate tensile stresses large enough to remove small piece of concrete, and are more applicable to shallow removal of small volumes of concrete.

The question regarding the removal of deteriorated concrete is when and how a sound substrate is achieved. Gaul [95] suggested the strength of the concrete at and near the surface can be evaluated by a pull out test. For epoxy and polyester protective barrier materials, the tensile strength of the concrete should be at least 0.7MPa.

2.3.2.3 Surface preparation

It is widely recognised that surface preparation is one of the most critical factors affecting the performance of a repair material. The repair will only be as good as the effect expended in surface preparation, regardless of the nature or quality of the repair material. The objective of surface preparation is to provide a sound, dry, even, level surface, free of dirt, dust, oil, and grease. However, the desired condition of the concrete surface may vary somewhat, depending on the type of repair being undertaken and the condition of the substrate.

The methods of surface preparation include chemical, mechanical, blast, flame cleaning, and acid etching.

When concrete is contaminated with oil, grease, etc., chemical cleaning, such as using detergents, and various proprietary concrete cleaners, can be used. This should be followed by vigorous scrubbing and thorough rinsing with water to remove all residues. Solvents should not be used to clean concrete since they will dissolve the contaminate and carry it deeper into the concrete.

Devices used for mechanical cleaning are, in general, of two types, rotary and impact. Rotary equipment includes rotary discs and grinders which are usually used on low strength substrates that do not have a steel trowelled finish. They are not effective on hard, dense concrete, which are likely to polish rather than abrade. Impact tools such as bush hammers, scabblers, and needle guns will effectively remove several millimetres of surface.

Blast cleaning includes wet and dry sandblasting, shot blasting, and water jetting. A sandblasting machine uses compressed air to eject a high speed stream of sand or other abrasive from a nozzle. The hardness of the concrete is important in determining

whether sandblasting is the most economical method for application other than light cleaning. Dust is a problem in the dry method of sandblasting, and clean up is another. Many US cities have placed restrictive regulations on sandblasting due to health and environmental problems [96]. Wet blasting applications are labour-intensive regarding the final clean up and of course also produce residual moisture. Sand remaining on the substrate will prevent proper adhesion of the repair material. Shot blasting uses metallic abrasives to scour the concrete surface. Shot, propelled by a rotating wheel, impacts on the concrete surface and rebounds into a recovery unit. The following three factors influence the depth of blasting methods[1]: size of the abrasive, amount of abrasive; and delivery pressure of the machine.

In a concrete practice note prepared by Murray [97], surfaces with different roughness and texture were produced by sandblasting and jack hammer (Fig. 2.16 and Fig. 2.17).

Water blasting consists of directing a high velocity, high pressure, water jet onto the concrete surface through a specially designed nozzle. The equipment can be used in applications ranging from laitance removal to hydrodemolition of concrete to depths of up to 30mm. Advantages of this method are as follows:-

(1) No dust is produced and the noise is minimum;

(2) There are no mechanical vibrations that might cause structural damage;

(3) The machine selectively removes deteriorated concrete and leaves good concrete intact;

(4) Rebars are not damaged as they might be by scarifiers or scabblers; and

(5) Removal of deteriorated concrete is faster than by conventional methods, such as with a jack hammer.

Flame cleaning is generally used to clean concrete surfaces that are to be coated with coatings or those that will receive resinous overlays. Depending on the properties of

the concrete, a surface scaling or partial melting of the surface layer is obtained. After flame cleaning, any melt residual or loose surface particles should be removed with a wire brush or surface scaler.

Acid etching has been used to remove laitance and dust. The acid will remove enough cement paste to provide a roughened surface which improves the bond of repair materials, but remaining acid residue, if not washed thoroughly, may have a detrimental effect on the bond strength. ACI committee 515 recommends that acid etching only be used when no alternative means of surface preparation can be used [1].

Researchers, to some extent, are trying to use laboratory facilities to produce some typical kind of surface conditions. By comparing bond strengths from differently prepared surfaces, the effect of surface preparation has been evaluated. The surface conditions include:

(1) Mechanically sound, but very smooth surfaces, such as saw cut surfaces [13, 18, 19, 34, 37, 41, 48, 62]; saw cut and sandpapered surfaces [13, 14], cast and slightly sandblasted surfaces [13, 19, 39, 42, 55]; and ground surface [48];

(2) Mechanical sound, fairly rough surfaces, such as sandblasted surfaces [17, 19, 73], and pneumatic needle gunned surfaces [15, 63];

(3) Mechanically sound, rough surfaces, such as water jetted surfaces [17, 19, 20], grit blasted surfaces [19], and sandblasted surfaces [73];

(4) Rough surfaces but with superficial defects or weak layers, such as fractured surfaces [18, 40, 43, 63, 73], and jack hammered surfaces [17, 20].

Surface conditions produced in laboratories also include:

(1) Surface set retarder produced rough surfaces [15];

(2) Acid etched surfaces [19, 40, 43]; and

(3) Artificially debonded surfaces [15, 63].

Test methods relating to results presented in this paragraph are based on tensile bond tests. Long, et al's results [40] showed that a mechanically sound but very smooth surface (saw-cut) can produce higher bond strength than a rough, but with superficial defects surface (split/chiselled). Tests carried out by Hindo[20], Silfwerbrand [17], Kuhlmann [13], Long, et al [19], and Austin and Robins [15, 16] also showed that in a tensile bond test, a sound substrate is very important in ensuring that full bond strength development can be achieved by a repair material. Surface defects, such as weak layer, microcracks, artificial debonding, always have a detrimental effect -- the tensile bond strength is greatly reduced. If soundness can be guaranteed, tensile strength will increase with an increase in surface roughness [18, 19], but the degree of increase varies with the materials used.

A limited study using the slant shear test has shown that failure stress is heavily dependent on surface roughness, and not sensitive to the existence of surface defects, such as microcracks [15, 63].

2.3.3 Moisture condition of the substrate

It is known that moisture condition affects bond strength development, but not many common conclusions have been drawn.

When a repair material is applied onto the substrate, water movement between these two materials will occur due to the unbalanced moisture conditions. If the substrate is dry, water will move from the repair material to the substrate, reducing the water/cement ratio at the bond interface. If free surface water exists, cement paste at the bond interface may by diluted [98]. The moisture condition of a substrate relates to

both the internal moisture condition inside the substrate and the surface moisture state. Unfortunately, most reports do not clearly distinguish between the two. Often, a substrate is simply defined as wet or dry.

In the concrete repair industry, it is generally recommended that concrete substrate is thoroughly wetted without any standing water before a repair material is applied [99-101]. However, some published data showed that a dry substrate produced higher bond strength [21, 63, 64, 102], whilst others showed that a prewetted surface produced stronger bond [15, 38]. In studies of bond between cement paste and aggregates, the common conclusion is that a dry aggregate produces a stronger bond [48, 103, 104].

Apart from reasons that unbalanced moisture condition affects water movement between a substrate and a repair mortar, Shaw [7] pointed out the effect of ambient temperatures on bond strength and the importance of prewetting of a substrate surface. Water loss at the interface between the repair material and the prepared concrete may prevent proper hydration of the cement matrix at this interface.

2.3.4 Bond coats

It is essential to obtain the best possible bond at the interface between existing concrete and the repair material. Prior to the introduction of polymer bond coats, it was the practice either to use nothing and rely on the surface preparation of the substrate, or to use a cement slurry. Both of these techniques gave excellent results in the laboratory, but in the field, the results were often disappointing [9]. This was the basic reason for the research and development of special bond coats (bond aids, bonding agents, etc. have the same meaning in this thesis).

A bond coat can function in two ways: improve the close contact between a repair material and the substrate; and improve the bond strength.

In [18], on a saw cut surface, the tensile bond strength of a sand/cement mortar was increased from about 1.2MPa without a bond coat to about 3.1 MPa with an epoxy bond coat. On a split surface, the bond strength was increased from about 0.7MPa to about 1.9MPa with an epoxy bond coat.

Generally, it is a requirement that a bond coat should be tacky when a repair material is applied [7, 8, 105], but the time needed for a bond coat to become tacky may vary between products from different manufacturers, and different polymer types.

Judge, et al's results [40], using a tensile bond test, showed a tacky condition doesn't always guarantee the best bond that can be achieved. Some dry bond coats produced higher bond strengths than tacky ones. It depended very much on the bond coats used. With three different acrylate bond coats, the bond strength was not very sensitive to the conditions of the bond coat (wet, tacky, or dry). Two other bond coats (Terpolymer and PAVc/VeoVa) achieved the highest bond strength under dry conditions, but an SBR bond coat showed complete loss of bond strength when becoming dry. Dixon and Sunley [43] also reported a very detrimental effect when repair material is applied to a dried SBR bond coat .

Also, applying a second bond coat to the dried first coat will not remedy the situation, rather a more dramatic decrease in bond strength has been recorded [38, 43]. Thus manufacturers require that if a bond coat becomes dry, it should be removed completely, the surface reprepared if necessary, and a new bond coat applied [100, 101, 106].

Whilst a strong brush may often be the easiest way to transfer the mixed material from the container to a vertical surface, it is vital to ensure that it is firmly worked into the roughened concrete surface by a scrubbing action with a stiff-bristled brush [1, 105].

2.3.5 Application of repair materials

After priming the substrate with a bond coat a period of drying may be necessary to wait until the bond coat develops to a near-dry tacky condition, meanwhile the mortar can be prepared. Polymer bond coats for cementitious mortar need a drying period, but polymer cement bond coats become tacky immediately and there should be no delay in placing the mortar [105].

The method of application depends on the conditions where the mortar is to be applied; for example, recasting or spraying for large areas like overlays, or hand applied systems for patch repair of small areas.

In laboratories, a repair is usually carried out by applying a repair mortar on top of a prepared substrate [17-19, 37, 48]. This is possibly the easiest way to ensure a close contact between a repair material and the substrate. But in practice, except for horizontal surfaces, repairs can also be carried out on a vertical surface or a soffit. This means taking the initial bond property of a repair material into consideration. In some cases, a shutter may be necessary if the depth is more than can be applied overhead in one pass.

Using the core pull-off test, the bond strength of an SBR modified mortar carried out by Naderi et al [107] was about equal to a sand/cement mortar applied to a wet surface without any bonding slurry. Visual examination of the cores indicated that the weakness of the SBR mortar appeared to be a result of inadequate bond between the

bond coat and the repair material. This suggests that this kind of repair material is highly sensitive to workmanship.

In order to see the effect of different operators on bond strength, Kuhlmann [37] reported results carried out by trainees participating in two different courses. When following the same standard procedure, test results showed very good reproducibility and single-operator precision.

2.3.6 Curing of repair

2.2.2

It is essential that all practical measures should be taken to ensure proper curing of the newly placed mortar. This can present some problems in those cases where the repaired areas are small and widely spaced [9, 10]. Even with reasonable attempts at curing, it is often found that fine hairline cracks develop around the perimeter of the repaired areas due to drying shrinkage [9]. Unless steps are taken to seal these cracks, they are likely to form the nucleus of fresh deterioration or they will tend to widen due to frost action. Thus curing has effects on both bond strength and the bulk properties.

Plum [108] conducted tests of the curing environment on polymer modified materials. The properties studied include compressive strength, flexural strength, elastic modulus in compression, and flexural creep. It was found that conditions of both temperature and humidity during the curing period had a significant effect on the final properties. Test results from [109, 110] demonstrated similar detrimental effect of improper curing on material properties.

The curing condition has different effects on different bulk properties. Vipulanandan, et al's results [22] showed that whilst the compressive strength of the polymer concrete investigated increased with increased curing temperature, the tensile splitting

strength and compressive modulus decreased. They used the compressive strength to judge the optimum curing condition.

Proper curing aims to maintain the moisture condition inside the repair material for suitable hydration and enhance the designed level of durability. Hence the surface layer is more vulnerable to improper curing than the inner bulk material. The surface layer (about 30-50mm) in thickness is most affected due to the high rate of evaporation of water from the surface layer. This could lead to surface problems from wear, deterioration, and poor durability [21, 53, 111, 112]. For example, the repair mortar should restore the alkaline conditions in the surrounding of the reinforcement, so it must be resistant to carbonation as much as possible. Test results from [53] demonstrated that a 3-day moist curing showed less carbonation depth than a 1-day moist curing.

In a repair work, early and effective curing is also important because it will reduce the early-age moisture losses usually leading to excessive volume changes and reduce the early-age stresses at the bond interface [112].

In [87], temperature ranged from a little above freezing to tropical temperature, with relative humidity from desert area to coastal area. The study was divided into two parts. For the first part, mixing of concrete patch repairs was carried out at laboratory temperature. Placing and finishing used an environmental chamber under test conditions. The repaired specimens were left in the chamber for 14 days and then transferred to a constant temperature room of 20°C and stored for a further 14 days before tests were carried out. For the second part, the repair material ingredients were conditioned and then mixed at the desired test conditions (10°C, 70%RH, and 40°C, 70%RH). The repaired specimens were subjected to curing conditions for 14 days and then tested after a further 14 days.

Test results (pull-off and twist-off tests) revealed that curing conditions affected the bond strength, but the influence differed for different repair materials. For example, an environmental condition of high humidity with low temperature was an ideal curing condition for unmodified OPC/sand mortar, but flowing concrete showed increased bond strength with an increase in humidity and temperature. The SBR modified mortar also favoured a high humidity environment, but the ideal temperature was 10-20°C. All other repair materials showed that with increased humidity, bond strength increased, whilst the acrylic modified cementitious mortar exhibited a reduction in bond strength for high levels of humidity.

Results from the second part of the programme revealed that materials mixed at room temperature generally gave higher bond strengths than those mixed at other temperatures, though the margin was very small between 10°C and 20°C. Greater reduction in bond strength occurred at high temperature (40°C) and low temperature (4-6°C).

Tests carried out by Lavelle [86] showed that whilst unmodified cementitious mortar benefited most from a wet curing environment, the acrylic modified mortar, with polymer/cement ratio varying from 10 to 20 percent, produced higher material strength (tensile, compressive, flexural strength, etc.) under a air curing situation. It was also pointed out in [86] that while air drying is recommended for curing acrylic latex-based mortars, care should be taken to avoid rapid dehydration, which can lead to surface cracking. Three curing conditions were adopted to see the effect on the properties of acrylic modified cementitious material and the corresponding bond strength. The three curing conditions were: (1) a 28-day air cure, (2) a 28-day wet cure, and (3) a 28-day air cure plus a 7-day water soak. For unmodified mortar, 28-day wet cure produced higher bond strength than 28-day air cured. But for the modified material, results showed that 28-day air cure produced higher shear bond strength.

In a Concrete Society report [10], it was reported that although the polymer acts to some extent as an integral curing membrane, separate curing with polythene sheet, damp hessian or a sprayed-on uniform film of proprietary curing membrane is essential in exposed conditions, especially in hot drying and cold windy conditions. Greater care is required with thin layers to prevent rapid early drying out which will interfere with the hydration of the cement. After the curing a period of air curing is necessary with polymer-modified mortars to allow full properties to be developed.

All these indicate the importance of proper curing on a repair system. In [105], it is recommended that where the area of a patch exceeds 0.75m^2 (or a 1m run of a narrow repair) it is advisable to finish the work 0.5m^2 at a time and apply curing protection before continuing. In [9] it is further recommended that where repairs of any magnitude are carried out, the whole surface of both the repair and the areas which have remained without repair, should be sealed with a durable coating.

2.4 Effects of environmental conditions on bond strength

2.4.1 Introduction

In order to design the repair for durability, the effect of the environment on the repair per se, as well as the effect of the same environment on the existing substrate, and the interface between the two materials should be considered. Then the combined effect on the composite system can be evaluated by careful analysis of the current processes involved. For example, some environments which are relatively harmless to the substrate may be harmful to the repair material and vice versa.

If the properties of the environment in which the repaired structure is to serve are known, the levels of the relevant properties that repair materials must have in that environment, to yield the desired performance, can be identified. When the

specification is properly prepared and complied with, the repair should possess such properties that as it interacts with the elements of the environment, it will not deteriorate. or work as expected.

First of all, the performance of repair materials and bond interface under different environmental conditions should be understood to provide information for material selection and evaluation of a repaired system. So far, most of research carried out has been on substrate concrete, with a small number on repair materials and just a few on bond performance.

2.4.2 Temperature effects

2.4.2.1 Effects of temperature on concrete

Temperature effects can be divided into low and high temperature effects. The effects can be seen in two aspects: (1) chemical change - dissociation or decomposition of hydrated products at high temperature; and (2) physical change - differential thermal expansion between aggregate and cement paste, evaporation of water at high temperature, icing of water at low temperature, and thermal stresses caused by these changes.

There are numerous papers discussing the effect of temperature on substrate concrete. The effect of high temperature can be summarised as follows [113]:

(1) The coefficient of thermal expansion - This is a variable quantity depending on the mix design and the type of aggregate used. Since aggregates make up the bulk of concrete, their properties will largely determine the concrete properties. Generally, the coefficient of thermal expansion of concrete varies between $7.4 \times 10^{-6}/^{o}C$ and $13 \times 10^{-6}/^{o}C$.

(2) Strength - Unless large temperature differentials are allowed to develop (as in a rapid heating), the compressive strength of concrete at elevated temperature is usually maintained up to about 300°C, but above this temperature a significant decrease can be anticipated (Fig. 2.18). The magnitude of the decrease depends on the nature of the aggregate and the initial moisture content of the specimen.

(3) Deformation - Modulus of elasticity decreases with increasing temperature (Fig. 2.18). The other aspect is the increased drying shrinkage when concrete is exposed to elevated temperature due to additional moisture loss from the paste (Fig. 2.19). The rate of shrinkage depends on the rate of moisture loss from concrete, depending on the following factors: initial moisture content, water/cement ratio, moisture content of the aggregate, specimen shape and surface moisture conditions. Creep will also increase with an increase in temperature.

At low temperatures, the mechanism is different from that at elevated temperatures. Moisture content and the progressive formation of ice play a direct role in the change of physical properties of hardened concrete. The content of evaporable water and the distribution of pores and voids in concrete have a direct relationship with performance of concrete at low temperature. In the hardened cement paste, water can be found in several states. Although there is no sharp division, the following classification is suitable according to Bjegovic, et al [114].

(1) Chemically bonded water is the water, bound by hydration process into hard compounds, making up cement gels.

(2) Interlayer water penetrates between layers of hard gel or intercrystallic space, as in clays. The thickness of such interlayers is about 1 manometer (10^{-9}m), and by removing the water, these spaces close and the hardened cement paste contracts.

(3) Adsorbed water is the water tied to the gel surface by surface forces. In the first layer, which is several water molecules thick, these forces are very strong, and this part is under great pressure. With increased distance these forces rapidly decrease.

(4) Free water is found in the capillaries and in large gel pores. It is sufficiently distant from the gel surface and is free from surface forces.

(5) As well as water, concrete voids contain air with a certain amount of vapour, depending on temperature and air pressure.

Gel pores are generally filled with water, and if the paste is saturated the capillary cavities will also be filled. However, the gel pores are so small that it is impossible for water to freeze unless the temperature drops far below normal. It is estimated that freezing can only occur at temperatures below -78^{o}C. Ice crystals cannot form since no more than probably a dozen or so molecules of water occupy the gel pores. In frozen concrete, therefore, water in the gel pores is supercooled but not frozen. Capillary cavities, on the other hand, are sufficiently large to accommodate ice crystals and water will freeze. Bubbles of entrained air are not generally filled with water unless the concrete becomes saturated by means of a vacuum or pressure. It was reported in [115] that small samples of ice have adhesive strength which is fifteen times greater in tension than in shear. Ice formed in capillary cavities will act in two ways: a) strengthen bond within paste, and b) exert pressure due to volume expansion.

If the evaporable water in a hardened concrete is less than that needed for saturation, both the actions will be small compared with fully saturated specimens. If there is no evaporable water in hardened concrete, no change in performance will be expected. For a saturated specimen with entrained air to mitigate the detrimental effect of expansion of ice, high strength increase has been observed [115]. From the above discussion, it can be seen that so long as concrete is properly cured, cooled slowly, and not exposed to freezing and thawing cycling, it will perform satisfactorily.

2.4.2.2 Effects of temperature on polymer-modified repair materials

Adding a polymer latex will modify the thermal response of the concrete/mortar. Both the polymer and cement will contribute to the overall performance of the modified product.

Unlike traditional materials of construction, the physical properties of a polymer are very sensitive to the effect of small temperature changes, and in particular to typical temperature variations which may be met in service, e.g.. -10^{o}C to 60^{o}C. By changing temperature some 20-30^{o}C upwards or downwards, one may transform a material which is hard and strong at, say, 20^{o}C to one which is hard and brittle at 0^{o}C, but soft and weak at, say, 40^{o}C. These changes have an obvious consequence in polymer modified mortar applications.

Due to the complexity of polymer properties and an endless variety of materials, it is not possible to present a detailed picture of the temperature effect on polymer materials. Each case should be related to a specific kind of material, and to a specific material composition. A comprehensive review of the properties of commonly available polymers and the consequence of polymer-concrete mismatch is given by Hewlett and Hurley[116].

For polymer modified concrete/mortar, because the majority of the bulk volume is occupied by coarse aggregate and fine aggregate, the temperature effect will be different from that on pure polymer materials. Vipulanandam and Paul [22] carried out research on the performance of epoxy and polyester polymer concrete with about 85 percent aggregate by weight. Although the compressive strength of the polymer concrete increased with increasing temperature up to 80^{o}C, other properties such as the tensile splitting strength, and the modules of elasticity, decreased.

Shivaprasad, et al [34] carried out tests on cold weather concrete patching materials. The materials used were a methyl methacrylate (MMA) based polymer concrete, another MMA of different brand name, (but nominally identical materials), a water-activated magnesium phosphate cement (MPC), a non-water, liquid-activated magnesium phosphate, and a polyurethane based polymer concrete. Because of their very special purpose for cold-weather patching, they are reviewed here rather than in the curing section. 100x200mm cylinders of the patching materials were cast in the cold room at a temperature of -9^{o}C. Three cylinders were tested for compressive strength 24 hours after casting. Specimens were allowed to thaw for 1 hour before testing to maintain a uniform condition during testing. Three additional cylinders were tested in the same way after a 7-day cold storage. Some showed an increase in compressive strength from the age of 1 day to 7 days, whilst others showed a slight decrease. It is also interesting to note the difference in strength between the two nominally identical MMA concretes.

2.4.2.3 Effect of temperature on bond strength

As a composite system, many factors have an effect, such as thermal stresses, changes in modulus, material properties, and shrinkage. It is very difficult to measure the temperature effect on bond strength without interaction with the factors mentioned above. Yeoh, et al [87] carried out both the core pull-off and the twist-off test with different repair materials. Because the temperature and humidity were maintained right after application of repair material to 14-day old substrate, the test results were discussed in section (2.3.6).

2.4.3 Shrinkage

2.4.3.1 Shrinkage of concrete

Volume changes accompany the loss of moisture from both fresh and hardened concrete. However, the term 'drying shrinkage' is generally reserved for hardened

concrete, while 'plastic shrinkage' is used for fresh concrete, since its response to loss of moisture is quite different. "Carbonation shrinkage', which occurs when hydrated cement reacts with atmospheric carbon dioxide, can be regarded as a special case of drying shrinkage. 'Autogenous shrinkage', which occurs when a concrete self-desiccates during hydration, is also a special case of drying shrinkage [113]. Among these, drying shrinkage is a much more important phenomenon. Inadequate allowance for the effects of drying shrinkage in concrete design and construction can lead to cracking or warping of the elements of the structure due to restraints present during shrinkage.

Shrinkage predictions involve many uncertainties, which include that due to: [117]

(1) measurement error;

(2) random variation of the environmental relative humidity and temperature;

(3) random variability of the material properties which results from the process of mixing, casting, and the curing of concrete;

(4) the random nature of shrinkage increments, which is a consequence of the stochastic nature of the microscopic physical mechanism of shrinkage; and

(5) the shrinkage prediction model itself (i.e., the shrinkage formula), both its form and the value of its parameters.

A detailed discussion on shrinkage can be found in [113, 117, 118].

All practical portland cement shrinks about 400 to 800 με due to drying, according to a Portland Cement Association document quoted by Ytterberg [118]. Schrader [21] reported that most good-quality conventional concretes shrink in the general range of 350 to 650 με. Different formulas have been proposed to describe the shrinkage

development, for example, the ACI recommendation [119], the CEB-FIP recommendation [120], and the BP model [117].

2.4.3.2 Shrinkage of repair materials

With a polymer modification, the shrinkage of many repair materials is very different from traditional concrete, in both the ultimate shrinkage and shrinkage pattern.

Emberson and Mays [5] conducted shrinkage tests on different repair materials, including resinous materials, polymer modified cementitious materials, and cementitious materials. Shrinkage tests included early shrinkage within the first 24 hours after placing and long-term shrinkage. Test results showed that the shrinkage was nearly entirely dependent on the repair material tested. No single formula could be followed. For example, in the category of resinous materials, polyester mortar showed early shrinkage taking place during the first 15-20 min (up to nearly 4,500 με) then nearly no change at all afterwards, but acrylic mortar showed nearly no shrinkage within 1-3 hours after placement, then gradually shrank to about 1,000 με within the next 20 hours. Long term shrinkage tests showed that epoxy mortar developed no shrinkage within 16 months. The magnesium phosphate modified cementitious mortar showed a sharp increase in expansion to about 1,100 με within about 50 days, then gradually decreased to a expansion of about 600 με within the next 15 months. The SBR modified mortar showed a shrinkage of about 540 με within the first month, then gradually developed to about 740 με within the next 15 months. The normal OPC/sand mortar shrank to about 700 με in one month and about 1,100 με in 16 months.

In selecting repair materials, Emmons and Vaysburd [112] pointed out that many pre-packaged repair materials, including some claimed by sales personnel to be 'low shrinkage' have high shrinkages well in excess of what is typical for concrete. Schrader [21] made a comparison of two commercial formulations of a very common packaged mortar product, (often sold as a low-shrinkage material) with typical concrete. One

commercial product showed over 2,000 με shrinkage, the other nearly 1,000 με, whilst the typical concrete showed just 400-500 με.

Curing may change shrinkage values, but shrinkage tests carried out by Kuhlmann [71] on a Styrene-Butadiene modified concrete showed differences only within the first few days. After that, shrinkages were nearly exactly the same. The curing condition for one group of specimen was of a 1-day damp cure followed by air cure, and the other, a 2-day damp cure followed by air cure.

Burge's test [23] showed the effect of polymer type on the shrinkage of modified products. The shrinkage of control concrete was about 500 με. The SBR modification had hardly any effect on shrinkage, and the shrinkage of styrene-acrylate modified mortar decreased with increasing polymer content. For polyvinylpropionate (PVP) modified mortar, the polymer addition increased the shrinkage value dramatically to more than 3,000 με when the polymer/cement ratio was 25 percent.

Clearly the test results mentioned above showed very significant differences in shrinkage values, and the strong dependence on polymer type and polymer content. In order to minimise stresses induced due to the differential shrinkage, a classification should be given as to define what shrinkage value is acceptable.

While Emberson and Mays [48] set a general requirement that curing and long-term shrinkage should be much less than that of substrate concrete, Emmons and Vaysburd [112] made it very clear that a target goal of drying shrinkage value for a repair material is 0%. A classification based on shrinkage was also presented by Emmons and Vaysburd (Fig. 2.20). By using this classification they found that only 15 percent of 46 surface repair materials tested can be labelled as low shrinkage, despite the fact that the manufacturers claimed them to be expansive, non-shrinking, or shrinkage-compensating.

If this classification is applied to categorise repair materials used in [53] based on the measured shrinkage, none can be labelled as low shrinkage, five fall within the medium shrinkage range, and the other five are high shrinkage materials.

2.4.3.3 Effects of shrinkage on bond performance

If the shrinkage is not free to develop, stresses will be generated which will affect the bond strength. Peier [42] reported a wedge test which was used to provide a quick evaluation of crack sensitivity and bond strength of a mortar. Peier divided repair materials into three categories: sealing mortar, thin layer mortar, and concrete replacing mortar, no cracks and no layer separation must occur for the thin layer mortar and concrete replacing mortar.

Rizzo and Sobelman [35] pointed out that while the standard prisms can be used to measure the long-term shrinkage, they can not be used to correlate easily to shrinkage cracking owing to the need to relate the shrinkage to the development of tensile strength and stress relaxation of a repair material. They reported an alternative method of evaluating crack tendency - the restrained shrinkage test. Casting the mortar around a rigid insert and recording the time when cracks occur, they claimed that this method was easy to carry out and gave useful results.

Either the restrained shrinkage test or the wedge test, a material may fail due to a weak bond, a low tensile strength, a high shrinkage, or low creep performance. If all the properties are available, a theoretical analysis can be carried out which can predict both the stress distribution and the stress development along the bond interface. Some research has been carried out on the structural performance of repaired slabs or beams [121-123], but not much on the bond performance.

2.4.4 Effects of temperature cycling

Al-Mandil, et al [89] carried out thermal cycling test on epoxy injected beams and slant shear cylinders (Fig. 2.21). After epoxy injection and proper curing, specimens

were subjected to thermal cycling (between 20°C and 70°C at 35%RH, with 2 cycles per day), and then tested in flexure for beams and compression for the slant shear cylinders. For solid and unrepaired beams, flexural strength were enhanced possibly due to the following two reasons:

(1) After thermal cycling, the age of the specimen was up to 80 days older than those tested at the beginning of the cycling; and

(2) The cycling may have contributed to the hydration of the remaining unhydrated cement.

For repaired beams, severe reduction in flexural strength was recorded. This means that as the number of thermal cycles increased, the epoxy products tended to lose their bonding strength and could eventually became structurally ineffective.

Solid cylinders showed slight increase in failure load up to 200 cycles, then a slight decrease from 200 to 300 cycles. Repaired specimens showed a much lower failure load compared to solid ones at the beginning of the cycling and then showed significant increase in the failure load (approaching that of solid specimens with increasing cycling numbers). No satisfactory explanation was given.

2.4.5 Effects of freeze/thaw cycling

2.4.5.1 Effects of freeze/thaw cycling on substrate concrete

Concrete subjected to repeated cycles of freezing and thawing may deteriorate rapidly, or it may remain in service for many years without showing signs of distress. Failure of the material may take the form of loss of strength, crumbling, or some combination of the two. The mechanisms of freeze/thaw damage can be attributed to hydraulic pressure and ice accumulation.

Water in the capillary pores of cement paste expands upon freezing. If the required volume is greater than the space available, the excess water is driven off by the pressure of expansion. If the pressure exceeds the tensile strength of the paste at any point, it will cause local cracking. In repeated cycles of freezing and thawing in a wet environment, water will enter the cracks during the thawing, only to freeze again later, and there will be progressive deterioration with each cycle.

Even when the hydraulic pressure is not great enough to damage the paste, pressure may build up because of the ice accumulation in the capillary pores. Water in the gel pores is under the influence of surface forces and thus does not freeze in the super cooled state until the temperature drops to the point at which it can freeze. In a practical situation, water will remain liquid as long as it remains in the gel. But because the super cooled water has a higher free energy than the ice in the capillaries, it can flow into the capillaries to freeze. In this way, ice accumulates in the capillaries, eventually exerting pressure on the capillary walls.

Tests on freezing and thawing cycle are usually carried out according to ASTM C666 [124], and damage to the specimen is assessed periodically by visual examination and by measurement of the dynamic modulus of elasticity. The resistance to freezing and thawing of a concrete is influenced by the following factors: air voids and distribution, w/c ratio, aggregate, and curing. Detailed discussion can be found in [23, 125-127].

2.4.5.2 Effects of freeze/thaw cycling on repair materials

Bordeleau, et al [128] studied the effect of SBR polymer modification on concrete properties with the polymer/cement ratio of 7.5 and 15 percent, respectively. One of the parameters investigated was the resistance to a freeze/thaw cycle in the presence of de-icing salt solution. The modified specimens were cured with wet burlap for one day then followed by air cure. The normal concrete specimens for comparison were moist

cured for 3 days. The results indicated that SBR in concrete improves very significantly the resistance of the concrete surface to freezing and thawing.

Lavelle [86] used acrylic modified cementitious mortars in a freeze/thaw test using ASTM C291 test methods. Visual examination was carried out after 60 cycles, which revealed very low penetration of water and salt into the acrylic modified mortar surface.

Balaguru, et al [31] carried out an experimental investigation on the freeze/thaw durability of epoxy resin polymer modified concrete. Specimens were subjected to a maximum of 900 cycles of freezing and thawing, using ASTM C666 procedure A. Results indicated that the resistance to freeze/thaw cycle depended on the polymer content. Specimens with a p/c ratio of 0.2 and 0.3 disintegrated when subjected to further freezing and thawing (beyond 300 cycles) while specimens with a p/c ratio of 0.6 withstood up to 900 cycles of freezing and thawing without extensive damage.

All these tests demonstrate the superior resistance of polymer modified cementitious mortar to freezing and thawing cycles compared with traditional concrete.

2.4.5.3 Effect of freeze/thaw cycling on bond strength

Tests carried out by Cady, et al [129] were targeted at the bond interface, but no test on bond strength was conducted. The test was designed to evaluate the durability and compatibility of overlays and bridge deck substrate treatment. The durability was judged based on visual examination of the substrate and overlay, such as severe deterioration, spalling, cracking, and weight loss. The compatibility was judged on the number of freeze/thaw cycles when debonding occurred. ASTM C666 method A was used, but the specified maximum number of cycles was increased from 300 cycles to 500 cycles. Pulse velocity measurement was also carried out. From the pulse velocity measurement, they mentioned that if debonding occurred, there should be a very

significant decrease in pulse velocity. But in some instances, the recorded variation in pulse velocity measurement was a reflection of surface deterioration rather than debonding. The durability and compatibility depended not only on repair materials used, but also on the substrate treatment. For example, for methyl methacrylate soak impregnation treated substrate, both latex modified concrete and polymer concrete showed good durability and compatibility, but the low-slump dense concrete showed severe spalling. All repair materials applied on untreated concrete showed slight spalling and compatibility was acceptable.

Shivaprasad, et al [34] included the ASTM C666 procedure A test to study the durability of cold-weather concrete patching materials. Specimens were subjected to 300 cycles of freezing and thawing. Weight and half-cell potential were measured prior to cycling and at intervals not exceeding 36 cycles. After cycling, specimens were fatigue tested in flexure to assess the effect of freeze/thaw on fatigue strength, and particularly on patch-substrate concrete bond strength. They also pointed out that weight loss results were not very meaningful, as they often reflected deterioration of the substrate concrete more than of the patch material. Tests showed some debond failures, but results varied significantly.

Ohama [66] reported long-term outdoor exposure involving frost action and weathering of polymer-modified mortar in comparison with conventional mortar and concrete. Excellent durability of latex-modified mortars in terms of adhesion to ordinary cement mortar after a 10-year outdoor exposure in Tokyo was obtained. In contrast to unmodified mortar-bonded specimens that failed within one year of outdoor exposure, most latex-modified mortar-bonded specimens had a satisfactory adhesion for practical use after the 10-year exposure period. The general trend of bond strength decrease was of a fast reduction in bond strength within the first 12 months, followed by a very slow decrease.

A study was also carried out by Lavelle [86] on the flexural bond strength of Portland cement mortars modified with two different acrylic polymers and exposed outdoor for five years. These exposures were carried out in the north-eastern part of the United States, and the specimens were subjected to at least 70 freeze/thaw cycles per year and 1300mm cumulative rain per year. It is surprising to find out from the tests that the flexural bond strength showed no reduction at all. Instead nearly a 40 percent increase in bond strength was recorded. The unmodified flexural bond specimens showed nearly constant bond strength during the 5-year long term out-door exposure.

2.5 Conclusions

From the above review, it is apparent that much work has been done, and this contributed significantly to the understanding of concrete repairs. Much of the work done has been of a trial nature, lacking a thorough and systematic approach. For example, some research has just used test methods to compare between repair materials. When conflicting results occurred, the explanation was often not satisfactory. Even though many bond test methods have been put forward, the evaluation of the methods has not received a systematic study. When conducting a test to select a repair material, the first question is which test method should be selected. Faced with this situation, the author chose the evaluation of test methods as the first part in this study. The test methods were evaluated based on some fundamental factors involved, such as the surface preparation, mismatch of material properties, and specimen geometries.

In the study of effect of workmanship on bond strength, much work has emphasised the importance of workmanship, however, a substantial proportion of the work was on surface preparation. In fact, workmanship also covers other aspects, including mistiming, compacting, and bond coat. A successful repair can only be obtained when all these are taken into consideration. Careful analyses of each factor and its influence

on the overall performance are thus desirable. Hence, the author carried out tests, most of which were designed to study those factors which have received little attention, and a small proportion to complement existing test results. This formed the second part in this study.

As mentioned earlier, much of the work which has been carried out was in the initial stage. Little work has been done on the effect of environmental conditions on bond strength. In this study, based on a thorough evaluation of bond test methods and systematic study of workmanship, the effect of environmental condition was further included in the research.

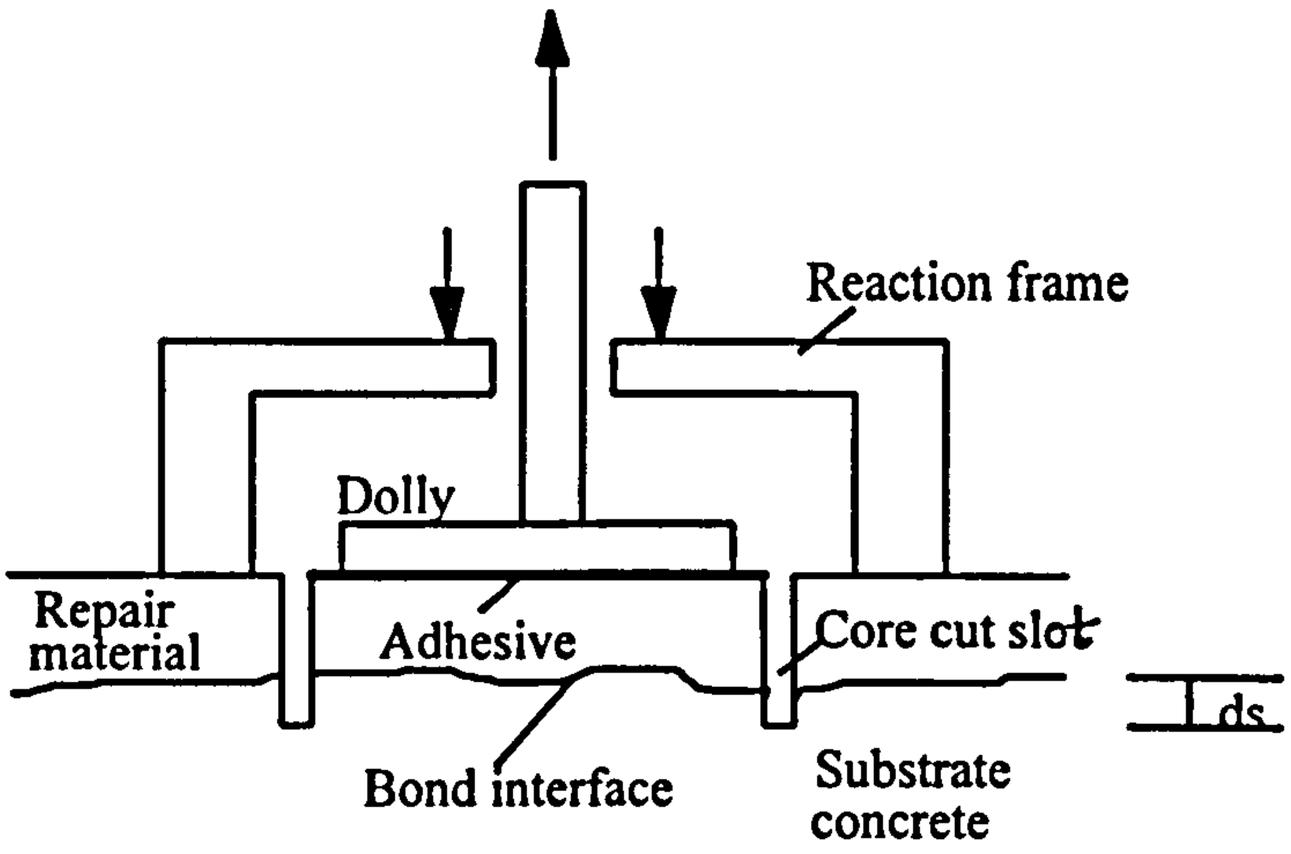

Figure 2.1 General test principle for a core pull-off test

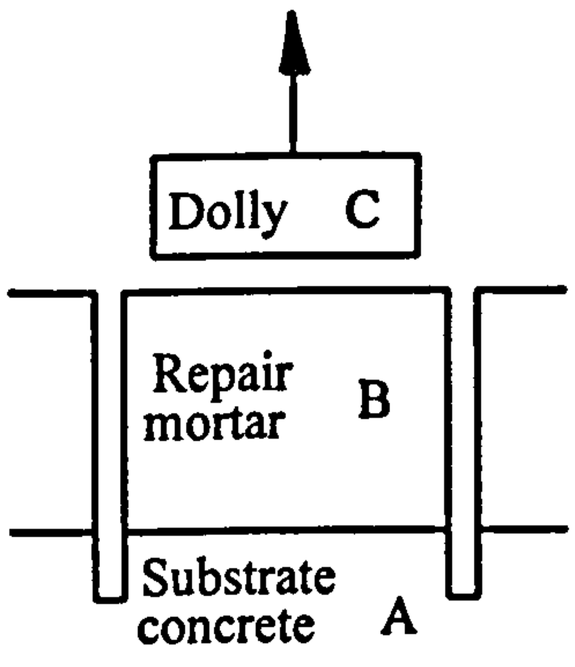

Bond failure at dolly
(110% B/C)

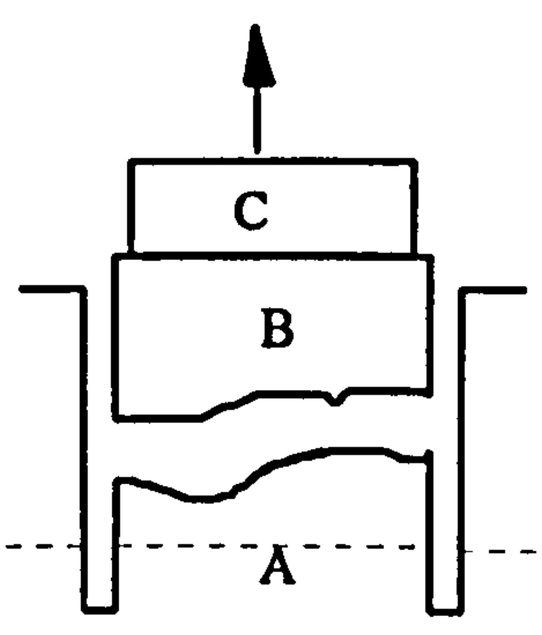

Cohesive failure of mortar
(100% B)

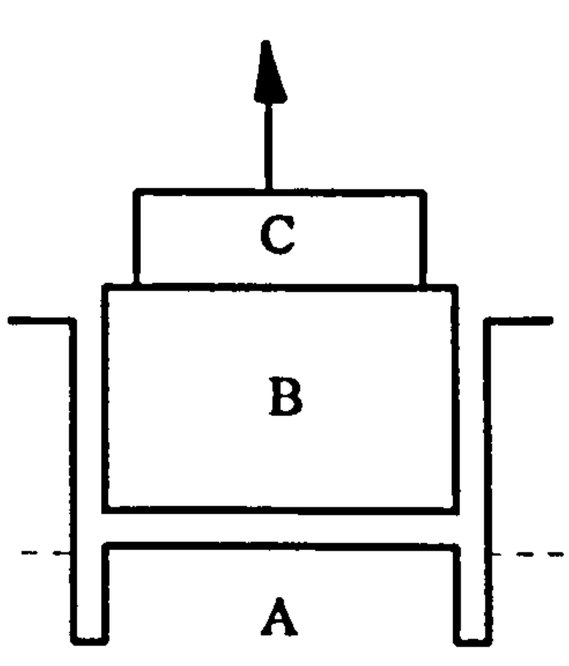

Bond failure
(100% A/B)

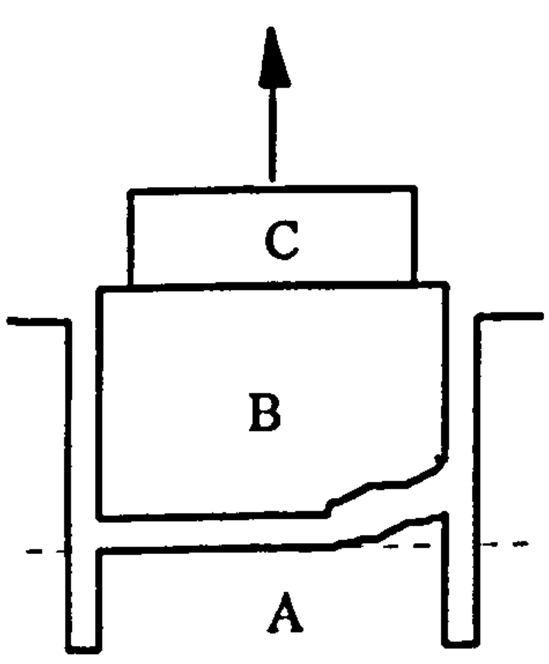

Partial bond failure and
cohesive failure of mortar
(60% A/B, 40% B)

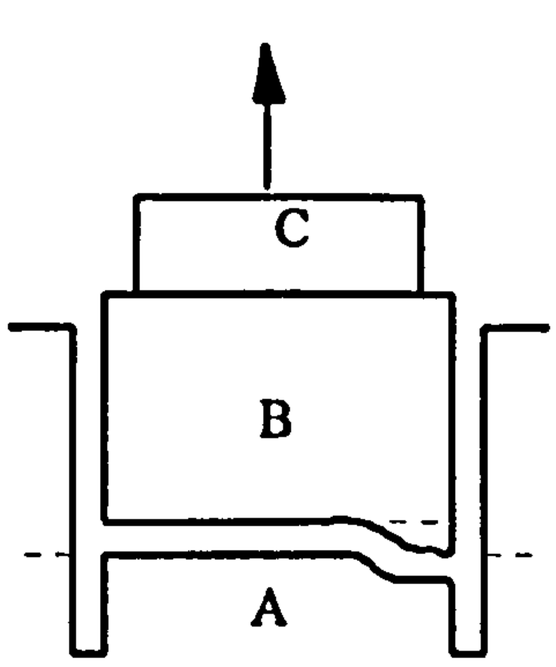

Partial bond failure and
cohesive failure of substrate
(60% A/B, 40% A)

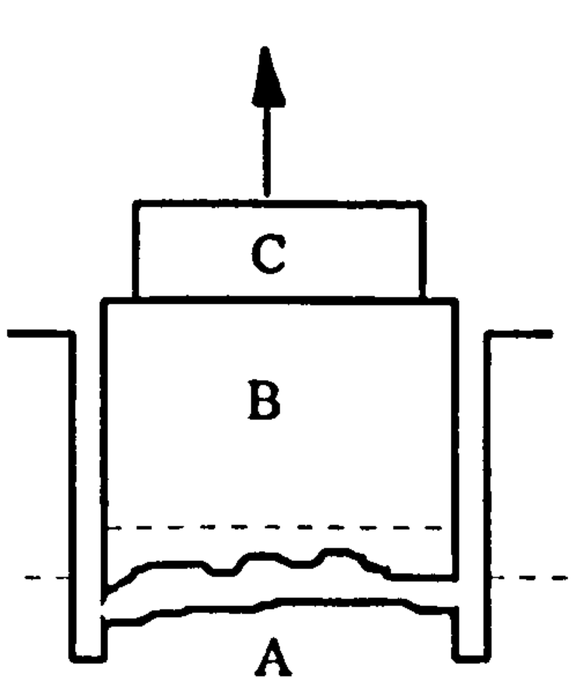

Cohesive failure of substrate
(100% A)

Figure 2.2 Possible failure modes from a core pull-off test

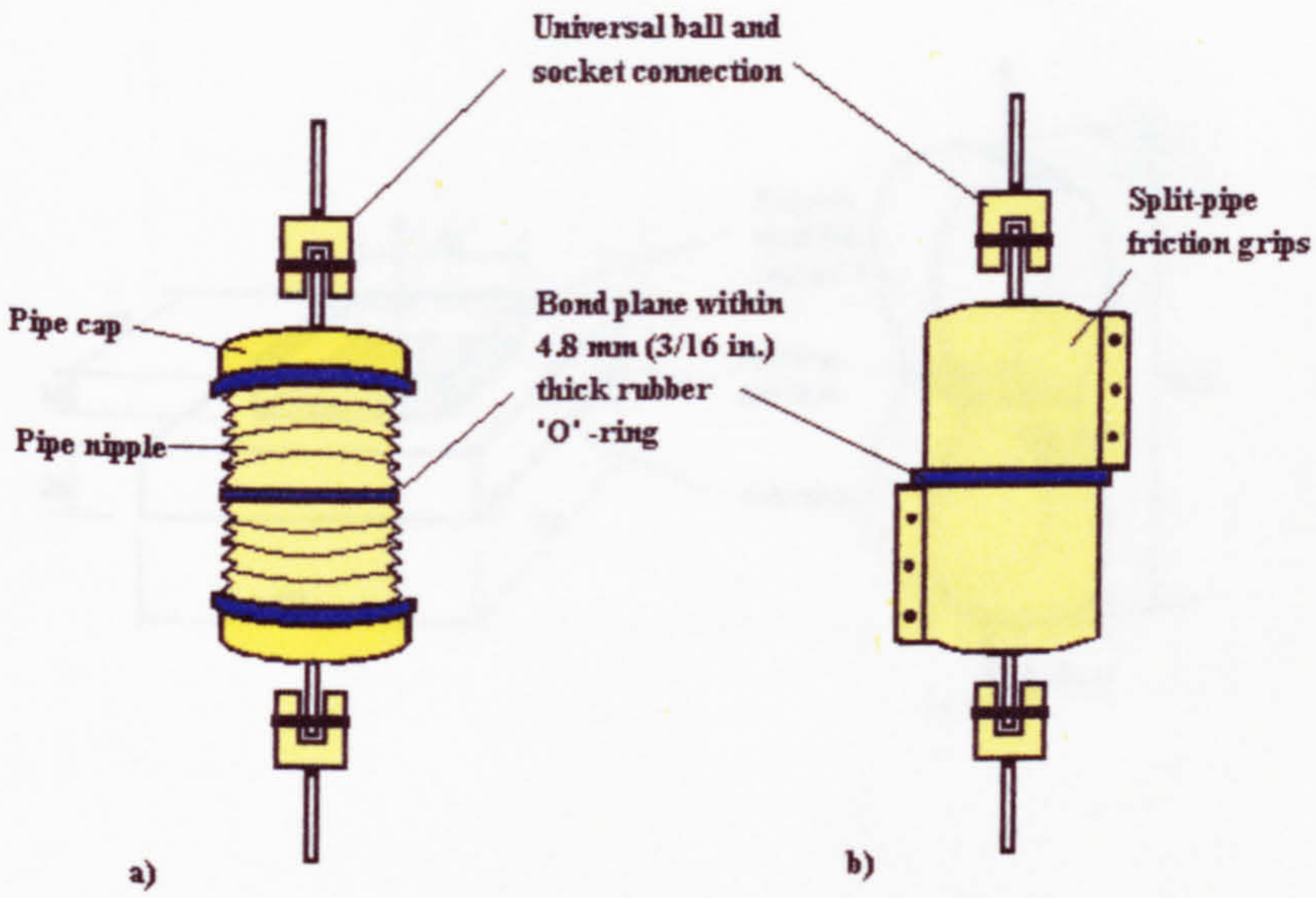

Figure 2.3 Tensile bond tests

a) Pipe-nipple grip tensile bond test b) Friction-grip tensile test

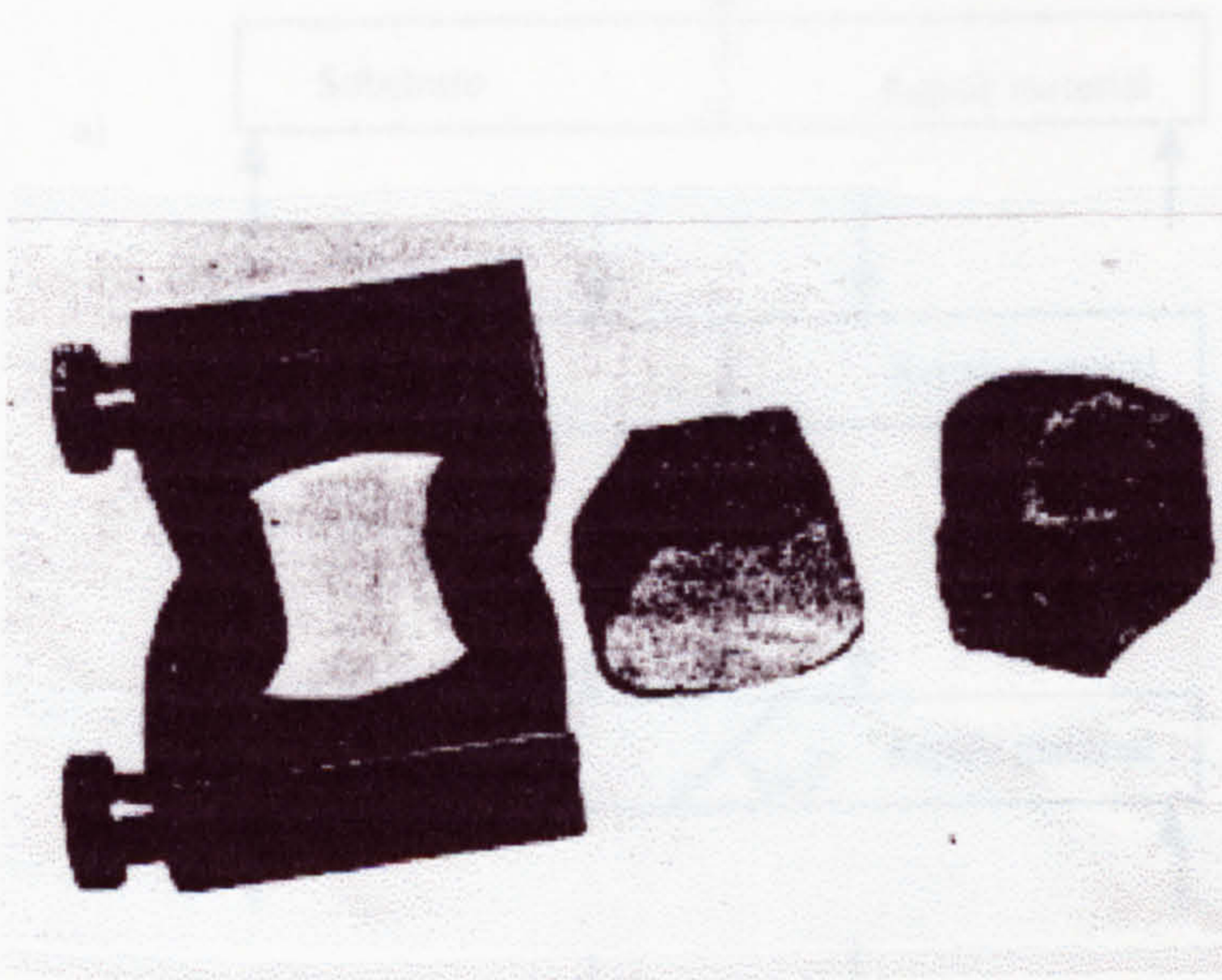

Figure 2.4 BS6319 : Part 7 mould and tested specimen (dog-bone test)

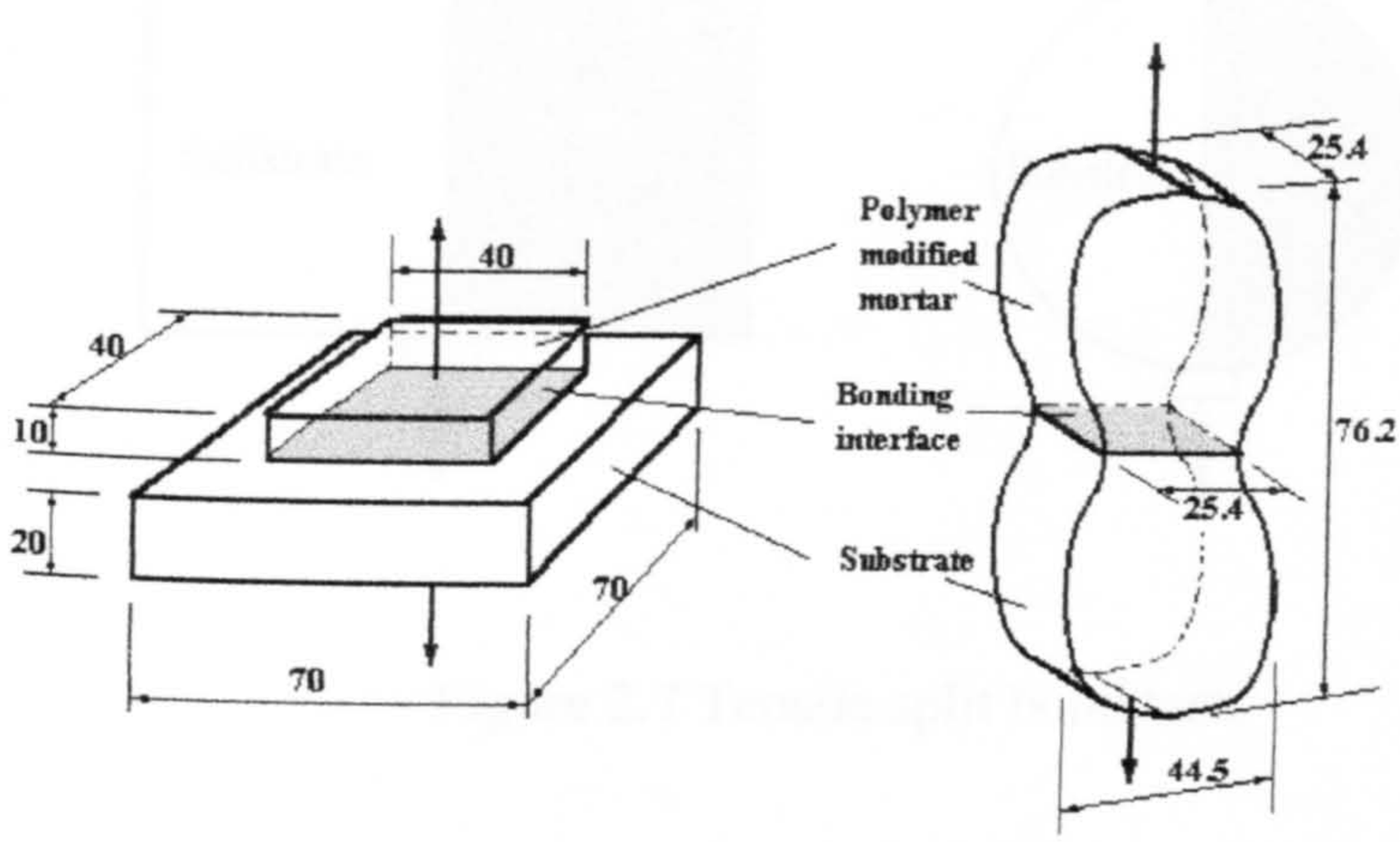

Figure 2.5 Tensile bond tests [ref.(14)]

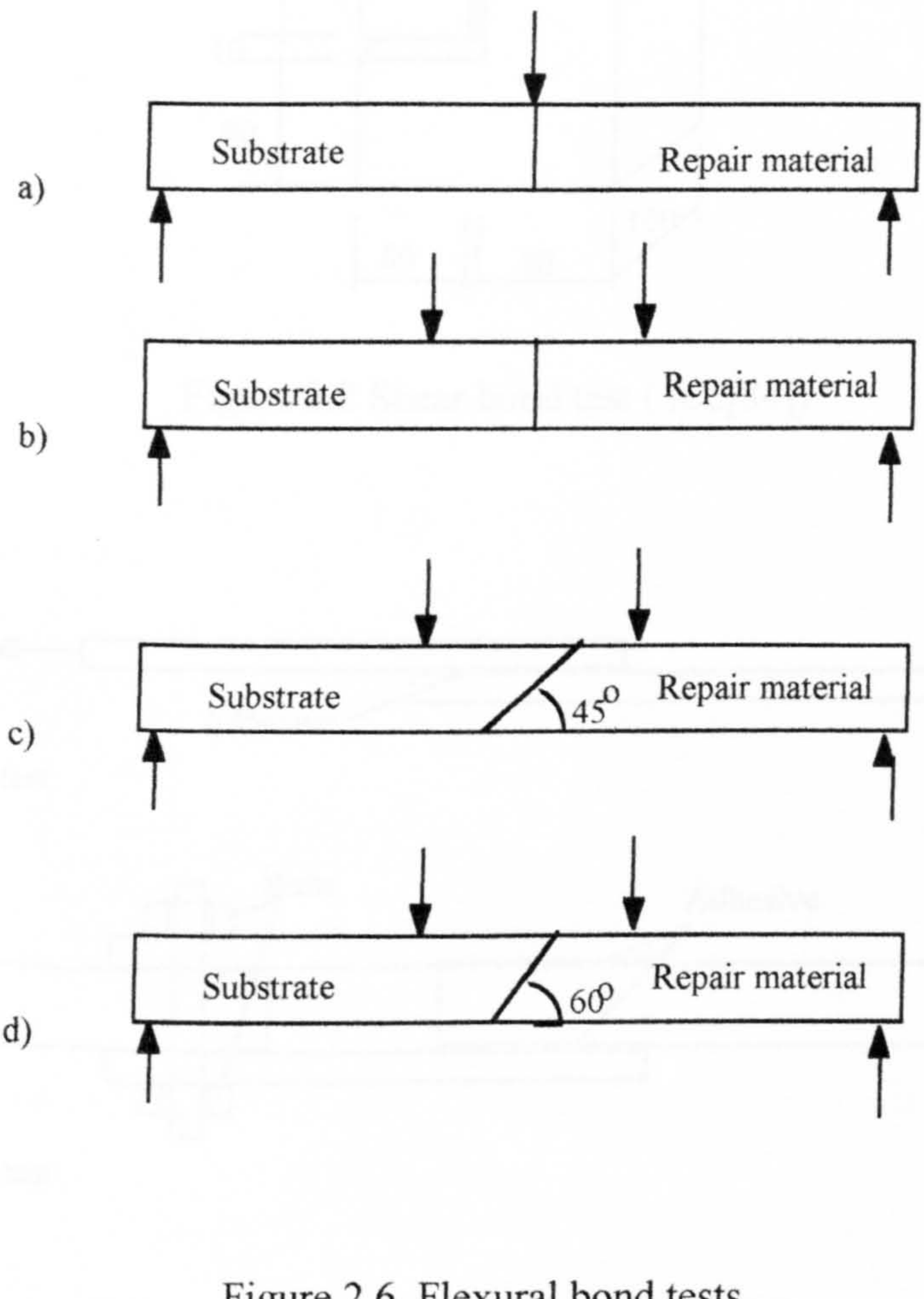

Figure 2.6 Flexural bond tests

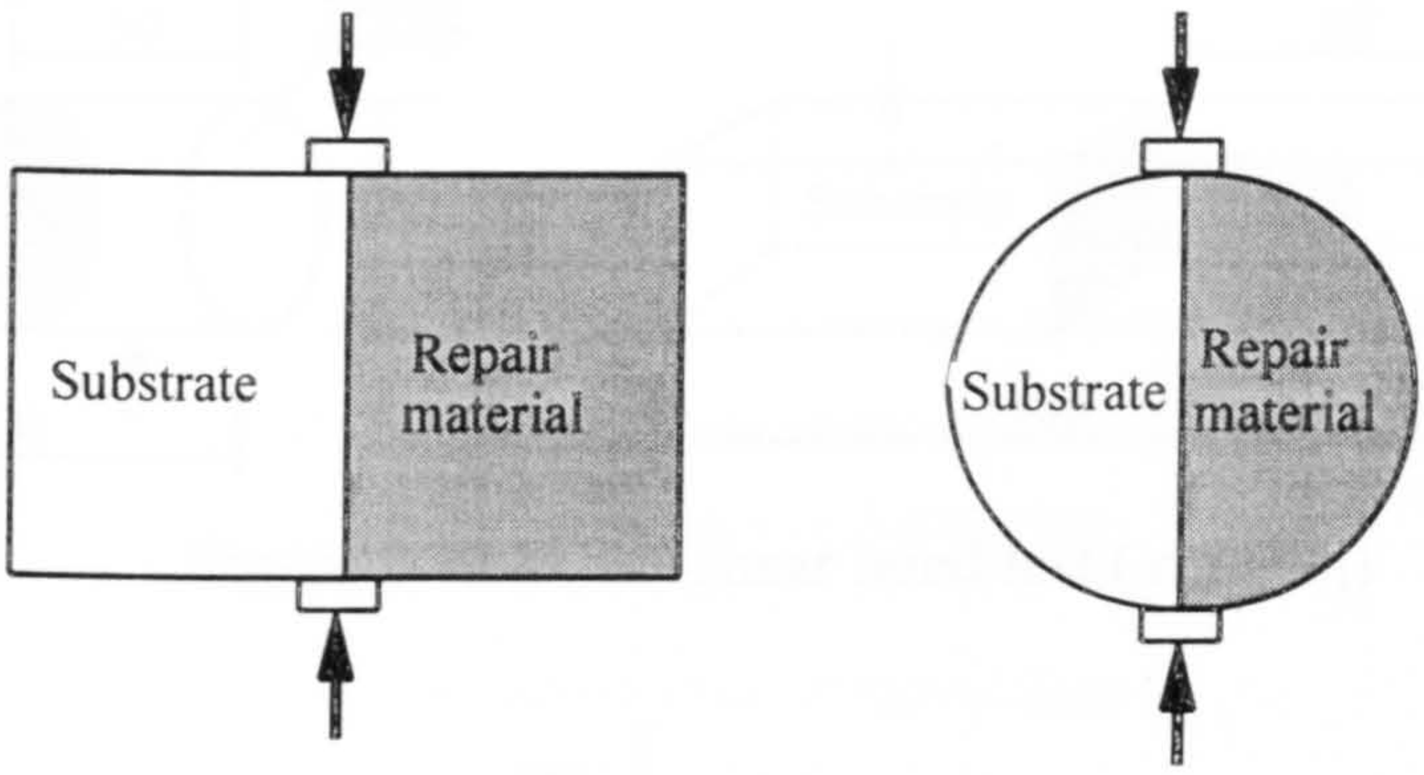

Figure 2.7 Tensile split bond tests

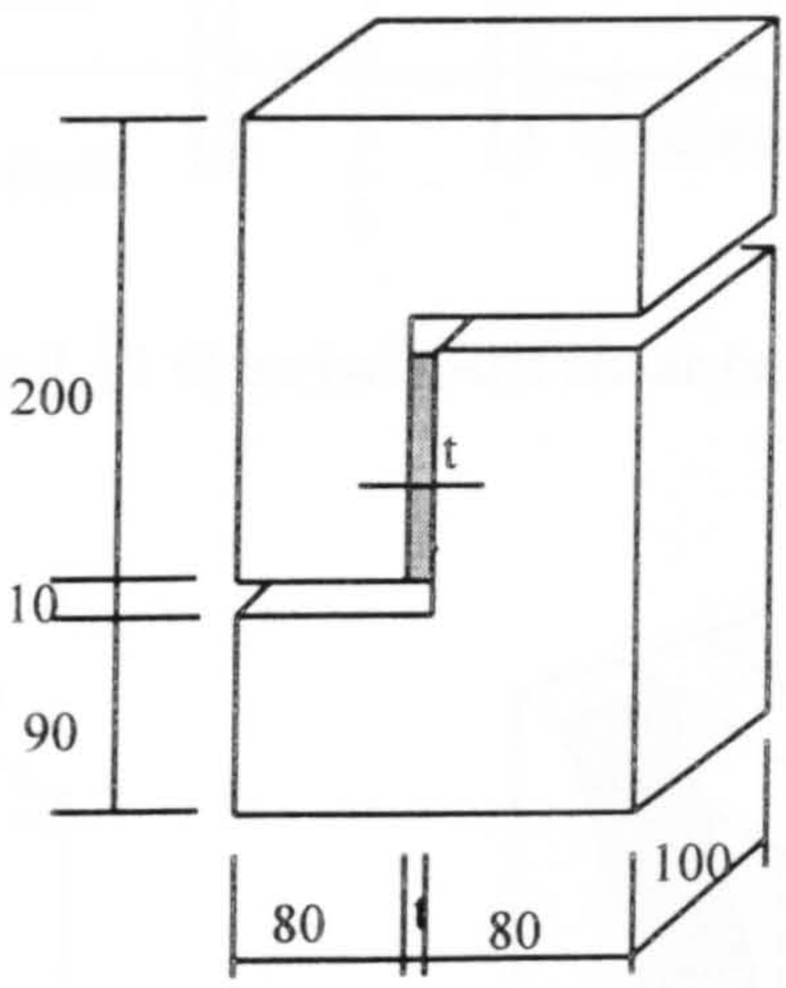

Figure 2.8 Shear bond test (ref.[84])

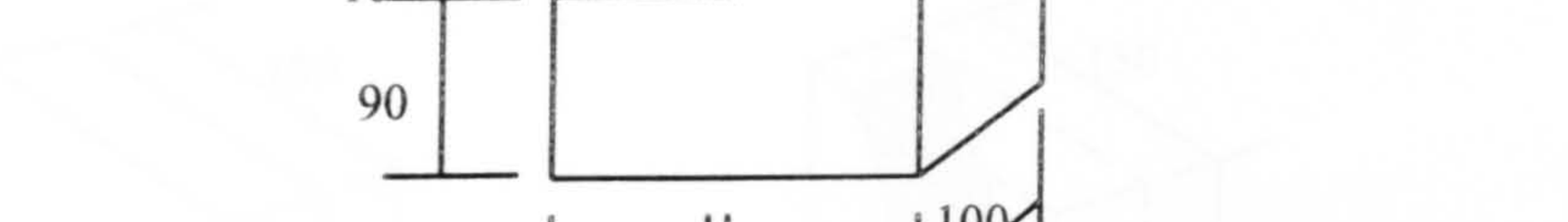

a) Single lap test

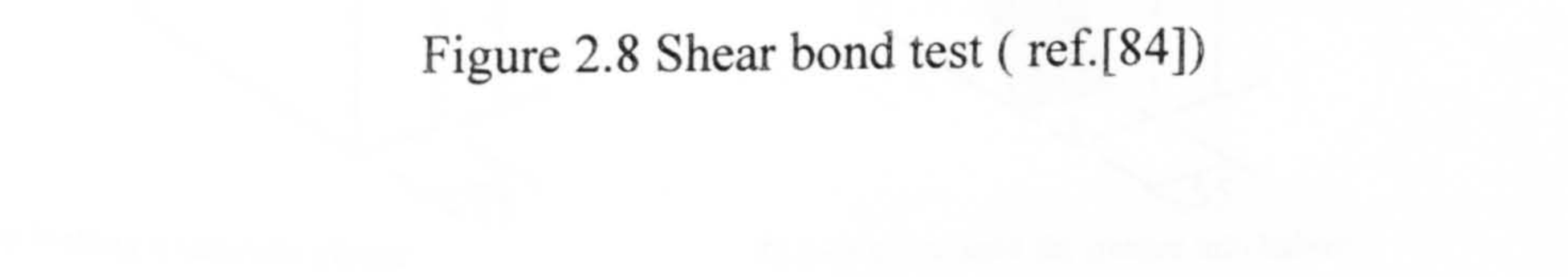

b) Double lap test

Figure 2.9 Shear bond test (ref.[70])

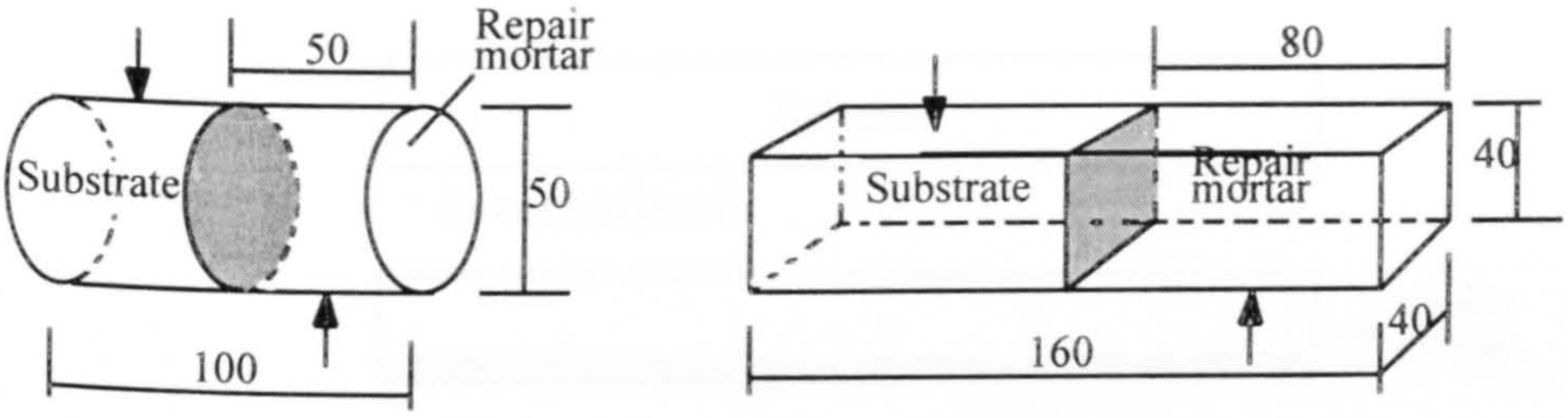

Figure 2.10 Direct shear bond test (ref.[14])

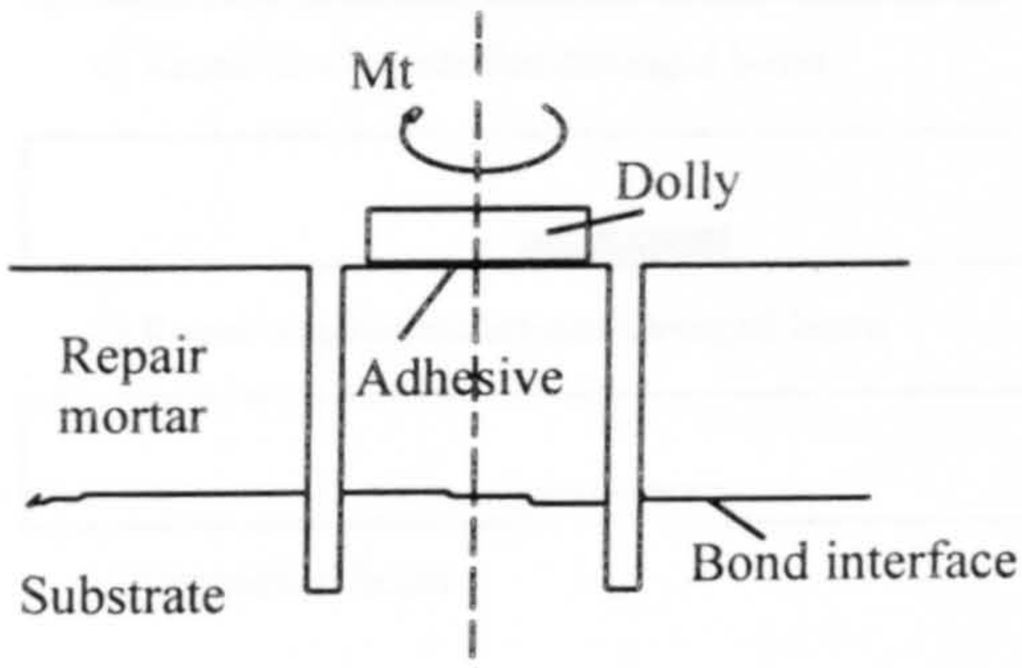

Figure 2.11 Core twist-off shear bond test

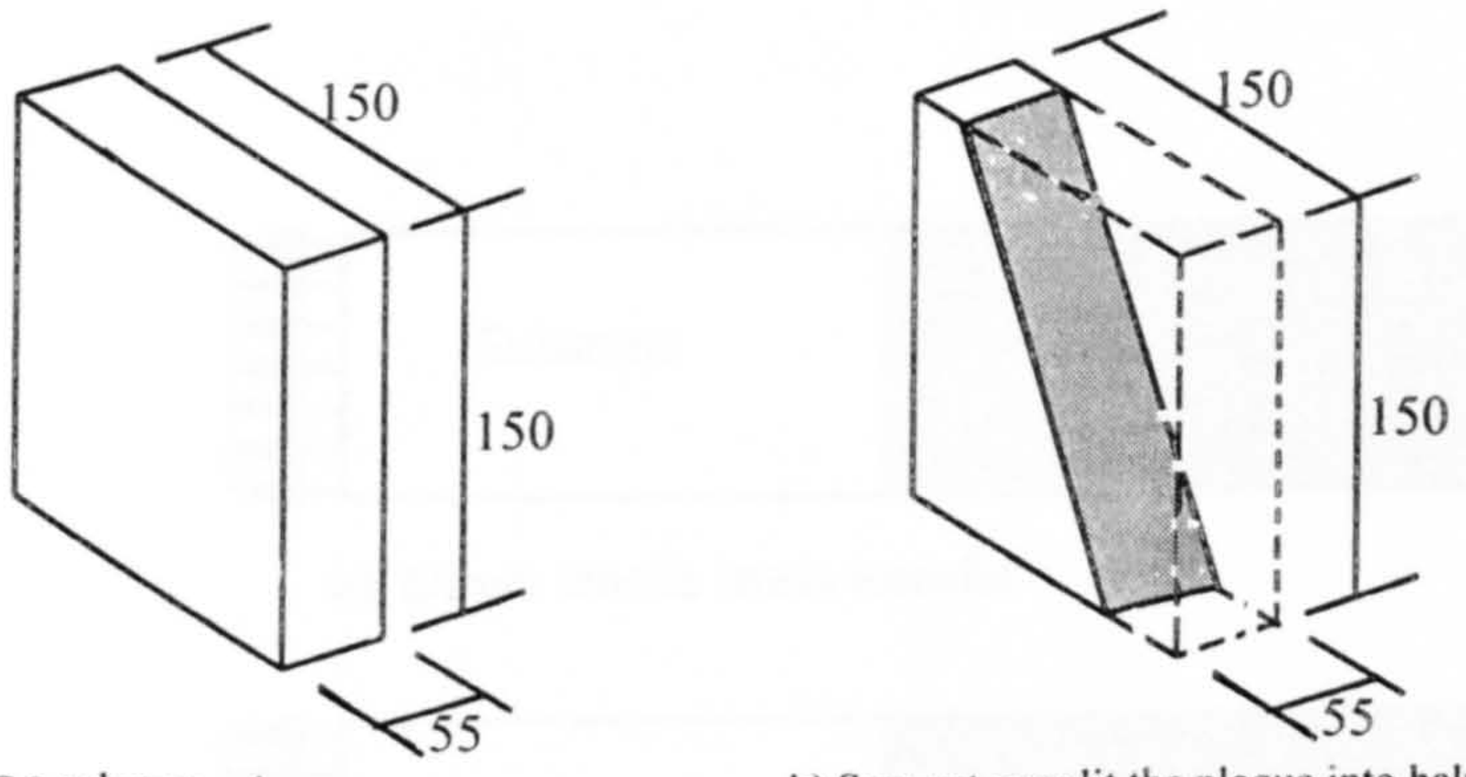

a) Making a substrate plaque

b) Saw cut or split the plaque into halves

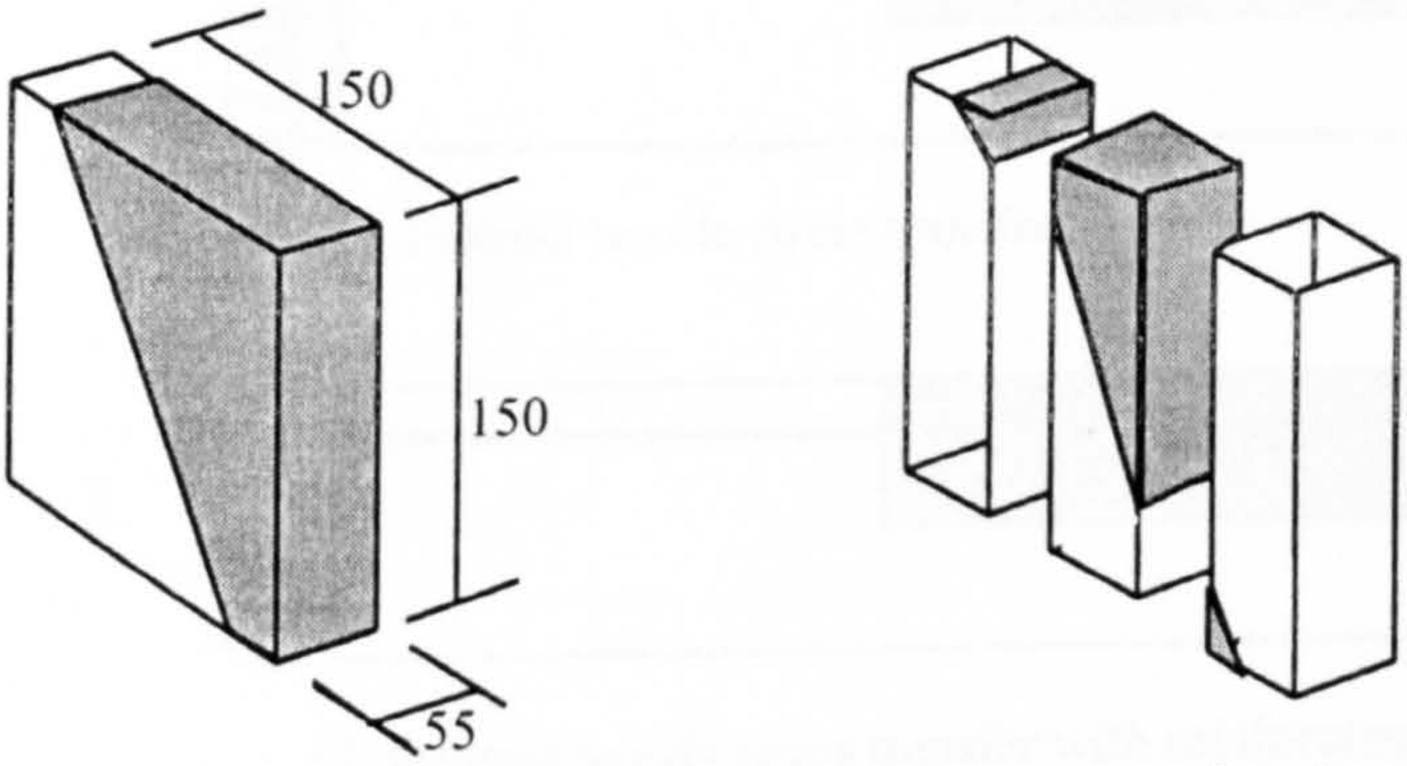

c) Applying repair material

d) The finally prepared specimen (the centre piece)

Figure 2.12 Making a slant shear specimen

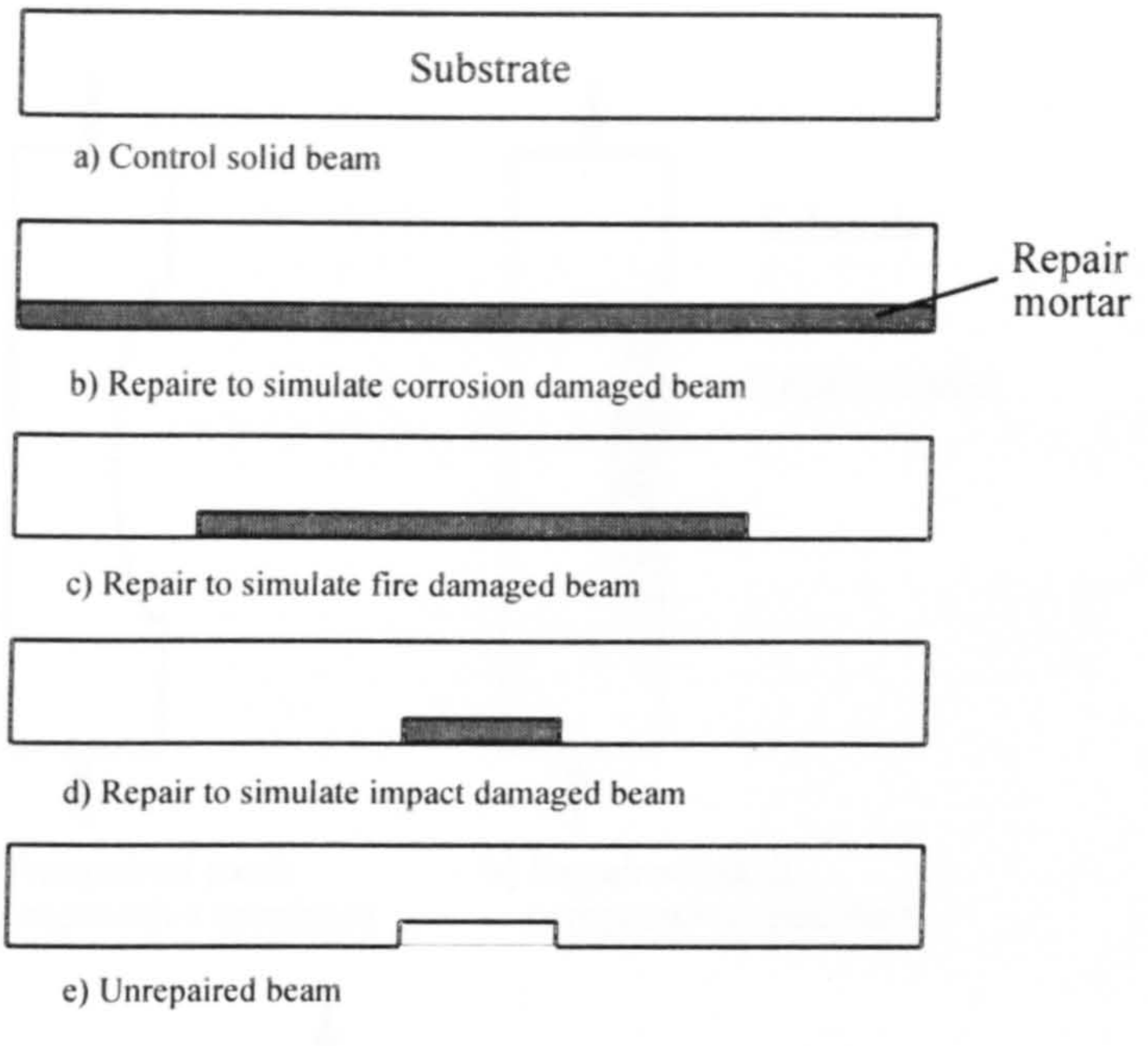

Figure 2.13 Flexural tests

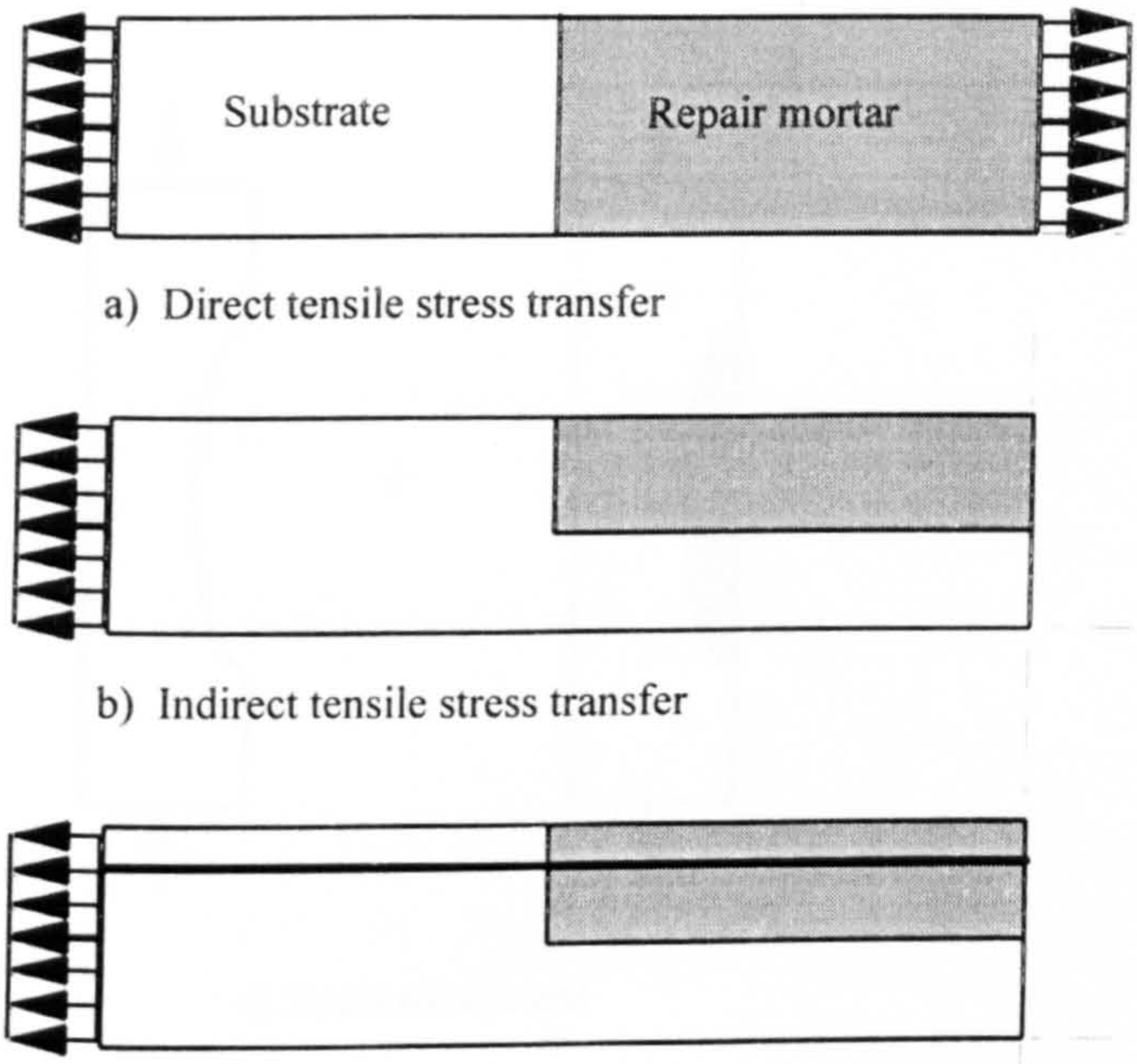

Figure 2.14 Patch repair tests (ref.[94])

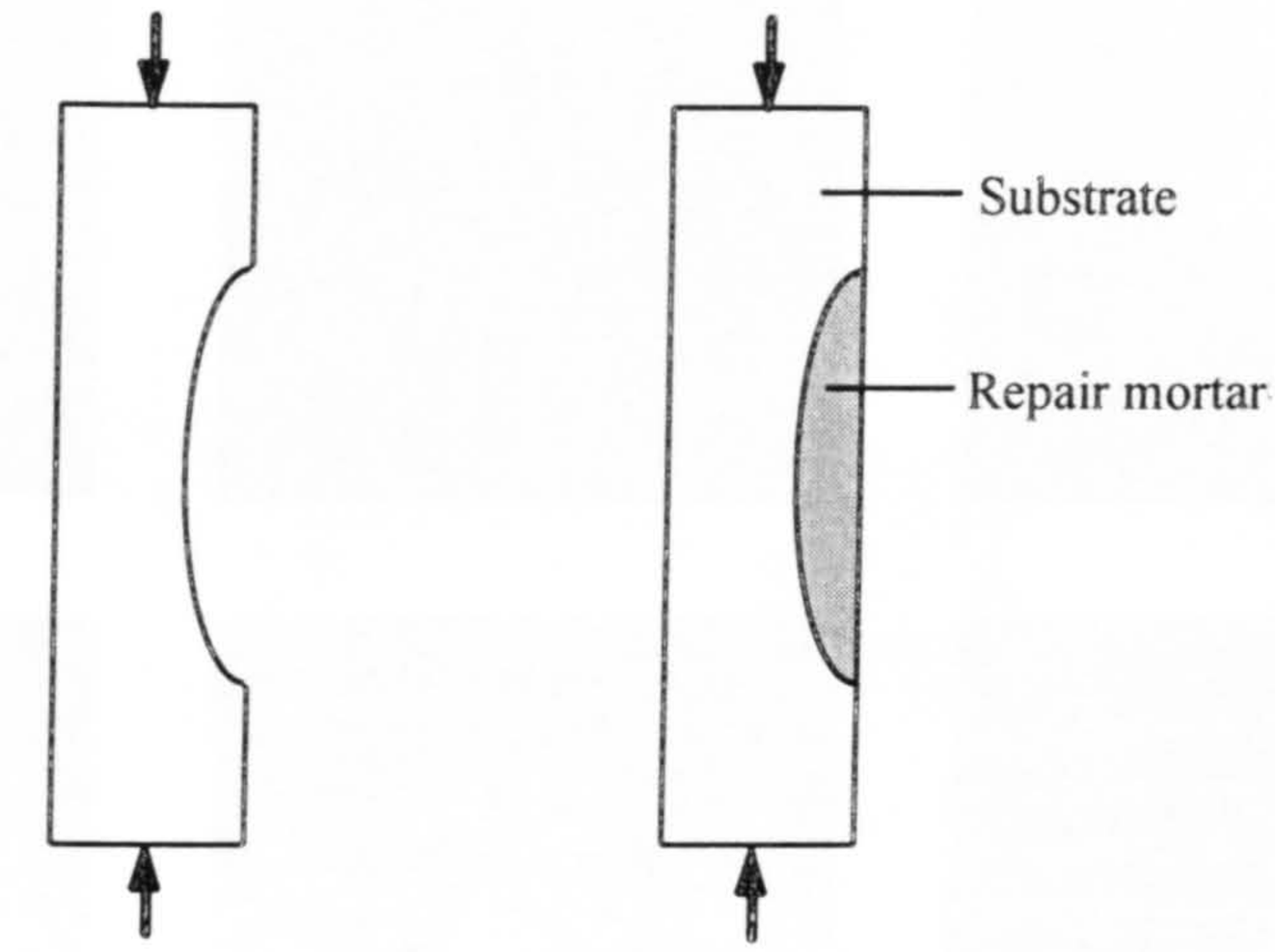

a) Unrepaired patch compressive specimen

b) Repaired patch compressive specimen

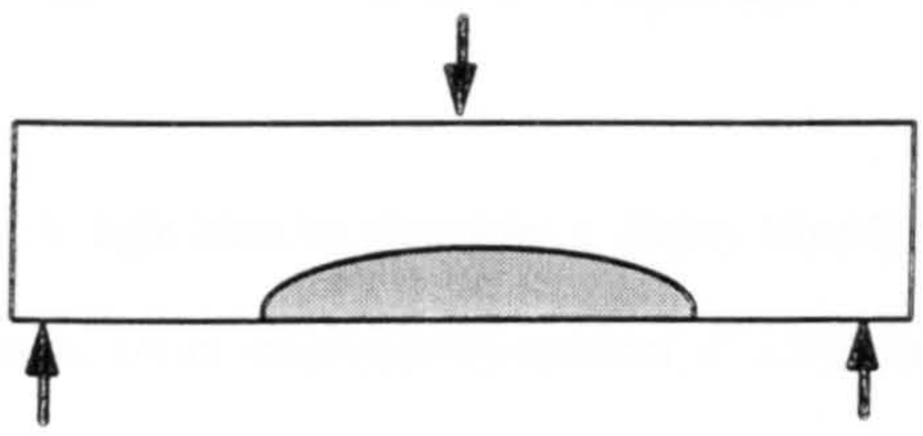

c) Repaired patch flexural specimen

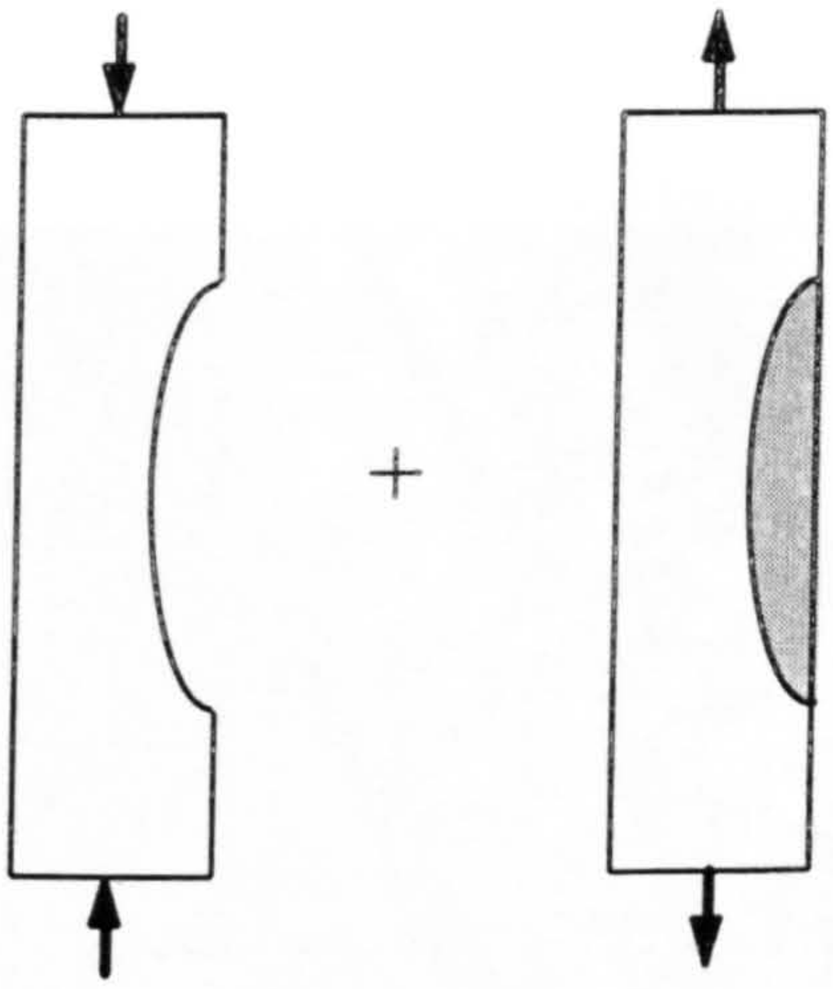

d) Patch tensile test

Figure 2.15 Patch repair tests

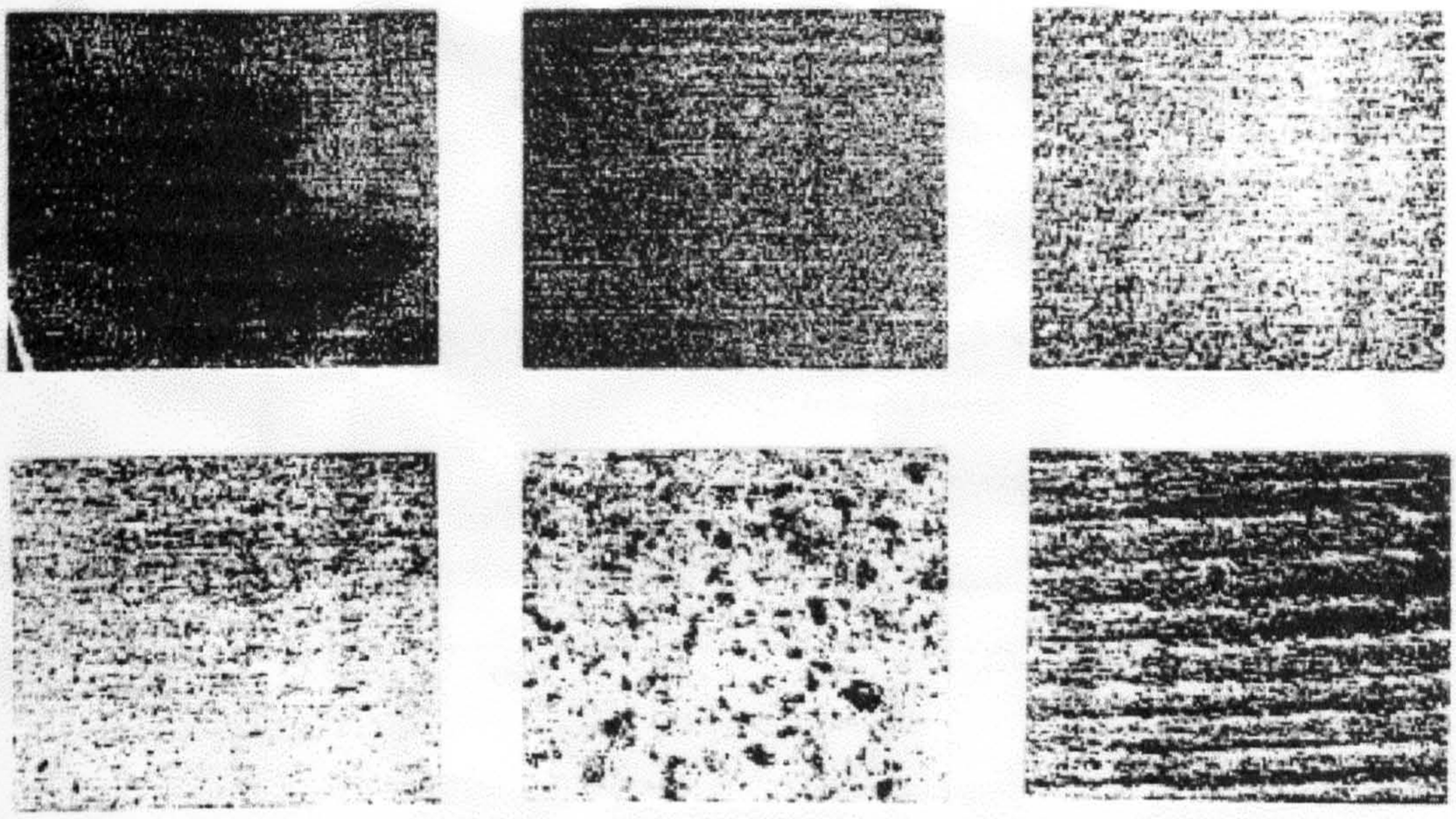

Top from left to right:
a: sandblast (too little, too light); b: light blast by shot blast c: Heavy blast by shot blast;
Bottom from left to right:
d: 1/8 in. amplitude by sand blast; e: 1/4 in. amplitude by scabbler; f: 1/8 in. or 1/4 in. amplitude by scarifier

Figure 2.16 Roughened concrete surfaces (copy from Ref.[96])

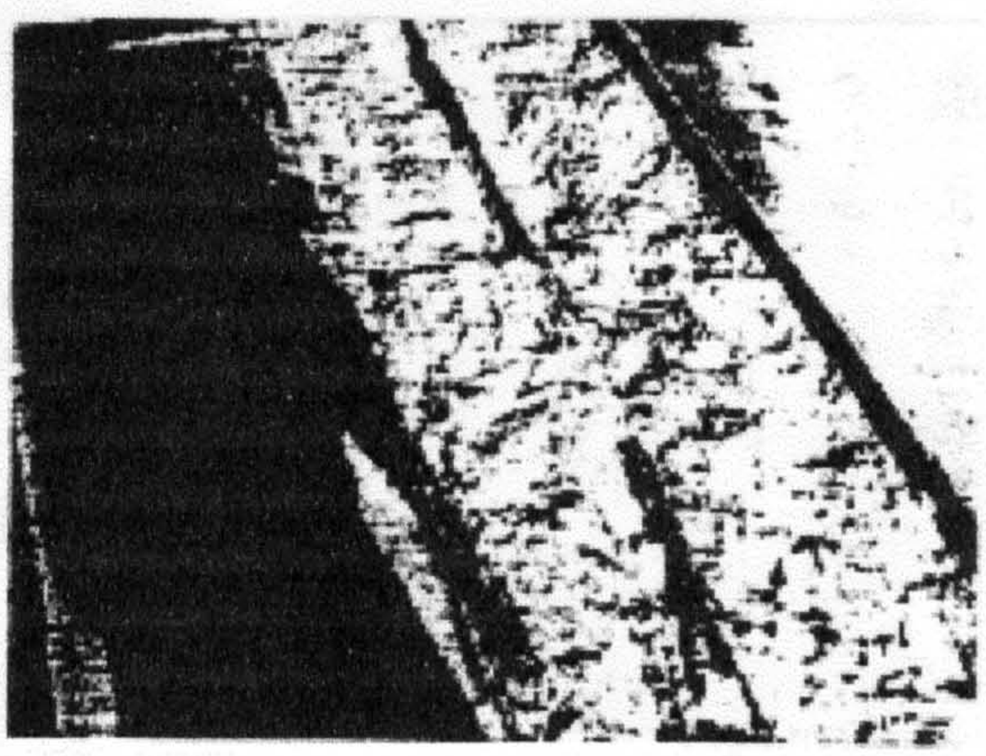

Figure 2.17 Fracture plane by jack hammer (copy from Ref.[96])

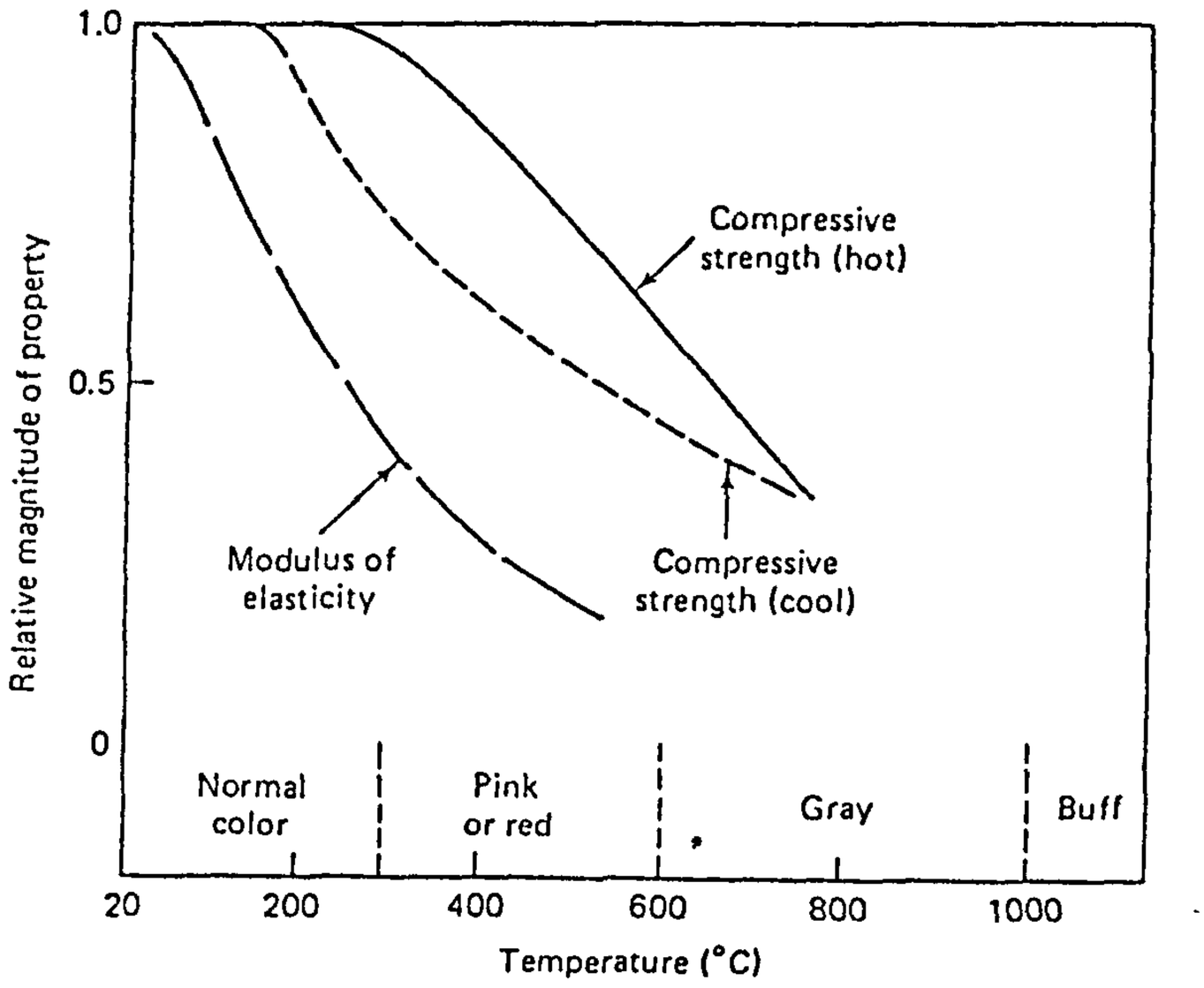

Figure 2.18 Effect of heating on strength and modulus of concrete (ref.[113])

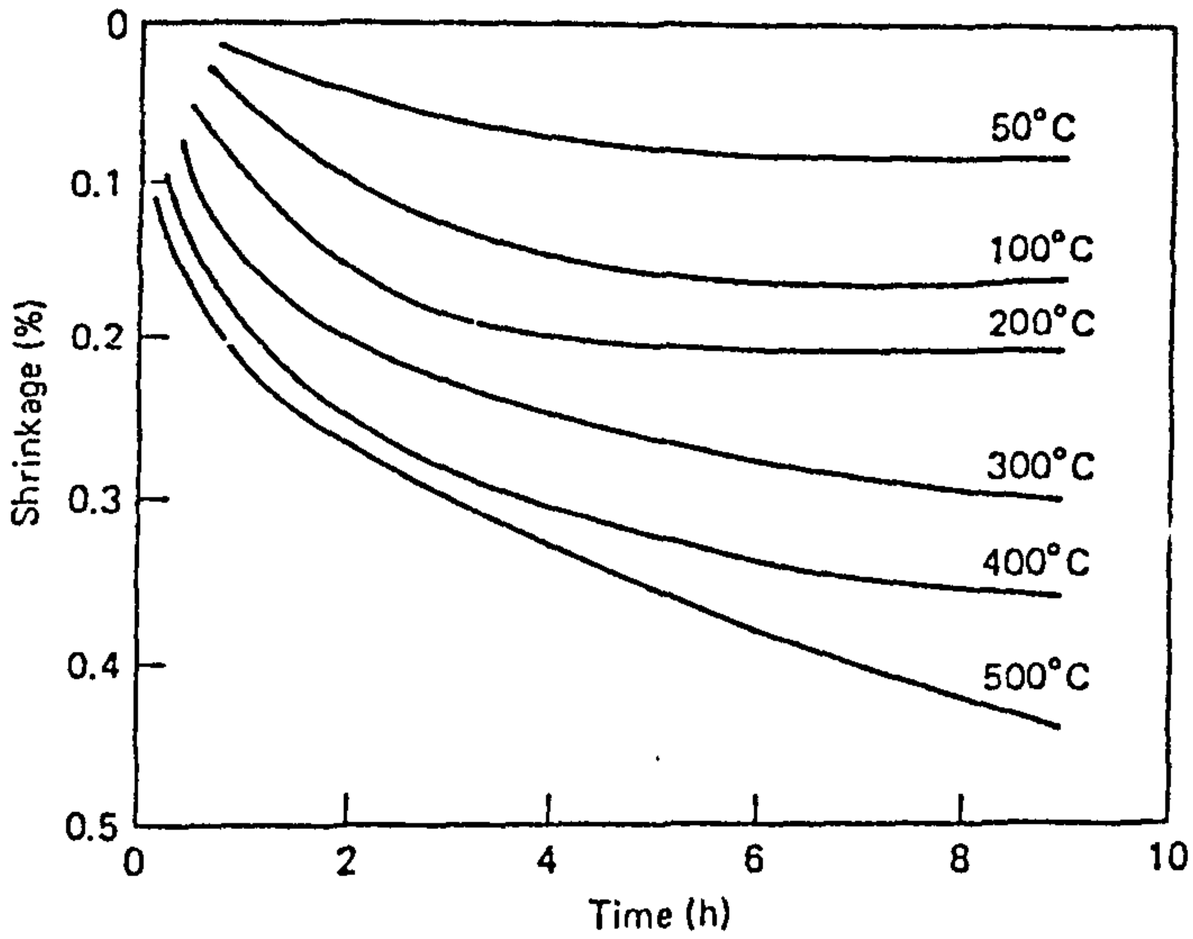

Figure 2.19 Effect of temperature on magnitude and rate of shrinkage (ref.[113])

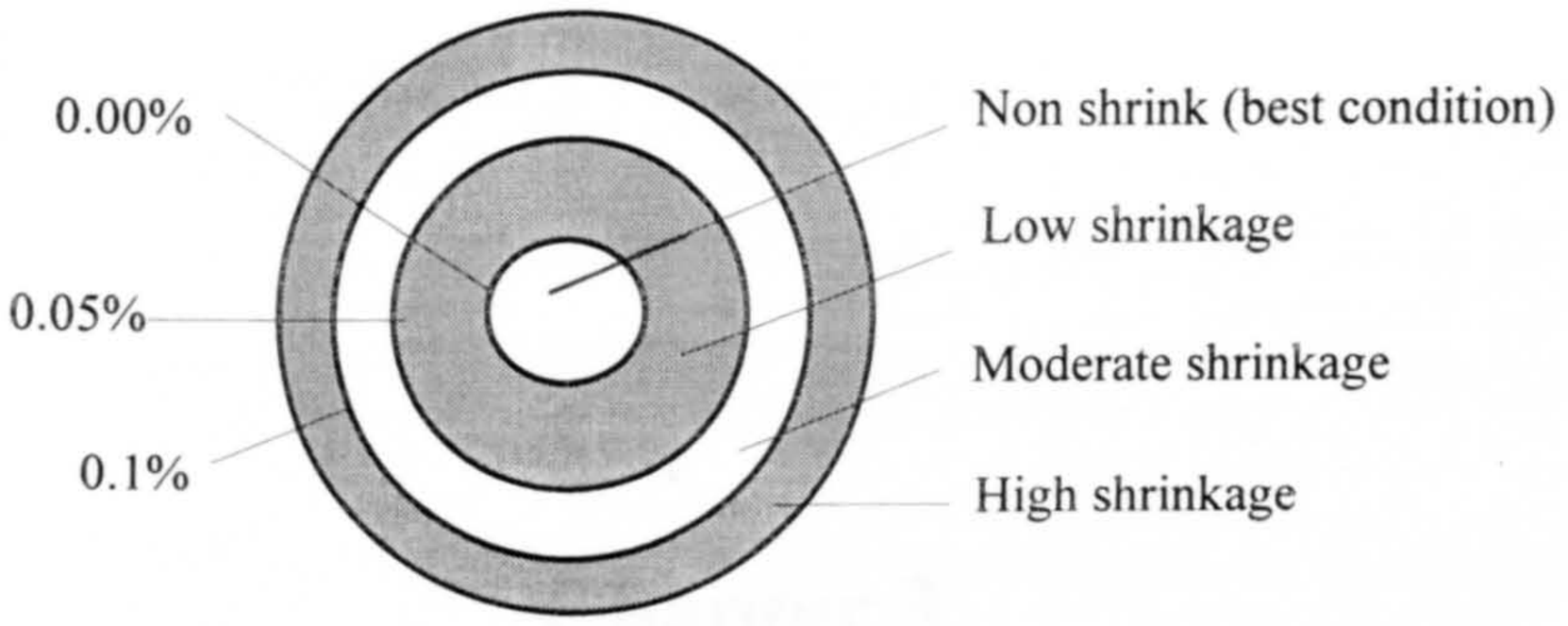

Figure 2.20 Shrinkage classfication (ref.[112])

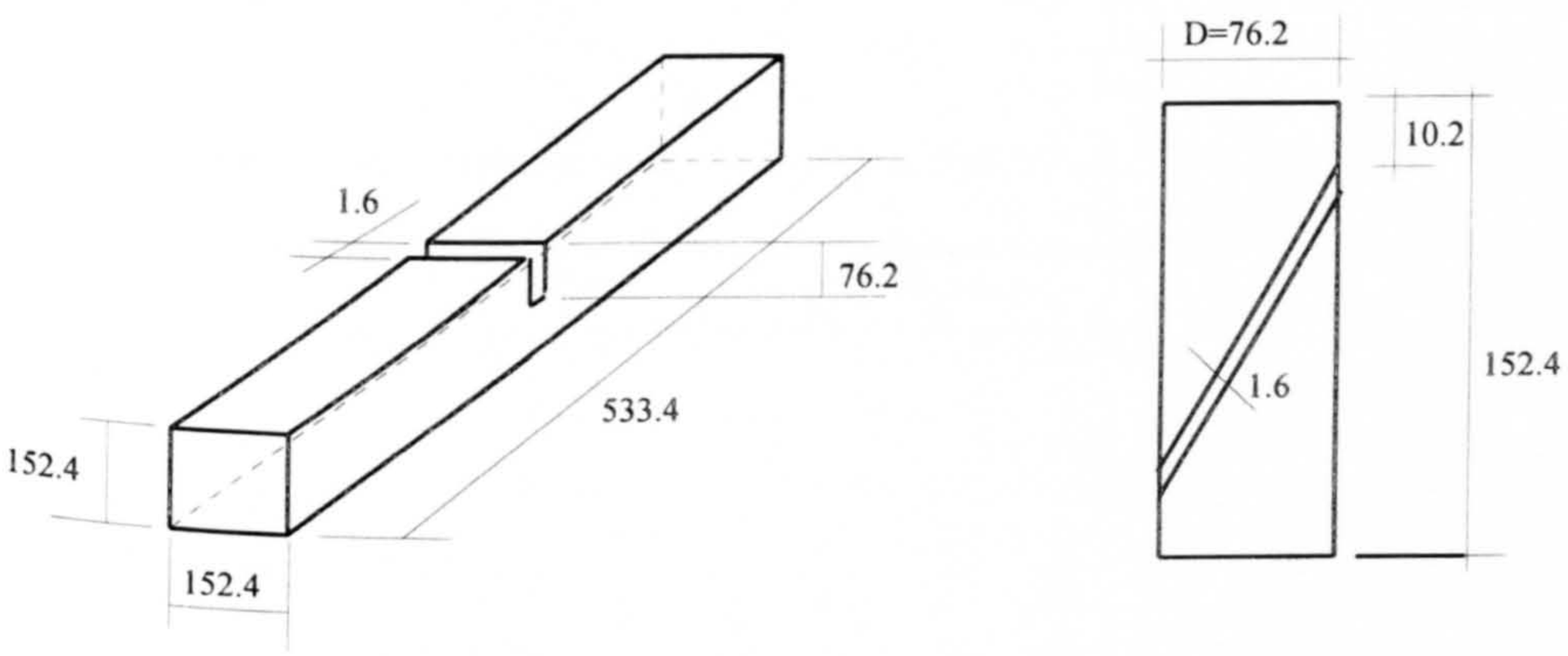

a) Flexural test

b) Slant shear test

Figure 2.21 Resin injection repaired specimens (ref.[89])

Chapter 3

MATERIALS AND TEST PROGRAMME

Chapter 3 Materials and test programme

3.1 Introduction

The main aims of the research programme were to see the effects of workmanship and environmental conditions on the bond performance of patch repair work. There are many factors involved in each category, e.g., surface roughness, moisture conditions, and curing methods in the workmanship, and thermal cycling and freezing and thawing cycles in the environmental conditions. Furthermore, repair materials perform differently under each condition. Both the test parameters and repair materials were kept within a limited range in order to focus attention on a few important issues.

3.2 Substrate concrete

3.2.1 Cement

Ordinary Portland cement from Castle Cement (Ketton) Ltd was used for all the substrate concretes. Table 3.1 and 3.2 show the typical chemical composition and requirement of physical properties of OPC in accordance with BS12, 1989.

3.2.2 Aggregate

Fine aggregate of 5mm down was washed river sand from Portaway Minerals (Elton) Ltd. A sieve analysis is given in Table 3.3. Coarse aggregate was river gravel of medium grade (5 - 10mm) from Hoveringham Quarry.

3.2.3 Mix details

The mix proportion by dry weight was as follows:

cement : fine aggregate : coarse aggregate = 1 : 2.3 : 2.3

water/cement ratio = 0.48

For the calculation of the proportion of materials, the density of concrete used was 2,400 Kg/m^3. Therefore, for 1m^3 of concrete the ratio of materials used is given below:

cement	: 394 Kg
fine aggregate	: 908 Kg
coarse aggregate	: 908 Kg
water	: 190 Kg

In the pilot studies, two other substrate mixes (1:1.6:3.0 w/c=0.45, and the mix suggested in BS 6319 Part 4) were used, but no material properties were measured.

3.2.4 Concrete Strength

Three 100x100x100 mm cubes randomly selected and cast from different batches were tested at different ages. The average 28-day compressive cube strength was 64.4 MPa with a coefficient of variation of 1.8%. Strengths at other ages ranged from 60.4 MPa (60 days) to 73 MPa (158 days) (Table 3.4).

The average core pull-off tensile strength was 3.03 MPa with a coefficient of variation of 5.2%. Nearly all tests failed at the end of the drilled cores where high stress concentration can be expected (Table 3.5).

Tensile splitting strength was calculated based on the equation suggested by Bangash [130].

$$f_{ct} = 0.55(f_c)^{0.5} \qquad (3.1)$$

where f_c is the cylinder compressive strength in MPa. If it is assumed that the cylinder strength is 80 percent of the cube compressive strength, f_{ct} can be worked out as varying from 3.82MPa (60 days) to 4.2MPa (158 days).

The flexural tensile strength was calculated based on the equation suggested by Bangash [130].

$$f_{fl} = 0.95(f_c)^{0.5} \qquad (3.2)$$

The flexural tensile strength would vary from 6.6 to 7.3 MPa.

3.2.5 Modulus of elasticity

The British Code of Practice (BS8110 : Part 1) [131] was used to predict the modulus of concrete, resulting in values ranging from 34.2GPa to 36GPa.

During the initial studies, the substrates were quite young when they were repaired, varying from 7 to 15 days. Later, the age of substrate was set about 3 months old, varying from 80 to 110 days, with a few exceptions. After repair, the age of the substrates would be around 130 days. The 130-day properties were adopted in the theoretical analysis.

3.3 Repair materials

In this work, the following repair materials were used and are listed below:

(1) an acrylic modified cementitious mortar (A1);

(2) an SBR modified cementitious mortar (SBR);

(3) a flowing concrete (F); and

(4) an OPC/sand mortar (S/C).

Selecting of repair materials should depend upon the feature under investigation. It should be emphasised that the purpose here is to develop our understanding and not to evaluate the relative performance of individual material. The repair materials used in this study were selected following consultation with other researchers in the field, in particular G Mays at the Royal Military College at Cranfield, and D. Cleland at Queen's University of Belfast. Research from all these institutions formed a systematic programme sponsored by the SERC.

The first three are proprietary products. The mix proportions of the proprietary products were recommended by the manufacturers. The mix ratio of the unmodified OPC/sand mortar was one portion of cement and two portions of sand by weight, with water/cement ratio of 0.4. Typical properties of these materials were measured and are shown in Table 3.6. The compressive strengths were measured using 70x70x70 mm cubes, according to BS4550 : Part 3 1978 [132], the moduli of elasticity were measured using 40x40x160 mm prisms according to BS6319 : Part 6 1983 [133], and the shrinkage was measured using 76x76x190mm (3"x3"x7.5") prisms.

Bond coats were used for the acrylic modified mortar and the SBR modified mortar following the manufacturers' recommendation. These bond coats were supplied by manufacturers specifically designed for the repair material recommended.

The proprietary repair materials were supplied in packages ranging from 25 Kg to 45 Kg per bag, yielding a coverage, when mixed with water, from 12.5 to about 22 litres.

Another proprietary acrylic modified cementitious light weight mortar (A2) was also used but only in the study of moisture conditions. No material properties were measured for this repair material.

Except for the drying shrinkage test in which the age of a repair mortar was about 120 days, the age of a repair mortar in other tests was set at 28 days. Due to some technical problems with testing equipment involved, most of the repairs were from 28 to 41 days at the time of test with a few exceptions.

3.4 Test programme

3.4.1 Workmanship test parameters

The following parameters were included in the workmanship study:

surface roughness	(SRI);
surface soundness	(SSD);
surface cleanliness	(SCL);
moisture conditions	(MCS);
application methods	(AMS);
bond coat mistiming	(BCM);
repair mortar mistiming	(RMM); and
curing methods	(CMS).

Each parameter can be influenced by workmanship. For example, the surface can vary from smooth to rough, and the substrate can be dry or wet. In order to compare the effects clearly, each factor was given a varying range and a standard condition was defined accordingly. Where possible, the selection of the varying range was based on previous research in which the possible variation of each factor has been studied. The standard conditions (which are highlighted) were in general reflecting the requirement for a good preparation and execution of the repair. But for the surface roughness, a medium rough surface was defined as the standard roughness because the surface texture was more representative of the site conditions (the definition of roughness

index (SRI) is given in Appendix 1). The simulation of these variations will be discussed in detail in Chapter 4. This influence was indicated by the variation of these parameters as shown below:

Surface roughness:	(1) smooth	SRI > 250mm	(SM)
(SRI)	(2) ***fairly rough***	***SRI = 225 mm***	***(FR)***
	(3) rough	SRI < 200 mm	(RF)
Surface soundness:	(1) ***sound, no surface defects***		***(GD)***
(SSD)	(2) weak, with surface defects		(WK)
Surface cleanliness:	(1) ***clean, no dust, no oil, etc.***		***(CL)***
(SCL)	(2) contaminated		(CT)
Moisture conditions:	(1) Saturated surface wet		(SW)
(MCS)	(2) Saturated surface dry		(SD)
	(3) ***Air dry surface wet***		***(AW)***
	(4) Air dry surface dry		(AD)
	(5) Bone dry surface wet		(BW)
	(6) Bone dry surface dry		(BD)
Applying methods:	(1) ***Hand applied***		***(HA)***
(AMS)	(2) vibrated		(VB)
Bond coat mistiming:	(1) ***No mistiming***		***(No)***
(BCM)	(2) about 30 minutes mistiming		(30)
Mortar mistiming:	(1) ***No mistiming***		***(No)***
(RMM)	(2) about 30 minutes delaying		(30)

Curing methods:	(1) no curing at all	(NO)
(CMS)	(2) ***covered with plastic sheet 3 days***	***(3d)***
	(3) covered with plastic sheet 7 days	(7d)

3.4.2 Environment test parameters

The following parameters were included in the study of environmental conditions:

Room temperature;	(RT)
High temperature curing followed by thermal cycling;	(HT-TC)
High temperature curing followed by drying shrinkage;	(HT-DS)
Low temperature curing;	(LT)
Low temperature curing followed by freeze/thaw cycles.	(LT-F/T)

Only one condition for each parameter was considered:

Room temperature (RT):	***temperature inside a laboratory;***
Drying shrinkage (DS);	leaving specimens inside a laboratory in dry conditions for about three months;
High temperature (HT):	40°C with 20% relative humidity;
Low temperature (LT):	4°C, no control on relative humidity;
Thermal cycling (TC):	Temperature changed from 10°C to 40°C, the relative humidity was also controlled; in total 42 cycles (Fig. 3.1);
Freeze/thaw cycle (F/T):	Only temperature was controlled, varying from -17°C to 5°C. Total F/T cycles was 33 for each material tested (Fig. 3.2).

3.4.3 Choice of test methods

Bond test methods were reviewed in section 2.2. They included tensile bond test (core pull-off test, dog-bone test, etc.), shear bond tests, slant shear tests, and patch repair tests. A tensile bond test is very sensitive to surface defects; the slant shear test is

currently the only one included in British Standards; and a patch test puts a repair material into a more realistic situation in which stresses are transferred indirectly. Consequently, the test methods selected for this project were:

(1) the core pull-off test (CP);

(2) slant shear test (SS);

(3) patch compressive test (PC); and

(4) patch flexural test. (PF).

3.4.4 Test combination

When selecting the combination of test parameters and test methods, due consideration was given to the current knowledge of workmanship and environmental conditions on bond strength (for example, there are many test results on surface preparation, only a few on mistiming, etc.); the selection were made in order to investigate mainly the effect of those parameters for which few firm conclusions have been drawn. Some additional specimens were used in the initial study to check and confirm some of the accepted knowledge on bond performance. The combination of test variables investigated is given in Table 3.6 as a matrix. For the core pull-off test, the effect of the different parameters was obtained by averaging at least five results, and for all other tests, at least three results.

Because mixing of part bags is not allowed by manufacturers, specimens for each group were so arranged that the repair material of each bag was fully used for each casting.

Table 3.1 Typical chemical composition of ordinary Portland cement (OPC)

	Typical chemical analysis							
	Analysis				Compound			
	Lima	Silica	Alumina	Iron Oxide	Tricalcium silicate (C3S)	Dicalcium silicate (C2S)	Tricalcium aluminate (C3A)	Iron compound (C4AF)
OPC BS12, 1989	65	21	5	3	59	16	8	9

Table 3.2 Requirement of physical properties of OPC in accordance with BS12

	Requirement of physical properties								
	Fineness min (m2/kg)	Setting time (vicat apparatus)		100mm mortar cube strength (MPa)			70.7mm concrete cube strength (MPa)		
	Air permeability	Initial, min (minutes)	Final, max (hours)	3 days min	28 days min	28 days max	3 days min	28 days min	28 days max
OPC BS12, 1978	275	45	10	25	47	67	15	34	52

Table 3.3 Sieve analysis of fine aggregate

B.S. sieve size (mm)	5.0	2.36	1.18	0.6	0.3	0.212	0.15	0.075
Passing rate (%)	99.4	79.2	66.5	57.4	23.2	7.8	2.1	0.2

Table 3.4 Compressive strength of the substrate concrete

Group	Age (days)	Cube strength (MPa)	Average cube strength (MPa)	Coefficient of variation (%)
GP6	28	65.3 64.7 63.1	64.4	1.8
GP12	54	64.9 64.0 64.0	64.3	0.8
GP1	60	61.1 58.4 61.6	60.4	2.9
GP11	60	68.0 69.1 70.7	69.3	2.0
GP10	61	58.7 68.3 67.8	64.9	8.3
GP8	65	65.6 63.4 66.5	65.2	2.4
GP9	68	68.5 69.0 66.3	67.9	2.1
GP2	70	65.4 69.7 69.3	68.1	3.5
GP4	126	69.8 71.9 69.7	70.5	1.8
GP3	131	72.8 72.9 73.1	72.9	0.2
GP5	158	72.6 74.8 72.2	73.3	1.9

Table 3.5 The core pull-off tensile strength of substrate concrete at 28 days

No	Failure load (KN)	σ (MPa)	Failure mode	average σ (MPa)	COV (%)
1	8.43	3.19	end of core	3.03	5.2
2	7.71	2.92	"		
3	8.45	3.20	"		
4	7.95	3.01	"		
5	7.53	2.85	"		

Table 3.6 Properties of the repair materials

Repair material	Cube strength (MPa)	Core pull-off tensile strength (MPa)	Elastic modulus (GPa)	One-month shrinkage (με)	Three-month shrinkage (με)
Acrylic modified mortar (A1)	49.6	2.02	26.1	270	590
SBR mordified mortar (SBR)	45.7	1.77	27.3	560	950
Flowing concrete (F)	68.2	2.14	29.1	350	510
OPC/sand mortar (S/C)	65.7	2.56	30.9	240	480

Table 3.7 Test combinations

1	2	3	4	5	6	7	8	9	10	11	12	13	14	15	16	17	18	19
Repair materials		Sand/cement mortar				Acrylic modified mortar				SBR modified mortar				Flowing concrete				A2
Specimen types / Test parameters		CP	SS	PC	PF	CP	SS	PC	PF	CP	SS	PC	PF	CP	SS	PC	PF	CP
Control specimens		x	x	x	x	x	x	x	x	x		x	x	x		x	x	
Surface roughness index	SM	x	x			x			x									
	MR	Standard surface roughness: medium rough																
	RF	x	x			x			x									
Surface soundness	S	Standard surface soundness: sound																
	W	x	x															
Surface cleanliness	CL	Standard surface cleanliness: clean																
	CT	x	x			x				x				x				x
Moisture condition	SW	x				x				x				x			x	x
	SD	x				x				x				x			x	x
	AW	Standard moisture condition: air dry surface wet																
	AD	x				x				x				x			x	x
	BW	x				x				x				x			x	x
	BD	x				x				x				x			x	x
Applying methods	HA	Standard applying method: by hand																
	VB	x	x															
Bond coat mistiming	NO	Standard parameter: no mistiming of bond coat																
	40	x				x	x			x	x		x					
Repair mortar mistiming	NO	Standard parameter: no mistiming of repair mortar																
	40		x		x	x	x			x	x		x		x		x	
Curing methods	NO	x		x	x	x		x	x	x		x	x	x		x	x	
	3d	Standard curing method: moist curing for three days																
High temperature curing followed by drying shrinkage		x		x	x	x		x	x	x		x	x	x		x	x	
High temperature curing followed by thermal cycling		x			x	x		x	x	x		x	x	x			x	
Low temperature curing		x			x	x		x	x	x		x	x	x			x	
Low temperature curing followed by freeze/thaw cycling		x			x	x		x	x	x		x	x	x			x	

Note: **Control specimens**: the parameters for control specimens are indicated by each standard parameter.

Bond test method:

CP: core pull-off test; SS: slant shear test;
PC: patch compressive test; PF: patch flexural test;

Parameters of workmanship:

SM: smooth surface; MR: medium rough surface;
RF: rough surface
S: sound surface; W: weak surface;
CL: clean surface; CT: contaminated surface;
SW: saturated surface wet; SD: saturated surface dry;
AW: air dry surface wet; AD: air dry surface dry;
BW: bond dry surface wet; BD: bond dry surface dry;
HA: Hand applied without vibration; VB: hand applied with vibration;
NO: no mistiming in mistiming group or no curing in curing group;
40: about 40 min. mistiming 3d: 3d moist curing ;
A2: light weight acrylic modified mortar

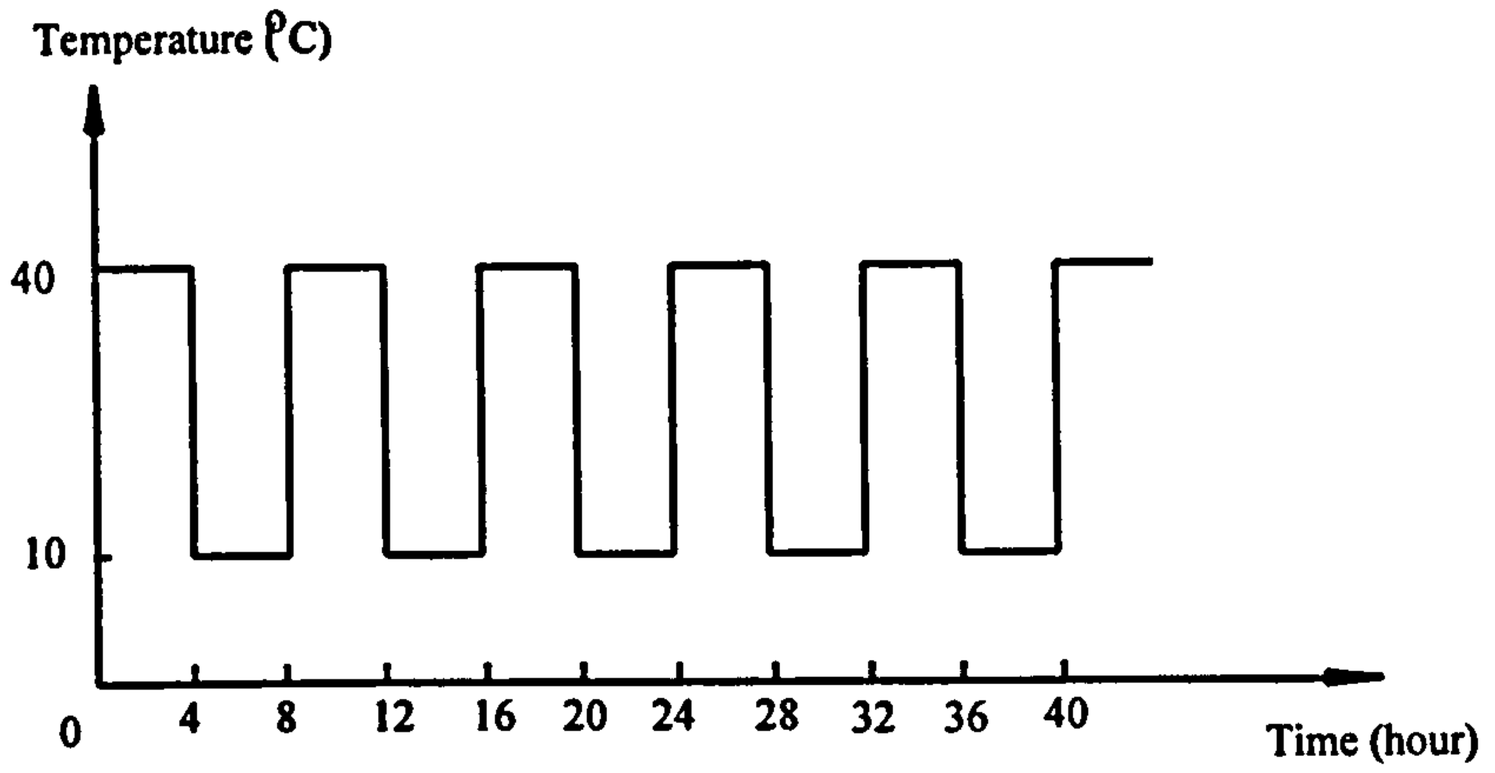

a) Temperature cycling

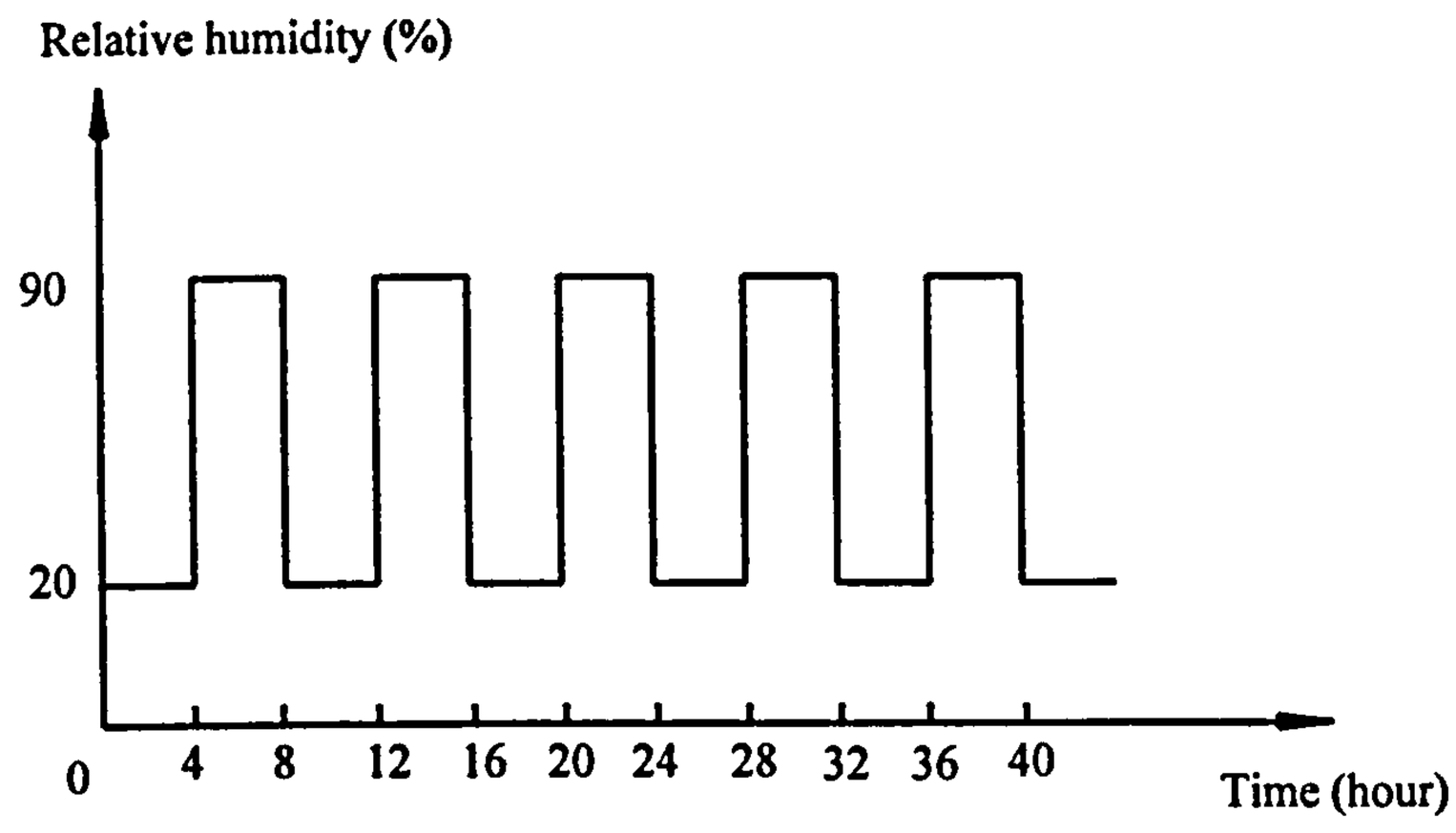

b) Relative humidity cycling

Figure 3.1 Thermal cycling

Figure 3.2 Freeze/thaw cycling

Chapter 4

EXPERIMENTAL AND ANALYTICAL METHODS

Chapter 4 Experimental and Analytical Methods

4.1 Introduction

In Chapter 3, the test programme was described, which included the test parameters and the specimen types. In this Chapter the methods used to prepare the specimens and to carry out the tests are described, along with the analytical techniques used to model the tests.

4.2 Experimental Methods

4.2.1 Test methods

4.2.1.1 The core pull-off test

The tests were carried out using a Limpet pull-off test equipment which applies a direct tensile force to the core (Fig. 4.1). The loading rate adopted followed the Limpet manufacturer's suggestion of 1 revolution every five seconds, roughly equal to 0.02 MPa/sec. When failure occurred, the Limpet showed the maximum load achieved. The failure mode for each result was recorded as the relative percentage of failure in the substrate, bond interface, and repair mortar.

4.2.1.2 The slant shear test

A Denison 600KN standard test machine was used for the slant shear test (Fig. 4.2). The loading rate was 60.5 KN/min, equivalent to about 20 MPa/min. The failure mode was recorded as bond failure or monolithic failure.

4.2.1.3 The patch compressive test

A Denison hydraulic compressive testing machine of 3,000 KN loading capacity was used for the patch compressive test in the first half of this project. Later, tests were

carried out using a newer 600KN Denison testing machine (Fig. 4.3) due to a fault in the old machine. A loading plate was put on top of unrepaired patch compressive specimens, and a few repaired ones at the early stage of this project, to ensure that load was axially applied (Fig. 4.4). For repaired specimens, failure mode was recorded as bond failure or monolithic failure.

4.2.1.4 The patch flexural test

A 100KN INSTRON universal test machine was used for the patch flexural test. The test was controlled by cross head movement at a constant rate of 0.15 mm/min. The loading arrangement is shown in Fig. 4.5. The failure mode was recorded as bond failure, or cracking of repair material. At the same time, load versus cross head movement was recorded by an X-Y recorder.

4.2.2 Specimen preparation

4.2.2.1 Substrate concrete

All substrate concretes were cast and vibrated on a vibrating table, and cured with polythene sheets for 24 hours before they were demoulded and put in a water tank for 6 days. After water curing most specimens were left in air to dry for three weeks before they were sandblasted, and a few were split after the curing to produce split surfaces for the initial studies. The general procedures to prepare the substrate for repair is shown in Fig. 4.6.

4.2.2.2 Specimens for the core pull-off test (CP)

100x100x500 mm and 50x100x500 mm substrate beams were cast. The 100x100x500 mm beams were line load split or saw cut along the longitudinal direction to produce two 50x100x500 mm substrates. After surface preparation, the substrate was moisture conditioned before the repair material was applied. The substrate was then put in the mould leaving a vertical repair area, and the repair material applied using gloved

hands; if necessary a metal rod was used to make sure that the repair material at the corner was adequately compacted (Fig. 4.7). The top of the repair mortar was pressed fairly hard using a steel trowel to compact and finish the repair. This method of compacting was used for all other kind of specimens. This produced a smooth and even loading surface, minimising the variation in failure load that could be caused by the unevenness of a steel trowel finished loading surface. After being covered using polythene sheet for three days, the repaired specimens were air cured inside the laboratory for about 3 weeks. About a week before the test was to be carried out, the repaired beam was core drilled from the side of repair mortar - five cores for each beam. The drilling depth into the substrate was controlled to about 15-20mm except for a few beams which were used to investigate the drilling depth effect. With these, the drilling depth was controlled to about 1-2 mm (just beyond the bond interface). Because water was used to cool the diamond core tip, the surface layer of the specimens were saturated after coring. Therefore, cored specimens were left in the laboratory to dry for about 2 days under air exposure. The top of the cores was sandpapered to remove any laitance, and then steel or aluminium dollies of 50 mm in diameter and 20 mm in thickness were glued to the top of the cores with 2-part epoxy resin. The epoxy resin was allowed at least 24 hours air cure before the tests were carried out.

4.2.2.3 Specimens for the slant shear test (SS)

The concrete substrate was prepared in the following ways:

(1) 150x150x55 mm plaques were cast, and when the plaque was at least two weeks old each was saw cut or line load split into two halves to produce two substrates.

(2) A wooden block of the shape of a saw cut substrate was inserted into the mould, then substrate concrete was poured into the remaining space. One substrate was produced from each mould.

After surface preparation and moisture conditioning, the substrate was put into the mould and the repair material applied. The repaired plaques were kept in the mould and covered using polythene sheet for three days. They were saw cut at the age of at least 14 days to produce a test specimen with a cross section of the size about 55x55 mm. The actual size was measured to calculate the stresses at failure (Fig. 2.12).

4.2.2.4 Specimens for the patch compressive test (PC)

A 100x400x512 mm slab with a formed circular cut-out of 25x200 mm was cast (Fig. 4.8). After surface preparation of the cut-out area and moisture conditioning, the repair material was applied. The repaired slab was covered with polythene sheet for three days followed by air cure. The slab was cut into five prisms before test. The variation of the width of the prism caused due to cutting was taken into consideration for stress calculation.

4.2.2.5 Specimens for the patch flexural test (PF)

A 100x310x450 mm slab with a formed rectangular cut-out of 25x180 mm was cast (Fig. 4.9). After surface preparation of the cut-out area and moisture conditioning, the repair material was applied. The repaired slab was initially covered with polythene sheet for three days unless otherwise stated, followed by air cure inside the laboratory. The slab was cut into three beams before test. The variation of the width of the beam was taken into consideration for stress calculation. A piece of steel strip was put on top of the beam to ensure that the load was uniformly applied over the width of the beam.

4.2.3 Surface preparation

The preparation consisted of two steps. The first step was to produce a substrate surface, and the second one was to finally prepare the surface to give the required roughness.

Four methods were used in the first step, and they are listed below:

(1) Formed surface (FM)

It is self evident that a formed surface is the surface in contact with the form-work during casting. After curing, a layer of laitence will form.

(2) Saw-cut surface (SC)

It is also self evident that a saw-cut surface is the surface that is being saw-cut. Both cement paste and aggregate will be cut through. A blade with a diamond saw tip was used.

(3) Line-load split surface (LS)

This was carried out on specimens for the core pull-off test and the slant shear test.

For the core pull-off test specimens, two steel bars of 14mm in diameter were put centrally on the top and bottom sides of the prism along the longitudinal direction. Then load was applied on the steel bars through the loading plate of the test machine until the concrete split.

For the slant shear test specimens, two steel wires of about 3mm in diameter were put on the top and bottom sides of the plaque along the specified direction. Then load was applied to split the plaque.

(4) Concrete set retarder produced surface (SR)

A concrete surface set retarder from Sika Limited, (a pink thixotropic emulsion), was used to roughen the concrete surface. The retarder was applied to the dry, clean form-work for the cut-out area and left to dry completely before casting the substrate concrete. After demoulding the following day the concrete surface in contact with the retarder was wire brushed to expose the coarse aggregate. The substrate so produced was then water cured for 6 days, followed by air cure.

Five methods were used in the second step, and they are listed below:

(1) No treatment (NT)

This means no further treatment was carried out to surfaces produced in the first stage.

(2) Wire brushing (WB)

An steel wire brush was used to further prepare the surface. Depending on the age and hardness of the substrate surface, the effect of using a wire brush was found to be very different.

(3) Needle gunning

A pneumatic needle gun was used for further surface preparation. Depending on the age and hardness of the substrate surface, the effect was again very different.

(4) Sand blasting (SB)

Sandblasting removed laitance and roughened the area where the repair was to be carried out by projecting sand particles at the concrete surface at high velocity. This was done by taking specimens to a specialist local company who carried out the blasting under University supervision. Grade 35 sand particles (maximum size 0.25mm) from Mansfield were used for the sand blasting, and the delivery pressure at the nozzle was about 0.5 MPa. By varying the operating time and the distance between the nozzle and the concrete, surfaces with different degrees of roughness were produced.

(5) Contaminating (CT)

Demoulding oil was brushed on the sound, roughened and dry surfaces, and left inside the laboratory to dry out overnight. After drying out, the visual difference between a contaminated and a clean surface was difficult to detect. The surfaces were then thoroughly washed with a waterjet and further moisture conditioning was carried out, as required, before the repair material was applied.

The methods for preparing substrate surfaces are indicated by joining the notations for the first step and the second step together. For example, FM-SB means a formed surface, then sand blasted, and LS-NT means a line load split surface with no further treatment, etc.

Surface roughness was measured using a surface roughness index (SRI) according to the draft European Standard : CEN TC 104 WGB : Draft EN YYY Part 1 [60]. The detailed procedure is given in Appendix 1.

4.2.4 Moisture conditioning

Most research carried out on this issue simply defines the substrate as wet or dry. In this study, both the moisture condition inside the substrate and at the surface were considered. The moisture condition inside the substrate was defined as saturated, air dry, and bone dry, and the condition at the surface as wet and dry. Six combinations of moisture condition were used in this project to study their effect on bond strength. The six moisture conditions and their designation are as follows:

saturated surface dry	(SD);
saturated surface wet	(SW);
air dry surface dry	(AD);
air dry surface wet	(AW);
bond dry surface dry	(BD); and
bone dry surface wet	(BW).

The moisture conditions were simulated in the following ways (Fig. 4.10):

For a saturated substrate, the specimen was kept in a water tank for three days before surface moisture condition was to be defined for repair. A bone dry substrate was simulated by putting the substrate concrete into an oven at a temperature about 80-

100°C for three days, followed by two days in air for it to cool down. The air dry substrate was obtained simply by leaving the specimen in air after six days initial curing in a water tank until the repair was to be carried out. Excluding the initial test in which the age of the substrate before repair was about 7 to 15 days, the age of the substrates used for the CP test before repair was carried out varied from 65 to 126 days for the S/C mortar repaired specimens, from 65 to 266 days for the A1 mortar repaired specimens, from 83 to 131 days for the SBR mortar repaired specimens, from 84 to 89 days for the A2 mortar repaired specimens, and from 84 to 132 days for the flowing concrete repaired specimens. In total, the age of 83% of all specimens varied from 84 to 132 days, 7.5% varied from 65 to 77 days, and 9.5% varied from 191 to 266 days.

The second aspect relates to the moisture condition at the surface. In this study, a wet surface was defined as what looked wet, but no free water, and a dry surface was defined as what had dried back from a wet look surface for 10-20 min.. For a saturated substrate, a dry surface was produced by taking the specimen out of the water tank about 60 min. before the repair was to be carried out. A wet surface was produced by taking the specimen out of the water tank about 20 min. before repair. If there still was free water after that time, compressed air was used to blow off the excess. If the surface tended to become dry during that period, a clean polythene sheet was used to cover the surface to prevent drying out.

For air dry and bone dry substrates, a dry surface was produced simply by leaving the specimen in air until the repair material was applied. Wire brushing and compressed air were used to blow off the dust on the surface. A wet surface was produced by sprinkling water for about 20 min., then blowing the excess off.

4.2.5 Curing of repaired specimens

The standard curing method used polythene sheet to cover the whole repaired specimen tightly for three days, followed by air cure. To simulate no curing of a

specimen, it was simply left uncovered in the laboratory after repair. A few test specimens were covered with polythene sheet for seven days.

4.2.6 Environmental conditioning

A FISONS FE 1000 climate cabinet was used for controlling the environmental conditions specified in section 3.4.2. The cabinet volume was $1m^3$ with an operating range of -40 to +100°C and 15 to 99% RH.

During the 3-day curing period, either at a high temperature (40°C) or low temperature (4°C), the repaired specimens were covered with polythene sheet. Air temperature and relative humidity outside the polythene sheet were used as controlling parameters, for high temperature curing, they were set at 40°C and 20%RH, and 4°C for low temperature curing (the relative humidity was not controlled in this case).

After the 3-day initial curing period inside the cabinet, the polythene sheet was removed, and further environmental conditioning which will be described below was started. For the drying shrinkage group, the specimens were removed from the environment cabinet and then left in air inside the laboratory until the repair was about 4 months old to be tested. For the thermal cycling group, the specimens remained in the cabinet for another week., and the cabinet was changed into the thermal cycling status as defined in section 3.4.2. After this, they were left in air until the test when the repair was 28 days old. The low temperature cured specimens were left in air after the initial 3-day curing period inside the cabinet until the test when the repair was 28-day old. For the freezing and thawing cycle group, the PC and PF slabs were taken out of the cabinet and saw cut into the prisms (with a cross section of 100x100mm). After immersing in water for 24 hours, the specimens were put into containers specially designed for this test. The containers were filled with water (about 3mm above the surface of the prisms), and then put back into the environmental cabinet for the

freezing and thawing cycling test. The water was checked regularly during thawing times and refilled if necessary.

4.3 Analytical methods

4.3.1 Finite element analysis

The PAFEC finite element system was used to carry out the finite element analyses. Materials were assumed to be linear-elastic. Eight noded isoparametric curvilinear quadrilateral elements and six noded isoparametric curvilinear triangular elements were used under different situations. The data file was generated using either the PAFEC Interactive Graphics system (PIG system) or data moduli method. For the reasons of simplicity, the data moduli method is used here to present the data files.

The finite element analyses were applied to the following cases:

(1) Effect of modulus mismatch on stress concentration over the bond interface in a direct tensile stress transfer situation (Fig. 4.11)

This model is to see the effect of modulus mismatch on stress concentration over a bond interface. Because of the symmetry about the longitudinal axes, only half of the specimen is modelled. Under the action of a longitudinal stress, the transverse deformation is affected by both the modulus E, and Poisson's ratio ν ($\varepsilon_y = -\nu\varepsilon_x = -\nu\frac{\sigma_x}{E}$). In this model, the effect of modulus mismatch is considered by changing either the modulus E or the Poisson's ratio ν. Uniform tensile stress of σ_o = 1 MPa is applied at the top side of the model. No change in stress distribution is obtained as long as $(E_c/\nu_c)/(E_m/\nu_m)$ remains unchanged.

(2) Effect of drilling depth into the substrate concrete on stress distribution over the bond interface in a core pull-off test (Fig. 4.12)

The core is modelled axisymmetrically about its central axis. Eight-noded isoparametric curvilinear quadrilateral elements are used in this model. To reveal only the effect of drilling depth on stress distribution over the bond interface, the properties of the substrate concrete and the repair material were selected in such a way that there is no modulus mismatch effect on stress distribution. Three drilling depths were considered: 2mm, 10mm and 15mm. Mesh density near the bond interface is modified accordingly for selected drilling depth. Loading and supporting condition is modelled based on the Limpet pull-off test equipment used: uniform tensile stress applied on the top of the core, and reaction provided by the metal ring some distance from the core centre.

(3) Effect of modulus mismatch on indirect stress transferring in a patch compressive test (Fig. 4.13)

Because of the sharp angle at the periphery of the bond interface, six-noded isoparametric curvilinear triangular elements were used to model the edge part of the repair mortar and eight-noded isoparametric curvilinear quadrilateral elements for the rest part. Uniform stress is applied at the top side of the specimen. Because of the symmetry about the horizontal central axis, only half the specimen is modelled.

(4) Effect of modulus mismatch on stress transferring in a patch flexural test (Fig. 4.14)

Half specimen is modelled and eight-noded isoparametric curvilinear quadrilateral elements were used.

(5) Effect of displacement simulated loading on eccentricity induced on unrepaired patch compressive specimens (Fig. 4.15)

Half of the specimen is modelled with eight-noded isoparametric curvilinear quadrilateral elements. The loading condition is simulated by specifying uniform displacement at the top side of the specimen. In contrast, the loading condition of uniform compressive stress is thought to represent the situation when a loading plate is used (Fig. 4.4). The stress distribution over the central cross section (the narrowest cross section) is plotted.

(6) Effect of modulus mismatch on stress distribution over the bond interface in a slant shear test (Fig. 4.16)

This model consists of three parts: the substrate concrete, the bond interlayer (the adhesive), and the repair mortar. In the case of two concrete blocks are bonded together by an adhesive, the repair mortar and the substrate concrete are assumed having the same material properties. The attention is focused on the modulus mismatch between the adhesive and the blocks. In the case of a repair mortar is applied on top of the substrate concrete, the bond interlayer and the repair mortar are assumed having the same material properties. Or in a more general way, all three materials are different from each other. Uniform compressive stress of σ_o = 10 MPa is applied on the top side of the specimen. The stress distribution over the bond interface is plotted against the horizontal distance from the edge of the specimen.

(7) Effect of difference in the coefficients of thermal expansion on stresses induced over the bond interface in a concrete overlay situation (Fig. 4.17)

Half the specimen is modelled because of symmetry. Temperature of -30°C is assigned to all nodes in the repair mortar. This will generate differential thermal deformation equivalent to a differential thermal strain of 300 με and because of the restraint provided by the substrate concrete thermal stresses will be generated. No external load is applied. No material property mismatch is considered.

All the PAFEC files are given in Appendix 2.

4.3.2 Simplified elastic analysis

Simplified linear elastic analysis was used to see the effect of modulus mismatch on stress transferred to the repair material in both a patch compressive and patch flexural test (Fig. 4.18).

Suppose the axial strain at the mid-height of the cross section is ε_0, and the curvature ϕ, the strain distribution over the central cross section can be expressed as

$$\varepsilon = \varepsilon_o + \phi(x - \frac{b}{2}) \qquad (4.1)$$

Integrating over the cross section, the axial load, P, and the bending moment, M, can be worked out.

$$P = \int_0^c E_c \varepsilon t dx + \int_c^b E_m \varepsilon t dx \qquad (4.2)$$

$$M = \int_0^c E_c \varepsilon t (x - \frac{b}{2}) dx + \int_c^b E_m \varepsilon t (x - \frac{b}{2}) dx \qquad (4.3)$$

where t is the thickness of the prism,

E_c, E_m are the moduli of substrate and repair mortar, respectively.

c is the width of the narrowest cross section of the substrate, and

b is the gross width of the substrate.

By substituting Eq.(4.1) into Eqs.(4.2) and (4.3), the following equations can be worked out.

$$\varepsilon_o K_{11} + \phi K_{12} = P \tag{4.4}$$

$$\varepsilon_o K_{21} + \phi K_{22} = M \tag{4.5}$$

or in another form

$$\begin{bmatrix} K_{11} & K_{12} \\ K_{21} & K_{22} \end{bmatrix} \begin{bmatrix} \varepsilon_o \\ \phi \end{bmatrix} = \begin{bmatrix} P \\ M \end{bmatrix} \tag{4.6}$$

where

$$K_{11} = t\,c\,E_c + t(b-c)E_m$$

$$K_{12} = \frac{t\,E_c}{2}\left[(c-\frac{b}{2})^2 - \frac{b^2}{4}\right] + \frac{t\,E_m}{2}\left[\frac{b^2}{4} - (c-\frac{b}{2})^2\right]$$

$$K_{22} = \frac{t\,E_c}{3}\left[(c-\frac{b}{2})^3 + \frac{b^3}{8}\right] + \frac{t\,E_m}{3}\left[\frac{b^3}{8} - (c-\frac{b}{2})^3\right]$$

$$K_{21} = K_{12}$$

In the case of a patch compressive test, P = Po, M = 0, and in the case of a patch flexural test, P = 0, M = Mo.

The longitudinal stresses in the substrate concrete at the central cross section can then be worked out:

$$\sigma_c = E_c \varepsilon \tag{4.7}$$

and the longitudinal stresses in the repair material at the central cross section:

$$\sigma_m = E_m \varepsilon \tag{4.8}$$

Stresses at the bond interface can be determined from Mohr's stress circle using the angle of the bond interface having the same abscissas:

$$\sigma_n = \sigma_o \cdot \sin^2 \alpha \qquad (4.9)$$

$$\tau_n = 0.5\sigma_o \sin(2\alpha) \qquad (4.10)$$

where σ_o is the stress in longitudinal direction, σ_n and τ_n are normal and shear stresses acting on the bond interface, respectively, and α is the angle between the bond plane and the longitudinal axis.

4.3.3 Shrinkage and creep considerations

This differs from the previous analyses in that the effect of time is taken into consideration.

Shrinkage and creep were considered in the following two cases:

(1) the repair material was applied symmetrically on a substrate; only longitudinal deformation would occur (Fig. 4.19); and

(2) the repair overlay situation, where due to the differential shrinkage, bending will be induced (Fig. 4.20).

4.3.3.1 Repair material applied symmetrically on a substrate

At any time t, the total strain in an uniaxially loaded specimen consists of a number of components, which include the instantaneous strain $\varepsilon_e(t)$, the creep strain $\varepsilon_c(t)$, the shrinkage strain $\varepsilon_{sh}(t)$, and the temperature strain $\varepsilon_t(t)$. Although not strictly correct, it is usual to assume that all four components are independent and may be calculated separately, and summed to obtain the total strain [134].

Ignoring the temperature effect, it can be seen from Fig. 4.19 that if shrinkage of the repair material is greater than that of the substrate concrete, tensile stress will be

developed in the repair material, and compressive stress in the substrate. At any time t, the total strain developed in repair mortar can be worked out by the principle of superposition as

$$\varepsilon_m = \varepsilon_{shm}(t,t_m) + \varepsilon_{em} + \varepsilon_{cm} \tag{4.11}$$

and the total strain in the substrate concrete:

$$\varepsilon_c = \varepsilon_{shc}(t,t_c) + \varepsilon_{ec} + \varepsilon_{cc} \tag{4.12}$$

where

ε_{shm}, ε_{shc} are the shrinkage strains in the repair material and the substrate concrete, respectively;

ε_{em}, ε_{ec} are the elastic strains in the repair material and the substrate concrete, respectively;

ε_{cm}, ε_{cc} are the creep strains in the repair material and the substrate concrete, respectively; and

t_m, t_c are the age of the repair material and the substrate concrete at the time when shrinkage starts.

Equilibrium requires that the following equation be satisfied:

$$\sigma_m A_m + \sigma_c A_c = 0 \tag{4.13}$$

Compatibility requires:

$$\varepsilon_m = \varepsilon_c \tag{4.14}$$

It can be seen that so long as the shrinkage strains, the constitutive relationship of materials, and the creep strains are known, shrinkage stress due to restraint provided by the substrate can be evaluated. But the determination of creep strains can be a very complicated problem.

Methods can be divided into several categories depending on the method used to determine the creep strain, or the creep coefficient. They include the effective modulus method, the age-adjusted effective modulus method, and the rate of creep method. Each one has its advantages and disadvantages. Bearing in mind that every method is based on many assumptions and only provides an approximate solution, it is better to determine the upper and lower limit of the shrinkage stresses. The actual effect of shrinkage and creep can be evaluated between these limits. It is not in the scope of this study to compare different methods. According to [134], the effective modulus method and the rate of creep method were adopted because they provide the lower and upper limit analyses. Detailed derivations are given in Appendix 3.

4.3.3.2 Repair overlay situation

Because of the differential shrinkage, the repaired beam will bend, and internal stresses develop.

An element of a composite beam, length d_X, is shown in Fig. 4.20b. The beam is made from two materials, the repair material (m) and substrate concrete (c), joined by a medium of assumed negligible thickness but having finite shear and normal stiffness.

Assuming that plane sections within each material remain plane, the strains can be expressed in terms of the displacements u and w, relative to the local x and z axes, respectively. For material m, the total displacement in the x-direction over depth z_m, denoted by u_m, is given by:

$$u_m = u_{mo} - z_m w_m^{'} \tag{4.15}$$

in which the subscript *m* denotes the repair material, and w_m' denotes the first derivative of w_m with respect to x. Similarly for material c:

$$u_c = u_{co} - z_c w_c^{'} \tag{4.16}$$

where u_{mo}, and u_{co} are displacements along the x-direction at the central axes within the repair material and the substrate concrete, respectively.

The strains in materials *m* and *c*, denoted by ε_m and ε_c, are given by:

$$\varepsilon_m = u_m^{'} = u_{mo}^{'} - z_m w_m^{''} \tag{4.17}$$

$$\varepsilon_c = u_c^{'} = u_{co}^{'} - z_c w_c^{''} \tag{4.18}$$

Stresses can now be related to strains by the moduli of the materials, E_m and E_c. For linear elastic behaviour, E_m and E_c are constants, for non-linear elastic and elastic plastic materials: E_m and E_c are functions of strain. Only linear elastic behaviour of materials is considered here. If ε_{fm} and ε_{fc} define the free strains due to shrinkage, creep, temperature, etc., the stresses σ_m and σ_c are given by:

$$\sigma_m = E_m(u_{mo}^{'} - z_m w_m^{''} - \varepsilon_{fm}) \tag{4.19}$$

$$\sigma_c = E_c(u_{co}^{'} - z_c w_c^{''} - \varepsilon_{fc}) \tag{4.20}$$

The axial forces N_m and N_c, and moments m_m and m_c are obtained by integrating the stresses, multiplied by an appropriate level arm in the case of moments, over the cross-sectional area of materials *m* and *c*, denoted by A_m and A_c. Hence:

$$N_m = \int \sigma_m dA_m \tag{4.21}$$

$$N_c = \int \sigma_c dA_c \tag{4.22}$$

$$m_m = -\int \sigma_m z_m dA_m \tag{4.23}$$

$$m_c = -\int \sigma_c z_c dA_c \tag{4.24}$$

Since the strains and stresses throughout the beam have been defined in terms of four independent displacement variables, four independent equations are required to obtain a solution. These four equations are obtained by considering the equilibrium of a small element of the beam and the compatibility of displacements at the interface between the two materials.

Resolving forces horizontally gives:

$$N_m + N_c = 0 \tag{4.25}$$

Resolving forces vertically and taking moments gives:

$$m_m + m_c + N_m \cdot e = 0 \tag{4.26}$$

The slip u_{mc} at the interface between materials *m* and *c* is the relative displacement in the x-direction of initially adjacent particles. Hence, if the shear stiffness of the joint per unit length is denoted by K_S, and z_{im} and z_{ic} are the z-coordinates of the interface in the two materials (z_{ic} is negative), then:

$$\tau = K_s u_{mc} = K_s[(u_{mo} - z_{im} w_m') - (u_{co} - z_{ic} w_c')] \tag{4.27}$$

in which τ is the shear force per unit length.

The separation at the interface between materials *m* and *c* is the relative displacement in the z-direction of adjacent particles. Hence, if the normal stiffness of the joint per unit length is denoted by K_n:

$$\sigma_n = K_n(w_c - w_m) \tag{4.28}$$

in which σ_n is the normal force per unit length. Equilibrium of an element of material m yields the equations:

$$\tau = N_m^{'} \tag{4.29}$$

$$m_m^{'} + \tau z_{im} - f_m = 0 \tag{4.30}$$

$$f_m^{'} - \sigma_n = 0 \tag{4.31}$$

The main equations can now be summarised as follows:

$$N_m = \int E_m(u_{mo}^{'} - z_m w_m^{''} - \varepsilon_{fm})dA_m \tag{4.32}$$

$$N_c = \int E_c(u_{co}^{'} - z_c w_c^{''} - \varepsilon_{fc})dA_c \tag{4.33}$$

$$m_m = -\int E_m(u_{mo}^{'} - z_m w_m^{''} - \varepsilon_{fm})z_m dA_m \tag{4.34}$$

$$m_c = -\int E_c(u_{co}^{'} - z_c w_c^{''} - \varepsilon_{fc})z_c dA_c \tag{4.35}$$

$$N_m^{'} + N_c^{'} = 0 \tag{4.36}$$

$$m_m^{\bullet} + m_c^{\bullet} - N_c^{\bullet} e = 0 \tag{4.37}$$

$$N_m^{\cdot} - K_s[(u_{mo} - z_{im} w_m^{\cdot}) - (u_{co} - z_{ic} w_c^{\cdot})] = 0 \tag{4.38}$$

$$m_m^{\bullet} - K_n(w_c - w_m) + N_m^{\bullet} e = 0 \tag{4.39}$$

Detailed derivation of the closed form solution is given in Appendix 4.

4.3.4 Bond strength criterion

4.3.4.1 Introduction

Bond strength criterion is the key to a thorough understanding of how a repair system behaves, but little information has been found on this issue. Robins and Austin [68] recently presented a unified failure envelope from their evaluation of concrete repair bond tests. The bond failure envelope enables a meaningful comparison of information from different test methods to be made. Based on related test results by the author and others, the concept of a bond strength criterion is proposed. In order to have a clear understanding of what a bond strength criterion is, a brief discussion is needed to differentiate between a material strength criterion and a bond strength criterion.

The strength criterion for a material depends on stresses acting on a material element, but in the case of a bond strength criterion, it is the stresses acting on bond interface that matters. Because a bond interface is the contact area between two materials, the actual failure will depend on the relative performance between repair materials and bond interface, i.e., if the failure envelope of a material is first reached, the failure will be controlled by material strength rather than by bond strength.

4.3.4.2 The shape of the bond strength envelope

Tests carried out by Long, et al [41] showed that the shear bond strength obtained from Coulomb's theory was much higher than that obtained from a shear bond test, (such as the twist-off test). Robins and Austin's work [68] using two differently graded sand/cement mortars showed the similar trend, but a more close examination revealed that in the combined stress state of compression and shear, the Coulomb's theory was found adequate to predict the bond failure strength, in the tension-shear stress state, also a linear form can be used to approximate the relationship. Thus, a bi-linear bond strength envelope is presented at present (Fig. 4.21). When more test results are available, the proposed envelope can be modified or updated. The establishment of this bi-linear bond strength envelope needs the following parameters: the tensile bond strength, σ_t, shear bond strength, τ_o, slant shear bond strength, σ_n and τ_n, and the internal friction angle, ϕ, (or the coefficient of friction, μ).

When all these parameters are known, the procedure to establish the bond strength envelope is described below (see Fig. 4.21)

For bond strength envelop a-c

$$\tau = a_1\sigma + b_1 \qquad (4.40)$$

Boundary conditions

$$\sigma = 0,\ \tau = \tau_o = \beta\sigma_t\ , \text{and}$$

$$\tau = 0,\quad \sigma = \sigma_t\quad (\sigma_t < 0,\ \beta < 0,\ \tau > 0)$$

where τ_o is the shear bond strength, σ_t is the tensile bond strength, and β is the shear/tensile bond strength ratio.

So

$$\tau = \beta(\sigma_t - \sigma) \qquad (4.41)$$

For bond strength envelop c-e

$$\tau = a_2\sigma + b_2 \tag{4.42}$$

Boundary conditions

$$a_2 = \mu$$

$$\sigma = \sigma_n, \tau = \tau_n \quad (\mu > 0, \sigma_n > 0, \tau_n > 0)$$

where μ is the coefficient of friction, σ_n and τ_n are the normal and shear stresses acting on the bond plane, respectively.

So

$$\tau = \tau_n + \mu(\sigma - \sigma_n) \tag{4.43}$$

At point c

$$\sigma_c = \frac{\beta\sigma_t + \mu\sigma_n - \tau_n}{\mu + \beta} \tag{4.44}$$

$$\tau_c = \frac{\beta(\mu\sigma_t - \mu\sigma_n + \tau_n)}{\mu + \beta} \tag{4.45}$$

4.3.4.3 Determination of parameters

For the determination of all the coefficients needed to establish a complete strength failure envelope, the tests results should be based on the same repair material, and same surface preparation. The determination of β should be obtained from τ_o and σ_t based on the same preparation procedures. Even though there are many test results available for the tensile bond strength, not many are available for the shear bond strength. Long, et al [41, 87] carried out both the core pull-off and twist-off tests which provided both the tensile and shear bond strengths needed while the surface condition remained comparable. Thus, their results were used for determining the coefficients, and the author worked out the following relationship.

$$\tau_o = \beta_1 \sigma_t + \beta_2 \qquad (4.46)$$

where β_1 and β_2 are coefficients, varying with surface preparation methods and repair materials. The coefficient of β used in the bond strength envelope establishment can be related to $\beta 1$ and $\beta 2$ as

$$\beta = (\beta_1 \sigma_t + \beta_2)/\sigma_t \qquad (4.47)$$

Table 4.1 shows the coefficient of β_1 and β_2.

For the determination of the coefficient of friction, test results from the following researchers were taken into consideration:

Frank [59]:	μ = 0.7 for a surface sandblasted after removal from the moulds (smooth),
Robins and Austin [68]:	μ = 0.8 for a smooth surface;
Alexander, et al [48]:	μ = 0.75 - 0.87 for a smooth surface;
ACI 318-83 [90]:	μ = 1.0 for concrete placed against a hardened concrete surface, with the surface roughened to a full amplitude of about 6 mm;
Robins and Austin [68]:	μ =1.1 for rough surface; and
Regan [63]:	μ = 1.4 for rough surface.

Values adopted in this research are shown in Table 4.2.

Table 4.1 Coefficients of β_1 and β_2

Surface preparation method	Saw cut surface	Split/rough	Split and shot blasted			
Repair material	different repair materials	different repair materials	SBR modified mortar	Acrylic modified mortar	Flowing concrete	Sand/cement mortar
β_1	0.88	2.18	2.56	1.14	1.11	1.25
β_2	1.56	0.59	0.66	1.59	1.22	0.81
Correlation coefficient			0.98	0.89	0.81	0.91

Table 4.2 Relationship between the coefficient of friction and surface roughness

Surface roughness	Smooth	Medium rough	Rough
Coefficient of friction, μ	0.75	1.0	1.25

Table 4.1 Coefficients of β_1 and β_2

Surface preparation method	Saw cut surface	Split/rough	Split and shot blasted			
Repair material	different repair materials	different repair materials	SBR modified mortar	Acrylic modified mortar	Flowing concrete	Sand/cement mortar
β_1	0.88	2.18	2.56	1.14	1.11	1.25
β_2	1.56	0.59	0.66	1.59	1.22	0.81
Correlation coefficient			0.98	0.89	0.81	0.91

Table 4.2 Relationship between the coefficient of friction and surface roughness

Surface roughness	Smooth	Medium rough	Rough
Coefficient of friction, μ	0.75	1.0	1.25

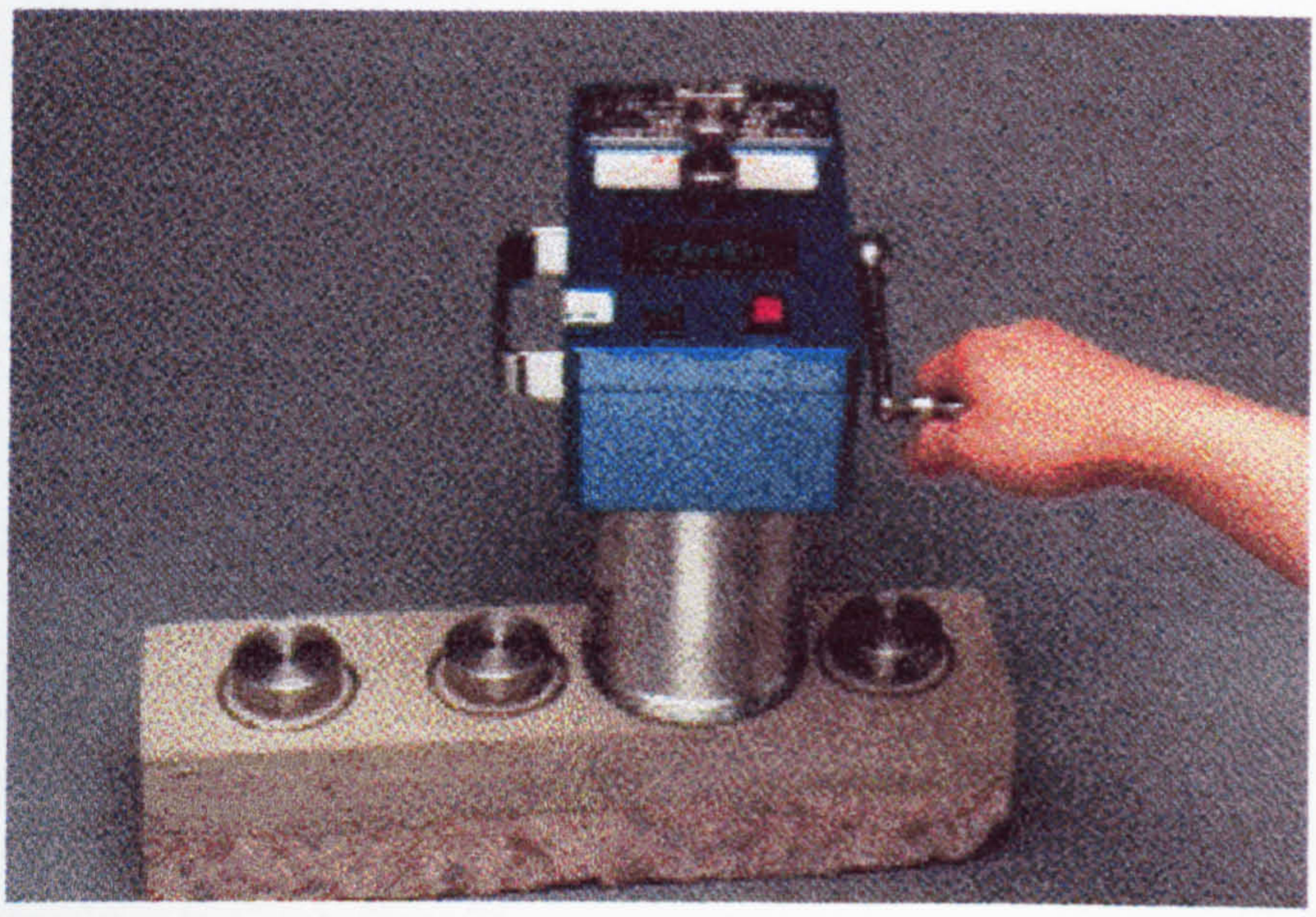

Figure 4.1 Core pull-off test set-up

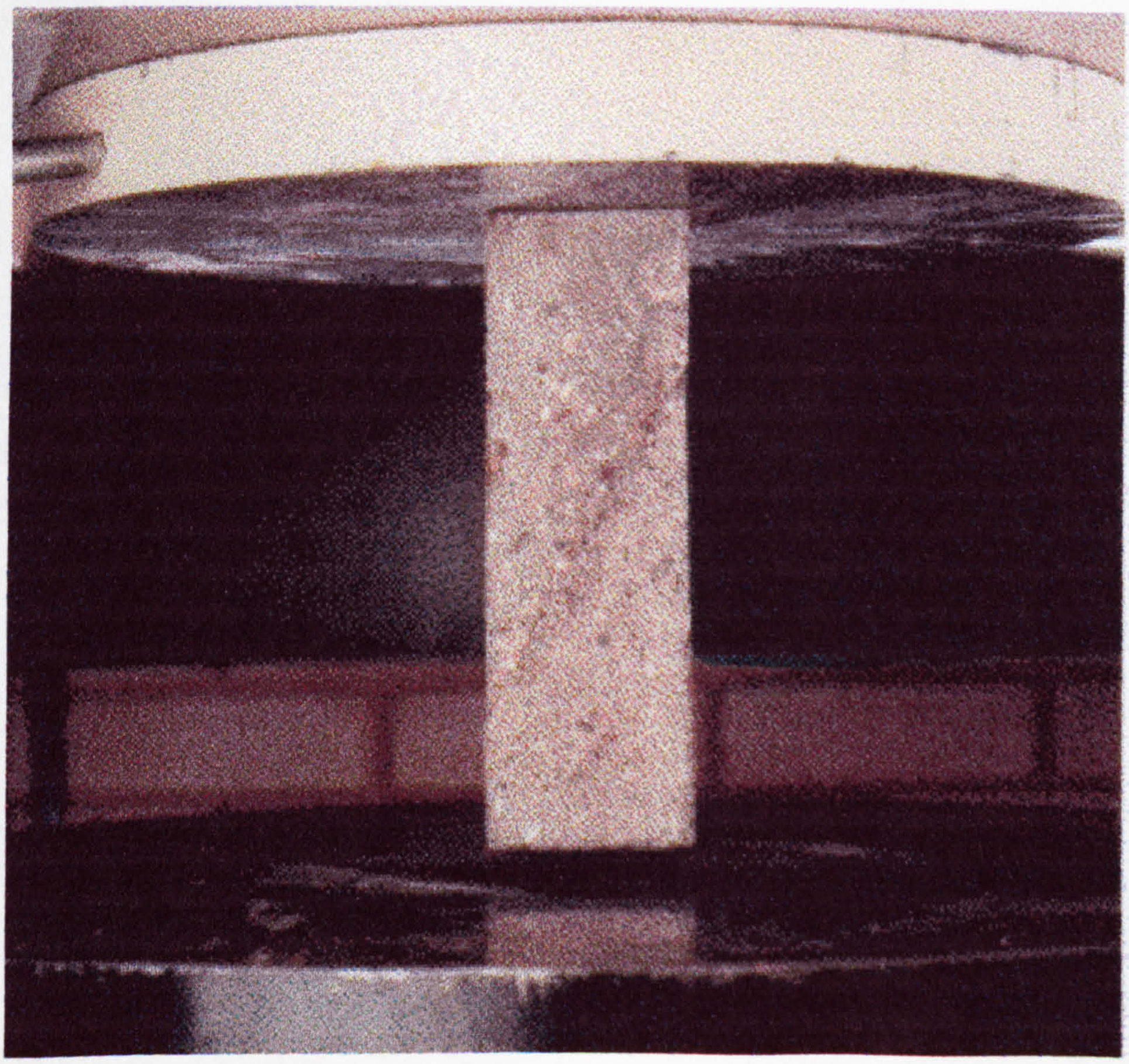

Figure 4.2 Slant shear test

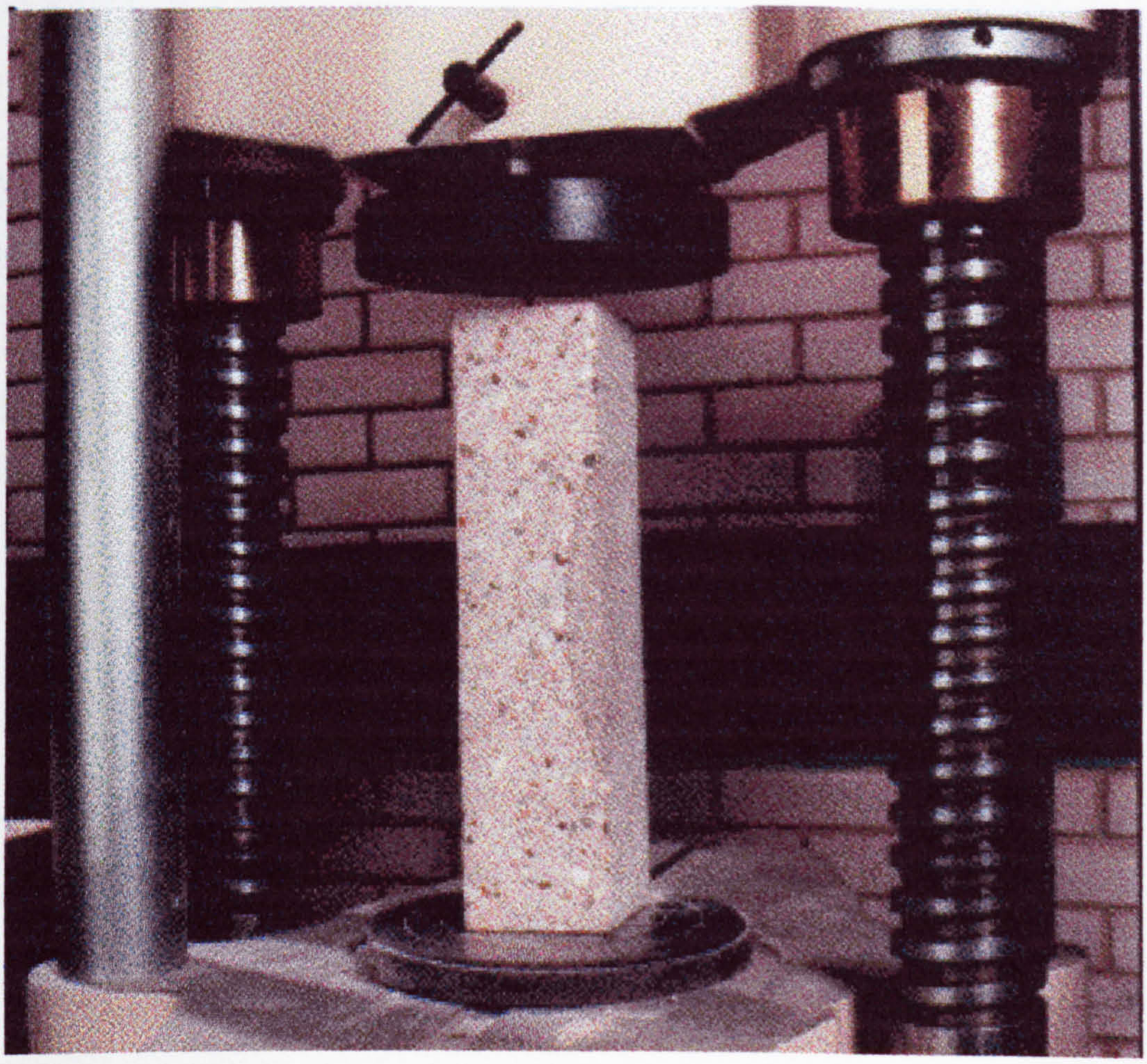

Figure 4.3 Patch compressive test

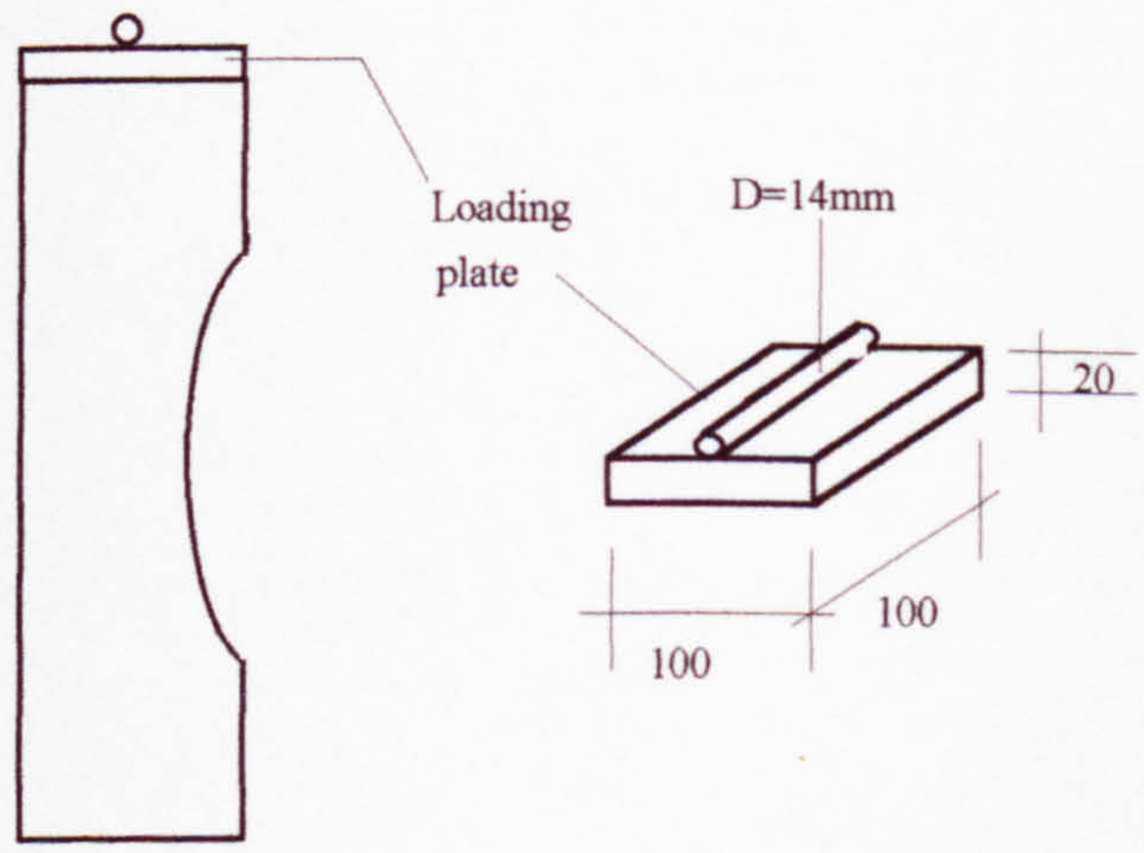

Figure 4.4 The loading plate for the patch compressive test

a) Test set-up

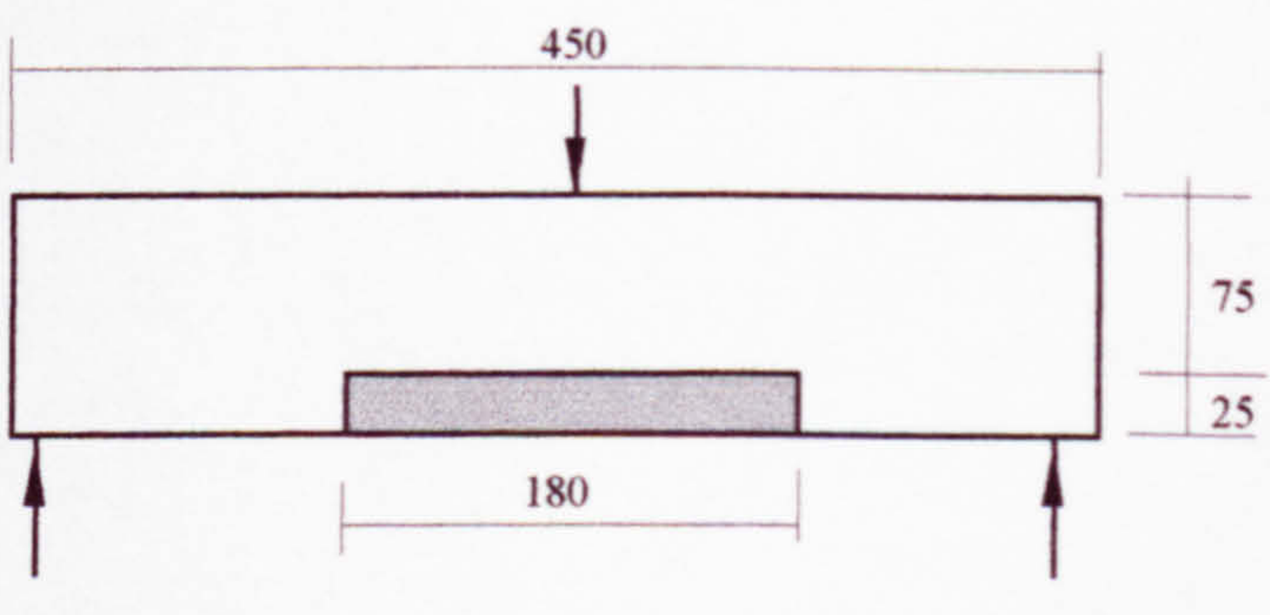

b) Specimen size

Figure 4.5 Patch flexural test

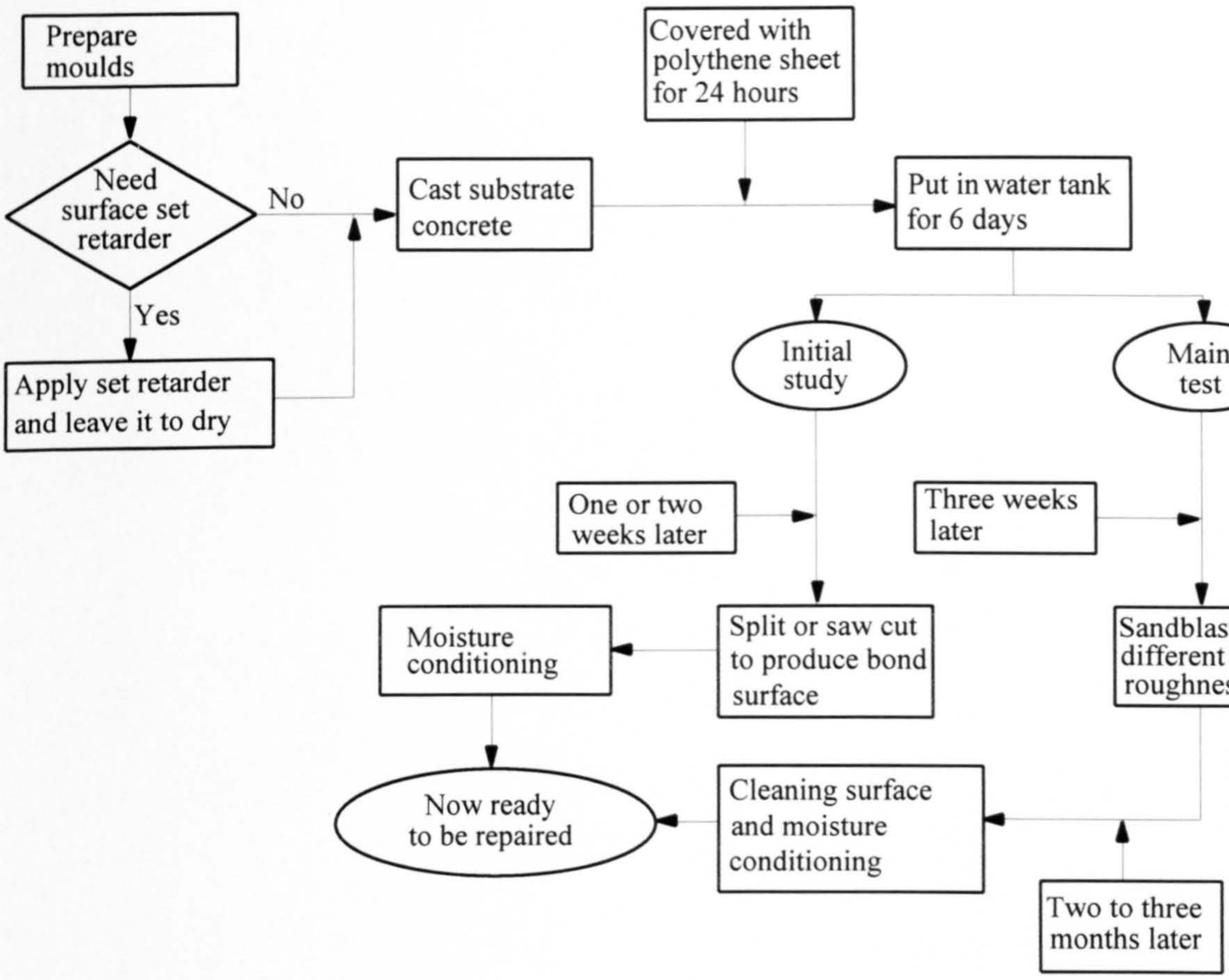

Figure 4.6 Making a substrate for repairing

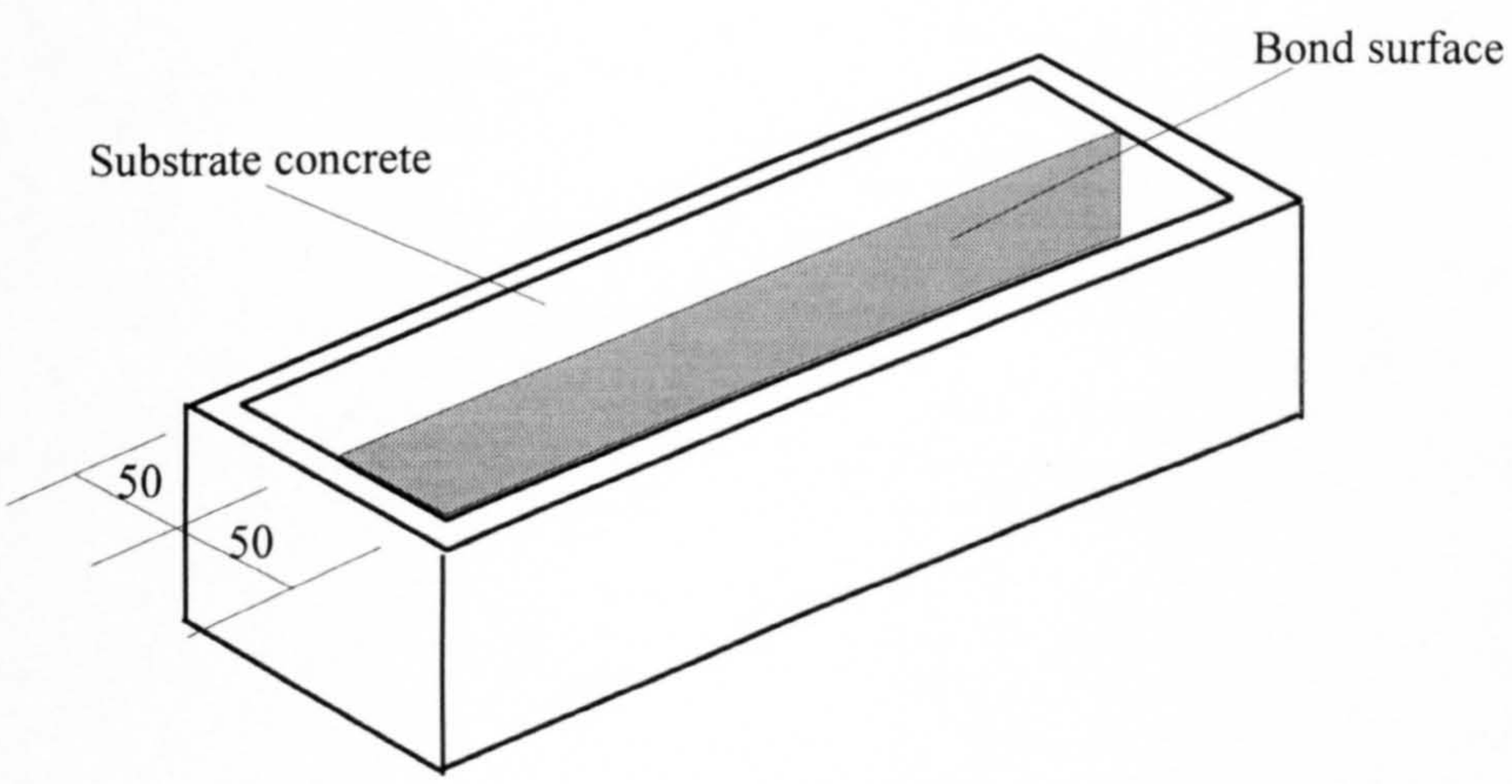

Figure 4.7 Preparing a repair for the core pull-off test

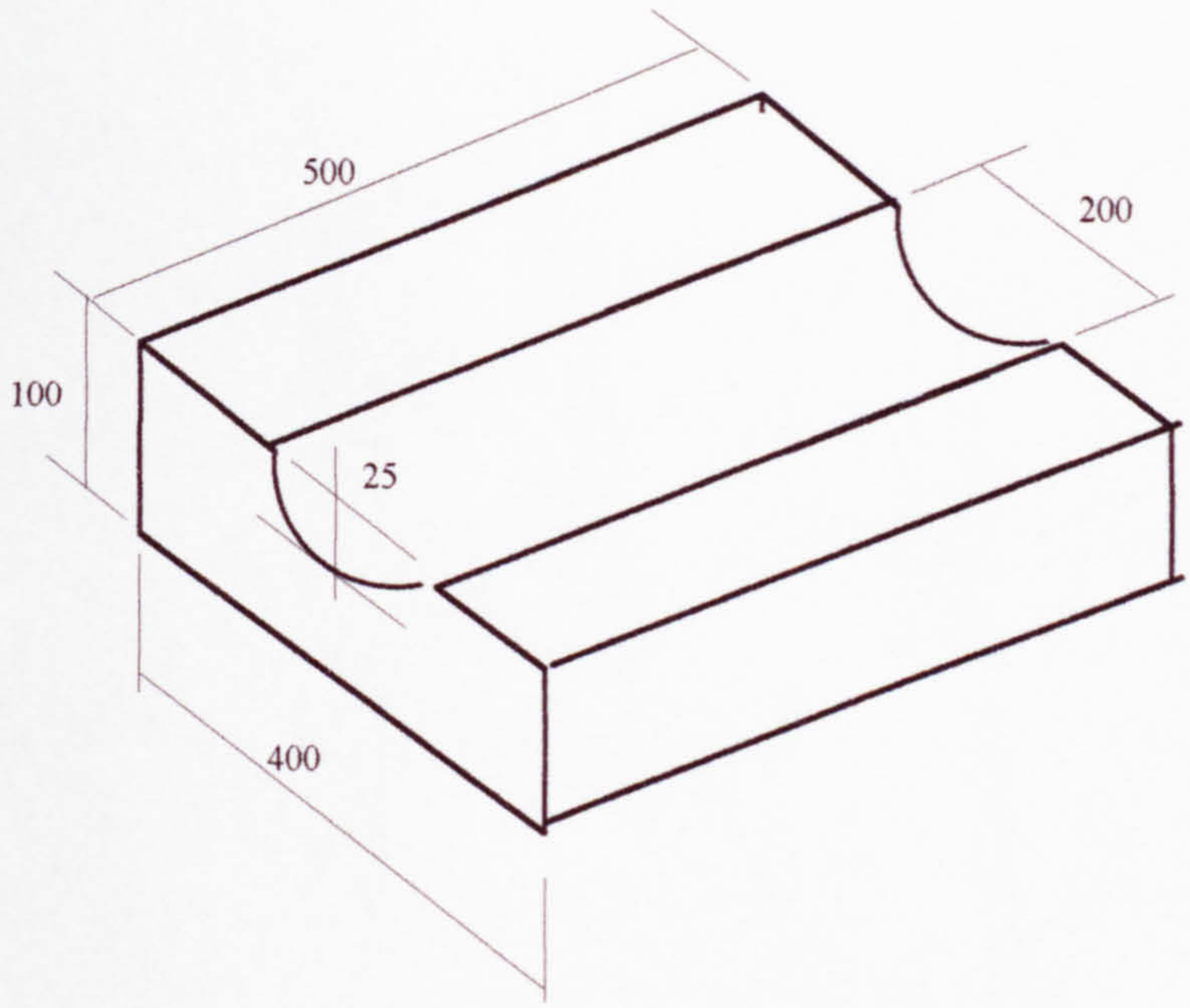

a) Specimen size

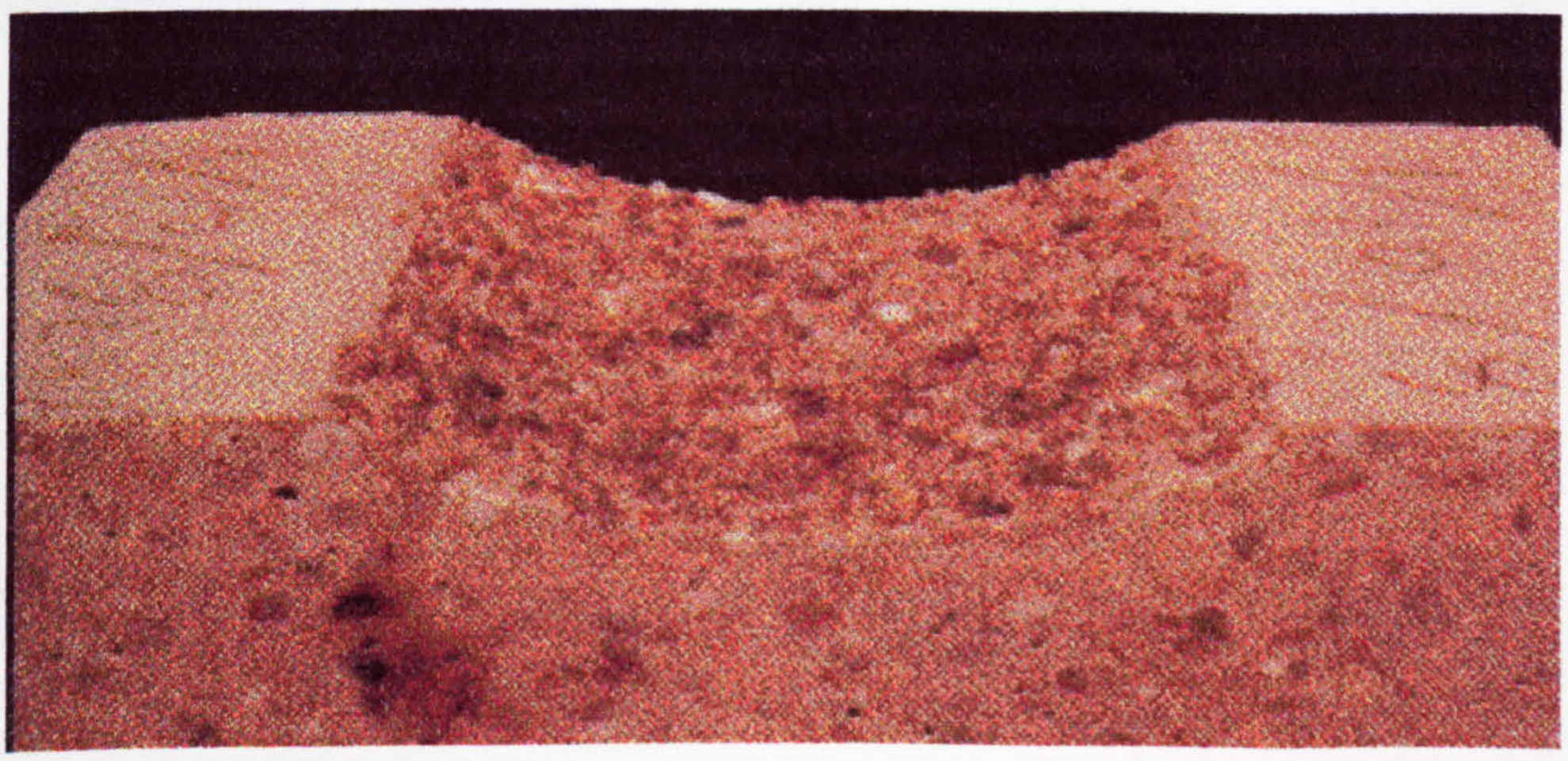

b) A roughened substrate by sand blasting for the patch compressive test

Figure 4.8 Details of a patch compressive specimen

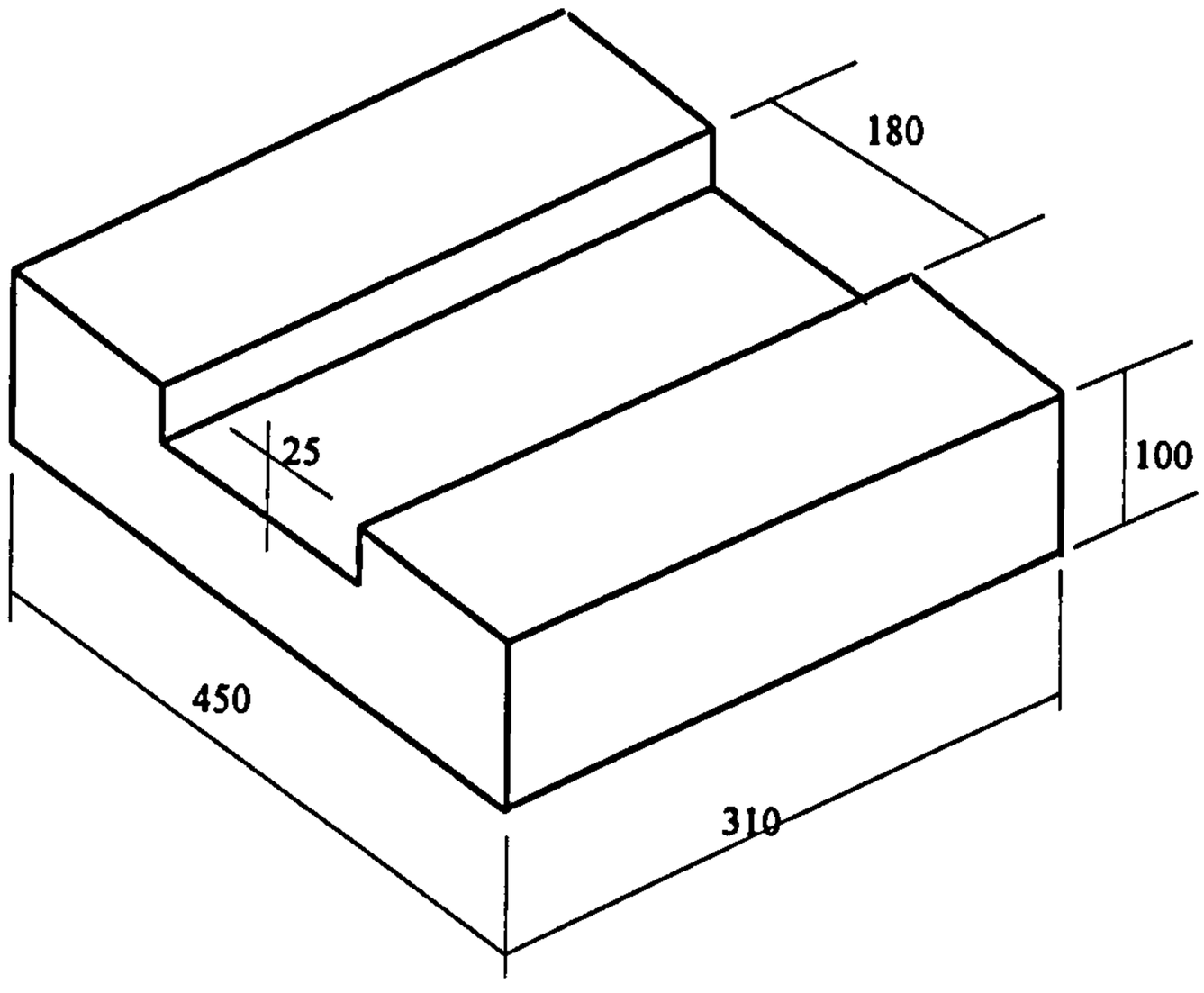

Figure 4.9 Slabs used for making patch flexural specimens

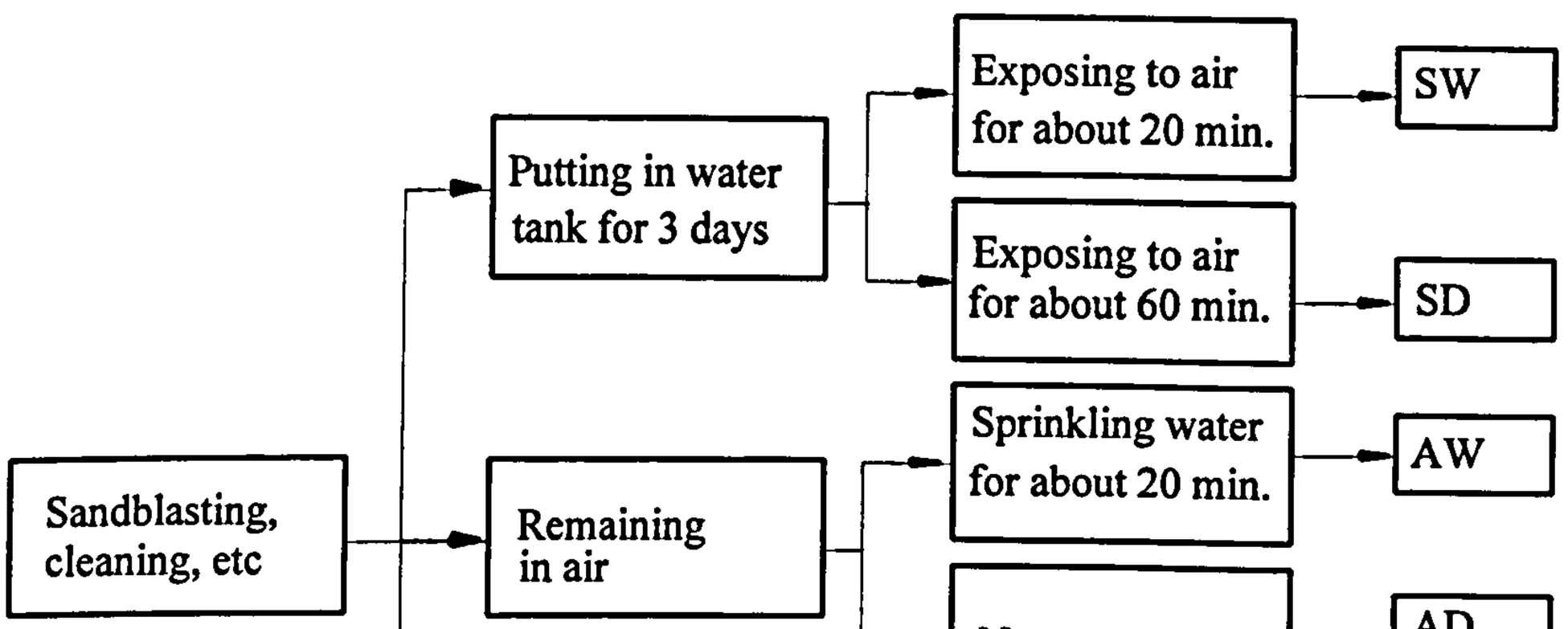

Figure 4.10 Simulation of the moisture condition of the substrate

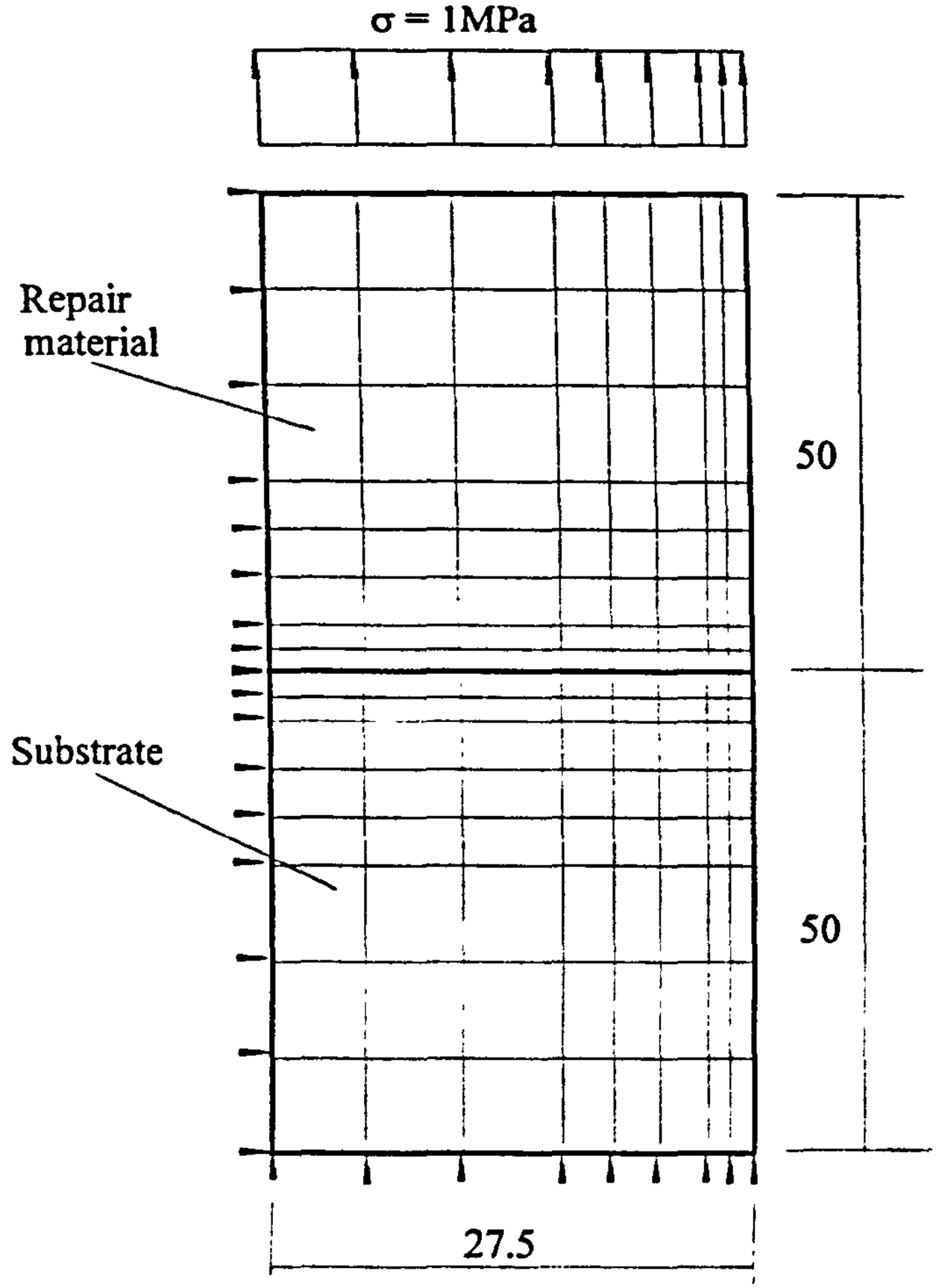

Figure 4.11 Finite element modelling of a bond interface under direct tensile stress

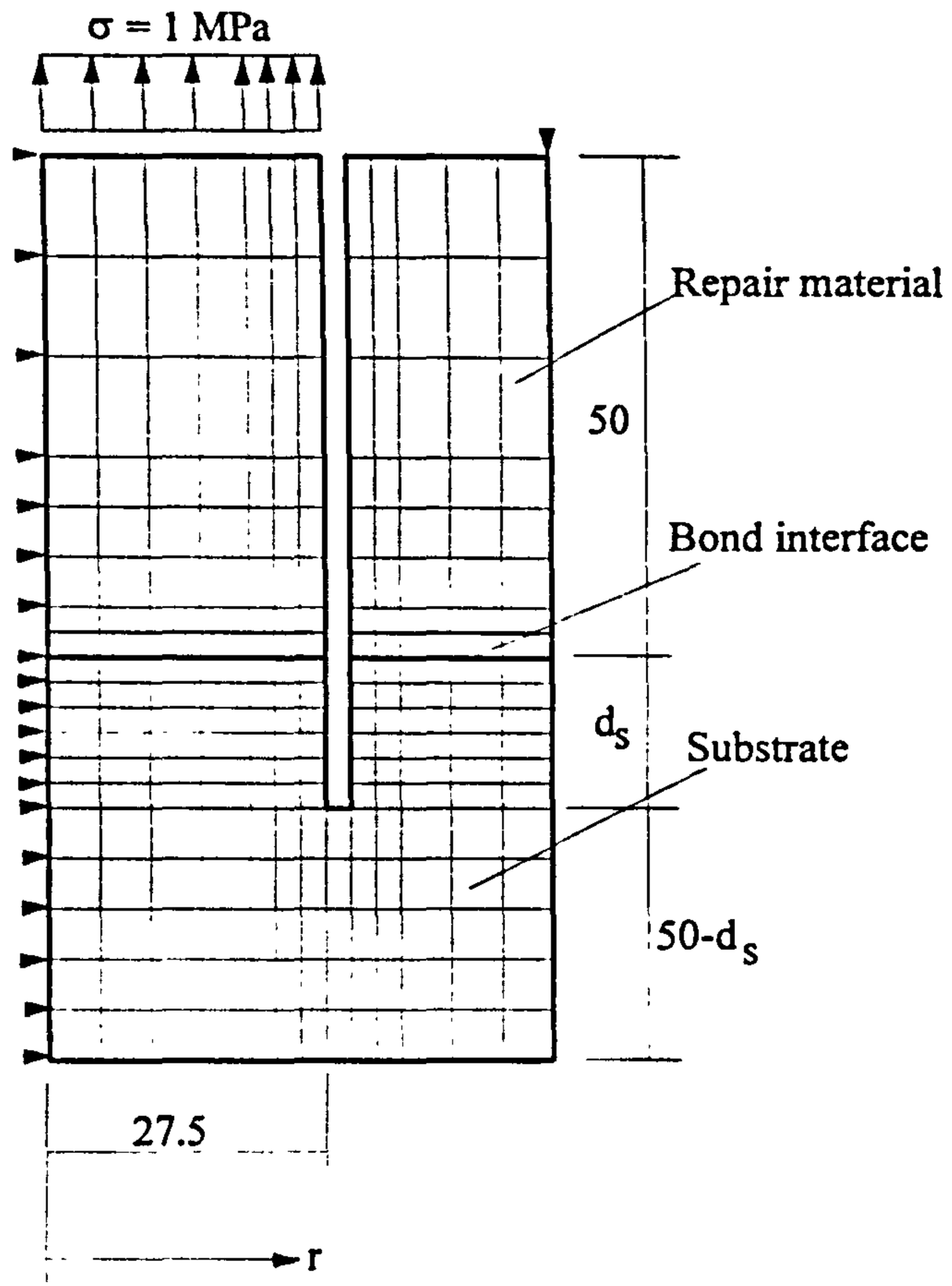

Figure 4.12 Finite element modelling of the coring depth effect in the core pull-off test

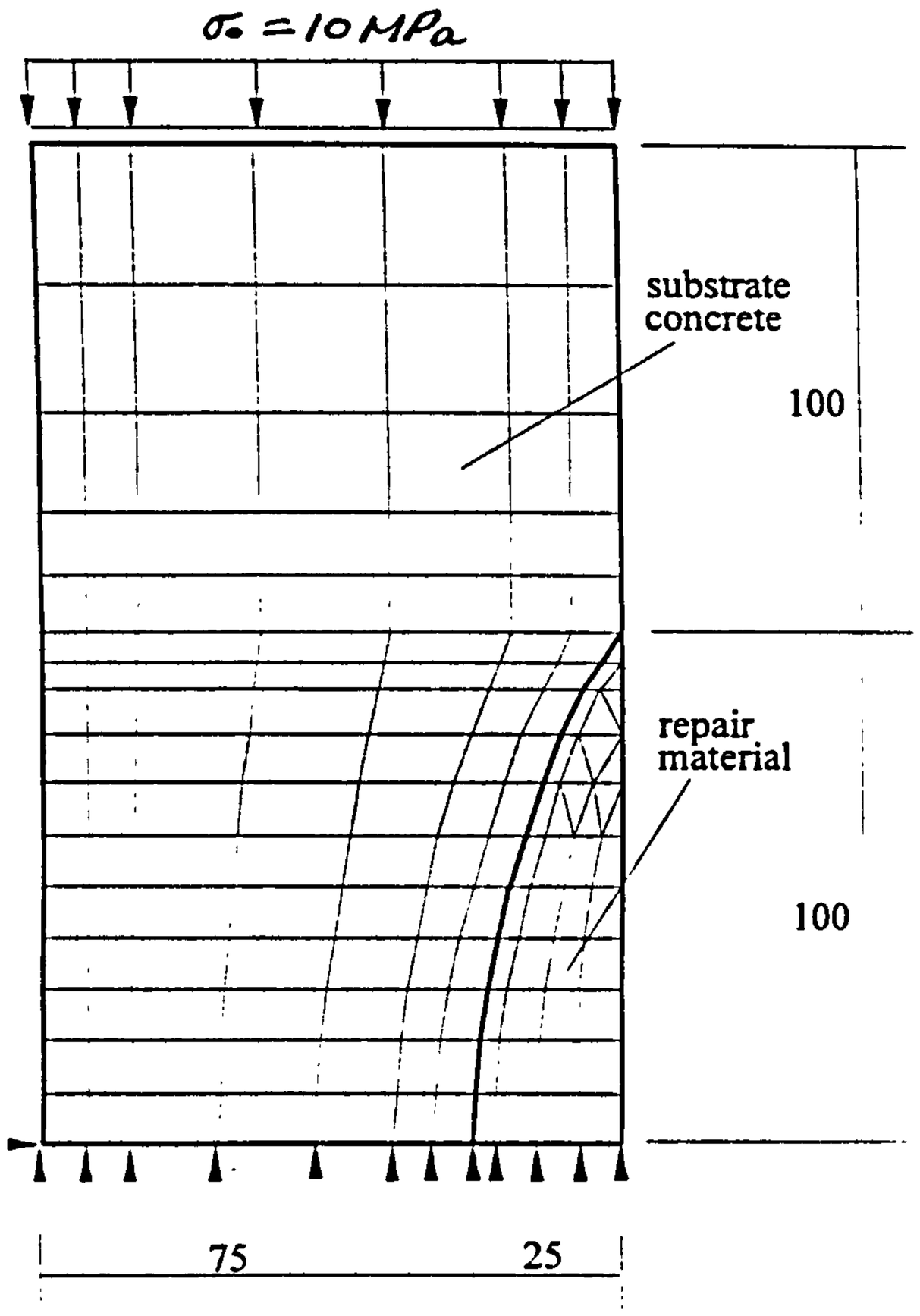

Figure 4.13 Finite element modelling of the effect of modulus mismatch in the patch compressive test

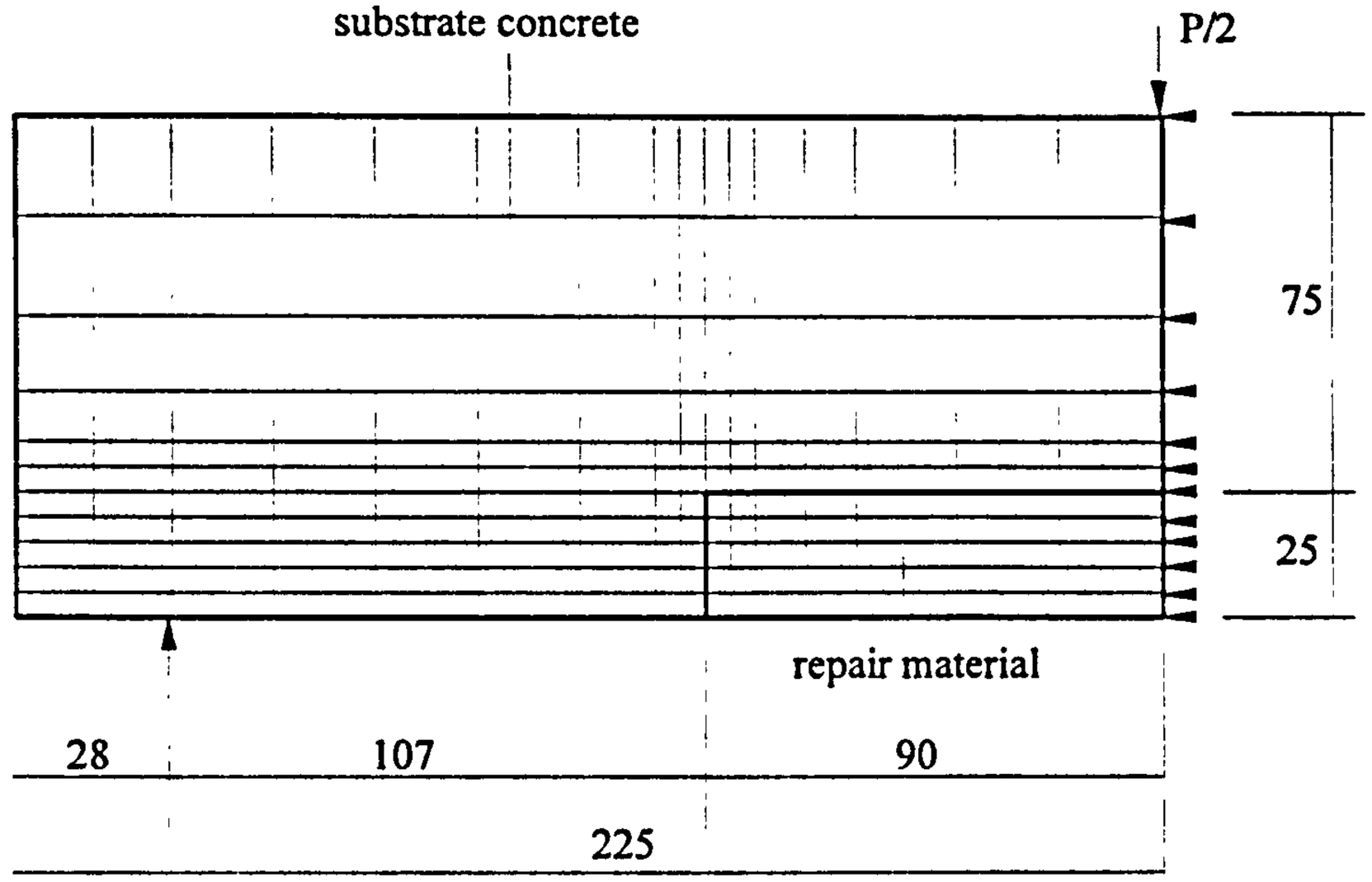

Figure 4.14 Finite element modelling of the effect of modulus mismatch in the patch flexural test

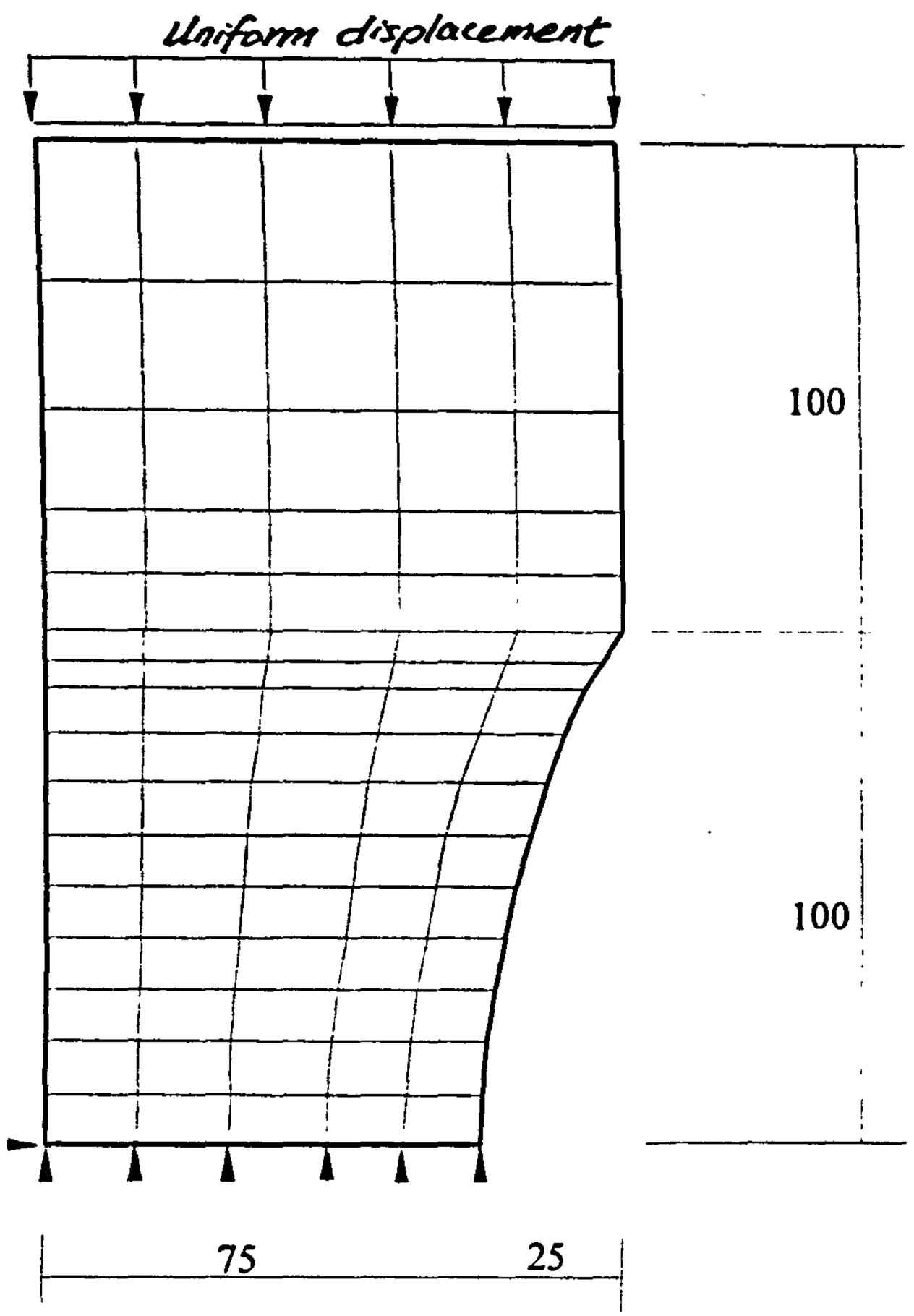

Figure 4.15 Modelling of the effect of uniform displacement simulated loading on eccentricity induced over middle cross section

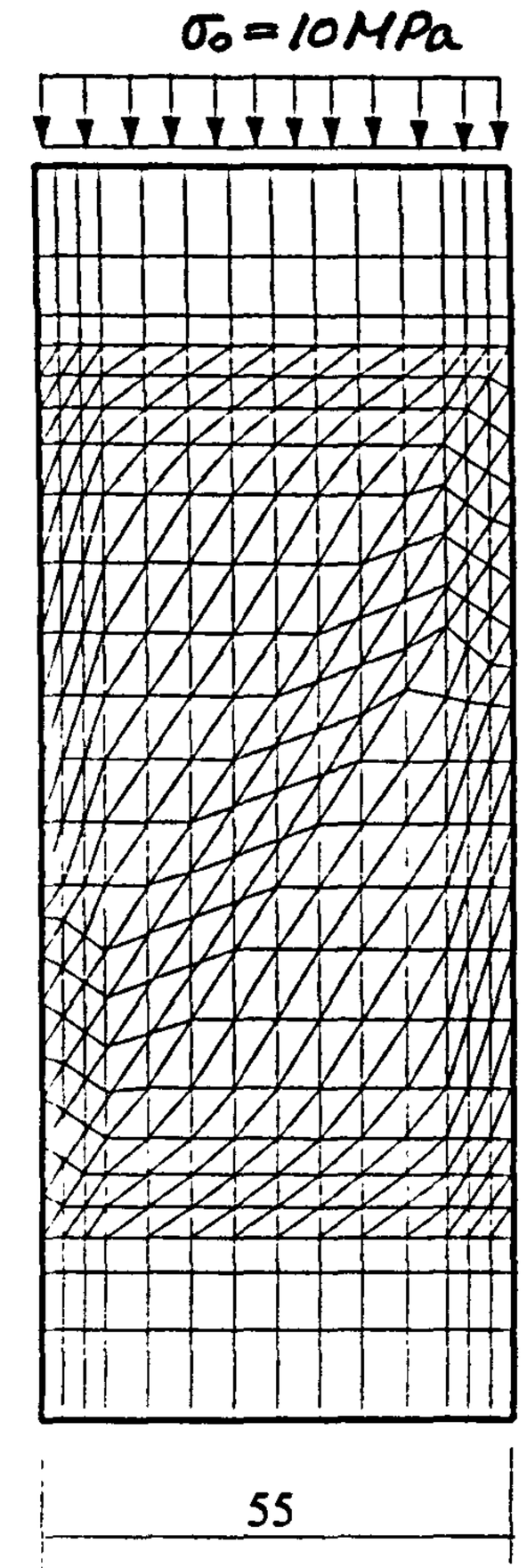

Figure 4.16 Modelling of the effect of modulus mismatch in a slant shear test

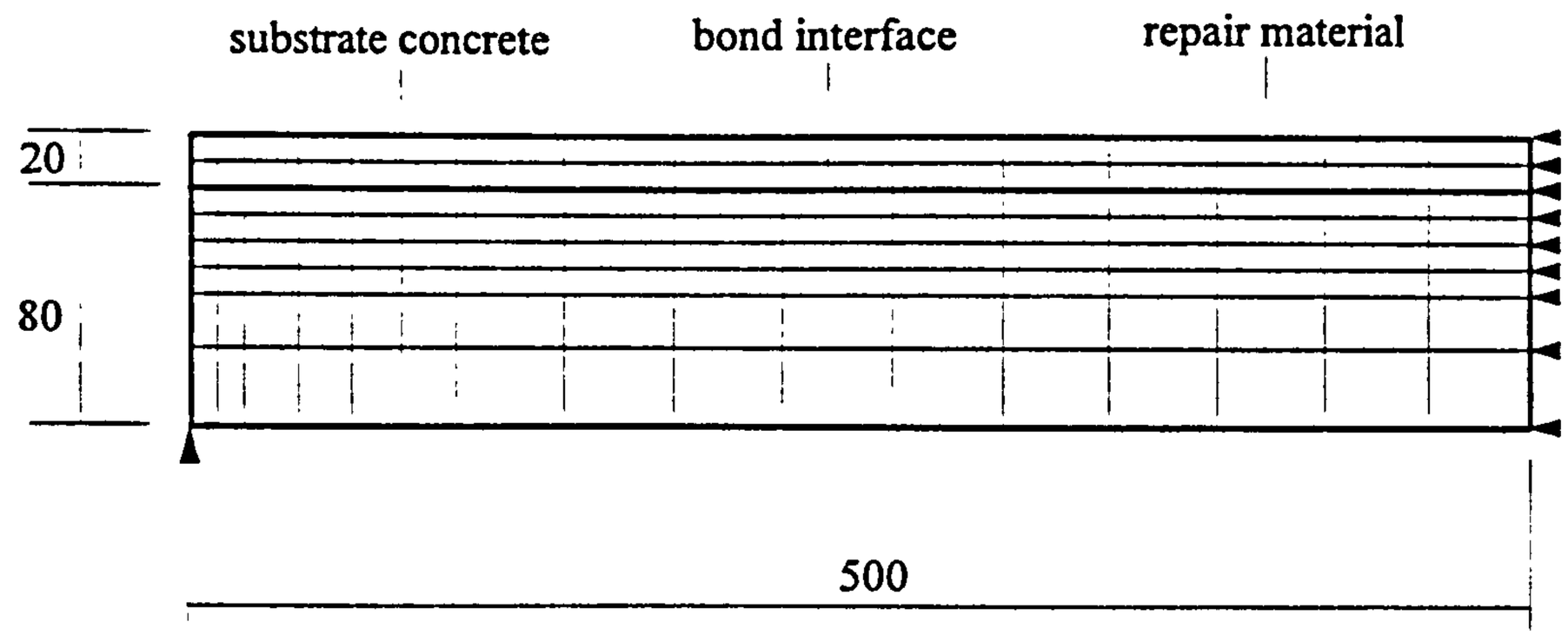

Figure 4.17 Modelling of differential thermal deformation on stresses induced over the bond interface

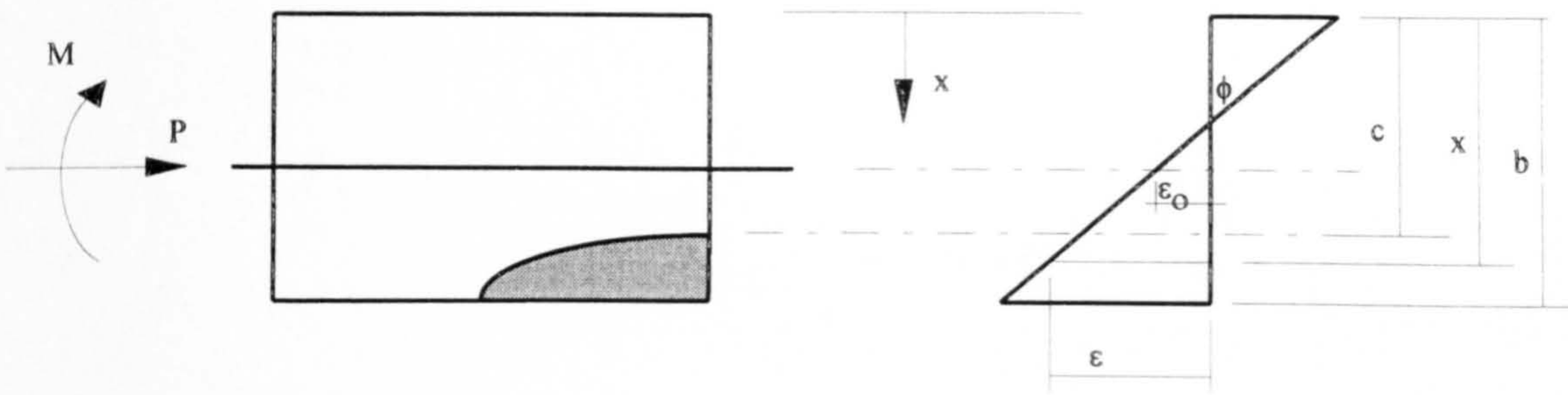

Figure 4.18 Simplified analysis of a patch repaired specimen

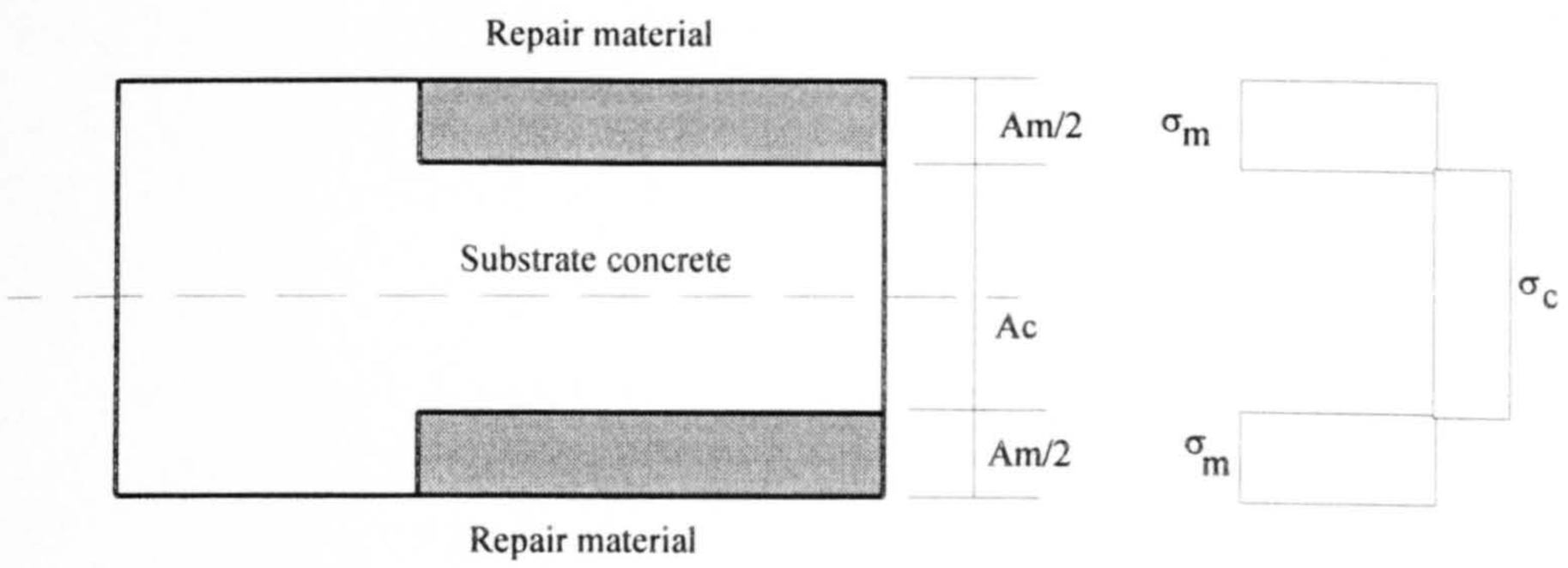

Figure 4.19 Repair material applied symmetrically to the substrate

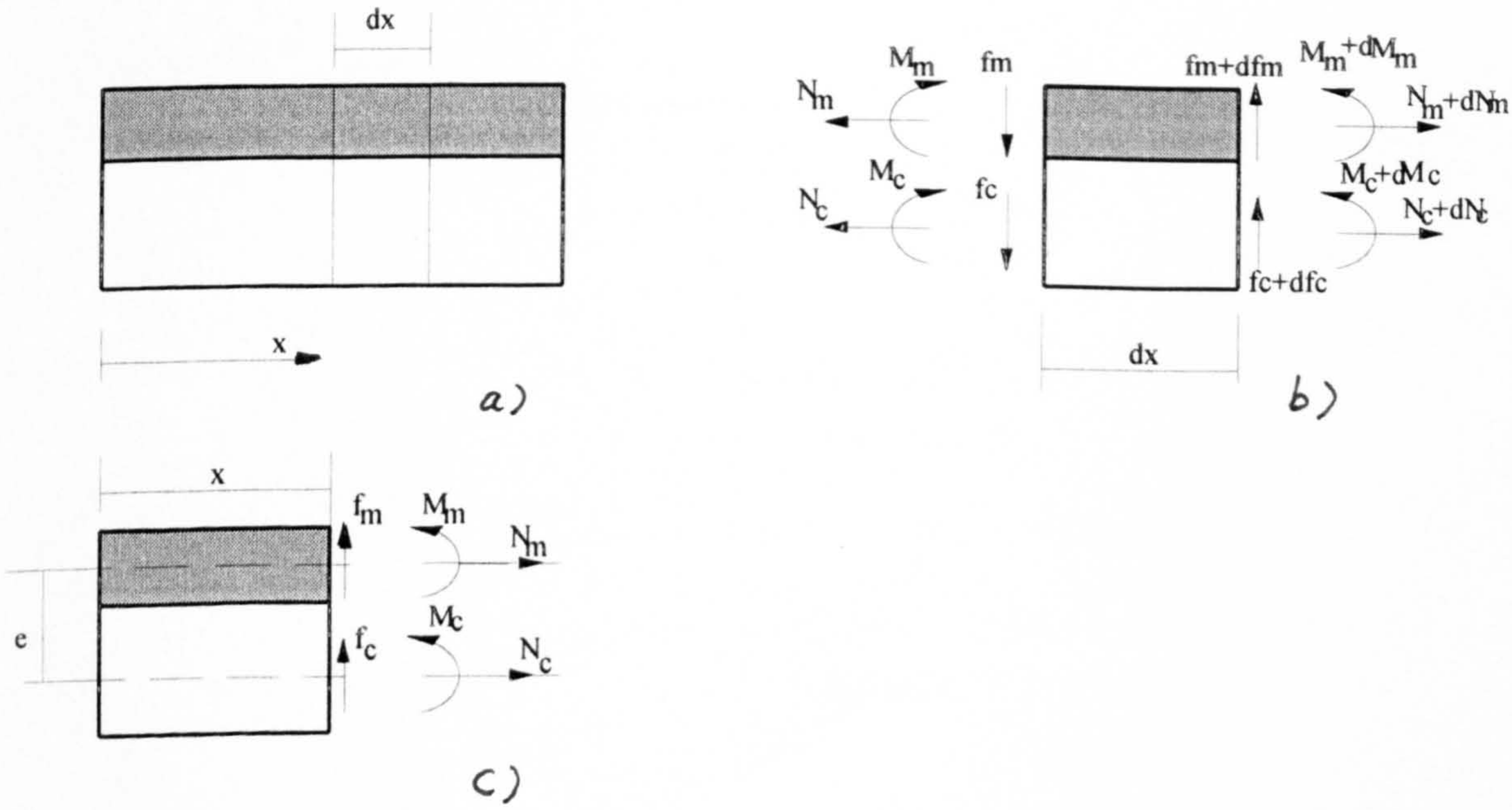

Figure 4.20 Internal stresses generated due to differential shrinkage in a repair overlay situation

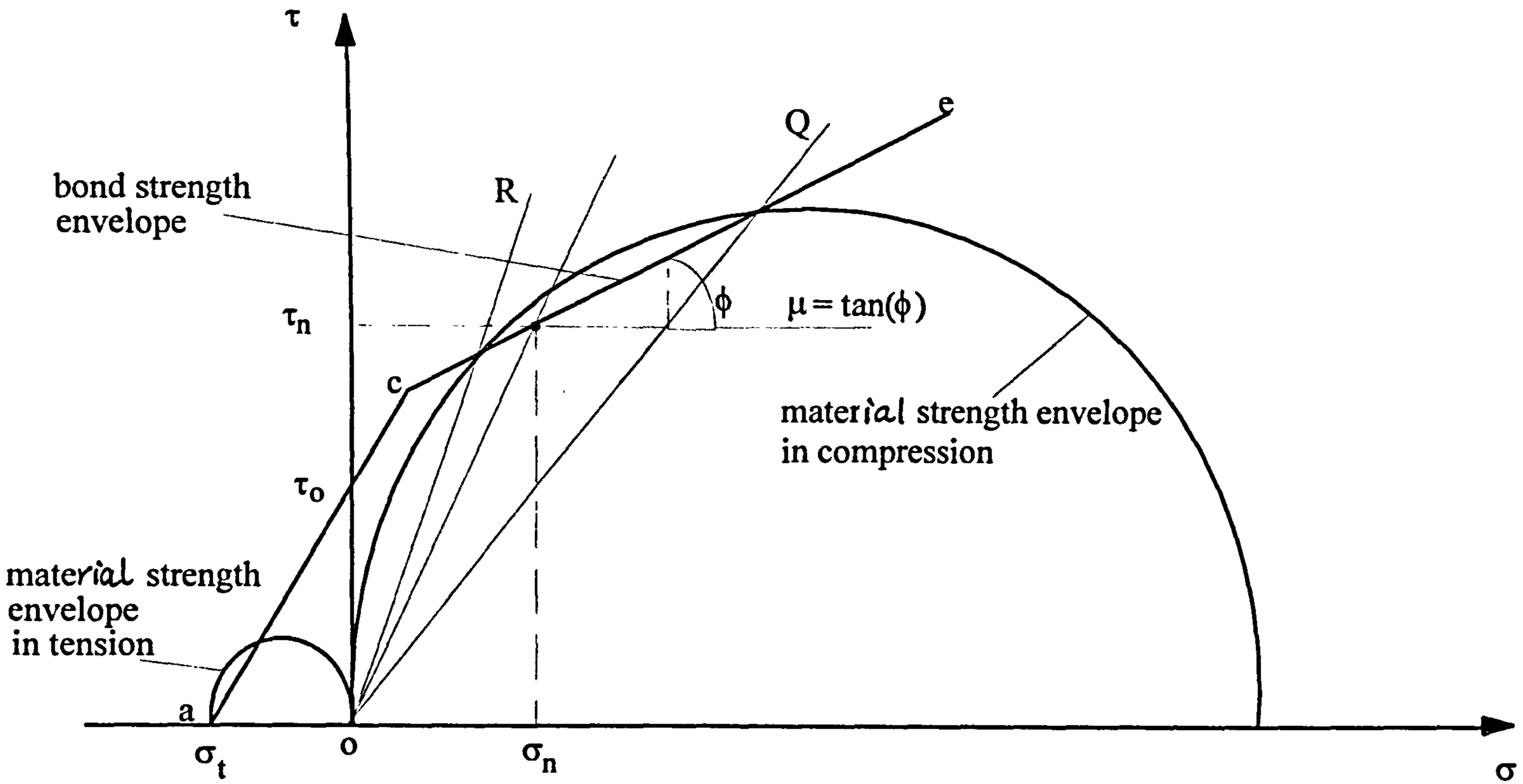

Figure 4.21 Establishment of a bond strength envelope

Chapter 5

EVALUATION OF BOND TEST METHODS FOR CONCRETE REPAIRS

Chapter 5 Evaluation of Bond Test Methods of Concrete Repairs

5.1 Introduction

Good adhesion of repair materials on concrete is of vital importance in the application of concrete patch repairs, and the bond strength developed depends on many factors. These factors include the chemical and physical properties of substrate concrete and repair material, and the care taken in the preparation and execution of the repair. The bond interface can be put into compression, tension, or multi-stress states. Thus the bond strength measured also depends on the stress state imposed on the bond interface. The effect of one factor under one stress state could well be different under another stress state.

The study of this intangible, adhesive property requires a physical test or tests that can both quantify the bond strength parameter and identify the failure mode. There have been numerous investigations of the bond of cementitious systems, and many of these have been concerned with the development of a suitable test. Little standardisation has yet occurred, although tensile pull-off tests are becoming increasingly favoured in site quality control testing.

One of the major problems associated with conducting any type of test is deciding what to measure, how to measure it, and how to interpret the test results. Some requirements have been put forward by different researchers for a bond test, as stated in section 2.1, but it was felt that a more appropriate approach would be to tackle the following questions to address the requirements for a bond test, and to evaluate bond test methods. These questions include:

(1) What kind of factors will influence conducting a bond test ?

(2) What are the responses of each test to the variation in test parameter involved to a specific test method ?

(3) Which factor /factors is crucial in ensuring the full development of the bond strength ?

(4) Which factors are important to achieve a durable repair ?, and

(5) What kind of a test can be used to monitor the quality of these crucial factors ?

Based on the answer to these questions, a better solution can be applied in real repairs so that a disadvantageous effect can be either mitigated, minimised, or even avoided by selecting a more appropriate repair material or by emphasising the vital importance of one or more procedures encountered during the preparation and execution of the repair. Emphasising the vital importance of the most important factors involved is a different approach to unnecessarily strict specifications and over-inspection based on a lack of understanding or even misconceptions. The latter will cause extra work and extra costs.

The factors that need investigating include: the effect of workmanship (such as the surface roughness, and surface soundness, etc.); the effect of material property mismatch (such as the modulus mismatch, and the differential deformation which may be caused by differential shrinkage or the differential thermal deformation, etc.); specimen geometry related effects (such as the variation of specimen size due to specimen preparation, and the secondary stress induced into the bond interface due to specimen geometry, etc.); and the stress state related factors (such as tensile stresses, shear stresses, etc. imposed on the bond interface). When a bond interface is put into a specific stress state, the discussion will be mainly concerned with the first three factors. The following sections discuss tensile, shear, slant shear, and patch bond tests

5.2 Tensile bond tests

5.2.1 Surface roughness and soundness

These two parameters depend directly on the method of producing the bond surface to be repaired. If the bond surface is produced by casting or saw-cutting, possibly followed by sand-blasting or needle-gunning, the surface is likely to be sound. But the roughness will vary depending on the size of grit or sand used, the amount of abrasive, and the delivery pressure [1, 9]. If the bond surface is produced by a vigorous mechanical method, such as hammering or splitting, the surface will be very rough, but microcracks will be induced just beneath the prepared surface [17, 18, 20, 40, 43, 63, 73]. Test results have showed that the tensile bond strength is very sensitive to the existence of microcracks at the bond surface. This is due to a reduction in the effective bond area and the stress concentration at the tips of microcracks, which will accelerate their development.

It can therefore be argued, that if failure occurs in a tensile bond test within the substrate but very near the bond interface, it is possibly caused by poor surface preparation (due to excessive mechanical action, for example) rather than the substrate reaching its tensile strength capacity. Also, the poor surface preparation prevents the development of the maximum bond strength that a repair material can achieve.

The author carried out some tests using a sand/cement mortar on surfaces with different roughness. There was a sharp increase from a smooth(saw-cut surface) to a slightly rough surface (slightly sand blasted), but the increase in bond strength from the slightly rough to the rough surfaces was not significant (Table 5.1). Cleland, et al's [19] recent test results on surface preparation techniques also revealed the importance of a sound substrate for strength development. Nine methods were used to prepare the split concrete surfaces. Among them, six methods were considered being able to

produce a sound substrate with varying degrees of roughness. However, the differences between the tensile bond strengths were very small, even though a rougher surface produced slightly higher bond strength. This indicates that a rougher surface produces a higher bond strength, but the increase may vary depending on the repair materials used.

Apart from microcracks, there also exist other kind of surface defects, which can be caused by chemical residue, contamination, dust, or even air voids entrapped at the bond interface (due to improper compaction). In a tensile test, these surface defects will reduce the measured bond strength.

However, the way these defects affect the test results can vary. For a vigorously and mechanically roughened surface, microcracks will be induced, but scattered randomly over the bond interface. For a randomly distributed surface defect, the ability of a test method to detect its existence depends on whether the surface is under a tensile stress state, and the level and uniformity of the tensile stresses imposed. In a direct tensile test, a nearly uniform tensile stress state is applied to the bond interface. Hence, so long as there are some surface defects, it is likely they will be detected, i.e., a reduction in the bond strength will be observed. In an indirect tensile test, such as the tensile splitting test, the stresses imposed over the bond interface are not evenly distributed, and also, compressive stresses near the edge of the bond interface will be expected. So if the surface defects happen to be in the compressive stress area, they will not be detected.

If surface defects are caused due to chemical residue, contamination, etc., they tend to be in a large area. When acid etching is used, the whole bond area could be affected. The large surface area defects should be easily detected by a tensile test, no matter whether a direct, or an indirect one. Knowing some surfaces had been contaminated by oil, the author used water-jetting and wire brushing to clean the surfaces before repair,

but the results still showed sharp reductions in bond strength (Table 5.2). This suggests that no matter how good the repair material, oil contamination has a very significant detrimental effect even though the surfaces were cleaned using normal methods.

5.2.2 Modulus mismatch

In a direct tensile test, stress variations, (especially stress concentrations at the edge of a bond interface) will be induced due to the modulus mismatch. Fig. 5.1 shows the results from an linear elastic finite element analysis with the mesh generation being shown in Fig. 4.11. Material properties used were: elastic modulus of 30GPa and 20GPa, and the Poisson's ratio of 0.2 and 0.13, respectively for the substrate concrete and the repair material. It needs to be pointed out that it is very difficult to see the direct relationship between the degree of stress concentration and the measured macro-level failure stress (or the bond strength). A bond strength only exists between two materials. Unless the intrinsic bond strength is known, the bond strength measured using the macro-level physical test will always include the effect of modulus mismatch. If the modulus varies, the intrinsic bond strength may also vary. A repair material with low modulus may suffer high stress concentration, but failure may still occur in the substrate if it has a high bond strength. An example of this situation is the case of epoxy bonded plates, where despite a very large modulus mismatch between the steel and epoxy resin/concrete (and hence very high stress concentration), the system can still generate a high bond strength. In contrast to this, the bond strength between a substrate concrete and a sand/cement mortar can only generate a modest bond strength even though the modulus mismatch is very small.

5.2.3 Differential deformation

The effect of the differential deformation, caused by either differential shrinkage or differential temperature deformation, should be considered. In a bond test, the

temperature effect is usually not included (unless in the consideration of the effect of environmental conditions). The shrinkage effect depends on the specimen size, shape, and the restraint provided by the substrate. In the dog-bone test, and the steel pipe grip tensile test, the effect of the shrinkage can be ignored because the specimens used are very small, and the ratios of the free surface areas to the bond area are very large. In other tests which involve large-size specimens, such as a slab or a beam used for the core pull-off test, shear and normal stresses will be generated along the bond interface. This could affect the measured failure load and the translation of test results.

Fig. 5.2 shows the shear and normal stresses generated along the bond interface due to the differential shrinkage using a linear elastic finite element analysis with the mesh generation being shown in Fig. 4.17. Material properties assumed were: $E_c=E_m=20GPa$, $\varepsilon_{shm}=300\mu\varepsilon$, $\varepsilon_{shc}=0$, and $\alpha_a = A_m/A_c = 0.1$. The results show that the stresses vary along the bond interface, with the maximum principal stress occurring near the periphery of the repair. At the edge of the bond interface, the principal stresses divert from the horizontal direction, and tensile stress components normal to the bond interface are generated. This tensile stress tends to lift the overlay or screed - a problem experienced with many repairs. Because old concrete also shrinks, the effect of shrinkage depends very much on the differential shrinkage between a repair mortar and the substrate concrete. The younger the substrate, the smaller the differential shrinkage will be. This must be taken into consideration when using laboratory results to predict the effect of shrinkage on buildings and other structures, because substrates used in the laboratory are generally much younger than the concrete used on actual sites.

5.2.4 Variation of specimen size and shape due to specimen preparation

How to put a bond interface into a uniform tensile stress state has been the subject of many studies, where the principal concern has been to minimise load eccentricity.

Even with care, the actual geometry achieved may differ from that which was intended, such as the core diameter and the coring depth. This kind of difference can cause some variation in the ultimate failure loads. Large variations in the failure loads have occasionally been recorded.

In the core pull-off test, this could be caused by the following three factors:

(1) unevenness of the loading surface;

(2) eccentricity induced due to dollies not being positioned axially; and

(3) eccentricity induced due to core drilling.

Unless the surface is very carefully levelled, a steel trowel finished surface (as in a repair overlay situation) will cause random eccentricities during coring, adhering of dollies, and mounting a test set-up. Little information has been found on this issue. In this study, in order to reduce the influence of these factors on variation of failure load, this problem was avoided by casting the repair material in such a way as to ensure that the loading surface was absolutely even and smooth (the casting procedure is referred to section 4.2.2.1 and Fig. 4.3).

When dollies were adhered on top of the cores, they tended to slip slightly before the epoxy was set (if the surface was sloping a little). Care was taken to make sure that the dollies were positioned properly until the epoxy set, thus minimising any eccentricities induced by this factor.

Eccentricities induced due to core drilling depend very much on the core drill. In the first part of this study, a fairly old core drill was used. After the pull-off tests, forty cores were cut in half and the eccentricities measured. The average eccentricity induced due to non-verticality was about 1.5mm in a depth of 50mm (corresponding to an angle of 1.7^{o}), with a coefficient of variation as high as 45%. The eccentricity was caused mainly during the core tip touching and leaving the specimen. This leads to a

theoretical increase in the maximum stress at the periphery of 20%. However, the variation in the measured bond strengths was much smaller. The difference between the theoretical and the observed behaviour may be due to at least two effects: stress relief caused by strain relief; and the probability that the weakest zone will not correspond with the area of highest stress. Nevertheless, care should always be taken to minimise load eccentricity, particularly in site applications. The measured high eccentricities (due to core drilling), led to the purchase of a new core drill that was used throughout the remainder of this project. Eccentricities measured from 15 cores using the new core drill were much smaller compared with the old one, around 0.28mm in a 50mm depth, corresponding to an angle of 0.32°.

For the two methods of the pipe-nipple grip and the friction-grip tests carried out by Knab and Spring[13], the same steel pipes and surface preparations were adopted. One would assume that these two methods would produce similar results, but bond strengths obtained from the friction-grip method were about 35% lower than those from the pipe-nipple grip method. Knab and Spring attributed this difference to possible eccentricities induced in the friction-grip method.

5.2.5 Secondary stress induced over the bond interface

A variety of specimen configurations have been proposed to measure the bond strength. It was found that secondary non-uniform stresses over the bond interface can be induced due to the methods of gripping/reacting with the specimen. Here, the term, 'secondary non-uniform stresses' is used to differentiate from that caused by the modulus mismatch.

In Ohama's work [14], specimens with sudden change in cross section joined at the bond interface, produced lower bond strengths than the specimens for the dog-bone test. This can be attributed to the additional stress concentration at the bond interface

caused by the sudden change of the cross section (Fig. 2.5). The other stress concentration occurring simultaneously at the bond interface is that caused by the modulus mismatch.

In the research carried out by Knab and Spring[13], and Kuhlmann[37], the applied load was transferred through the internal circumference of the steel pipes to the substrate and the repair material. Because of the sudden change in the cross section, the stress distribution over the bond interface could be greatly influenced.

In the core pull-off test, the influence of the steel dolly and the reaction frame depends on the drilling depth d_s of the core into the substrate concrete (Fig. 2.1), and the thickness of the repair mortar. Fig. 5.3 shows the drilling depth effect based on a finite element analysis; the mesh generation was shown in Fig. 4.12. The material properties assigned for the repair material and the substrate respectively were elastic moduli of 20 and 30 GPa and Poisson's ratios of 0.13 and 0.2. These gave a uniform stress distribution over the bond interface when the drilling depth is large (>50mm). From Fig. 5.3 it can be seen that the shallow cuts give rise to significant stress non-uniformity. For the 5mm drilling depth adopted in other research [18, 42, 54], the results show that the ratio of the tensile stress at the bond periphery to the assumed uniform stress can be as high as 1.5. This non-uniformity of stress distribution is caused solely by the shallow drilling depth. Other reports on core pull-off tests [5, 20] made no mention of the drilling depth. Clearly if they were of the order of 5 mm, which could possibly be due to either poor workmanship on site or even not knowing the effect of the drilling depth in the laboratory, high stress concentrations could have resulted. The FE analysis suggests that shallow drilling depth will underestimate the real bond strength, and ignorance of the drilling depth effect may be one of the main causes of difficulties in reproducing and comparing test results. Increasing the drilling depth reduces the stress variation which is within 4% of the uniform (>50mm) value when the depth exceeds 15mm. Tests carried out by the author demonstrated this effect

(Table 5.3). From the Table, it can be seen that the failure stresses with 1-2mm drilling depth were about 18% lower than those with 15mm drilling depth. It is also relevant that when failure occurs consistently in the substrate concrete (due to the bond strength exceeding the tensile strength of the substrate), the failure plane is usually located at the end of the drilling core in the area of high stress concentration. It can be concluded that the proposed drilling depth of 15 ± 5mm in the draft European Standard [60] is a sensible value which should minimise this type of error.

If the thickness of a repair mortar is small, the influence of the relatively stiff metal dolly glued to the top of the core might become significant. Bungey, et al [80] have analysed the effects of dolly thickness and drilling depth when measuring the surface tensile strength of concrete using a pull-off arrangement. Their results show that the shallower the drilling depth, the higher the measured strength. This can be explained as follows. The load is applied through the centre of the dolly, causing stresses in the centre area to be higher than those at the periphery, despite the rigidity of the metal discs. On the other hand, the restraint provided by the rest of the concrete at the tip of the core tends to result in higher stress at the periphery rather than in the middle of the core. The actual stress distribution depends on the combination of these two actions; the first effect tends to compensate partially for the effect of the latter, reducing the stress non-uniformity. Thus the deeper the core, the higher the net stress concentration will be, which corresponds to lower failure loads. In contrast to this, in the core pull-off bond test, the deeper the drilling into the substrate, the smaller the effect of the restraint at the tip of the core on the stress distribution over the bond interface. Also, the thicker the repair material, the smaller the effect of the metal dollies on stress distribution over the bond interface. Tests on the effect of different dolly materials (both steel and aluminium) were carried out by the author. No effect on the bond strength was apparent with either the sand/cement mortar (50mm thick), or the acrylic modified cementitious mortar (A1, 40mm thick). Bungey, et al [80] have also shown

that the stiffness of the dolly does not affect the cohesive failure strength of concrete in the tensile pull-off test if the drilling depth is greater than 20mm.

5.3 Shear bond tests

5.3.1 Introduction

Shear bond tests are not common in evaluating bond strength. The limited studies include the twist-off shear tests by Long, et al[41, 87], and direct shear bond tests [14, 48, 85, 86].

Before discussions of the factors which might influence measured results, it is necessary to make clear whether it is possible to measure the shear bond strength, or under what conditions. From Mohr's circle of stress, the pure shear stress state can be viewed as a combination of equal tension and compression in directions at 45° to the shear direction (Fig. 5.4). Assuming the material considered has different strengths in tension, compression, and shear, symbolically, potential failure will occur in the direction determined by the following equation:-

$$\text{Potential failure} = \max \{\sigma_c/f_c, \sigma_t/f_t, \tau/\tau_o\} \rightarrow 1.0$$

In the pure shear stress state, $\sigma_c = \sigma_t = \tau$, this means the failure will occur depending on the relative value of f_c, f_t, and τ_o. The following discussion includes comments on the roles of f_c, f_t, and τ_o in measuring and interpreting shear bond test results.

5.3.2 Surface roughness and soundness

These two factors affect the test results in two different ways. But first a brief discussion is required about materials behaviour prior to a discussion of the shear bond strength.

For a tension-weak brittle material such as concrete, sand/cement mortar, and other cementitious based materials, the compressive strength is far greater than the corresponding tensile strength. Under a shear stress state, failure is usually dominated by tensile cracking rather than shear slipping. This can be demonstrated by the failure mode of a concrete cylinder under a torque. This means that even if a shear stress is imposed, failure load is an indication of the tensile strength, rather than the expected shear strength of the material. To explain this, a material is defined in three levels: micro-level, meso-level, and macro-level, an approach adopted in fracture analysis of concrete [135]. At the micro-level, concrete consists of crystals of calcium silicate hydrate with primary and secondary bonds. The layered absorbed water around the crystals also plays an important role. The meso-level considers the composite nature of concrete and distinguishes between hardened cement paste, aggregate, and a bond layer between these two constituents. At the macro-level, concrete is modelled as a homogeneous isotropic material. Based on this definition, the macro-level failure mode of concrete under a torque can be explained more clearly at the meso-level. Usually, the bond between cement paste and aggregates is the weakest part of the concrete composite and the work needed to overcome the resistance in Fig. 5.5b will be higher than that in Fig. 5.5a, which means that failure will initiate in the form of tensile cracking at the principal tensile stress direction rather than shear slipping along the shear direction. At the macro-level, coarse aggregates are viewed as evenly distributed within the concrete and concrete can be modelled as a homogeneous material. If a shear line is there, it is bound to pass through several aggregates and failure will be initiated in tensile cracking at other direction. This supports the explanation given in Fig. 5.5 no matter what kind of surface textures the coarse aggregates have because the surface texture of the aggregate mainly affects the meso-level bond strength. The measured macro-level strength will not be affected by how the element is loaded relative to its element axis, so long as the ratios between the principal stresses remain constant. The surface texture of the coarse aggregate will

affect the tensile bond strength between the cement paste and the aggregate at the meso-level. As a consequence, the macro-level tensile and compressive strengths of concrete will be affected [48], but the nature of the failure, tensile cracking rather than shear slipping, will not be changed.

In concrete repairs, the nature of the repair puts the bond between the substrate and the repair material into the macro-level rather than the meso-level, and the surface roughness will affect both the results and their interpretation. If the bond interface is completely straight and smooth, such as a saw-cut surface, a shear line can pass through the bond interface completely, with no need to overcome any extra resistance caused by mechanical interlock. In such cases, the difference between the tensile bond strength and the shear bond strength may become very small and the possibility of measuring the shear bond strength is increased. In reality, no bond surface is completely straight and smooth, and a contribution by mechanical interlock, due to the rough and uneven surface texture, exists. Shear bond strength will be much higher than the corresponding tensile bond strength (Fig. 5.6). So, when a shear stress is imposed on the bond interface, the failure will also be initiated by tensile cracking, rather than shear slipping.

This means that a shear bond test will generally reflect the tensile bond property of a repair material, and should correlate well with results from tensile bond tests.

Using the twist-off shear test, a torque is applied to the composite system. Based on the discussion presented above, it can be expected that a tensile crack will initiate at the periphery of the bond interface because of the lower tensile bond strength. But, due to the higher tensile strengths of both the substrate concrete and the repair material, cracks initiated in the bond interface cannot propagate into the repair material or the substrate. More work is needed to overcome the resistance, and new microcracks will occur somewhere along other parts of the periphery of the bond interface and develop

gradually into the internal bond area until failure occurs. This means that even though the failure will occur in the form of tensile cracking, the failure stress will be higher than that that would be expected from a direct tensile bond test. If the tensile bond strength is higher than the tensile strength of the repair material or the substrate, tensile cracking will initiate somewhere else in the repair material or the substrate, depending on the relative tensile strengths of these two materials. In this case, the roughness effect is not important. The twist-off shear and the core pull-off tests carried out by Yeoh, et al [87] showed that the shear bond strength is much higher than the tensile strength, and at the same time, the two methods showed similar trends concerning the influence of environmental conditions.

A sound substrate concrete is of great importance in ensuring bond performance in a tensile test. But in a shear test, such as the twist-off test, surface defects such as microcracks may not be easily detected. This is possibly due to the fact that in the twist-off test, stresses are unevenly distributed, and the possibility that microcracks, if there are any, are randomly scattered. If the surface defects are located in a less stressed area, the effect cannot be easily detected. Tests were carried out on both chisel-hammer split surfaces, and saw-cut surfaces by Cleland, et al[18]. The twist-off test showed nearly no difference in failure loads between the two differently prepared surfaces, whilst the pull-off test detected reductions in bond strength due to microcracks caused by splitting (Fig. 5.7). The test results can be interpreted in two ways. Firstly, the results indicate that the load carrying capacity of a twist-off test is not sensitive to surface preparation. The strict requirement for a very sound surface preparation can be relaxed a little if the load carrying capacity is the main concern. Secondly, if the repair is to re-establish the protective layer of the reinforcement from further ingress of detrimental agents, such as moisture or chloride ions etc., ensuring a good bond and minimising sources for potential deterioration are the key issues to achieve the goal. From this point of view, it can be argued that failing to detect the

surface defects will increase the possibility of long term problems, and the twist-off test is not suitable for detecting the existence of the surface defects.

Direct shear bond tests were carried out by Ohama, et al [14] along with direct tensile bond tests. Generally, they showed similar effects of polymer modification on bond strengths, i.e., the bond strength was enhanced by increasing polymer/cement ratio, and the shear bond strengths were higher than the corresponding tensile bond strengths. This indicates that either of these methods can be used to select and compare between different repair materials so long as the substrates used are the same. But the quantitative correlation between the tensile and shear bond test results was not very good.

5.3.3 Modulus mismatch

In a shear bond test, modulus mismatch also affects stress distribution over the bond interface. But according to the discussion presented in the section of tensile bond test, this effect is usually linked with the unknown intrinsic bond strength which is determined by the chemical components of the materials considered. Changing the chemical component, both the modulus and the intrinsic bond strength will change. The measured shear bond strength includes both effects. The most important effect in real repair work is how load is shared between the repair and substrate which will be dealt with later in the section on patch test (section 5.5).

5.3.4 Differential deformation

This effect, as discussed in section 5.2.4, depends on the size and geometry of the specimens used for carrying out the shear bond tests. For the direct shear tests used by Ohama, et al [14], the effect can be ignored because the restraint provided by the substrate is very small. But for the direct shear tests carried out by Tayabji [85] and the

twist-off test by Yeoh, et al [87], the effect depends on the size of the slabs or beams where cores were drilled. The analysis is exactly the same as that shown in section 5.2.4.

5.3.5 Variation of specimen size and shape due to specimen preparation

In the shear bond test, the way the shear stress is applied and the selection of the bond cross section, may influence bond strength measurement.

In the twist-off shear bond test, the shear stress is not uniformly distributed. Depending on the shape of the cross section, the ratio of the failure load to the load corresponding to the maximum strained fibre reaching the maximum stress will vary. This is explained below. Because of friction stress (or the post-peak stress), a cylinder under a torque will not fail when the maximum strained fibre reaching the shear strength. For a rough surface, the friction shear stress developed will be higher than that with a smooth surface. Assuming the shear stress - shear strain relationship is as shown in Fig. 5.8a, the effect of the friction shear stress can be determined and is shown in Fig. 5.8b, a detailed derivation being given in Appendix 5. It can be envisaged that for a hollow cylinder cross section, the post-peak effect will be reduced significantly.

In a direct shear bond test, the shape of the cross section influences the uniformity of the shear stress distribution over the bond interface. Thus, the average stress based on gross area will vary accordingly. From theory of the strength of materials, shear stress distribution and the ratio of maximum shear stress to the average stress can be worked out.

For a rectangular cross section:

$$\tau = \frac{6P}{bH^3}\left(\frac{H^2}{4} - h^2\right) \tag{5.1}$$

$$\frac{t_{max}}{\tau_o} = \frac{3}{2} \cdot \frac{P}{bH} / (\frac{P}{bH}) = \frac{3}{2} \tag{5.2}$$

For a circular cross section:

$$\tau = \frac{4P}{3\pi R^4}(R^2 - h^2) \tag{5.3}$$

$$\frac{\tau_{max}}{\tau_o} = \frac{4}{3} \cdot \frac{P}{\pi R^2} / (\frac{P}{\pi R^2}) = \frac{4}{3} \tag{5.4}$$

Figs. 5.9 and 5.10 show the shear stress distribution over the rectangular and circular cross section, respectively. The detailed derivation is given in Appendix 6. Because of the higher non-uniformity of the shear stress over the rectangular bond interface, it can be expected that the shear bond test with a rectangular cross section, will produce lower failure stresses than those with a circular cross section. In a total of 10 cases tested by Ohama, et al [14] (three polymer cement ratios: 5%, 10%, and 20%, respectively, three polymer types: styrene-butadiene rubber (SBR), ethylene-vinyl acetate (EVA), and polyacrylic ester (PAE) and one group with no polymer at all), 9 cases showed that a rectangular cross section produced lower shear bond strengths; only 1 showed a very slightly higher bond strength (Fig. 5.11).

5.3.6 Secondary stresses induced over the bond interface

It has been demonstrated in the above section that the shape of the bond interface affects shear bond test results, but the stress ratios presented in Fig. 5.11 are higher than the elastic predictions. If the specimen sizes used by Ohama, et al [14] are examined, it can be found that the length of the circular shear specimens was 100mm, and the length of the rectangular ones 160mm. If the distance between the shear loads is not very small, secondary bending stress will be induced. From figures presented by

Ohama, et al [14], the distance was not given, but it appears that it was shorter in the circular cases than in the rectangular cases. If this is so, the higher secondary bending stresses in the specimens with rectangular cross section would also produce lower failure loads. Detailed test information is needed before a satisfactory answer can be given.

Tayabji [85] reported the shear bond test on a bridge deck. Cores of about 94mm in diameter were cut from test sections of the repaired bridge deck. Direct shear test equipment was used. It is interesting to note that with the increase in scarification depth achieved using hydrojetting, which was equal to the repair thickness, the measured shear bond strengths decreased dramatically (Fig. 5.12). One would assume that for this real repair, deeper scarification by hydrojetting would produce a stronger bond, because a sounder substrate was produced. No explanation can be given here unless the detailed loading conditions are obtained.

For both the cases from [14] and [85], it is important to know the distance between the loading point and the bond interface, and whether this distance changed during different tests.

For the twist-off test, if a torque is exerted by a horizontally applied force, a secondary bending stress will also be introduced (Fig. 5.13).

Assuming a failure will occur when the principal tensile stress reaches a certain value:-

$$\sigma'_{max} = \tau_o \sqrt{1 + (\frac{H}{L})^2} \qquad (5.5)$$

where τ_o is the maximum shear stress at the periphery of the core cylinder. Keeping σ^t_{max} constant, Fig. 5.14 shows the achievable maximum shear stress τ_o based on a elastic analysis It shows that so long as the L/H ratio exceeds 3 (or H/L < 0.3), the secondary bending effect can be ignored and the maximum stress is about the maximum shear stress.

5.4 Slant shear test

5.4.1 Introduction

This method puts a bond interface under a combined stress state of compression and shear. The philosophy associated with this method is that if failure occurs monolithically, the bond is good.

Changing the bond direction, shear and normal stresses acting on the bond interface will change accordingly. But failure is not just dependent on the shear stress component. It depends on a specific combination of shear and normal stresses. Although some researchers claim that the slant shear test represents the typical stress state experienced in a real structure, the real bond directions and real stress conditions will differ from those adopted in the test. Hence, it is very important to know how to apply results obtained from the slant shear test to predict bond performance at other bond directions. Also, we need to know how to use the slant shear test to analyse the effect of workmanship and other factors.

Some researchers select this method because they claim that it produces a stress state fairly typical in service [38, 59, 63, 84]. Others prefer this method because they claim that it is sensitive to variations in the bond strength [38], or it produces consistent test results [13].

5.4.2 Surface roughness and soundness

It is known that compressive stresses can be transmitted through a microcrack. The contribution of compressive stresses acting on the bond interface cannot be ignored in the interpretation of results from the slant shear test.

The author carried out the following tests on the effect of surface roughness and soundness (see Table 5.4 and Fig. 5.15). In the first series of tests, specimens were line load split into two halves. Bonding surfaces of the first group of specimens were further treated using needle gunning to produce the rough and sound surfaces, whilst the second group received no further treatment. It is known that there are microcracks associated with a split surface as shown by Cleland et al's results on tensile bond test [18], but results from the second group showed no reduction in the bond strengths at all, rather, slight increases were recorded. In the latter case, this could be related to the higher degree of roughness associated with the untreated split surfaces. In the second series of tests, three groups of specimen were prepared in the following ways: (1) formed surfaces then needle gunned (sound, but very smooth), (2) sandblasted surfaces but contaminated with demoulding oil (rough but contaminated), and (3) sandblasted surfaces (rough and sound). From the results, it can be seen that a rough but contaminated surface may produce a higher bond strength than a sound, but very smooth, surface. Austin and Robins [15], and Climaco and Regan [63] carried out slant shear tests on split surfaces prepared in such a way that the potential tensile bond strength was zero. They found that the failure loads were as high as 50 percent of the solid control specimens, which means that in a slant shear test the effect of surface roughness is very significant.

Based on all the results mentioned above, it is clear that the performance of a slant shear test is affected by both chemical adhesion and mechanical interlock. For the same quality substrates and repair materials, it can be assumed that the chemical adhesion does not change unless the surface is contaminated, regardless of the surface roughness. But the contribution of the mechanical interlock increases with increasing surface roughness, and can even change the failure mode from a bond failure to a monolithic failure.

Changing the bond direction will change the potential bond failure load. The relationship can be described using the Coulomb theory: a shear failure will occur if the following equation is satisfied:

$$\tau_n = c + \mu\sigma_n \tag{5.6}$$

or

$$\tau_n = c + \tan(\phi)\cdot\sigma_n \tag{5.7}$$

where τ_n is the shear stress acting on the bond interface;

σ_n is the normal stress acting on the bond interface;

c is the adhesion strength;

μ is the coefficient of friction; and

ϕ is the internal friction angle, $\phi = \tan^{-1}(\mu)$.

Using the relationships that $\tau_n = 0.5\sigma_o\sin(2\alpha)$,and $\sigma_n = \sigma_o\sin^2\alpha$, (see Fig. 5.16), the external stress required to produce a shear failure along the bond direction can be worked out as:

$$\sigma_o = c[\cot\alpha + \tan(\tan^{-1}\mu + \alpha)] \tag{5.8}$$

where α is the angle between the bond interface and the longitudinal axis.

In order to produce a clearly defined bond failure, it is better to select the bond direction that corresponds to the minimum bond failure load. Under this condition, the critical angle, or the critical bond direction, and the minimum bond strength can be worked out as following.

$$\sigma_o = 2c\cdot\tan(45+\frac{\phi}{2}) \tag{5.9}$$

$$\tau_{cril} = c(1+\sin\phi) \tag{5.10}$$

$$\alpha_{crit} = 45 - \frac{\phi}{2} \tag{5.11}$$

Fig. 5.17 shows the variation of σ_o/c with the bond angle, α, Fig. 5.18 shows the variation of σ_o/c with coefficient of friction, μ. From Fig. 5.17 and Fig. 5.18, it can be concluded that:

(1) The external stress required to produce a shear failure along the bond interface varies with the bond direction selected;

(2) There exists a bond direction, (the critical bond direction), α_{crit}, at which direction the required external stress to produce a shear bond failure is minimised;

(3) The coefficient of friction, μ, affects the determination of the critical bond direction; and

(4) A rougher surface will produce a higher bond strength. The increase can become very significant depending on the bond angle selected.

The material may also fail, so when the external stress, σ_o, is greater than the compressive strength of the weaker material, a cohesive failure will occur. From this a further conclusion can be drawn:

(5) If a cohesive failure occurs at the critical bond direction, changing the bond direction will not produce a bond failure. But if a cohesive failure occurs at some other angles, bond failure may still be possible if the bond plane angle is moved closer to the critical bond angle.

Results from different researchers have shown that surface roughness affects the value of the coefficient of friction (see section 4.3.4.3). This suggests that the critical bond direction will change with the surface roughness. Accepting that different roughness are used in the slant shear test, suggests that a cohesive failure obtained using the

method in BS 6319: Part 4 will not necessarily guarantee a cohesive failure at other angles.

The adhesion strength, c, can be determined by intersecting the bond strength envelop with the vertical axis. However, under high ratio of shear/compression stress state, the failure should be determined by the bond strength criterion described in section 4.4.4.

5.4.3 Modulus mismatch

5.4.3.1 Introduction

Modulus mismatch causes local stress concentration as in the case of tensile bond and shear bond tests. But in a slant shear test, modulus mismatch may also induce a eccentricity. The mismatch can occur between a concrete and an adhesive when two concrete blocks are bonded together by the adhesive, such as in the case of resin injection, or between a concrete substrate and a repair material (Fig. 5.19a and b), but the effect on the stress distribution and eccentricity is different.

5.4.3.2 Effect of modulus mismatch on the stress distribution over the bond interface

For the case a in Fig. 5.19, when two concrete blocks are bonded together by an adhesive, the effect is mainly localised at the edge. For the normal stresses acting on the bond interface, the stress level at the vicinity of the edge of the bond is higher than the assumed uniform value when the modulus of the adhesive is lower than that of the concrete. In the middle of the bond area, the normal stresses are slightly smaller than the assumed uniform stress (Fig. 5.20a). In contrast to this, the shear stresses acting on the bond interface are smaller in the vicinity at the edge, and higher (but very close to the uniform stress) in the middle area (Fig. 5.20b). The material properties assumed were: $E_{c1} = E_{c2} = 30GPa$, $\nu_{c1} = \nu_{c2} = 0.2$, $E_m = 0.67E_c$, $\nu_m = 0.2$. In both cases, the applied direct stress $\sigma_0 = 10MPa$. stresses are nearly uniformly distributed in the central area. The effect of the modulus

mismatch is localised in the edge, as in the case of a tensile test where modulus mismatch causes stress concentrations near the edge of the bond interface.

When there is a modulus mismatch between the substrate concrete and the repair material, the effect of the mismatch on stress distribution is different from that in Fig. 5.20. Fig. 5.21a and b show the normal and shear stress distributions obtained from a finite element analysis, the mesh generation being shown in Fig. 4.16. The shear stress distribution follows one pattern, and the normal stress distribution follows another. The results show that if there is a modulus mismatch, the actual stress distributions along the bond interface will differ from what are assumed. When the modulus of the repair material is lower than that of the substrate, the general trend is for an increase in stress at the ends of the interface, with the maximum normal and shear stresses occurring at the side with least repair material depth. When the modulus ratio is greater than 0.7, both the stress distributions tend to be uniform with some variations at the edge of the bond interface.

It was mentioned earlier that the effect of modulus mismatch is usually linked with the unknown intrinsic bond strength which is determined by the chemical components of the materials and other factors. The point raised here is that if the adhesive used in Fig. 5.19a is same as the repair material used in Fig. 5.19b, and failure in both cases is controlled by bond failure, will the bond strength be same with each other despite the different patterns of stress distribution ? More work needs to be done to clarify and establish the relationship.

5.4.3.3 Effect of modulus mismatch on eccentricity

Generally speaking, so long as the specimen is centrally placed in the test machine, the ball system of the test machine will ensure that the load is axially applied. But due to the small size of the cross section (about 55x55mm), a load applied on the specimen is possibly better simulated by a uniform displacement. If the repair material

and the substrate have the same modulus, the uniform displacement applied at the top of specimen is equivalent to an axial load. But if there is a modulus mismatch, eccentricity can be induced.

To demonstrate this, an FE analysis and a simple linear elastic analysis were carried out. The mesh generation for the FE analysis is shown in Fig. 4.16. The eccentricity induced due to a uniform displacement, based on the elastic analysis, is given below (Detailed derivation is given in Appendix 7).

$$e = [\frac{\frac{bK_2}{2} + K_1}{K_2} \ln \frac{K_1 + bK_2}{K_1} - b] / \ln \frac{K_1 + bK_2}{K_1} \qquad (5.12)$$

where $K_1 = s\beta_t + s + L$

$K_2 = \beta_t \cot\alpha - \cot\alpha \quad (\beta_t \neq 1)$

$\beta_t = E_m/E_c$

When $\beta_t = 1$, e=0, i.e., no eccentricity will be introduced.

The finite element analysis and the linear elastic analysis agree very well. Fig. 5.22 shows the eccentricities induced due to the modulus mismatch using the eq.(5.12). The eccentricities induced will increase the maximum compressive stress of the slant shear specimens, the degree of increase being also shown in Fig. 5.22. For a standard specimen (L=155mm and length/width ratio of about 2.8), the increase in the maximum stress is about 10% when the modulus ratio is 0.6, and about 5% when the modulus ratio is 0.8. If the length of the specimen can be increased, the effect of the modulus mismatch will gradually be reduced to a local area and the eccentricities will be reduced significantly. If the length of the specimen can be increased to 300mm (the length/width ratio of 5.5), the increase in the maximum stress is less than 5% when the modulus ratio is 0.6, and only about 2% when the modulus ratio is 0.8. In [63], the ratio of the length to the width of the cross section was 6.7, and the effect of the

modulus mismatch on eccentricity induced can be ignored for commonly used repair materials.

5.4.4 Differential deformation

For the slant shear test, the ratio of the free surface areas of the repair material to the bond area is much greater than that in a slab or in a beam. And due to the nature of the small size of specimens, restraint provided by the substrate is very small, therefore the effect of differential deformation can be ignored.

5.4.5 Variation of specimen size and shape due to the specimen preparation

The main factors are the variations of the bond plane angle and the surface roughness. Depending on the method used to produce a bond surface, the achieved bond angle may differ slightly from what it is expected. The method suggested in BS6319 :Part 4 was found not to produce consistent bond directions, and Austin and Robins [15] drew the same conclusion. The line load split method produces more consistent bond directions with microcracks induced and very rough surface textures. Cut and formed surfaces produce the most consistent bond directions, and different roughness can be obtained by sandblasting. Fig. 5.23 shows examples of the bond planes obtained.

Variation in the bond plane angle will affect the failure load, but the effect depends on the difference between the bond angle selected, α, and the critical bond angle, α_{crit}, which is related to the surface roughness. If α is very close to α_{crit}, the variation of the failure loads caused by a small variation in α will also be very small and can be neglected. If α differs significantly from α_{crit}, a small variation in the bond direction may cause a significant variation in the failure load. Fig. 5.24 shows the variation in the failure load due to a one degree variation in the bond angles. If α_{crit} is 28^{o},and α is 30^{o}, a one degree variation in the achieved bond angle may only cause less than 1%

variation in the failure load. But if α_{crit} is 18^o (corresponding to a very rough surface), and the selected bond direction, α, is still 30^o, the effect of a one degree variation in the achieved bond angle could cause variations in failure load of about 12%.

Secondly, in the study of the relationship between the variation of specimen sizes and shape, the surface roughness has to be considered. It has been shown that the bond angle selected should be very close to the critical bond direction in order to test the minimum slant shear bond failure load. The critical bond direction bears a direct relationship with the surface roughness. But a bond angle is produced prior to roughening the surface. This means that unless it can be guaranteed that the critical bond angle, corresponding to the achieved roughness, matches the bond angle selected, the variation of the bond angle should always be taken into consideration.

Based on the relationship between surface roughness and the coefficient of friction adopted in this study (section 4.3.4.3), the following bond direction is suggested. For a smooth surface, α should be selected around 27^o; for a medium rough surface, α around 23^o; and for a rough surface, α around 19^o. For a sharp angle, it might be difficult to make the specimen. A simple way round this problem is to use a smooth surface at the normal 30^o direction. Strengths at other directions or other roughness can be derived from the bond strength criterion developed in this study (see section 4.3.4). For example, in Table 5.4, the failure stress of the smooth surface slant shear specimen was 26MPa. By using the bond strength criterion, the failure stress corresponding to a rough surface can be determined as:

$$\sigma_{RF} = \frac{\sin\alpha\cos\alpha - \mu_{SM}\sin^2\alpha}{\sin\alpha\cos\alpha - \mu_{RF}\sin^2\alpha}\,\sigma_{SM} = 53\ \text{MPa}$$

The measured failure stress for the rough surface was 50.4MPa. Because the actual failure stress was very close to the material strength, it indicates that the failure was possibly controlled by the material strength rather than by the bond strength.

5.5 Patch repair tests

5.5.1 Introduction

In many situations the bond strength methods mentioned above do not represent the real conditions of repair systems in practice.

For example, Perry and Holmyard [56] reported tests on repaired domes and corresponding slant shear tests. They found that results obtained from the slant shear test on small, well-prepared specimens were not directly comparable to the results obtained from the repaired domes.

Ainsworth, et al [2] reported pull-off stress requirements used by the Hong Kong Housing Authority. Their experience of large numbers of pull-off tests has shown that in-situ pull-off stresses rarely approached the minimum laboratory bond strength. They draw the conclusion that the in-situ pull-off test results cannot be compared directly with that from the laboratory bond tests.

A question may then be asked as to under what circumstances, can the results obtained from these simple tests be applied to a real repair situation ? Little information has been found. In order to tackle these problems, Austin and Robins [15, 16] initiated the idea of patch repair systems which put repairs into more realistic conditions, so that the interaction within the system can be evaluated. Firstly, they pointed out the difference in stresses between several current bond test methods and patch repairs. Load is applied directly to the repair when using the core pull-off, the slant shear tests

and others. In a real patch repair system, stresses imposed on the bond interface and the repair material result from different trends in deformation between the substrate concrete and the repair material, which bears a direct relationship with the modulus mismatch. A repair material with a lower modulus will share less load than a repair material with a higher modulus. It can be argued that the current bond test methods are mainly for the measurement of bond strength, whilst the repair systems require further research aimed at the interactions between the substrate, the repair material, and the bond between these two materials. The study for the latter case requires a thorough understanding of the mechanical, thermal and chemical behaviour of the whole repair system. Fig. 5.25 shows the procedures for a mechanical analysis of a repair system. Without results obtained from bond strength measurement, it will be difficult to know the meaning a failure load obtained from a repair system. Examples can be given below.

Fig. 5.26 shows two specimens with same substrates but repaired with different materials. Suppose the specimen 'a' fails at load 'P1', and the specimen 'b' fails at load 'P2'. If the repair material in 'b' has a higher modulus than that in 'a', stresses transferred through the bond interface in 'b' will be higher than that transferred in 'a' under the same level of external load. The specimen 'b' may fail at a lower failure load than the specimen 'a' (i.e., $P_2 < P_1$) even though the repair material in 'b' could have a higher direct tensile bond strength than that of the repair material in 'a'. A higher direct tensile bond strength does not necessarily guarantee a higher failure load in the repair system considered.

Another example shows the importance of the geometry of the cut-out in interpreting test results. Fig. 5.27 shows two specimens with the same repair material and same surface preparation except for the geometry of the cut-out; one with a rectangular cut-out, and the other with a circular one. Test results may show that the specimen with a rectangular repair fails due to inadequate bond strength, whilst the specimen with the

circular repair may produce a monolithic cracking failure. It is not sufficient to draw the conclusion that the specimen 'b' has a repair material with adequate bond strength.

Similar research into repair systems includes studies carried out by Kudlapur, et al [34], Peier [42], Perry and Holmyard [56], Cairus[91], Emberson and Mays [94], and Ramirez [93, 136]. The analysis by Emberson and Mays [94] showed the importance of modulus mismatch on stress transfer. Because their interest was in the composite behaviour at a low stress level, neither the failure load nor the failure mode were available.

For all of these tests, what goal do we want to achieve ? To have structures re-strengthened ? To re-gain the protection for reinforcement ? Or just simply for the purpose of aesthetics. Some reports of the evaluation of repair materials omit the purpose of the repair in the design of the patch repair test. One example is shown in Fig. 5.28. Because reinforcement was used in the specimen, if failure is controlled by the yielding of the reinforcement, no contribution from the repair material to the ultimate bending capacity will be expected. If failure is controlled by the crushing of the concrete in the compressive zone, again, no contribution from the cracked repair material to the ultimate bending capacity can be expected. Hence, by measuring the ultimate bending capacity of a reinforced concrete beam to evaluate the efficiency of the repair material, repaired and unrepaired specimens will show no difference.

It can thus be seen that discrepancies in the interpretation of results between the repair system and direct bond tests can be attributed to a lack of understanding of what the repair material may contribute or how it functions in a repair system.

5.5.2 Selection of repair systems

In order to evaluate repair materials or repair systems, the stress state in the system has to be known, together with the bond strength criterion. The behaviour of the system is described by a set of characteristic mechanical properties containing the bulk

properties of various materials (e.g. compressive strength, modulus of elasticity, linear thermal expansion coefficient, etc.), and bond properties.

Bulk properties differ essentially from bond properties because they only characterise one material. Bond properties characterise the special properties between two materials, and in addition, will be affected by workmanship and other factors.

The application of bulk properties to predict the performance of a structural element is generally straight forward, following well-established knowledge of mechanics and various numerical methods. The effect of configuration and size of the specimen is well acknowledged and has been integrated into the design procedures. But for the analysis of repair systems, configuration and size have received little attention. Therefore it is important to select the repair systems which can be used to evaluate a repair material and to predict its contribution more effectively.

In order to have a better understanding of how a repaired work will behave, the author defines the repairs into two categories : lab-repair and site-repair.

A lab-repair is the kind of repair that will be carried out in a laboratory with the objective of assessing how the repair system will function under critical situations. If all the factors which influence the behaviour of a repair system are viewed as variables, the purpose of a lab-repair and its corresponding research are to see the effects of these variables on the performance of the repair work, and under what situations the repair will fail at the minimum load, and what the failure mode and controlling parameters will be. Then by changing some of the crucial variables, a better performance of the repair system can hopefully be achieved.

A site-repair is the repair that will be carried out on real structures. Its purpose is not to test the bond performance of repair materials, but to achieve the desired target, such

as to restore the structural integrity, maximise the service life of repaired structure, minimise the cost for repairing (based on properties of repair materials given) and expand the experience or information obtained from lab-repairs. Because it is known that the bond is usually the weakest part in the composite, procedures should be taken to put the bond in the most favoured conditions, such as changing the geometry, putting the bond mainly into compression, (rather than the combined stress state of compression and shear), choosing the most appropriate repair material, and applying some protective coat, etc.

Austin and Robins [15] carried out patch compressive tests with different geometry of cut-out (Fig. 5.29). Suppose a repair mortar has the same modulus as that of the substrate, the effect of the modulus mismatch can be neglected temporarily, and the attention can be focused on the geometry selection. Based on their test results, a circular cut-out of 200x25mm was chosen because it produced the lowest failure load compared with other geometry of cut-out.

This can be verified by using the bond strength criterion proposed in section 4.3.4. With the combined stress state of compression and shear, the external stress, σ_o, required to produce a bond failure can be worked out as indicated by eq.(5.6). Fig. 5.17 shows the relationship between σ_o/c and α. Whether for a smooth, a medium rough, or a rough surface, the circular cut-out of 200x25mm specimen will produce the lowest failure load among the situations considered. If this cut-out is selected for the lab-repair for the purpose of studying the bond quality, it should definitely be avoided in site repairs. In site repairs a circular cut-out of 100x50mm will work much better than the previous one (in fact, a rectangular one is preferred for this special case ignoring stress concentration at corners).

Based on the experimental studies by Austin and Robins [15], and the author's trial tests and theoretical verification, two geometries of cut-out were selected for this patch

repair study. One is called the patch compressive test, and the other, the patch flexural test (Fig. 4.3 and Fig. 4.5). In the patch compressive test, the stress state at the bond interface is very similar to that in a slant shear test. In the patch flexural test, the stress state at the bond interface is similar to that in a tensile test.

It is now clear that if a comparison is to be made between the patch tests and other bond test methods, it should be between a patch compressive test and the slant shear test, or between a patch flexural and a tensile bond test. Indiscriminate comparison will not provide much useful information.

Also, in order to study the contribution of a repair material on a patch repair test, the load carrying capacity of unrepaired specimens should also be known.

Six unrepaired patch compressive specimens were tested. The specimens were divided into two groups: one with a loading plate to ensure that the external load was axially applied on the specimen (see Fig. 4.4), and the other group without such a loading plate, the axiality of the external load was dependent on the loading system of the test machine. Because of the fairly big proportion of the cut-out on the whole cross section, with and without a loading plate did make difference in the failure load (Tab. 5.5). For the group with a loading plate, the average failure load was 235KN which was 28% lower than that without the loading plate (300KN). This difference would affect the interpretation of test results that whether a increase in failure load was caused by the contribution of bond/repair material or by the loading system. To verify this, both a simple elastic prediction and an FE analysis were carried out. Fig. 5.30 shows the stress distribution over the narrowest cross section. In Fig. 5.30, with a loading plate means the external load is axially applied, and without the loading plate means the external load is simulated by a uniform displacement at the top of the specimen. Predictions from the simple elastic analysis agreed well with that from the FE analysis. The FE analysis on specimen without a loading plate revealed that under

a uniform displacement loading condition, the distance between the free surface of the cut-out and the end of the specimen was not long enough to ensure the uniform displacement being equivalent to uniform stress. This resulted a shifting of load from the centre of the gross cross section towards the centre of the net cross section of about 6.3 mm. Assuming the compressive strength is 80% of the cube strength [113, 138], predicted failure loads from both analyses were 199 and 269KN, respectively, an increase of 35%. The predicted loads were slightly lower than the test results, about 15% and 10% for the case with and without the loading plate, respectively.

Unrepaired patch flexural specimens were tested at different ages. Some solid beams were also tested. The failure loads are shown in Table 5.6. The predicted failure loads were obtained assuming the maximum strained fibre reaching the flexural tensile strength which was determined by eq.(3.2), and agreed well with the test results (the average ratio of P_o/P was 1.07, with a coefficient of variation of 8%). When the failure load of a repaired specimen is greater than that of the unrepaired ones, it is certain that the increase in the ultimate bending capacity is due to the repair material and the bond strength achieved. When the failure load of a repaired specimen is not greater than that of the unrepaired ones, it may be difficult to tell when the repair material fails. Still using the relationship between the compressive strength and the flexural tensile strength (eq.(3.2)), Fig. 5.31 shows the range of flexural tensile bond strength where the contribution of a repair material to ultimate bending capacity can be measured. It is clear that below a certain value of the flexural tensile bond strength, the failure load will be the same as an unrepaired one, and over a certain value, the repaired specimen will behave like a solid beam and failure is by cracking of the substrate.

After surface preparation, the actual size of the cut-out will be different from that of the initially formed cut-out. It varies with the roughness induced. In this study, it was found that for a rough surface, a thickness of about 5mm was removed; for a medium rough surface, a thickness of about 3mm was removed, and for slightly sandblasted

smooth surface, hardly any change at all. The geometry adopted in this study is shown in Fig. 5.32. In the patch repair systems, there are four possible failure modes (using the modulus ratio being unity as an example, see Fig. 5.31):

(1). The bond or the repair mortar fails at a load which is lower than P_o, and the system fails at P_o, (due to the variation in the material properties, some variation in the failure load can be expected). This can be viewed as the lower limit of the failure load;

(2). The bond and the repair material remain intact and the substrate fails at a load P_1, which is greater than the failure load of the unrepaired specimens, P_o. This can be viewed as the upper limit of the failure load;

(3). The failure of the bond leads to a simultaneous failure of the repaired specimen. The load is designated as P_3, ($P_o<P_3<P_1$); and

(4). The failure of the repair material (cracking or crushing) leads to a simultaneous failure of the repaired specimen. The load is designated as P_4, ($P_o<P_4<P_1$).

5.5.3 Surface roughness and soundness

Surface roughness and soundness affect test results, but the effect is linked with the material strengths and the modulus mismatch.

For the patch compressive test, due to sandblasting, the actual geometry of the cut-out and the bond angle at the periphery of the cut-out will vary as shown in Fig. 5.32. The effect of the roughness in a patch compressive test is marked by the change in the geometry of the cut-out. Fig. 5.33a shows the predicted external stress required to produce a bond failure, and Fig. 5.33b, the external stress to produce a substrate failure. The predicted failure stress of the repaired specimen will be the lower one of the values presented in Fig. 5.33a and Fig. 5.33b, and is shown in Fig. 5.33c. In Fig. 5.33, βt defines the modulus ratio of the repair material to the substrate. The

calculation is based on the following assumptions: (1) A slant shear specimen with a smooth surface fails at an externally applied stress of 20MPa due to debonding; and (2) The compressive strength of the substrate is 50MPa (cube strength f_{cu}=62.5MPa).

It can be seen that the external stresses required to produce the substrate failure do not vary much with the surface roughness. When the modulus ratio is 0.4, the variation of the potential substrate failure loads is about 4% from a very rough to a very smooth surface. The variation will be smaller with the increasing modulus ratio. But the external stresses required to produce the bond failure vary significantly with the surface roughness.

If there is a significant modulus mismatch, the repaired patch compressive specimen will behave just like an unrepaired one, the maximum compressive stress in the concrete corresponding to the bond failure load is much higher than the substrate material strength. This suggests that in this case the patch compressive specimen will fail in the form of a crushing of the substrate concrete far earlier than debonding can occur. This also suggests that the surface roughness will not affect the test results. With a decrease in the modulus mismatch, both the potential bond failure stress and the maximum compressive stress in the substrate will reduce sharply. The possibility of a bond failure is increased. If the failure is being dominated by the performance of the bond, a rougher surface will produce a higher failure load. For example, in Fig. 5.33a,, the failure stress is about doubled from smooth to rough surfaces for all the cases of modulus mismatch considered. In terms of the predicted failure stress of the repaired specimens, the increase in failure load from smooth to rough surfaces depends on the modulus ratio, βt. For low modulus repair material, for example, βt=0.4, the increase is about 15%, when βt is 0.7, the increase is 90%, and over 110% when βt is 0.9. Because the stress state in the patch compressive test is very much dominated by the existence of compressive stresses along the bond interface, it can be

assumed that some local surface defects will not affect the overall mechanical performance based on results from the slant shear tests.

For the patch flexural test, sandblasting will change the size of the cut-out but will not change the bond angle. From the discussions on tensile bond tests, it is known that a rougher surface usually produces a slightly higher failure load, but the effect is related to the specific repair material concerned. Tests carried out by the author and by Cleland, et al [19] showed that the acrylic modified cementitious repair mortar and the flowing concrete were not sensitive to surface roughness. The plain sand/cement mortar and the SBR modified cementitious mortar preferred a rougher surface. But in the patch flexural test, the most important aspect is the load sharing between the repair material and the substrate concrete; which is directly related to modulus mismatch. As in the patch compressive test, when the modulus ratio is very low, it is the substrate that controls the failure, and the roughness and soundness will have no contribution to the bending capacity of the repaired specimen.

5.5.4 Modulus mismatch

It has been demonstrated that modulus mismatch affects the level of stress transferred from the substrate to the repair material. The effect can be viewed in the following two ways: the effect on bond performance, and the effect on the performance of the repaired specimens.

With a low modulus repair material, while the tendency of bond failure is reduced, the substrate takes a higher load. If stresses in the substrate reach the material strength, material failure will occur. The evaluation should be based on the optimisation design principal that the material and the bond fail simultaneously. This will let the repaired specimen have the maximum load carrying capacity.

Fig. 5.34 shows the effect of modulus mismatch in a patch compressive test assuming that a slant shear specimen with a smooth surface fails at an external stress of 20MPa due to debonding, and the compressive strength of the substrate concrete being 40MPa (Fig. 5.34a) and 50MPa (Fig. 5.34b), respectively. The lower value between the substrate and bond failure stress is the predicted failure stress of the repaired specimen. Failure load can be worked out by multiplying the stress with the area of the cross section. Fig. 5.35 shows the effect of modulus mismatch in a patch flexural test. The potential failure stress is referred to the tensile stress at the most strained fibre of the repaired patch flexural specimen, and is only a nominal stress because the modulus mismatch was not considered. The failure load can be worked out using the following equation:

$$P = \frac{4bh^2\sigma}{3L} \tag{5.13}$$

where b is the width of the specimen;

h is the height of the specimen;

L is the supporting span of the specimen; and

σ is the potential failure stress of a patch flexural specimen.

From Fig. 5.34 and Fig. 5.35, it can be seen that with an increase in the modulus of the repair material, more load is shared by the repair material, and the failure tendency is shifted from the material failure (crushing in a patch compressive specimen, or cracking in a patch flexural specimen) to the bond failure. At a particular value of modulus mismatch, the substrate concrete and the bond will fail simultaneously. The above studies clearly show that in the patch tests, the modulus mismatch has a very important role in the interpretation of test results. Knowing the effect of the modulus mismatch, better design can be achieved in real repairs by taking the effect into consideration. For example, for the repair of concrete columns, if we know that the bond area will be put into a compressive stress state, a material with similar modulus

to that of the substrate and a rectangular cut-out will work more effectively than a low modulus, high bond strength repair material. But in a soffit repair, it is the latter type of repair material that will contribute in a more effective way. Fig. 5.36 shows the comparison between patch compressive test results conducted by Austin and Robins [15] and the predicted failure stress using the bond strength criterion developed (see section 4.3). The theoretical prediction was based on the following data from [15]: f_{cu}=54.5MPa, f_c=0.8f_{cu}, a patch compressive specimen with rough surface and 204x26mm circular cut-out failed at an external stress of 35.2MPa, the repair material being M0.4. It clearly shows that for cut-out with large bond angles, the failure stress was increased even though the repair material was the same one.

5.5.5 Differential deformation

This is considered in two cases: symmetric and non-symmetric. Because no test results was found on this issue, the following discussions are mainly based on the theoretical prediction.

5.5.5.1. Symmetric repair (Fig. 4.17)

If there is a differential deformation due to the shrinkage or the temperature change, stresses will be induced at the bond interface.

In section 4.3.3, the basic formulas were derived. It has been mentioned that the effective modulus method (EMM) and the rate of creep method (RCM) were used to evaluate the shrinkage effect.

For the effective modulus method, creep is treated as a delayed elastic strain and is taken into account simply by reducing the elastic modulus for concrete. The shrinkage stress developed in the repair mortar is determined by the following equation:-

$$\sigma_m = \varepsilon_{em} E_m = \frac{E_m(\varepsilon_{shm} - \varepsilon_{shc})}{1 + \phi_m(t, t_m) + \beta_t \alpha + \beta_t \alpha \phi_c(t, t_c)} \tag{5.14}$$

For the rate of creep method, the following differential equation is obtained:-

$$\dot{\sigma}_m + \sigma_m F_1(t) + F_2(t) = 0 \tag{5.15}$$

where

$$F_1(t) = \frac{\dot{\phi}_m + \alpha \beta_t \dot{\phi}_c}{1 + \alpha \beta_t}$$

$$F_2(t) = \frac{\dot{\sigma}_{shm} - \beta_t \dot{\sigma}_{shc}}{1 + \alpha \beta_t}$$

Where

ε_{shm}, ε_{shc} are the shrinkage strains of the repair material and the substrate concrete at time t, respectively;

ϕ_m, ϕ_c are the creep coefficients of the repair material and the substrate at time t, respectively;

β_t is the modulus ratio, $\beta_t = E_m/E_c$;

α is the area ratio, $\alpha = A_m/A_c$;

t_m, t_c are the ages of the repair material and the substrate at the time being loaded, respectively (in this case it is the start of the drying out);

$\dot{\phi}_m$, $\dot{\phi}_c$ are the differentiations of ϕ_m and ϕ_c with respect to the time t, respectively;

$\sigma_{shm} = E_m.\varepsilon_{shm}$, $\sigma_{shc} = E_c.\varepsilon_{shc}$;

$\dot{\sigma}_{shm}$, $\dot{\sigma}_{shc}$ are the differentiations of σ_{shm} and σ_{shc} with respect to the time t, respectively.

The Runge-Kutta method [140] was used to obtain the numerical solution for the differential equation (see Appendix 3).

Using ACI recommendations for shrinkage and creep quoted in [134],

$$\varepsilon_{shm} = \frac{t}{35+t}\varepsilon^{*}_{shm} \tag{5.16}$$

$$\varepsilon_{shc} = (\frac{t+t_c}{35+t+t_c} - \frac{t_c}{35+t_c})\varepsilon^{*}_{shc} \tag{5.17}$$

$$\phi_m = \frac{t^{0.6}}{10+t^{0.6}}\phi^{*}_{m} \tag{5.18}$$

$$\phi_c = (\frac{(t+t_c)^{0.6}}{10+(t+t_c)^{0.6}} - \frac{t_c^{0.6}}{10+t_c^{0.6}})\phi^{*}_{c} \tag{5.19}$$

where $\varepsilon_{shm}{}^{*}$, $\varepsilon_{shc}{}^{*}$ are the ultimate shrinkage values of the repair mortar and the substrate, respectively, and $\phi_m{}^{*}$, $\phi_c{}^{*}$ are the ultimate coefficients of creep of the repair mortar and the substrate, respectively.

Fig. 5.37 shows the shrinkage stresses developed in the repair mortar due to the differential shrinkage. It was assumed that the ultimate creep coefficients of both the substrate and the repair material were 2.35, which was determined according to ACI 209 method and using the mix ratios of the substrate concrete, and the ultimate shrinkage strains of both the materials were 500με. Other material properties assigned were: Ec= 30GPa, β_t=E_m/E_c=0.6, α=0.1. Also shown in Fig. 5.37 is the predicted shrinkage stresses without considering the creep effect.

The results from the effective modulus method (EMM) and the rate of creep method (RCM) defines the range of shrinkage stresses. Without considering the creep effect, the shrinkage stresses predicted are much higher than those when the creep effects are considered.

Fig. 5.38 shows the effect of the age of substrate on the shrinkage stresses. Because both the substrate and the repair mortar will shrink, the younger the substrate, the smaller the differential shrinkage will be. When the age of the substrate is one month old, the shrinkage stress is about 60% of that when the substrate is 10 years old, about 85% when the substrate is three months old, and about 97% when the substrate is one

year old. Clearly results obtained from a young substrate will underestimate the shrinkage stress. The age difference between a laboratory specimen and a real structure which needs to be repaired has to be taken into consideration.

Fig. 5.39 shows the effect of repair area ratio. With increasing repair area ratio, the restraint provided by the substrate becomes smaller and, as a consequence, the shrinkage stresses decrease. When the area ratio is 0.1, the shrinkage stress is about 97% of that when the ratio approaches zero, and about 85% when the area ratio is 0.5. This suggests that the area ratio also needs to be considered.

5.5.5.2. Non-symmetric repair

Based on the formulas presented in section 4.3.3, the following equations can be obtained (see Appendix 4):

$$\tau = \frac{-[(1+\phi_m)E_cI_c + (1+\phi_c)E_mI_m]}{e(1+\phi_m)(1+\phi_c)} w^{(3)} \tag{5.20}$$

$$\sigma_n = \frac{E_mI_m}{1+\phi_m} w^{(4)} + \frac{(1+\phi_m)E_cI_c + (1+\phi_c)E_mI_m}{e(1+\phi_m)(1+\phi_c)} z_{im} w^{(4)} \tag{5.21}$$

where w is the deflection of the repaired beam. Fig. 5.40 shows the shear stress distribution at 28 days, Fig. 5.41 the normal stress distribution, and Fig. 5.42 the tensile stress distribution in the repair material. Material properties assumed were: $E_c=E_m=K_s=30GPa$, $\varepsilon_{shc}=\varepsilon_{shm}=500\mu\varepsilon$, $\phi_c=\phi_m=2.35$, $\alpha=0.1$.

For the bond, the critical region lies at the edge area where the tensile and shear stresses reach their peak values. For the sections away from the edge, both the tensile and shear stresses decrease sharply to nearly zero. This agrees with the finite element analysis carried out by Letsch [138]. In contrast to this, the tensile stresses in the repair material reach their peak value at the centre area. This suggests that the possible

failure mode could either be cracking/delamination in the vertical direction at the edge of the repair as the case in [139], or cracking in the horizontal direction at the centre area in the repair mortar [42]. In [139], cracking in the substrate concrete at the edge of the bond interface was observed. This was obviously caused due to high tensile stresses at the edge and that the bond strength exceeded the tensile strength of the concrete.

5.5.6 Variation of specimen size

For the patch tests specially designed for this project, the thickness of the cut-out will affect the stress transferred to the repair material and the actual bond angle at the periphery in a patch compressive test.

In a patch compressive test with a repair material having a very low modulus, it is usually the substrate that controls the failure load. With the increasing thickness of the cut-out, net cross section of the substrate concrete is reduced. This will lead to a higher compressive stress being generated at the side in contact with the repair material; the potential failure load of the repaired specimen is reduced. When the repair material has a similar modulus to that of the substrate, it is usually the bond that dominates the failure load. With an increase in the thickness of the cut-out, the bond direction at the periphery of the repair area diverts further from the critical bond direction. As a consequence, the potential bond failure load of the repaired specimen is increased. If this load is higher than that which can cause a material failure, the failure mode is changed due to the size variation. When the modulus of the repair material is very low, the failure load of the repaired specimen with a rough surface will be slightly lower than those with smooth surfaces due to the decrease in the net cross section, about 4% when the modulus ratio is 0.4, and just 1% when the modulus ratio is 0.8. When the modulus of the repair material is high, the failure load of the repaired specimen with a rough surface will be higher than that with a smooth surface

depending on the bond strength and repair material used. Hence, the effect of the variation of specimen size has to be considered together with the modulus mismatch.

For a patch flexural test, the length and the depth of the cut-out will be affected by the surface preparation. The effect is similar to what has been described for the patch compressive test. When the modulus of the repair material is very low, it is the substrate that controls the failure. Roughening the surface will lead to thickening of the cut-out, thus the net cross section of the substrate is reduced. As a consequence, the potential failure load will be reduced. By increasing the modulus of the repair material, higher stress will be transferred through the bond interface to the repair material, but if the debonding load is less than the failure load of the unrepaired specimen, it is still the substrate that controls the ultimate failure load.

5.5.7 Comparison between the patch tests and other test methods

In the section describing the selection of repair systems (5.5.2), it was mentioned that the comparison should be made between the patch flexural and a tensile bond tests, or between the patch compressive and the slant shear tests. The comparison should be based on same test parameters, such as surface roughness and environmental conditions. Based on the tests carried out in this project, Fig.5.43 shows the comparison between the patch flexural and the core pull-off tests using the sand/cement mortar (Fig. 5.43a) and the acrylic modified cementitious mortar (Fig. 5.43b). They showed fairly good correlation.

5.6 Discussion

5.6.1 General

One of the major problems associated with conducting any type of test is deciding what to measure, how to measure it, and how to interpret the measurement. Rather

obviously, the test selected must be able to study one or more of the factors that will influence the performance of a system, and ideally the crucial ones. In interpreting bond test results, it is important to remember that the goal is to evaluate the response and environments for situations where the material or detail can be employed successfully, as well as those situations where it cannot be so employed. In the previous sections, factors which affect results of the bond test methods have been discussed. These factors include those related to workmanship, material property, and geometry of specimens. Due to different stress states induced at the bond interfaces, the response of those test methods to factors involved are different. This forms the basis for the evaluation of the test methods.

5.6.2 Surface roughness and soundness

Generally, the tensile bond tests are very sensitive to surface defects. If the surface defects are randomly distributed, the capability of a tensile test method to detect the existence of these defects depends on whether the stress imposed on a bond surface will cover the affected area. For the core pull-off test, the more cores that are drilled in a prepared area, the higher the possibility that the defects can be detected. For the dog-bone test or the pipe-nipple grip and the friction grip tests, stress is imposed on the whole prepared surface area. If there are some surface defects, they will to be detected. For the tensile splitting and the patch flexural tests, stresses along the bond interface vary significantly. In the tensile splitting test, tensile stresses are generated in the central area, and compressive stresses at the edge. In the patch flexural test, tensile stresses are generated at the edge rather than in the central area. So the ability to detect the existence of surface defects depends on whether the surface defects happen to be in the tensile stress area. Also, when debonding occurs before the external load reaches the failure load for an unrepaired specimen, the effect of surface preparation cannot be effectively evaluated.

If surface defects are uniformly distributed throughout the bond area, such as the chemical residue associated with surface set retarder, and acid etched surfaces, they will be easily detected. When surface soundness is guaranteed, tensile bond strength will increase with roughness, but this may be partially offset by the difficulty in achieving good compaction.

The slant shear, the patch compressive, and the twist-off shear tests are not sensitive to surface defects. They are highly influenced by the surface roughness. For the first two methods, the roughness affects the friction coefficient, thus affecting the critical bond angle. For the bond orientation suggested in BS 6319, Part 4, if the bond surface is smooth, it tends to produce the lowest bond failure load. If the bond surface is rough, the critical bond angle changes from the standard 30° angle to a sharp angle of about 19°, which can make the measured failure load upto 45% higher than that corresponding to the critical bond angle.

If a repair is to be carried out in a harsh environment, it is very important to minimise the possibility of further deterioration. In this case, detecting surface defects and ensuring proper bond are the right way to achieve the targeted goal. Thus it can be seen that tensile tests are good for this purpose.

If a repair is for structural strengthening and the sources for further deterioration have been blocked, a slant shear test can be used. But there is an intrinsic problem associated with the slant shear test - the dependence of the critical bond angle on the surface roughness. Unless we can make sure that the critical bond angle corresponding to the roughness achieved will be very near to the bond angle produced during the surface preparation, the measured failure load will always be higher than that which would occur at the critical bond angle. Because it is very difficult to control the surface roughness, the effect of surface roughness on failure load should be taken into consideration when evaluation of a repair material is to be made.

All the tensile bond test methods are sensitive to the existence of surface defects, such as microcracks. The dog-bone test method has the advantage that it can be used to measure the early bond strength, and it is easy to operate. The core pull-off test needs more preparation before testing, such as coring, leaving to dry, and adhering dollies. Because of the possible disturbance during core drilling, the core pull-off test is not suitable for measuring early-age bond strength. But it has the greatest advantage that it can be used in both laboratories and on site. This is important because different specimen sizes, and different test configurations may cause variation in failure load, which sometimes can make the interpretation of result difficult. Hence, the core pull-off test is more suitable for applying laboratory results to in-situ quality control, as reported in [2].

The pipe-nipple grip and the friction grip tensile bond tests involve more work than the core pull-off and the dog-bone tests. Also, the sudden change in the cross section near the bond interface due to the steel pipe will cause much higher secondary stress induced over the bond interface, which will affect the interpretation of the results. The effect is similar to the coring depth effect in the core pull-off test.

As has been stated in Chapter 2, there are not many indirect tensile test results available, especially those that are directly comparable with other tensile bond test methods. Tensile splitting bond tests were carried out by Cairns [82] using repaired cylinders. The measured strengths were about 1.7MPa. Because no further information was given, such as the age at testing, compaction method, and surface preparation, it is very difficult to comment on whether or not this value indicates a good bond property.

Flexural tests can be viewed as overlay repairs, such as that shown in Fig. 2.13b, or patch repairs (Fig. 2.13c and d, and Fig. 2.15c). Because for both cases, tensile stress will be generated at the edge of the repair, the importance of a sound substrate is

obvious. In both cases, the effect of modulus mismatch has to be considered, together with the knowledge of the failure loads of unrepaired specimens.

5.6.3 Modulus mismatch

In a direct tensile test, a stress concentration will always be generated at the edge of the bond interface so long as there is a modulus mismatch. This is the intrinsic nature of a contact problem. Unless meso-level bond strength criterion can be developed, the effect of this contact modulus mismatch is always included in the measured macro-level tensile bond strength.

In an indirect tensile bond test, modulus mismatch affects the results in two ways: firstly, as stated earlier, the contact modulus mismatch, which will result in stress concentrations at the edge of the bond interface, and secondly, the modulus mismatch which affects the level of load transferred to the repair material. The lower the modulus a repair material has, the lower the load transferred to the repair will be.

In a slant shear test, the effect of modulus mismatch affects the stress distribution in the following ways:

(1) If two concrete blocks are joined by an adhesive as in the case of resin injection, stress concentration is localised at the edge of the bond interface. This is similar to what happens in a direct tensile test - stresses at places other than the edge are nearly uniformly distributed.

(2) If the substrate is repaired with a repair material having a different modulus, the stress distribution along the bond interface will differ quite significantly from what is usually assumed. The general trend is for an increase in stress at the ends of the interface with the maximum normal stresses and shear stresses occurring at the side with least repair material

depth (E_m<E_c). When the modulus ratio is greater than 0.7, the effect is very small and can be ignored.

(3) If the load applied to the specimen is simulated by a uniform displacement at the top of the slant shear specimen, the modulus mismatch will induce eccentricity, which will cause a reduction in failure load. Based on an elastic FE analysis, when the modulus ratio is 0.5, the maximum stress will be increased by 13% compared with the axially loaded solid specimen. When the modulus ratio is 0.6, the maximum stress increase is about 10%, and for a modulus ratio of 0.8, the increase is less than 5%. For the repair materials used in this project, the modulus mismatch varies from about 0.74 for the acrylic modified cementitious mortar to about 0.83 for the sand/cement mortar. Thus, the modulus effect can be ignored for the straight forward bond test methods.

For the patch tests, the important aspect of modulus mismatch is that it affects stress transferred to the repair material. When the modulus ratio of the repair material to the substrate concrete is 0.7, stress transferred to the repair material will be about 7 percent lower than that when there is no modulus mismatch in a patch compressive test, and about 13 percent lower in a patch flexural test.

5.6.4 Differential deformation

The effect of differential deformation depends on the size and shape of specimens used. For the slant shear, the dog-bone and the tensile split tests, this can be ignored. For the pull-off and the twist-off test, it cannot because most of the time, slabs or beams are used as the testing areas. The effect depends on the size of beams or slabs used. Tensile and shear stresses will be generated at the edge of the bond interface. If these stresses exceed the bond strengths during the hardening time, delamination may

occur. If there is a disturbance to the bond strength development, the bond strength eventually achieved may be reduced. If these stresses are below bond strength during hardening, the effect will decrease rapidly during core drilling as much of the stress will be relieved. For site repairs, no core will be drilled unless it is for the purpose of quality control. While these stresses will not affect the core pull-off test results, they will definitely affect the overall performance. To mitigate the effect, one can either select a repair material that exhibits a small differential deformation, or thicken the edge at the bond interface to put the bond into a less disadvantageous condition (Fig. 5.43) [1].

In the patch compressive test, the shrinkage of the repair material will generate tensile stresses in the repair material and compressive stresses in the areas in contact with the bond interface. When the external stress is applied, the effect of the shrinkage may increase the overall failure load if the failure is controlled by the bond. It may also decrease the overall failure load if the failure is controlled by the crushing of the substrate concrete. In contrast to this, in the patch flexural test, the effect of the shrinkage may reduce the overall failure load if the failure is controlled by the bond, or increase the overall failure load if the failure is controlled by the substrate.

5.6.5 Variation of specimen size

In the core pull-off test, the possible variation of the specimen size can be caused by the core drilling and surface levelling. In this project, these factors were minimised using a good quality core drill and a special casting procedure. For the dog-bone, the pipe-nipple grip, and the tensile split test, this effect can be ignored.

In the slant shear and the patch compressive tests, a small variation in the bond angle may cause a significant variation in the failure loads, especially when the selected

bond direction is 30 degrees, and the surface is rough. When the bond surface is smooth, the slant shear test can produce consistent results.

The variation of specimen size also includes the variation in cross section. In a direct shear test, the shear stress distribution over the bond interface is not uniform, with higher shear stress occurring at the neutral axis position. For a circular cross section, the theoretical ratio of the maximum shear stress to assumed uniformly distributed stress is 1.33, and for a rectangular cross section, the ratio is 1.5. The higher the ratio, the lower the measured failure load will be. In a direct shear bond test, this needs to be taken into consideration.

5.6.6 Secondary stress induced at the bond interface

Secondary stresses can sometimes be induced over the bond interface due to unnoticed factors which include unnoticed restraint and the secondary bending effect, which will affect test results.

In the core pull-off and the twist-off test, the coring depth into the substrate affects the uniformity of stress distribution over the bond interface. The lower the coring depth, the higher the effect will be. To avoid this effect, a drilling depth of more than 15mm is suggested. This is in agreement with the value in the draft European Standard [60]. In the twist-off and the direct shear test, the secondary bending effect plays an important role. In a slant shear test, it is the eccentricity caused by modulus mismatch that counts. In the patch tests, this effect can be ignored. Knowing the possible sources of these secondary stresses will lead to better design and conducting of bond tests, and the bond strength measured will be a better reflection of the performance of the repair material.

5.6.7 Concluding remarks

(1) The tensile test methods are able to detect surface defects, such as microcracks. The slant shear or other tests that put a bond interface under a combined stress state of shear and compression are not suitable to detect surface defects.

(2) In the slant shear test, the bond angle selected should be very near to the critical bond angle which is determined by the surface roughness. By doing so, if a cohesive failure occurs, then at any other bond angles no bond failure will occur. If the actual bond angle is different from the critical bond angle, a cohesive failure will not necessarily exclude bond failure at other orientations, which are usually the weakest part in a repair composite.

(3) If the soundness can be guaranteed, the core pull-off and the core twist-off tests will usually predict the same trend in bond strength measurement, but the absolute values of bond strengths are different. The twist-off results tend to be higher than the pull-off results. The difference is much higher for a rough surface than a smooth surface.

(4) If the bond surface is very smooth, results obtained from the slant shear test can be very consistent, but if the bond surface is rough, the results can vary significantly depending on the method employed to produce the surface.

(5) A patch test can compare with other straight forward bond tests provided that: (a) the stress state induced over the bond interface, or at the critical position is similar to what will occur in the straight forward bond test method; and (b) the modulus mismatch is taken into consideration.

(6) In a patch test, the modulus mismatch affects the stress state in the substrate, the repair material, and the bond interface. The actual failure load depends on the relative level of stresses to their failure criteria. The maximum failure load will be achieved when the bond and the material (the weaker one of the substrate and the repair material) fail simultaneously. Thus a repair with no modulus mismatch may not produce the highest failure load.

(7) The selection of the bond test methods should be based on information about the deterioration, prevention of further deterioration, and the stress states which will be imposed over the bond interface. For the commonly experienced repairs, the damages are caused mainly due to corrosion of reinforcement, which will result in the form of spalling of concrete cover, etc. The tensile bond strength becomes very important in ensuring the success of the repair. Thus, a tensile bond test is the best method. For the purpose of direct comparison between laboratory results and site results, the core pull-off test should be preferred.

Table 5.0 Combinations relating to bond test methods

1	2	3	4	5	6	7	8	9	10	11	12	13	14	15	16	17	18	19	20
Repair materials		Sand/cement mortar				Acrylic modified mortar				SBR modified mortar				Flowing concrete				A2	Table & Figure number where test details can be found
Specimen types / Test parameters		CP	SS	PC	PF	CP	SS	PC	PF	CP	SS	PC	PF	CP	SS	PC	PF	CP	
Control specimens		x	x	x	x	x		x	x	x		x	x	x		x	x		T(5.1 5.2 5.4) F(5.31 5.43)
Surface roughness index	SM	x	x			x			x										T(5.1)(5.4) F(5.31)(5.43)
	MR	Standard surface roughness: medium rough																	
	RF	x	x			x			x										T(5.1)(5.4) F(5.31)(5.43)
Surface soundness	S	Standard surface soundness: sound																	
	W	x	x																T(5.4)
Surface cleanliness	CL	Standard surface cleanliness: clean																	
	CT	x	x			x				x				x				x	T(5.2)
Moisture condition	SW																		Note: T(5.2) means Table (5.2), and F(5.31) means Figure (5.31)
	SD																		
	AW	Standard moisture condition: air dry surface wet																	
	AD																		
	BW																		
	BD																		
Applying methods	HA	Standard applying method: by hand																	
	VB																		
Bond coat mistiming	NO	Standard parameter: no mistiming of bond coat																	
	40																		
Repair mortar mistiming	NO	Standard parameter: no mistiming of repair mortar																	
	40																		
Curing methods	NO																		
	3d	Standard curing method: moist curing for three days																	
High temperature curing followed by drying shrinkage																			
High temperature curing followed by thermal cycling																			
Low temperature curing																			
Low temperature curing followed by freeze/thaw cycling																			

Note: **Control specimens**: the parameters for control specimens are indicated by each standard parameter.

Bond test method:

CP: core pull-off test; SS: slant shear test;
PC: patch compressive test; PF: patch flexural test;

Parameters of workmanship:

SM: smooth surface; MR: medium rough surface;
RF: rough surface
S: sound surface; W: weak surface;
CL: clean surface; CT: contaminated surface;
SW: saturated surface wet; SD: saturated surface dry;
AW: air dry surface wet; AD: air dry surface dry;
BW: bond dry surface wet; BD: bond dry surface dry;
HA: Hand applied without vibration; VB: hand applied with vibration;
NO: no mistiming in mistiming group or no curing in curing group;
40: about 40 min. mistiming 3d: 3d moist curing ;
A2: light weight acrylic modified mortar

Table 5.1 Effect of surface roughness on the tensile bond strength

Surface roughness	Age (days)		Bond strength (MPa)	Number of tests	Number of bond failures
	substrate	mortar			
Smooth	37	30	0.27	5	5
Slightly rough	37	30	1.54	5	5
Rough	35	28	1.76	5	5

Table 5.2 Effect of surface contamination on the tensile bond strength

Repair material	Contaminated			Control		
	SRI (mm)	Age (days) (M)	Bond strength (MPa)	SRI (mm)	Age (days) (M)	Bond strength (MPa)
S/C	230	28	0.34	230	28-31	1.53
A1	230	35	0.77	285	41	2.85
SBR	230	28	0.43	230	28	1.53
F	200	28	0.98	200	28	2.03
A2	230	28	0.76	230	28	1.73

Table 5.3 Effect of coring depth into the substrate on the tensile bond strength

Age (days)		SRI (mm)	Moisture condition	Failure load (MPa)	Coring depth (mm)	Stress ratio	Notes
substrate	mortar						
80	31	285	SD	2.51	1-2	0.82	sand blasted surface
85	36	285	SD	3.06	15		
148	31	210	SD	1.61	1-2	0.78	Set retarder produced surface
148	31	210	SD	2.06	15		

Table 5.4 Effect of surface roughness and cleanliness on the slant shear test results

Surface roughness	Surface preparation method	Surface cleanliness	Age (days)		Failure stress (MPa)
			substrate	mortar	
rough	LS-NT	clean	70	28	49.5
rough	LS-WB	clean	56	28	45.6
smooth	FM-NG	clean	112	14	26.0
rough	FM-SB	clean	97	14	50.4
rough	FM-SB	contaminated	97	14	42.0

Table 5.5 Comparison between the predicted and measured failure load of the unrepaired patch compressive specimens

Age (days)	f_c (MPa)	Predicted failure load, Po (KN)	Measured failure load, P (KN)	P/Po	Note
28	53.1	199	251	1.26	With loading plate
28	53.1	199	227	1.14	
28	53.1	199	227	1.14	
28	53.1	269	316	1.17	Without loading plate
28	53.1	269	282	1.05	
28	53.1	269	301	1.12	

Table 5.6 Comparison between the predicted and measured failure load of the unrepaired patch flexural specimens

Age (days)	f_c (MPa)	f_t (MPa)	Predicted failure load Po (KN)	Measured failure load P (KN)	Po/P
28	51.2	6.80	6.47	5.56	1.16
37	51.2	6.80	6.47	6.05	1.07
43	51.2	6.80	6.47	5.91	1.09
139	58.4	7.26	6.91	7.15	0.97
176	58.4	7.26	6.91	7.17	0.96
188	58.4	7.26	6.91	6.33	1.09
28	51.2	6.80	11.5	9.4	1.22
139	58.4	7.26	12.3	12.1	1.02

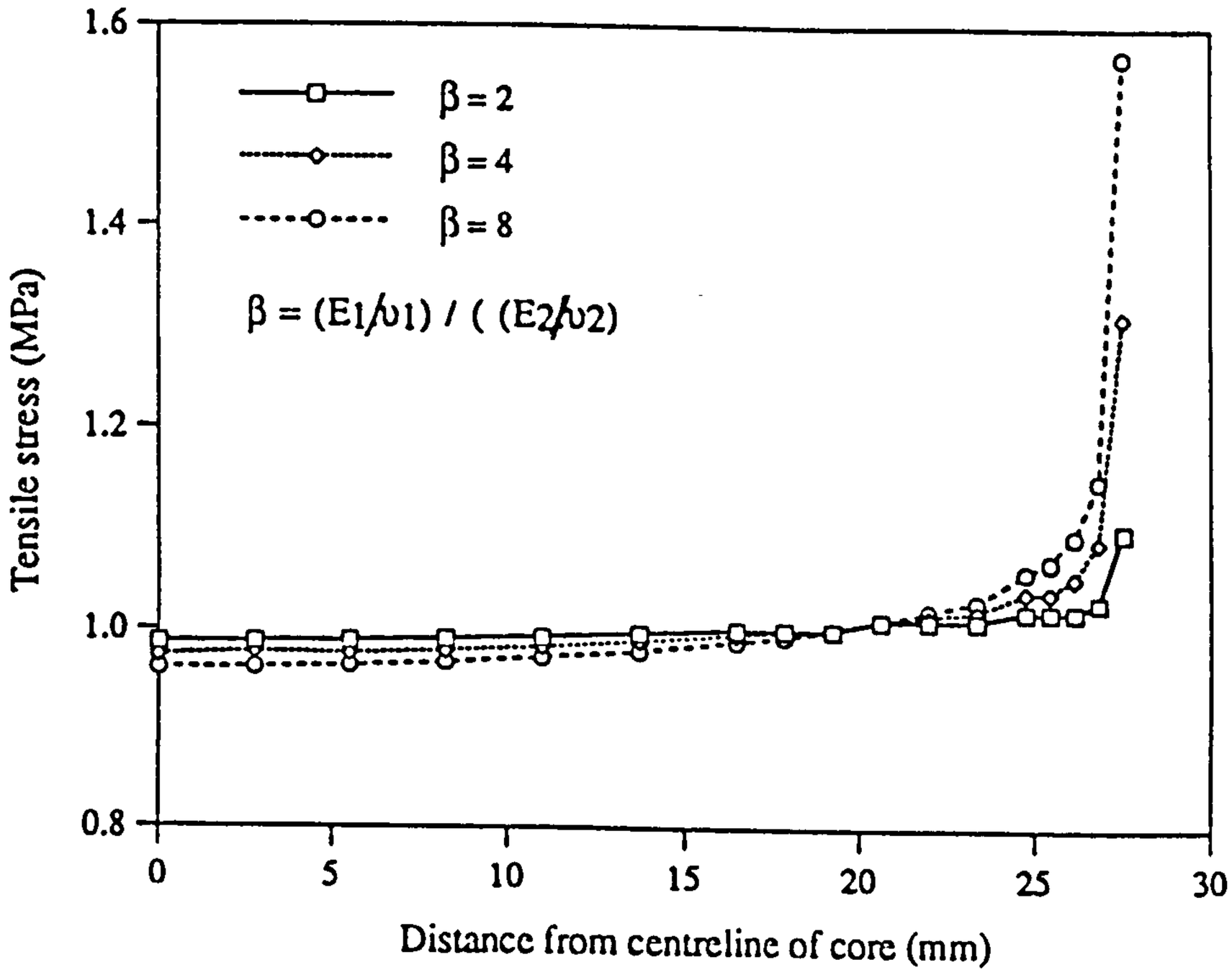

Figure 5.1 Stress distribution in a tensile bond test due to modulus mismatch

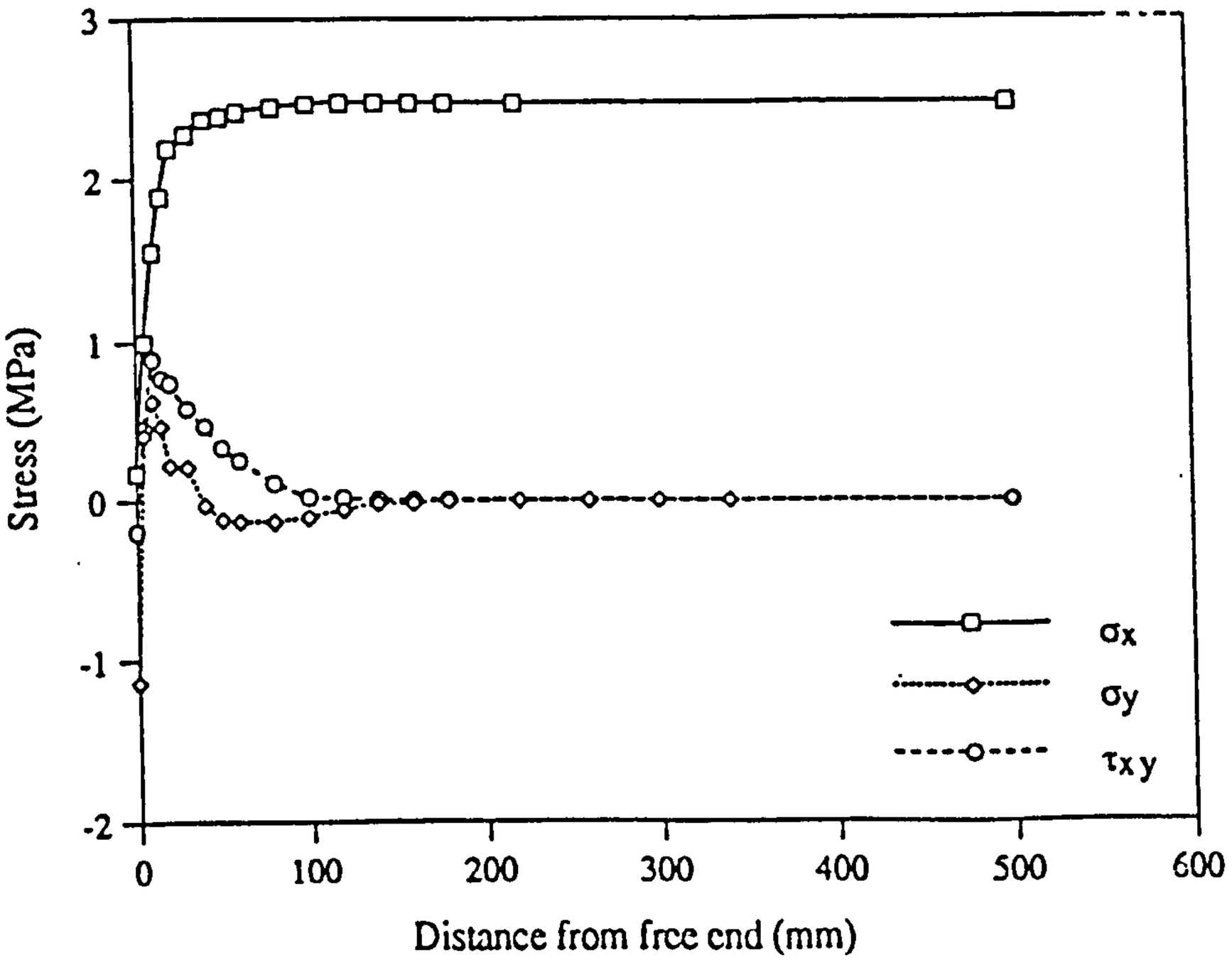

Figure 5.2 Stress distribution over the bond interface due to differential shrinkage

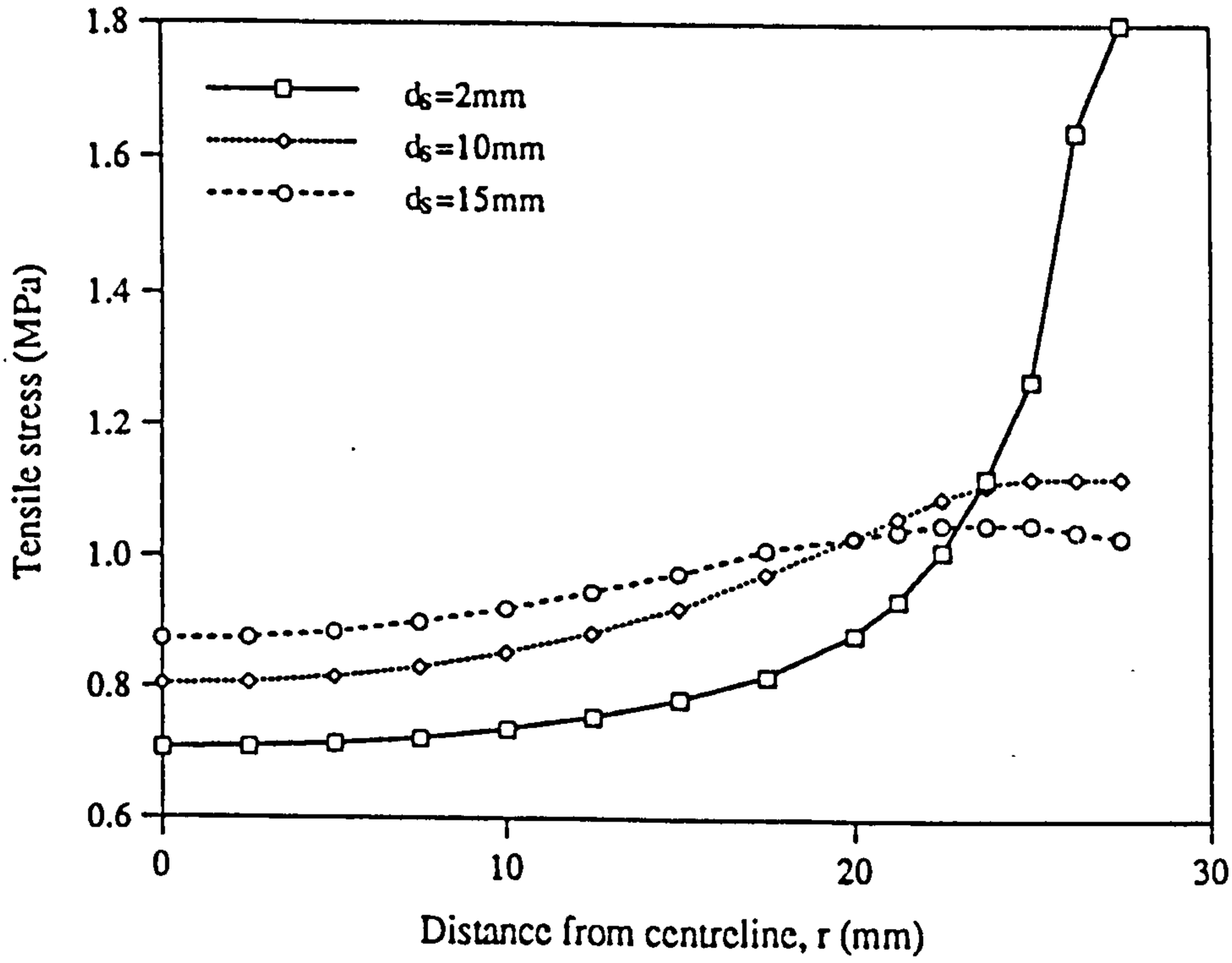

Figure 5.3 Effect of coring depth into the substrate on stress distribution over the bond interface

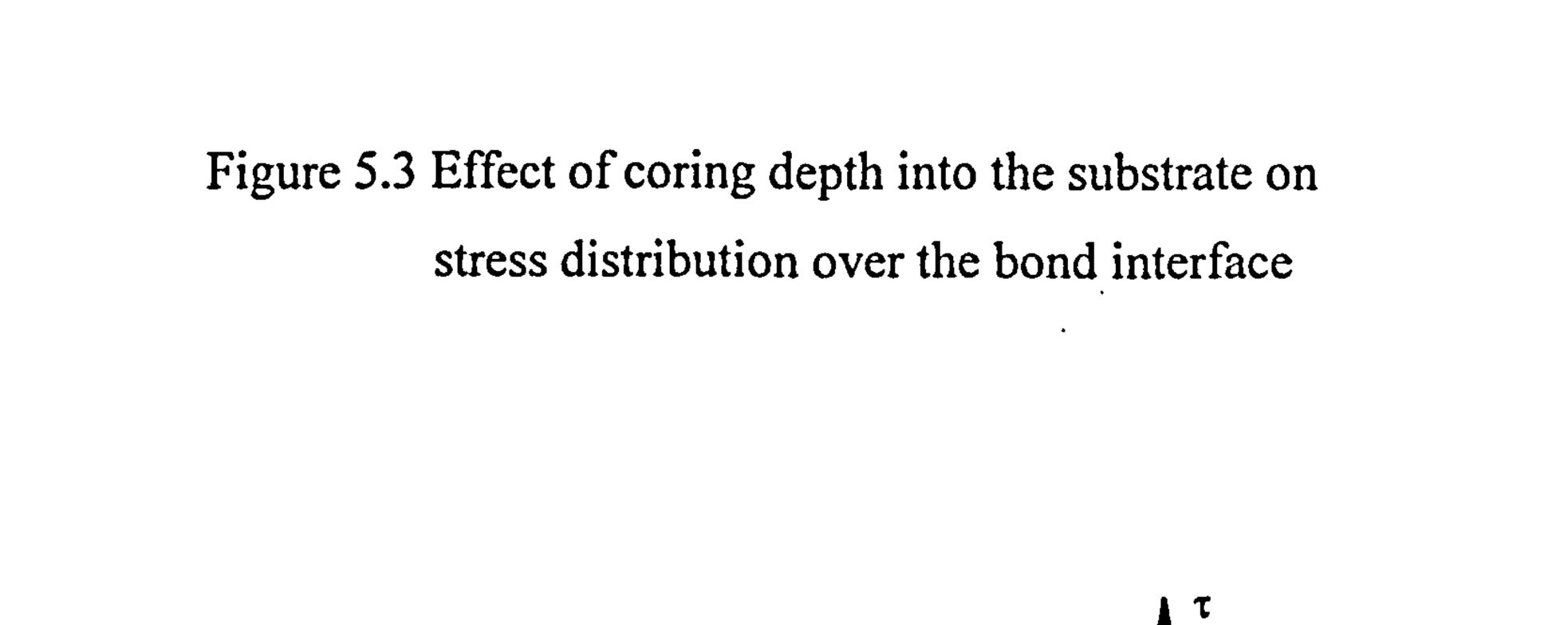

Figure 5.4 Mohr's circle of stresses

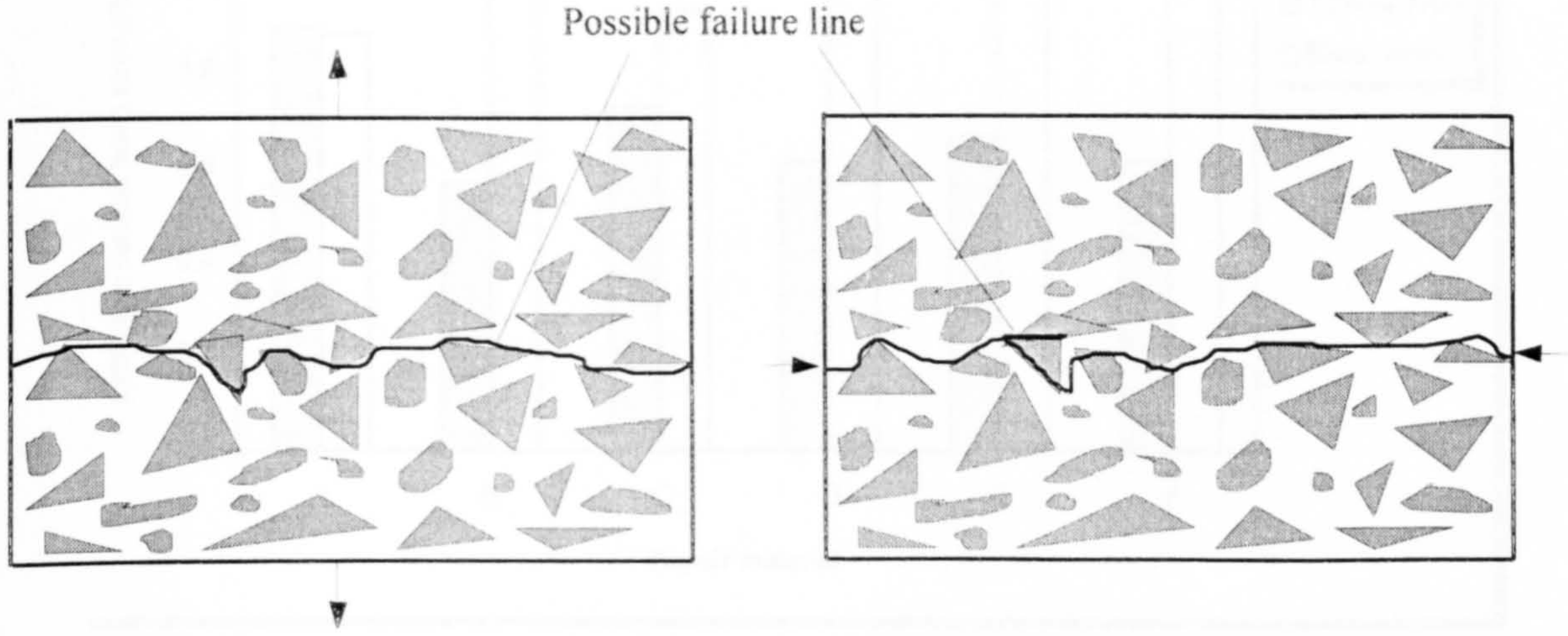

a) under a tensile stress

b) under a shear stress

Figure 5.5 Solid concrete under tensile and shear stresses

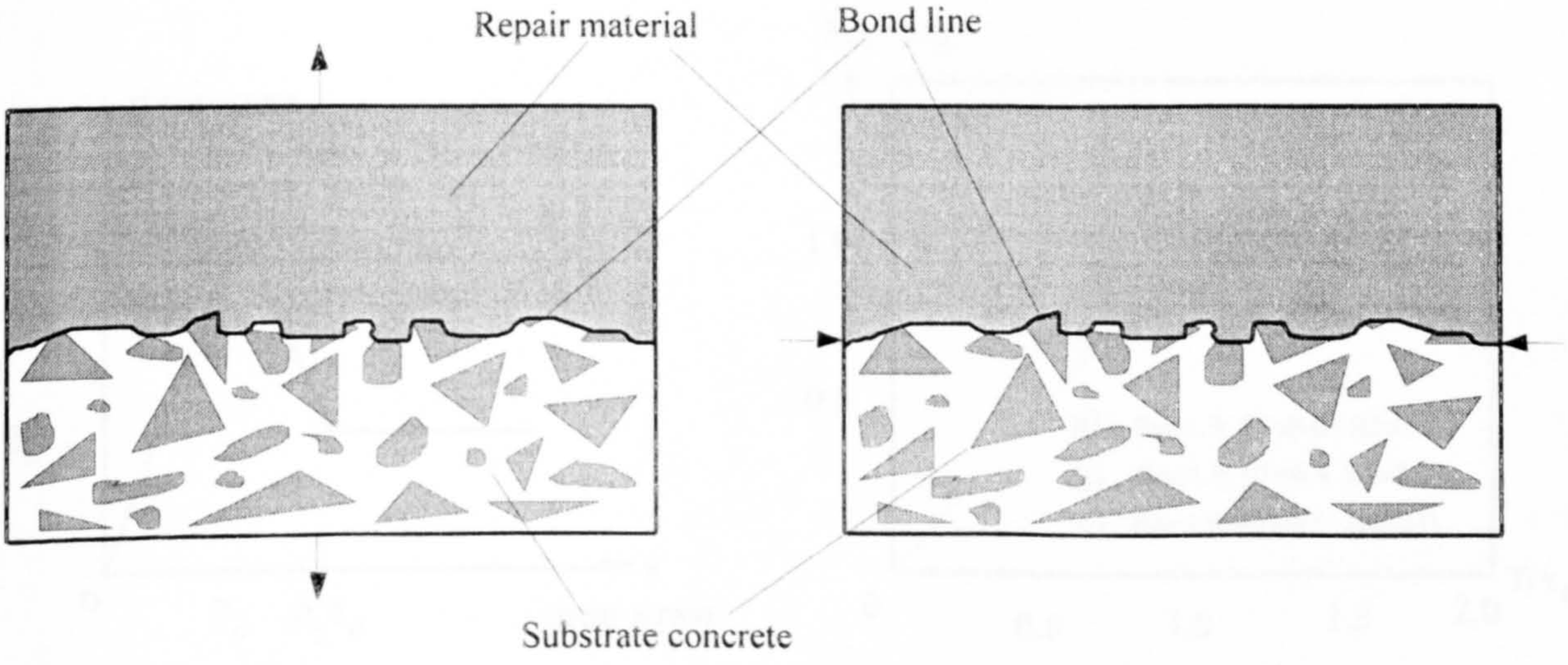

a) under a tensile stress

b) under a shear stress

Figure 5.6 A repair element under the tensile and shear stresses

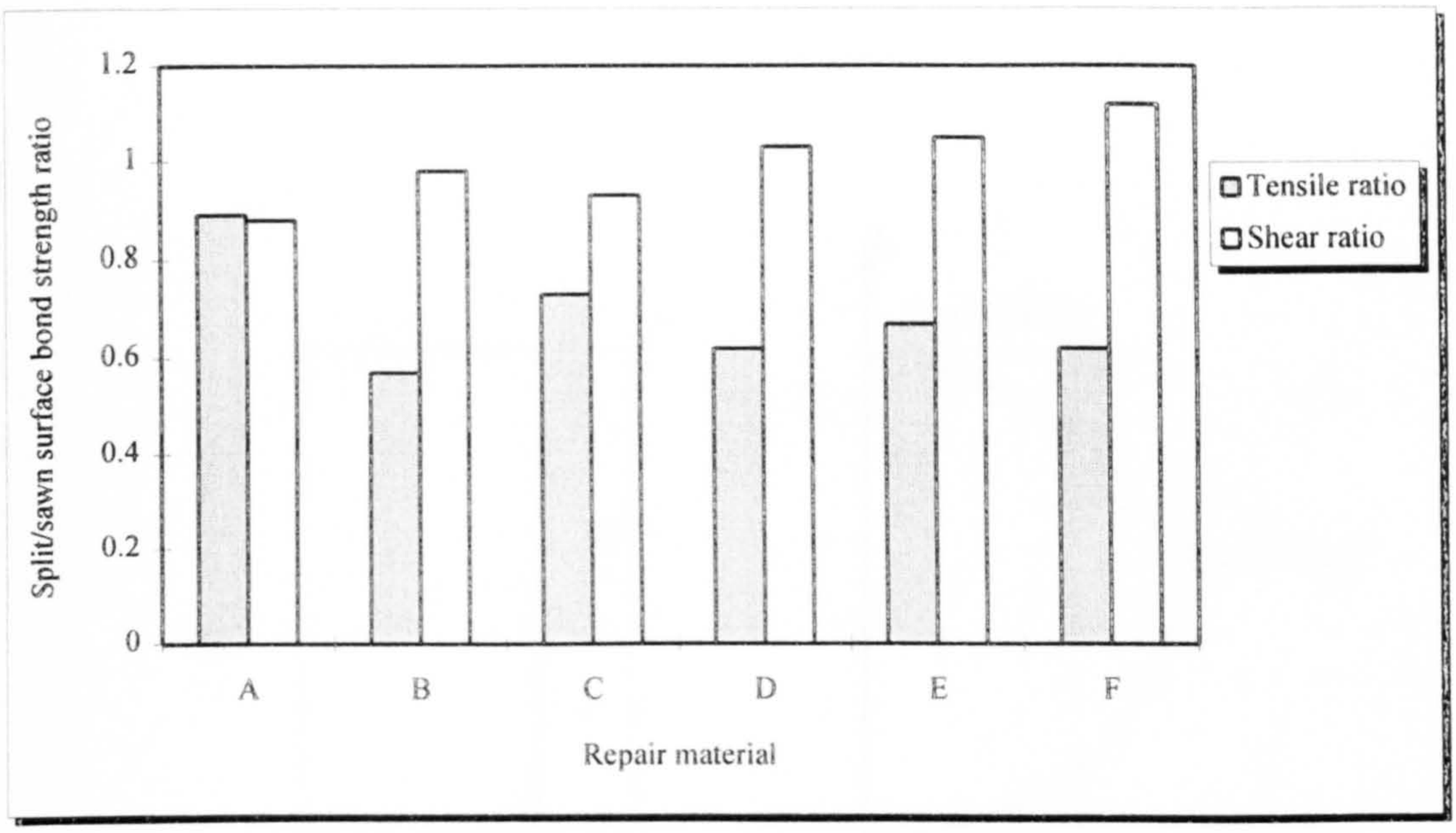

Note: A: SBR mortar; B: plain mortar; C: acrylic mortar; D: plain mortar + OPC bond coat; E: plain mortar + acrylic bond coat; F: plain mortar + epoxy bond coat

Figure 5.7 Effect of surface defects on tensile bond strength

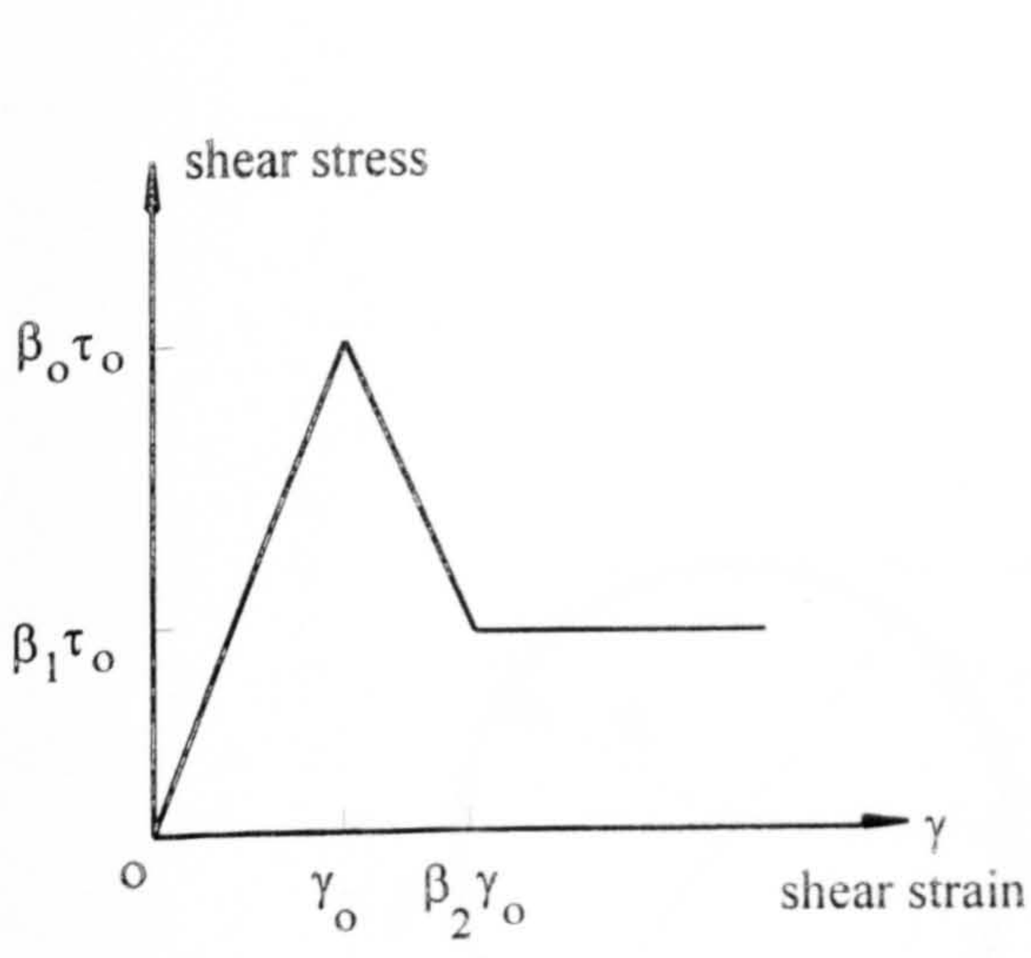

a) Bond shear stress - shear strain relationship

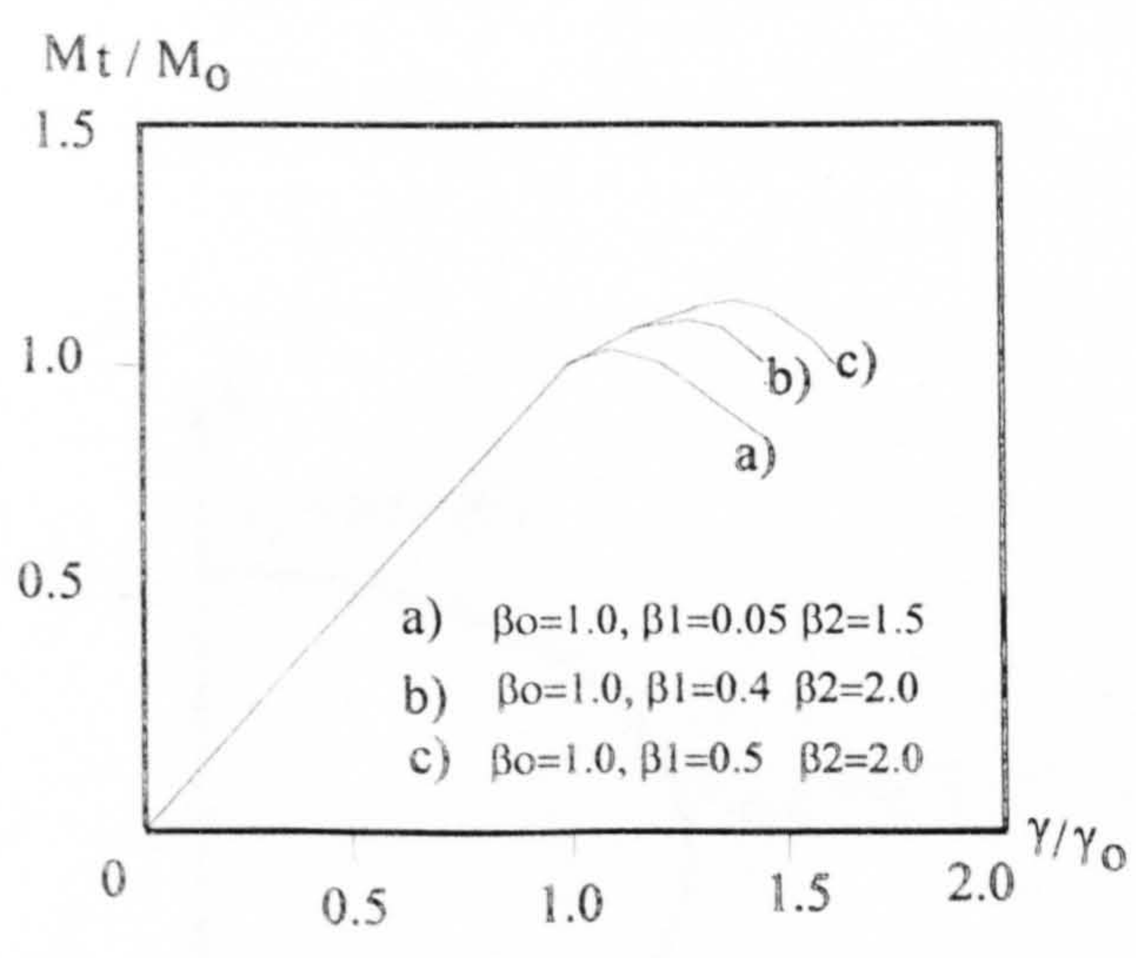

b) Increase in twisting moment due to post peak resistance compared with elastic prediction

Figure 5.8 Effect of post-peak resistance on failiure load of twist-off test

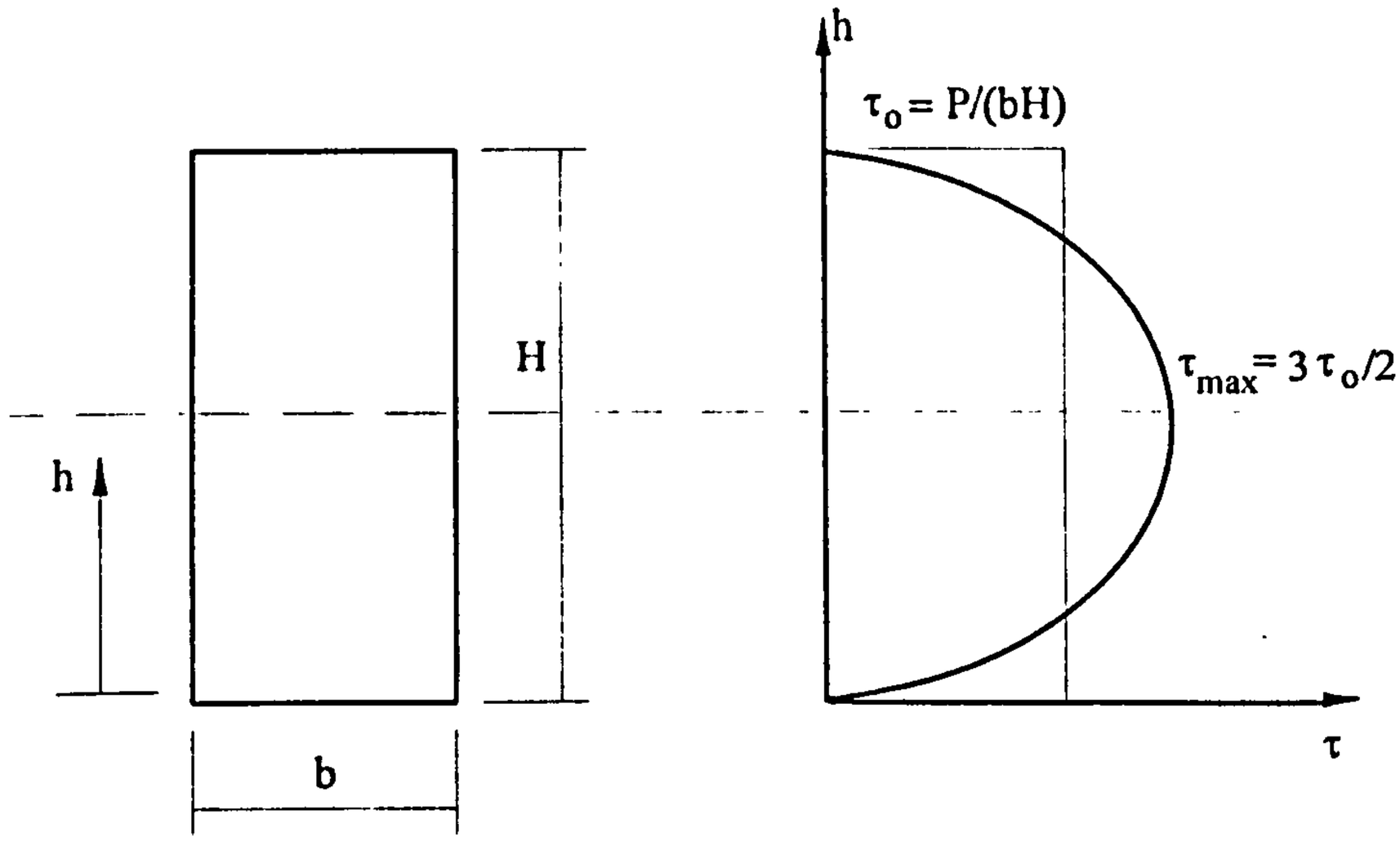

Figure 5.9 Shear stress distribution in a direct shear bond test using a rectangular cross section

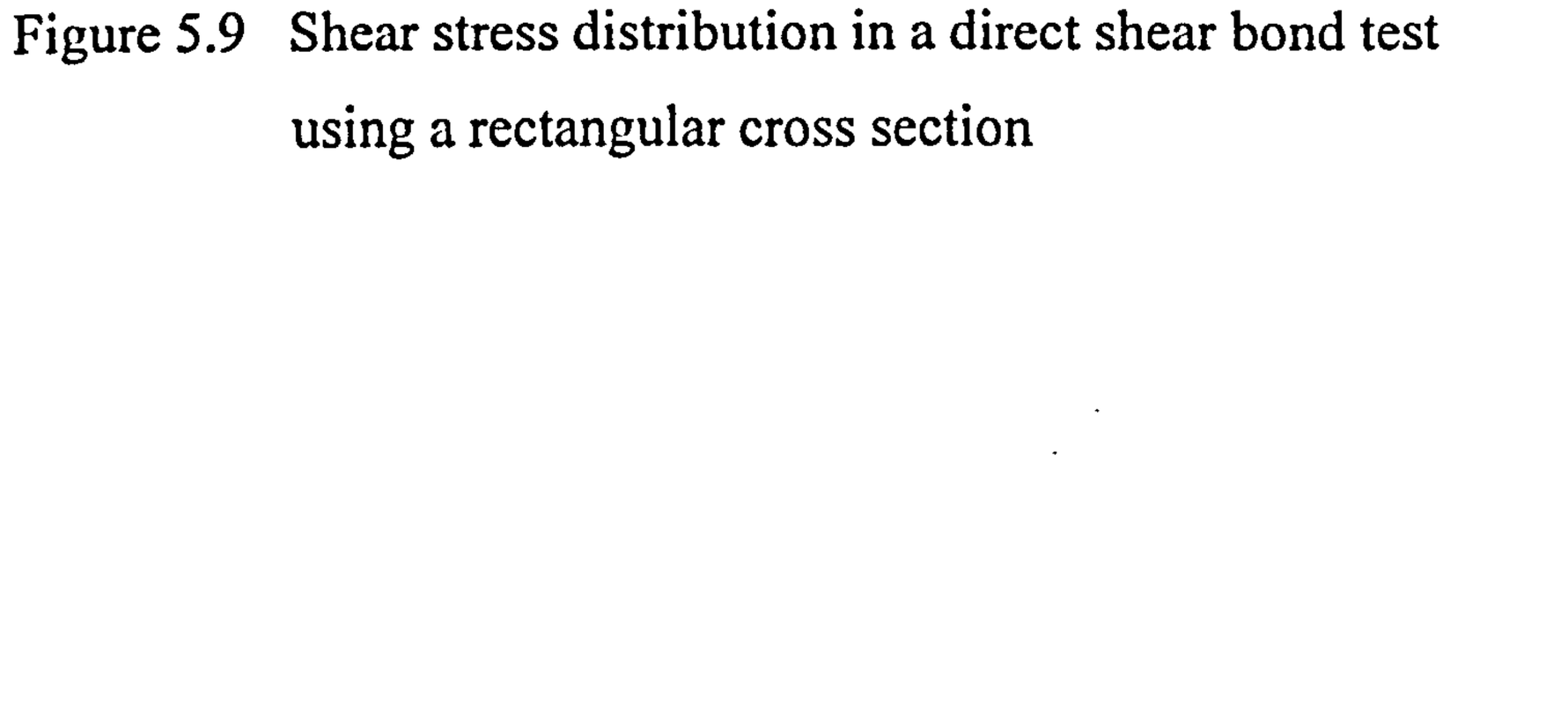

Figure 5.10 Shear stress distribution in a direct shear bond test using a circular cross section

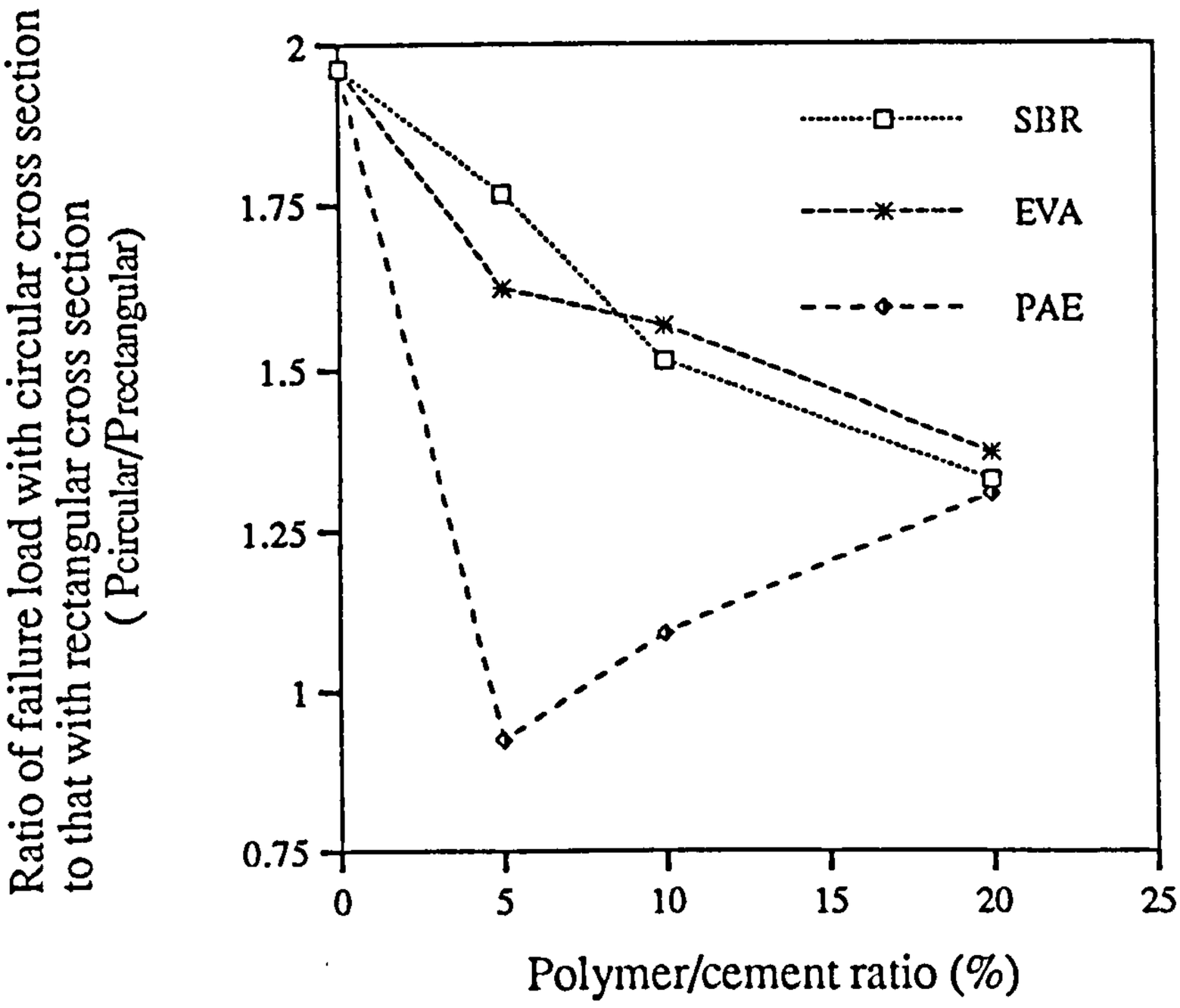

Fig.5.11 Effect of the shape of bond interface on shear bondstrength
(Results from ref.[14])

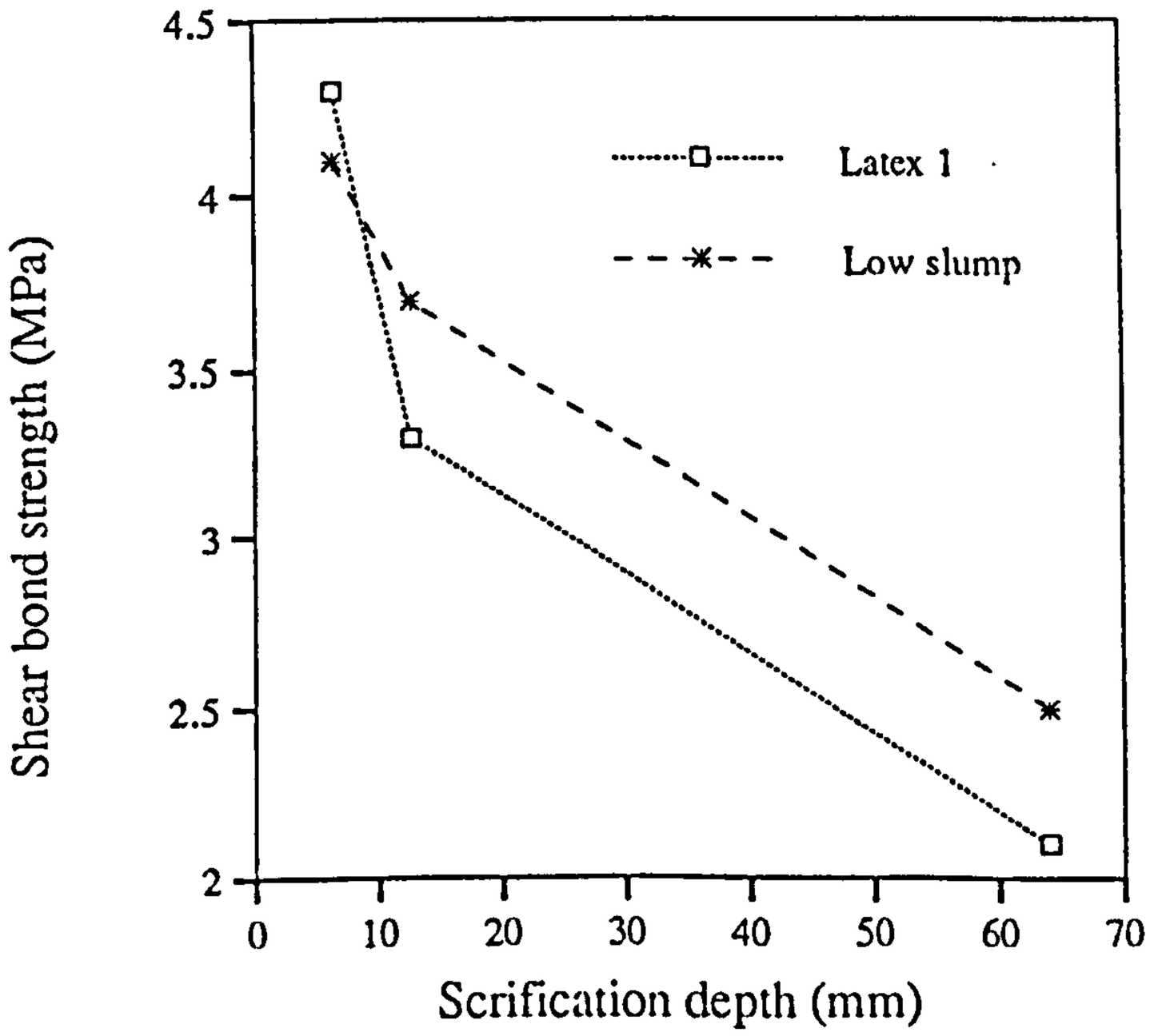

Fig. 5.12 Effect of scarification depth on shear bond strength
(Results from [85])

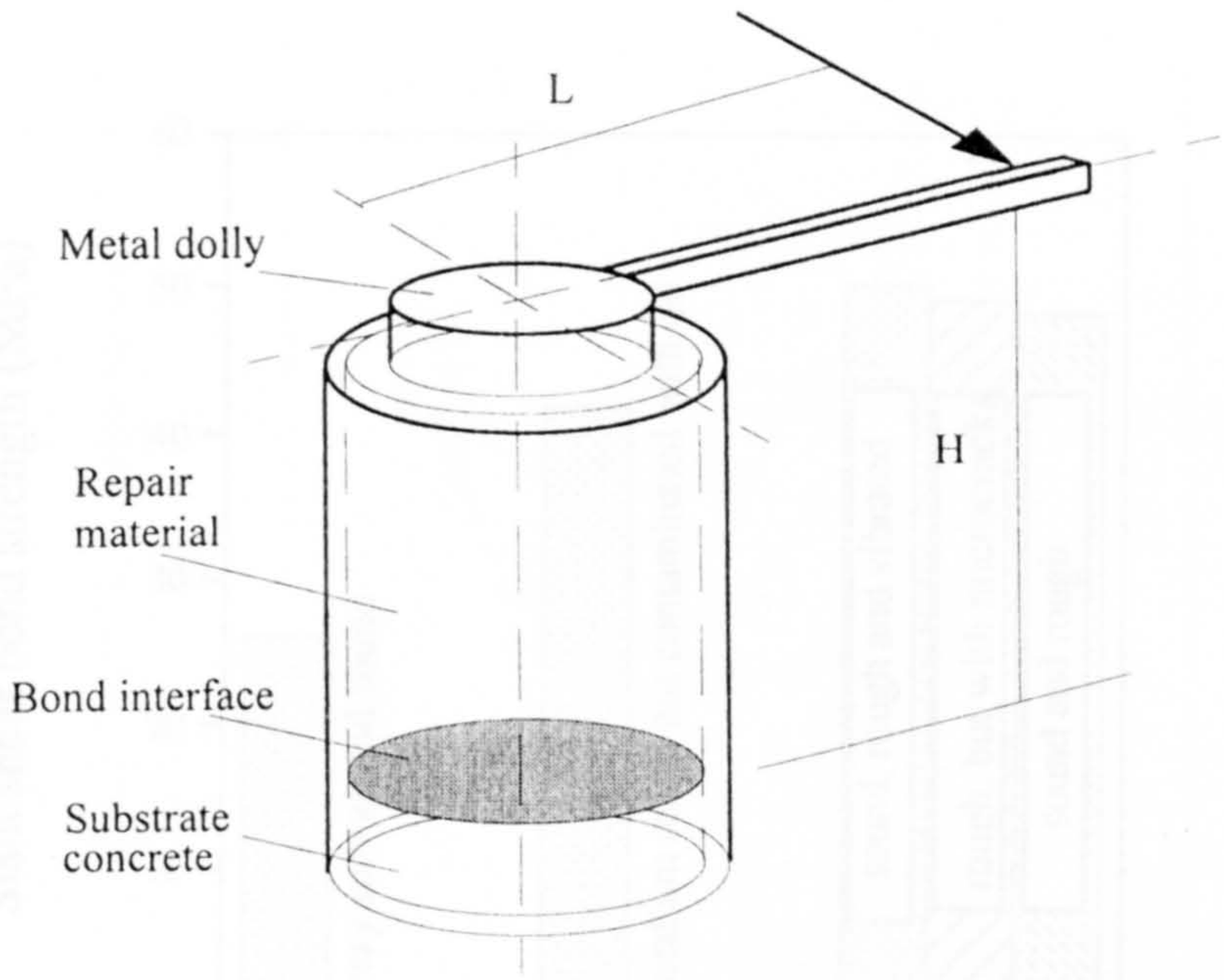

Figure 5.13 Twist-off shear bond test

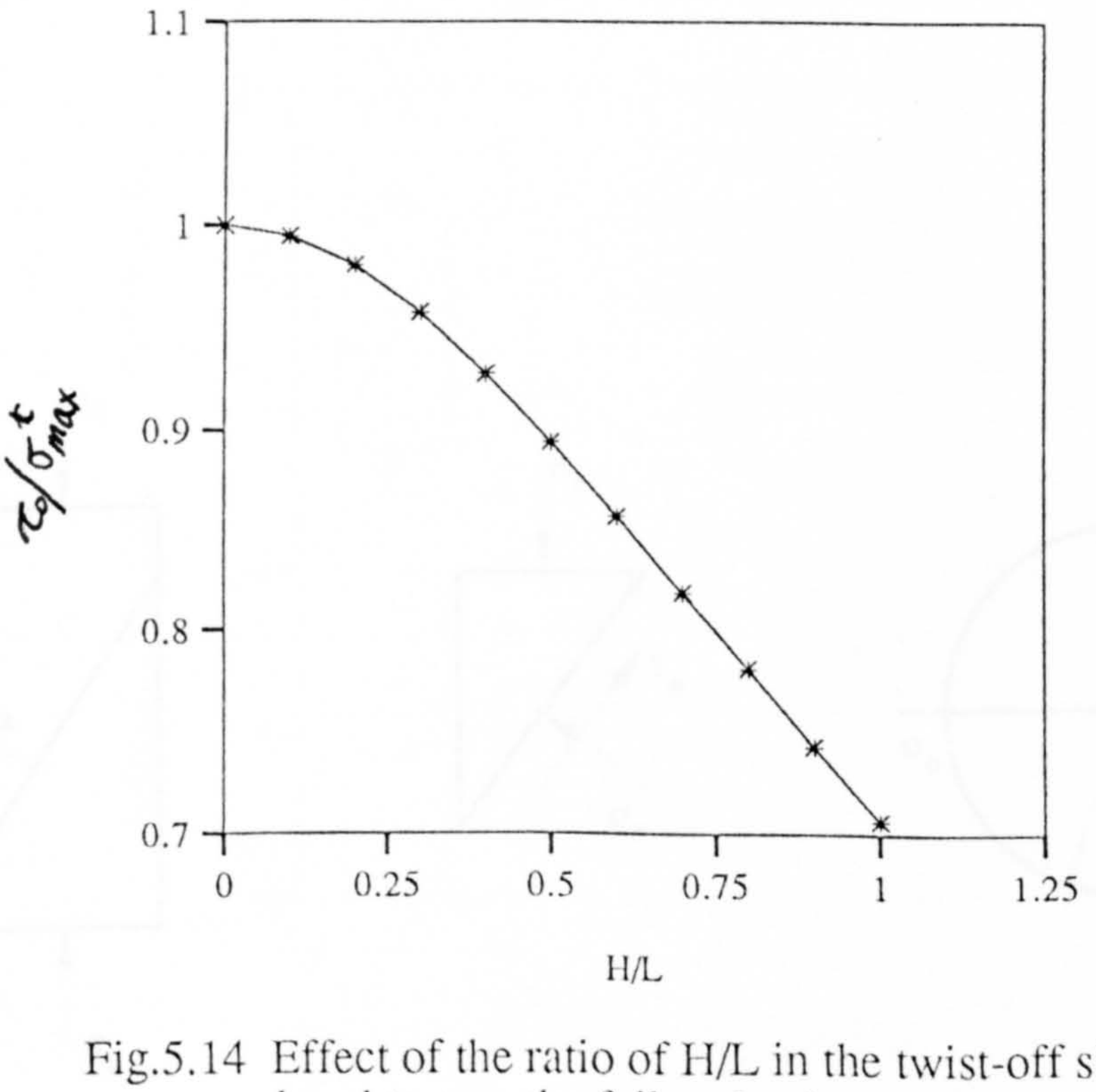

Fig.5.14 Effect of the ratio of H/L in the twist-off shear bond test on the failure load

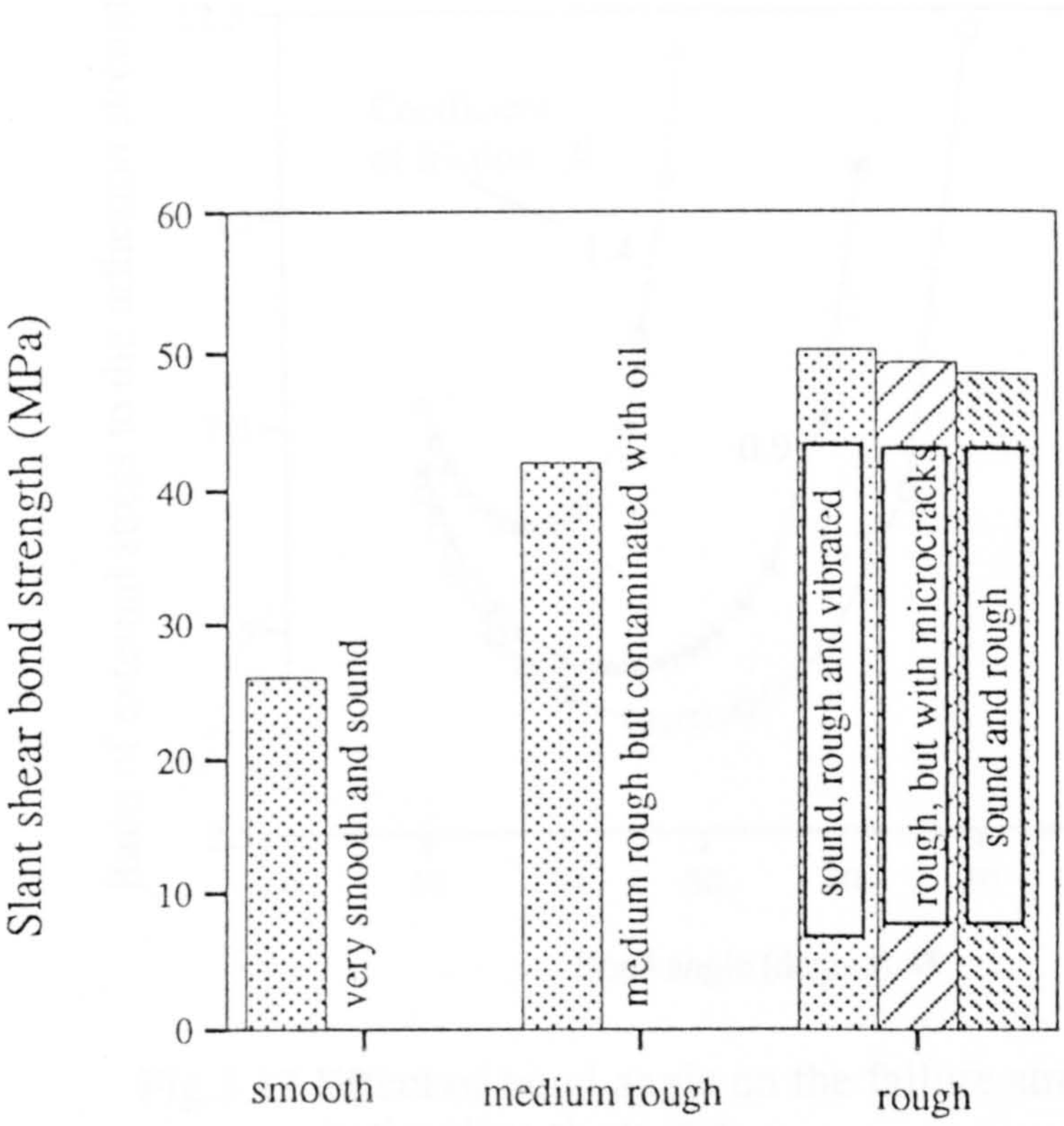

Fig.5.15 Effect of surface soundness and roughness on the slant shear bond strength

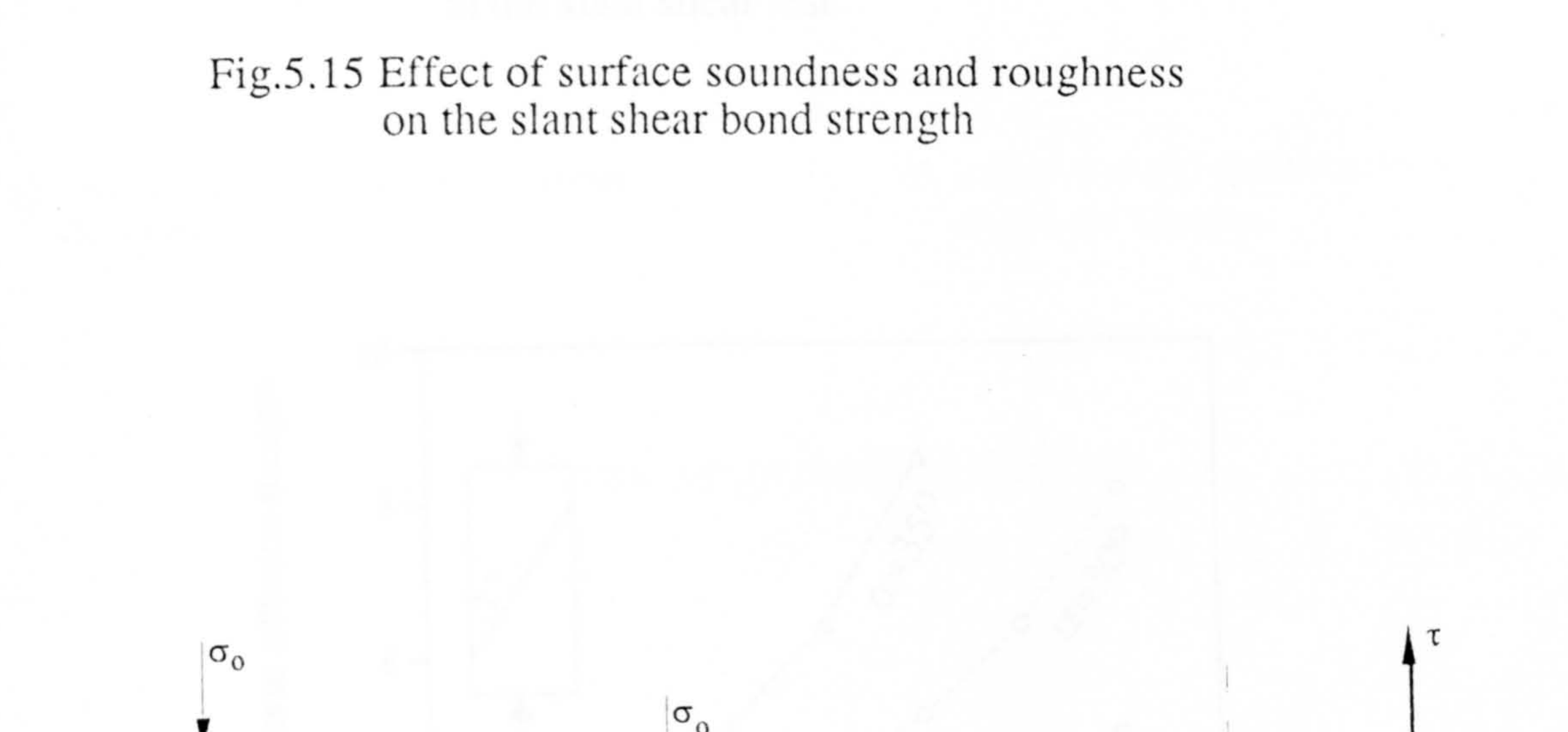

Figure 5.16 Stress state in a slant shear specimen

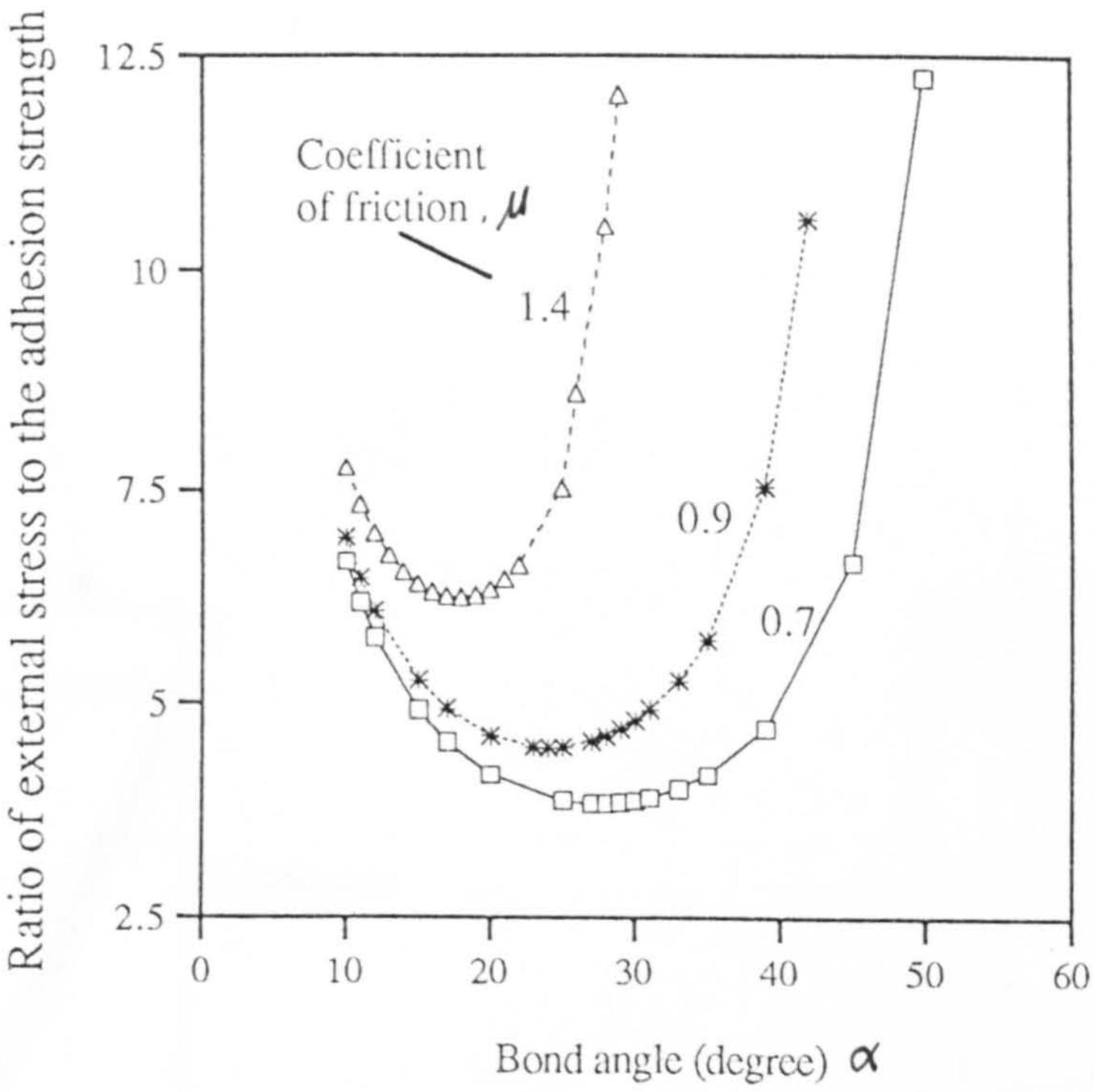

Fig.5.17 Effect of bond angle on the failure stress in the slant shear test

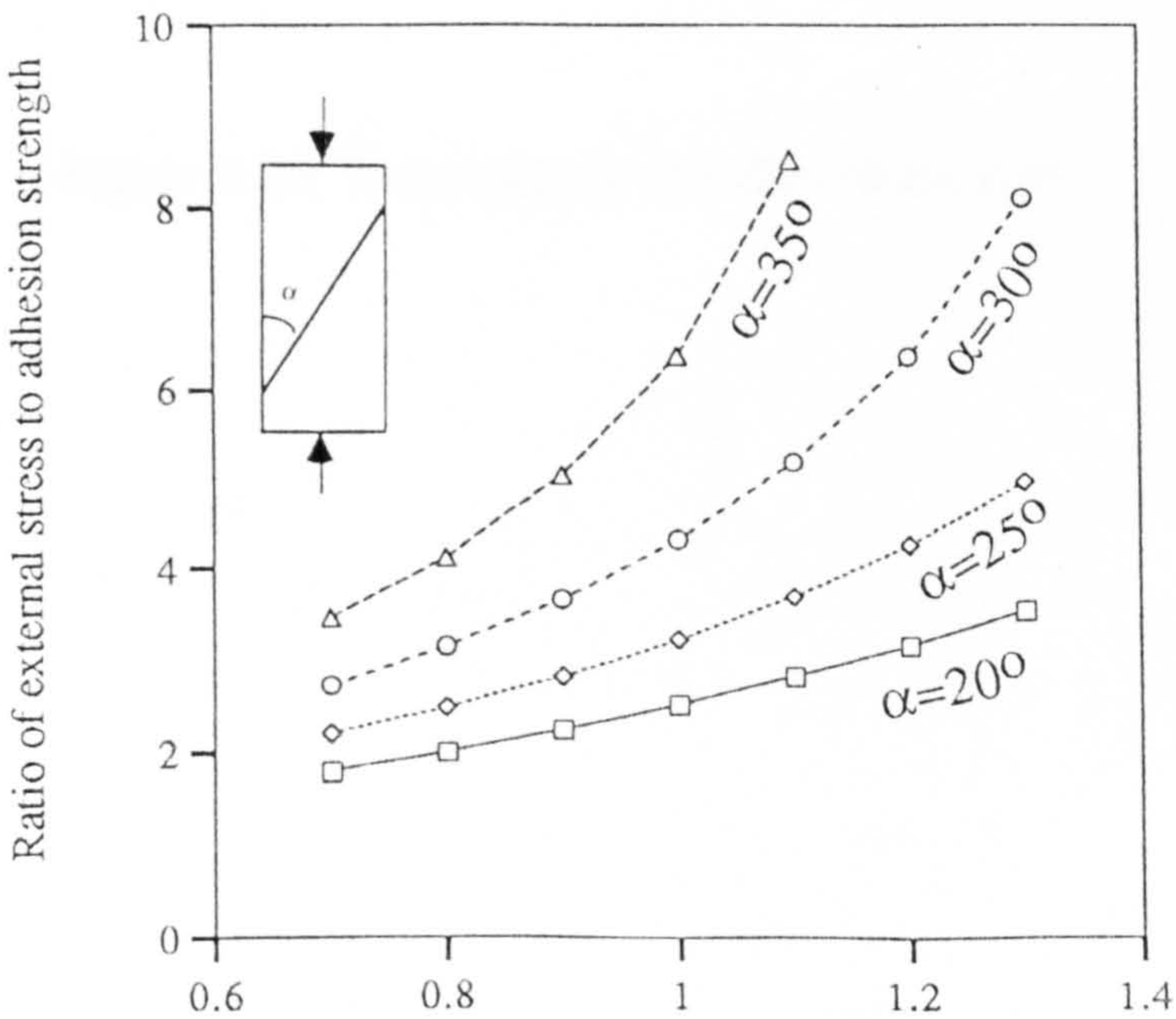

Fig. 5·18 Effect of surface roughness on shear/compression test

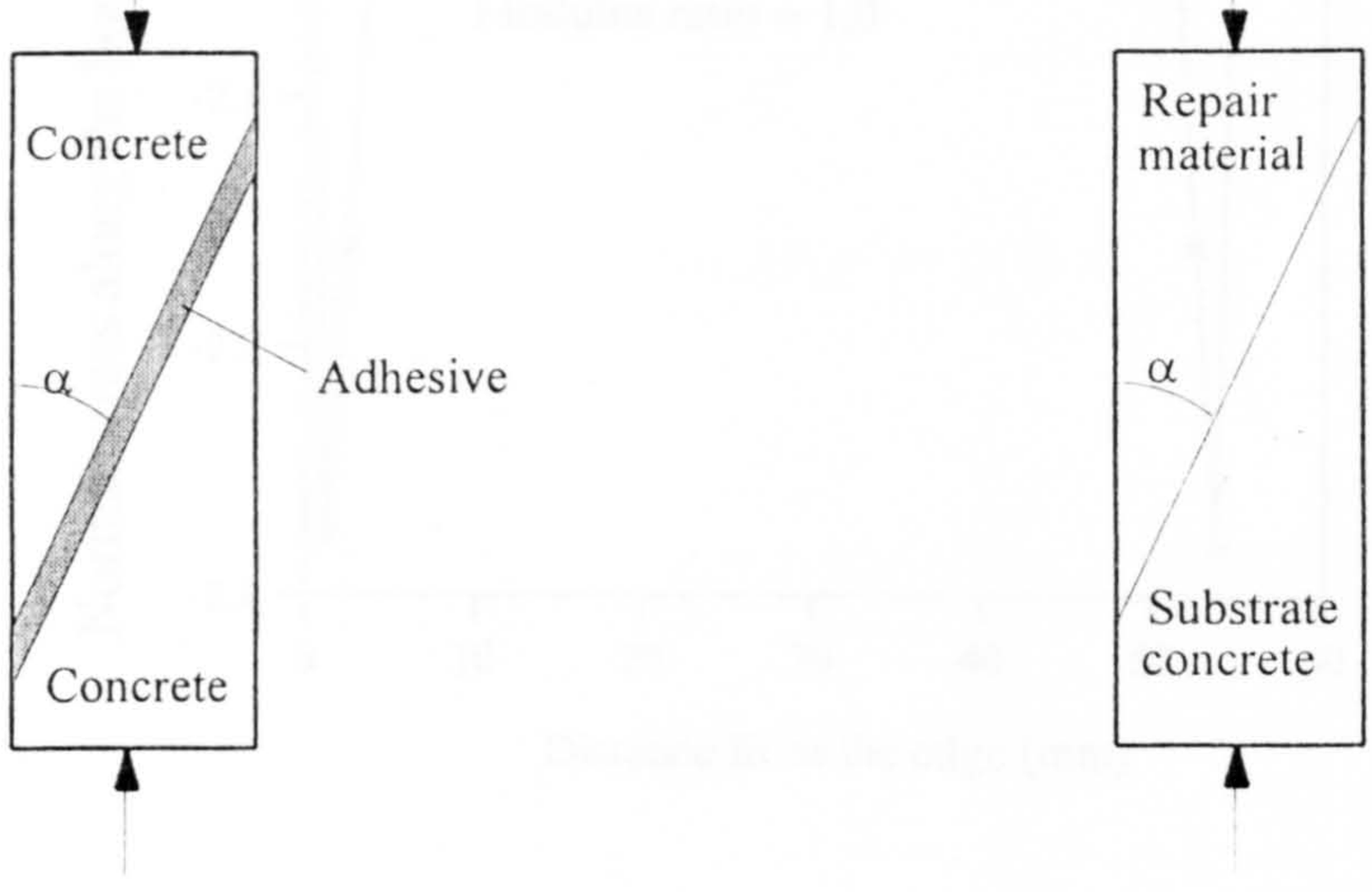

a) Two concrete blocks bonded together by an adhesive

b) Repair material applied onto a substrate concrete

Figure 5.19 Two cases in the slant shear test

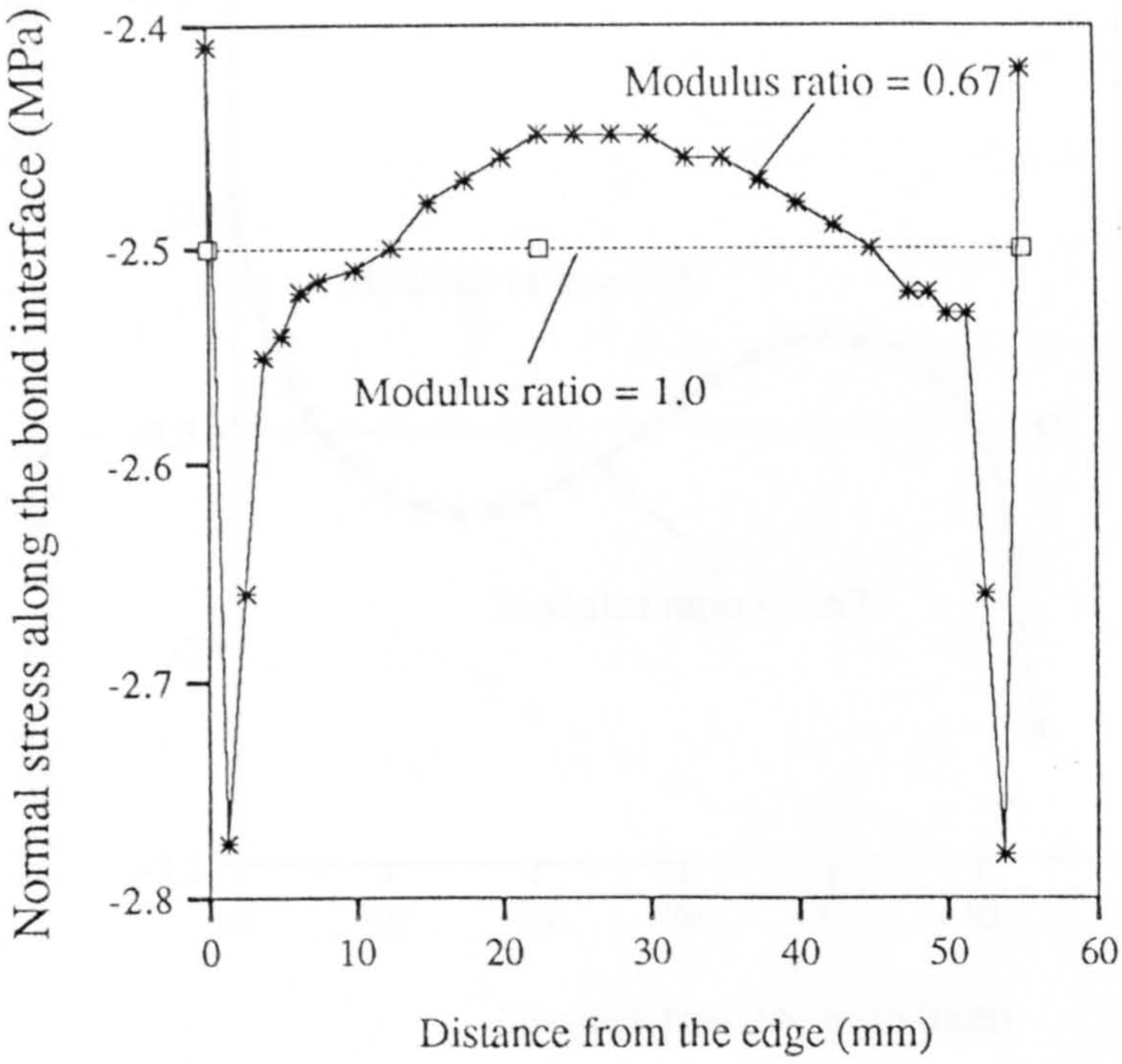

a)

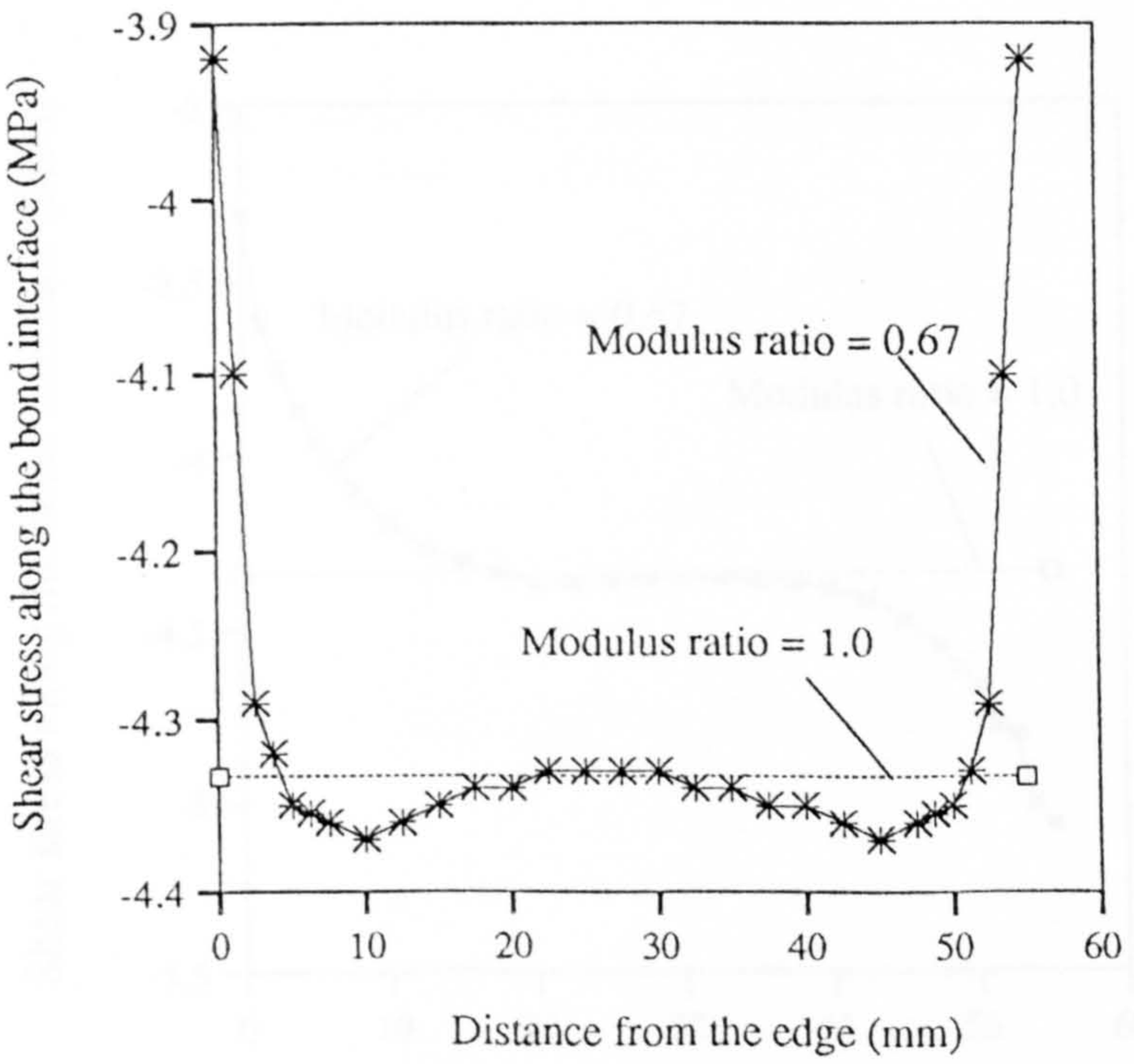

b)

Fig.5.20 Effect of modulus mismatch on stress distribution when two concrete blocks are bonded together by an adhesive

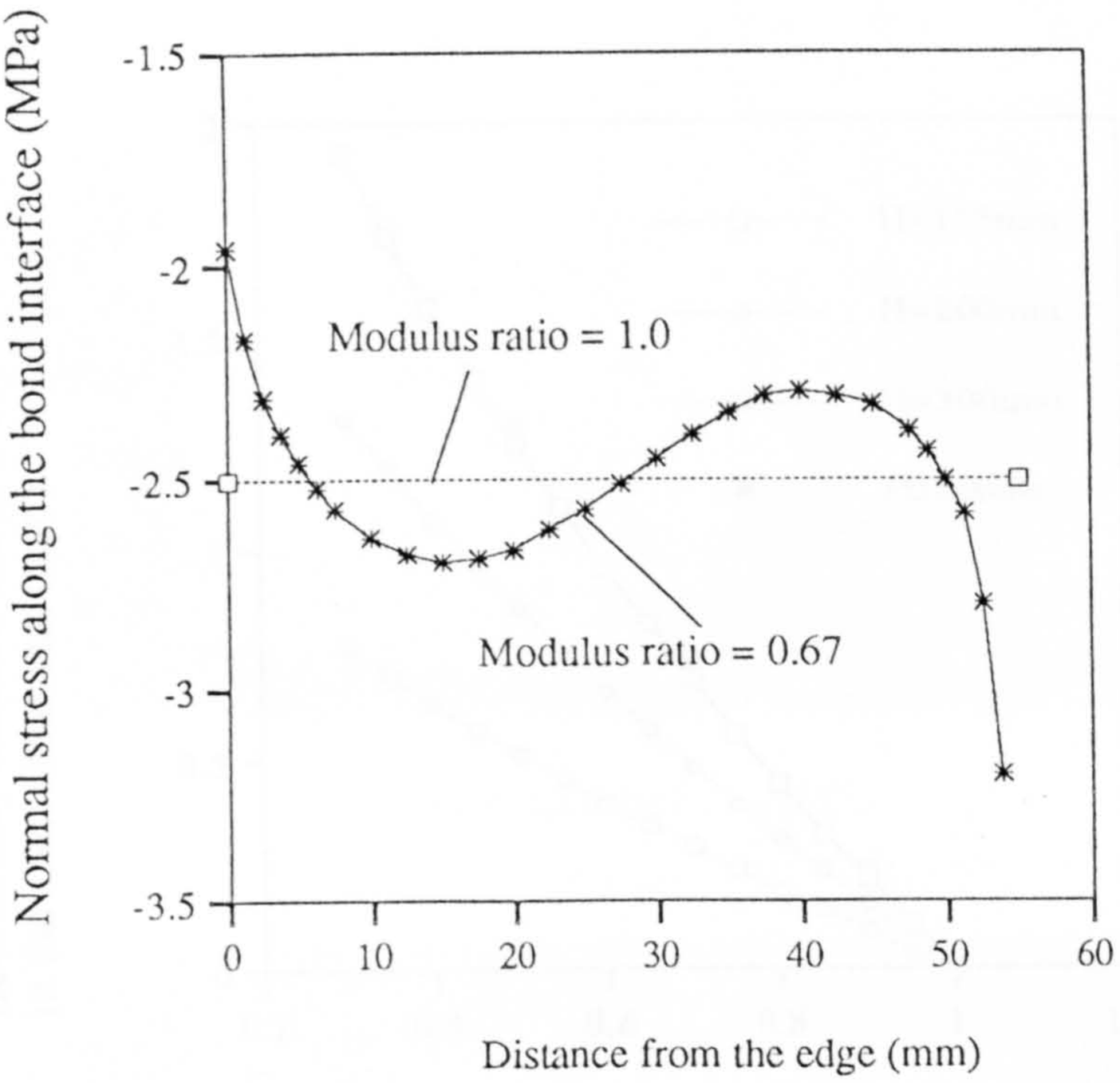

a)

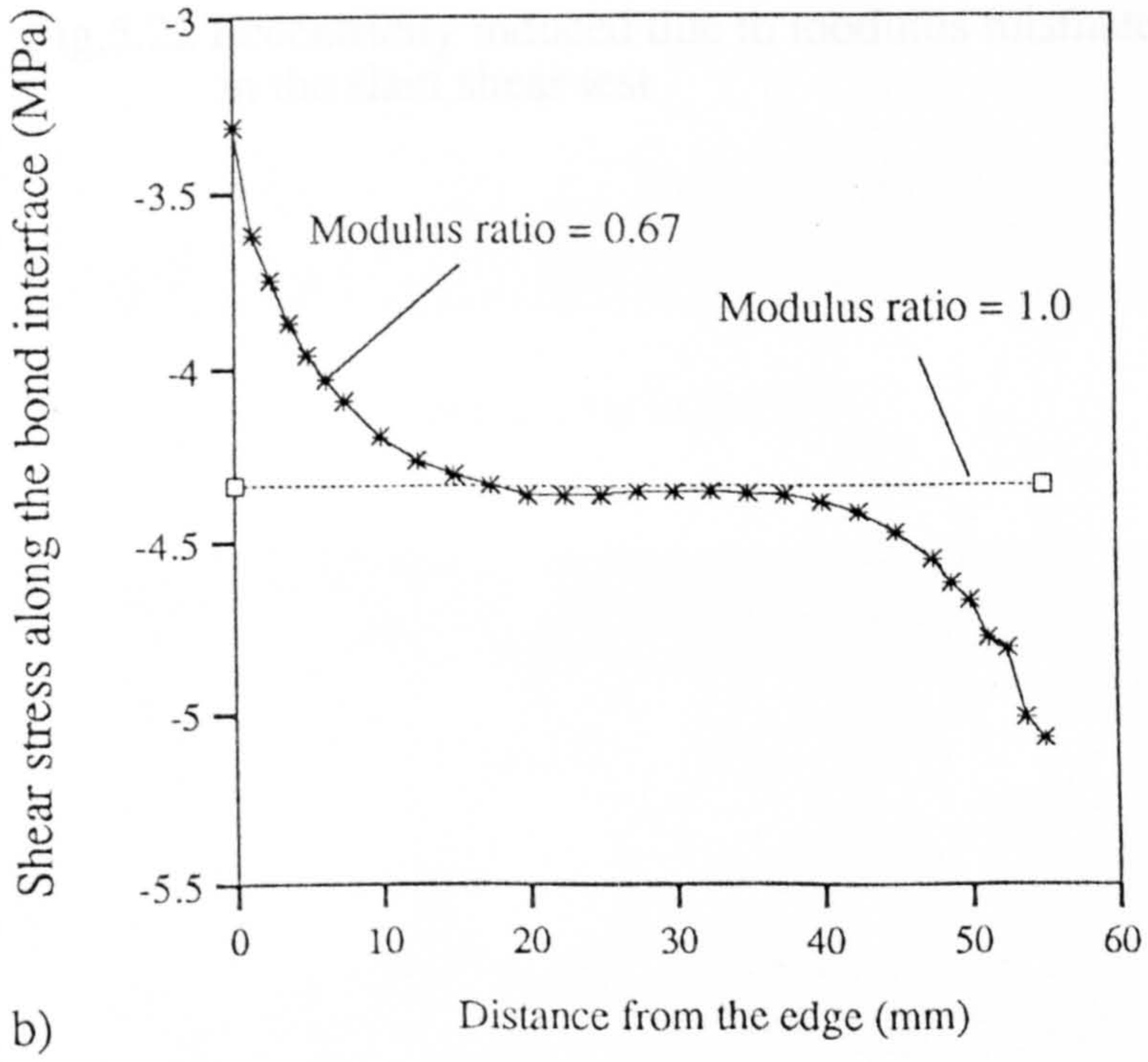

b)

Fig.5.21 Effect of modulus mismatch on stress distribution along the bond interface in a slant shear test when a repair material is applied onto a substrate

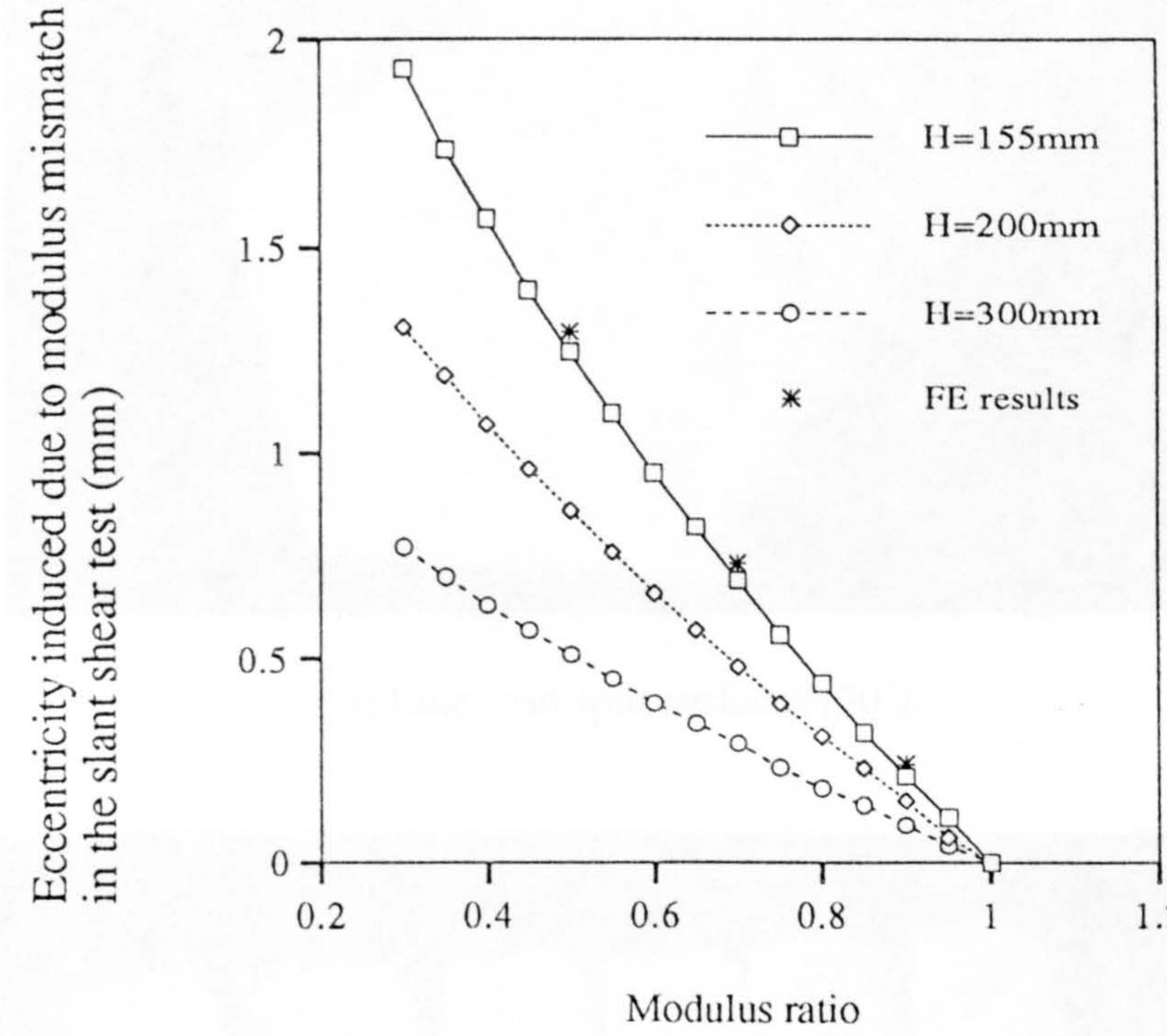

Fig.5.22 Eccentricity induced due to modulus mismatch in the slant shear test

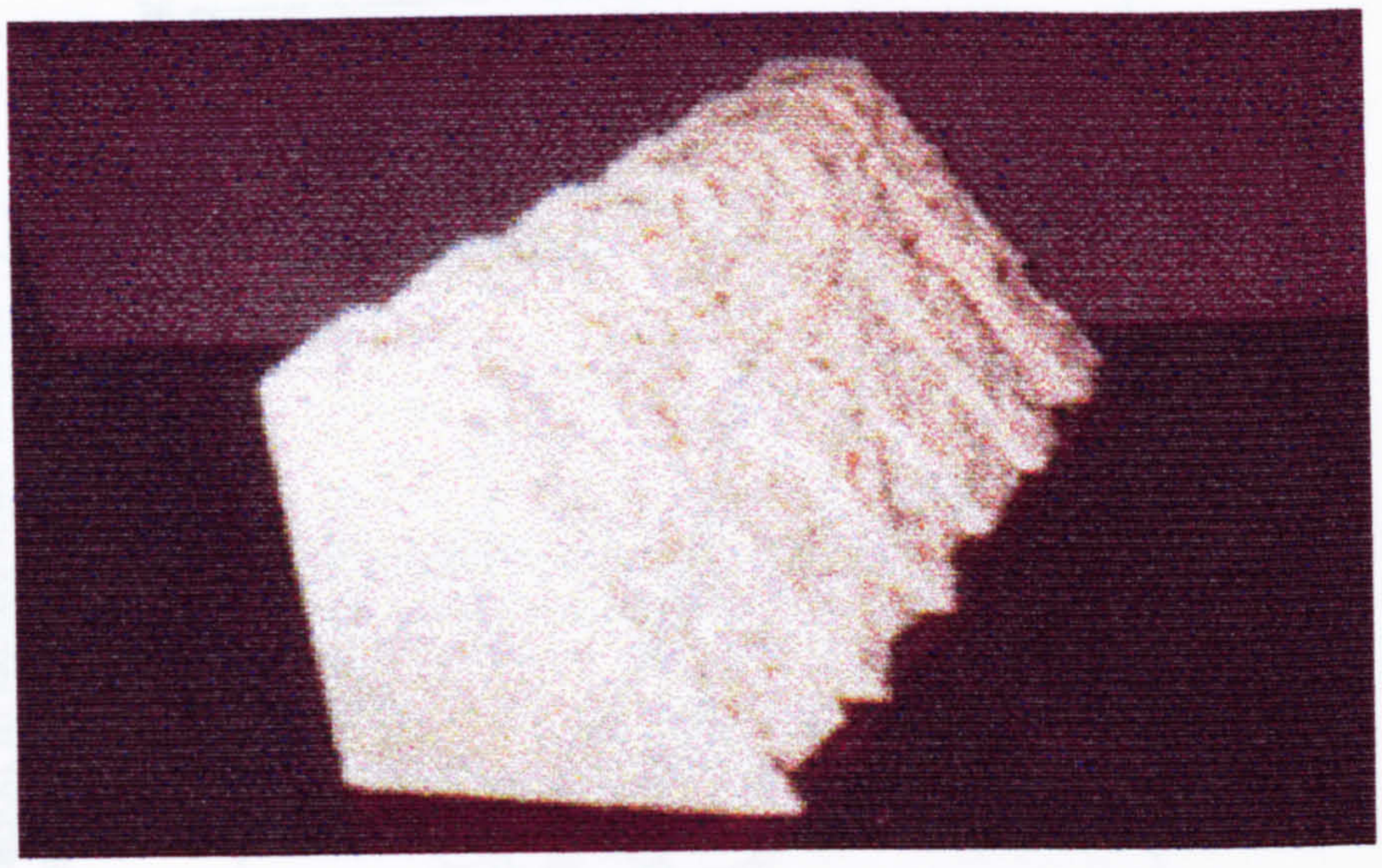

a) Line load split surfaces (30°)

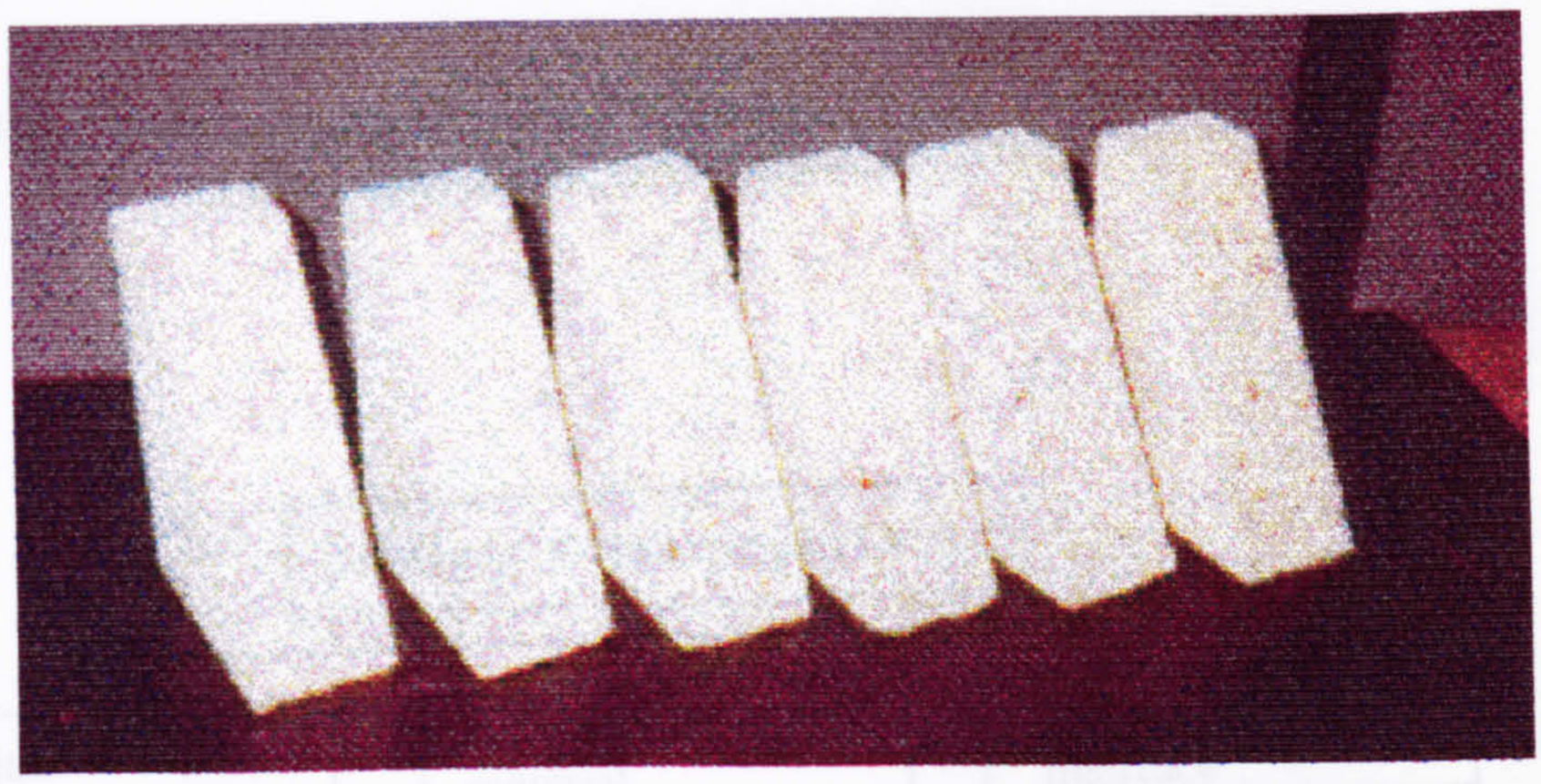

b) Saw cut surfaces (30°)

c) Surfaces produced using BS6319 : Part 4 method

Figure 5.23 Bond surfaces produced with different method

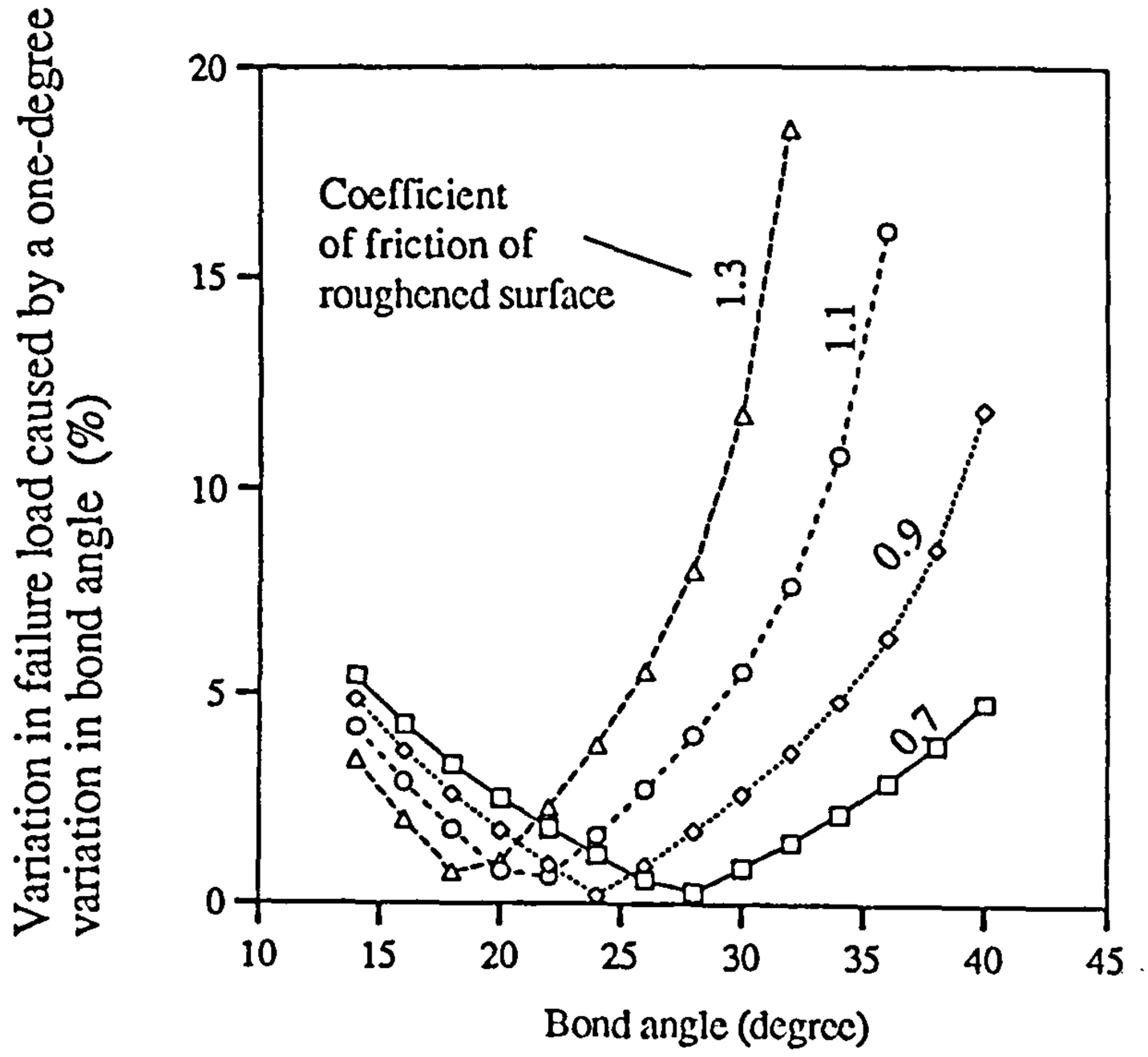

Fig.5.24 Variation in failure load due to one-degree variation in the bond angle in the slant shear test

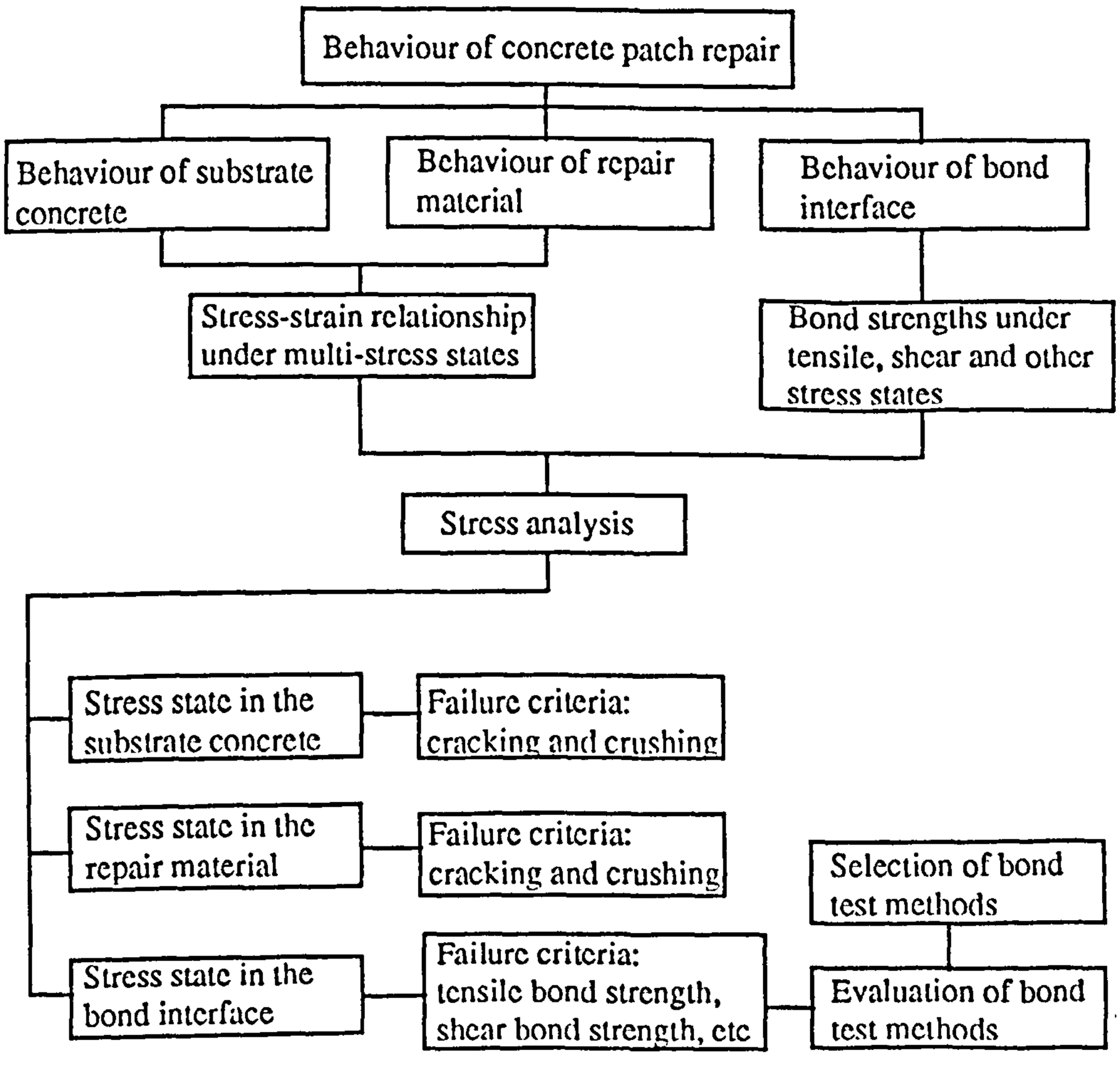

Fig.5.25. Procedure for analysis of a repair system

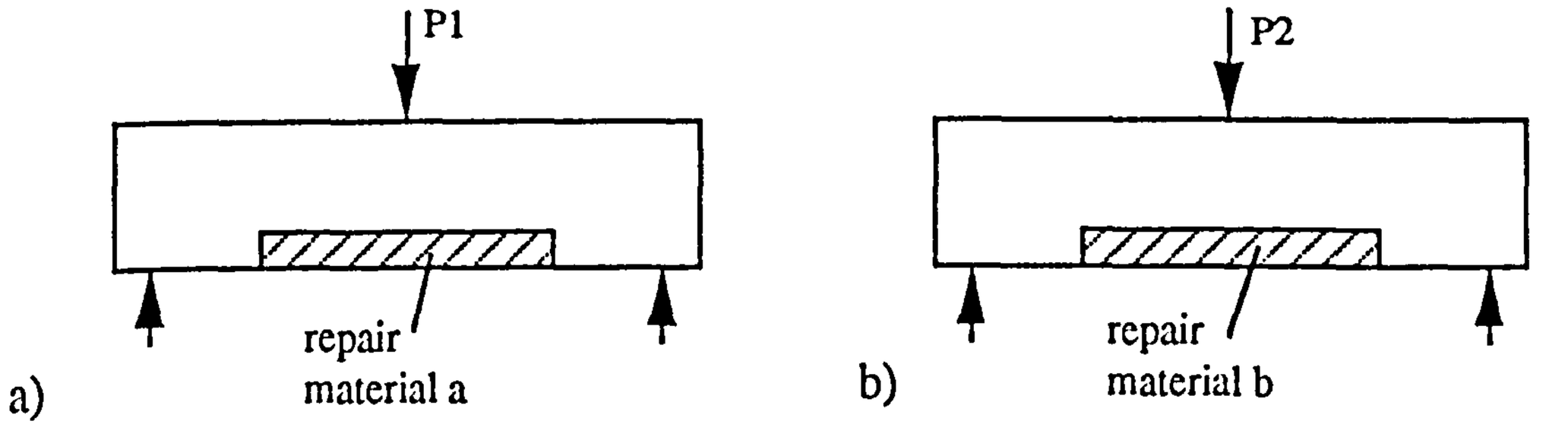

Fig.5.26 Patch flexural specimens repaired with different repair material

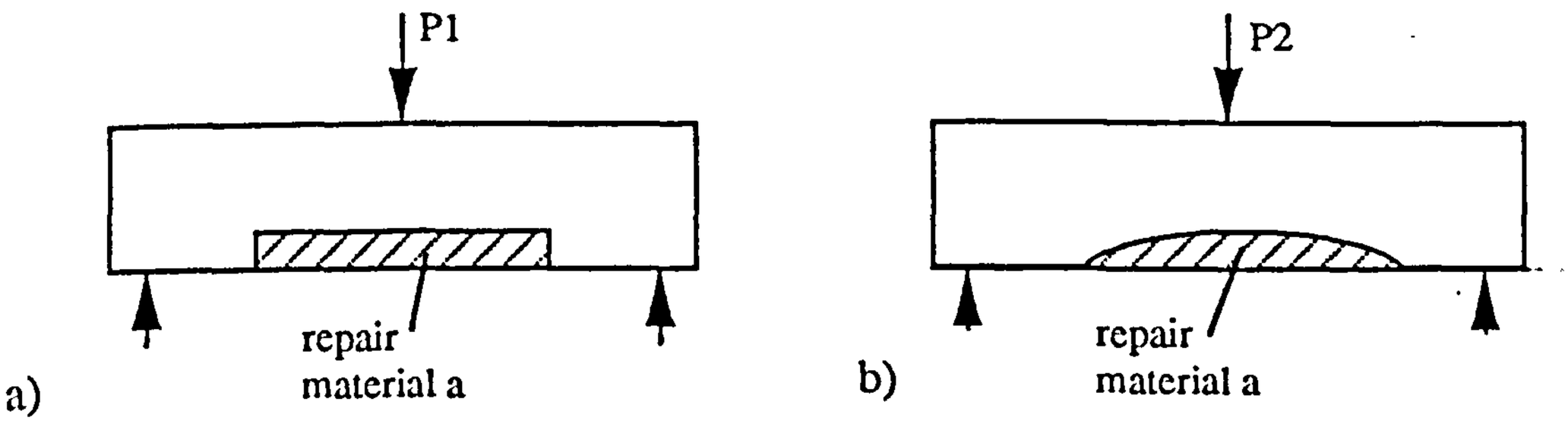

Fig.5.27 Patch flexural specimens with different geometry of cut-out

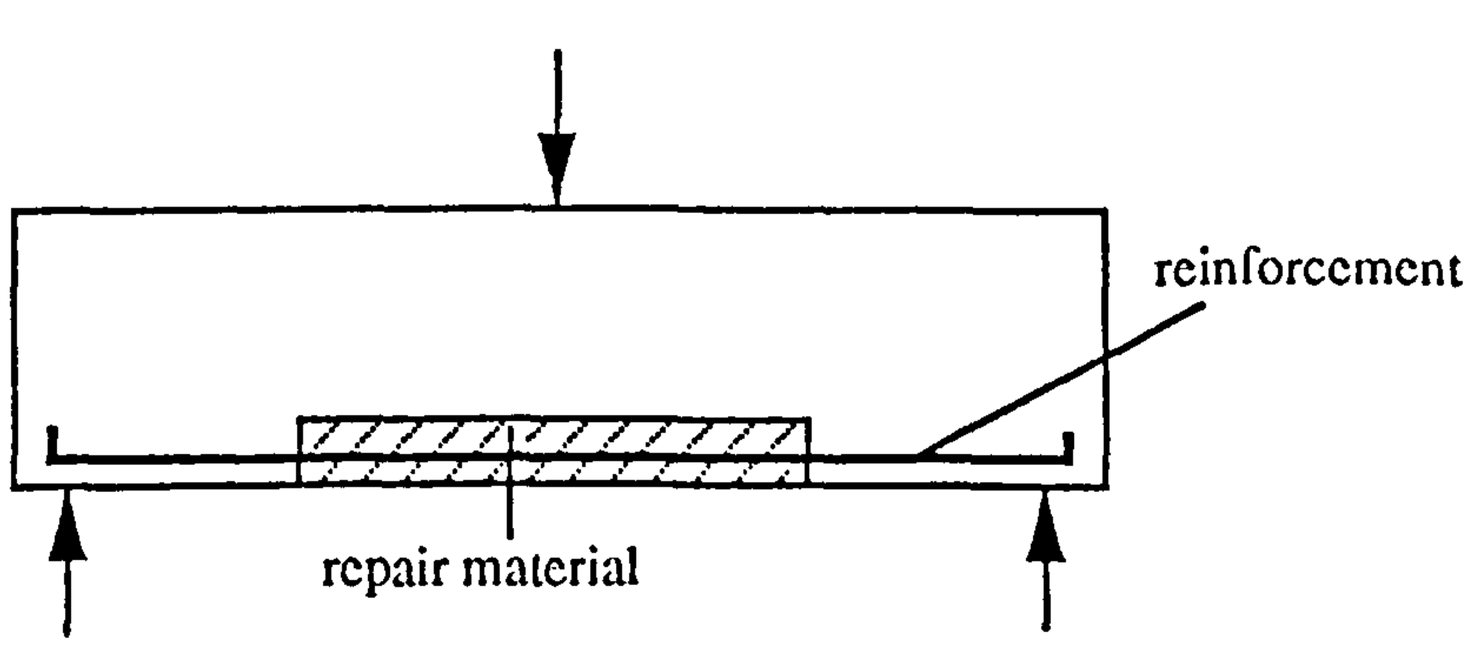

Fig.5.28 Patch flexural specimen with reinforcement

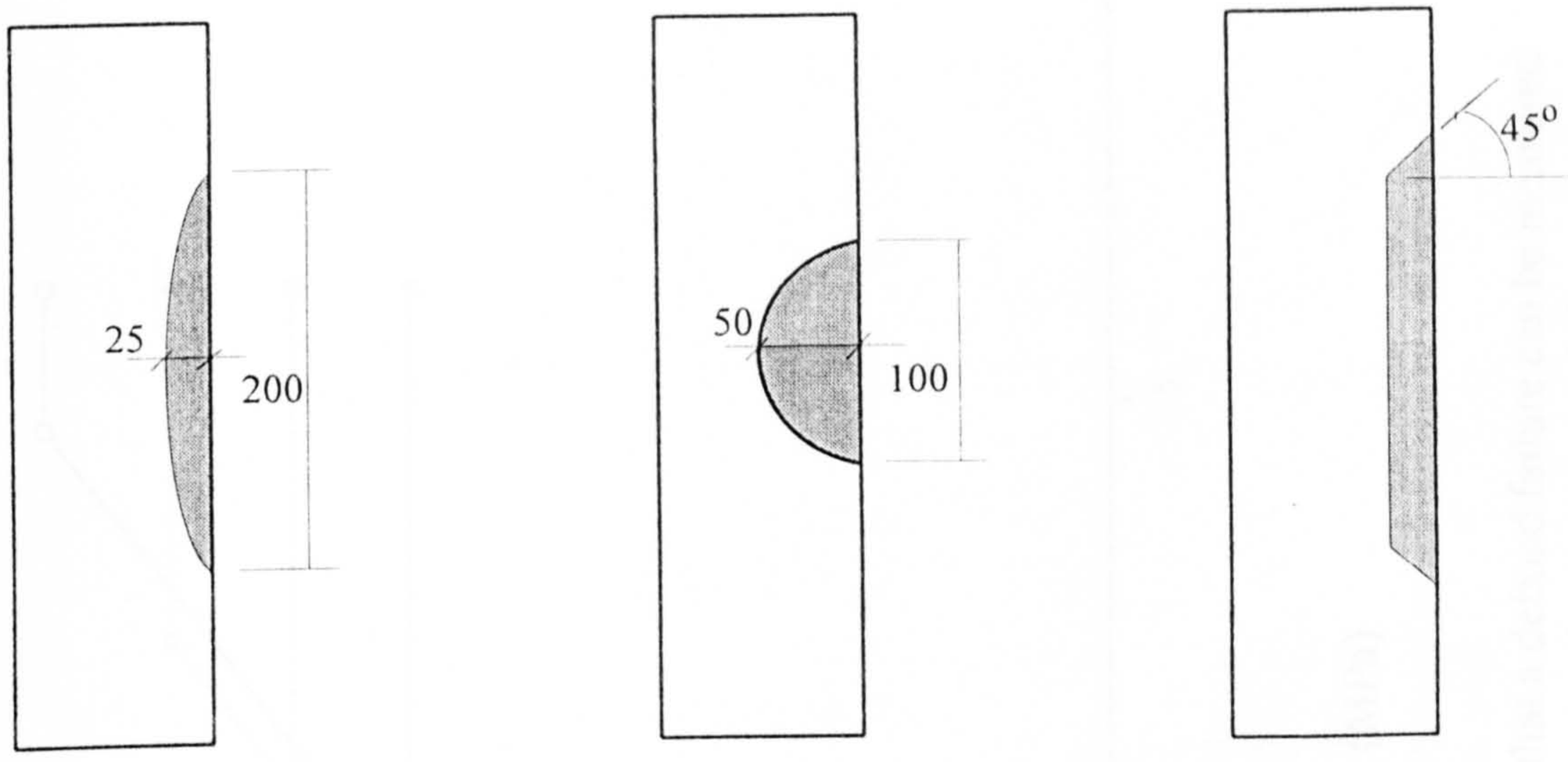

a) b) c)

Figure 5.29 Patch compressive specimens with different geometry of cut-out

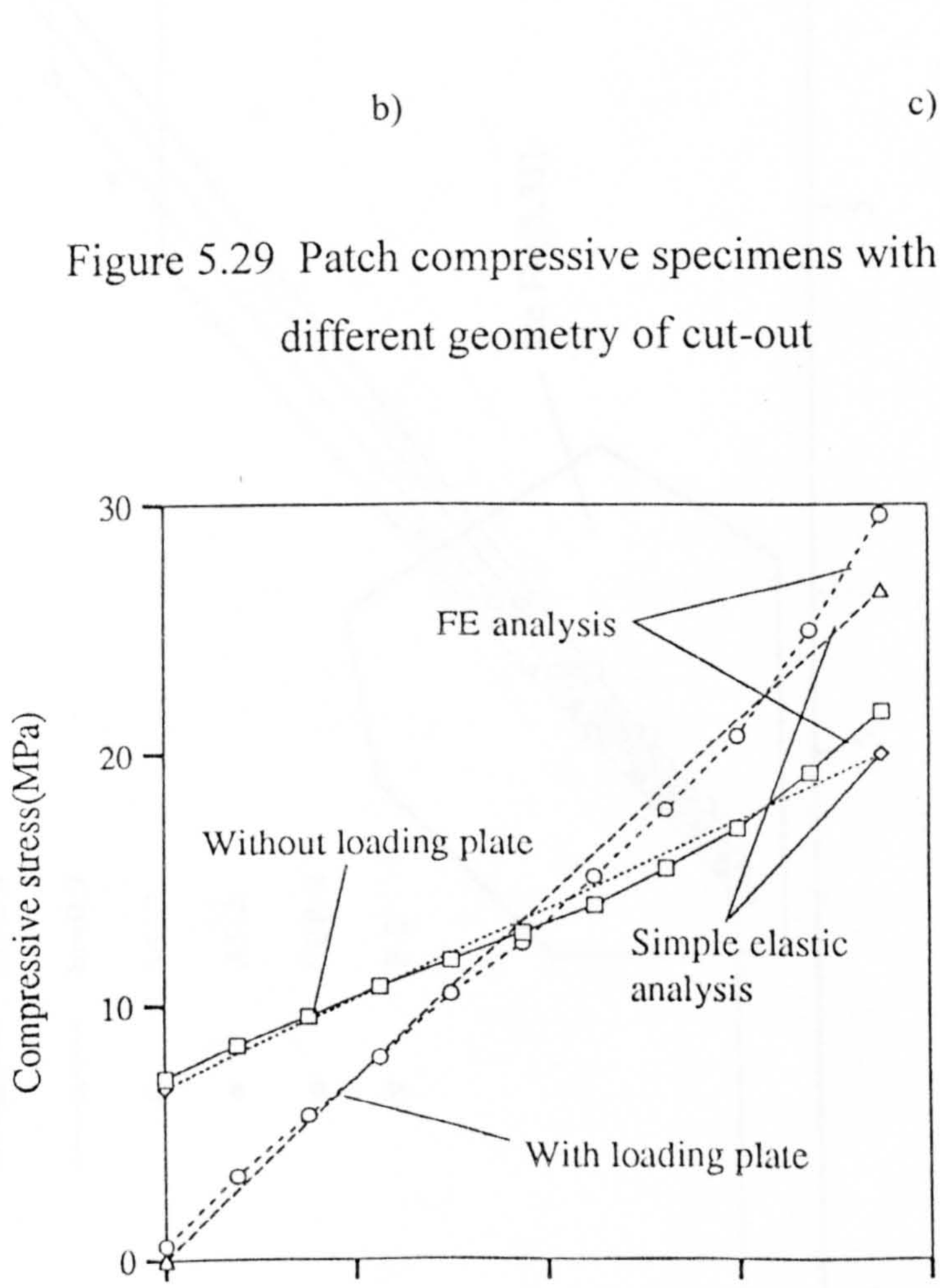

Fig.5.30 Compressive stress distribution over the narrowest cross section of an unrepaired patch compressive specimen

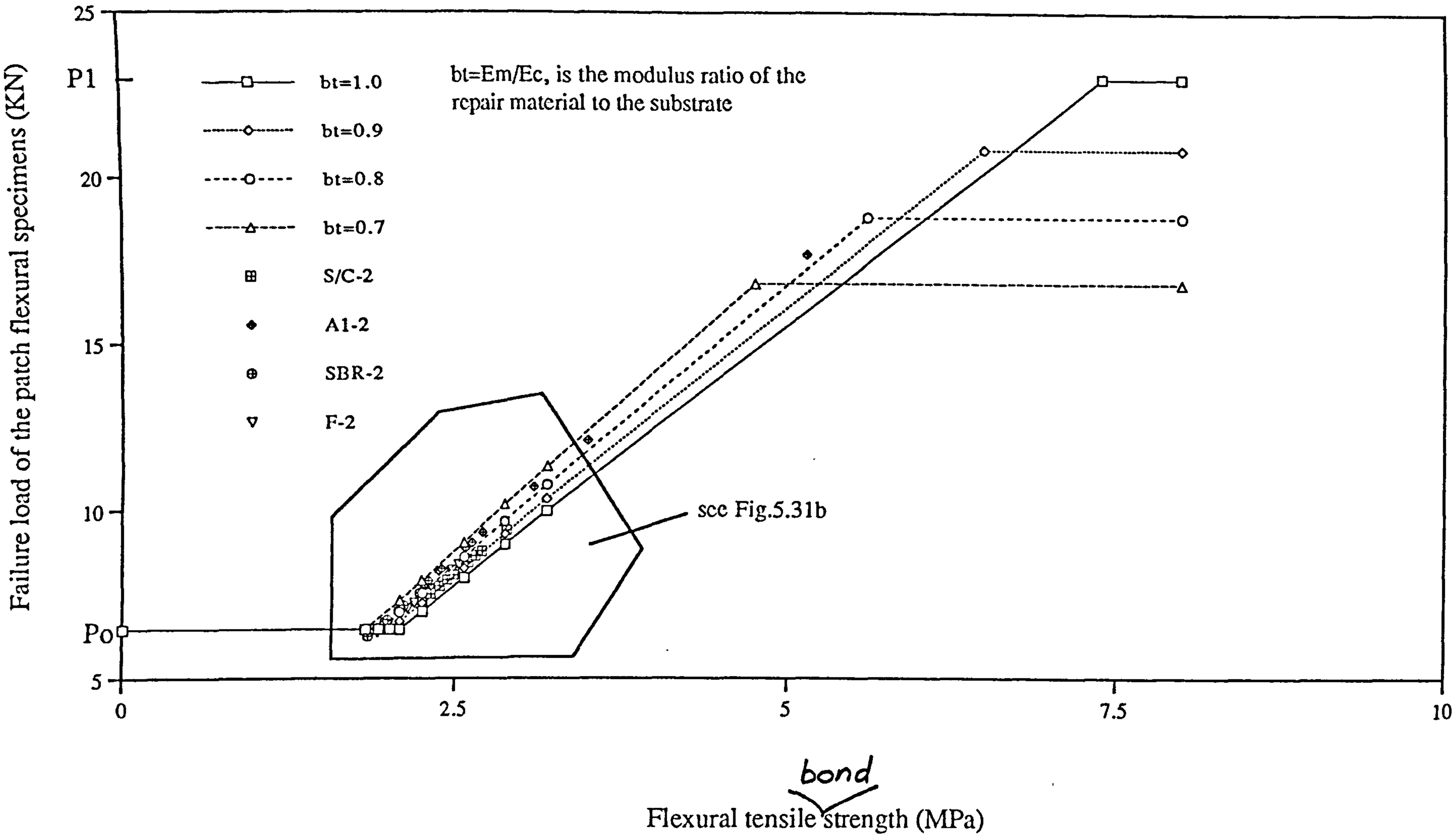

Fig.5.31a The varying range of the patch flexural specimens that a debond failure can be measured

p_1 is obtained based on the condition that concrete at the bond interface fails due to tensile strength is reached.

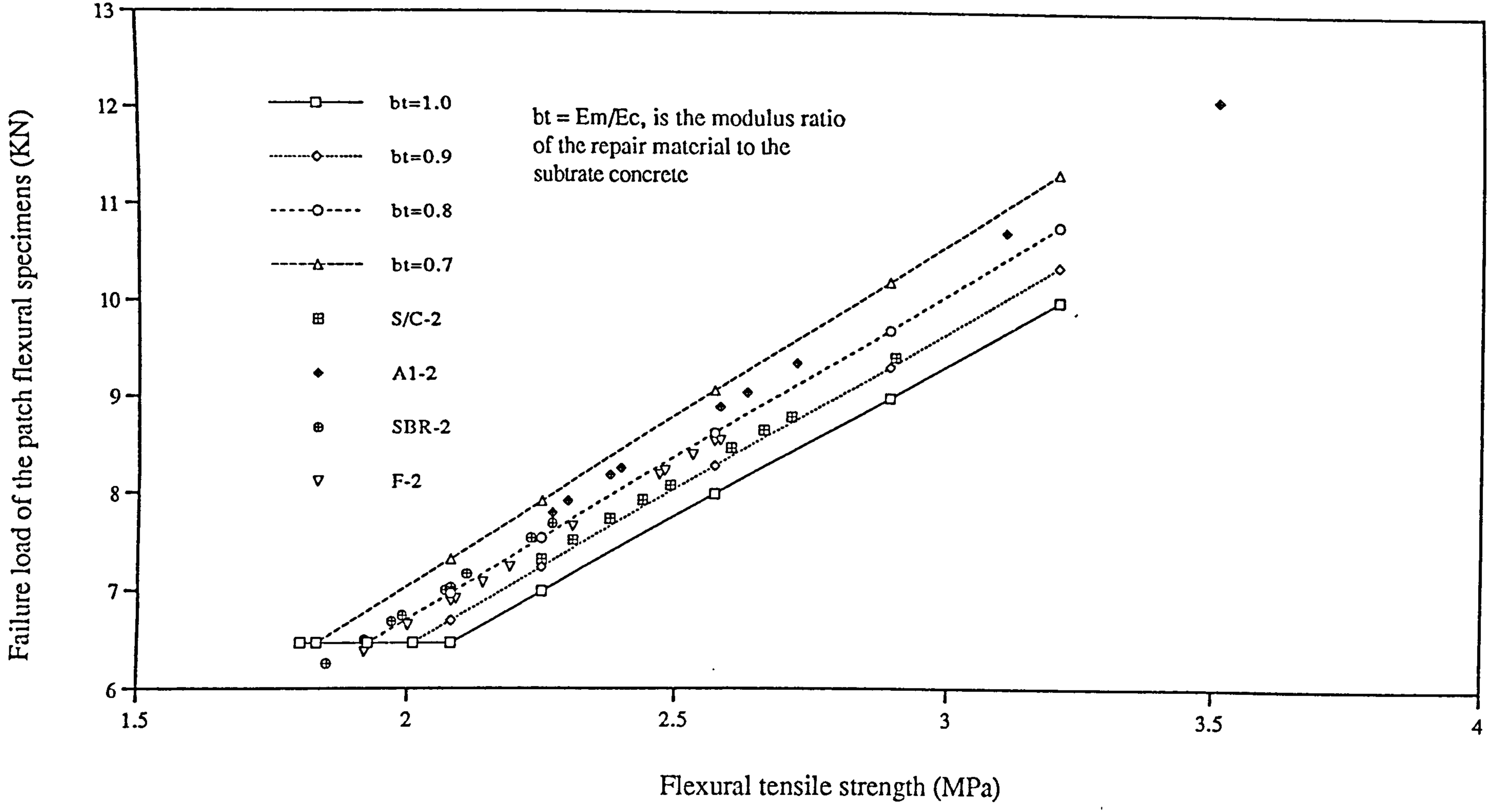

Fig.5.31b The varying range of the patch flexural specimens that a debond failure can be measured

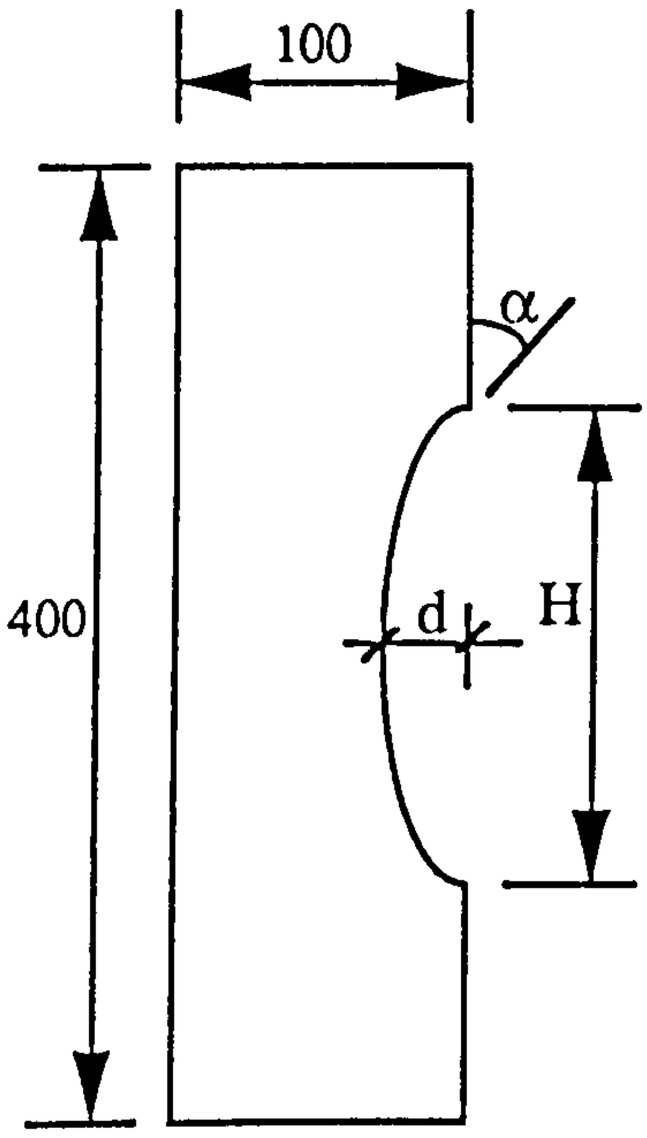

Surface roughness	Bond angle at the periphery of the cut-out, α	H (mm)
smooth	28.07	200
medium rough	29.53	212.45
rough	30.45	220.45

a) Patch compressive specimen

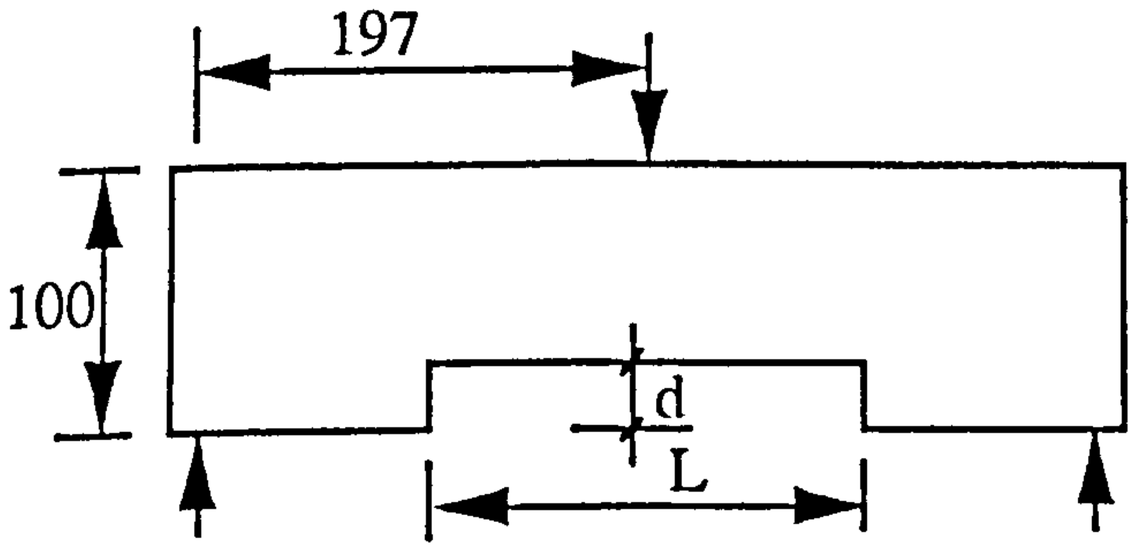

Surface roughness	d	L
smooth	25	180
medium rough	28	186
rough	30	190

b) Patch flexural specimen

Fig.5.32 Geometry of the cut-out used in the theoretical analysis

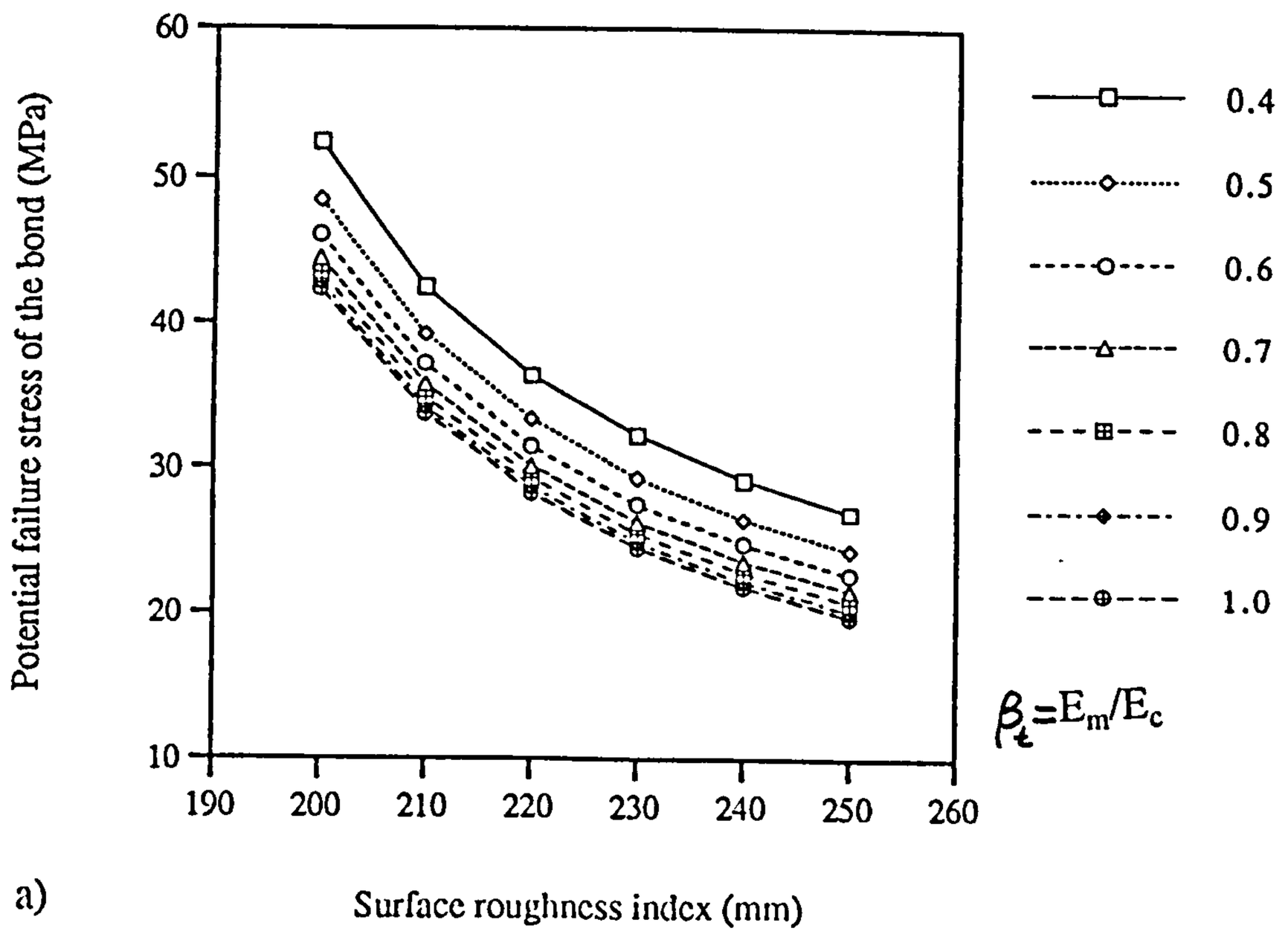

a)

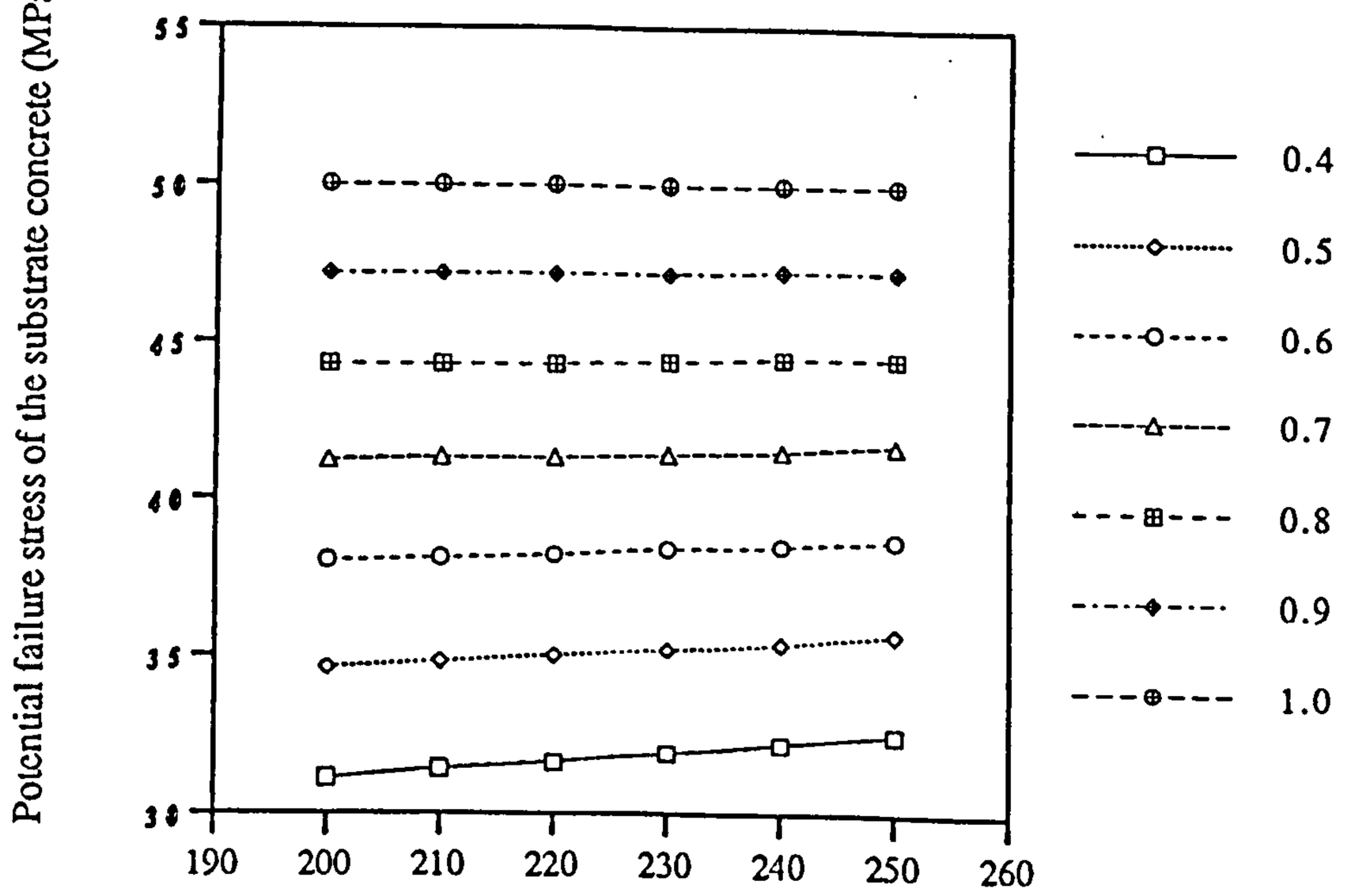

b)

Figure 5.33 Effect of surface roughness on the potential failure stress of the patch compressive specimens

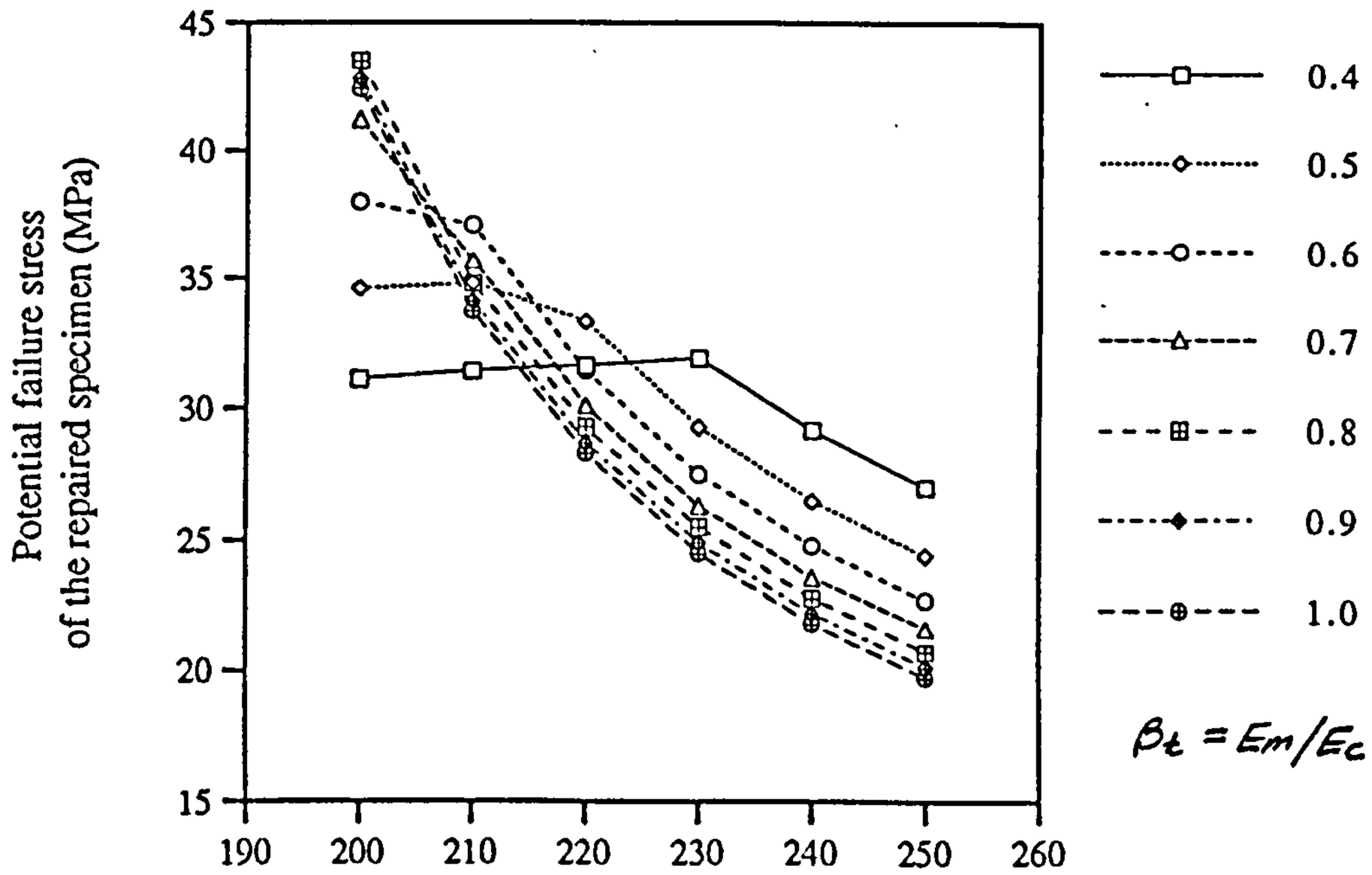

Figure 5.33 Effect of surface roughness on the potential failure stress of the patch compressive specimens

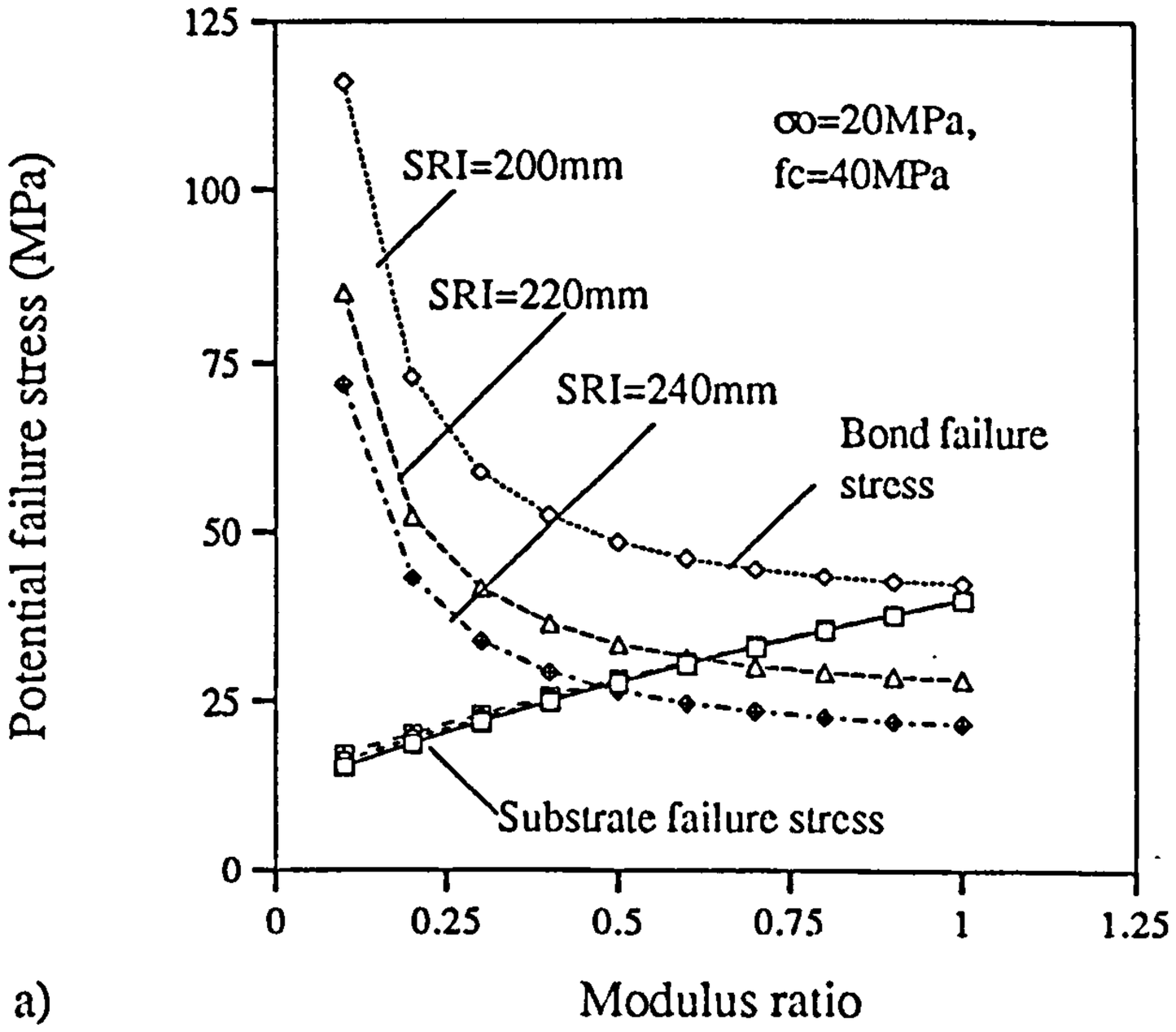

Figure 5.34 Effect of modulus mismatch on the potential failure stress of the patch compressive specimens

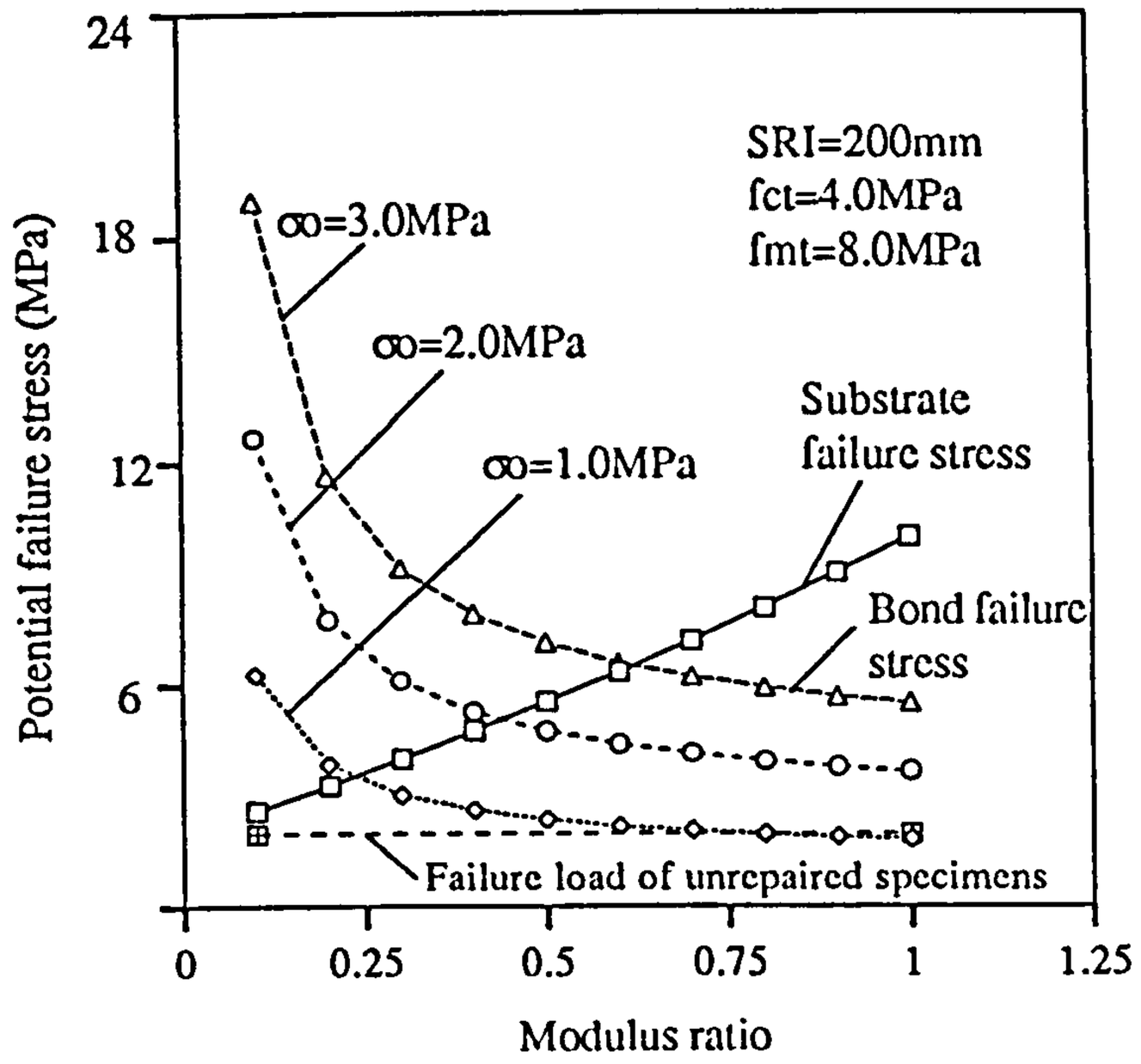

a)

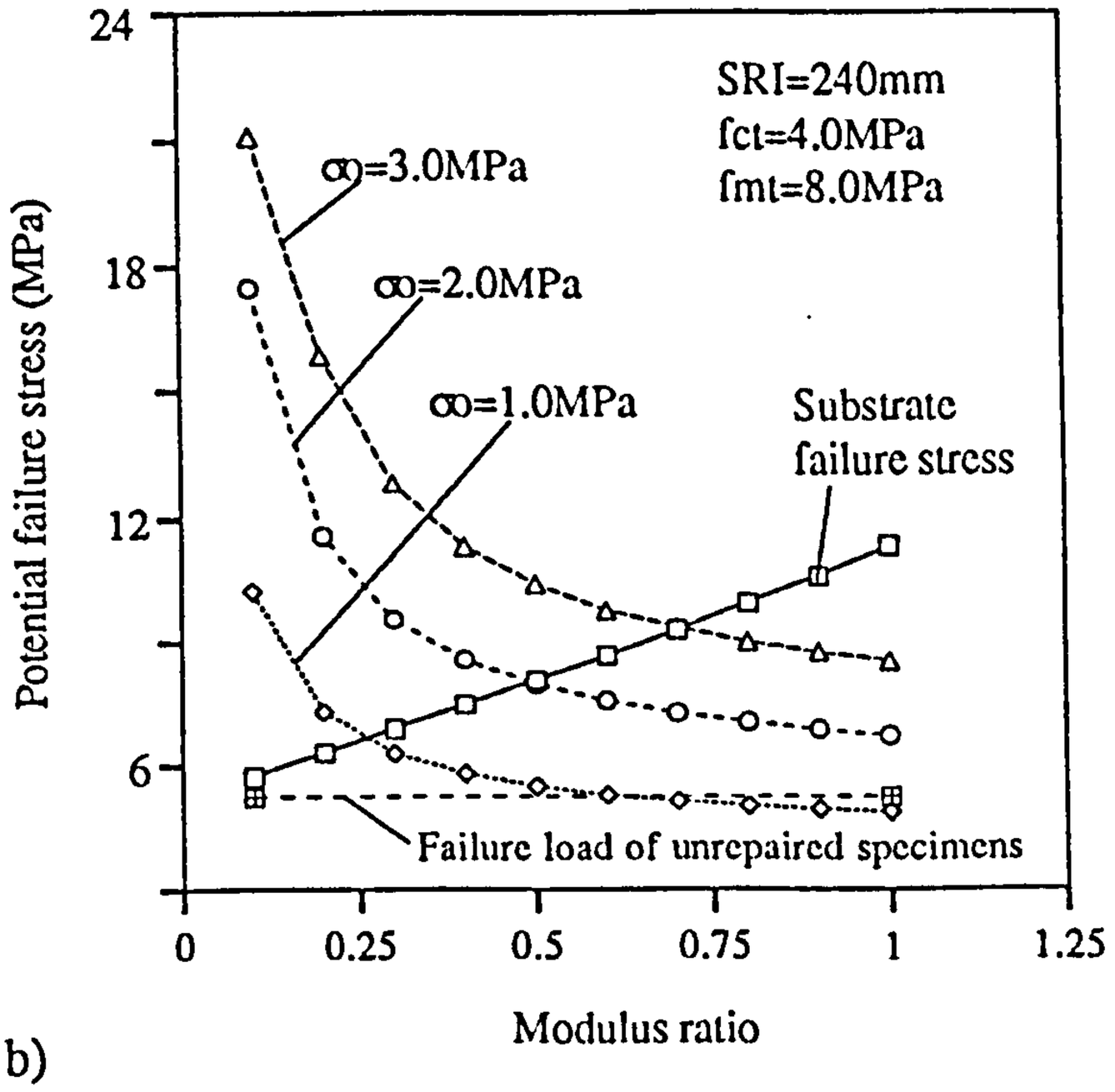

b)

Figure 5.35 Effect of modulus mismatch on the potential failure stress of the patch flexural specimens

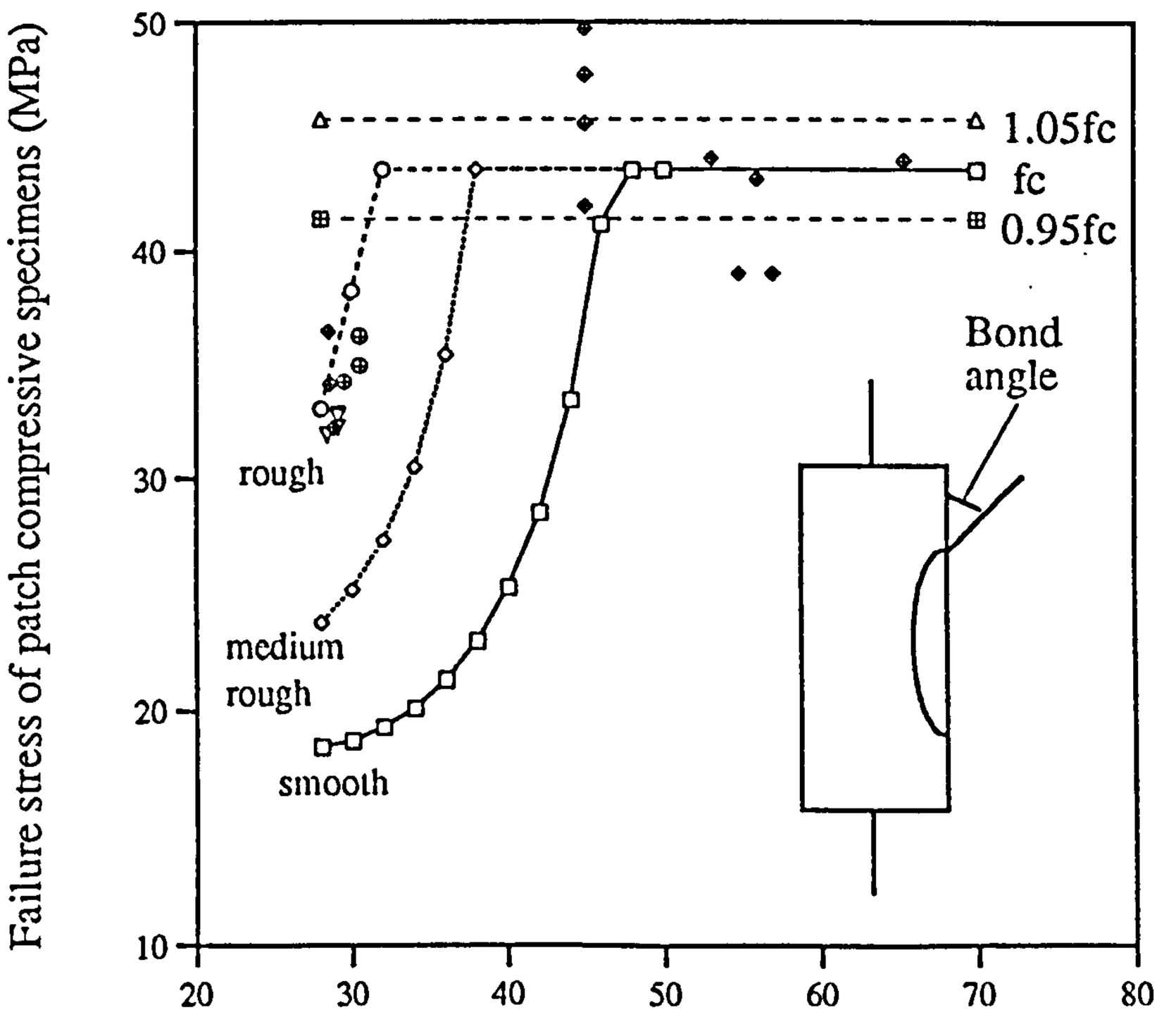

Fig.5.36 Effect of bond angle on failure stress of patch compressive specimens

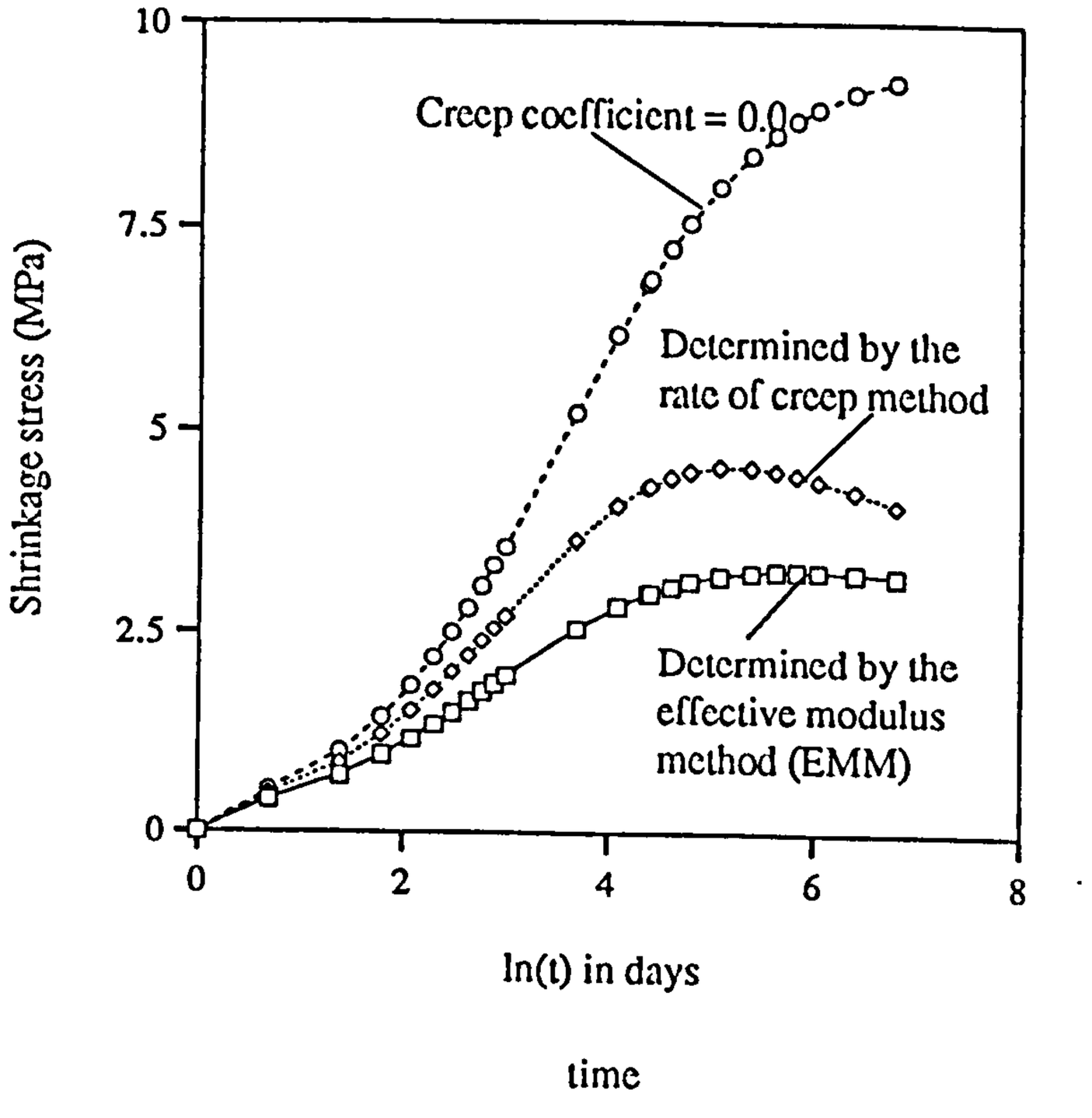

Fig.5.37 Shrinkage stress development considering the creep effect

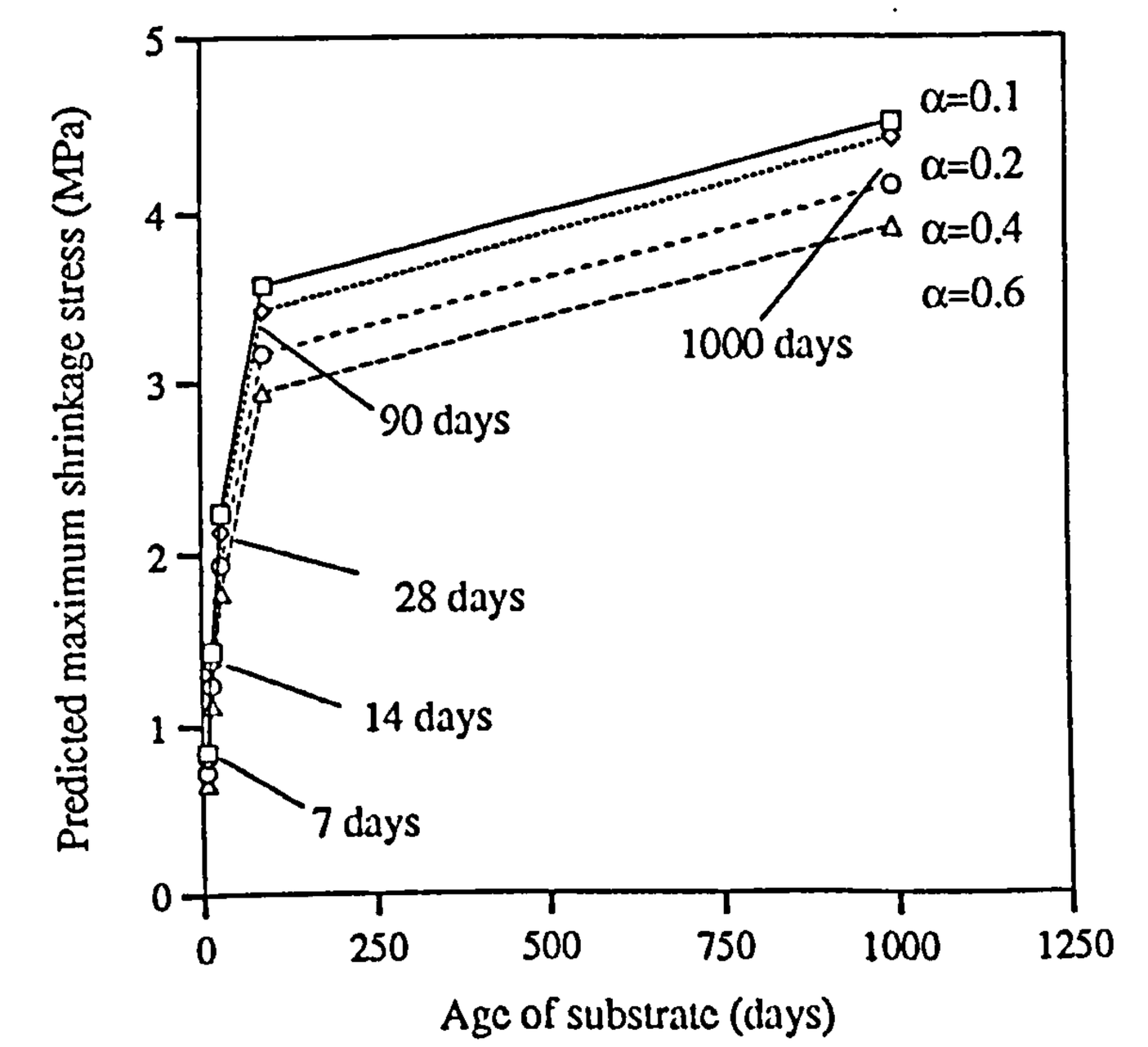

Fig.5.38 Effect of age of the substrate on the maximum shrinkage stress

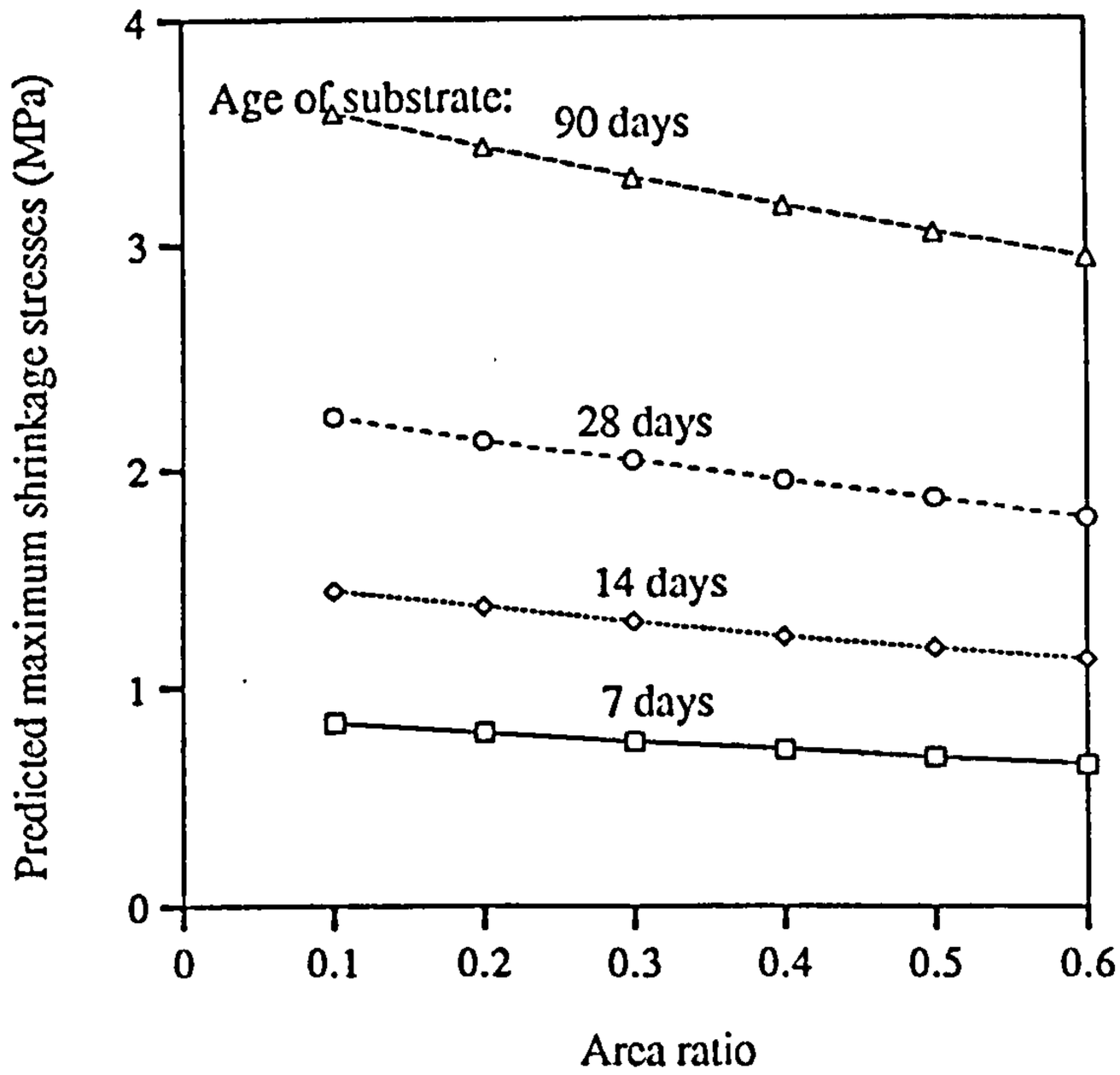

Fig.5.39 Effect of area ratio on the maximum shrinkage stress

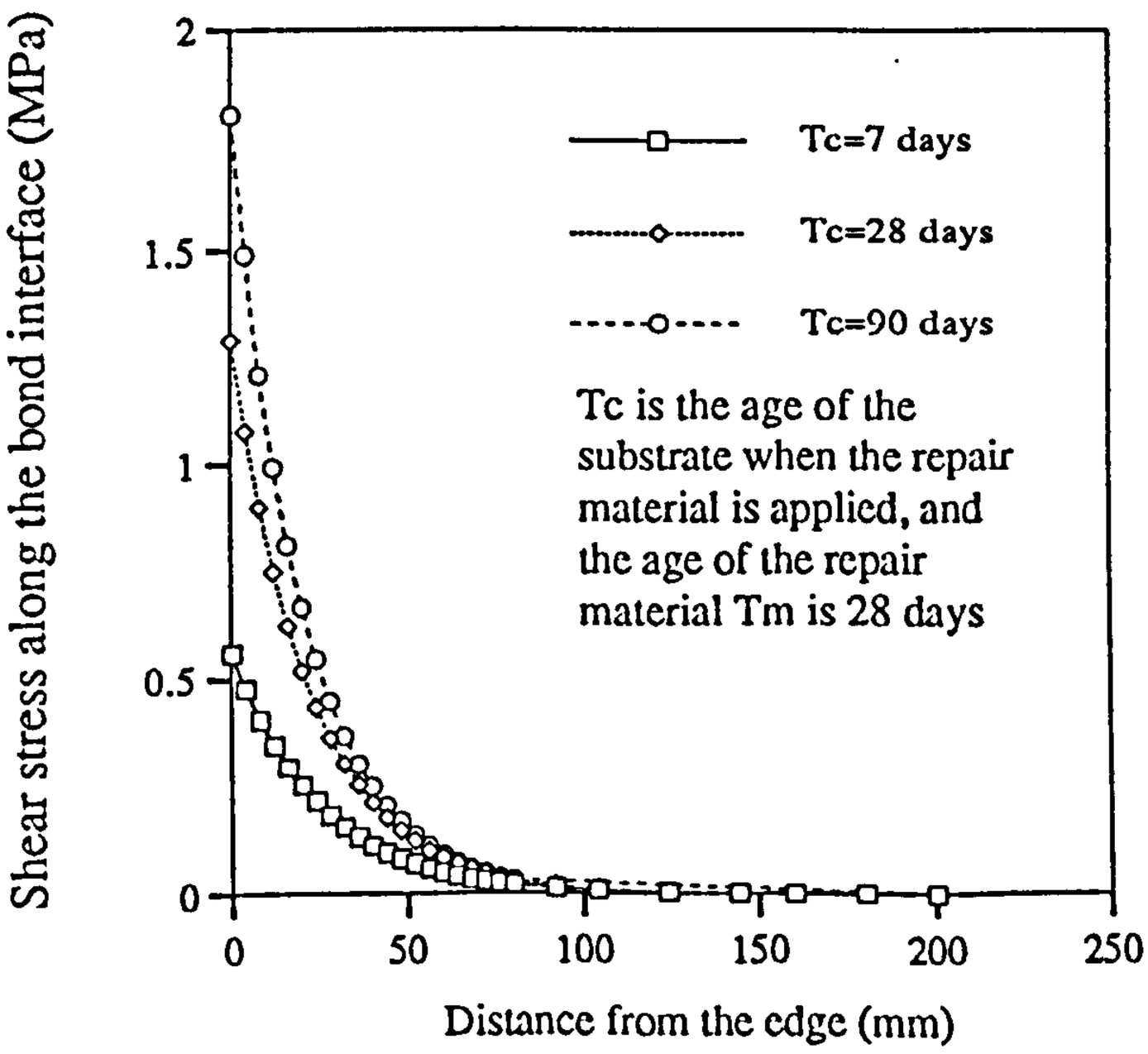

Fig.5.40 Shear stress distribution along the bond interface due to differential shrinkage

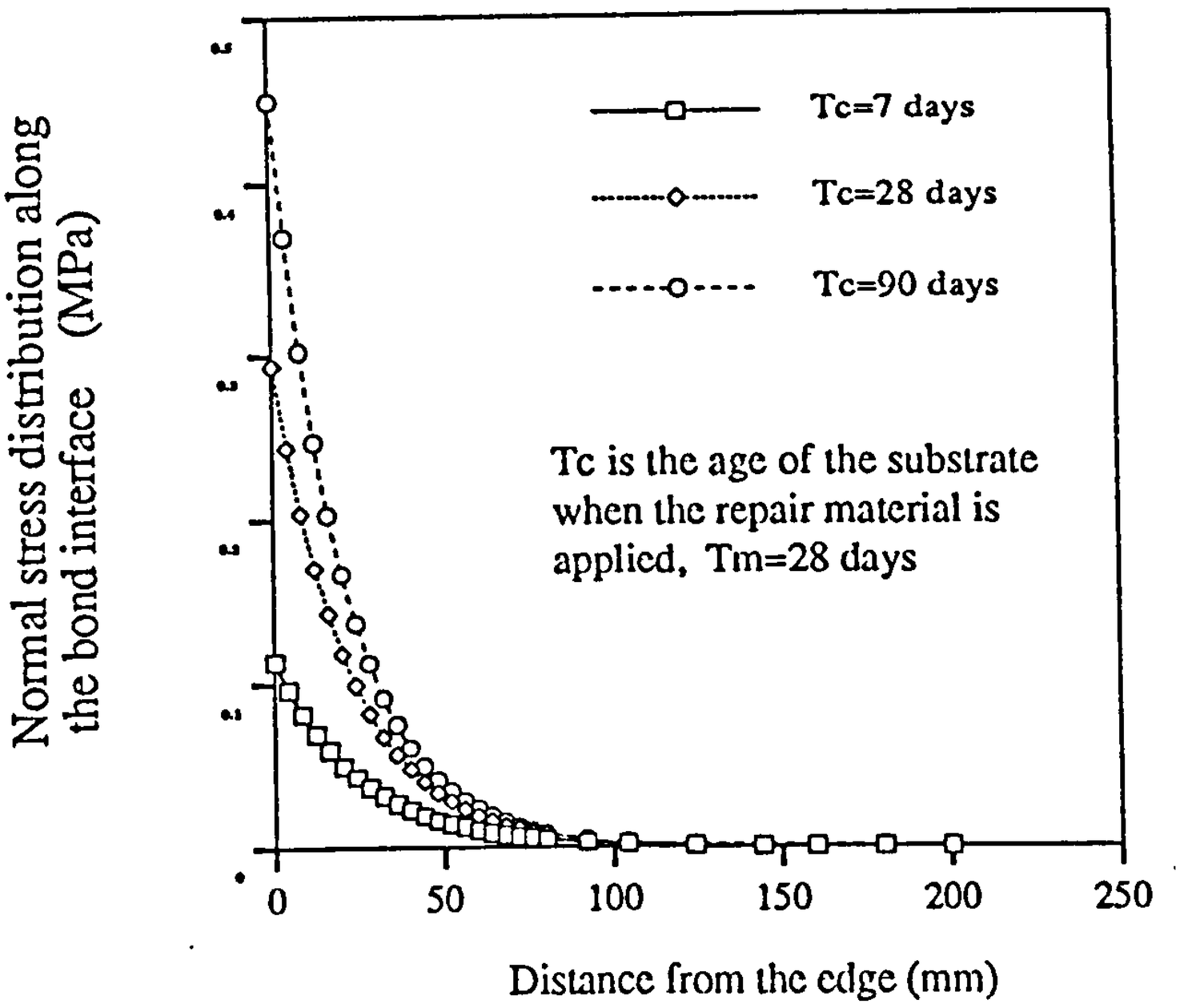

Fig.5.41 Normal stress distribution along the bond interface due to differential shrinkage

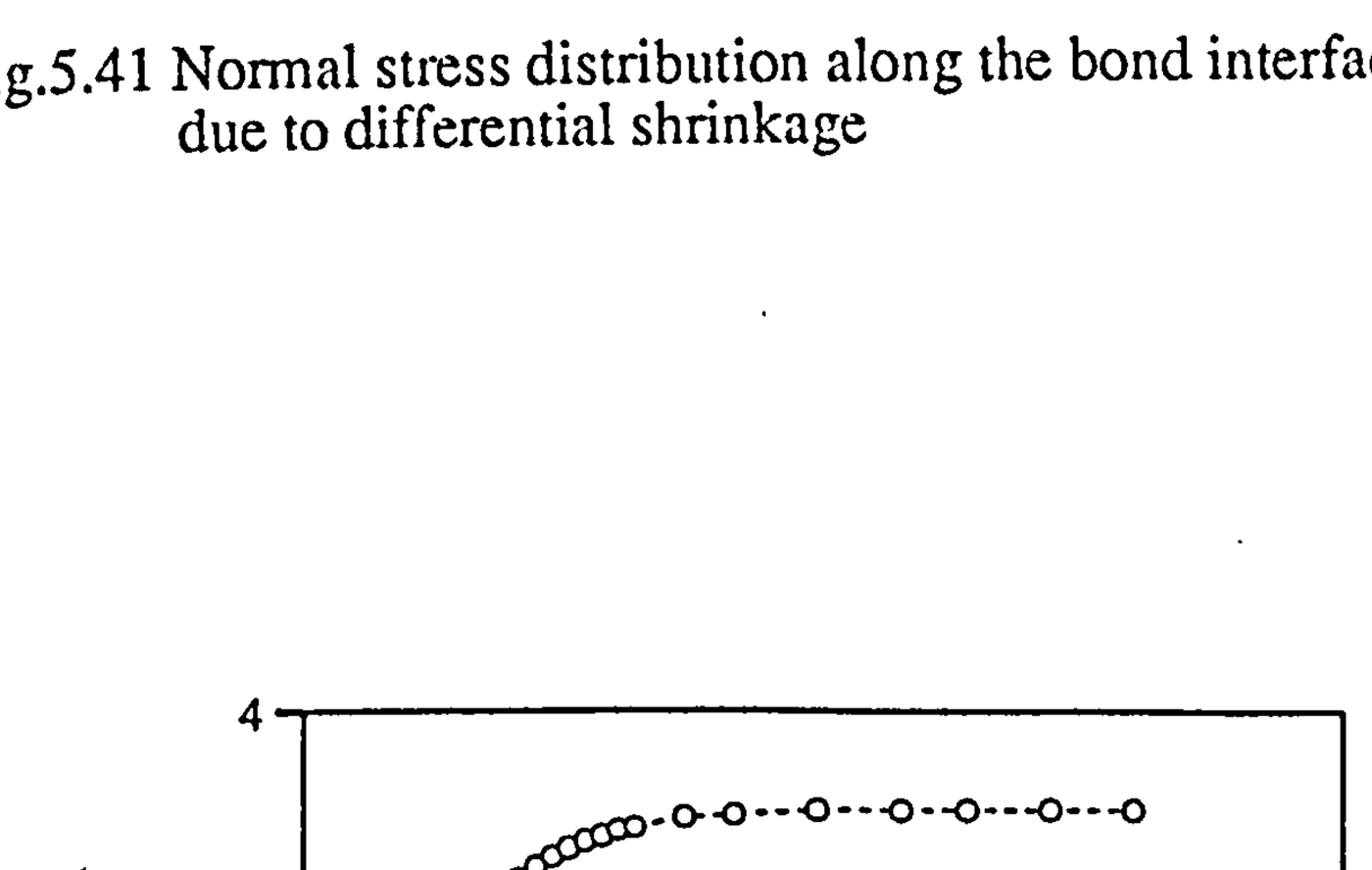

Fig.5.42 Tensile stress distribution in the repair material due to differential shrinkage

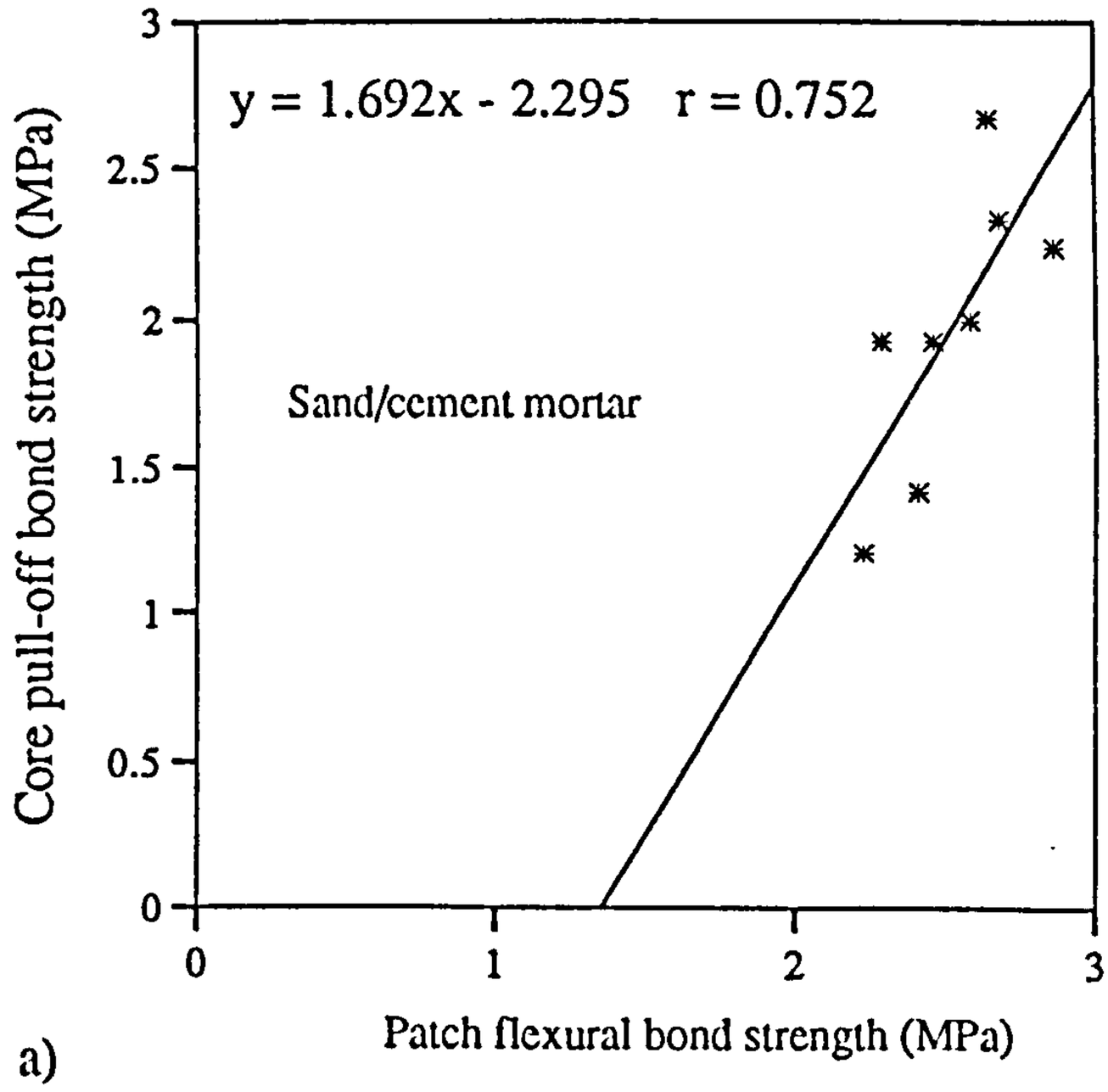

a)

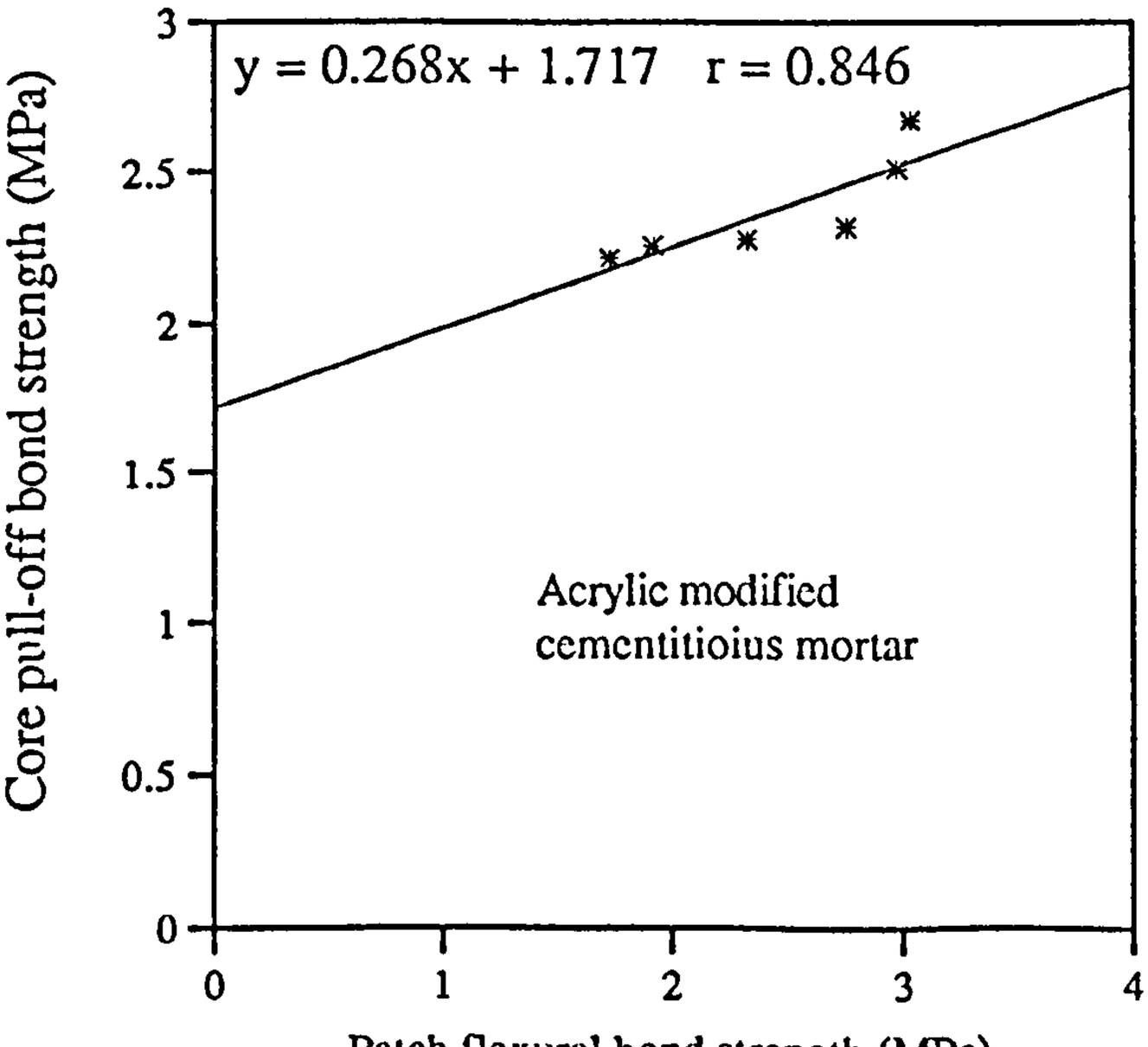

b)

Fig.5.43 Comparison between the patch flaxural and the core pull-off tests

Chapter 6

EFFECT OF WORKMANSHIP ON BOND STRENGTH

Chapter 6. Effect of workmanship on bond strength

6.1 Introduction

Data obtained from questionnaires and interviews with engineers and contractors with extensive experience indicated that poor workmanship is the prime cause of short term failures[6]. But workmanship covers many aspects, such as removal of deteriorated concrete, surface preparation, application of a bond coat, and installation of a repair material. A careful study of each factor involved is required to improve our understanding of the effects of workmanship and hence increase the possibility of success.

6.2 Surface preparation

6.2.1 Presentation of test results

Table 6.1 and Fig. 6.1 show the pull-off test results using the sand/cement (S/C) mortar applied to surfaces prepared by four different methods. Because the substrates were originally in a sound condition, it can be assumed that the surface soundness was good, but the roughness was different for the first three cases. The line load splitting produced loose particles at the surface. However, sound surface was still obtained after needle gunning. Ranking the roughness from low to high follows the order of saw-cut with no further treatment which is extremely smooth (SC-NT), saw-cut then needle gunned which is quite smooth (SC-NG), formed surface and sandblasted which is fairly rough (FM-SB), and line load split then needle gunned which is very rough (LS-NG). It is surprising that the SC-NT surfaces produced very low tensile bond strength (all hand applied specimens failed during core drilling, resulting in virtually no bond strength). The finished surfaces using the SC-NG method were still very smooth, but some tiny voids were exposed after needle gunning. Temporarily ignoring

the results from the SC-NT surfaces, which will be discussed later, test results presented in Table 6.1 and Fig. 6.1 show clearly that rougher surfaces produced higher failure loads with the S/C mortar.

Table 6.2 and Fig. 6.2 show the pull-off test results obtained with the contaminated surfaces. Demoulding oil was brushed on the sound, rough and dry surfaces. After drying out overnight, there was no visual difference between the contaminated and clean surfaces. Even though the contaminated surfaces were thoroughly washed with waterjet and wire brushed before applying the repair mortar, the tensile bond strengths were still reduced dramatically.

Table 6.3 and Fig. 6.3 show the pull-off results from surface set retarder roughened surfaces. Even though the surfaces were rough, the tensile bond strengths were slightly lower than those from the sandblasted surfaces, 6% with the sand/cement mortar, and 18% with the acrylic modified mortar.

Table 6.4 and Fig. 6.4 show the slant shear test results for the various surfaces. The formed surfaces were very sound and smooth, but the roughness was changed after needle gunning or sandblasting. Failure stresses in Fig. 6.4 show that they varied significantly with the surface roughness. When the repair mortar was vibrated on formed surfaces, the slant shear bond strengths obtained with the medium rough surfaces (SRI=230mm) and rough surfaces (SRI=200mm) were about 60% and 100% higher than that with the smooth surfaces, respectively. For the line load split surfaces, the surfaces with no further treatment produced the highest bond strengths whilst the needle gunned surfaces produced slightly lower bond strengths.

6.2.2 Influence of preparation method

Roughness, soundness, and cleanliness are the three issues related directly to the methods employed to remove deteriorated concrete and the methods for further treatment. In section 2.3.2, various methods were discussed, such as spalling, blasting,

and cutting. Mechanical methods remove the surface layer. Unless chemical methods are used, such as acid etching or chemical detergents, it is the roughness and soundness that dominate the quality of the prepared surface.

A sound and rough surface is desirable except when they are to be coated and painted, where a smooth surface is sometimes preferred. Many methods have been used both in laboratories and on construction site to prepare bond surfaces. These methods include: pneumatic hammering [17, 20, 62, 63, 142-145], scarification [145-147], splitting [15, 18, 19, 43, 63], sandblasting [17, 19, 38, 42, 72, 144-148], grit blasting; [5, 19, 60, 144, 149], water jetting [17, 19, 20, 85, 142, 143, 147], saw-cutting [13, 15, 18, 37, 50, 52, 73], and sand papering [13, 14, 37, 50].

In Chapter 4 (section 4.2.3), the surface preparation methods are described which include:

(1) Formed surface;

(2) Saw-cut surface;

(3) Line-load split surface; and

(4) Set retarder produced surface.

Formed surface

Formed surface is sound, but the surface cleanliness depends on whether the laitance is thoroughly removed. If the formed surface is needle gunned or wire brushed at the age of about 24 hours, a rough surface can be obtained, but after curing in a water tank, the surface is still covered with laitance. Further treatment is needed to clean the surface. A few substrates were produced at the early stage of this project, but no bond test was carried out.

If the substrate is first cured in a water tank for a few days, then the surface is very difficult to roughen by needle gunning. In Table 6.4, the formed then needle gunned

surface produced the lowest slant shear bond strength even though the surface is clean and sound. In contrast to this, a fairly rough surface (formed and sand blasted FM-SB) produced much higher slant shear bond strength even though the surface is contaminated intendedly.

When a formed surface is sand blasted, the laitance can be thoroughly removed and different surface roughness can be obtained by adjusting the distance between the nozzle and the surface and the operating time (Fig. 6.5). The sand blasted specimen has not only a roughness which is associated with the big area surface profile (macro roughness), but also roughness which is associated with the local area of paste and the surface of aggregate (meso roughness).

In Cleland, et al's work [19], where the delivery pressure of the sand stream was 0.7MPa, only smooth surfaces were produced. In Silfwerbrand's work [17], the sand blasting also produced smooth surfaces. It was found in the author's work that rough surfaces can be produced using sand blasting method by adjusting the operating time and the distance between the nozzle and the concrete surface. Even though the substrate concrete in this project was of high strength (about 64MPa), rough surfaces were produced by prolonging the operation time and adjusting the distance between the nozzle and the surfaces. The roughness achieved varied from very smooth (SRI=285mm) to very rough (SRI < 200mm) (Fig. 6.6). Also shown in Fig. 6.6 are surfaces with different roughness using different mix ratios for the substrate concrete. From left to right follows the sequence of the mix ratios from the following sources: Loughborough (with river aggregates), Belfast, Loughborough (with crushed aggregates), and BS6319: Part 4. After sand blasting, more coarse aggregates were exposed for rougher surfaces. This is especially so for the substrates using the mix ratios from Belfast and BS6319: Part 4 which contain a higher proportion of coarse aggregates. In contrast the line load split surfaces, even though very rough, did not have much coarse aggregate exposed. Based on the comparison between surface textures and advice from site engineers, the Loughborough mix ratio with river

aggregates was chosen for the substrates for the rest of the tests. This had a low proportion of coarse aggregate to give a sandblasted texture with a reasonable amount of paste as often obtained on site after mechanical or water cutting.

Saw-cut surface

Saw cutting produced extremely smooth and straight surfaces. The surface debris produced during cutting was removed with water jet. In terms of surface roughness, it had neither macro roughness nor meso roughness. When needle gunning was used to roughen the surface, only very tiny bits were removed, which produced surfaces with only very slight meso roughness but no macro roughness. The saw cut surface represents the situation of extremely smooth and very sound surfaces, but in reality, it is very rare to have this kind of surface to receive a repair material.

Line-load split surface

The fractured surfaces produced by this method are very rough with the surface roughness index definitely less than 200mm. Unlike sand blasted surfaces, on which nearly all coarse aggregate located near the surface were exposed after the blasting, cement paste was quite often found covering the coarse aggregate, thus making the surface looked having a high proportion of cement paste. Substrates using the four mixes mentioned above were also line load fractured, but the difference of surface textures was much smaller compared with the ones which were sand blasted (Fig. 6.7).

Loose particles were found on the fractured surfaces, some of them were so loose that a bare hand could remove them. When needle gunning was used, a substrate with sound and very rough surface was obtained.

Surface set retarder produced surface

Surface set retarder, as it is called, delays the strength development near the surface. When a substrate was demoulded at the age of 24 hours, the surface in contact with the retarder was so weak that a wire brush could remove all the cement paste at the

surface and exposed the coarse aggregate. After this the substrate was cured in a water tank for a few days then followed by air cure inside a laboratory until receiving a repair material.

Because much of the cement paste at the surface was removed by the wire brushing, the surface had a very high proportion of coarse aggregate, which was not representative of site conditions. Also, wire brushing removed only cement paste, causing no effect on surface texture of coarse aggregate. For the river gravel used in the substrate, its smooth surface texture remained unchanged, which is not like the effect of sand blasting which causes the aggregate surface to be roughened slightly.

The cleaning of the residue of surface set retarder and laitance was not easy. The surface was cleaned vigorously with water jet and wire brushing, but when becoming dry, it still looked like there was some residue over the surface.

The combined effect of surface residue and smooth aggregate surface made this kind of surface less suitable for receiving a repair material. With the core pull-off test, the tensile bond strength was reduced by 6% with sand/cement mortar, and 18% for the acrylic modified mortar compared with sand blasted surfaces (Fig. 6.3). With the slant shear test, the bond strength was reduced by 20% (Fig. 6.4).

Other surface preparation methods

One method which is often quoted is the water jetting. The efficiency of water jetting depends on the water pressure and the operating time, but generally a sound and rough surface can be produced. A longer operating time will produce a rougher surface. However, undesirable wormholes around and behind the aggregates can be created if the water jet aims at one area for too long [143]. This may cause problems in compaction, especially when a repair material is hand applied. One example is the tensile tests conducted by Silfwerbrand [17], where the water jet method produced

much rougher surfaces than those by sandblasting, but the average bond strength was about 17% lower. The pressure of the water jet was not given, but it was reported that about a 20mm thickness of concrete was removed. It was reported in [19] that when the pressure of the water jet was 28MPa, laitance was thoroughly removed, and also the upper portion of fine aggregate and the top surface of coarse aggregate were exposed. When the pressure of the water jet was 70MPa, both the fine and coarse aggregates were exposed. The water jetting pressure was just 21 MPa in [147], thus only light removal of concrete surface could be expected (it in fact was a final cleaning method).

Sand papering hardly changes the original roughness. If this method is adopted as the further preparation method on a formed or saw-cut surface, the smooth surfaces will remain smooth except for some sand scratches.

6.2.3 Effect of stress state

The response of bond performance to surfaces prepared by different methods depends on the stress state imposed on the bond interface and the type of repair material.

Under a tensile stress state, a sound substrate is very important in ensuring the full development of the potential bond strength because failure occurs at the weakest part of the composite. When soundness is achieved, the bond strength will increase with increasing surface roughness. But the difficulty in achieving good compaction on a rough interface may partially offset the benefit of a rough surface, as shown in Silfwerbrand's test results [74]. While the general trend of the roughness effect holds, the relative increase in bond strength varies with the repair materials.

Sand/cement mortar

A rougher surface corresponds to a higher bond strength. Under a tensile stress state, the increase was fast from extremely smooth surface (SC-NT) to smooth surface (SC-

NG), but much slower from smooth to rough surface (LS-NG) (Fig. 6.8). Good compaction, such as by vibration, increased the absolute value but the trend is quite similar. If the lower bond strength associated with hand application is because that there exist air voids at the bond interface, the air voids, together with other surface defects, such as chemical residue, produce lower tensile bond strength compared with well compacted repair. Ignoring the SC-NT case because it is rare in practice, the vibrated repair produced tensile bond strength about 35% higher than the hand applied.

Using the bond strength criterion described in Chapter 4 (section 4.3.4), the roughness can be seen more clearly for other stress states. Based on the tensile bond strength of 1.41 MPa and the slant shear bond strength of 37.3 MPa obtained with the medium rough surfaces, and assuming that the cube strengths of the substrate and the sand/cement mortar are 60 MPa and the cylinder strength is 80% of the cube strength, Fig. 6.9 shows the effect of surface roughness on performance of repaired specimens. The adhesion strength c can be determined as

$$c = \tau_{,,} - \mu\sigma_{,,} == 16.15 - 9.325 = 6.83 \quad MPa$$

The strength at other roughness can be worked out using the strength criterion:

$$\sigma_{o} = \frac{c}{\sin\alpha\cos\alpha - \mu\sin^{2}\alpha}$$

For smooth and rough surfaces, the failure stress should be 27.8 MPa and 56.6 MPa. respectively. The actual failure stresses were 26.0 MPa, and 50.4 MPa, and for the set retarder produced surface, assuming the friction coefficient is 1.1, the predicted failure stress is 36.3 MPa, the actual failure stress is 30.2 MPa. The other way to increase the failure stress is to increase the bond angle. Based on the calculation, when the bond

angle is greater than 42 degrees, the failure will be controlled by the material strength rather by the bond strength.

Based on tests results obtained with the sand/cement mortar repaired specimens, the effect of surface roughness is shown in Fig. 6.10. It reveals that the effect of roughness is influenced by the surface inclination. With a bond angle less than the normally selected angle of 30 degree, 20° or 25° as demonstrated, the increase in failure load due to a rougher surface is nearly the same with the tensile test. At 30°, the increase in failure load from smooth to medium rough surface is about the same with the tensile test, but the increase from medium rough to rough surface nearly double the increase from the tensile test. With a bond angle of 35°, a rougher surface can increase the failure load by an amount much greater than that can be achieved with a tensile test. This reflects the fact that with a higher bond angle the normal to shear stress ratio is increased, and the contribution by the normal stress component is again confirmed.

<u>Acrylic modified cementitious mortar</u>

Fig. 6.11 shows the core pull-off test results using the acrylic modified cementitious mortar which was applied on two different substrate concrete each with different roughness. If the total of 50 results is averaged the mean bond strength is 2.75 MPa, with a coefficient of variation of only 11.6%. The low coefficient of variation indicates that the acrylic modified mortar was not sensitive to surface roughness and that it also produced very high tensile bond strength. Assuming that the test results follow the normal distribution, the bond strength will vary from about 2.66 to 2.84 MPa at a 95% confidence level, or from 2.63 to 2.87MPa at a 99% confidence level. This clearly shows the good and consistent bond performance demonstrated by this repair material. The same repair product used in [19] showed similar results, with the core pull-off bond strengths ranging from 2.81 to 2.98MPa on cast surfaces. It was observed that when a bond coat was applied, all newly coated surfaces tended to be

very smooth regardless of the original roughness. The smaller effect of the surface roughness on the polymer modified materials may be partly due to the fact that a bond coat was used with most of the modified materials.

Under the combined stress state of shear and compression, the average nominal failure stress of the slant shear specimens is 42.2Mpa. Because with a bond coat the surface is very smooth even though the initial surface before applying the coat is quite rough. This indicates the roughness effect is not very significant for this kind of repair material.

SBR modified cementitious mortar

The tests carried out in [19] and [73] showed that the effect of roughness on the SBR modified cementitious mortar was more significant than that on the acrylic modified mortar, but less than that on the sand/cement mortar. The increase in bond strength from smooth to rough surfaces was about 30%.

Flowing concrete

The high flowing and wetting characteristics associated with the flowing concrete ensure good surface contact with the substrate. However, the increase in bond strength from smooth to rough surfaces was just 8% based on test results carried out by Cleland, et al [19]. This might be caused due to the quite high bond strength of the flowing concrete, and partly to workmanship.

For all these repair materials, the effect of surface defects dependes on stress state imposed. Under a shear stress state, the effect of the surface conditions is similar to that in a tensile test so long as the surface is sound [97]. If there are some surface defects, shear bond tests carried out by Cleland, et al [18] showed that the effect of these defects on bond strength is very small. This is in agreement with findings from the evaluation of bond test methods, and also this indicates that if the load carrying capacity is of main concern, the effect of the surface defects can be ignored under this kind of stress state.

Under a combined stress state of compression and shear the effect of surface roughness becomes very significant. This is because a rougher surface corresponds to a higher coefficient of friction which will enhance the contribution of the compressive stress component to the overall bond strength. Table 6.4 shows that a rough surface produced much higher failure loads than a smooth surface. The prediction of bond failure loads under various surface roughness can be done using the Coulomb failure criterion, which was discussed in section 5.4. If the bond surface is not contaminated, i.e., the adhesion strength is not affected, the existence of microcracks has little detrimental effect on the failure load.

6.2.4 Conclusions

It can be seen from the discussions above that the response of the bond performance to the surface preparations depends on the stress states imposed on the bond interface, and the repair material selected. Specification of the surface preparation technique should take all these factors into consideration. For a repair area that will be put under a tensile stress state, the importance of the surface soundness of a substrate should be emphasised. For repair areas that will be put under a compressive stress state, bond will not be a problem if the load carrying capacity is of main concern. For areas that will be put under a combined stress state of compression and shear, the bond performance is not sensitive to the existence of microcracks, so the stringent requirement for a sound substrate can be relaxed a little. To date, there is not a well established document which states clearly when a substrate can be accepted as a sound substrate. Specifications are often project related. For example, it was suggested by Gaul [95] that the tensile strength of the concrete should be at least 0.69MPa for surface coatings. In a concrete overlay situation, it was required that the average pull-off strength should be at least 1.1MPa, with no single results below 0.83MPa [149]. In

[1], it is suggested that removal of damaged material is continued until aggregate particles are being broken rather than simply pried loose from the matrix.

Cleanliness must also be properly defined. To detect this kind of surface contamination, the water drop test can be used [95]. Oily conditions exist if water is sprinkled on the surface and stands in droplets without spreading out immediately, indicating that the surface is contaminated, which will interfere with the adhesion of most repair materials. Some bond surfaces which were intentionally contaminated in this project, were subsequently wire brushed and water jetted before applying the repair material with the aim of mitigating the detrimental effect, but the effort was fruitless. This suggests that bond surfaces contaminated with oily substance can not be improved by the wire brushing and water-jetting (low pressure). If only the surface is contaminated, the oily substance may be removed by chemical cleaning with detergents, caustic sodas solutions, or trisodium phosphate [95]. A vigorous scrubbing action should be carried out during the washing procedure. It is important to thoroughly flush the surface of the concrete with clean water to remove all traces of the loosened oil as well as the cleaning solution. If the body of the concrete has been saturated with oil, grease, or fat over a long period of time, even a well executed surface cleaning may not be enough for the surface preparation. Methods other than chemical cleaning should be considered that will remove a substantial depth of concrete (e.g. high pressure water jetting).

The texture of the prepared surface has received little discussion so far. In order to produce a bond surface that is representative of site conditions, or in order to apply the laboratory findings to site repairs, the texture of the prepared surface also needs to be discussed.

The author's results on saw-cut surfaces with no further treatment (SC-NT) demonstrated complete loss of bond strength during core drilling when the S/C mortar

was hand applied, and very low bond strength (0.27MPa) when the mortar was vibrated. Results on SC-NG surfaces ,even though the surfaces were still very smooth, showed a tensile bond strength of about 1.2MPa. This may be attributed to the difference in the micro-level surface texture. After saw cutting, the surface looked as if it had been polished: extremely smooth. Also, some tiny voids on the surface had been filled with very fine cutting debris. This will adversely affect the bond strength development. Alexander, et al's results [48] on water-saw surfaces showed similar trends.

Kuhlmann [37] used three different methods to prepare bond surfaces: (1) cut; (2) cut and sand papered; and (3) cut and sandblasted. All methods produced very smooth surfaces. However, at the micro-level, the sand papered and the sand blasted surfaces may have some scratches or tiny voids scattered over the surface. The tensile bond strengths measured using the pipe nipple grip method showed little difference. Similar results were also obtained by Alexander, et al [48]. In contrast to this, the surface set retarder produced surfaces that had a rough profile at the macro-level, but the surface of the river coarse aggregates still retained their original smooth texture. With sand blasting both a macro-level roughness and roughening of the surfaces of coarse aggregates can be obtained. Hence, the lower bond strengths obtained from the set retarder surfaces may be attributed partly to some chemical residue, and partly to the extreme smooth surface texture of the coarse aggregates.

6.3 Moisture condition

This section deals with the effect of variation in the moisture state of the substrate/repair system on bond strength. The test results and some general observations are presented first, followed by:

(1) discussion of the test results, looking at each of the four repair materials in turn; and

(2) a wider discussion examining how changes in the substrate concrete, repair material and curing environment (from those investigated here) might affect bond performance.

6.3.1 Presentation of test results

Both moisture condition inside the substrate and at the surface layer were investigated, with the former considering three levels: saturated, air dry and bone dry, and the latter considering two levels: wet (no free water) and dry. By combining the conditions inside the substrate and at the surface layer, six levels of moisture condition were simulated: saturated surface wet, saturated surface dry, air dry surface wet, air dry surface dry, bond dry surface wet, and bond dry surface dry.

Table 6.5 shows the core pull-off test results of five different repair materials, and Figures 6.12 to 6.16 show the results of each material in a graphic form. Table 6.6 and Fig. 6.17 show the patch flexural test results of the flowing concrete. It can be seen that the moisture conditions did not produce a general trend on the bond strength with their effects varying between the different repair materials.

Sand/cement mortar

The surface moisture condition had little effect on the sand/cement mortar. The difference between results from the wet and dry surfaces was about 2% for saturated and air dry substrates, and about 8% for the bone-dry substrates. The data were analysed using the t statistical test [150], and the results are shown in Table 6.7. Formulae used for the statistical analysis are given in Appendix 8. The test results suggested that it is the moisture condition inside the substrate that affects the bond strength. The bone dry substrates produced the highest bond strength (2.35MPa), followed by the saturated substrates (1.81MPa). The air dry substrates produced the

lowest bond strength (1.43MPa), about 40% lower than that obtained with the bone dry substrates.

Acrylic modified cementitious mortar

Neither the moisture condition at the surface layer nor inside the substrate appeared to affect the bond strength of the acrylic modified mortar. The bond strengths achieved varied from 2.61 to 2.85MPa. Examination of the failure modes revealed that of the 75 test results presented in Table 6.5, only 23 (about 31%) failed at the bond interface. The lower bond failure rate indicates that the bond strength of this acrylic modified material is very good and that the effect of moisture condition on the bond strength is very small. If all 75 test results are averaged, the mean bond strength is 2.80MPa with a coefficient of variation of only 10.6%.

SBR modified mortar

With the SBR modified mortar, the saturated surface wet and the bone dry surface dry substrates produced similar, high bond strengths. These two situations represent the two extremes of moisture condition in a substrate, the former being very wet, and the latter very dry. The general effect of the surface moisture condition is not clear. For the saturated substrate, the bond strength obtained with the wet surfaces was about 17% higher than that obtained with the dry surfaces. But with an air dry substrate, the bond strength obtained with a wet surface was about 30% lower than that with a dry surfaces. For the bone dry substrate, the difference in bond strengths between these two surface moisture conditions was very small.

Flowing concrete

Test results with the flowing concrete showed clearly that a dry surface produced a higher bond strength than a wet surface. The wettest substrate (saturated surface wet) produced the lowest bond strength, and the driest substrate (bone dry surface dry) produced the highest bond strengths with the core pull-off test. Patch flexural tests

were also carried out on the flowing concrete to study the effect of moisture condition. The failure loads with the saturated substrate were slightly lower than that of the unrepaired beams. Because the failure load of a repaired specimen should not be lower than that of an unrepaired one, this indicates that the difference was caused by variation of the substrate properties. The bone dry surface dry substrate produced the highest failure loads with the patch flexural tests, which confirmed the results obtained from the core pull-off tests.

Lightweight acrylic modified cementitious mortar

The light weight acrylic modified cementitious mortar appeared unaffected by moisture condition, the two extreme states (saturated surface wet and bone dry surface dry) producing the highest and the lowest bond strengths (1.42 and 1.73MPa). If all the results are averaged, the mean bond strength is 1.56MPa with a coefficient of variation of 10.4%.

6.3.2. General observations

It is generally believed that the imbalance in moisture conditions in the substrate and the repair material affects bond strength development. Recent studies by Bretor, et al [151] using scanning electron microscopy and x-ray diffraction have shown that the water/cement ratio and crystallisation in the transition zone are different from that in the bulk materials, indicating a difference in the properties. It is obvious that bond strength will be affected by many factors relating to the properties of the substrate, the repair material, and the environmental conditions. Study carried out by Carles-Gibergues, et al [152] showed that the nature of cement can mask the influence of other parameters like the saturation state of the substrate. A thorough understanding will not be achieved unless these factors are taken into consideration. The following discussion deals with some of the important issues relating to: the moisture condition

of the substrates; the properties of the repair materials; the properties of the substrate; and some other factors.

6.3.3 Substrate moisture condition

The substrate moisture condition consists of both moisture condition inside the substrate and at the surface layer. The effects are different in the way they affect the bond strength development.

Sand/cement mortar

When the internal moisture condition is considered, its effects on the bond strength are not very clear (Fig. 6.12). The bone dry substrate produced the highest bond strength, whilst the air dry substrate produced the lowest bond strength. Schrader [21] reported a repair where concrete was cast onto an old concrete. The shear bond strengths on the dry substrate surfaces were about 20% higher than those on saturated substrate (prewetted for 18 months). In [48], the effect of internal moisture condition was found to be related to the absorption capability of the aggregates. For low absorption aggregates there is no significant difference between the tensile bond to 'saturated surface dry' and oven dry materials. Aggregates of high absorption showed a 50% increase in bond strength if these porous materials were dried before bonding. In Austin and Robins' work [15], wet surfaces were obtained by leaving the concrete substrate in the curing tank until required. The 'dry' surfaces were obtained by allowing the specimens to dry out in air overnight. Hence, the first group can be defined as saturated surface wet, and the second group is somewhere between a saturated surface dry and an air dry surface dry condition. Among the 14 comparative groups, eight showed no significant difference at both confidence levels, four groups showed the dry substrates produced higher bond strength, only two groups suggest that a wet substrate worked better than a dry one.

When the surface moisture condition is considered, the test results in Fig. 6.12 shows that its effect on the sand/cement mortar is not significant. The t statistical analysis shown in Table 6.7 suggests that there is no significant difference at confidence level of 99% between dry and wet surface moisture conditions. The slant shear tests conducted by Wall and Shrive [38] showed no clear effect of surface moisture condition. If the statistical analysis is based on the failure loads one can draw the conclusion that there is a significant difference at confidence level of 99%, suggesting a wet surface is beneficial to the bond strength. However, if the material strengths are taken into consideration, we find that the failure loads of the surface dry group were nearly same as the higher material strength, indicating that failure was controlled by the material strength rather than by the bond strength. This is verified by the failure mode where no bond failure was obtained. In [63], a new concrete was cast against an old concrete and the moisture condition investigated was focused on the surface layer which was sometimes pre-wetted before applying the repair material. The test results suggest that pre-wetting the substrate surface was slightly detrimental to the bond strength. Tests conducted by Monteiro [73] on surface moisture condition showed mixed trends. The t statistical analysis of these test results is shown in Table 6.8.

It is generally thought that a dry surface tends to pull cement paste from the new mixture into closer contact with the surface, and as the surface absorbs excess mix water, it reduces the water/cement ratio at the bond interface, thereby increasing bond strength and reducing shrinkage at the bond interface. However, if a substrate is so dry that a part of mixing water is sucked off into the substrate before any solvable and reactive components in the cement paste are formed, the repair mortar will not adhere firmly to the old concrete.

It can be seen from these tests that the moisture condition both inside the substrate and at the surface layer influenced the bond strength of the sand/cement mortar, but the

effect varied quite significantly, which indicates the effect of moisture condition may depend on a particular substrate and a particular mix ratio.

Acrylic modified cementitious mortar

The effect of the moisture condition on the acrylic modified mortar, both inside the substrate and at the surface layer, was not significant (Fig. 6.13). When the moisture condition inside the substrate was concerned, the bond dry substrate produced the lowest bond strength which was only 3% lower than that with the saturated or air dry substrates. When the surface moisture condition was concerned, the difference between results from wet and dry surfaces was less than 3% with the saturated and air substrates and about 8% with the bone dry substrates, and the statistical analysis showed no significant difference at both confidence levels (Table 6.7 and Fig. 6.13). Further, if all 75 test results of the A1 material in Table 6.5 are averaged the mean bond strength of all the moisture conditions is 2.8MPa, with a coefficient of variation of 10.6%. Statistically, no mean bond strength of each moisture condition was significantly different from the mean value at both confidence levels. These test results reflect the non-stringent requirement that the surfaces should only be dampened for this acrylic modified material.

With another acrylic modified cementitious mortar (A2) the effect of the moisture conditions on the tensile bond strength was also not significant. The saturated surface wet substrates (very wet moisture condition) produced the highest bond strength, the bone dry surface dry substrates (very dry) produced the lowest bond strength, this agrees with the trend with the first acrylic modified mortar. However, the absolute value of the tensile bond strength was not high even compared with the normal sand/cement mortar. The tensile bond strength of the A2 mortar varied from 1.42MPa to 1.73MPa. If all 24 test results of the A2 mortar are averaged, the mean bond strength is 1.56MPa, with a coefficient of variation of 10.4%. According to the manufacturer's suggestions, the substrate should be thoroughly soaked with water (any

excess water being removed) prior to the application of the bond coat, which can be defined as a saturated surface wet requirement. The test results support the manufacturer's requirement.

SBR modified mortar

The effect of the moisture condition on the SBR modified cementitious mortar varied considerably. The bond strength with the saturated surface wet substrate was 17% higher than that with the saturated surface dry substrate, but the bond strength with the air dry surface wet substrate was 30% lower than that with the air dry surface dry substrate. The bone dry substrates showed little difference in the tensile bond strength between a wet and dry surface. Tests carried out by Monterio [73] also showed mixed trends (Table 6.8).

The effects of moisture conditions on other unspecified latex-modified repair materials have also been reported by Schrader[21] and Austin and Robins [15]. In [21], the air dry substrates produced higher bond strength than pre-wetted substrates. In [15], the wet surfaces produced higher core pull-off bond strength than the dry surfaces, but nearly the same slant shear bond strengths using a commercial repair mortar.

The requirements for the moisture conditions depend on the type and the content of the polymer. The polymer particles form a cover around the cement grains if the dispersion is added in sufficient concentration to the mortar to improve its flexibility. In this way the hydration products of the cement cannot contribute in an appreciable manner to the bond and the bond is based mainly on the properties of the polymer system. In practice, the bonding dispersions used are less concentrated and, therefore, the crystalline bonds of the cement in the cement mortar can contribute to the bond. Hence, it is suggested by Ainsworth, et al [2] that natural or artificial drying of the concrete surface up to a certain content will be beneficial, but a visible water film on

the surface should be avoided. Also, the moisture content within a depth of about 10 to 20mm should normally not exceed 4 percent by weight, with a maximum of 6%. But in the ACI committee 503 report [152], it is reported that polymer adhesives tolerate a wide range of moisture conditions in the plastic concrete and the hardened substrate. When polymer is used to modify the properties of concrete and mortar (mainly the bond strength), it can be expected that the effect of the moisture conditions will be less significant for the polymer modified materials than that for the plain sand/cement mortars.

Flowing concrete

Flowing concrete is a blend of Portland cements, graded aggregates, and additives which impart controlled expansion in both the plastic and hardened state whilst minimising water demand. The aggregate grading is designed to aid uniform mixing and eliminate segregation under pumping pressures. It is not a polymer modified cementitious mortar, and the flowing characteristic makes it different from the common sand/cement mortar and concrete. Thus, a separate discussion is presented for the flowing concrete.

Tables 6.5 and 6.6 show the moisture effect on bond strength using the core pull-off test and the patch flexural test, respectively, and Figures 6.16 and 6.17 show the results in graphic form. Table 6.7 shows the statistical analysis. It can be seen in Figs. 6.16 and 6.17 that the pull-off test results suggest a dry surface is superior to a wet one, whilst the patch flexural tests showed only very small difference between the two surface moisture conditions. From both the tests, the bone dry surface dry substrates produced the highest bond strength. The statistical analysis showed no significant difference at both confidence levels from the patch flexural tests, and also no significant difference between the air dry surface wet and the air dry surface dry ones from the core pull-off tests.

If the failure loads of the unrepaired beams are considered in the interpretation of the test results, it can be seen that the failure loads of the patch flexural beams with both the saturated surface wet and the saturated surface dry substrates were slightly lower than that of the unrepaired ones, which suggests that debond may have occurred even before the beams reached the failure load of unrepaired specimens. Thus, the failure loads should be considered to be the same as the unrepaired ones.

6.3.4 Influence of changes in repair material constituents

The response of the bond performance to moisture conditions can be influenced by the repair material, and its mix constituents, for example, the w/c ratio, aggregate/cement ratio, aggregate type, polymer type, and polymer content.

Sand/cement mortar

With the S/C mortar used in [48], the test results showed an increased material strength (compressive strength and the modulus of rupture) with decreasing w/c ratio down to 0.3, but the modulus of rupture of bond showed the peak value at a w/c ratio of 0.4. If the w/c ratio of 0.3 is the optimum value for the material strength for that material concerned, it may not be the optimum value for the bond strength. Increasing or decreasing the w/c ratio at the bond interface due to the substrate moisture condition will change the bond strength accordingly. If the original w/c ratio is designed for a saturated substrate, a reduced bond strength can be expected if part of the mixing water is sucked off from the mortar due to a very dry substrate.

Two grades of S/C mortars were used by Austin and Robins [15]: M40 and M30, with the w/c ratios of 0.4 and 0.5, respectively. Table 6.9 shows the bond strength ratio. The bond strengths with the M40 mortar were about 13% lower than those with the M30 mortar. This difference can be attributed partly to the difference in the w/c ratios, and partly to the effort to properly compact the mortars. In contrast to the tensile bond

strength, the compressive strength of the M40 mortar was about 13% higher than that of the M30 mortar. This clearly demonstrates that a higher material strength does not necessarily correspond to a stronger bond.

Polymer modified cementitious mortar

With polymer modified mortars, attention should be paid to the difference between laboratory produced materials and commercially available materials. The addition of polymer latex will generally improve the properties of fresh concrete. The latex also entrains a considerable amount of air due to the action of the emulsifying surface active agent that stabilises the latex. Indeed, it may be necessary to suppress the air entrainment by the addition of an antifoaming agent to keep the entrained air within reasonable limits[13].

Two repair materials using the same kind of latex but one with an anti-foaming agent, and the other without, were tested by Knab and Spring [13] using different test methods. Results from all the tests showed clearly that the one with the anti-foaming agent produced much higher bond strength. If the effect of the excess air is ignored, the much lower bond strength measured using the polymer latex (without an anti-foaming agent) may lead someone to draw the conclusion that this kind of polymer (or this particular product) is inefficient in improving the bond strength.

It is known that polymers themselves normally show considerable shrinkage. How can we imagine that when a kind of polymer is mixed with concrete, a low shrinkage material is produced. There must be other admixtures which will compensate the shrinkage effect.

Because due to commercial reasons the mix composition for most repair materials is unknown, the discussion can only be based on the physical performance shown by each individual repair material together with some general trends and general

knowledge of that particular polymer system concerned. For example, the substrate surface is required only to be dampened prior to the application of the bond coat of the A1 mortar, whereas the SBR modified mortar is required to be thoroughly soaked with water but no free water on the surface. If a repair mortar is required to be applied with a bond coat, the moisture condition mainly affects the bond between the substrate and the bond coat and the time required to let the bond coat become tacky, which will be discussed in later sections.

Flowing concrete

The flowing concrete was found to be very easy to fill in the mould without any extra effort. The examination after the tests showed very good contact at the bond interface. But slight segregation was observed when handling a small volume of the flowing concrete. This might cause some variation in bond properties from patch to patch, and partly explains the fairly high coefficient of variation. It should be pointed out that this kind of repair material is not suitable for small patch repairs.

6.3.5 Influence of changes in substrate concrete properties

The permeability of the substrate concrete will affect the rate of water movement between the repair mortar and the substrate, depending on the mix ratio, especially the w/c ratio, curing condition, and curing time. Generally, it is the permeability of the cement paste that affects the permeability of a concrete, but the microcracks at the cement paste-coarse aggregate bond interface may also contribute to the increase in permeability. In this study, in order to limit the testing parameters, only one substrate mix was used. The discussion presented here is mainly based on tests conducted by other researchers, and hopefully this can arouse interest for further research.

Alexander, et al's tests [48] showed that for aggregates of low absorption, there was no significant difference between the tensile bond strength to saturated surface dry and

over-dry materials. Aggregates of high absorption showed up to a 50% increase in bond strength if these porous materials were dried before bonding. They draw the conclusion that the increased bond strength associated with dry absorbent aggregates was probably due to a reduction in the w/c ratio at the bond interface.

Usually, more water than that needed for hydration of the cement is added to the concrete mix to achieve a proper workability, and a slight reduction in w/c ratio at the bond interface will enhance the bond strength. But if the w/c ratio is reduced below the level for proper hydration, a weak bond will result. An extreme case can be demonstrated by applying an S/C mortar onto an oven-dry brick (high porosity); only a very low bond strength will be generated.

For quality controlled concrete, the variation of the permeability should not affect the bond strength significantly. But in order to determine if there is too much moisture in the concrete the following test was suggested initially by Gaul [95]. A 1.2x1.2m polythene sheet is taped to the surface of the substrate concrete when the ambient conditions of sunlight, temperature, and humidity are the same as will exist during application of the barrier, and left in place for a length of time which is equivalent to that required for the barrier system to cure after it has been applied. If in this length of time, visible moisture collects under the polythene sheet, it is highly likely that moisture conditions in the concrete will interfere with a good bond for most barrier systems.

One area which so far has not received much attention is the type of aggregates in the concrete mix. Two different types of aggregates: limestone and granite, were used to study the bond between polymer modified cement paste and aggregate by Su, et al [50]. Polymer dispersions used include: a styrene acrylate (SA), a copolymer of vinylpropionate and vinylchloride (VVC), and an acrylate with a coupling agent (ACA). The results showed very significant difference between these two kind of

aggregates. With the plain cement paste, the bond strengths at 180 days were about 1.5MPa with the granite and about 3.3 MPa with the limestone. With the SA modified cement paste, the bond strengths at 180 days were: with the limestone, if the polymer content was less than 15%, hardly any bond strength at all; if the polymer content was 25%, very high bond strength, nearly 5MPa; with the granite: steady increasing bond strength up to about 4.5MPa with the increasing polymer content to about 25%. For VVC modified cement paste (polymer/cement ratio: 15%), the bond strengths with both limestone and granite reached their peak values at 7 days, with the former being about 1,8MPa and the latter only 1.0MPa.

In a situation of concrete repair, the bond between the repair material and the aggregate in a substrate will affect bond strength. Tests conducted by Su, et al [50] cast some doubt on direct comparability of results from different sources because many different types of aggregates have been used, further research is needed to see the significance of the aggregate types affecting bond properties in concrete repairs.

6.3.6 Influence of curing condition

In a laboratory study, the attention is usually focused on the moisture movement between the substrate and the repair mortar due to the unbalance of moisture conditions. In fact, moisture exchange takes place not only at the transition zone, but also at surfaces exposed to the air. In the lab-repair, it might be the former moisture exchange that affects the bond strength, whilst in the real repair, the latter moisture exchange may become the dominating factor.

Shaw [7] pointed out that applying conventional concrete, sprayed concrete, sand/cement or polymer modified mortars at high ambient temperatures will cause problems to bond because water loss at the interface between the repair material and

the prepared concrete may prevent proper hydration of the cement matrix at this interface.

Schrader [21] pointed out the beneficial effect of wetting the surface and letting it dry back from the standpoint of evaporating cooling, especially for slabs and reinforcing steels exposed to the sun. A hot surface can cause fast setting, drying, and excessive stiffening of the mix at the interface. Curing also accounts for the moisture loss from the bond interface. If a repair is not properly cured, the surface layer (about 30 -50mm in thickness) is mostly affected due to the high rate of evaporation [111]. The affected layer is coincident with normal patch repair thickness, this puts bond interface in an influential range from curing. Bond interface beyond this range may not be affected by improper curing. But it should be born in mind that it is the periphery of the bond that is under risk, and also it is the periphery where further deterioration could occur due to a weak bond, poor impermeability, and invasion by detrimental substrate.

From the discussion above, it can be seen that the requirement for a thorough wetting the substrate is mainly for compensating the fast moisture loss resulting from a high ambient temperature, windy weather, and improper curing. An indiscriminate requirement for thorough wetting may not be beneficial in all cases.

6.4 Bond coats

6.4.1 Test results and test observations

Tables 6.10 and 6.11 show the effect of bond coat on the S/C mortar and polymer modified mortars using the core pull-off test, and Tables 6.12 and 6.13 show the effect of bond coats on patch compressive and patch flexural tests conducted in the range of repair materials. Figs. 6.18 and 6.19 show the tensile results in graphic form. The test results

clearly show that if applied properly a bond coat can increase the bond strength quite significantly.

Sand/cement mortar

Only the acrylic modified bond coat was applied with the sand/cement mortar. Clearly, the bond strength of the sand/cement mortar was enhanced with this kind of bond coat, with the increase being most significant with the core pull-off test (nearly 75%). With a patch compressive test, the bond strength was increased from 35.2 to 43.6 MPa with a smooth surface (SRI = 285 mm), and from 41.3 to 48.4 MPa with a rough surface (SRI = 190 mm). When the bond coat was dry at the time of applying the sand/cement mortar, the tensile bond strength was much lower than that without a bond coat.

The application of a bond coat in the patch compressive test also enhanced the bond strength, but the degree of increase was far less significant than that in a tensile situation. Applying the sand/cement mortar on the acrylic bond coat, the patch compressive tests showed around a 17% increase in failure loads for the rough surfaces, and a 24% increase for the smooth surfaces. This is as expected because with a bond coat the interface between the bond coat and the S/C mortar tends to be very smooth. If the original surface is rough, a bond coat will function in the following two ways: by enhancing the adhesion strength, and reducing the roughness effect.

Acrylic modified mortar

This repair material is supplied with a specially formulated bond coat which is in a fairly good running state after mixing. Without this coat the tensile bond strength was just 0.75 MPa, about 55% of that of the sand/cement mortar. With this coat the tensile bond strength was 2.82 MPa, 15% higher than that of the sand/cement mortar with the same bond coat. No matter what the original surface roughness was, all surfaces looked fairly smooth after applying the bond coat. The bond coat gradually becomes

tacky with increasing exposing time. 40 -60 min. after mixing, the surface layer of the coat was getting dry, but below this surface layer the coat was still wet and tacky. This mistimed bond coat received freshly mixed mortar to simulate a bond coat mistiming situation. The reduction in tensile bond strength was less than 3%.

With the patch compressive test, the increase due to the bond coat was not significant. The patch compressive bond strength at an age of 14 days was increased from 26.3 MPa without a bond coat to 29.4 MPa with the bond coat, the increase being 12%. A 40 min. mistiming in the bond coat did not cause any decrease in bond strength, rather, a 10% increase was recorded.

SBR modified mortar

This product also comes with a specially formulated bond coat. Unlike the acrylic modified bond coat which was in a fairly good running state, the SBR modified bond coat was in a tacky condition immediately after mixing. The tensile bond strength with the bond coat was 1.53 MPa, which is about 9% higher than that of the sand/cement mortar without a bond coat. When the SBR modified mortar was applied without the bond coat, the tensile bond strength was only 0.93 MPa. When the bond coat was mistimed by 40 min., a 25% reduction in bond strength was recorded. With the patch compressive test a 40 min mistiming caused a 9% decrease in the bond strength.

6.4.2 General observations

The aim of a bond coat is to improve bonding between hardened concrete and newly placed cement-based materials such as concrete and mortar. Prior to the introduction of polymer bonding agents, it was the practice either to use nothing and rely on the preparation of the surface of the base concrete, or to use a cement slurry. Both of these techniques gave excellent results in the laboratory, but in the field, the results were often disappointing.

Hence it can be seen that the purpose of a bond coat is to achieve an effective adhesion between the repair and the old concrete to make up for the defects that may be encountered on site. The Concrete Society [10] suggest that where a hand-applied resin or cementitious mortar repair system is used, the concrete surface is normally coated with a bond coat. The repair material should be applied while the bond coat is still tacky.

For a hand-applied cementitious mortar, a bond coat of polymer-latex-cement slurry, or neat latex (according to the manufacturer's recommendations) is normally applied to the prepared surface. Depending upon the porosity of the concrete, it is usually necessary to dampen the concrete with clean water to minimise suction immediately before applying the bond coat, otherwise the open time of the bond coat will be short. The bond coat should be mixed to a smooth creamy consistency and applied by brush as a uniform coat; the repair mortar must be applied while this coat is still tacky.

There are different kinds of polymers, but if a polymer is to be incorporated into the repair mortar, it is usual for it to be incorporated also into the bond coat. For resin systems, the bond coat is usually a resin of similar nature to that forming the binder in the repair mortar. All proprietary resin repair systems provide both bond coat and repair mortar.

6.4.3 Effect of different repair materials

The tensile bond strength of the S/C mortar was increased from 1.41MPa to 2.46MPa using an acrylic bond coat (Fig. 6.18). In [18], the bond strength of an S/C mortar was increased from about 1.20MPa without a bond coat to about 1.94MPa with S/C grout, and to about 2.4MPa with the acrylic bond coat on the saw cut surfaces. This agrees very well with the author's test results.

The importance of a bond coat for polymer modified mortars is more obvious than that for an S/C mortar. Two additional comparative tests were carried out to see the influence of a bond coat on the tensile bond strength of the A1 mortar and the SBR modified mortar. With the bond coat recommended by the manufacturer the bond strength was 2.82MPa with the A1 mortar and 1.53MPa with the SBR mortar. However, without a bond coat, the bond strength was reduced to 0.75 and 0.93MPa, respectively, which are much lower than that achieved using a sand/cement mortar only. There is no test data on polymer modified mortar with other kinds of polymer modified bond coat as this is not practical. The interesting issue is that quite a few kind of bond coats are compatible with normal sand/cement mortar. If a bond coat can increase the bond strength of the sand/cement mortar, the repair cost can be reduced considerably, which is very beneficial to the construction industry.

6.4.4 Effect of timing of repair application

In order to achieve the most effective adhesion using a bond coat, care must be paid to the timing of the application of the repair onto the bond coat. Generally, a repair material must be applied while the bond coat is still tacky, otherwise, a dramatic drop in bond strength can be expected [1, 38, 43, 105]. Three cases of mistiming can occur: (1) applying fresh mortar onto a dried bond coat; (2) applying dried mortar onto a fresh/tacky bond coat; and (3) applying dried mortar onto a dried bond coat. In practice, case (3) will not happen. In this section the focus is on the case (1): applying fresh mortar onto a bond coat of varying degree of dryness, whilst case (2) will be dealt with in the next section.

To simulate different dryness of a bond coat, the bond coat was mixed and applied onto a ready prepared substrate, and the repair mortar was mixed about 2 to 3 minutes before the specified mistiming of the bond coat was reached, say 40 min. and 60 min..

Judge et al's results [40], using a core pull-off test, showed that a tacky bond coat produced nearly in all cases very good bond strength, which though may not be the best bond strength that could be achieved. But the optimum condition of a bond coat to produce the best bond depends very much on the particular type of a bond coat. For example, with three different acrylate bond coats, the bond strengths achieved were not very sensitive to the condition of the bond coat, whether they were wet, tacky, or dry. The terpolymer and PAVc/VeoVa bond coat achieved the highest bond strengths under dry conditions but an SBR bond coat showed complete loss of bond strengths when becoming dry. Dixon and Sunley [43] also reported a detrimental effect when the repair material was applied to a dried SBR bond coat.

Applying a second bond coat to the dried coat will not remedy the situation. In [43], the application of a double layer SBR bond coat showed a dramatic decrease in bond strength. Serious reduction in bond strength with double bond coats also occurred with acrylic dispersions [105], and the PVA bond coat [38].

From all the above test results, it can be seen that even though sometimes a tacky bond coat may not produce the optimum bond strength, it nearly always produces an acceptable result. Thus the requirement for a tacky bond coat is justified..

A dried bond coat is usually detrimental and can be identified easily. The real problem is sometimes related to judging when a bond coat will develop into a tacky condition so that the repair material can be mixed. Depending on the ambient temperature, wind speed and solar radiation, the time required for a bond coat to become tacky will vary. When the freshly mixed acrylic modified mortar was applied on an acrylic bond coat which had been left exposed for about 40 - 60 min, no detrimental effect on bond strength was observed. When the freshly mixed SBR repair mortar was applied on an SBR bond coat which had been left exposed for about 40 min, a 30% reduction in the

tensile bond strength was recorded and the statistical analysis showed a significant difference at both confidence levels of 95% and 99%. Unlike the acrylic bond coat used with the A1 material, which was in a state of fairly low viscosity after mix, the SBR bond coat was in a tacky state immediately after the mix, which shortened the open time of the SBR bond coat.

In [38], exceeding the PVA manufacturer's recommended pot life by about 20 min did not adversely affect the bond strength. If moisture loss from the bond coat can be prevented, the bond coat will still function well despite a longer delay. In this project, a bond coat was mixed in a small mixer. It was applied on up to three specimens at a time, whilst the remainder in the mixer was covered tightly. In this way, the bond coat could be kept in a wet condition for at least 60 min..

Since the re-application of a polymer-cement bond coat is not recommended, it follows that great care must be taken to apply this type of bond coat just in advance of the mortar or concrete application. But as the rate of drying of any water-based material can be so variable and unpredictable, there is always a risk that premature drying may occur. If it does, the only way to prevent a weak bond is to wet-scrub back to the clean concrete and start again.

6.5 Installation (by hand or casting)

In section 6.4, the problems with mistiming of a bond coat were discussed. This section will discuss how to obtain good installation of repair material. The compaction of a repair material can be influenced by a few factors, such as the workability of the repair material, and the method of installation (by hand or casting). In this research programme, installation by hand means the repair material was applied into the mould with gloved hands layer by layer and if necessary a metal rod was used to make sure that the repair material at the corner was adequately compacted. installation by vibration means the compaction of the repair material was achieved using a vibrating table. This is viewed as the ultimate degree of compaction which can be achieved with a gloved hand.

6.5.1 Test results and test observations

The effect of the degree of compaction on the core pull-off bond strength can be seen in Table 6.1. The vibrated group with surfaces which were saw cut and received no further treatment had a bond strength of 0.27MPa, whilst the hand applied group with same surfaces showed complete loss of bond during core drilling. The hand applied group with surfaces which were saw cut and needle gunned produced a bond strength of 1.2MPa, whilst the vibrated group had a bond strength of 1.57MPa, which was 31% higher. The bond strength obtained from the vibrated group was also higher than that from the control specimens.

The effect of compaction can also be seen with the slant shear test (Table 6.4). The vibrated group with the formed and then sand blasted surfaces had a slant shear bond strength of 42MPa, which is about 13% higher than that from the hand applied group. But for the line load split and needle gunned surfaces, the slant shear bond strength from the vibrated group was about 4% lower than that from the hand applied group. It needs to be emphasised that the slant shear strengths from both groups slightly exceeded the weaker material strength.

Not only the compacting method, but also the workability of a repair material will affect the degree of compaction. In Tables 6.11 to 6.13, a 40-60min mistiming of the acrylic modified mortar applied on freshly mixed acrylic modified bond coat caused around a 12% reduction in the core pull-off strength, but no reduction in the patch compressive strength. A 40min mistiming of the SBR modified mortar applied on freshly mixed SBR modified bond coat caused about a 40% reduction in the core pull-off strength. In the patch compressive test, a reduction in the failure load was recorded, but this was much smaller than that in the core pull-off test, only about 5%, and in the patch flexural test the failure load was slightly lower than those unrepaired specimens, which makes the interpretation of test results difficult. For the S/C mortar and the flowing concrete no reduction in the patch compressive failure load was recorded. In the patch flexural test, the reduction in bond strength was only 2% for the S/C mortar, and about 9% for the flowing concrete.

6.5.2 Discussion of the test results

The above results clearly demonstrate the importance of proper compaction on bond strength. They also showed that the effect is different under different stress states. The variation of compaction depends on the workability of the repair material, the shape of the area where repair is to be carried out, the access to the repair area, and the method used to apply the repair material. Operator differences also cause variations in compaction.

In this project, about a third of the repair material was poured into the mould each time. For the core pull-off test, a metal rod was used to compact the repair material except in the case of the flowing concrete. When the mould was filled, a steel trowel was used to press the top part of the repair material and to produce an even repair surface. No problem was experienced with the sand/cement mortar in achieving reasonable compaction, however, some compacting difficulties were encountered with the acrylic modified mortar at the beginning of this project due to loss of workability. These were overcome later by covering the remaining mortar in the container with polythene sheet to maintain the workability. The loss of workability of the SBR mortar was more significant than that associated with the A1 material, and more effort was requested to compact it.

It was easier to achieve good compaction with the patch compressive and the patch flexural specimens. Because a bond coat is usually used with a polymer modified material, the contact between a tacky bond coat and high workability repair material is likely to be good. But when moisture evaporates from the repair material causing significant reduction in the workability, this can make compaction very difficult.

In this project all the repairs were carried out under favourable conditions and did not require a high initial bond strength to maintain bond strength. Practically the repair

can be carried out on high-rise buildings, bridges, etc., and the position can be horizontal, vertical, or overhead, which will require high initial bond strength.

Generally, the mixed mortar should be packed into place a little at a time, taking particular care to compact the first layer firmly onto the primed surface. The best method of doing this will depend on the situations; it may be simply to pack the material into the cavity if it is bounded on all sided by concrete in one plane, but when forming an arris it will often be necessary to use some form of support to one face. If the repair is shallow this may just be a hand-held board or trowel, but more substantial repairs will require a fixed shutter.

During the installation of repair material the workability of a repair material has to be maintained otherwise weak bond can result. This can happen for large area repairs and those carried out in hot weathers.

Unlike a bond coat which sometimes require a period of time to develop into a tacky condition, a repair material can be applied on a bond interface right after mixing. Any delaying in application will cause reduction in workability, and consequently, very substantial effort is required to compact the repair material well.

A 60min. delaying in installing the acrylic modified mortar caused 12% reduction in tensile bond strength even though results from the patch compressive test showed no adverse effect at all. This can be explained below. If the loss of workability resulted in some air voids at the bond interface, the tensile bond test is much more sensitive than the patch compressive test to detect the existence of surface defects.

A 40 min delaying of the SBR modified mortar in installing caused a substantial reduction in bond strength. The bond strength of the mistiming group was about 40% lower than that of the control specimens. The statistical analysis confirmed the difference at both confidence levels. This indicates that the SBR mortar is fairly

sensitive to the mistiming. In other tests using the SBR mortar, the problem of possible mistiming was overcome by: (1) using the maximum amount of water allowed in the manufacturer's technical data sheet; and (2) covering the remaining mortar in a container with polythene sheet to prevent moisture loss and maintain workability.

6.6 Curing

6.6.1 Presentation of test results

Table 6.14 and Fig. 6.20 show the effect of curing on the tensile bond strength development. All results except the one with the new flowing concrete showed some adverse effect on the bond strength due to receiving no curing precautions. Those specimens which needed to be properly cured were covered with polythene sheet tightly for 3 days to prevent moisture loss, and those with no curing precautions were simply left uncovered in the laboratory. The curing effect on the patch flexural tests is shown in Table 6.15 and Fig. 6.21, and the patch compressive test in Table 6.16 and Fig. 6.22.

Sand/cement mortar

Without covering with polythene sheet, bond strength of the sand/cement mortar was reduced. When the age of the specimens were around 28 days, the tensile bond strength was reduced by 14%, the patch flexural bond strength, 8%, and the patch compressive bond strength, 5%. The tensile bond strength suffered severe reduction when the age of the specimen was about 70 days.

Acrylic modified mortar

The acrylic modified mortar experienced a substantial decrease in bond strength with the core pull-off test. For the substrates with AW moisture condition, a 43% reduction was recorded, and for the substrate with the SD moisture condition, a 30% reduction

was recorded. Ignoring the effect of moisture condition, the reduction is 35%. With the patch flexural and patch compressive tests only 4% and 5% reductions in bond strength were recorded.

SBR modified mortar

The bond strength reduction of the SBR modified mortar was not significant in either the core pull-off test (6% reduction), or the patch compressive test (2% reduction). In the patch flexural test, because the failure loads of the uncovered specimens were slightly lower than that of the unrepaired specimens, which can only be explained as being due to the variation of the substrate properties; it is difficult to quantify the curing effect. If the failure modes are checked, it is found that no bond failure occurred either in the properly cured or uncovered specimens. This indicates that the tensile bond strength of the SBR mortar is low. But all the failure modes from the pull-off and the patch compressive tests clearly showed bond failures.

Flowing concrete

Curing had no effect on the flowing concrete with either the pull-off or patch compressive tests. The patch flexural tests showed around a 10% reduction in bond strength.

6.6.2 General observation

It is generally recognised that proper curing is important in ensuring full bond strength development, but with polymer modification the optimum curing environment for a repair material may be different from that for traditional concrete and sand/cement mortars.

In order to have a better understanding of the effect of the curing on the bond strength, the effect of curing on the material properties must be addressed.

For normal concrete and sand/cement mortars, the properties are developed through the gradual hydration of cement. When Portland cement is mixed with water, its constituent compounds undergo a series of chemical reactions which are responsible for the eventual hardening of concrete and mortar. The aim of curing is to ensure as much hydration as possible at reasonable cost. Theoretically, there is enough water in concrete to ensure complete hydration without additional water being supplied if the w/c ratio is over a certain limit, for example, 0.42 as stated in [113]. However, in practice, water is lost from the paste by evaporation, or by absorption of water by aggregate or formwork. Once enough moisture is lost from the concrete, hydration will stop and strength development is arrested.

For polymer modified cementitious materials, the properties will depend on the combined reaction of polymer and cement.

It needs to be emphasised that for polymer materials: (1) their physical properties are uniquely different from that of cement; (2) organic polymer materials cover an extremely broad range of chemical/physical types; (3) polymer properties are sensitive to the effect of relatively small temperature changes and they are also time dependent; and (4) the ultimate properties can be markedly affected by the environment in which the material is applied and cured.

The contribution to the ultimate performance from the polymer modified cementitious materials comes from two processes: the hydration of cement and the coalescence of the latex. The chemistry and reaction processes of cement hydration occur the same way as in a conventional mortar and concrete. However, while the hydration is taking place, water is being consumed and removed from the latex. This will concentrate the latex particles and bring them closer together with the continual removal of water, both by cement hydration and evaporation. The latex particles eventually coalesce into a film which is interwoven throughout the hydrated cement particles, coating these particles and the aggregate surface with a semi-continuous plastic film. This film is

responsible for maintaining moisture around the cement particles, eliminating the need for a continuous wet cure but permitting the cement hydration process to continue. During the initial curing period, however, proper covers such as damp burlap and polythene sheet must be used to prevent excessive moisture loss before the Portland cement begins to harden.

6.6.3 Discussion of the test results

In this test programme the curing conditions were simulated by either covering the repaired specimens tightly or leaving the repaired ones uncovered inside the laboratory, which therefore varied with the local ambient temperature and humidity. The implementation of this kind of comparative study of curing conditions was to see the effect on the bond strength if the repaired area was either covered or exposed to air. This kind of curing method is different from the one adopted in Yeoh, et al's research, in which the temperature and the relative humidity were kept constant, for example, the controlled environment set at 10°C, 70%RH, or 40°C, 70%RH. This curing method can reveal ideal curing conditions for each repair material, but it is difficult to apply the test results directly to real repairs. For example, the relative humidity varies significantly from day time to evening, so does the ambient temperature. The varying environmental conditions should be taken into consideration. At the moment, it is difficult to make a direct comparison between the results from this project and the results from [87].

The test results demonstrate that exposing the repaired area without any covering sheet is detrimental to bond strength, with the reduction rate depending on individual repair material.

Sand/cement mortar

The reduction of bond strength is in the range of 5 to 10% except the group with an age of 73 days showing a decrease of about 40%. But if it is compared with the

control specimens, the reduction is 7%. If it is assumed that the curing method only influences the intrinsic bond strength (adhesion strength), the reduction rate obtained with different test method can be averaged and this results in an average reduction rate of 8.5% for the sand/cement mortar.

Based on studies on material strength of concrete, the strength development is achieved by continuing hydration of cement. In the case of bond strength development of sand/cement mortar, we can also assume that hydration of cement dominates the bond strength. Exposing the repaired area to air will lead to high rate of moisture evaporation from the mortar, which indicates that ensuring proper hydration of cement is a good method of curing. This may be achieved by maintaining or adding water to the mortar.

Yeoh, et al's test [87] confirmed that a high humidity environment is an ideal curing condition for the sand/cement mortar. Thus, unmodified sand/cement mortar should be protected from moisture loss during the first few days after repair is carried out. Both methods of maintaining moisture by covering the repaired area and adding water by creating a high relative humidity environment are recommended.

Acrylic modified cementitious mortar

The significant decrease in tensile bond strength is not expected as it is generally thought that the film generated through polymerisation can partly act as curing membrane. But the reduction in bond strength from both the patch compressive and patch flexural tests are very small, about 5%.

The contribution to the ultimate performance from the polymer modified cementitious materials comes from two processes: the hydration of cement and the coalescence of the latex, with the former favouring a high humidity environment and the latter not favouring high humidity even though water tolerant polymers can be formulated.

In [86], the acrylic polymer was used to modify the cement mortar. Three curing regimes for the unmodified cement mortar were used: (1) a 28-day air cure, (2) a 28-day wet cure, and (3) a 28-day air cure plus a 7 day water soak, and two curing regimes for the acrylic modified mortar: (1) a 28-day air cure, and (2) a 28-day air cure plus a 7-day water soak.

The 28-day wet cure produced the highest properties for the unmodified cement mortars, whilst the 28-day air cure produced the lowest properties. The 7-day water soak after 28-day air cure compensated partly for the adverse effect of the air cure, but the later remedy of a 7-day water soak was far less effective than the initial wet curing. These results are in agreement with the author's and the findings from ref.[87].

For the acrylic modified mortar, the 28-day air curing produced much higher properties (the tensile, compressive, flexural, and impact strengths, and the shear bond strength) than those 28-day air cured followed by a 7-day water soak. The most affected properties were the tensile, flexural, and the shear bond strengths. Because all these are related to the tensile properties, it is not surprising to find that the reduction ratios were quite similar to each other (with the p/c ratio varying from 0.1 to 0.2, the average decrease in the tensile, flexural, and the shear bond strengths caused by the 7-day water soak was 0.59, with a coefficient of variation of 11%). The compressive strengths were reduced by about 10%, which is far less significant than the effect on the flexural properties. These tests indicated the very detrimental effect of water soaking on the polymer network inside the modified mortar, but were unable to suggest whether better properties could be achieved by covering the specimens with polythene sheets for the first few days.

If the effect of curing in [86] was focused on material properties, tests conducted in [87] was directly on the bond strength with different temperature and humidity. The test results in [87] revealed that both high and low humidity environment caused substantial damage to bond strength, about 15% decrease in core pull-off and core

twist-off bond strength.. The highest bond strength was obtained at a relative humidity of 70% and ambient temperature of 20°C, and is nearly same as the bond strength of the control specimens in the author's test.

Based on these test results it is possible to draw the conclusion that a too high or too low humidity environment is not beneficial to bond strength development of acrylic modified cementitious mortar. A good and practical curing method is to cover the repaired area for the first few days to ensure proper hydration of cement, and then expose the area to ensure the formation of polymer films.

<u>SBR modified mortar</u>

The bond strength reduction of the SBR modified mortar was not significant in either the core pull-off test (6% reduction), or the patch compressive test (2% reduction). Though the reduction is small, the results suggest that preventing moisture loss is beneficial to an SBR modified mortar.

In [87], test results clearly reveal that the SBR modified mortar favours a high relative humidity environment. The core pull-off bond strength at 70%RH was about 15% lower than that at 95%RH, and the bond strength at 40%RH was even lower, about 30% less. Showing the similar trend the bond strength obtained with the twist-off test at 70%RH was 10% lower than that at 95%, and 25% lower at 40%RH. The highest bond strength obtained was 7% higher than that of the control specimens in the author's test.

Studies on curing of SBR modified mortar recommend damp curing for the first few days followed by air curing [71]. It is reported that a one day damp curing followed by exposing to air can be a successful procedure if the weather condition is mild, but prolonged damp curing may be required if the temperature and wind condition are not favourable. Curing examples include initial damp curing for 24 hours followed by an

air cure for an airport department ramp [146], and for a bridge deck and garage floor [87].

All these test results suggest an initial damp curing for the SBR modified mortar, but when as to expose the repair area to air there is no common conclusion. Based on the test results and discussion, it is recommended that a minimum of 3-day damp curing be adopted.

Flowing concrete

The core pull-off and the patch compressive tests showed no reduction in bond strength, but a 10% decrease in patch flexural test was recorded. This suggests that flowing concrete should be protected from drying in the first few days. In [87], higher bond strength was obtained with higher relative humidity environment. Because the bond strength development is mainly based on cement hydration, an initial damp curing for a few days is recommended.

Based upon the test results and discussions above, it is clear that the ideal curing conditions vary with repair material. High humidity is good for plain sand/cement mortar but may not be ideal for polymer modified repair mortar. Preventing moisture loss by covering repaired areas is a practical method of proper curing.

6.7 General discussion of the effect of workmanship on bond strength

In order to achieve a durable and cost-effective repair, the workmanship has to be considered carefully. The above sections have discussed individually various workmanship issues. In the case of a bond failure, questions will be raised as to whether it is caused by incorrect workmanship, and if so, which aspect of the workmanship is at fault.

Because of the significant differences in chemical and physical properties between polymers and cement based materials, the effect of workmanship on each individual material has to be established. A factor favouring concrete may be detrimental to polymers, such as the curing regime for the two different materials. Without this knowledge, it will be difficult to achieve the best results.

For some aspects of workmanship the requirement for both the unmodified mortars and the polymer modified mortars is similar. For example, a sound substrate is required for both kinds of materials. Because of the difference in bonding performance and the use of a bond coat, a rough surface is not very important for polymer modified cementitious materials. This can be demonstrated with the acrylic modified mortar having tensile bond properties that exceed the tensile strength of concrete with either smooth or rough surfaces. In a laboratory, the issue is usually how to roughen a surface, but on construction sites, roughness will usually not be a problem due to cutting, chiselling or scarification, the issue is how to achieve a sound substrate, or when a sound substrate is achieved.

It is not just the moisture imbalance between the substrate and the repair material that affects the water movement, but also the weather conditions, and the curing method. In some cases, the latter effect can be more significant. For example, in hot weather moisture evaporation from the repair mortar may dominate the moisture movement leaving not even enough water for proper hydration of the cement. For most of the laboratory based results, the temperature and the wind conditions are much less significant than the in-situ conditions. More moisture loss can be expected in hot weather conditions. This has to be taken into consideration when applying laboratory results to guide site repairs.

Trial tests need to be carried out to find out how long is needed to let the bond coat become tacky, then the correct timing limits can be specified for mixing of the repair material. Under no circumstances should a second bond coat be applied if the first

coat becomes dry. For materials which do not need a bond coat, the repair materials should be applied immediately after mixing.

The major issue with installation of a repair material is how to achieve good compaction. Test results in the project demonstrated that compaction can be a problem especially with hand applied mortar. This problem can become worse if the workability of repair material is reduced or if the repair is carried out on soffit or vertical surfaces. Adding extra water is banned by manufacturers. Good practice is to carefully plan the timing of the final moisture condition, the bond coat if there is one, and the repair material, and to maintain workability by preventing moisture loss.

The curing requirements are different for unmodified cement mortars than for the polymer modified mortars. The comparison between different materials should be based on the optimum curing conditions for each individual material. Quite often, this aspect has been ignored in comparing different results. For example, in [154], all unmodified and modified specimens were covered by a plastic sheet after two hours, were demoulded after 24 hours, and were stored in laboratory air at about 18°C. Specimens for the shrinkage studies were stored in a conditioning room at 18+0.1°C and 65% relative humidity. This kind of curing condition may be beneficial for polymer modified mortars, but definitely is not so for unmodified mortars. If this difference goes unnoticed the contribution of a polymer can be overestimated. Also, if a polymer modified mortar is wet cured and compared with the normal S/C mortar, the contribution of the polymer can be underestimated.

Some other factors also need to be considered. For example, how a high bond strength can be achieved. In [5] because the substrate strength was fairly low, with the tensile splitting strength at 2.1 MPa, and the core pull-off strength 1.68MPa, the maximum bond strengths which could be achieved were limited by the low tensile strength of the substrate. Even with very good repair materials, such as epoxy mortar, polyester

mortar, and flowing concrete, the average failure stresses were in the range of 1.35 to 1.75MPa, which was far below results obtained from this project and from [19].

To summarise, workmanship covers many aspects, some are easy to be identified. During the whole repair procedure, each one has to be properly addressed and monitored.

6.8 Conclusions

Based on test results from this project and other researches, the following conclusions can be drawn.

(1) Workmanship covers many aspects, such as surface preparation, moisture condition, and curing method. To achieve a good repair every aspect has to be addressed properly.

(2) A rougher surface produces a higher bond strength, but the increase depends on each individual repair material. Sand/cement mortar favours a rough surface under different stress state. Polymer modified mortars are not very sensitive to surface roughness because a bond coat tends to decrease this effect.

(3) Bond strength depends on stress state imposed. Under a tensile stress state the surface soundness is the most important issue as surface defects will result in stress concentration which may cause premature bond failure. Under a combined stress state of compression and shear, the surface roughness can contribute significantly to resist bond failure. But this contribution can be replaced by selecting a bond plane with a high normal/shear stress ratio.

(4) The effect of moisture condition on bond strength varies with different repair material. The effect of moisture conditions at the surface layer and inside the substrate can be different. The acrylic modified cementitious

mortar was the least affected with tensile bond strength varying from 2.61 to 2.85 MPa for all moisture conditions studied. The flowing concrete favours both surface dry and inside dry. Saturated and surface wet condition should be avoided. In case of different weather conditions, an air dry surface dry substrate is recommended.

(5) Bond coat improves the contact between a repair mortar and substrate. The optimum condition for a bond coat to receive a repair material varies, but a tacky condition will produce a good, though may not the best, bond. Preventing moisture loss can partly decrease the detrimental effect of mistiming.

(6) Mortar mistiming will lead to loss of workability, which makes the compaction by hand very difficult and eventually results in weak bond. Thus a repair mortar should not be mixed until a few minutes before the bond coat becomes tacky, and then applied immediately after mixing.

(7) The requirement for a most efficient curing depends on how bond strength is gained. Bond strength developed through cement hydration favours a wet curing environment, but bond strength developed through formation of polymer films prefers quite often a drier environment. The sand/cement mortar, the flowing concrete, and the SBR modified mortar prefer high relative humidity environment, but the acrylic modified mortar favours a relative humidity around 70%RH. In view of the nature of patch repair, covering the repaired area tightly with polythene sheet is a good and practical way of curing.

Table 6.0 Combinations relating to workmanship

1	2	3	4	5	6	7	8	9	10	11	12	13	14	15	16	17	18	19	20
Repair materials / Test parameters / Specimen types		Sand/cement mortar				Acrylic modified mortar				SBR modified mortar				Flowing concrete				A2	Table and Figure numbers where test details can be found
		CP	SS	PC	PF	CP	SS	PC	PF	CP	SS	PC	PF	CP	SS	PC	PF	CP	
Control specimens		x	x	x	x	x	x	x	x	x		x	x	x		x	x		T(6.1 - 6.6, 6.10, 6.11, 6.13) T(6.14, 6.16) F(6.11)
Surface roughness index	SM	x	x			x													T(6.1)(6.4) F(6.11)
	MR	Standard surface roughness: medium rough																	
	RF	x	x			x			x										T(6.1)(6.4) F(6.11)
Surface soundness	S	Standard surface soundness: sound																	
	W	x	x																T(6.4)
Surface cleanliness	CL	Standard surface cleanliness: clean																	
	CT	x	x			x				x				x				x	T(6.2)(6.3)
Moisture condition	SW	x				x				x				x			x	x	T(6.5)(6.6)
	SD	x				x				x				x			x	x	T(6.5)(6.6)
	AW	Standard moisture condition: air dry surface wet																	
	AD	x				x				x				x			x	x	T(6.5)(6.6)
	BW	x				x				x				x			x	x	T(6.5)(6.6)
	BD	x				x				x				x			x	x	T(6.5)(6.6)
Applying methods	HA	Standard applying method: by hand																	
	VB	x	x																T(6.1)(6.4)
Bond coat mistiming	NO	Standard parameter: no mistiming of bond coat																	
	40	x				x	x			x		x	x						T(6.10) - (6.13)
Repair mortar mistiming	NO	Standard parameter: no mistiming of repair mortar																	
	40		x		x	x	x			x		x	x		x		x		T(6.11) - (6.13)
Curing methods	NO	x		x	x	x		x	x	x		x	x	x		x	x		T(6.14) - (6.16)
	3d	Standard curing method: moist curing for three days																	
High temperature curing followed by drying shrinkage																			
High temperature curing followed by thermal cycling																			
Low temperature curing																			
Low temperature curing followed by freeze/thaw cycling																			

Note: **Control specimens**: the parameters for control specimens are indicated by each standard parameter.

Bond test method:

CP: core pull-off test; SS: slant shear test;
PC: patch compressive test; PF: patch flexural test;

Parameters of workmanship:

SM: smooth surface; MR: medium rough surface;
RF: rough surface
S: sound surface; W: weak surface;
CL: clean surface; CT: contaminated surface;
SW: saturated surface wet; SD: saturated surface dry;
AW: air dry surface wet; AD: air dry surface dry;
BW: bond dry surface wet; BD: bond dry surface dry;
HA: Hand applied without vibration; VB: hand applied with vibration;
NO: no mistiming in mistiming group or no curing in curing group;
40: about 40 min. mistiming 3d: 3d moist curing ;
A2: light weight acrylic modified mortar

Table 6.1 Effect of surface preparation method on the tensile bond strength of the sand/cement mortar

Repair material	Sand/cement mortar							
Surface preparation method	Formed surface then sand blasted (medium rough)		Saw cut no further treatment (smooth)		saw cut and needle surface gunned (smooth)		Line load needle split and gunned (rough)	
Method of installation	Hand applied		hand applied	Vibrated	hand applied	Vibrated	hand applied	Vibrated
Age (days)	28-35	79	30	30	30	30	28	74
Number of tests	15	10	5	5	5	5	5	5
Number of bond failures	15	10	5	5	5	5	5	5
Tensile bond strength (MPa)	1.41	2.20	0	0.27	1.2	1.54	1.76	2.27
Coefficient of variation	30	18.4	0	21	17	19.7	28.7	17.6

Table 6.2 Effect of surface contamination on the tensile bond strength

Repair material	S/C		A1		SBR		F		A2	
Surface preparation method	FM-SB		FM-SB		FM-SB		FM-SB		FM-SB	
Surface cleanliness	CL	CT	CL	CT	CL	CT	CL	CT	CL	CT
Age (days)	28-35	28	28-38	35	28	28	28	28	28	28
Number of tests	15	5	25	5	5	5	5	5	5	5
Number of bond failures	15	5	4	5	5	5	5	5	4	5
Tensile bond strength (MPa)	1.41	0.34	2.76	0.77	1.53	0.43	2.03	0.98	1.67	0.76
Coefficient of variation (%)	30	33	12.4	37	17	10	23	26	4.4	12.8

Note: S/C: Sand/cement mortar; A1: Acrylic modified mortar;
SBR: SBR modified mortar; F: Flowing concrete;
A2: Light weight acrylic modified mortar.
FM-SB: Formed surface then sand blasted
CL: Clean surface CT: Contaminated surface

Table 6.3 Comparison between tensile bond strength with set retarder produced and sand blasted surfaces

Repair material	Sand/cement mortar		Acrylic modified mortar	
Surface preparation method	Formed surface then sand blasted (FM-SB)	Surface set retarder produced than wire brushed (SR-WB)	FM-SB	SR-WB
Surface roughness index (mm)	230	<200	285	190
Age (days)	28-35	14	28-38	28-31
Number of tests	15	5	25	13
Number of bond failures	15	3	4	10
Tensile bond strength (MPa)	1.41	1.33	2.76	2.25
Coefficient of variation (%)	30	12.7	12.4	28.9

Table 6.4 Effect of surface preparation methods on the slant shear bond strength of the sand/cement mortar

Repair material	Sand/ cement mortar							
Surface preparation method	Formed surface then needle gunned	Formed surface then sand blasted (FM-SB)		FM-SB	Set retarder produced and wire brushed	Line load split and not further treatment	Line load split and needle gunned	
Surface cleanliness	Clean (CL)	Contaminated	CL	CL	CL	CL	CL	CL
Method of installation	Vibrated (VB)	VB	VB	Hand applied	Hand applied	Hand applied	Hand applied	VB
Surface roughness index (mm)	>285	230	200	230	210	<190	<190	<190
Age (days)	14	14	14	14	14	28	28	28
Number of tests	3	3	3	3	6	3	3	6
Number of bond failures	3	3	3	3	6	2	0	3
Slant shear bond strength (MPa)	26.0	42.0	50.4	37.3	30.2	49.5	45.6	43.7
Coefficient of variation (%)	7.0	9.8	1.7	15	18.8	12.8	17.6	13.5

Table 6.5 Effect of moisture condition on the tensile bond strength

Repair material	Surface preparation method	Age (days)	Number of tests	Number of bond failures	Moisture condition	Tensile bond strength (MPa)	Coefficient of variation
Sand/cement mortar	Formed surface then sand blasted	28	5	5	SW	1.82	12.5
		28	5	5	SD	1.81	20
		28-35	15	15	AW	1.41	30
		28	5	5	AD	1.44	22
		28	5	5	BW	2.44	9
		28	4	4	BD	2.25	12.3
Acrylic modified mortar	Formed surface then sand blasted	41	10	6	SW	2.8	10.6
		28-41	35	8	SD	2.82	11.2
		41	10	2	AW	2.85	8.9
		41	10	3	AD	2.77	9.8
		31	5	3	BW	2.61	15.9
		31	5	1	BD	2.83	7.1
SBR modified mortar	Formed surface then sand blasted	28	5	5	SW	1.90	8.0
		28	5	5	SD	1.63	8.1
		28	5	5	AW	1.53	17.0
		28	5	4	AD	2.18	9.4
		28	5	5	BW	1.97	14.6
		28	5	5	BD	1.91	11.0
Flowing concrete	Formed surface then sand blasted	28	5	5	SW	1.14	26.0
		28	5	5	SD	2.16	12.0
		28	5	5	AW	2.03	23.0
		28	5	4	AD	2.38	16.0
		28	5	5	BW	1.93	15.0
		28	5	1	BD	2.86	10.0
Light weight acrylic modified mortar	Formed surface then sand blasted	28	5	5	SW	1.73	4.3
		28	5	5	SD	1.49	8.9
		Not available for this AW group					
		28	5	4	AD	1.67	4.4
		28	4	4	BW	1.44	10.8
		28	5	5	BD	1.42	7.5

Table 6.6 Effect of moisture condition on patch flexural specimens

Repair material	Flowing concrete						Unrepaired specimen
Surface preparation method	Formed surface		then sand blasted				
Age (days)	30	30	28	28	30	30	
Number of tests	3	3	3	3	3	3	
Number of bond failures	2	0	1	0	0	2	
Moisture condition	SW	SD	AW	AD	BW	BD	
Failure load (KN)	6.65	6.38	7.67	7.09	8.40	8.54	6.84
Flexural bond strength (MPa)	1.99	1.90	2.29	2.11	2.49	2.54	
Coefficient of variation (%)	11.4	7.9	11.3	6.0	9.9	5.6	9.6

Table 6.7 The t-statistical analysis of the effect of moisture condition on bond strength

Repair material	Parameter varied	Mean bond strength (MPa)		Confidence level	
		first moisture condition	second moisture condition	95%	99%
Sand/cement mortar	SW : SD	1.82	1.81	N	N
	AW : AD	1.41	1.44	N	N
	BW : BD	2.44	2.25	N	N
Acrylic modified mortar	SW : SD	2.80	2.82	N	N
	AW : AD	2.85	2.77	N	N
	BW : BD	2.61	2.83	N	N
SBR modified mortar	SW : SD	1.90	1.63	Y	N
	AW : AD	1.53	2.18	Y	Y
	BW : BD	1.97	1.91	N	N
Flowing concrete	SW : SD	1.14	2.16	Y	Y
	AW : AD	2.03	2.38	N	N
	BW : BD	1.93	2.86	Y	Y
Light weight acrylic modified mortar	SW : SD	1.73	1.49	Y	N
	BW : BD	1.44	1.42	N	N
Flowing concrete (patch flexural test)	SW : SD	1.99	1.90	N	N
	AW : AD	2.29	2.11	N	N
	BW : BD	2.49	2.54	N	N

Table 6.8 Effect of moisture condition on tensile bond strength (Based on test results from ref.[73])

Repair material	Surface preparation method	Parameter varied	Mean bond strength (MPa)		Confidence level	
			first moisture condition	second moisture condition	95%	99%
Sand/cement mortar (M40)	water-jet	SW : SD	1.96	1.95	N	N
	washing	AW : AD	2.63	2.36	N	N
	sand blasting	SW : SD	1.62	2.44	Y	Y
		AW : AD	1.5	2.28	Y	Y
	splitting	SW : SD	2.20	1.41	Y	Y
		AW : AD	1.68	1.60	N	N
	sawing	SW : SD	1.13	1.12	N	N
		AW : AD	0.86	0.93	N	N
SBR modified mortar	sand blasting	SW : SD	3.28	2.62	Y	Y
		AW : AD	2.85	2.81	N	N

Table 6.9 Tensile bond strength of sand/cement mortar with different mix ratio (Based on test results from ref.[15])

Surface condition	Tensile bond strength (MPa)		Bond strength ratio (M40/M30)	Average bond strength ratio	Coefficient of variation (%)	Note
	M40 mortar	M30 mortar				
C/W	2.22	1.73	1.283	0.8725	25.6	C: cracked surface S: sawn surface N: needle gunned surface M: middle debonded E: edge debonded W: surface wet D: surface dry
C/D	1.51	1.57	0.962			
S/W	2.04	1.48	1.379			
S/D	1.87	2.45	0.763			
N/W	1.38	2.38	0.58			
N/D	2.03	1.93	1.05			
M/S/W	0.91	1.24	0.734			
M/S/D	1.55	1.73	0.896			
M/N/W	1.26	1.58	0.797			
M/N/D	1.65	1.73	0.954			
E/S/W	0.86	1.54	0.558			
E/S/D	0.65	1.34	0.485			
E/N/W	1.50	1.59	0.943			
E/N/D	1.29	1.55	0.852			

Table 6.10 Tensile bond strength of the sand/cement mortar with and without a bond coat

Bond coat	condition	Tensile bond strength (Mpa)	Coefficient of variation (%)
No bond coat	(control specimens)	1.41	30
With A1 bond coat	dry	0.68	29
	tacky	2.46	14

Table 6.11 Tensile bond strength of polymer modified mortars with different bond coat condition *and mortar mistiming*

Repair material	Bond coat condition	Number of tests	Number of bond failures	Mistiming (min.)	Tensile bond strength (Mpa)	Coefficient of variation (%)
Acrylic modified mortar	control (tacky)	35	8	0	2.82	11.2
	No bond coat	5	5	0	0.75	36
	Coat mistiming	10	3	40-60	2.74	7.6
	Mortar mistiming	10	7	60	2.49	25.0
SBR modified mortar	control (tacky)	5	5	0	1.53	17.0
	No bond coat	10	10	0	0.93	22.0
	Coat mistiming	5	5	40	1.12	14.0
	Mortar mistiming	5	5	40	0.92	15.0

Table 6.12 Patch compressive test results with different bond coat condition and mortar mistiming

Repair material	Surface roughness index (mm)	Age (days)	Number of tests	Number of bond failures	Bond coat condition	Mistiming (min.)	Nominal slant shear bond strength (Mpa)	Coefficient of variation (%)
Sand-cement mortar	190	28	3	1	No bond coat	0	41.3	6.4
	230	28	5	5	No bond coat	0	34.2	21
	285	28	3	0	No bond coat	0	35.2	13
	190	28	2	1	A1 bond coat	0	48.4	**
	285	28	2	0	A1 bond coat	0	43.6	**
	190	28	3	0	No bond coat, mortar mistiming	40	43.1	6.7
Acrylic modified mortar	200	14	2	2	No bond coat	0	26.3	**
	285	14	2	2	tacky	0	29.4	**
	230	28	7	4	tacky	0	42.2	13.4
	230	28	3	0	coat mistiming	40	46.9	6.5
	230	28	3	3	mortar mistiming	40	46.7	1.4
SBR modified mortar	230	28	3	3	tacky	0	35.0	4.0
	230	28	4	4	coat mistiming	40	32.7	6.9
	230	28	3	3	mortar mistiming	40	33.1	1.7
FLowing concrete	230	28	4	0	No bond coat	0	37.6	3.6
	230	28	4	1	mortar mistiming	40	38.3	4.0

Table 6.13 Patch flexural test results with different bond coat condition and mortar mistiming

Repair material	Surface roughness index (mm)	Age (days)	Number of tests	Number of bond failures	Bond coat condition	Mistiming (min.)	Failure load of patch flexural specimen (KN)	Coefficient of variation (%)
sand-cement mortar	230	51	3	3	No bond coat	0	7.94	5.5
	230	28	3	3	mortar mistiming	40	7.75	2.1
SBR modified mortar	230	30	3	0	tacky	0	7.18	6.6
	230	28	3	0	coat mistiming	40	7.01	9.6
	230	28	3	0	mortar mistiming	40	6.75	12.3
Flowing concrete	200	30	3	3	No bond coat	0	7.67	5.3
	230	28	3	0	mortar mistiming	40	6.92	5.3
Unrepaired specimen							6.84	9.6

Table 6.14 Effect of curing on tensile bond strength

Repair material	S/C				A1				SBR		F		
Age (days)	28-35	79	35	73	28-35	41	35	35	28	38	28-31	28	31
NTS	15	10	5	10	25	10	5	10	5	5	5	5	5
NBF	15	10	5	10	4	2	4	9	5	5	5	5	1
CMS	3d		No		3d		No		3d	No	3d	No	
σ (MPa)	1.41	2.20	1.21	1.31	2.76	2.85	1.64	1.92	1.53	1.44	2.03	1.55	2.69
COV	30	18.4	20	38.8	12.4	8.9	27.6	17	17	12.7	23	35	18

S/C Sand/cement mortar; A1: Acrylic modified mortar; SBR: SBR modified mortar;
F: Flowing concrete; NTS: Number of tests; NBF: Number of bond failures;
CMS: Curing method; 3d: covered with polythene sheet for 3 days;
No: No covering at all; σ : Tensile bond strength; COV: Coefficient of variation.

Table 6.15 Effect of curing method on patch flexural specimens

Repair material	Age (days)	Number of tests	Number of bond failure	Curing method	Failure load (KN)	Coefficient of variation (%)
S/C	51	3	3	3d	7.94	5.5
	28	3	3	No	7.33	11.8
A1	28	5	3	3d	8.23	9.7
	28	3	3	No	7.93	5.1
SBR	30	3	0	3d	7.18	6.6
	28	3	0	No	6.26	10.1
F	30	3	1	3d	7.67	7.0
	28	3	1	No	6.90	15.2

Table 6.16 Effect of curing method on patch compressive specimens

Repair material	Age (days)	Number of tests	Number of bond failure	Curing method	Failure load (KN)	Coefficient of variation (%)
S/C	41	2	2	3d	42.7	**
	41	3	3	No	40.5	3.5
A1	28	4	2	3d	42.2	5.5
	28	3	3	7d	39.1	4.4
	28	3	3	No	40.2	9.0
SBR	28	3	3	3d	35.0	4.0
	28	4	4	No	34.3	6.5
F	28	4	0	3d	37.6	3.6
	28	4	0	No	40.5	9.3

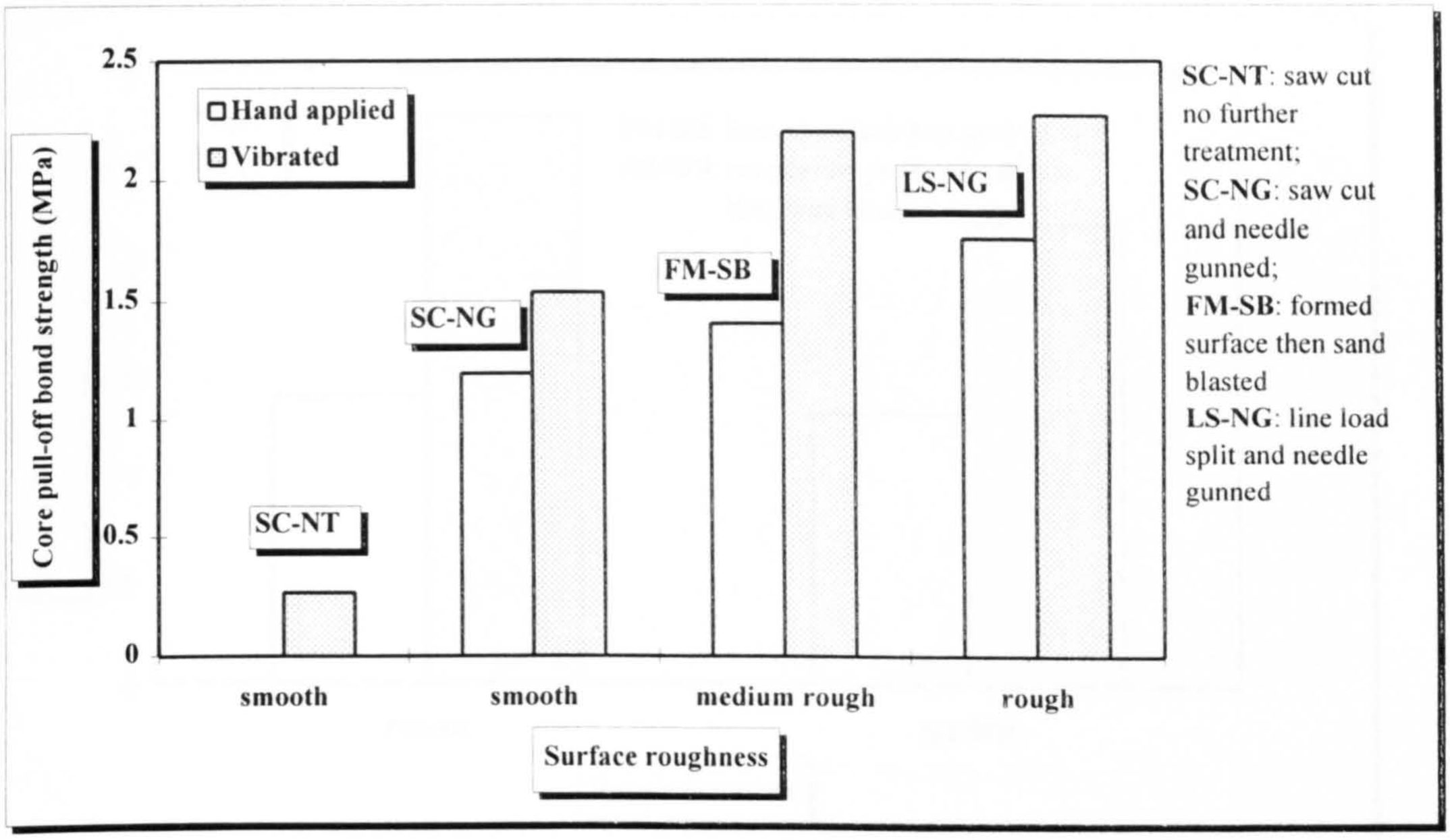

Figure 6.1 Effect of surface roughness on the core pull-off bond strength

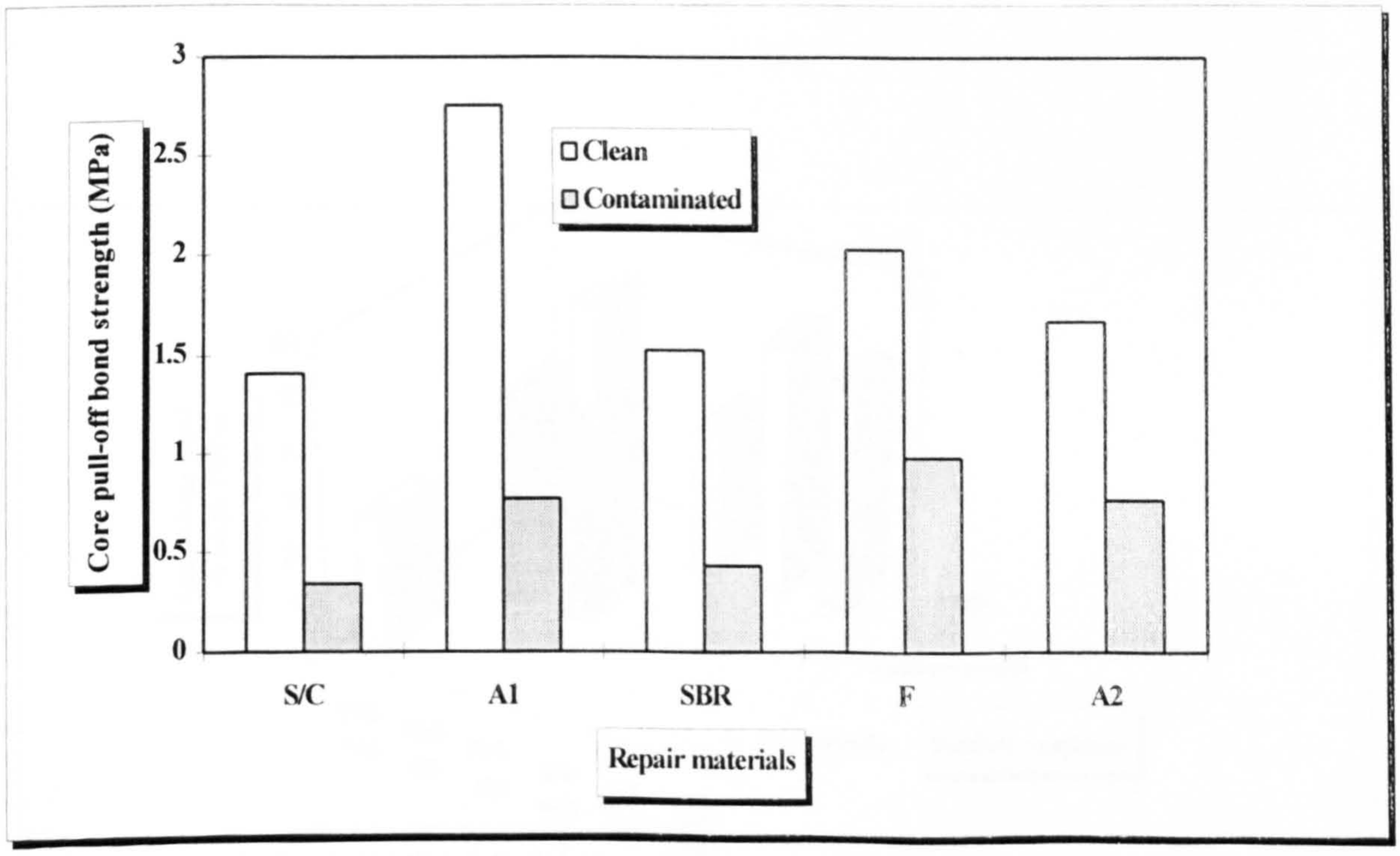

Figure 6.2 Effect of surface contamination on the core pull-off bond strength

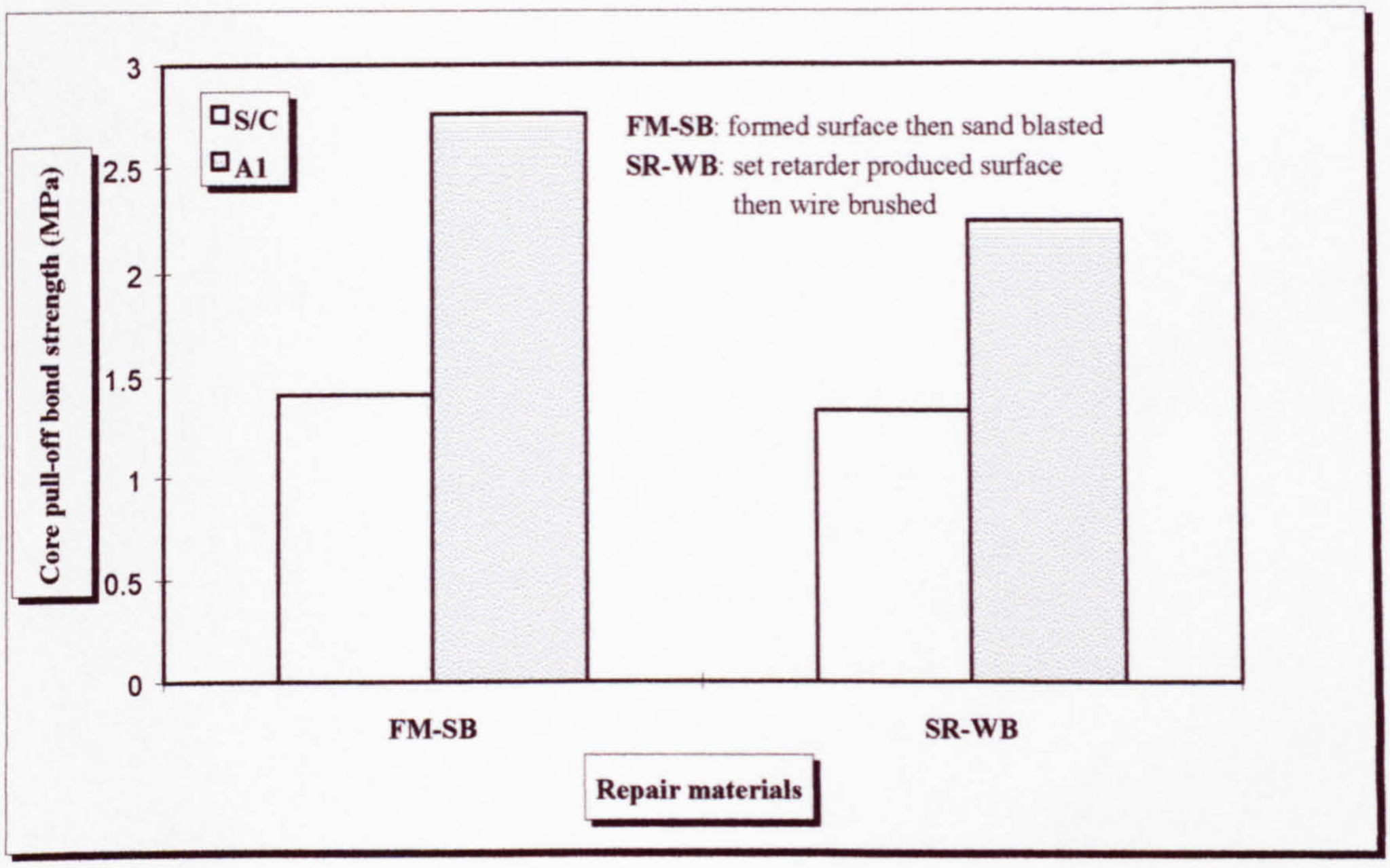

Figure 6.3 Comparison between tensile bond strength with surface set retarder produced and sand blasted surface

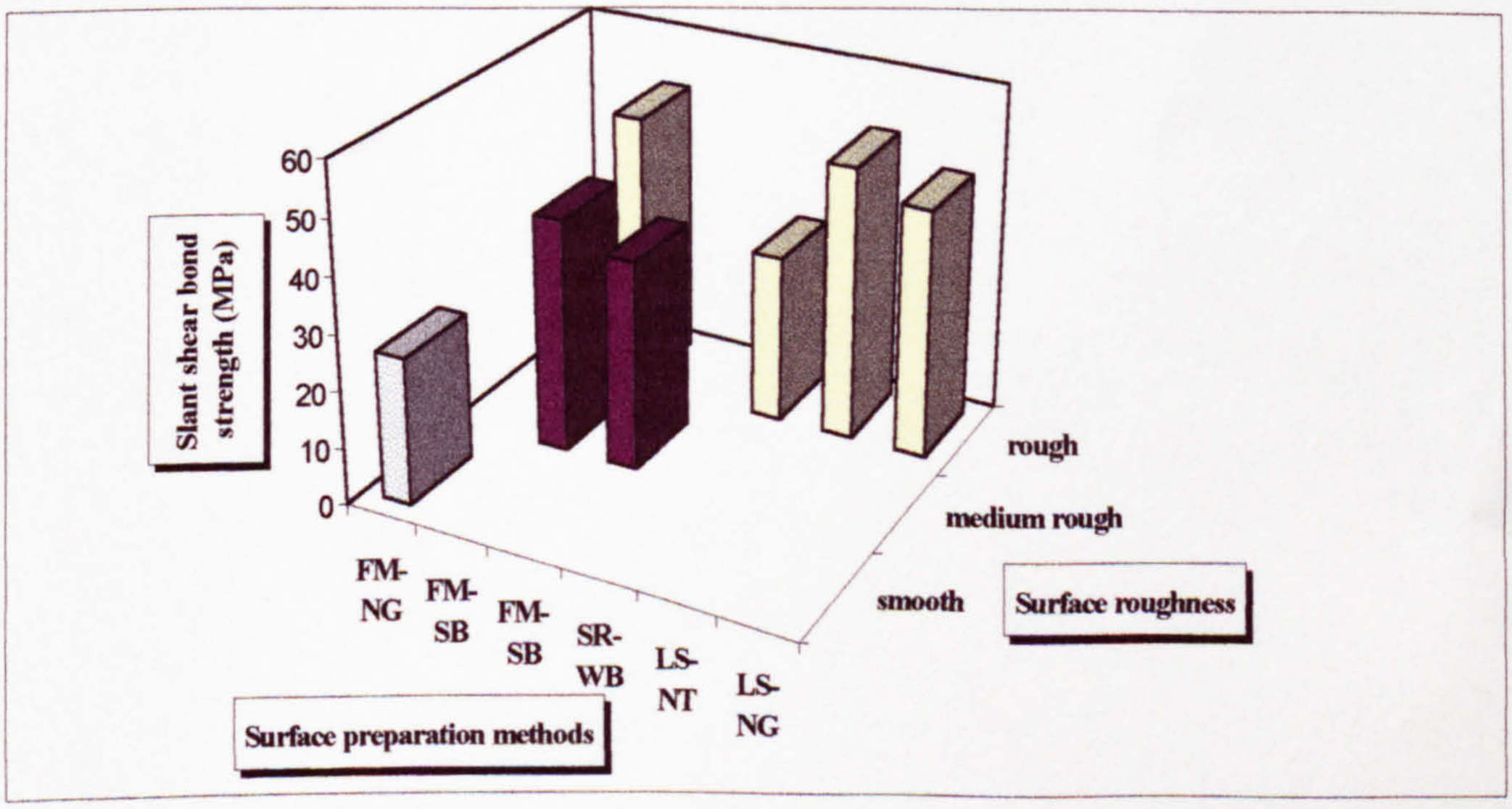

Figure 6.4 Effect of surface preparation methods and surface roughness on the slant shear bond strength

Figure 6.5 Sand blasted and split surfaces

a) sand blasted, medium rough b) sand blasted, rough c) Split surface, rough

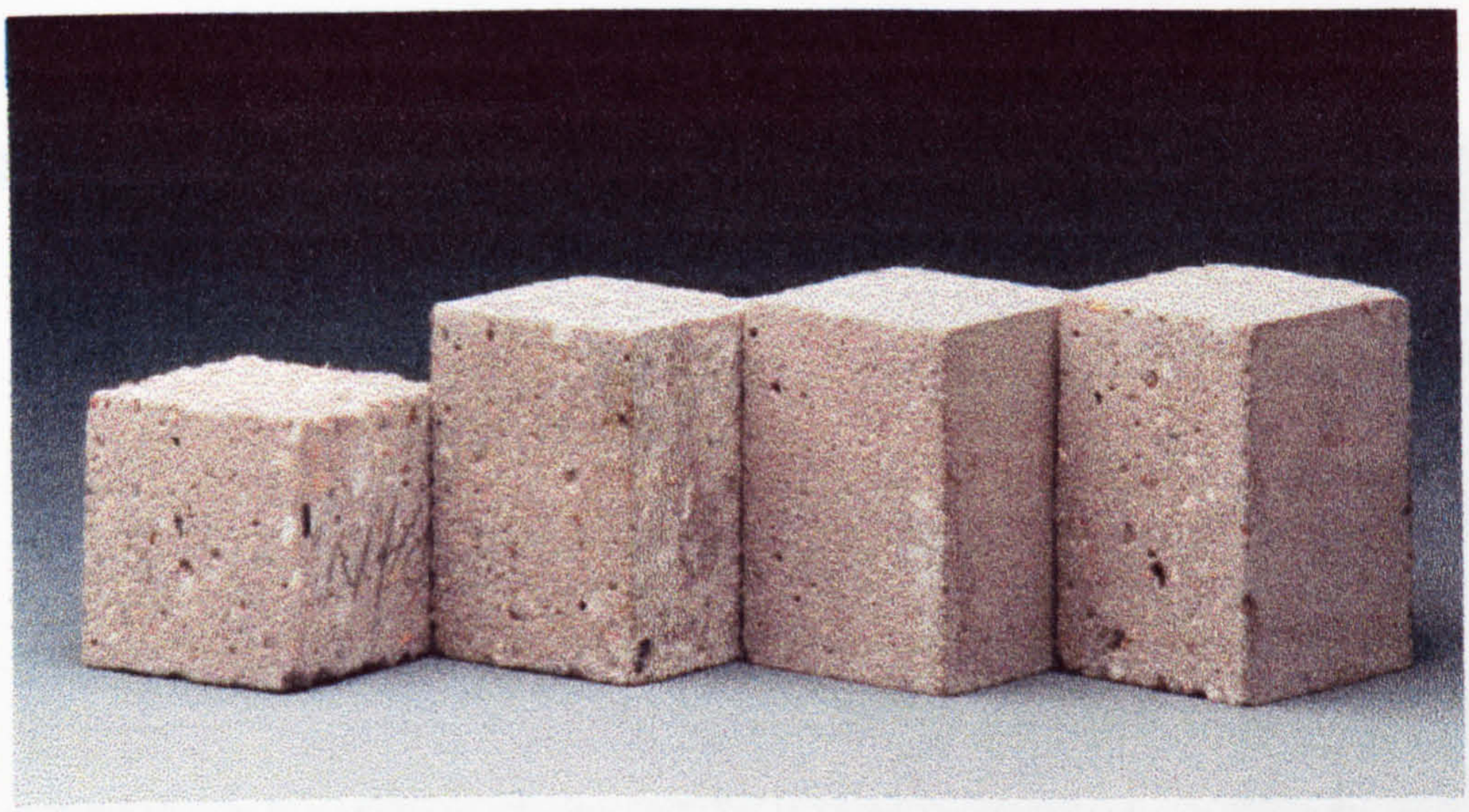

Figure 6.6a Smooth surfaces by sand blasting with different substrate mixes from the following sources

a) Loughborough (with river aggregate) b) Queen's University (Belfast)
c) Loughborough (with crushed aggregate) d) BS6319: Part 4

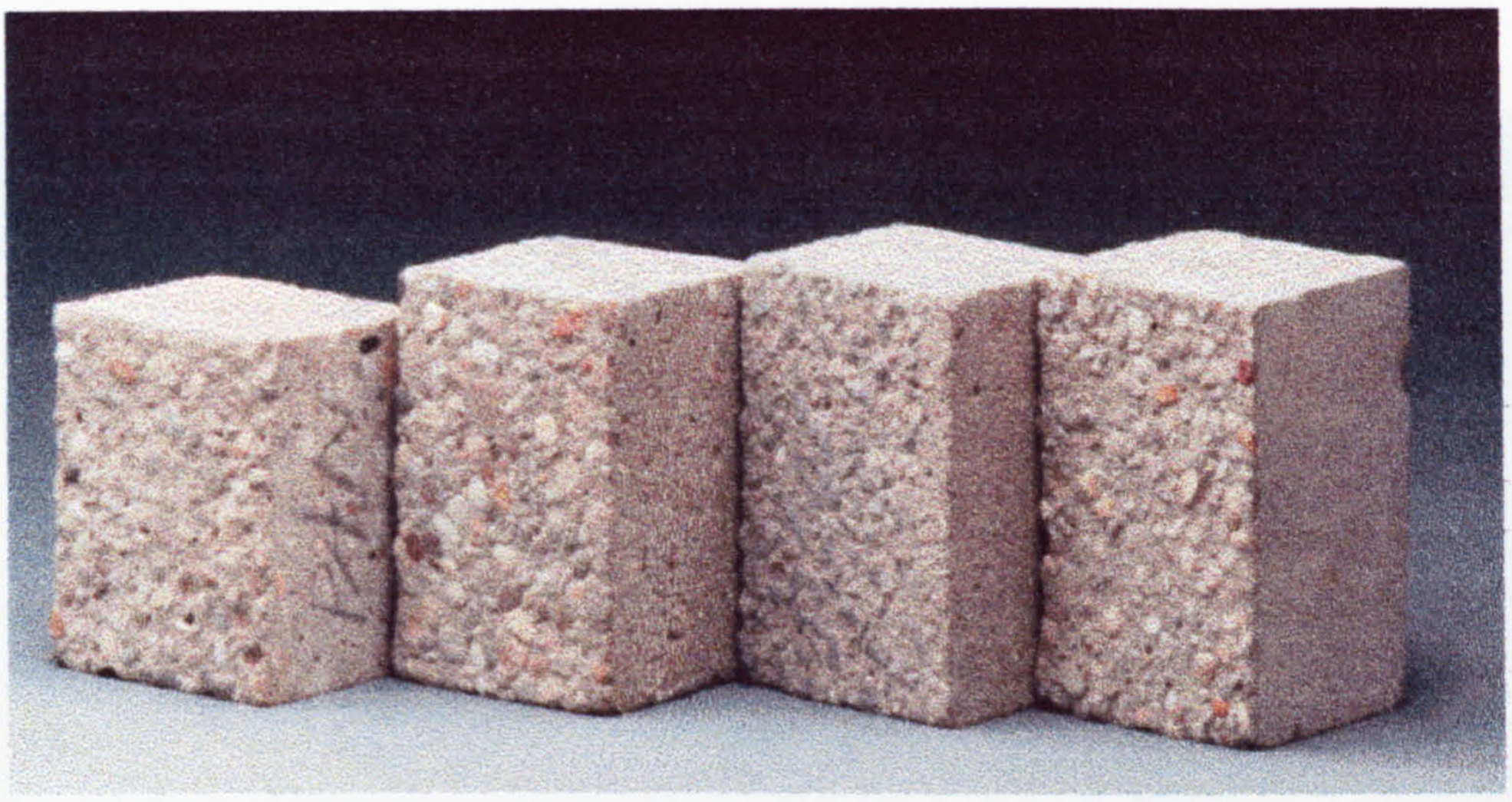

Figure 6.6b Medium rough surfaces by sand blasting

a) Loughborough (with river aggregate)
b) Queen's University (Belfast)
c) Loughborough (with crushed aggregate)
d) BS6319: Part 4

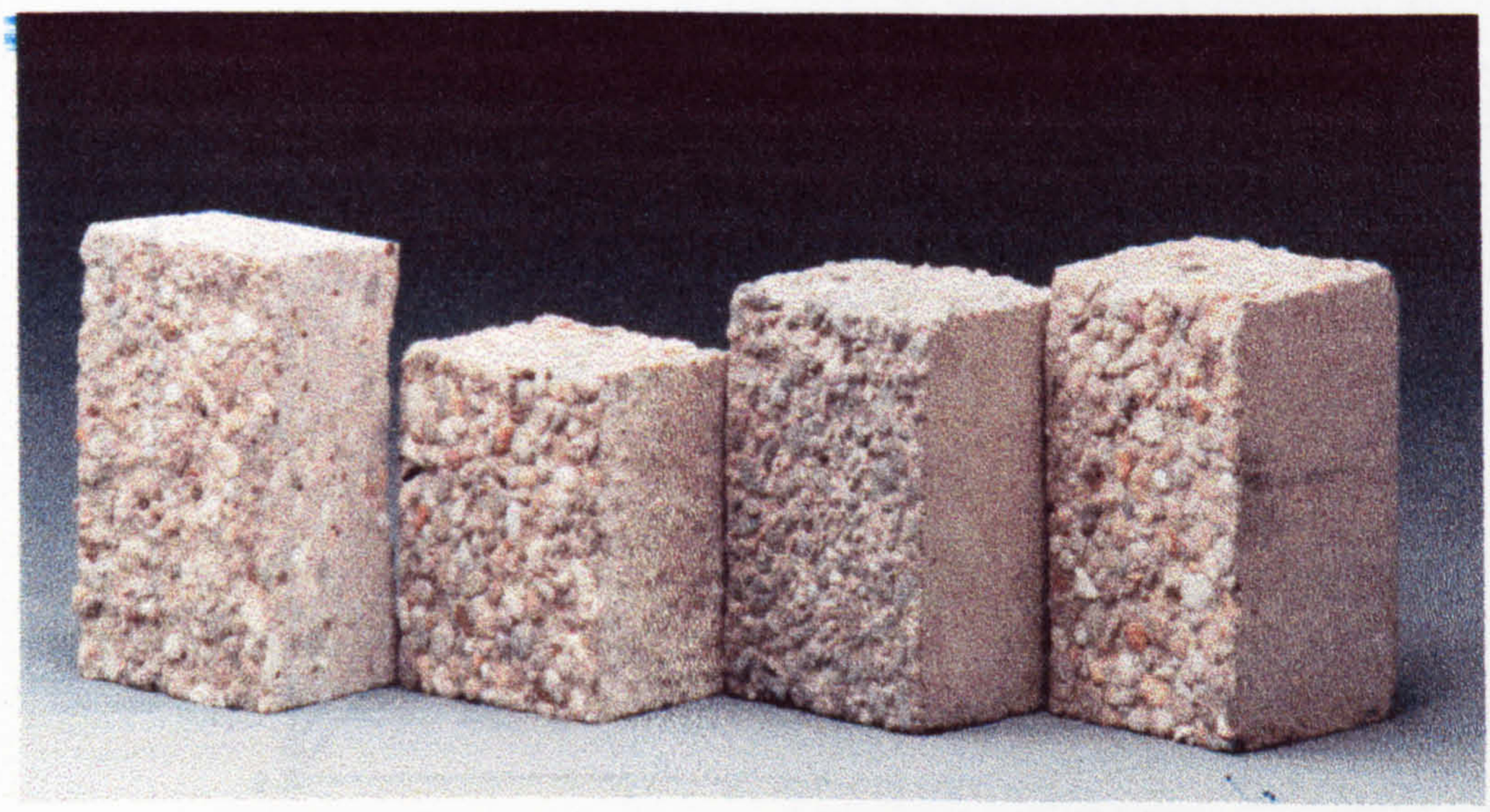

Figure 6.6c Rough surfaces by sand blasting

a) Loughborough (with river aggregate)
b) Queen's University (Belfast)
c) Loughborough (with crushed aggregate)
d) BS6319: Part 4

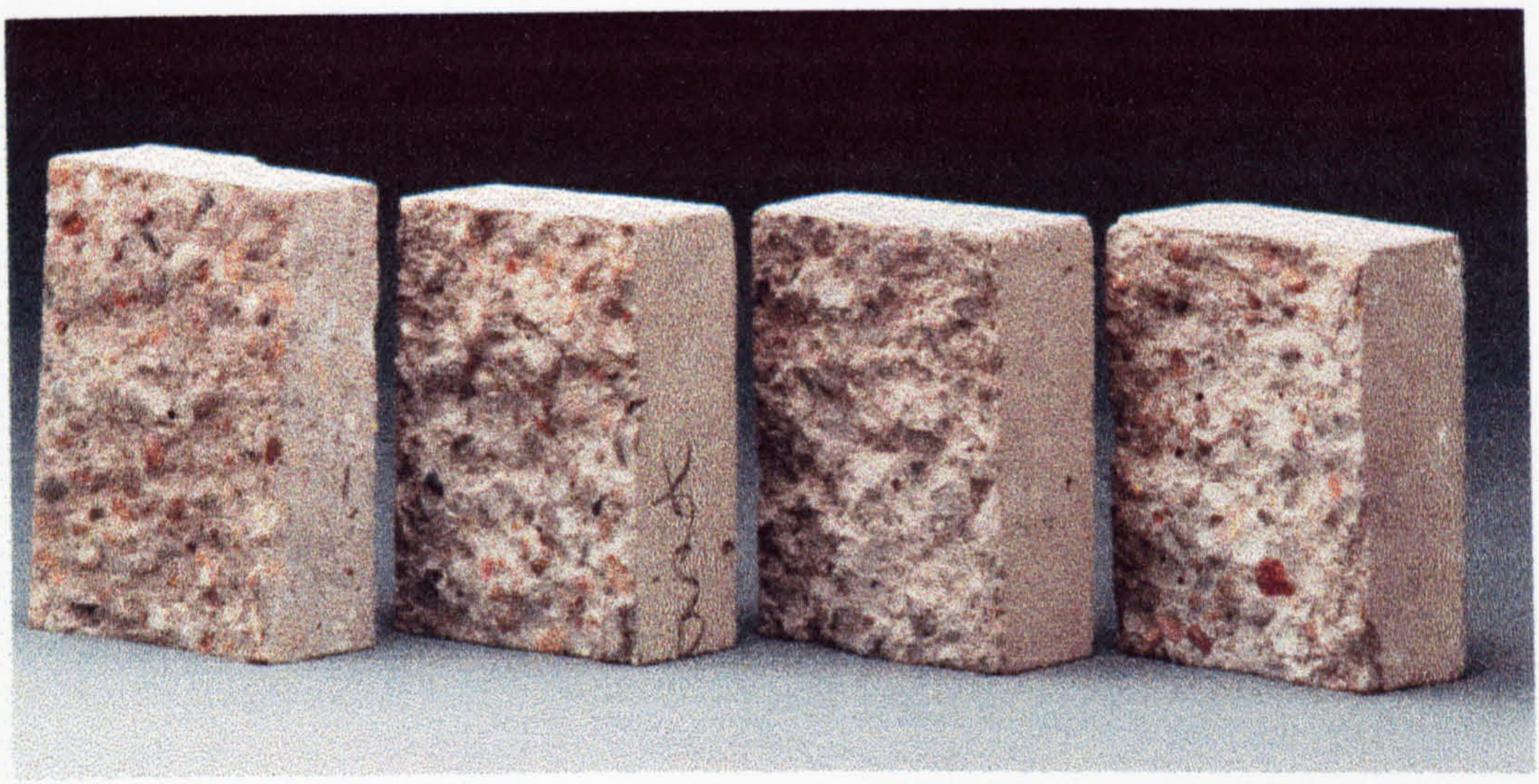

Figure 6.7 Line-load split surfaces

a) Loughborough (with river aggregate)
b) Queen's University (Belfast)
c) Loughborough (with crushed aggregate)
d) BS6319: Part 4

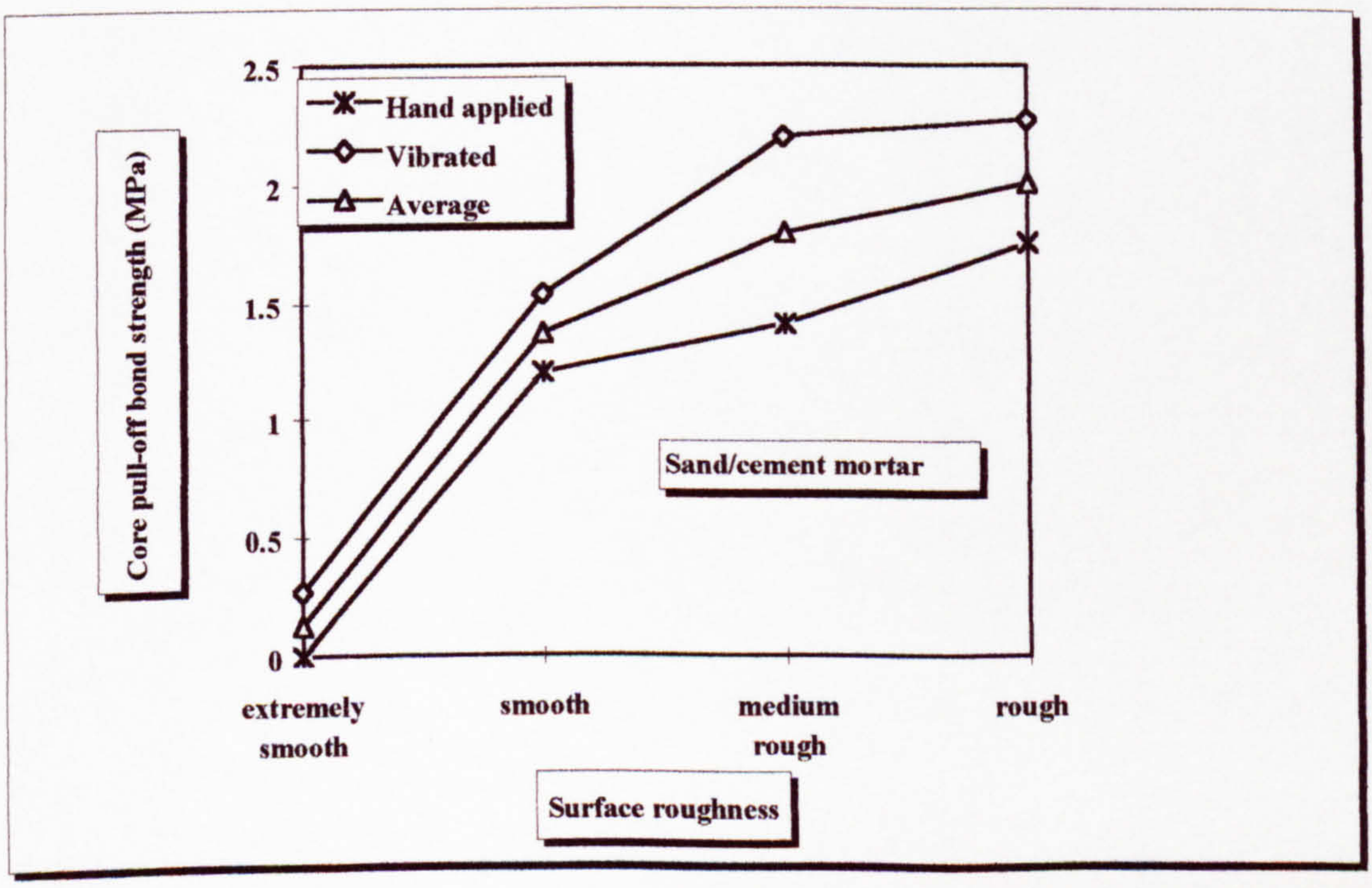

Figure 6.8 Surface roughness on tensile bond strength of the sand/cement mortar

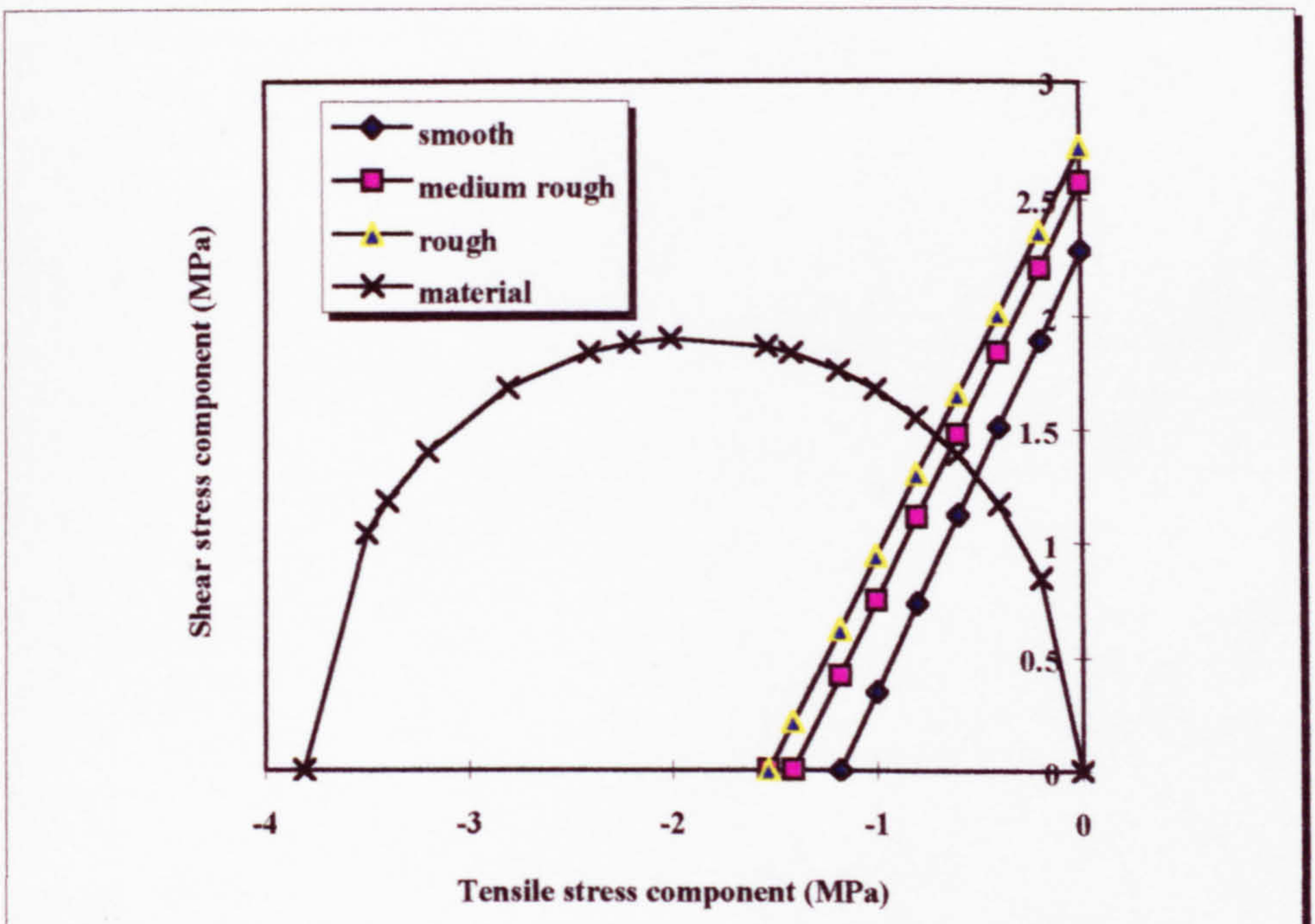

a) Shear/tensile stress state

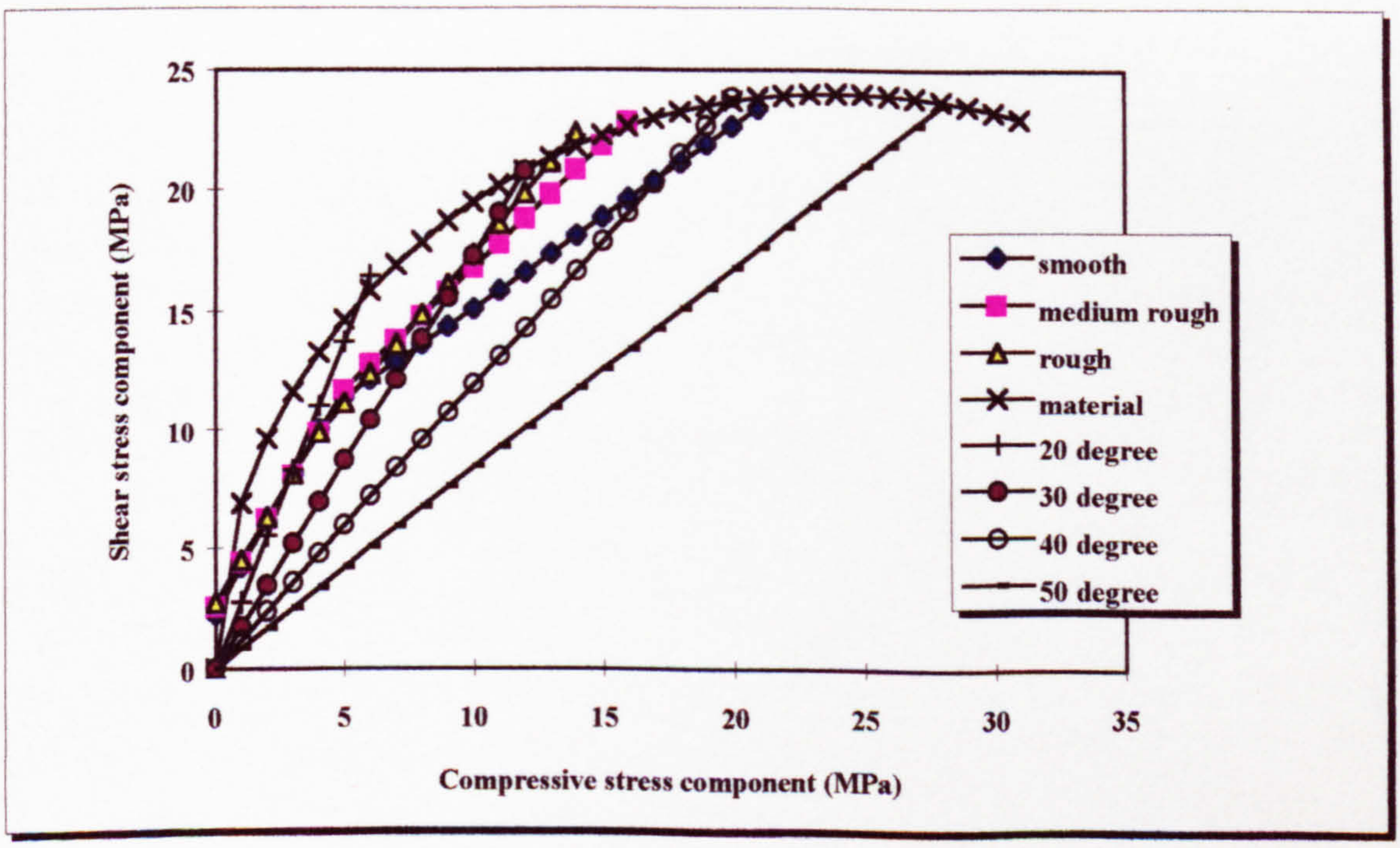

b) Shear/compressive stress state

Figure 6.9 Comparison between test results and predicted bond strength

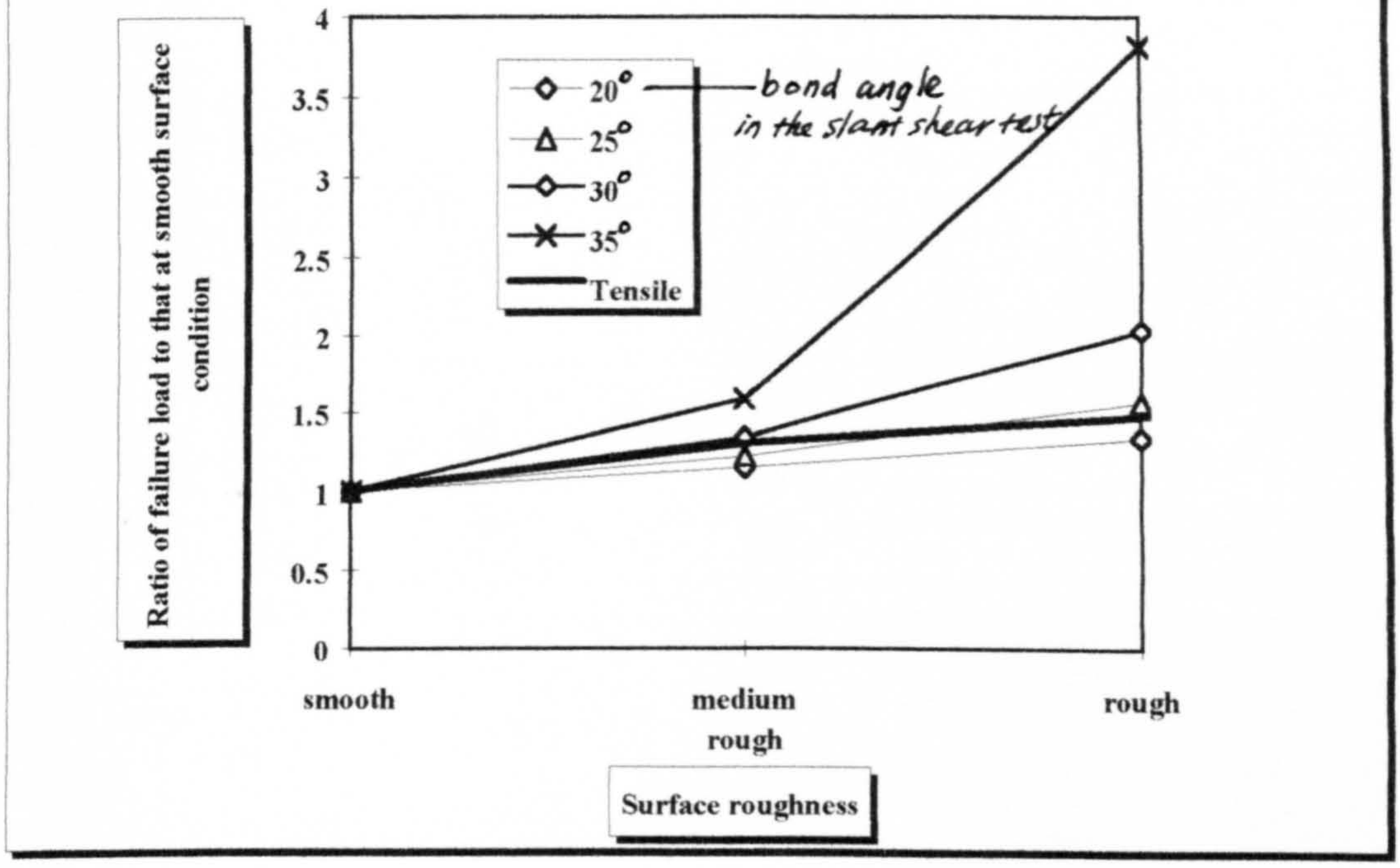

Figure 6.10 Effect of surface roughness under different stress states

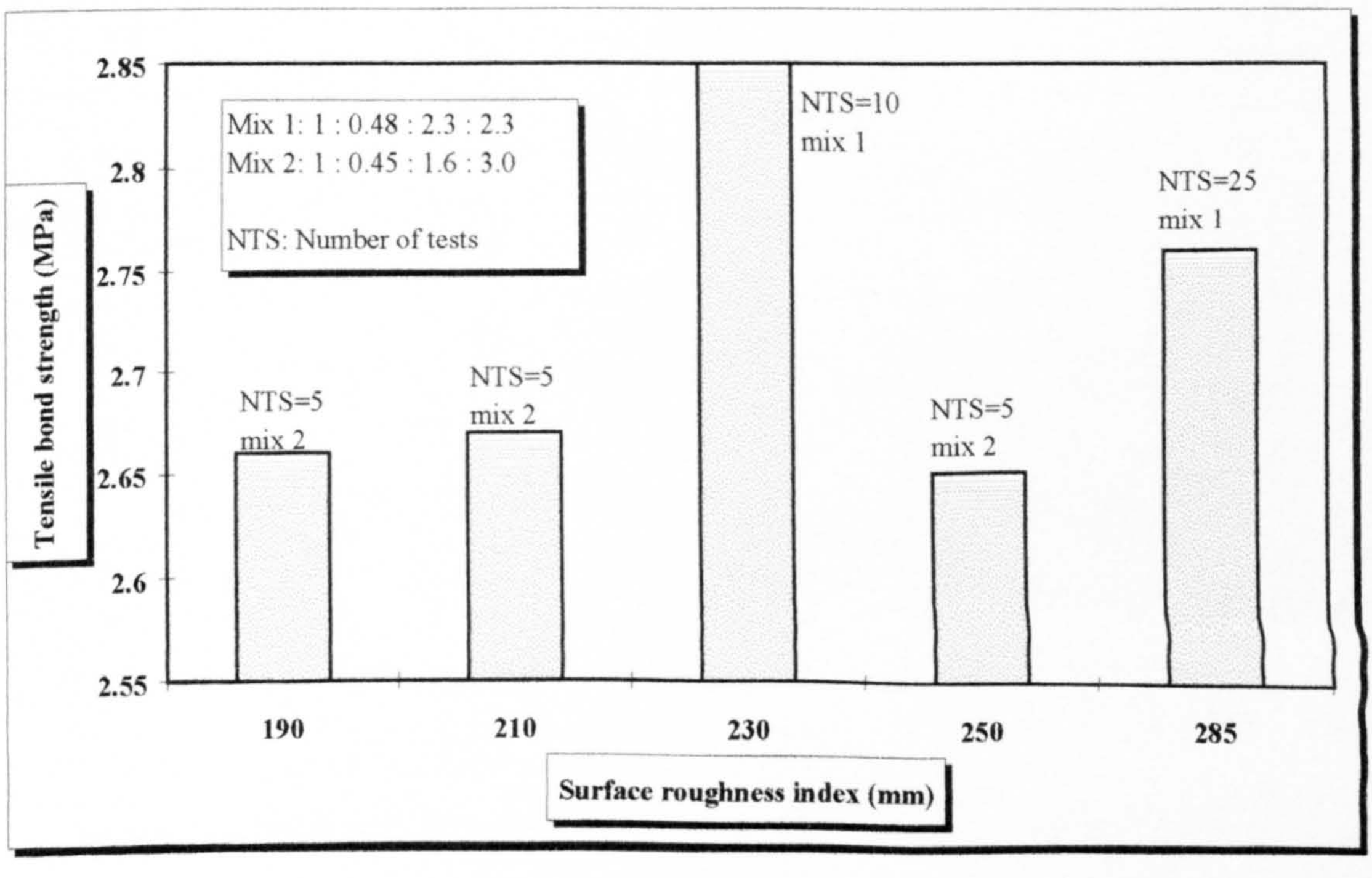

Figure 6.11 Tensile bond strength with the acrylic modified mortar

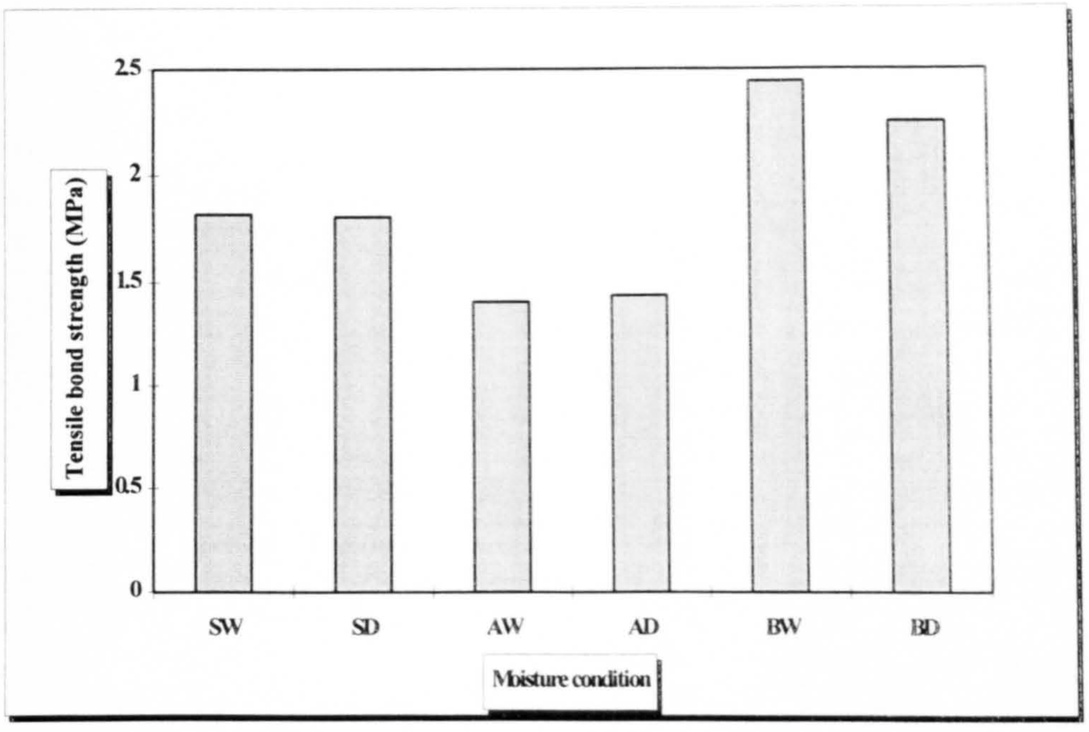

Figure 6.12 Effect of moisture condition on tensile bond strength with the sand/cement mortar

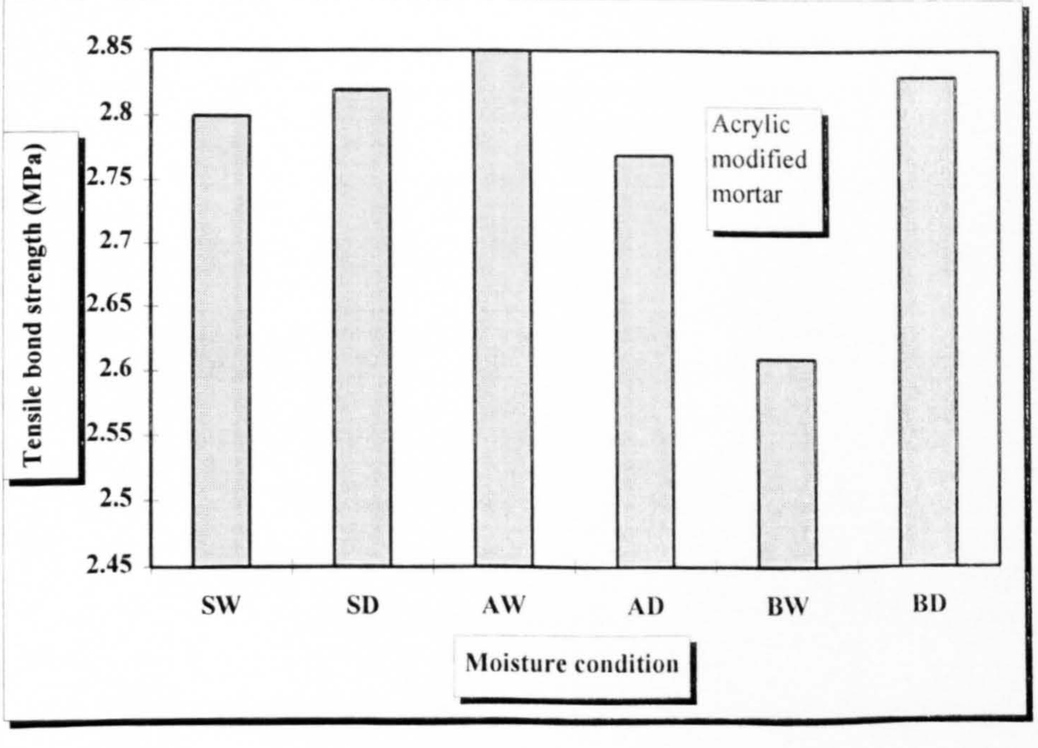

Figure 6.13 Effect of moisture condition on the tensile bond strength of the acrylic modified mortar

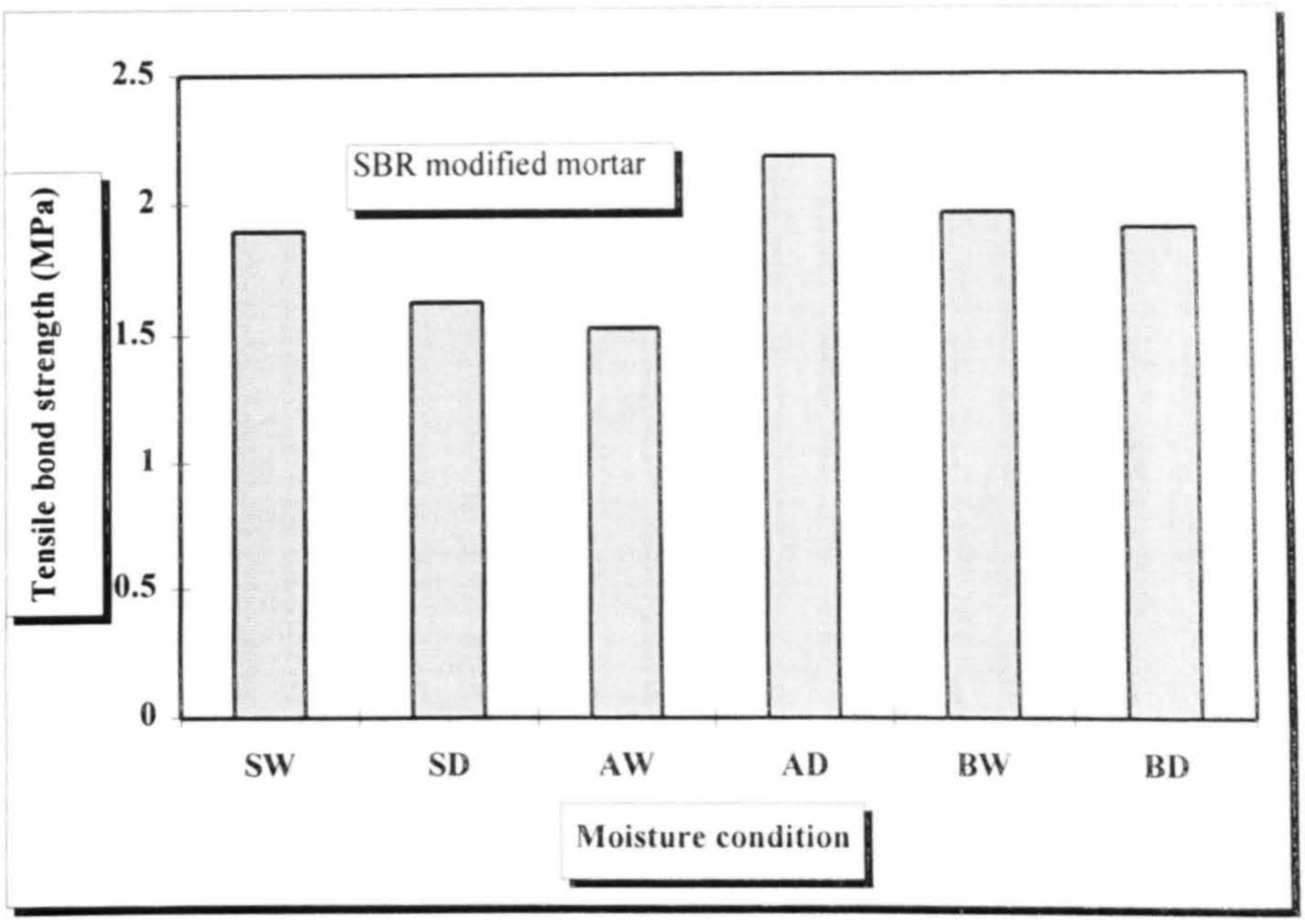

Figure 6.14 Effect of moisture condition on the tensile bond strength of the SBR modified mortar

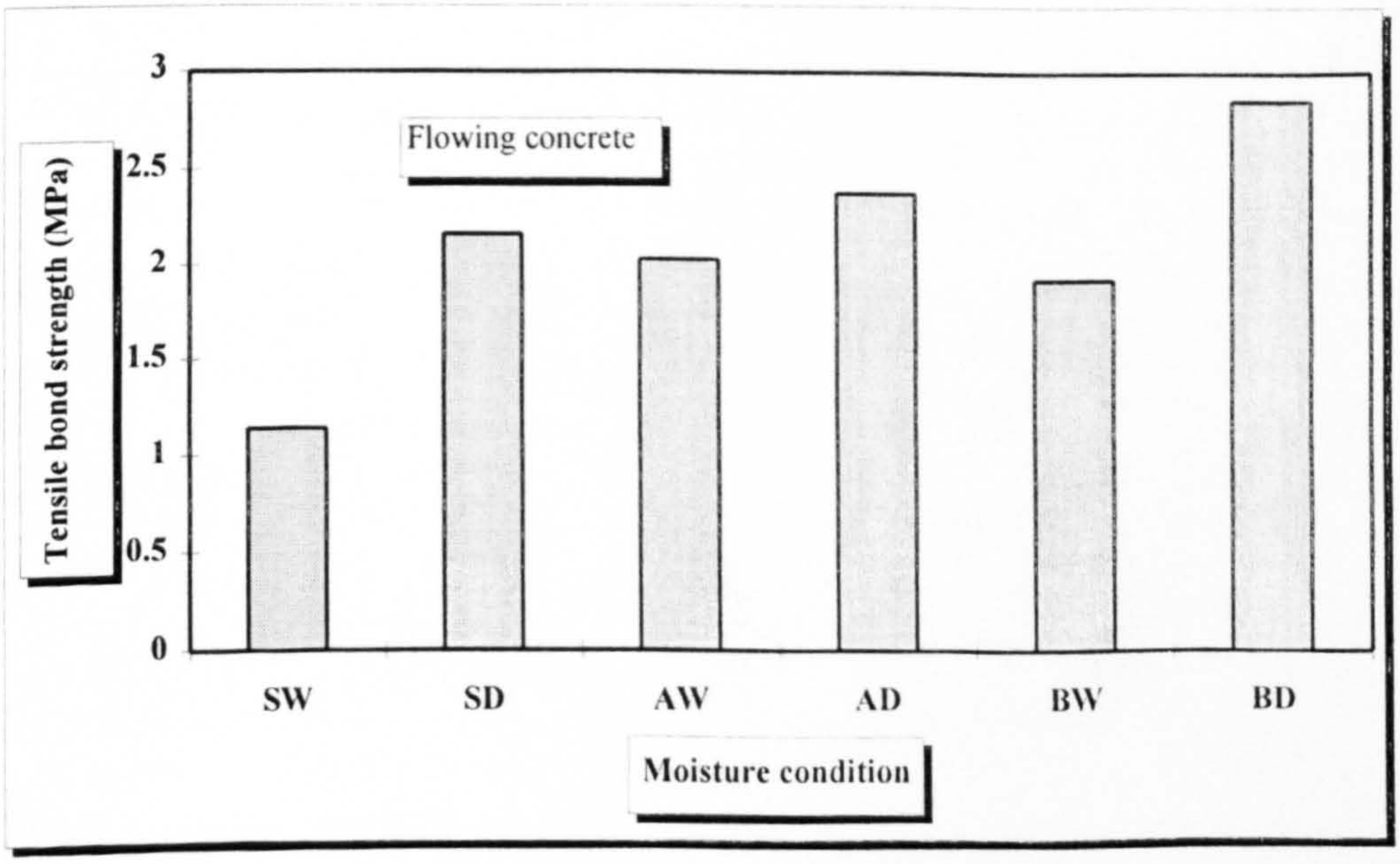

Figure 6.15 Effect of moisture condition on the tensile bond strength of the flowing concrete

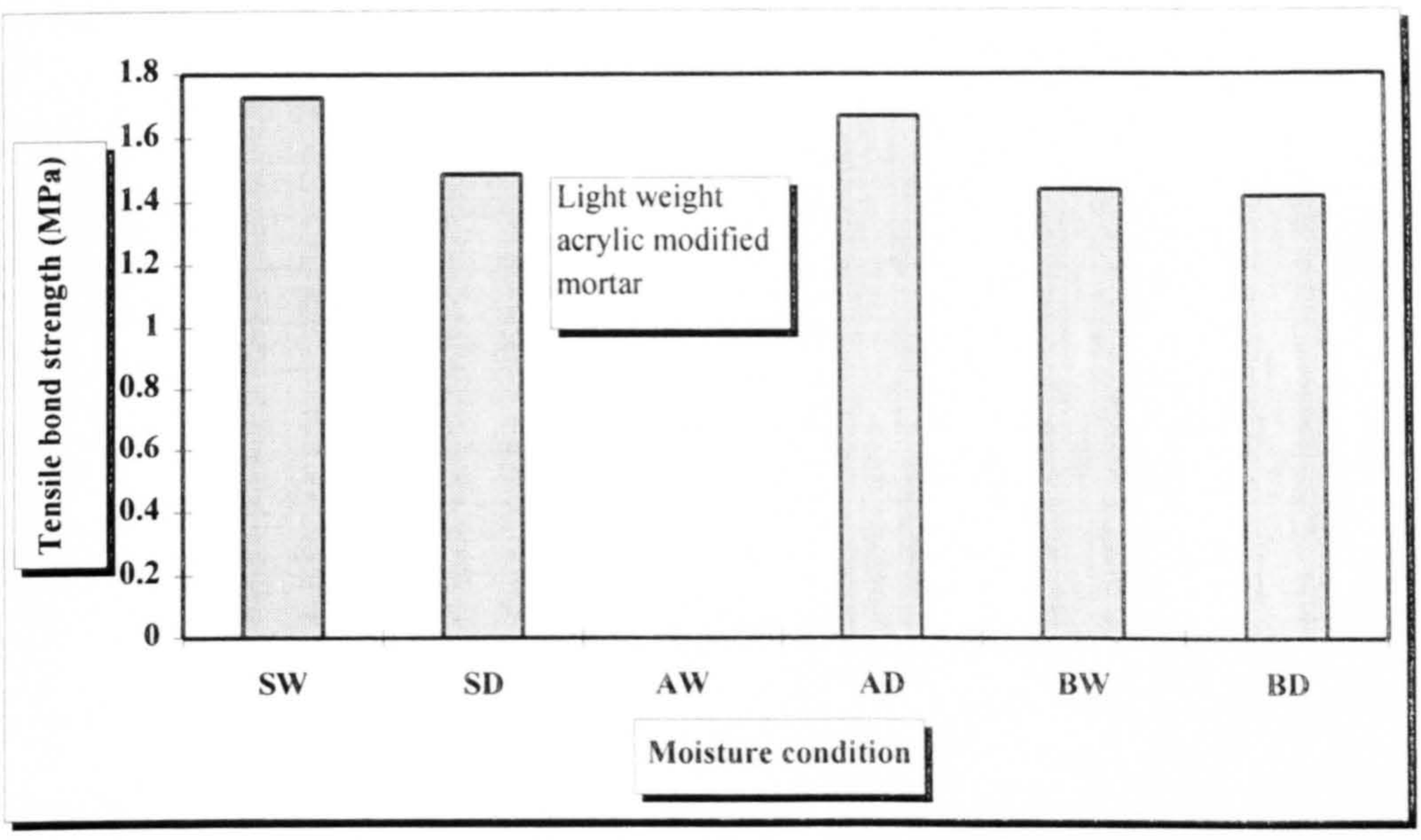

Figure 6.16 Effect of moisture condition on the tensile bond strength of the light weight acrylic modified mortar

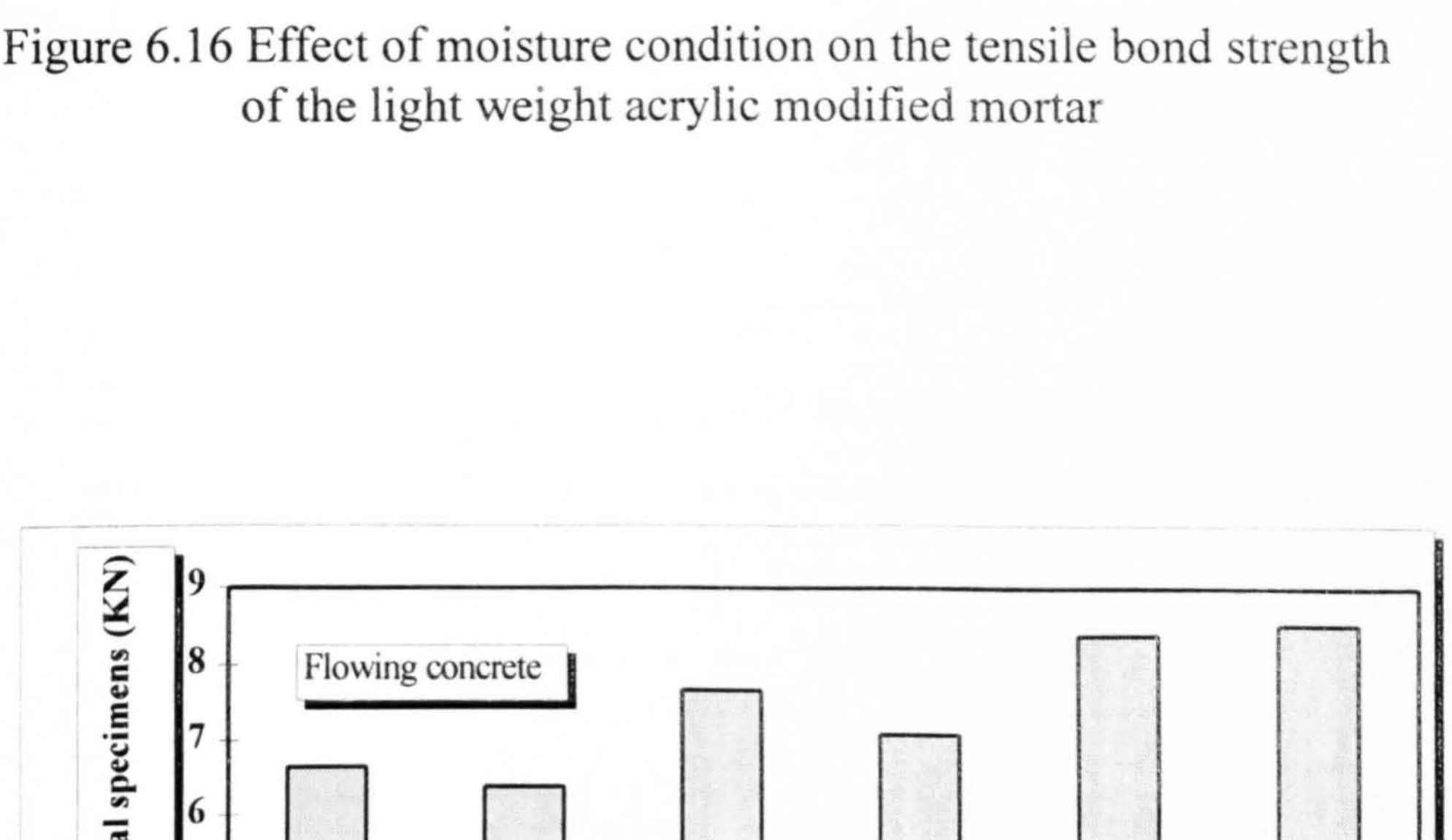

Figure 6.17 Effect of moisture condition on patch flexural specimens

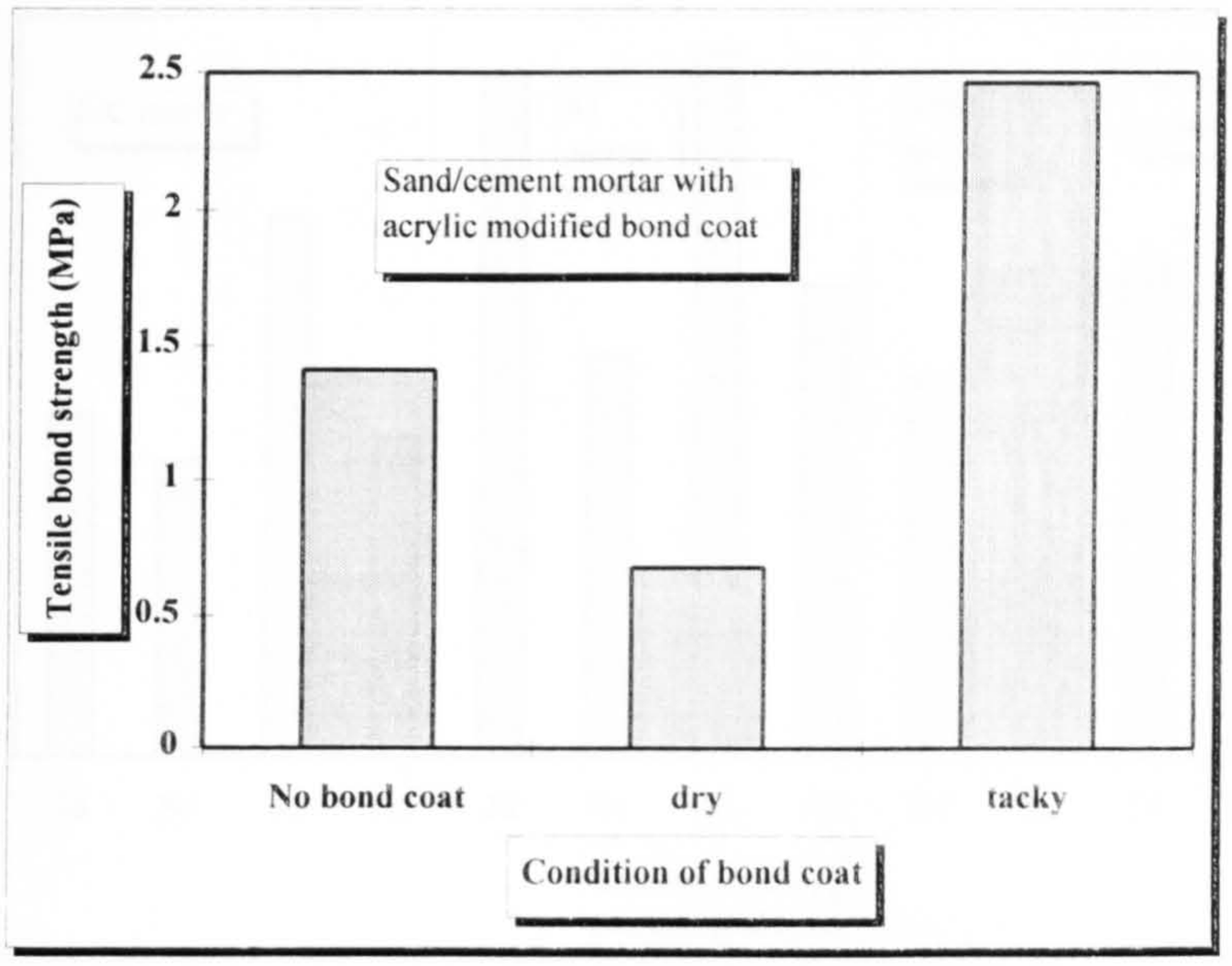

Figure 6.18 Effect of a bond coat on tensile bond strength of sand/cement mortar

Figure 6.19 Effect of bond coat on tensile bond strength
of polymer modified mortars

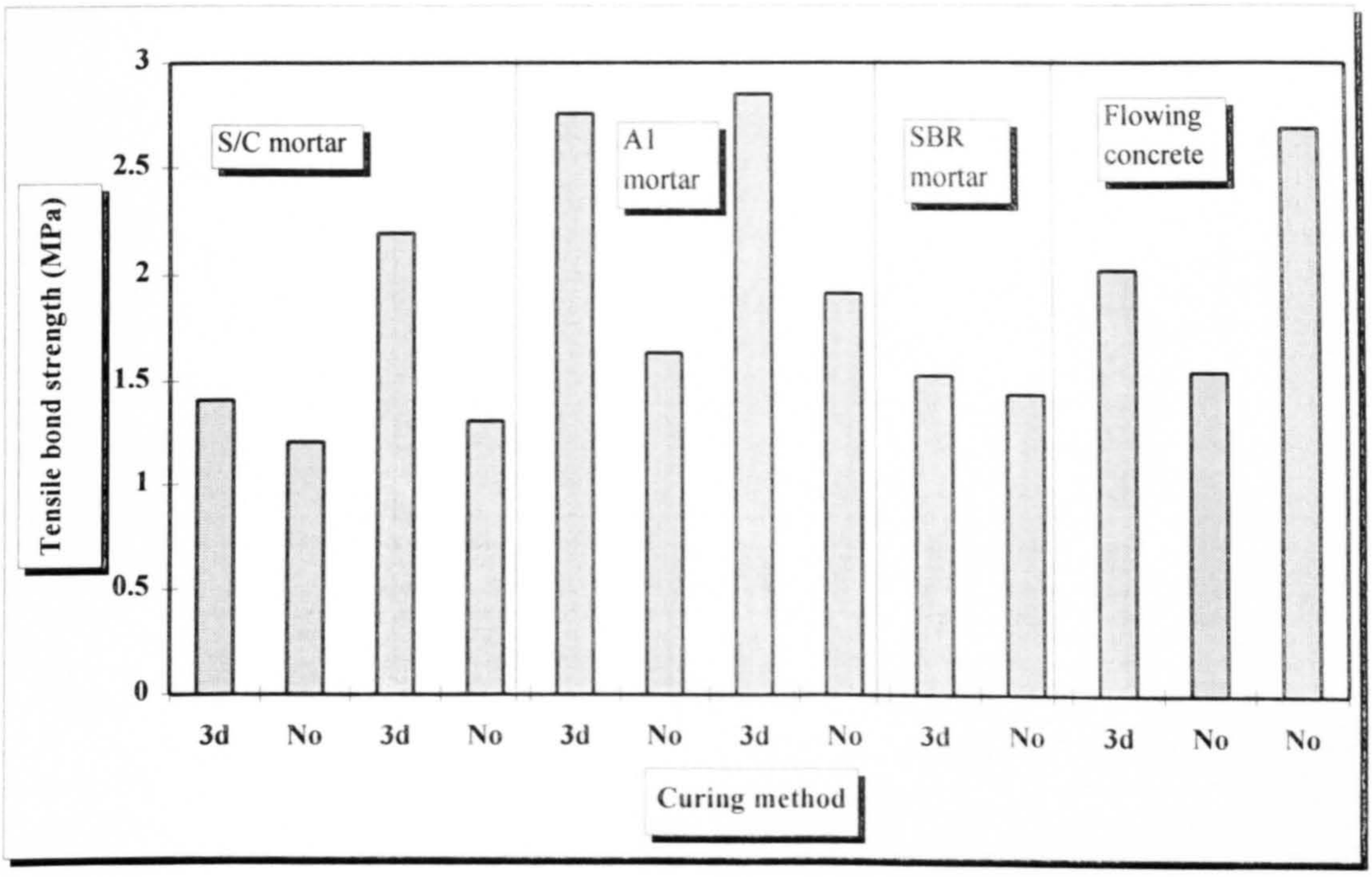

Figure 6.20 Effect of curing method on tensile bond strength

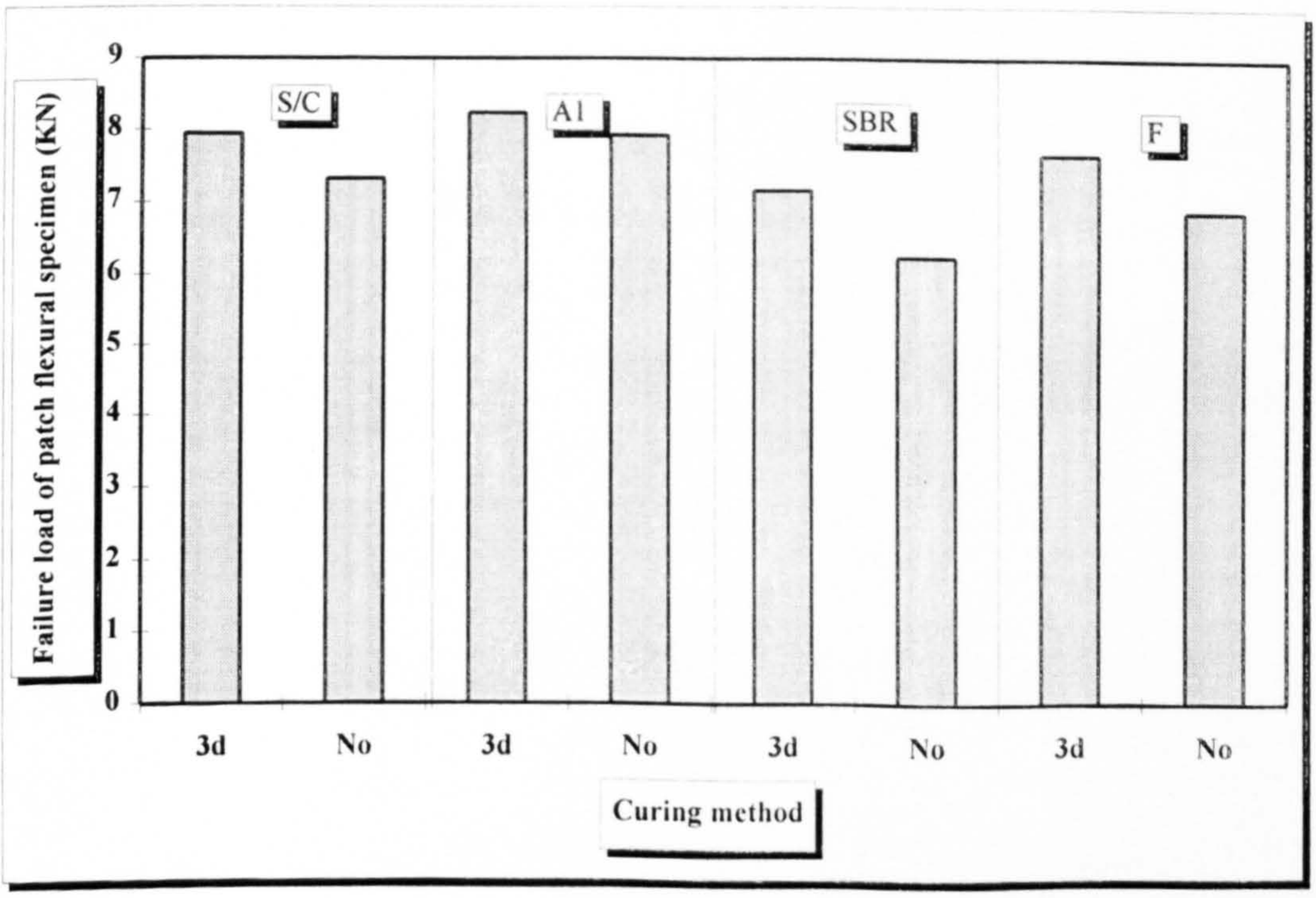

Figure 6.21 Effect of curing method on failure load of patch flexural specimens

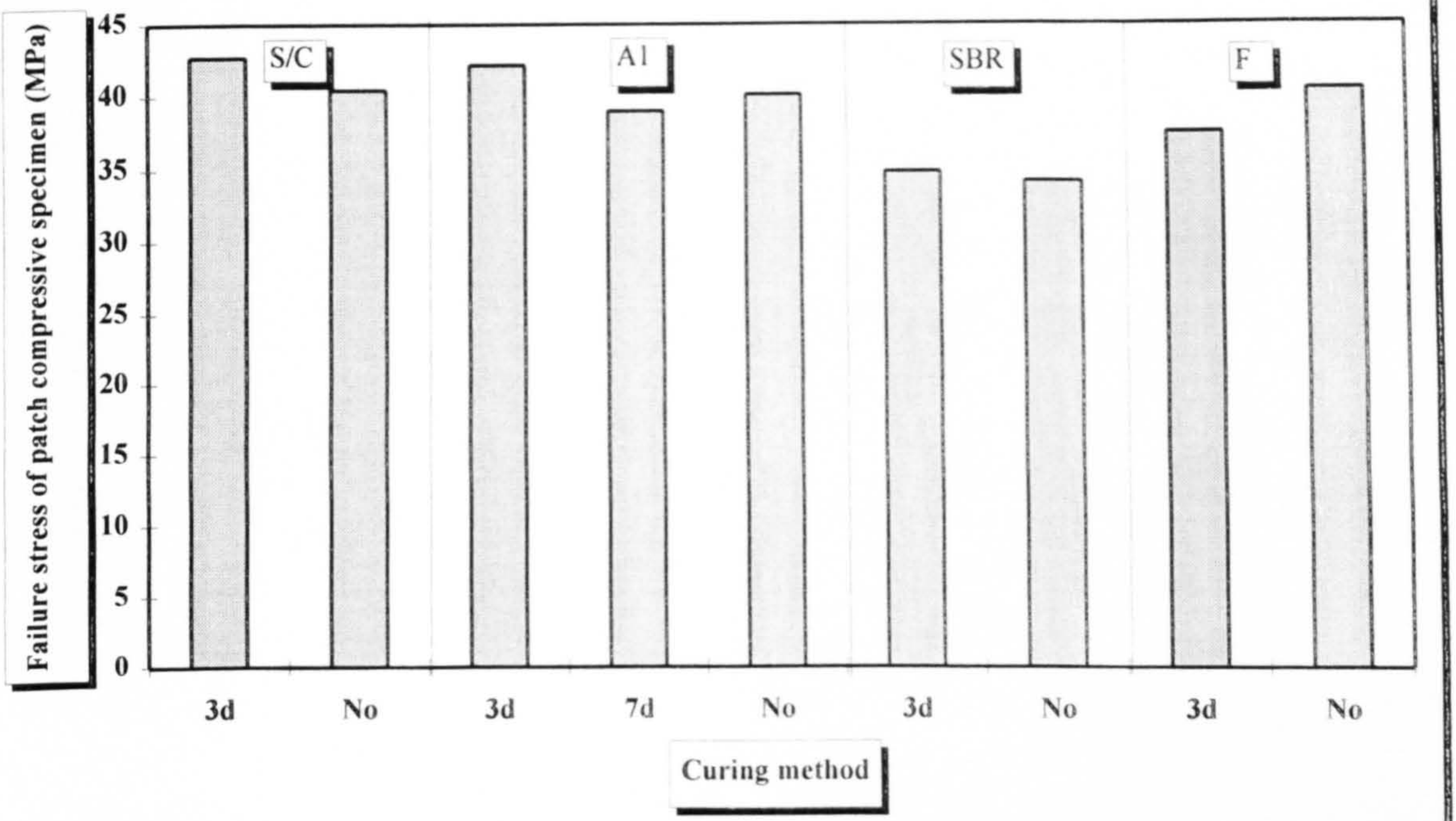

Figure 6.22 Effect of curing method on failure stress of patch compressive specimens

Chapter 7

EFFECT OF ENVIRONMENTAL CONDITIONS ON BOND STRENGTH

Chapter 7. Effect of environmental conditions on bond strength

7.1 Introduction

In order to design a repair for durability, the effect of environmental conditions on the repair material, the substrate concrete, and the interface between the two should be considered independently. Then the combined effect on the repair system can be evaluated by careful analysis of the processes involved. For example, some environmental conditions which are relatively harmless to the substrate may be harmful to the repair material, and vice versa.

If the properties of the environment in which the repaired structure is to serve are known, the levels of the relevant properties that repair materials must have in that environment to yield the desired performance may be selected. When the specifications are properly prepared and complied with, the repair possessing such properties will work satisfactorily as it interacts with the elements of the environment.

As reported in Chapter 4, the following environmental conditions were considered in this project: high temperature curing followed by drying shrinkage, high temperature curing followed by thermal cycling, low temperature curing, and low temperature curing followed by freezing and thawing cycles.

7.2 High temperature curing and drying shrinkage

7.2.1 Test results and general comments

Within the first 24 hours after placing the repair material, all specimens (not just the repair area) were sealed using polythene sheet inside the laboratory. After that, the specimens were demoulded and transferred to the environmental cabinet to receive a

high temperature curing for three days. Polythene sheet was also used to cover the specimens inside the environment cabinet which was set at 40°C and 20%RH. After the 3-day high temperature curing period, all specimens were taken out of the cabinet and left inside the laboratory to experience drying shrinkage.

Tables 7.1 to 7.3 and Figs. 7.1 to 7.3 show the effect of high temperature curing and drying shrinkage on results obtained from the core pull-off, the patch compressive , and the patch flexural tests. A few exceptions which were put in the oven at a later stage are also included in the tables.

Sand/cement mortar

Results from all three tests demonstrated increase in bond strength. The increase in tensile bond strength was nearly 40%, however, the increase in the patch compressive and patch flexural tests are quite modest, 13% and about 5%, respectively (Fig. 7.4). It also can be seen that although age affects bond strength, the effect is trivial

Acrylic modified cementitious mortar

Bond strength of the acrylic modified mortar was increased with all test methods. Because the bond strengths of the control specimens under different stress state were high, any increase in bond strength due to high temperature curing is unlikely to be very significant.

With the core pull-off test, the bond strength was increased by about 8%. It needs to be pointed out that no bond failure occurred with the high temperature cured specimens. In this case, the increase in bond strength can be viewed as a lower limit, i.e., the tensile bond strength was increase by at least 8% (Fig. 7.4).

The increase in bond strength with the patch compressive test was 3%. All three specimens failed due to debonding. Groups with an age ranging from 105 to 111 days also showed increases in bond strength, about 9%.

The failure load of patch flexural specimens was also increased, by 9% at the age of 50 days, and 14% at 135 days. An exceptional very high failure load was obtained with the group which had been cured at room temperature for 181 days.

An additional test was carried out to see the effect of high temperature curing on tensile bond strength to substrate of varying roughness. Although the surface roughness of the substrate varied from smooth to rough (the surface roughness index varying from 250 to 190 mm), the bond strength changed little.

SBR modified mortar

The bond strength with the SBR modified mortar was enhanced by the high temperature curing, and the increase was nearly 30% with the core pull-off test, followed by 21% with the patch compressive test, and 5% with the patch flexural test (Fig. 7.4). All specimens with the core pull-off and patch compressive tests failed at the bond interface, but the failure of patch flexural specimens was dominated by cracking in the repair mortar.

Flowing concrete

The core pull-off test showed no difference, whilst the patch flexural test produced 11% higher failure load (Fig. 7.4).

7.2.2. Discussion of the test results

7.2.2.1 Sand/cement mortar

The increases in the bond strengths could be attributed partly to the high temperature curing, and partly to the age difference (the age of the control specimens was 28-35 days, whilst that of the specimens which received high temperature curing was from 77 to 136 days). Clearly, the test results suggest that this kind of curing regime is beneficial.

Because high temperature will not change the repair geometry, or the surface roughness, it can be assumed that only the intrinsic bond strength will be affected. Using the bond strength envelope, this indicates that the slope of each line forming the bond strength envelope will not change. This is explained in Fig. 7.5. The inner bond strength envelope corresponds to the control specimens, and the outside envelope corresponds to high temperature cure specimens. It can be seen that in tensile stress state the increase in bond strength is significant and there is still potential for improvement in bond performance. In shear/compression stress state, the increase in bond strength is not significant and the bond failure range is reduced. This suggests that improvement in the intrinsic bond strength will not benefit the overall performance of the repaired specimen very much. Maybe an effective way to increase the failure load in shear/compression stress state is to select a bond direction far away from the critical bond direction which is related to surface roughness (see section 5.4.2).

Test results from [87] indicate that both temperature and humidity affect the bond strength development. The core pull-off and twist-off tests showed that 10-20^{o}C was the optimum curing temperature for the unmodified sand/cement mortar based on the 28-day bond strength. When the relative humidity (RH) was high (95%), the temperature effect was not significant. When the RH was low (40%), the core pull-off bond strength was only about 0.2MPa at 40^{o}C, and 0.8MPa at 10^{o}C. The maximum tensile bond strength from the core pull-off test was 1.28MPa under the optimum curing condition, which was about 10% lower than the core pull-off bond strength of the control specimens obtained from this project (1.41MPa).

Clearly, curing temperature and the RH affected the test results. Curing at 40^{o}C showed increased bond strength in this project, compared with the decreased strength in [87]. This difference can be attributed to the following reasons:

(1). In this project specimens were covered with polythene sheet for the first three days inside the environmental cabinet. Even though the RH inside the cabinet was very low, (the set RH was 20%, and the measured RH was about 30%), the actual RH beneath the sheet could be much higher than that value.

(2). Specimens used in [87] were exposed to the environment right after casting. Moisture movement can occur between a repair material and the air if there is a moisture imbalance. Moisture can be lowered by evaporation if the RH is low, or it can be increased if the air is saturated, the lower the RH, the higher the rate of evaporation. Rapid evaporation of moisture may not maintain enough water in the mortar to let the cement hydrate properly.

(3) The initial 24-hour proper curing at room temperature adopted in this project may be one of the most important reasons that accounts for the different bond strength with that in [87].

Based on the test results and the above discussion on concrete materials, the main factor affecting the bond properties in this research is the rate of moisture evaporation from the repair mortar. The higher the ambient relative humidity, the slower the rate of moisture evaporation. This possibly explains the results from [87] that even at high temperatures the decrease in bond strength was very small if the relative humidity was high. Also, initial proper curing may be critical to bond strength development in later stage.

The other factor which may affect the bond strength at high temperatures is the rate of cement hydration. From the study of concrete materials, it is reported in [113, 155, 156] that the higher the ambient temperature, the faster the rate of cement hydration. High rate of cement hydration will lead to non-uniform distribution of the hydration products leaving weak zones in the cement paste. This has some detrimental effects on the material strength and durability even though the early age strength can be enhanced. Concrete cast at different temperatures but cured at 21^{o}C produced varying

strengths, and 4°C casting temperature produced compressive strength 10% higher than the casting temperature of 21°C. When the curing temperatures were varied, both Verbeck and Helmuth's results quoted in [113] and Klieger's results quoted in [157] suggest that 13°C is the optimum curing temperature for both the 28-day and 90-day compressive strength. The effect of the rate of cement hydration on bond strength, however, depends on which is more significant between the early age enhancement and the detrimental effect of non-uniform distribution of hydration products.

It can be expected that the optimum curing regime for the bond might be different from that for the material strength. Based on tests carried out by Yeoh, et al [87], Fig. 7.6 shows the effect of curing temperature and relative humidity on the sand/cement mortar using the core pull-off and twist-off tests. In Fig. 7.6a, the horizontal axis represents the relative humidity, and the vertical axis the ratio of tensile bond strengths at different RH to the maximum tensile bond strength at that same curing temperature. This ratio is defined as the RH coefficient, γ_{RH}, i.e.,

$$\gamma_{RHi} = \frac{\sigma(t, RH_i)}{\{\sigma(t, RH_j)\}_{\max...(j=1,3)}} \tag{7.1}$$

In Fig. 7.6c, the horizontal axis represents the curing temperature, and the vertical axis the ratio of local maximum shear bond strength at temperature t_i to the maximum shear bond strength from all parameters, i.e.,

$$\gamma_{ti} = \frac{\{\sigma(t_i, RH_j)\}_{\max...(j=1,3)}}{\{\sigma(t_k, RH_j)\}_{\max...(k=1,3,j=1,3)}} \tag{7.2}$$

From the core pull-off test (Fig. 7.6a), the detrimental effect of low RH was accelerated by high temperature, resulting in a bond strength at 40%RH of only 19% of that cured at 95%RH when the temperature was 40°C. When the ambient

temperature was 10-20°C, the decrease at 40%RH was about 30%. When the RH was 70%, high temperature still caused greater reduction in bond strength than room temperatures (10-20°C). It is interesting to note that when the ambient temperature was 10-20°C, the reduction in core pull-off bond strength from 95%RH to 70%RH was less than 5%. The temperature effect shows that 10°C is the optimum curing temperature for the sand/cement mortar (Fig. 7.6c). The local maximum tensile bond strength at 10°C and 20°C (1.28MPa for both cases), which was also the maximum bond strength from all parameters tested, was about 8% higher than the bond strength at 40°C. The temperature coefficient, γ_t, showed an approximate linear relationship with the curing temperature.

Based on test results from this project and from [87], it can be concluded that high temperature mainly affects bond strength of sand/cement mortar indirectly through moisture evaporation. When the moisture evaporation can be prevented either by covering with polythene sheet or by maintaining a high relative humidity environment, the evaporation effect can be ignored. Higher temperature also causes faster cement hydration which can increase bond strength. A low relative humidity environment should be avoided especially during the first few days of curing.

7.2.2.2 Acrylic modified mortar

The failure loads of the specimens repaired with the acrylic modified mortar were also enhanced slightly after high temperature curing. However, the failure mode by each test method was different: the core pull-off specimens failed in the substrates; the patch compressive specimens failed due to debonding; and the patch flexural specimens failed by debonding with a few exceptions where the cracking in the repair mortar occurred. Thus with the core pull-off test the failure loads should be viewed as the lower limit of the bond strength under that particular stress state. Because the control specimens also had a high proportion of substrate failure the difference is merely an indication of the change of properties of the substrate concrete. In [113], it

is reported that concrete dried before testing showed an increase in strength. This can be used to explain the slight increase in failure loads when the repaired specimens were cured at high temperature. Under this condition, the moisture level inside the substrate was lowered, which might result in higher internal friction on a macroscopic scale. For oven-dried specimens, the increase in strength is about 10 to 15% [113]. In this study, the moisture levels inside the specimens which were kept in the environmental cabinet were higher than the oven-dried ones because the temperature inside the cabinet was set at 40°C, whereas that in the oven was 80°C and 120°C, respectively. Consequently, smaller increases in failure loads would be expected. The increases in the core pull-off bond strengths was 5% when the age of the repair was 74 days, and about 10% when the repair was 136 days.

The increase in failure load with the patch compressive test was less than 3%. The dominant failure mode of debonding for both the control specimens and the high temperature cured specimens and the very small difference in the failure loads suggest that the bond strength of the acrylic modified mortar under the combined stress state of shear and compression was not affected. In the interpretation of test results, the strengths of the substrate and the repair material have to be taken into consideration. The compressive strengths of the substrate and the acrylic modified mortar were 58.4MPa and 39.7MPa, respectively. When the modulus mismatch is taken into account, the compressive stress carried by the acrylic modified mortar was 40.7MPa, which was nearly same as the material strength, and the maximum compressive stress in the substrate was 51.6MPa. Lower modulus resulted in the repair material sharing less load. This explains why the nominal failure stress could be greater than the weaker material strength. The average failure load of all the patch compressive specimens repaired with the acrylic modified mortar in Table 7.2 was 42.5 MPa, with a coefficient of variation of 9.5% (the age of the repair: 28-46 days, and the age of the substrate: 136-233 days).

Additional temperature effect tests were also conducted and the results were included in Table 7.2. A week before tests were due to be carried out, these specimens were put in an oven at 80°C and 120°C, respectively, for three days, then left exposed for another two days to cool down. This regime produced an increase in failure load of about 10%, and the failures were mainly cohesive. The lower moisture content may have contributed to the higher increase in failure loads.

The increase in failure load was about 10% with the patch flexural test. Because nearly all the specimens which were high temperature cured failed due to debonding, it can be assumed that the increase was due to the increase in the bond strength. In Table 7.3, one group of specimens repaired with the acrylic modified mortar had a very high failure load, 115% higher than the control specimens. The reason for this increase was not clear, but it is assumed to be an exceptional freak result.

Tests were also carried out on the effect of high temperature curing on the acrylic modified mortar when substrates of varying surface roughness were used with the core pull-off test (Table 7.4). The mix ratio of the substrate was 1:1.6: 3.0 (cement: fine aggregate : coarse aggregate) with the w/c ratio of 0.45. The roughness varied from smooth to rough, but the failure stresses showed no difference. This also confirmed the observations from the surface preparation section (section 6.2.2) that the roughness effect on the acrylic modified mortar with a tensile test was very small and can be ignored. The average failure stress was about 4% lower than that of the control specimens. This suggests that the effect of high temperature curing (up to 40°C) on the acrylic modified mortar is very small and can be ignored.

In [87], the test results demonstrated that the specimens repaired with the acrylic modified mortar had a lower bond strength when they were exposed to a high temperature. The decrease was accelerated by high levels of relative humidity. The optimum curing environment was 20°C with 70%RH. The difference in ambient

condition compared with this research has been discussed in the above section. Clearly, the results suggest that the acrylic modified mortar does not prefer a very humid environment.

If the effects of the curing temperature and humidity are analysed separately, results from [87] can be shown more clearly in Fig. 7.7. Fig. 7.7a shows the RH coefficient, γ_{RH}, or the relative effect of moisture conditions on the core pull-off test at three RH levels (40%, 70%, and 95%) compared with the local maximum pull-off bond strength at the same temperature level (see eq. 7.1). Fig. 7.7b shows the relative effect of the moisture conditions on the twist-off test compared with the local maximum twist-off bond strength at the same temperature level. Fig. 7.7c shows the temperature coefficient, γ_t, the ratio of the local maximum bond strength at different temperatures to the maximum bond strength among all parameters studied.

It is interesting to note that when the RH was above 70%, temperature had little effect on bond strength either with the core pull-off test or with the twist-off test. When the RH was 40%, higher temperature caused more reduction in bond strength with the pull-off test. It has been pointed out in section 6.6.2 that the contribution to bond performance from polymer modified cementitious mortar comes from two processes: the hydration of cement and the coalescence of latex. Test results in Fig. 7.7 suggest the moisture condition may be more important than the temperature. Low relative humidity and high temperature will accelerate moisture evaporation resulting in not enough water for cement hydration. Based on tests carried out in this project and in [87], we can conclude that preventing moisture loss (rather than increasing or decreasing moisture) to make up for the temperature variation is more effective than keeping temperature constant to make up for moisture variation. And in fact it is the first case that is easy to operate on construction site. Ignoring the temperature effect on the RH coefficient at low RH levels (which will cause an error of 20% at 40°C), the

effect of curing conditions on the bond strength can be expressed in the form of eq.(7.3).

$$\sigma = \sigma_o \cdot \gamma_t \cdot \gamma_{RH} \qquad (7.3)$$

where σ_o -- the bond strength at the optimum curing condition (the maximum bond strength among all parameters studied);

γ_t -- coefficient of the curing temperature;

γ_{RH} --coefficient of the relative humidity;

γ_t and γ_{RH} for the core pull-off test are shown in Table 7.5, and γ_t and γ_{RH} for the twist-off test are shown in Table 7.6.

Equation (7.3) has the advantage that it can be incorporated into the theoretical analysis package. More work needs to be done to verify eq.(7.3) and to see whether it is always the best practical way to cover the acrylic modified mortar repaired area to account for the effect of the ambient temperature and to achieve the best possible repair.

7.2.2.3 SBR modified mortar

The high temperature curing followed by drying shrinkage produced increases in bond strength with the SBR modified mortar. The increase in the bond strength using the core pull-off test was 33%, and was significant at a 95% confidence level. The increase in failure load of the patch compressive specimen was 21%, and was significant at both confidence levels of 95% and 99%. The failure modes from both tests were in the form of debonding, and suggest that the improvement in bond performance was the result of increases in bond strength. There are possible two reasons to explain the increase in bond strength. First, it is the cement hydration which is accelerated by high temperature, and second, higher rate of coalescence of the SBR latex at higher temperature. The increase in failure load of the patch flexural specimen was 5%, but the failure was in the form of cracking in the repair mortar.

In [87], both the pull-off and the twist-off tests showed increased bond strengths with increasing RH from 40% to 95%, and the highest bond strength was 1.63MPa, 7% higher than the results obtained from the control specimens in this project (1.53MPa). This difference may be due to the higher relative humidity environment in [87]. The core pull-off strength of the SBR modified mortar was 1.40MPa in [5], which is slightly lower than that in this research. This could be partly attributed to the shallow core drilling (see section 5.2.5). The results in [87] (Fig. 7.8) also suggest that the effect of curing temperature and the relative humidity can be expressed as a two coefficient equation as shown by the eq.(7.3). Test results with the twist-off test showed similar trends, and the coefficients were given in Table 7.5 and 7.6, respectively. Based on test results in this research and in [87], it is possible to draw the conclusion that the SBR modified mortar prefers a high curing temperature and humid environment. Water adding may be more efficient than water maintaining for proper bond strength development. When the repair received a proper initial curing for 24 hours, the bond strength was increased under high temperature. When the repair was subjected to high temperature without initial proper curing, lower bond strength was obtained.

7.2.2.4 Flowing concrete

For the flowing concrete, the bond strength with the core pull-off test showed no change, whilst the failure load from the patch flexural test was increased by 11%. This indicates that the flowing concrete is not sensitive to curing temperature. In [87], the tensile bond strength of the flowing concrete increased from 1.82 to 2.41MPa with increasing temperature and humidity. The maximum bond strength was about 20% higher than that from the control specimens in this project. If the local maximum bond strengths at 10 and 20°C are compared with that of the control specimens in this project, the ratios are 1.09 at 20°C, and 1.0 at 10°C. Results from both the pull-off and the twist-off tests indicate that the flowing concrete prefers a curing environment with

higher temperatures and high humidity. The curing effect can also be expressed in the form of eq.(7.3) and is shown in Fig. 7.9. The temperature and relative humidity coefficients for the flowing concrete are given in Table 7.5 and 7.6.

7.2.3 Effect of drying shrinkage

7.2.3.1 Drying shrinkage of the repair materials

In the study of the effects of high temperature curing on the bond performance, it should be pointed out that during setting shrinkage stresses will be induced within the repair system due to differential shrinkage. This means that the bond strength must be capable of resisting the corresponding shrinkage stresses and the early development of good tensile bond strength is a prerequisite for achieving a good long-term bond [105]. Thus both the development of bond strengths and shrinkage stresses affect the interpretation of test results after ageing.

In order to evaluate shrinkage stresses, knowledge of both the substrate concrete and the repair materials is required. Fig. 7.10 shows the measured shrinkage curves for the repair materials used in this project. The results demonstrated that the sand/cement mortar and the flowing concrete, the two which have no polymer modification, had smaller shrinkage than the acrylic modified and SBR modified mortars.

<u>Sand/cement mortar</u>

Three samples were tested, two of them had very consistent results, whilst the third one was much higher than the first two. But the trend of shrinkage demonstrated by three specimens are very similar (Fig. 7.10a). Based on the average values, it can be seen that the shrinkage of the sand/cement mortar developed to about 100 με within the first three days, which was followed by a gradual development to 240 με at 28 days. Except the value at 35 days, shrinkage developed at a slower rate approximately linearly to 90 days at which it was about 480 με. In [5], the shrinkage measured was 700 με at one month. It should be pointed out that results from this project and from

[5] were not directly comparable because the starting age of measurement was different. In this project the shrinkage measurement was not started until after three days proper curing using polythene sheet, whilst in [5] the measurement was started from the first day. According to a Portland Cement Association document quoted by Ytterberg [118], all practical Portland cement concrete shrink about 400 to 800με. Supporting tests include those conducted by Altmann [158] with the maximum shrinkage ranging from 600 to 800με at 700 days. In order to see whether the results agree with recommendations, the ACI 209 method is used for predicting ultimate shrinkage. Based on results at 28, 53, and 90 days, the ultimate shrinkage predicted is 570 με, which is at the middle of the Portland Cement Association's suggestion.

Acrylic modified mortar

All three specimens showed very consistent results. The shrinkage developed to about 100 με within the first three days, 270 με at 28 days, and 590 με at 90 days (Fig. 7.10b). Because there are few test result available pertaining to the shrinkage pattern and shrinkage value of this kind of product, the prediction of the ultimate shrinkage is also made with the ACI 209 method. Following the same procedure with the sand/cement mortar, the ultimate shrinkage can be predicted of being 660 με. This agrees well with the data provided by the manufacturer (700 με).

SBR modified mortar

This repair material developed quite substantial shrinkage with values about doubling those associated with the sand/cement mortar, for example, 560 με compared with 240 με at 28 days, and 950 με against 480 με at 90 days. In [5], the shrinkage measured was 540 με at one month, but the difference in the starting age of measurement should not be forgot. The ultimate shrinkage predicted with the ACI 209 method is 1250 με.

Flowing concrete

A high proportion of shrinkage of the flowing concrete was developed within the first 28 days which accounts for nearly 70% of the total shrinkage developed within three

month time, with the shrinkage value being 350 με and 510 με, respectively. Again, with the ACI 209 method, the ultimate shrinkage can be determined being approximately 700 με, which agrees quite well with the data provided by the manufacturer (650 με).

In order to see the effect of shrinkage on a repair system, some theoretical analyses were carried out (see Chapter 4.3.3), which reveal that there are three main factors which affect the consistency and interpretation of the test result: (1) the age of a substrate when a repair material is applied; (2) the total shrinkage of the substrate; and (3) the shrinkage of the repair material.

7.2.3.2 Effect of the age of a substrate

This will determine how much shrinkage has developed before a repair material is applied. According to ACI 209 method of predicting shrinkage values [119], the concrete can only have shrunk about 45% of its total potential shrinkage (or the ultimate shrinkage) when the age of the substrate is 30 days, or about 70% at 90 days. From 90 to 180 days, the concrete will only shrink a further 5 to 12% of the total shrinkage. The younger the substrate, the smaller the differential shrinkage.

In [48], the long term tests were carried out to see the effect of age on bond and paste strengths. Within the first month, the paste strength was much higher than the bond strength, and reached its maximum value at about 28 days with no change at all in later stage. The bond strength reached its maximum value, which was the same as the paste strength, at the age of about 4 months with no change after that. This suggests that the bond strength increased at a much slower rate than that for the material strength. Fig. 7.11 shows the shrinkage stress variation due to the difference in the age of the substrates for the patch flexural tests. The material properties assumed were: $E_m = E_c$ =30 GPa, $\varepsilon^{\bullet}_{shm}$ = 400 με and $\varepsilon^{\bullet}_{shc}$ = 400 με. When the age of the substrate is 30 days old, the maximum tensile shrinkage stress in the repair mortar is about 40% lower than

that when the substrate is 120 days old. When the substrate is 90 days old, this is just 7% lower than that if the substrate is 120 days old. When an external load is applied on the repaired specimen, the failure point will be affected by both the shrinkage stresses and the stresses generated by the external load. So for the purpose of comparing different test results, the age of substrates should be kept constant.

In this project, the ages of the substrate concrete at the time of repairing varied from 98 to 147 days for the sand/cement mortar repaired specimens. Within the first 28 days after repairing, the substrate would have developed about 2 to 5% of the total shrinkage. Supposing $\varepsilon^{*}_{shc} = 400\mu\varepsilon$ and using the measured shrinkage at 28 days, the variation in the differential shrinkage caused due to this age difference is less than 4% and can be ignored. The age of the specimens repaired with the acrylic modified mortar varied from 46 to 151 days, with most around 90 days (the younger substrates were used at the beginning of this project). For the specimens repaired with the SBR modified mortar and the flowing concrete, the ages of the substrates varied from 74 to 109 days. Thus, the effect of this age difference on the differential shrinkage stresses can be ignored for the purpose of comparing relative bond performance.

7.2.3.3 Effect of the total shrinkage of the substrate concrete

The second factor which affects test results and result interpretation is the total shrinkage of the substrate concrete. The previous discussion on the age of the substrate suggests that if the substrate is young the differential shrinkage is lower than that with an old substrate. In fact, the differential shrinkage is not only influenced by the age of a substrate, but also by its total shrinkage. A young substrate with a very low shrinkage may result in higher differential shrinkage than an old substrate with high total shrinkage. The effect of total shrinkage is shown in Fig. 7.12. It reveals that with the total shrinkage varying from 400 to 800 με, the relative difference between the maximum shrinkage stress in the repair mortar is much smaller with old substrates than that with a young substrate even though the absolute value of the shrinkage stress

associated with the former case can be much higher. For example, when the age of the substrate is 30 days, the maximum shrinkage stress in the repair mortar can vary from about 0.3MPa to about 1.4MPa assuming the ultimate shrinkage of the substrate is 800με and 400με, respectively. The ultimate shrinkage of the repair mortar is assumed constant at 400με. When the age of the substrate is 120 days, the maximum shrinkage stress will vary from about 2.0MPa to 2.3MPa, and becomes less sensitive to the shrinkage value of the substrate. It can be envisaged that in practical repairs where the substrate can be much older than the laboratory specimens the effect of the total shrinkage on variation of maximum shrinkage stress can be ignored and an average total shrinkage would be acceptable in such instance.

7.2.3.4 Effect of total shrinkage of the repair mortar

The third factor which affects the test results is the shrinkage of the repair material. Manufacturers do not always provide the shrinkage value, and sometimes claim their products being of low shrinkage, such as 'only 0.1%', which is actually a significant amount of shrinkage (1000με). A polymer modified material may not have the same shrinkage value as another one modified by the same polymer, because many other admixtures will affect the final shrinkage values. Fig. 7.13 shows the shrinkage stress induced using the repair materials with different shrinkage values. The ultimate shrinkage of the substrate was again assumed to be 400με. Among the four repair materials tested, the SBR modified mortar had a high shrinkage, over 1200 με, which may be partly responsible for lower bond strength measured.

It should be pointed out that creep also plays an important role in determining the shrinkage stress. Some discussions were made in section 4.3.3. Unfortunately, no test data has been found on the effect of creep on concrete repairs.

7.2.4 Conclusion

From the test results and discussions above, it can be concluded that the effect of temperature varies with each repair material. If the repaired specimens are covered properly and receive proper curing for at least 24 hours, the high temperature curing (up to 40°C) can be beneficial to the bond strength with the sand/cement mortar and the SBR modified mortar. Although this environment enhanced performance of the acrylic modified mortar and flowing concrete, the increase is so small that can be ignored. The increase in bond strength also depends on stress state induced in the bond interface, but generally, the core pull-off bond strength showed the highest increase.

7.3 High temperature curing followed by thermal cycling

7.3.1 Test results and general comments

After high temperature curing at 40°C for three days, the specimens were subjected to the thermal cycling described in Fig. 3.1 for 14 days, and left in air until testing. The effects of the high temperature curing and thermal cycling (HT-TC) on the core pull-off tests, patch compressive tests, and patch flexural (PF) tests are shown in Tables 7.7 to 7.9 and Figures 7.14 to 7.17. The effects are different with each repair material, and also vary under different stress state.

Sand/cement mortar

Bond strengths were enhanced with two test methods conducted, especially the tensile bond strength which was increased from 1.41 to 2.23, nearly a 60% increase. The failure load with the patch flexural test was increased from 7.94 to 9.42 KN. It is interesting to note that while all 15 core pull-off tests with the control specimens failed at the bond interface, the high temperature curing and thermal cycling produced one

failure in the concrete substrate. Also a failure in the form of cracking in the repair mortar was produced with the patch flexural test.

Acrylic modified mortar

Bond strengths of the acrylic modified mortar showed a different trend after high temperature curing and thermal cycling, while the bond strength of the core pull-off test was reduced slightly by 5 percent, patch compressive and patch flexural bond strengths were increased by 3 and 25 percent, respectively.

When the failure mode with the core pull-off test is checked, a high proportion of bond failure (70%) was obtained compared with the control specimens which had just 16% bond failures. With the patch flexural tests, even though the bond strength was increased by 25%, this group of specimens produced 100% bond failure compared with the control specimens, for which the proportion of bond failure was 60%. Three additional patch compressive tests were conducted. The first group were covered one day and left in air one day before they were put into the environmental cabinet; the bond strength was hardly affected. The second group followed the normal high temperature curing and thermal cycling procedure, but were immersed in water for seven days before test; this caused 10% reduction in bond strength compared with the group which just received high temperature curing and thermal cycling. The third group also followed the normal thermal cycling procedure but were put in an oven at 120°C for 3 days followed by two days cooling down in air before test. The bond strength was increased by 7% due to being put into the oven, or by 10% compared with the control specimens.

SBR modified mortar

Three tests were conducted with the SBR modified mortar. The core pull-off and patch compressive tests showed 3% increase, whilst failure load of the patch flexural specimens was reduced by 10%. All core pull-off and patch compressive specimens

failed at the bond interface, in contrast to this nearly all patch flexural specimens failed due to cracking of the mortar.

Flowing concrete

The core pull-off strength was reduced by 15% from 2.03 to 1.75 MPa, however, the failure load of the patch flexural specimens was increased by 7% from 7.67 to 8.2 *KN*. All core pull-off specimens failed at the bond interface, whilst only one in three failed similarly with the patch flexural test.

7.3.2 Discussion of the test results

7.3.2.1 General

This environment differs from the previous one only in the period after high temperature curing. Thus, it may be assumed that apart from variation of bond strengths themselves any major change in bond strength is due to the difference in the following on curing environment. Thermal cycling usually has two effects on a repair system. The first one is related to the hydration of cement and the second to thermal stresses generated at the bond interface due to differential thermal deformation. To determine the thermal stresses knowledge of the coefficients of thermal expansion of both the substrate and repair materials is required.

7.3.2.2 Coefficients of thermal expansion

Substrate concrete

The coefficient of thermal expansion of the substrate concrete is a variable quantity depending on the mix design and the type of aggregate used, and can be estimated from the volume of mortar and coarse aggregate. Because cement paste has a high thermal expansion, the coefficient will also depend on the cement content. The variation over the normal range of cement contents may not be as great as changing the

type of aggregate. For concrete made with limestone sand and crushed limestone, the coefficient of thermal expansion is about $7x10^{-6}/^{o}C$ [113], or from $7x10^{-6}$ to $12x10^{-6}/^{o}C$ [8].

Repair materials

No test was carried out on measuring the coefficient of thermal expansion in this research, the following data were based on Emberson and Mays' results [5].

The coefficient of thermal expansion of the sand/cement mortar was dependent on the ambient temperature. When the temperature was between -60°C and 20°C, the coefficient of thermal expansion was $5.8x10^{-6}/^{\circ}C$, and $9.4x10^{-6}/^{\circ}C$ between 20 and 60°C. The coefficient of thermal expansion of the SBR modified mortar was $14.3x10^{-6}/^{\circ}C$ in a temperature range of -60°C to 20°C, and $10.9x10^{-6}/^{\circ}C$ from 20 to 60°C. For the flowing concrete, the ambient temperature did not influence the value which was $11.5x10^{-6}/^{\circ}C$.

7.3.2.3 Effect high temperature curing and thermal cycling on the repaired specimens

Thermal cycling usually has two effects on a repair system. The first one is related to the hydration of cement and the second to thermal stresses generated due to differential thermal deformation.

It is known that the hydrate reaction that takes place in concrete is exothermic and that the amount of heat produced usually causes the temperature of the repair mortar to rise. Because of the small amount of repair volume, the heat generated during hydration will dissipate rapidly into the air and the surrounding substrate concrete, and this can be ignored in the analysis.

Sand/cement mortar

Based on test results of high temperature curing in section 7.2, the bond strength of the sand/cement mortar was enhanced, and the increase can be attributed to the increase in

the intrinsic bond strength. During the thermal cycling, further increase would be expected.

Thermal stresses will also be generated because of differential thermal deformation. It has been discussed earlier that the coefficient of thermal expansion of the substrate concrete is about $7x10^{-6}$ to $12x10^{-6}/^{o}C$, and $(5.8\text{-}9.4)x10^{-6}/^{o}C$ for the sand/cement mortar in a temperature range from -60 to 60°C. Because the temperature change in the thermal cycling was from 10 to 40°C, the coefficient of thermal expansion would not expected to change significantly, and a single value of $9.4x10^{-6}/^{o}C$ is used in the calculation of thermal stresses.

The difference in the coefficients of thermal expansion is about $2.5x10^{-6}/^{o}C$. As a result, the differential thermal deformation generated due to a 20°C fluctuation in temperature is equivalent to 50 με. The thermal stresses can be worked out using the methods presented in Chapter 4. The maximum shear and normal stresses along the bond interface in a core pull-off specimen are 0.45MPa and 0.2MPa, respectively, the maximum tensile stress in the repair mortar is 0.75MPa. For the patch repair specimens, the maximum tensile stress generated at the bond interface is 0.75MPa. During thermal cycling, the maximum shear stress will vary between -0.45 to 0.45MPa, and the maximum normal stress between -0.2 to 0.2MPa for the core pull-off specimens. The maximum tensile stress will vary between -0.75 and 0.75MPa in a patch repaired specimen.

Unless microcracks develop at the bond interface during thermal cycling, no reduction in bond strength would be expected because at the time of testing stresses generated due to differential thermal deformation would have vanished. Test results with the sand/cement mortar suggest that bond strength development at high temperature might dominate the final bond strength.

Acrylic modified mortar

In section 7.2 of high temperature curing and drying shrinkage, it has been discussed that high temperature curing slightly enhanced the bond strength of acrylic modified mortar. In [87], test results reveal that though 40°C was not the optimum curing temperature variation of cure pull-off bond strength varied from 2.60 to 2.89 MPa in the temperature range from 10 to 40°C with relative humidity of 70%. Thus, the effect of temperature on the bond strength development can be temporarily ignored, and the attention here is the thermal stresses. Unfortunately, no test results on the coefficient of thermal expansion have been found. Based on results presented in Figure 7.17, we can assume that the effect of high temperature curing and thermal cycling is very small and can be ignored.

SBR modified mortar

Test results with high temperature curing and drying shrinkage demonstrated that bond performance of the SBR modified mortar was improved quite significantly. With the thermal cycling, bond strengths with the core pull-off and patch compressive tests changed little, whilst the failure load with the patch flexural test was reduced quite significantly. The difference in bond performance between these two environmental conditions can be viewed as the results of thermal stresses generated during the cycling.

The coefficients of thermal expansion are (7-12)x10^{-6}/°C for the substrate concrete, and 14.3x10^{-6}/°C in a temperature range of -60 to 20°C, and 10.9x10^{-6}/°C in a temperature range of 20 to 60°C for the SBR modified mortar. Because the thermal cycling was between 10 and 40°C, the coefficient of thermal expansion is assumed to be 10.9x10^{-6}/°C. This means that the difference between coefficients of thermal expansion can be 3.9x10^{-6}/°C. Assuming 20°C as the standard temperature at which there is no thermal stress generated, a temperature fluctuation of 20°C could generate quite high thermal stresses along the bond interface. In a repaired beam for the core

pull-off test, the maximum shear and normal stresses along the bond interface are 0.7 and 0.33 MPa, respectively, and the maximum tensile stress in the repair mortar is about 1.2 MPa. In the patch compressive and patch flexural specimens, the maximum tensile stress generated at the bond interface is 1.2 MPa which is about 80% of the tensile bond strength with the control specimens. Thus it can be assumed some microcracks were produced with the patch compressive and flexural specimens due to the thermal cycling. At the time of testing, a patch compressive specimen was under compressive stress and the microcracks could close and transmit stress effectively, which means that the effect of the thermal cycling can be ignored with the patch compressive specimen. In contrast to the patch compressive specimen, a patch flexural specimen was under bending and the repaired area was under tensile stress. The existence of microcracks will thus reduce the failure load of a patch flexural specimen. This is demonstrated by a significant decrease in failure load with the patch flexural specimens. With the core pull-off specimen, the small difference in bond strength with the control specimens suggests that a small amount of microcracks were generated but their detrimental effect on tensile bond strength was made up by the increase in bond strength due to high temperature curing.

Flowing concrete

The test results with the flowing concrete repaired specimens showed mixed trend, a 15% decrease with the core pull-off test, whilst a 7% increase with the patch flexural test. More test results are needed before any conclusion can be drawn.

7.3.3 Other influencing factors

Changing the amplitude of thermal cycling will change the magnitude of thermal stresses generated. The effect depends on the relative level to the bond strength. Little published information is available on this aspect. If changes in the material properties are ignored, the effect of thermal cycling is equivalent to a cyclic load, under which

stress concentrations are generated at the tip of some microcracks. An increase in the number of cycles will cause the microcracks to develop, thus reducing the effective area when the cyclic stress exceeds a certain level. When these microcracks develop into such a scale that the effective area is not able to undertake the load, fracture will occur. The stress range determines the maximum number of cycles. Examples of concrete beams under cyclic loading were presented in [135]. When the applied stress level was 80% of the static strength, the maximum number of cycles was about 20. This was increased to 100 cycles when the applied stress was 65% of the static strength. When the stress level was below 55% of the static strength, failure did not occur even after 1000 cycles. Bond tests under different number of thermal cycles are required to establish the relationship of stress ratio and maximum thermal cycles.

7.3.4 Conclusion

Thermal cycling affects bond performance in two different ways: temperature effect on cement hydration, and cycling of thermal stresses generated due to different coefficients of thermal expansion.

The bond strength of the sand/cement mortar was increased after the high temperature curing and thermal cycling. The acrylic modified mortar suffered very slightly with the core pull-off test, but showed some improvement with the patch flexural test. Thus it can be assumed that the effect of this thermal cycling is very small on the acrylic modified mortar. The SBR modified mortar has a high coefficient of thermal expansion which can results in high thermal stresses during thermal cycling. The test results with this repair mortar suggest that it is not suitable to be used in similar situations, especially where tensile stresses along a bond interface would be expected.

7.4 Low temperature curing

7.4.1 Test results

Repair materials in this project were cast at room temperature, covered with polythene sheet, and then demoulded and transferred after 24 hours to the environmental cabinet which was set at 4°C. This means that within the first 24 hours, the repair was properly cured at room temperature. Within the first three days in the environmental cabinet, the specimens were also covered with polythene sheet. After that period of time, the specimens were taken out of the cabinet and left exposed inside the laboratory.

Table 7.10 and Fig. 7.18 show the effect of low temperature curing on the core pull-off test results, Table 7.11 and Fig. 7.19 the effect on the patch compressive test, and Table 7.12 and Fig. 7.20 the effect on the patch flexural test. The effect of low temperature curing varied with each repair material.

<u>Sand/cement mortar</u>

The increase in tensile bond strength was very significant, from 1.41 MPa to 2.68 MPa, with the latter being very near to that of the acrylic modified mortar of the control specimens. This increase was supported by reduced number of bond failures. Failure load with the patch flexural specimens was increased by 10%, which was supported by reduced proportion of bond failures.

<u>Acrylic modified mortar</u>

Lower bond strengths were obtained with all three test methods. The tensile bond strength was reduced by 30% with a 100% bond failure compared with only 16% of the control specimens. Failure loads with the patch compressive and flexural specimens were reduced by 13% and 5%, respectively. Both patch compressive and flexural specimens showed higher rate of bond failures compared with their control counterparts.

SBR modified mortar

Low temperature curing caused reduction in bond strength with the SBR modified mortar. The reduction was quite significant with the core pull-off test with a 30% decrease being recorded. The patch compressive specimens suffered a 5% decrease in failure load, whilst the patch flexural specimen showed very slightly decrease. Bond failures were recorded with all core pull-off and patch compressive specimens. However, failure in the patch flexural specimens were in the form of cracking in the repair mortar.

Flowing concrete

The core pull-off and the patch flexural tests were carried out with the flowing concrete, and both produced higher bond strength. The increase with the former test was 30%, and two in five tests failed in the substrate. Compare with the control specimens, all five tests failed at the bond interface. The increase in failure load with the patch flexural test was 7%, and no bond failure was recorded.

7.4.2 General comments

Cold weather or low temperature curing may affect the properties of cementitious based materials in the following ways: (1) freezing of concrete while saturated and of low strength; (2) slow development of strength; and (3) thermal stresses on cooling to ambient temperature (if the fresh concrete is heated during curing).

Obviously, the effect depends directly on the magnitude and duration of the ambient temperature. ACI committee 306 [159] gives the following definition of cold weather which is defined as a period when, for more than 3 consecutive days, the following conditions exist: the average daily temperature is less than 5^{o}C and the air temperature is not greater than 10^{o}C for more than one-half of any 24-hour period. The average

daily air temperature is the average of the highest and the lowest temperature occurring during the period from midnight to midnight.

To help offset the problems of (1) and (2), the casting temperature of concrete or mortar should not be too low. If the ambient temperature is not too low, the heat of hydration, together with adequate insulation of exposed surfaces and formworks, should protect the concrete or mortar from freezing in its early life.

When the ambient temperature is very low, insulation may not be sufficient to maintain a temperature that is adequate for strength development and prevents freezing. In this case, the concrete needs to be heated by an external heat source.

7.4.3 Discussion

It is known that a low initial curing temperature followed by a normal curing will lead to higher strength for plain concrete or mortar than if it had been cured at a normal temperature for the total time, while a high initial curing temperature followed by a normal curing will have some detrimental effect. When polymers are incorporated into the mix design, their properties may also be changed by the low temperature curing. However, what is of interest here is the effects on the bond between two materials, not the strength of the individual component.

Sand/cement mortar

With the sand/cement mortar repaired specimens, the core pull-off tests produced large increase in the bond strength (90%), and the patch flexural test modest increase (9%), both demonstrated that the bond strength was enhanced.

It has been shown by Alexander, et al [48] that bond strength between cement paste and aggregate develops at a much slower rate than that of the strength of the material which is made of the same aggregate and cement paste. When a repair is cured at low

temperature, the bond strength may develop much slower than that at room temperatures, but the hydration products may be more uniform than those produced when cured at higher temperatures. It is known that if the 3-day and 7-day compressive strength are used to guide the curing temperature of concrete, high temperature curing would have been chosen as the preferred choice. However, in the study of bond performance, it is usually the 7-day and 28-day bond strengths that are measured. Whether the bond strength will catch up later and how the early curing may influence later age bond strength development are questions which require more research work.

The influence of low temperature curing on bond strength was studied by Yeoh, et al [87] and involved mixing, casting, and curing at 4°C and 6°C, respectively. The specimens were stored at the specified temperature for 14 days before testing at 28 days after repair. Test results showed that curing at 6°C caused a decrease in bond strength and there was a further sharp decrease from 6°C to 4°C. The low casting temperature and the much longer initial curing time may have accounted for the difference between these test results and those found in this project.

<u>Acrylic modified mortar</u>

All three tests with the acrylic modified mortar produced lower bond strength than that of the control specimens. The bond strength was reduced by 30% in the core pull-off test, 13% in the patch compressive test, and 5% in the patch flexural test. If it is assumed that the contribution of cement to the bond strength is increased, based on the results of the sand/cement mortar and flowing concrete, the cause of these reductions in the bond strength of specimens repaired with a polymer modified mortar seems to be related to the polymer systems used. Tests carried out in [87] of low temperature curing also produced lower bond strength with the value at 4°C was about half the that cured at 20°C. Clearly all these results suggest the importance of protecting polymer modified mortar repaired areas from low temperature in the early ages.

SBR modified mortar

Low temperature curing caused damage to bond strength of the SBR modified mortar. The tensile bond strength was reduced to only about 1.1 MPa, which is much lower than the bond strength of a normal concrete which can be achieved under the control situations. Though the reduction associated with the patch compressive and patch flexural tests were much smaller than the core pull-off test, the detrimental effect of a low temperature curing is obvious. The results in [87] with longer low temperature curing showed larger reduction than that in this project. Compared with the acrylic modified mortar, both suffered damage to their bond strength, which can be viewed as the damage to the polymer systems incorporated. Heating or protecting procedures should be incorporated into the repair during winter seasons or where low temperature will be experienced in the early ages after repair.

Flowing concrete

As with the sand/cement mortar, the flowing concrete samples also exhibited increase in bond capacities, neither of these materials containing a polymer. The increase in the core pull-off bond strength was significant with the flowing concrete repaired specimen (29%), but the increase was 7% with the patch flexural test. In contrast to these results, tests carried out in [87] produced much lower bond strength than those cured at room temperatures. This means that a short period of low temperature curing may be beneficial to the bond strength of flowing concrete, but a longer period of low temperature curing causes reduction in bond strength and should be avoided.

More work is needed to verify the findings from this project, and if they are true, recommendations should be made to guide cold-weather repairs.

7.5 Low temperature curing followed by freezing and thawing cycles

7.5.1 Test procedures and test results

All the specimens were firstly low temperature cured at 4°C for 3 days. After that, the specimens were saw cut into required sizes with cross section of 100x100mm, each saw-cut piece was put into a specially designed plastic containers with gaps of about 3mm around the specimen and then water was filled into the container. These specimens were immersed in water for 24 hours before subjecting to freeze/thaw cycles. During the heating period of the cycles, the specimens were checked regularly to see whether there was any sign of deterioration, such as cracking or delamination, and the containers were refilled with water if necessary.

After 33 cycles (5 hours per cycle and 7 days in total freezing/thawing time) all specimens were taken out from the environmental cabinet and left exposed inside the laboratory. All repair materials and the edge of bond interface showed no sign at all of any distress, nor did the saw cutting surfaces of the substrates. Only very slight crumbling was noticed at the casting surfaces of the substrate. This is considered to be due to the weak surface layer - the surface laitance.

Sand/cement mortar

Table 7.13 and Fig. 7.22 show the effect of freezing and thawing cycles on the core pull-off specimens. The bond strengths of the sand/cement mortar after the freezing/thawing cycles were increased in both the core pull-off test (65%) and patch flexural test (11%) (Figs. 7.22 and 7.24). The increase in bond strength was accompanied by a decrease in bond failure rate from 100% to 80% with the pull-off test, and from 100% to 67% with the patch flexural test.

Acrylic modified mortar

Results with all three test methods with the acrylic modified mortar showed decreased bond strength (Figs. 7.22 to 7.25). The reduction was 15% with the pull-off test, 11%

with the patch compressive test, and 3% with the patch flexural test. The rate of bond failure was increased from 16% to 80% with the pull-off test, and from 57% to 100% with the patch compressive test. The patch flexural specimens failed due to cracking in the repair mortar.

SBR modified mortar

The core pull-off test produced little change in the bond strength, the patch compressive test a 6% decrease in failure load, but a 7% increase being recorded with the patch flexural test. No change in bond failure rate was found (Figs. 7.22 to 7.25).

Flowing concrete

The core pull-off bond strength was increased by 25% with the flowing concrete, this is accompanied by a drop in bond failure rate from 100% to 60%. However, failure load of the patch flexural specimens was reduced by 5% without a change in bond failure rate (Figs. 7.22, 7.24, and 7.25).

7.5.2 General discussion of freezing and thawing on materials

Water in the capillary pores of cement paste expands upon freezing. If the required volume is greater than the space available, the excess water is driven off by the pressure of expansion. If the pressure exceeds the tensile strength of paste at any point, it causes local cracking. In repeated cycles of freezing and thawing in a wet environment, water can enter the cracks during the thawing period, only to freeze again later, thus causing progressive deterioration with each cycle.

The capability of a repair system to resist freezing and thawing cycles depends on its constituents: the substrate, the repair material, and the bond. The general method to study the effect of freeze/thaw cycle on a particular kind of material is to measure the weight loss and change of the dynamic modulus of elasticity. But in the case of bond performance, these two measurements are not suitable as they often reflect the

deterioration of material rather than the bond. The compatibility between a concrete overlay and the substrate concrete was judged by Cady, et al [129] on the number of freeze/thaw cycles when debonding occurred. Quite often, the specified number of cycles was increased with the aim of producing debonding. Although this method can be used to demonstrate the superior performance of polymer modified repair materials, as shown by Balaguru, et al's results [31], it cannot provide much information about the reduction in bond strength as a result of cycling. Thus it was decided in this project that the repaired specimens would be subjected to a limited number of freezing and thawing cycles and then the residual bond strength was measured.

7.5.3 Discussion of the test results

Sand/cement mortar

In section 7.4, the low temperature cured sand/cement mortar specimens had shown an increased bond strength, which was attributed to the more uniform hydration products. Because of the young age of the repair, the addition of freezing and thawing cycling has two effects on a repair system: accelerating hydration of the repair material and at the bond interface during heating; and forming ice inside the repair system and at the bond interface during freezing. The second effect depends on the water content inside the repair material as well as the air content, but generally causes accumulating deterioration. Because the number of freeze/thaw cycles was just 33 in this project (compared with the normal requirement of 300 cycles according to ASTM C666), it was expected that this cycling process would not cause severe reduction in bond strength. But the significant increase in bond strength was not expected.

If the comparison is made between two ambient conditions: low temperature curing and low temperature curing plus freezing and thawing cycling, the results presented in Figs. 7.21 and 7.25 suggest that the lower increase in the latter case is due to the effect of freezing and thawing cycles.

Acrylic modified mortar

The bond strengths of the specimens repaired with the acrylic modified mortar were reduced, but the reduction was lower than that of the low temperature curing group, namely 25%, 11%, and 3% with the pull-off, patch compressive, and patch flexural tests on the freeze/thaw group, compared with 32%, 13% and 5% on the low temperature curing group. The reduction in bond strength does not support tests on the materials, such as that by Lavelle [86]. Very low penetration of water and salt into the acrylic modified mortar surface after 60 freeze/thaw cycles was recorded by Lavelle. Whether the reduction in bond strength with this material was mainly caused due to early age low temperature curing needs more work. This preliminary study showed some detrimental effects of low temperature curing and freeze/thaw cycling on the bond strength of the acrylic modified mortar.

SBR modified mortar

The bond strengths from both the core pull-off and patch compressive tests with the SBR modified mortar showed hardly any change, the result from the patch flexural test was slightly lower than that from the control specimens. Compared with results from the low temperature curing group, the freeze/thaw cycling caused no further reduction in bond strength, rather the results suggest some improvement in the bond performance. This can be demonstrated by much smaller variation in the bond strength: +2.6% with the pull-off test (increase in bond strength), +6% with the patch compressive test, and -7% with the patch flexural test (decrease in bond strength) from the freeze/thaw group, and -30%, -5%, and -2%, respectively (decrease in bond strength), from the low temperature curing group. This improvement in bond performance may be due to the following two reasons: (1) the moisture content is not high and (2) the heating period may increase the contribution by polymers incorporated. Compared with high temperature curing and low temperature curing, it seems that the performance of polymers may be quite severely impaired by low temperature environment.

It should be mentioned that tests on material properties under freezing and thawing cycles, such as those conducted by Ohama [13], Shivaprasad, et al [34], Lavelle [86], and Cady, et al [129], demonstrated superior bond performance of polymer modified repair materials. Compared with tests carried out in this project, the main difference is the initial low temperature curing that might have impaired the bond strength, especially the proportion that should be contributed by the polymer systems

Flowing concrete

The core pull-off test produced 25% higher bond strength after the freezing/thawing cycles, however, the patch flexural test showed slight decrease in failure load. The results with both tests was lower than their counterpart of low temperature curing group. Similar to the sand/cement mortar, it seems the freezing/thawing cycles impaired bond strength development.

More work is needed to verify the detrimental effect of the initial low temperature curing and the relationship between deterioration of bond strength and freezing/thawing cycles.

7.6 General discussion and conclusions

Three test methods were used to study the effect of environmental condition on bond strength. Generally, all the three methods showed similar trends on the effects of the environmental conditioning. The relative variation in the bond strength cannot be compared directly because each test set-up was different and the influence of each factor involved would not be the same. For example, the variation of the tensile bond strength with a core pull-off test can vary from the lower bound of zero bond strength to the upper bound of the tensile strength of the substrate concrete. However, the lower bound of the failure load is increased to a fairly high level with the patch compressive and patch flexural tests with which the lower bound is controlled by the failure load of an unrepaired specimen, consequently the relative change in bond strength is reduced.

The workmanship was discussed in Chapter 6, in which the effect of environmental conditions need not to be considered in the interpretation of test results because all the tests were conducted inside the laboratory and the temperature variation can be considered as small and changing very slowly. But in studying the effect of environmental conditions, variation of workmanship may have to be considered. This variation of workmanship may be due to different levels of skill of different operators or the skill of a single operator but developed at different times. Test results from different sources with the sand/cement mortar have shown significant variation in the tensile bond strength, ranging from 1.21MPa [5] to 1.96MPa [73]. This indicates that the bond strength of the sand/cement mortar can be highly influenced by the workmanship. Even though all the tests in this research programme were conducted solely by the author, the gaining in skill in carrying out the repair work may have contributed partly to an increase in the core pull-off bond strength with time. Results from the patch compressive and the patch flexural tests were less affected by compaction because these two kind of specimens were easy to make.

In contrast to this, the compaction for the acrylic modified mortar and the flowing concrete was less influential. Mistiming of repair could cause fairly severe problems for compaction, especially with the SBR modified mortar, but this problem was prevented by using polythene sheet to seal the remaining mortar inside a container during the repairing. Thus the effect of workmanship on interpretation of test results pertaining to environmental conditions can be ignored as the rests were conducted in the later stage of this research programme.

Based on the test results and the discussions in each section, the following conclusions can be drawn:

(1) For the sand/cement mortar repaired specimens, results from all test methods and from all the environmental conditions considered showed different degrees of increase in the bond strengths. The increase under

different environmental conditions with the core pull-off test followed the order from high to low of: low temperature curing, low temperature curing followed by freeze/thaw cycling, high temperature curing followed by thermal cycling, and high temperature curing and drying shrinkage. The increase with the patch flexural test followed the order of the high temperature curing followed by thermal cycling, low temperature curing followed by freeze/thaw cycling, low temperature curing, and high temperature curing and drying shrinkage. The low increase with the patch flexural test suggests that in a real repair, the effect of variation in bond strength on load carrying capacity of a repaired specimen has to be considered in the light of the loading condition and geometry of cut-out. For the design or evaluation purpose, it can be assumed that the environmental condition considered had no detrimental effect on the sand/cement mortar repaired specimens.

(2) The acrylic modified mortar is a very good repair material with high bond strengths measured with the core pull-off test (very near the material strength), patch compressive test and patch flexural test. It can be seen that any significant increase in bond strength is difficult to be measured, although high temperature curing did show an increase in bond strength. Results from the thermal cycling group showed a mixed trend, but the reduction in bond strength with the core pull-off test was very small and can be neglected. This suggests that the thermal cycling had no detrimental effect on the acrylic modified mortar. Results from both the low temperature curing and low temperature curing followed by freeze/thaw cycling showed decreases in bond strengths, with smaller effect from the second group. This suggests that initial low temperature curing is very detrimental to the polymer system used. Either avoiding casting at winter seasons or protecting the repair from low temperature is recommended.

(3) The bond strengths of the SBR modified mortar are similar to plain sand/cement mortar under normal conditions. In a high temperature curing

environment, the SBR modified mortar showed quite substantial increase in bond strength, but because of high shrinkage of the mortar, the contribution of high temperature curing to bond strength was impaired by thermal cycling. In low temperature curing environment, these strengths were seriously affected, which may be explained by the fact that the polymers were seriously affected. Similar detrimental effect of initial low temperature curing was observed with acrylic modified mortar. Thus, the same recommendation for the acrylic modified mortar is also suggested, i.e., low temperature curing should be avoided.

(4) For the flowing concrete, results from both the high temperature curing, and low temperature curing showed increases in bond strength, but tests with the thermal cycling group and the freeze/thaw cycling group showed some mixed trend. This may be related to thermal stresses generated due to differential deformation. Another factor which may influence the interpretation of test results is that the flowing concrete is not recommended for shallow patch repair. Some segregation of aggregates was observed in the slant shear test.

(5) The study into the effects of environmental conditions was initial in scope, in that only one variable was studied in each condition. Results with all three test methods have demonstrated that they are able to show the effect of environmental conditions on a repair system. One important aspect in carrying out environmental testing is to eliminate other factors' influence by controlling the consistence of the workmanship involved. The study highlighted the importance of protecting polymer modified cementitious materials from low temperature curing.

Table 7.0 Combinations relating to environmental conditions

1	2	3	4	5	6	7	8	9	10	11	12	13	14	15	16	17	18	19	20
Repair materials		Sand/cement mortar				Acrylic modified mortar				SBR modified mortar				Flowing concrete				A2	Table number where test details can be found
Specimen types / Test parameters		CP	SS	PC	PF	CP	SS	PC	PF	CP	SS	PC	PF	CP	SS	PC	PF	CP	
Control specimens		x		x	x	x		x	x	x		x	x	x		x	x		T(7.1-7.3 7.7-7.16)
Surface roughness index	SM																		
	MR	Standard surface roughness: medium rough																	
	RF																		
Surface soundness	S	Standard surface soundness: sound																	
	W																		
Surface cleanliness	CL	Standard surface cleanliness: clean																	
	CT																		
Moisture condition	SW																		
	SD																		
	AW	Standard moisture condition: air dry surface wet																	
	AD																		
	BW																		
	BD																		
Applying methods	HA	Standard applying method: by hand																	
	VB																		
Bond coat mistiming	NO	Standard parameter: no mistiming of bond coat																	
	40																		
Repair mortar mistiming	NO	Standard parameter: no mistiming of repair mortar																	
	40																		
Curing methods	NO																		
	3d	Standard curing method: moist curing for three days																	
High temperature curing followed by drying shrinkage		x		x	x	x		x	x	x		x	x	x		x	x		T(7.1) - (7.3)
High temperature curing followed by thermal cycling		x			x	x		x	x	x		x	x	x		x	x		T(7.7) - (7.9)
Low temperature curing		x			x	x		x	x	x		x	x	x		x	x		T(7.10) - (7.12)
Low temperature curing followed by freeze/thaw cycling		x			x	x		x	x	x		x	x	x		x	x		T(7.13) - (7.15)

Note: **Control specimens:** the parameters for control specimens are indicated by each standard parameter.

Bond test method:

CP: core pull-off test; SS: slant shear test;

PC: patch compressive test; PF: patch flexural test;

Parameters of workmanship:

SM: smooth surface; MR: medium rough surface;

RF: rough surface

S: sound surface; W: weak surface;

CL: clean surface; CT: contaminated surface;

SW: saturated surface wet; SD: saturated surface dry;

AW: air dry surface wet; AD: air dry surface dry;

BW: bond dry surface wet; BD: bond dry surface dry;

HA: Hand applied without vibration; VB: hand applied with vibration;

NO: no mistiming in mistiming group or no curing in curing group;

40: about 40 min. mistiming 3d: 3d moist curing ;

A2: light weight acrylic modified mortar

Table 7.1 Effect of high temperature curing and drying shrinkage on tensile bond strength

Repair material	Curing temp. (°C)	Age of repair (days)	Number of tests	Number of bond failures	Tensile bond strength (MPa)	Coefficient of variation (%)
Sand/cement mortar	room temp.	28-35	15	15	1.41	30
	40	77	10	10	1.92	25.5
	40	136	5	5	2.0	12.3
Acrylic modified mortar	Room temp.	28-35	25	4	2.76	12.4
	40	74	10	0	2.91	6
	40	136	5	0	3.04	0.2
SBR modified mortar	Room temp.	28	5	5	1.53	17
	40	122	5	5	2.03	15
Flowing concrete	Room temp.	28	5	5	2.03	23
	40	122	5	4	2.04	20

Table 7.2 Effect of high temperature curing and drying shrinkage on failure load of patch compressive specimens

Repair material	Curing temp.	Age of repair (days)	Number of tests	Number of bond failures	Nominal failure stress (MPa)	Coefficient of variation (%)
Sand/cement mortar	Room temp.	28	3	0	35.2	13
	40	46	2	2	39.8	**
Acrylic modified mortar	Room temp.	28	11	6	42.2	11
	40	46	3	3	43.3	2
	Room temp.	105-111	6	1	43.3	10
	80*	105	6	2	47.8	3
	120*	111	3	0	46.8	4
SBR modified mortar	Room temp.	28	3	3	35.0	4.0
	40	112	3	3	42.5	4

Note: * The specimens were put in the oven at the temperature specified 5 days before testing.

Table 7.3 Effect of high temperature curing and drying shrinkage on failure load of the patch flexural specimens

Repair material	Curing temp.	Age of repair (days)	Number of tests	Number of bond failures	Nominal failure stress (MPa)	Coefficient of variation (%)
Sand/cement mortar	Room.	51	3	3	7.94	5.5
	40	49	3	3	8.09	5
	40	135	3	2	8.47	4
Acrylic modified mortar	room temp.	28	5	3	8.23	10
	40*	49	3	3	9.05	9.3
	40	50	3	3	8.9	4
	Room temp.	181	3	1	17.7	11
	40	135	3	2	9.38	3
SBR modified mortar	Room temp.	30	3	0	7.18	6.6
	40	113	3	0	7.55	5
Flowing concrete	Room temp.	30	3	1	7.67	7
	40	113	3	2	8.55	9.5

Note * means the repair mortar was exposed to the air after repairing rather than sealed with polythene sheet before being transferred to the environmental cabinet.

Table 7.4 Effect of high temperature curing on core pull-off bond strength to substrate of varying roughness

Repair material	Acrylic modified mortar		
Age (days)	74		
Moisture condition	Air dry	surface wet	
Curing temperature (oC)	40		
Number of tests	5	5	5
Number of bond failures	1	4	0
Surface roughness index (mm)	190 (rough)	210 (quite rough)	250 (smooth)
Tensile bond strength (MPa)	2.66	2.67	2.65
Coefficient of variation (%)	8.8	15.0	14.0

Table 7.5 Temperature and relative humidity coefficients for the core pull-off test (from data of Yeoh [87])

Repair material	σ_o (MPa)	γ_t $(10 < t < 40^oC)$	γ_{RH} $(40\% < RH < 100\%)$
Sand/cement mortar	1.28 [87] 1.21 [5] 1.41*	$2.34x10^{-3}$ t + 1.09	$-1.224RH^2 + 2.58RH - 0.346$
Acrylic modified mortar	2.89 [87] 2.76 *	$-2.77x10^{-3}$ t + 1.03	$-1.753RH^2 + 2.748RH - 0.065$
SBR modified mortar	1.63 [87] 1.53 *	$-6.74x10^{-3}$ t + 1.06	$0.188RH^2 + 0.31RH + 0.536$
Flowing concrete	2.41 [87] 1.75 [5] 2.03 *	$4.98x10^{-3}$ t + 0.80	$-0.327RH^2 + 0.66RH + 0.668$

Note: * means that the tests were conducted by the author.

Table 7.6 Temperature and relative humidity coefficients for the twist-off shear bond test (from data of Yeoh [87])

Repair material	σ_o (MPa)	γ_t $(10 < t < 40^oC)$	γ_{RH} $(40\% < RH < 100\%)$
Sand/cement mortar	2.79 [87]	$-5.73x10^{-3}$ t + 1.048	$0.794RH^2 - 0.39RH + 0.654$
Acrylic modified mortar	5.29 [87]	$-5.482x10^{-3}$ t + 1.043	$-1.842RH^2 + 2.56RH + 0.111$
SBR modified mortar	4.84 [87]	$-5.57x10^{-2}$ t + 1.025	$-0.376RH^2 + 0.98RH + 0.408$
Flowing concrete	3.93 [87]	$1.27x10^{-3}$ t + 0.948	$-0.242RH^2 + 0.6RH + 0.649$

Table 7.7 Effect of high temperature curing and thermal cycling (HT-TC) on the core pull-off bond strength

Repair material	Curing environment	Age (days)	Number of tests	Number of bond failure	failure stress (MPa)	Coefficient of variation (%)
Sand/cement mortar	Room temperature	28-35	15	15	1.41	30.0
	HT-TC	31	5	4	2.23	32.0
Acrylic modified mortar	Room temperature	28-35	25	4	2.76	12.4
	HT-TC	32	20	14	2.64	14.8
SBR modified mortar	Room temperature	28	5	5	1.53	17.0
	HT-TC	28	5	5	1.57	16.0
Flowing concrete	Room temperature	28	5	5	2.03	23.0
	HT-TC	28	5	5	1.75	16.0

Table 7.8 Effect of high temperature curing and thermal cycling (HT-TC) on the nominal failure stress of patch compressive test

Repair material	Curing environment	Age (days)	Number of tests	Number of bond failure	Nominal failure stress (MPa)	Coefficient of variation (%)
Acrylic modified mortar	Room temperature	28	7	4	42.2	13.4
	HT-TC (1)	31	5	4	43.2	2.6
	HT-TC (2)	46	3	3	43.3	12.8
	HT-TC (3)	56	2	1	39.3	**
	HT-TC (4)	56	3	3	46.3	1.6
SBR modified mortar	Room temperature	28	3	3	35.0	4.0
	HT-TC	28	3	3	36.4	3.3

Note: (1) Two days covered in air before being put into the environmental cabinet;
(2) One day covered in air before being put into the environmental cabinet;
(3) immersed in water for seven days before test; and
(4) Put in oven at 120°C for 3-day and 2-day cooling down in air before test.

Table 7.9 Effect of high temperature curing and thermal cycling (HT-TC) on the patch flexural failure load

Repair material	Curing environment	Age (days)	Number of tests	Number of bond failures	Failure load (KN)	Coefficient of variation
Sand/cement mortar	Room temperature	51	3	3	7.94	5.5
	HT-TC	28	3	2	9.42	7.6
Acrylic modified mortar	Room temperature	28	5	3	8.23	9.7
	HT-TC	63	6	6	10.32	6.7
SBR modified mortar	Room temperature	30	3	0	7.18	6.6
	HT-TC	28	3	1	6.5	1.8
Flowing concrete	Room temperature	30	3	1	7.67	7.0
	HT-TC	28	3	2	8.2	3.2

Table 7.10 Effect of low temperature curing on the core pull-off bond strength

Repair material	Curing environment	Age (days)	Number of tests	Number of bond failure	failure stress (MPa)	Coefficient of variation
Sand/cement mortar	Room temperature	28-35	15	15	1.41	30.0
	4°C	35	5	3	2.68	5.9
Acrylic modified mortar	Room temperature	28-35	25	4	2.76	12.4
	4°C	35	5	5	1.88	8.6
SBR modified mortar	Room temperature	28	5	5	1.53	17.0
	4°C	31	5	5	1.07	16.2
Flowing concrete	Room temperature	28	5	5	2.03	23.0
	4°C	31	5	3	2.61	15.0

Table 7.11 Effect of low temperature curing on the nominal failure stress of the patch compressive specimens

Repair material	Curing environment	Age (days)	Number of tests	Number of bond failure	Nominal failure stress (MPa)	Coefficient of variation
Acrylic modified mortar	Room temperature	28	7	4	42.2	13.4
	4°C	28	3	2	36.7	14.5
SBR modified mortar	Room temperature	28	3	3	35.0	4.0
	4°C	28	3	3	33.1	5.6

Table 7.12 Effect of low temperature curing on failure load of the patch flexural specimens

Repair material	Curing environment	Age (days)	Number of tests	Number of bond failure	failure stress (MPa)	Coefficient of variation
Sand/cement mortar	Room temperature	51	3	3	7.94	5.5
	4°C	28	3	2	8.66	6.9
Acrylic modified mortar	Room temperature	28	5	3	8.23	9.7
	4°C	28	3	3	7.81	3.2
SBR modified mortar	Room temperature	30	3	0	7.18	6.6
	4°C	28	3	0	7.04	8.2
Flowing concrete	Room temperature	30	3	1	7.67	7.0
	4°C	28	3	0	8.24	5.1

Table 7.13 Effect of low temperature curing and freezing and thawing cycles (LT-F/T) on the core pull-off bond strength

Repair material	Curing environment	Age (days)	Number of tests	Number of bond failure	failure stress (MPa)	Coefficient of variation
Sand/cement mortar	Room temperature	28-35	15	15	1.41	30.0
	LT-F/T	35	5	4	2.32	11.5
Acrylic modified mortar	Room temperature	28-35	25	4	2.76	12.4
	LT-F/T	35	5	4	2.33	18.7
SBR modified mortar	Room temperature	28	5	5	1.53	17.0
	LT-F/T	38	5	5	1.57	14.4
Flowing concrete	Room temperature	28	5	5	2.03	23.0
	LT-F/T	28	5	3	2.52	17.4

Table 7.14 Effect of low temperature curing and freezing and thawing cycles (LT-F/T) on the nominal failure stress of the patch compressive specimens

Repair material	Curing environment	Age (days)	Number of tests	Number of bond failure	failure stress (MPa)	Coefficient of variation
Acrylic modified mortar	Room temperature	28	7	4	42.2	13.4
	LT-F/T	28	3	3	37.5	3.2
SBR modified mortar	Room temperature	28	3	3	35.0	4.0
	LT-F/T	28	3	3	37.1	4.9

Table 7.15 Effect of low temperature curing and freezing and thawing cycles (LT-F/T) on failure load of the patch flexural specimens

Repair material	Curing environment	Age (days)	Number of tests	Number of bond failure	Failure load (KN)	Coefficient of variation
Sand/cement mortar	Room temperature	51	3	3	7.94	5.5
	LT-F/T	28	3	2	8.8	0.5
Acrylic modified mortar	Room temperature	28	5	3	8.23	8.7
	LT-F/T	28	2	0	8.0	**
SBR modified mortar	Room temperature	30	3	0	7.18	6.6
	LT-F/T	28	3	0	6.69	14.0
Flowing concrete	Room temperature	30	3	1	7.67	7.0
	LT-F/T	28	3	1	7.25	9.1

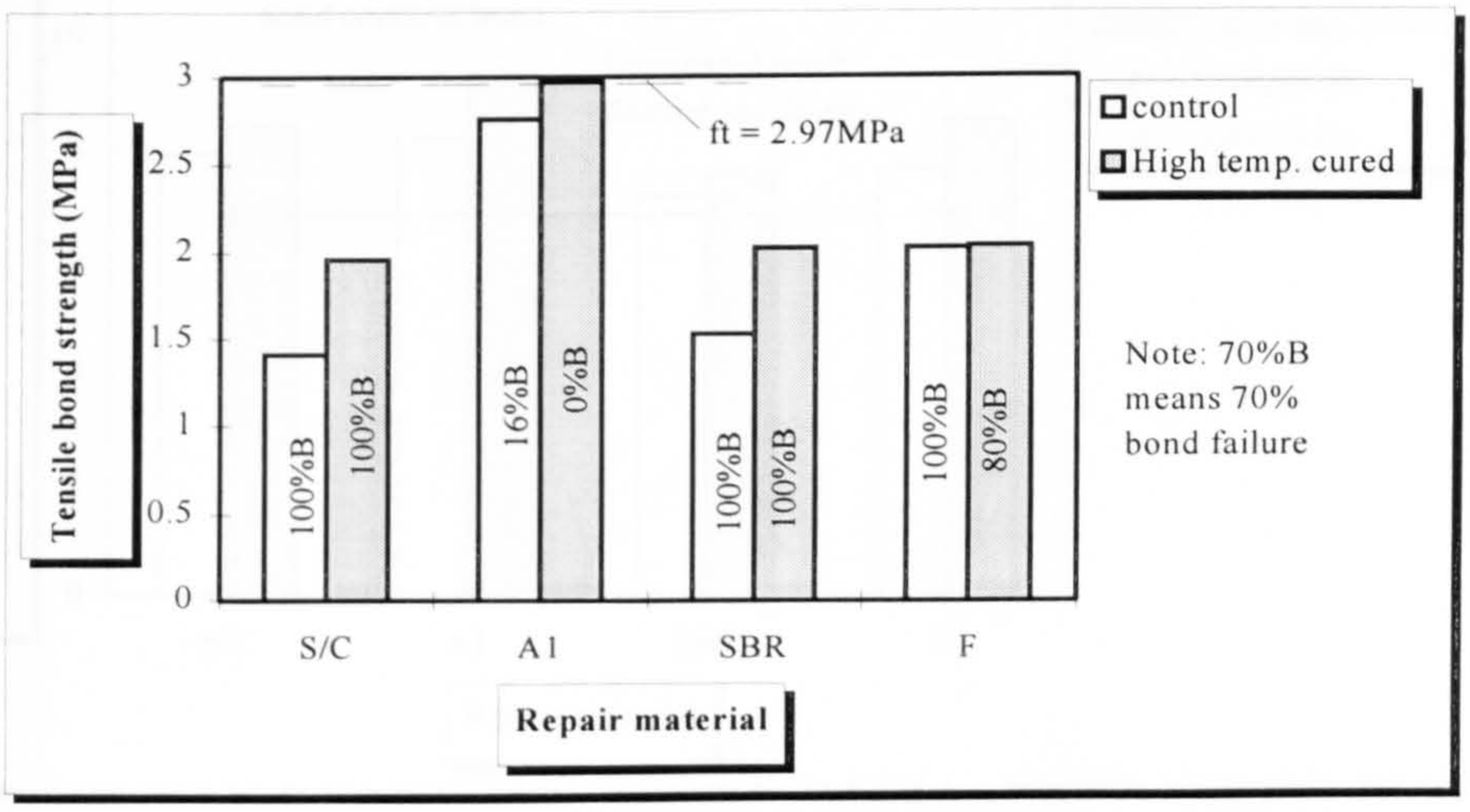

Fig. 7.1 Effect of high temperature curing and drying shrinkage on core pull-off bond strength

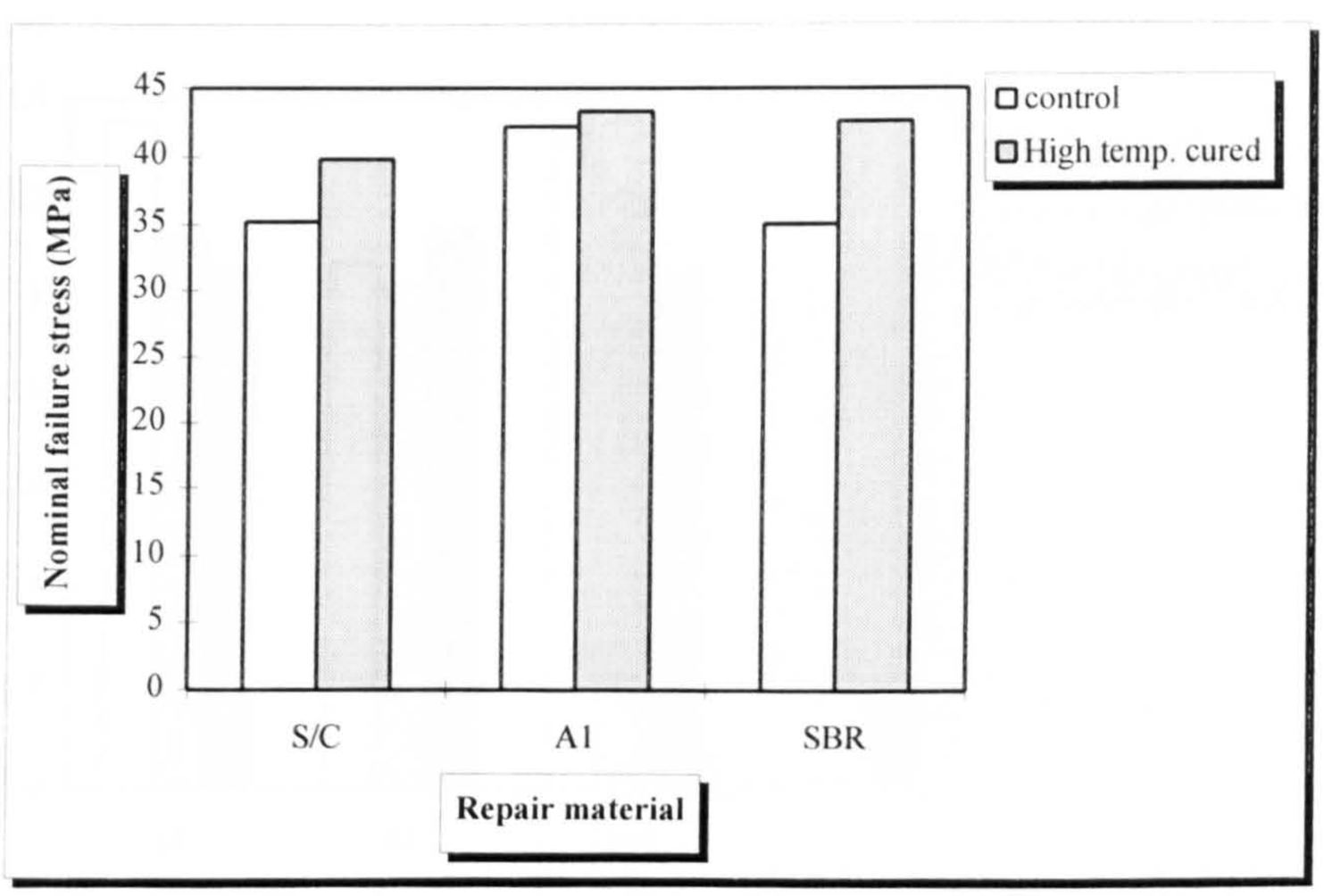

Fig. 7.2 Effect of high temperature curing and drying shrinkage on nominal failure stress of patch compressive specimens

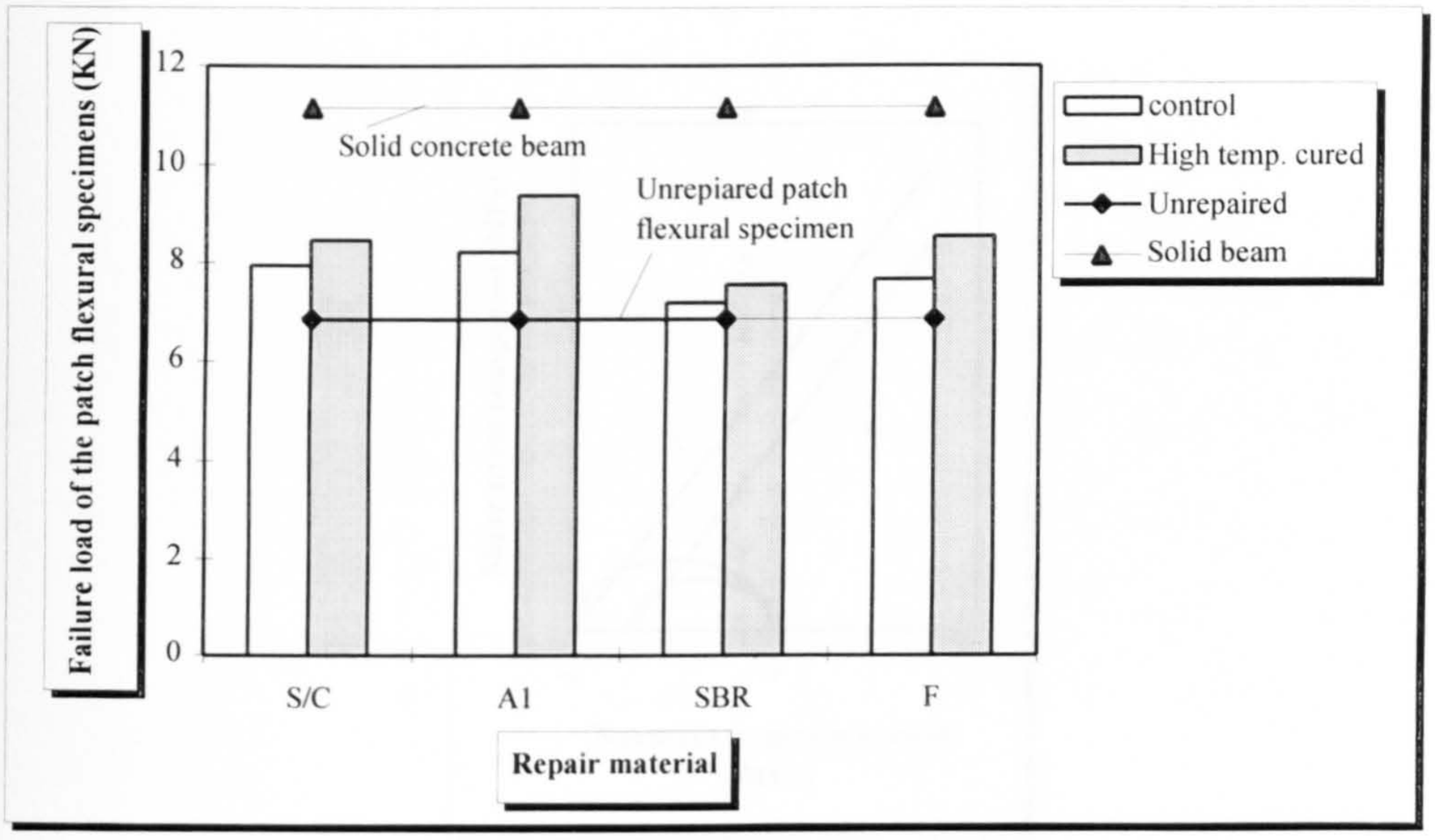

Fig. 7.3 Effect of high temperature curing and drying shrinkage on failure loads of patch flexural specimens

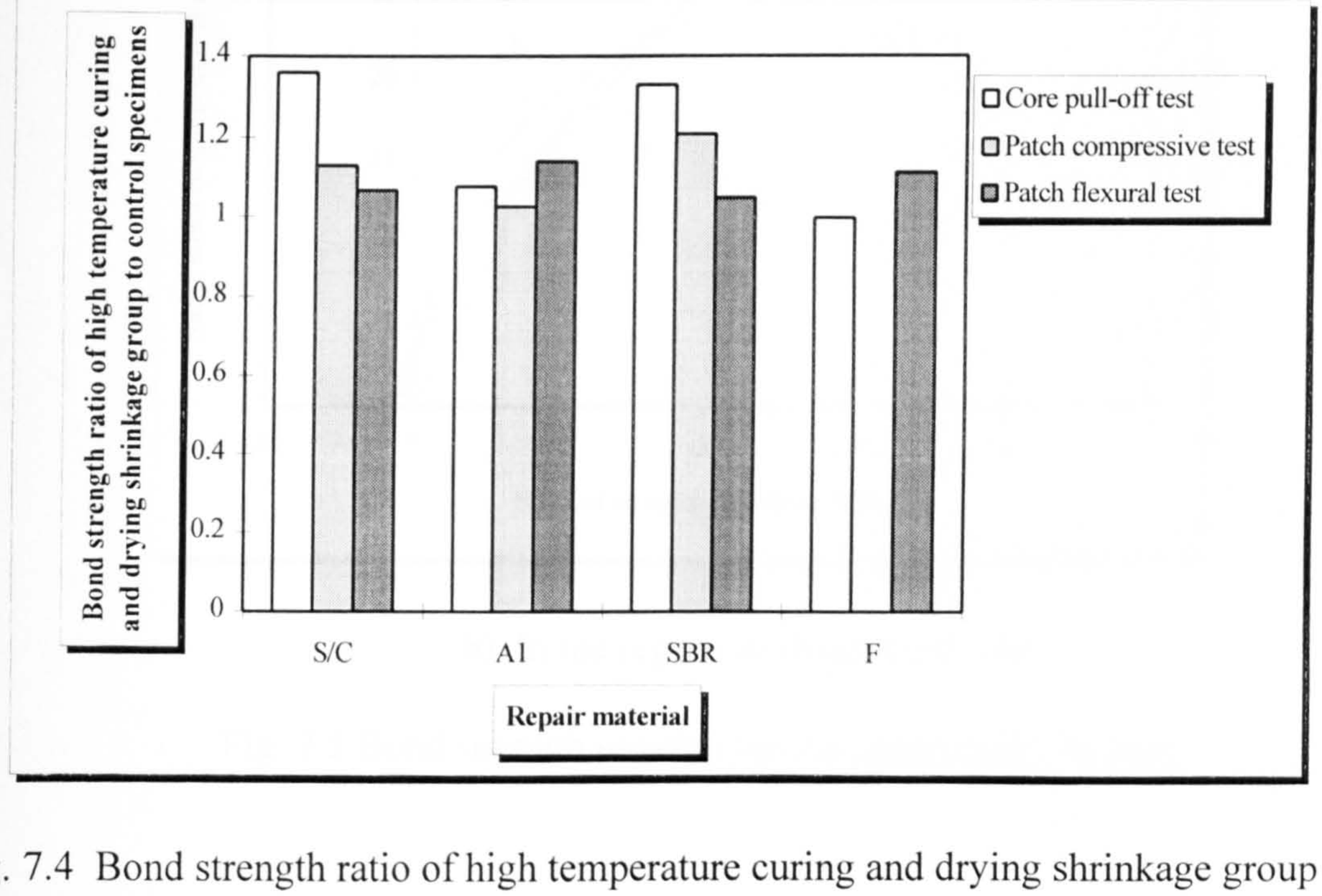

Fig. 7.4 Bond strength ratio of high temperature curing and drying shrinkage group to the control specimens with different test methods

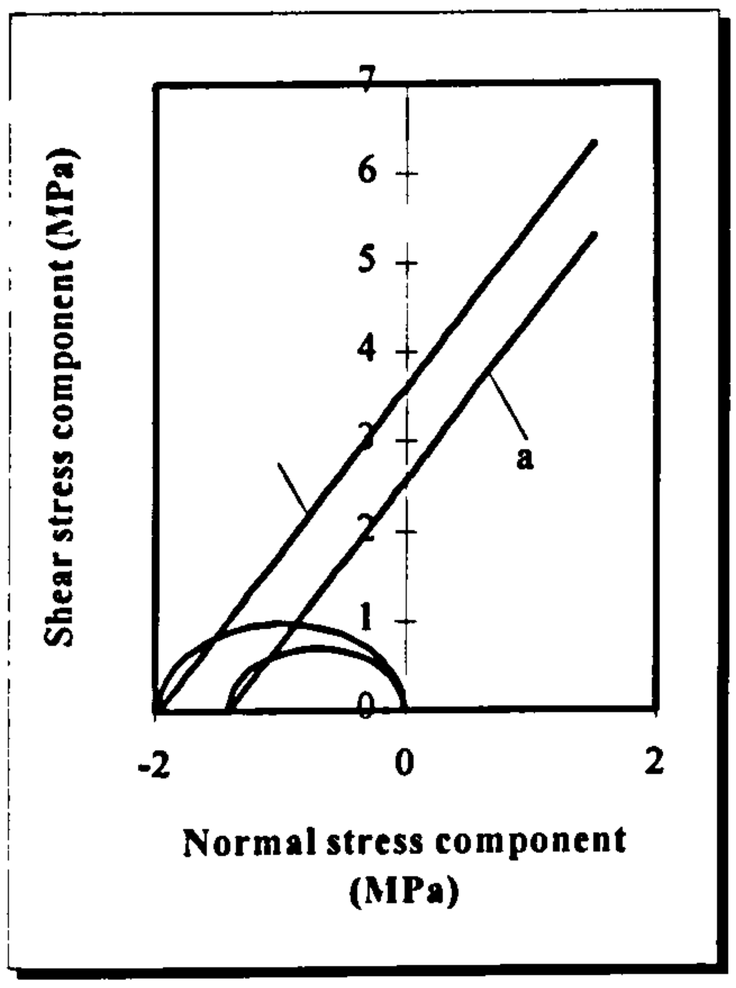

a) In the region of shear/tension

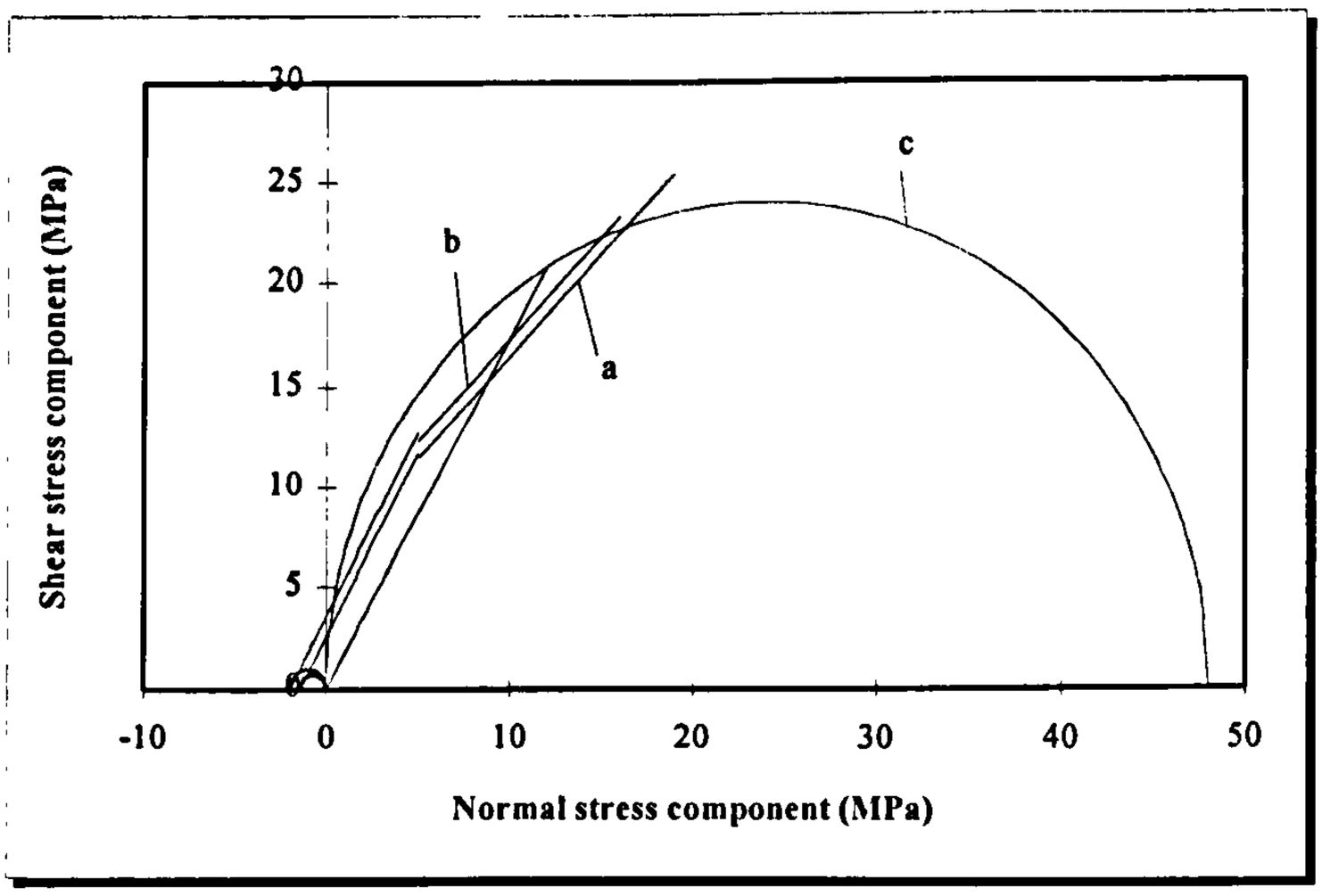

b) In the region of shear/compression

Fig. 7.5 Bond strength envelop for the sand/cement mortar

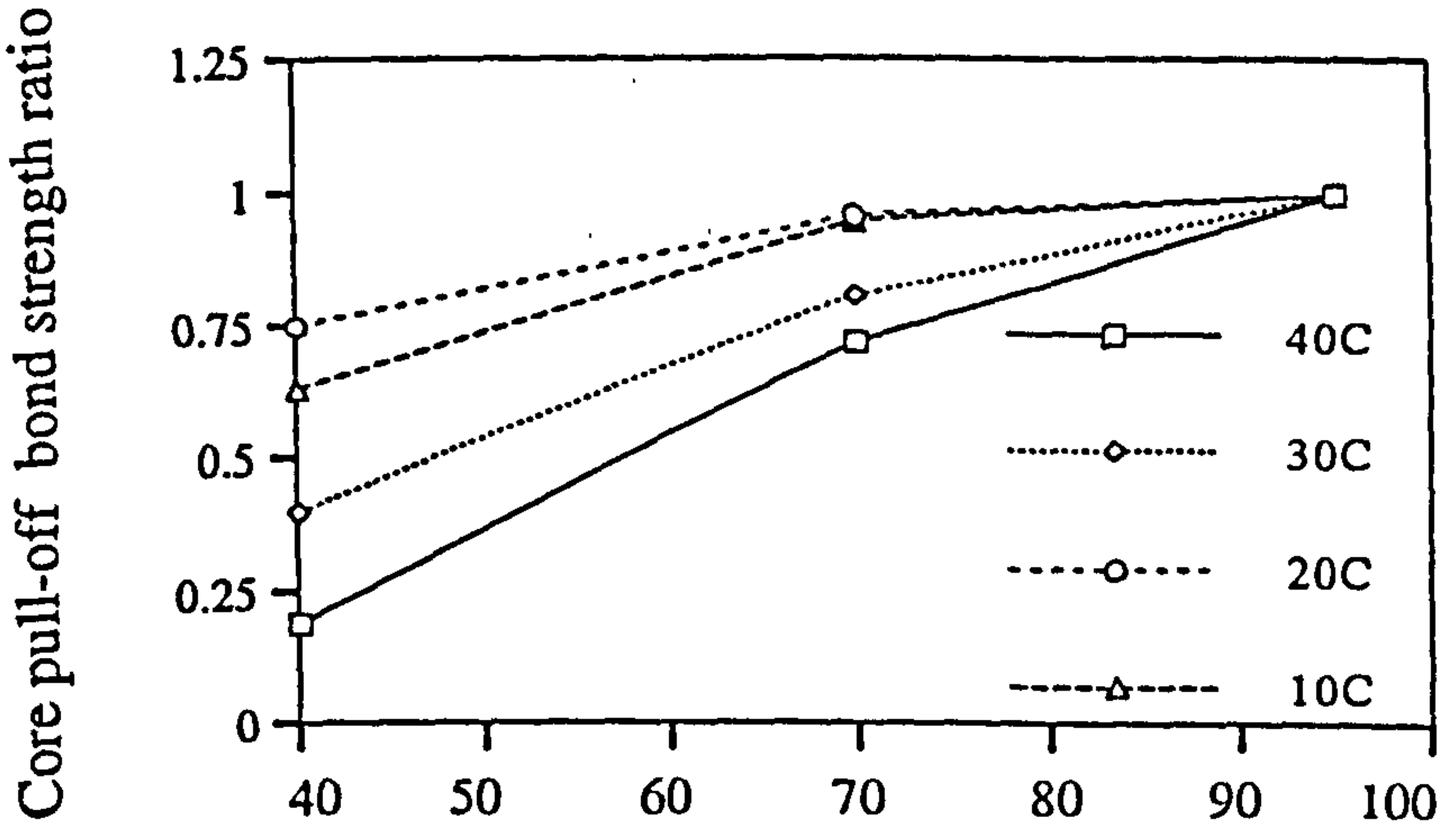

a)

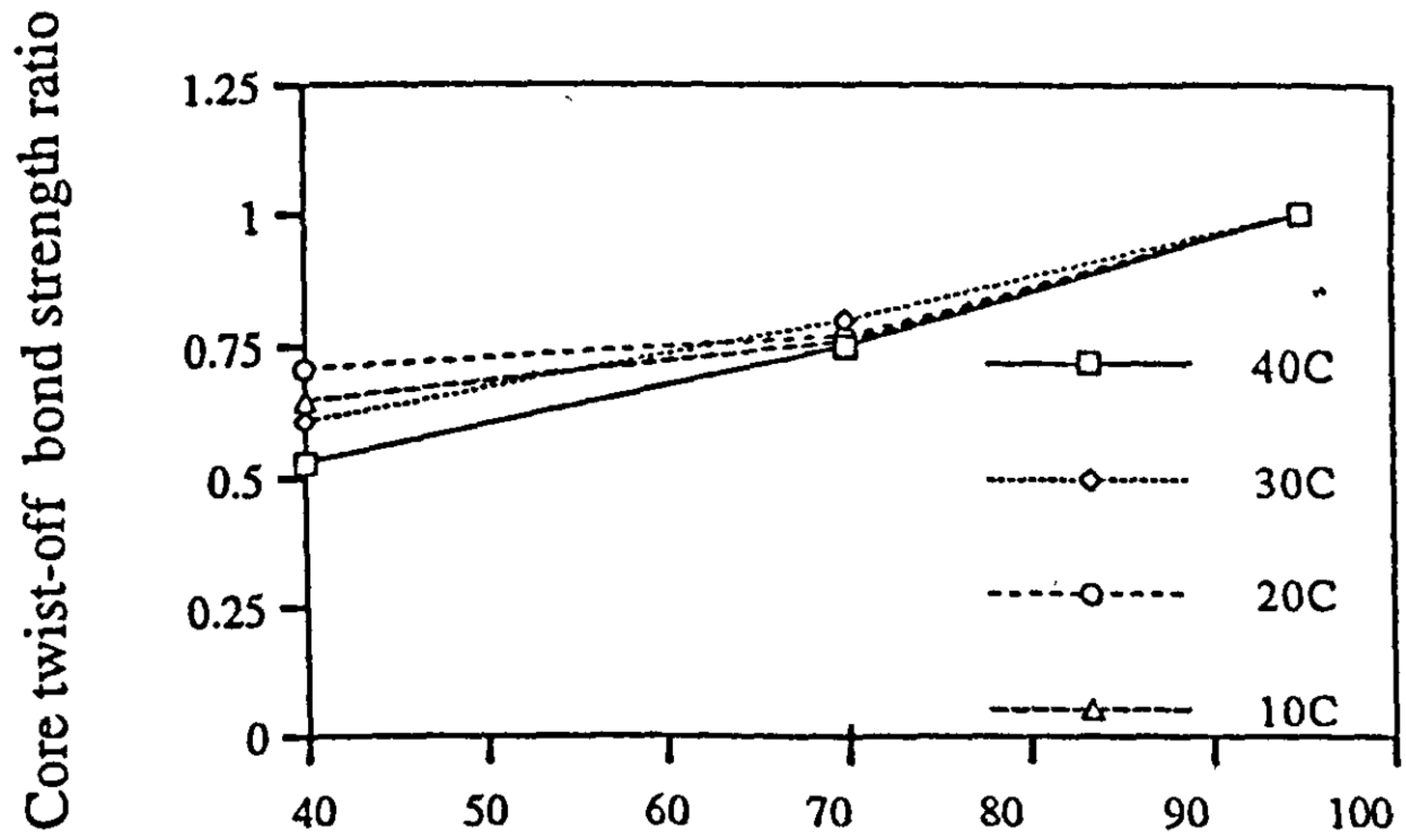

b)

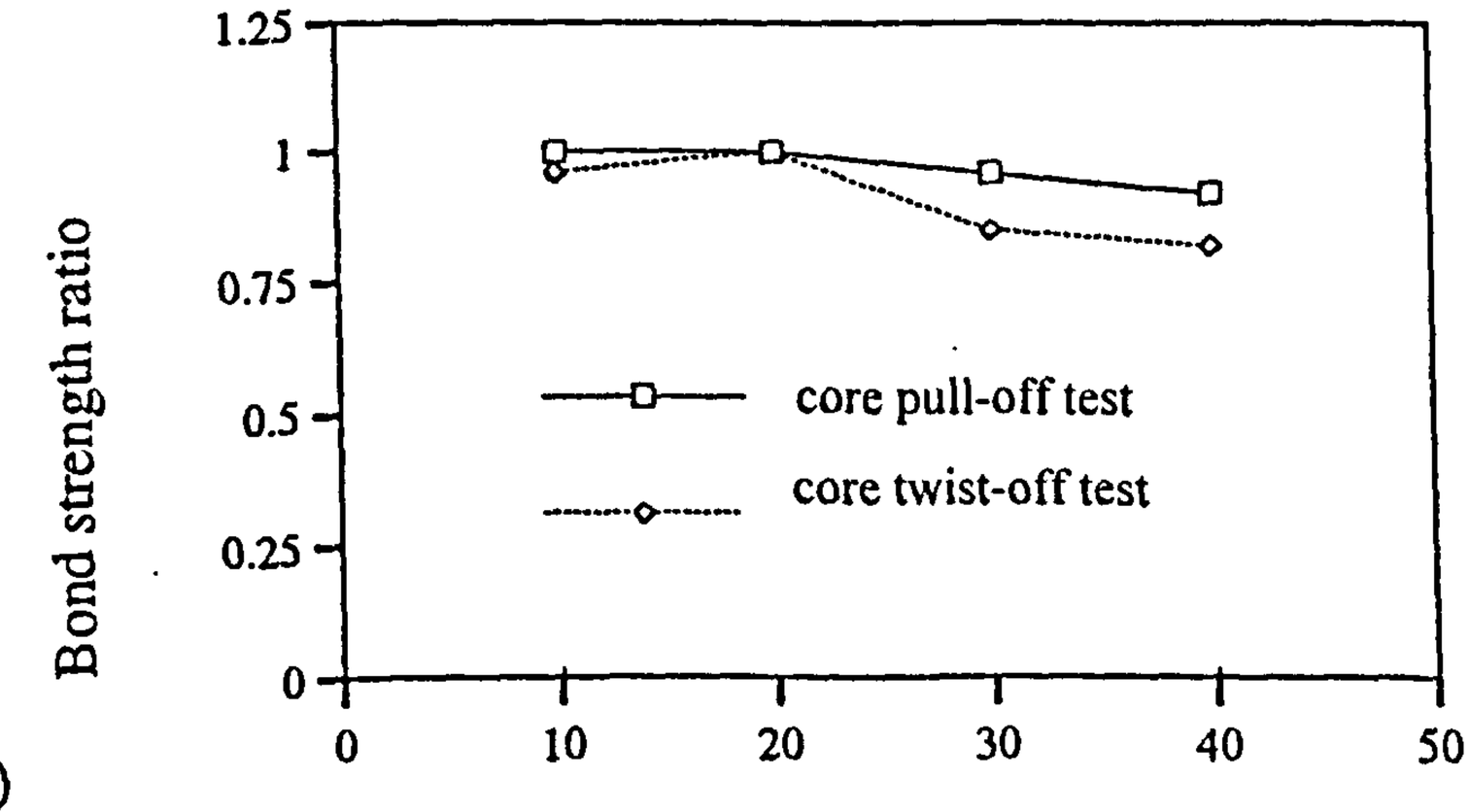

c)

Figure 7.6 Effect of curing on the core pull-off and twist-off bond strength of the sand/cement mortar (after Yeoh, et al [87])

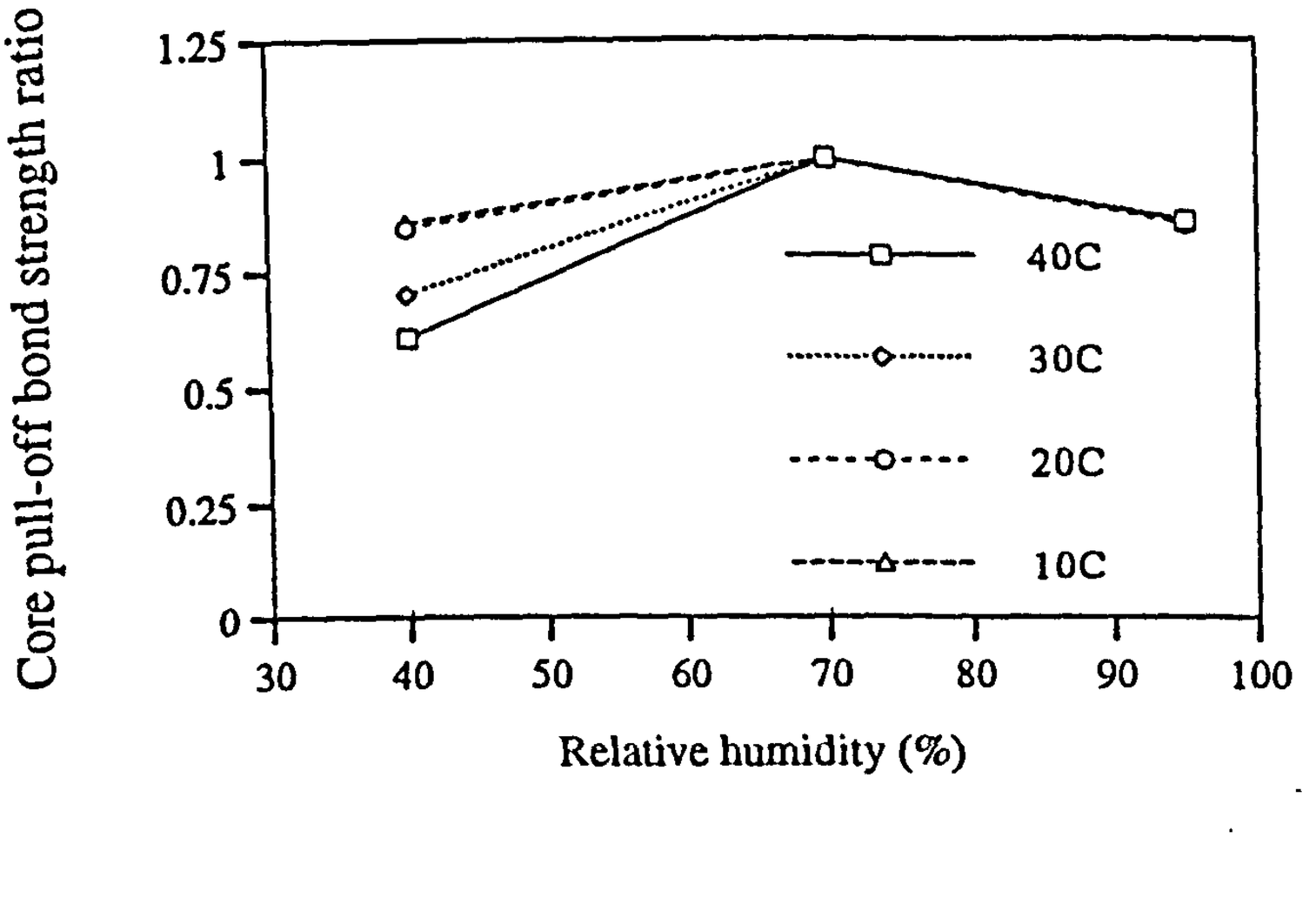

a)

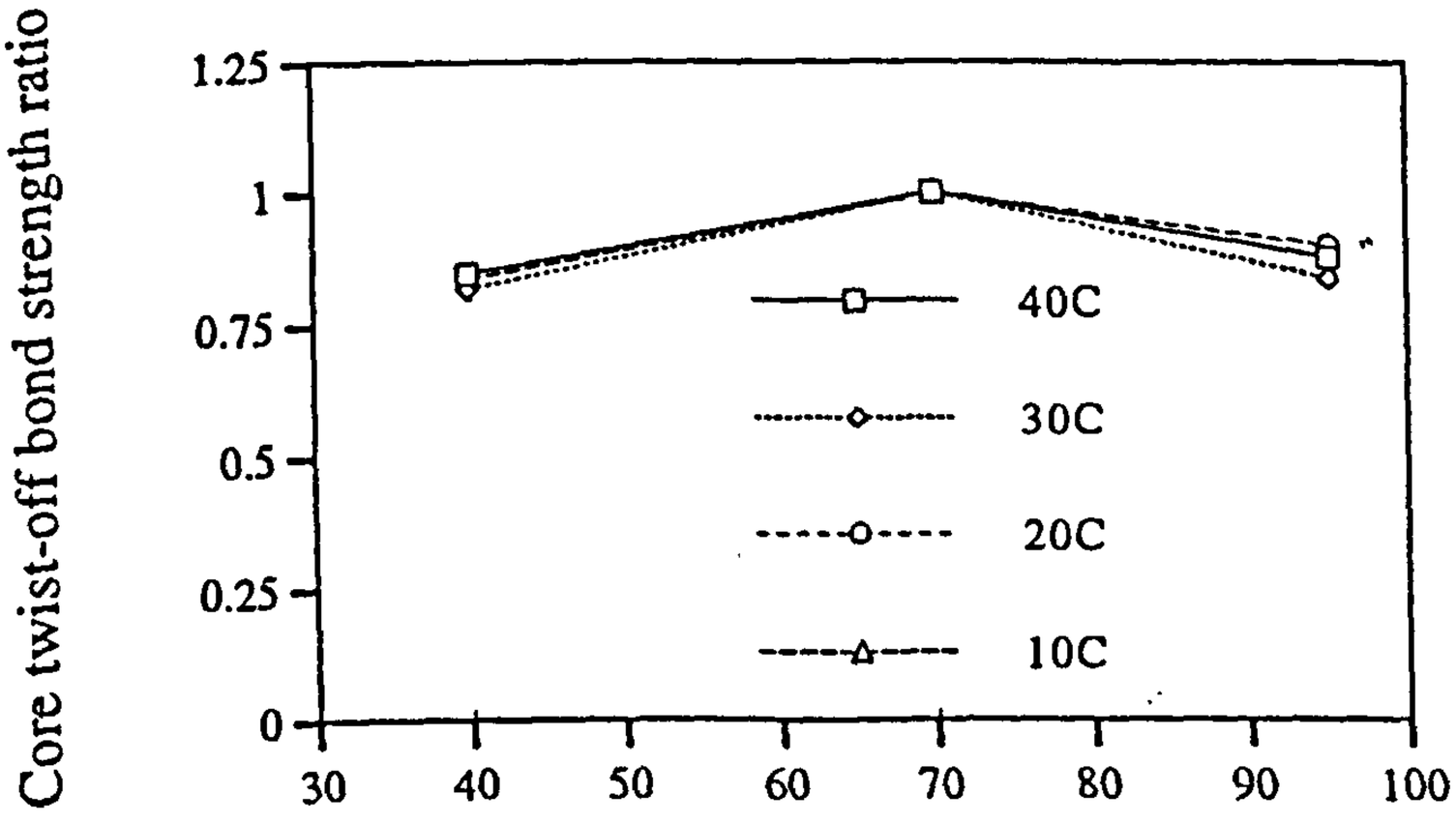

b)

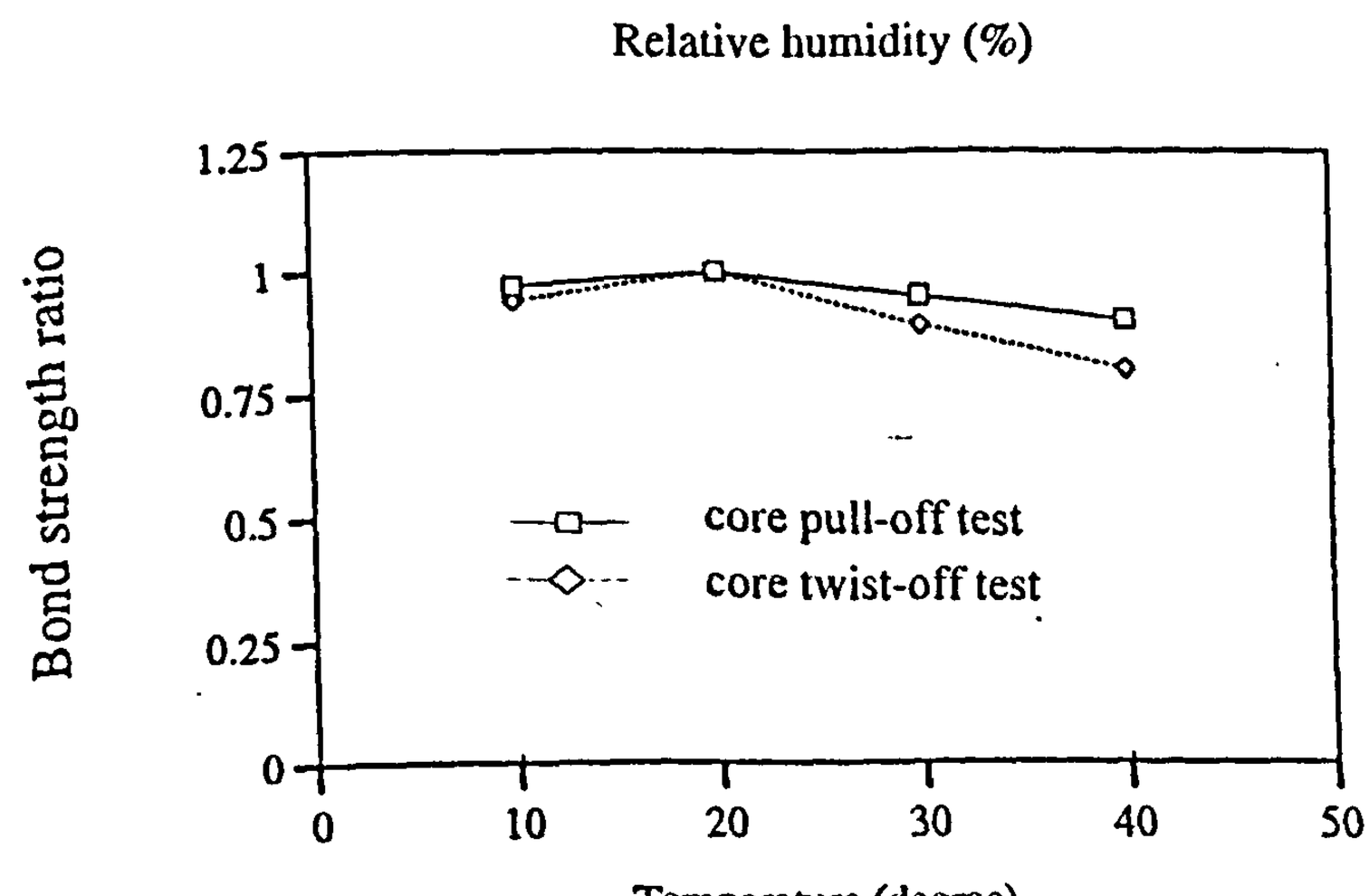

c)

Figure 7.7 Effect of curing on the core pull-off and twist-off bond strength of the acrylic modified mortar (after Yeoh, et al [87])

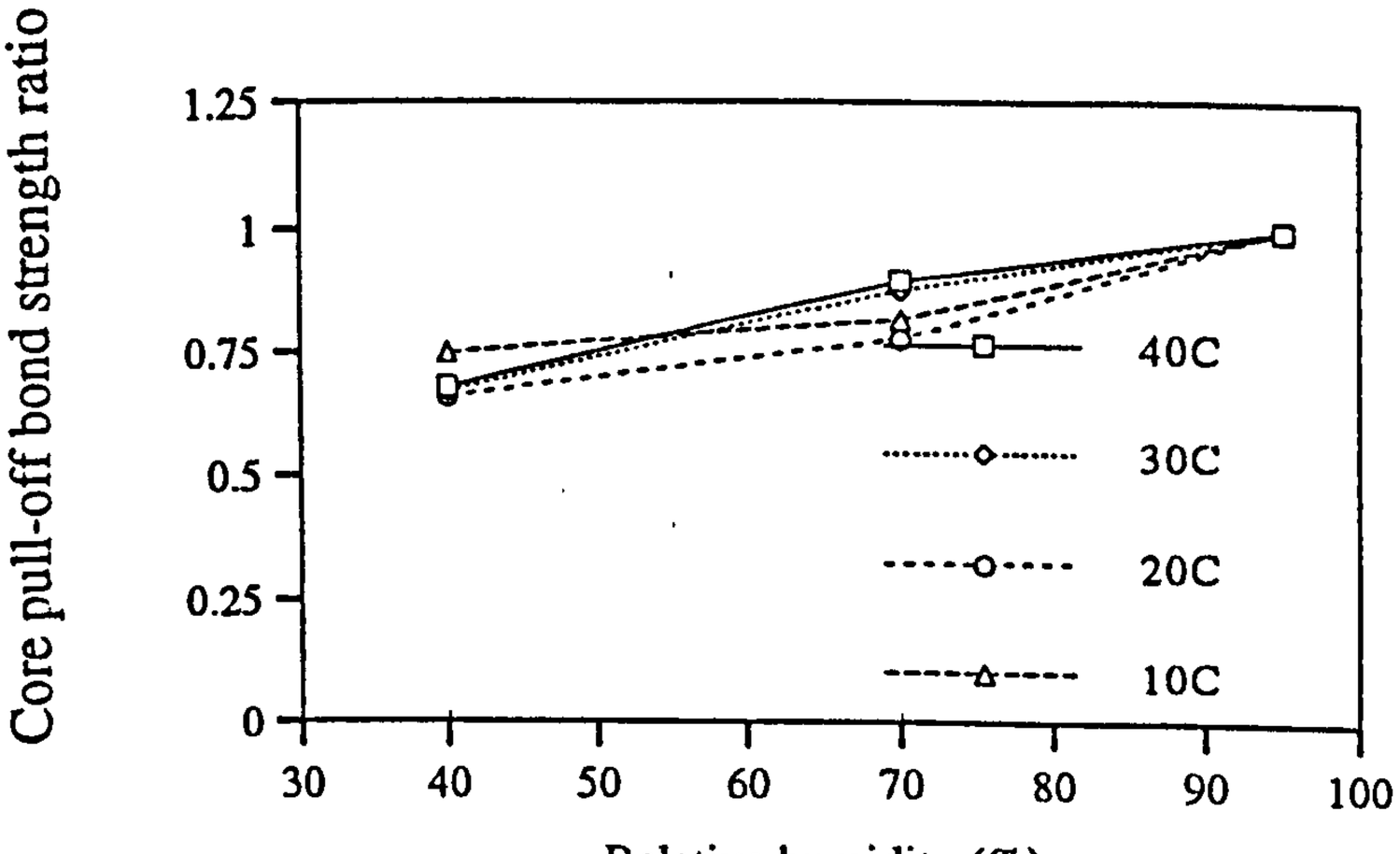

a)

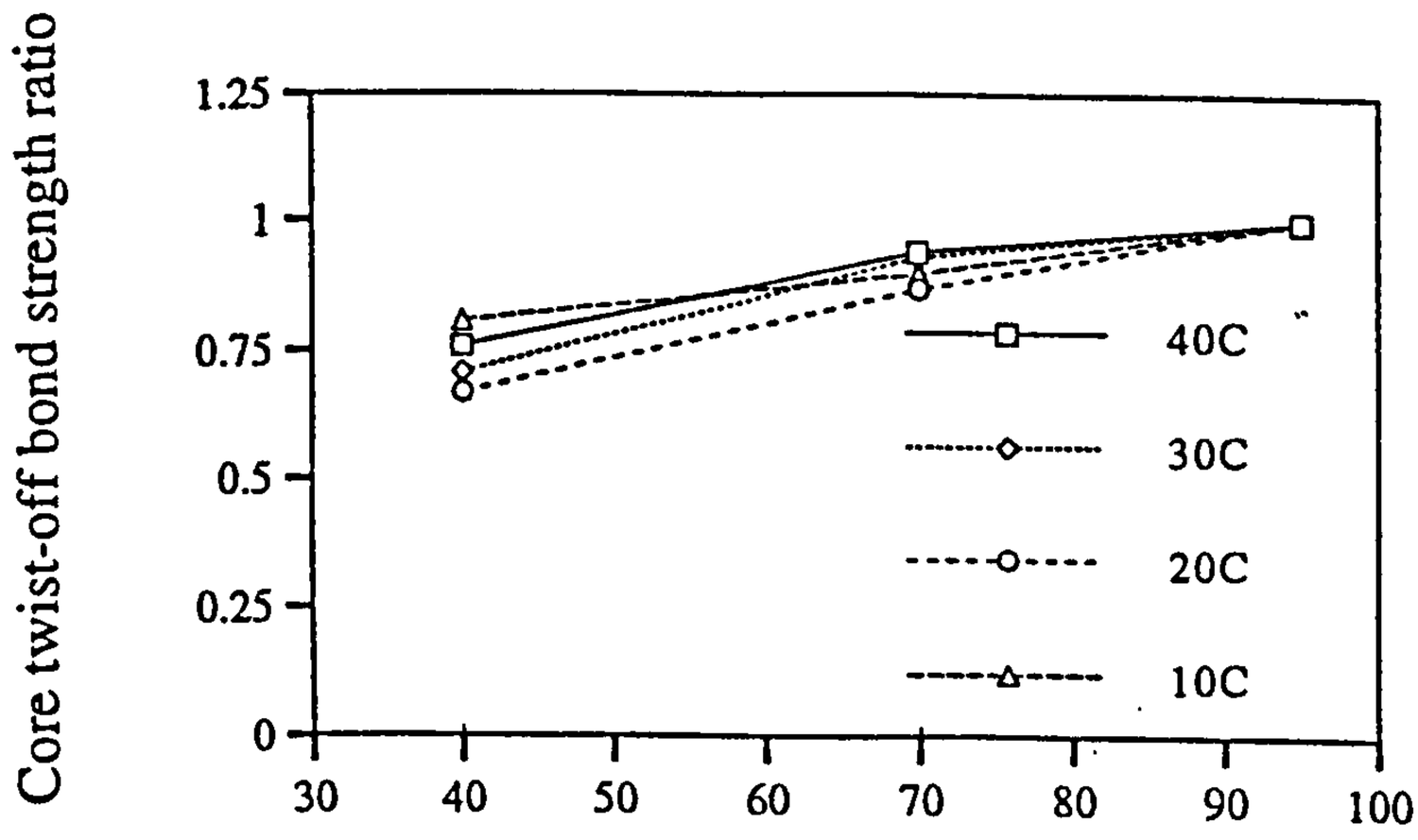

b)

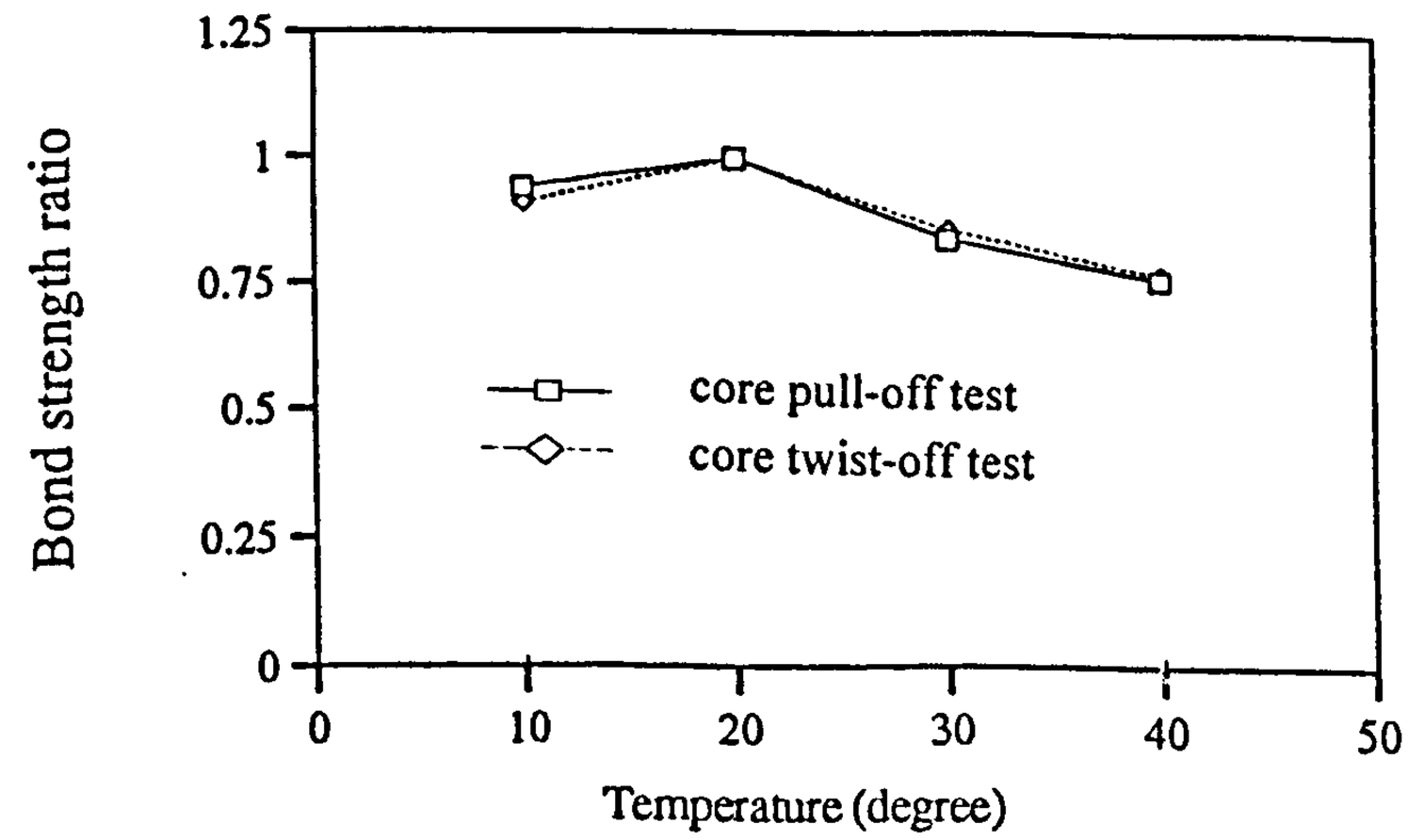

c)

Figure 7.8 Effect of curing on the core pull-off and twist-off bond strength of the SBR modified mortar (after Yeoh, et al [87])

a)

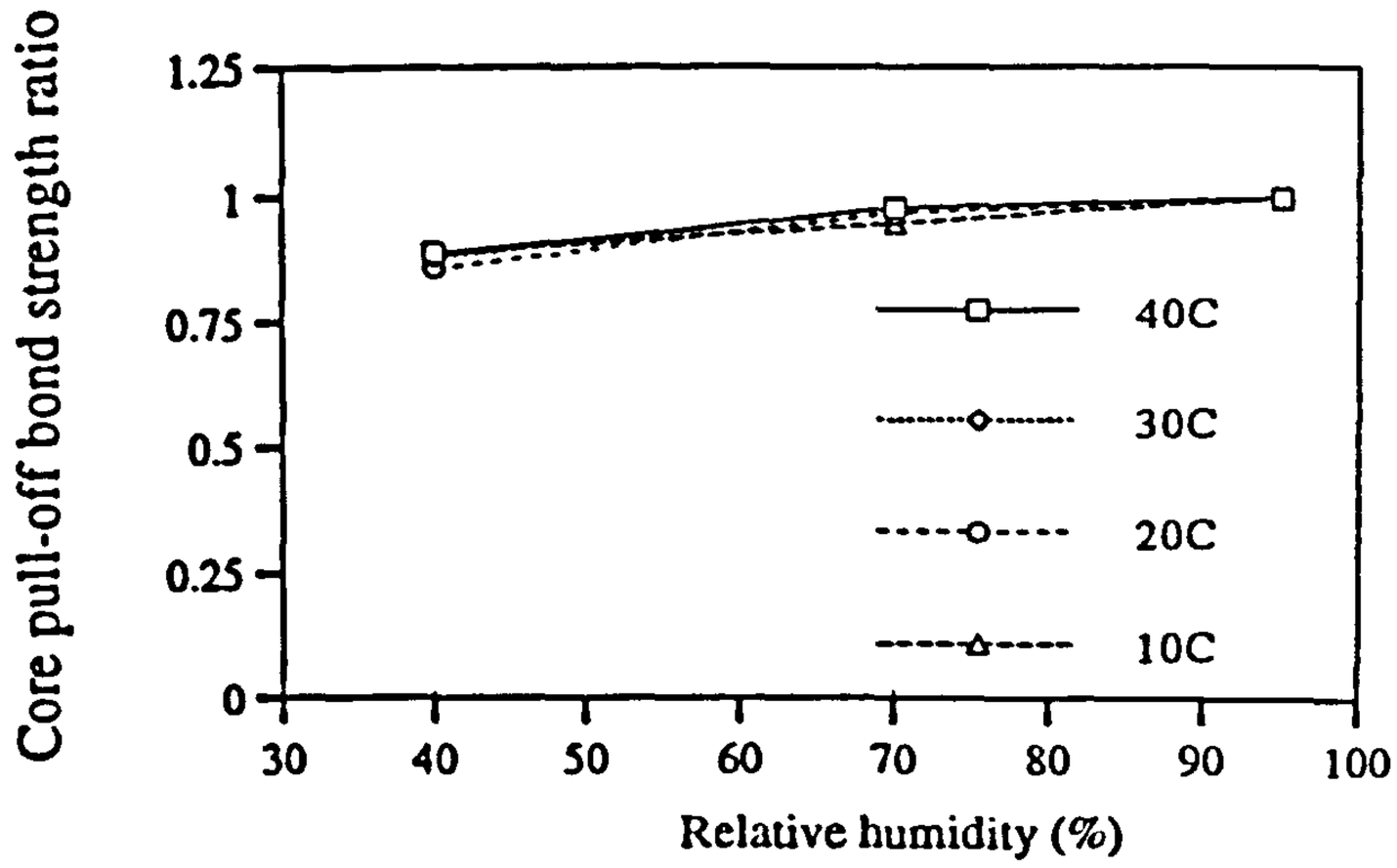

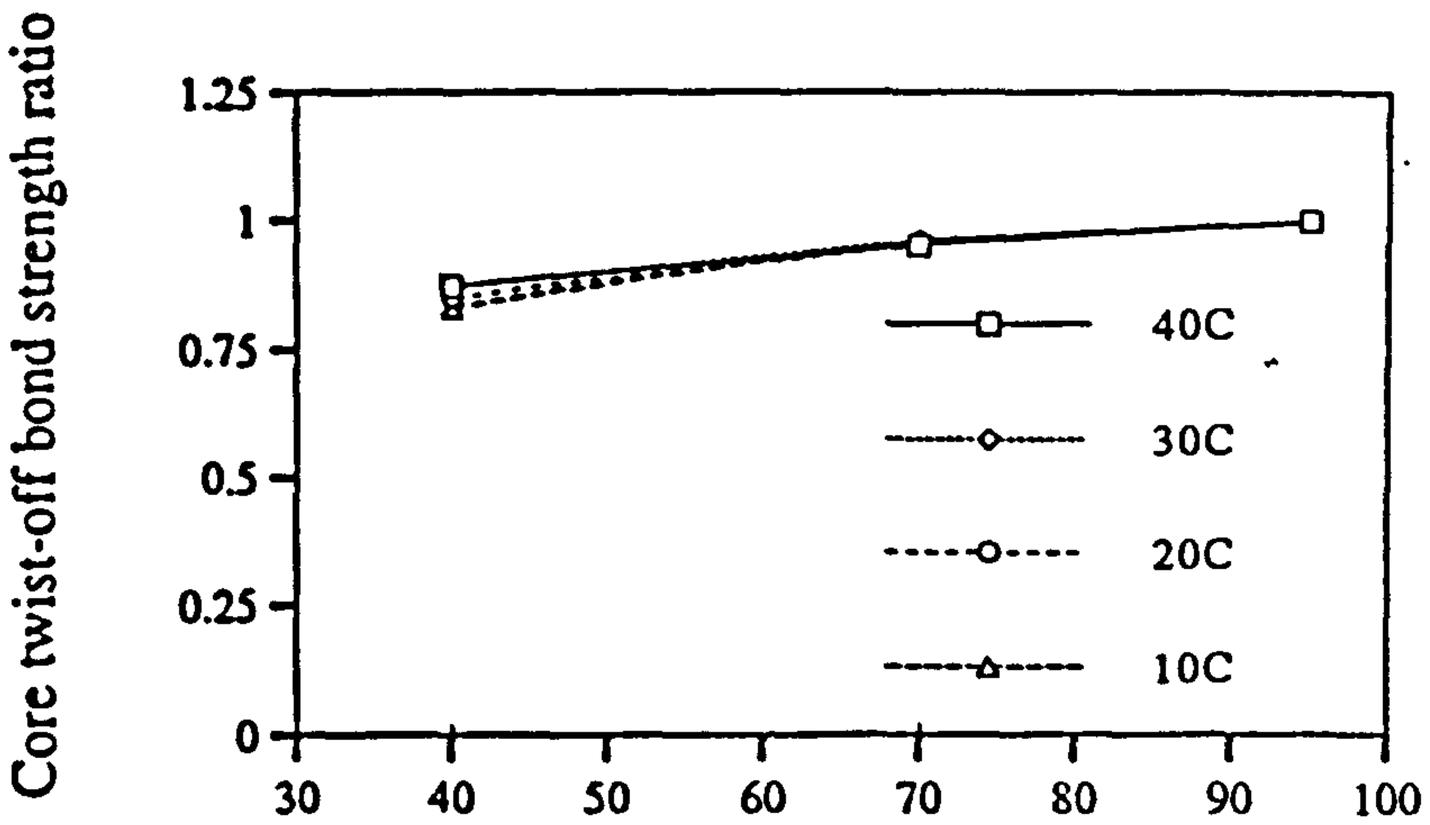

b)

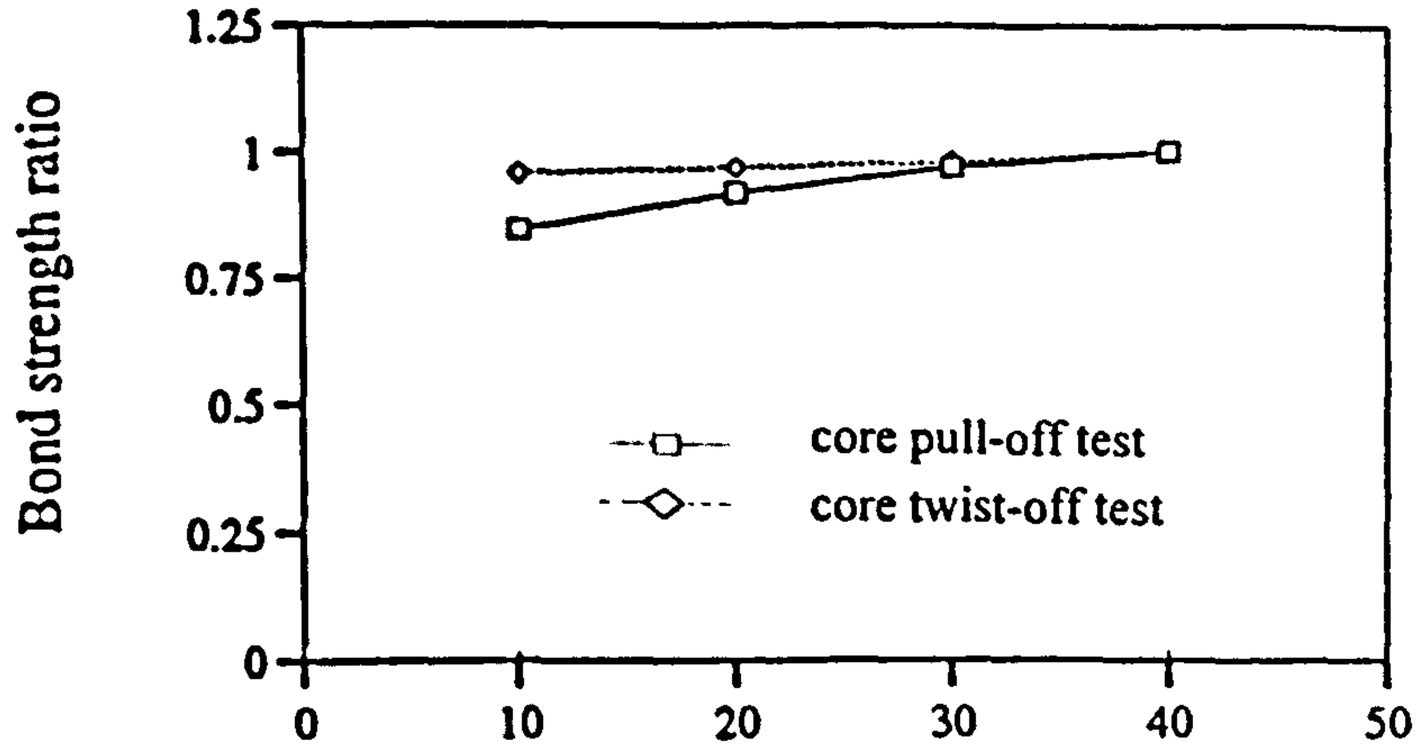

c)

Figure 7.9 Effect of curing on the core pull-off and twist-off bond strength of the flowing concrete (after Yeoh, et al [87])

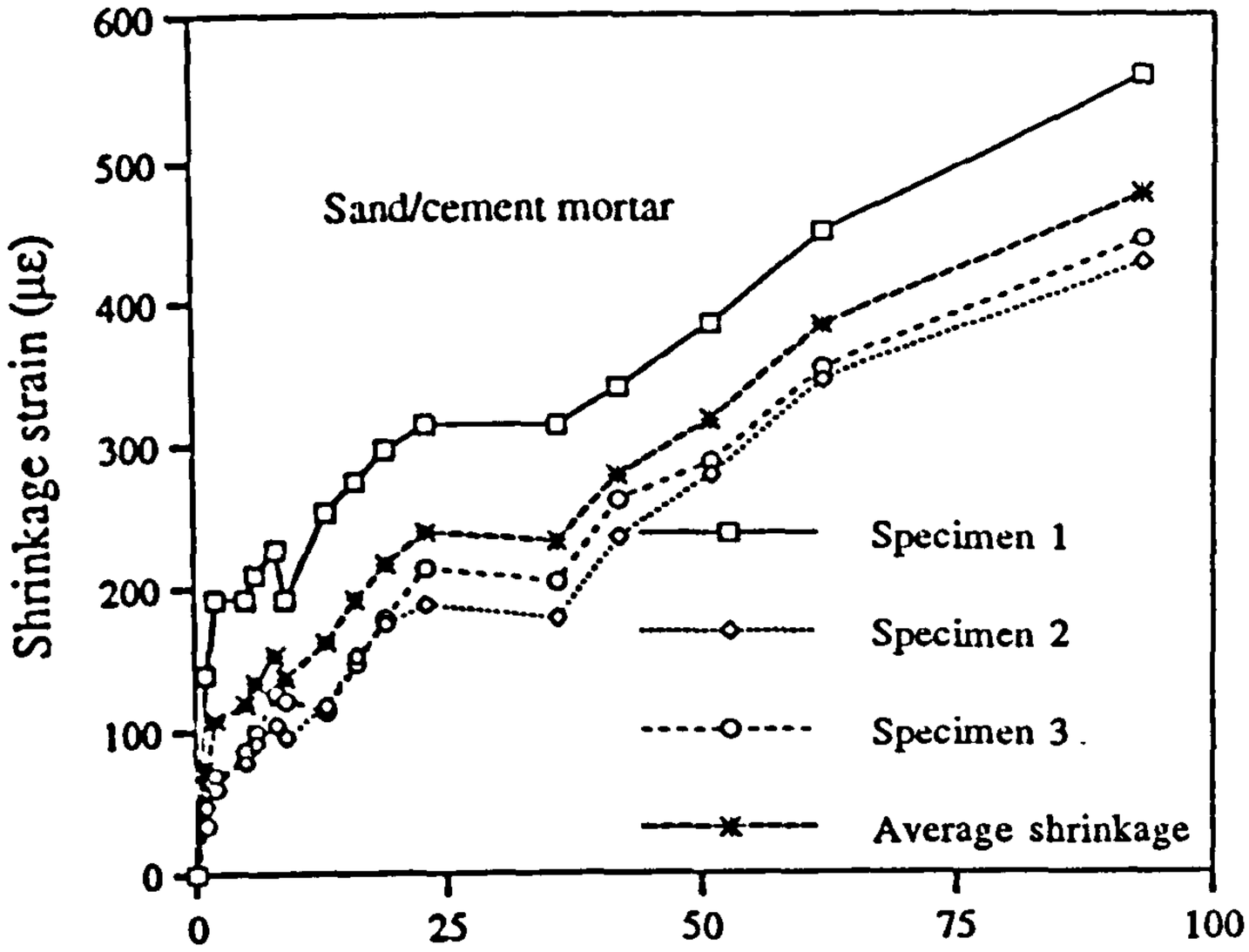

a)

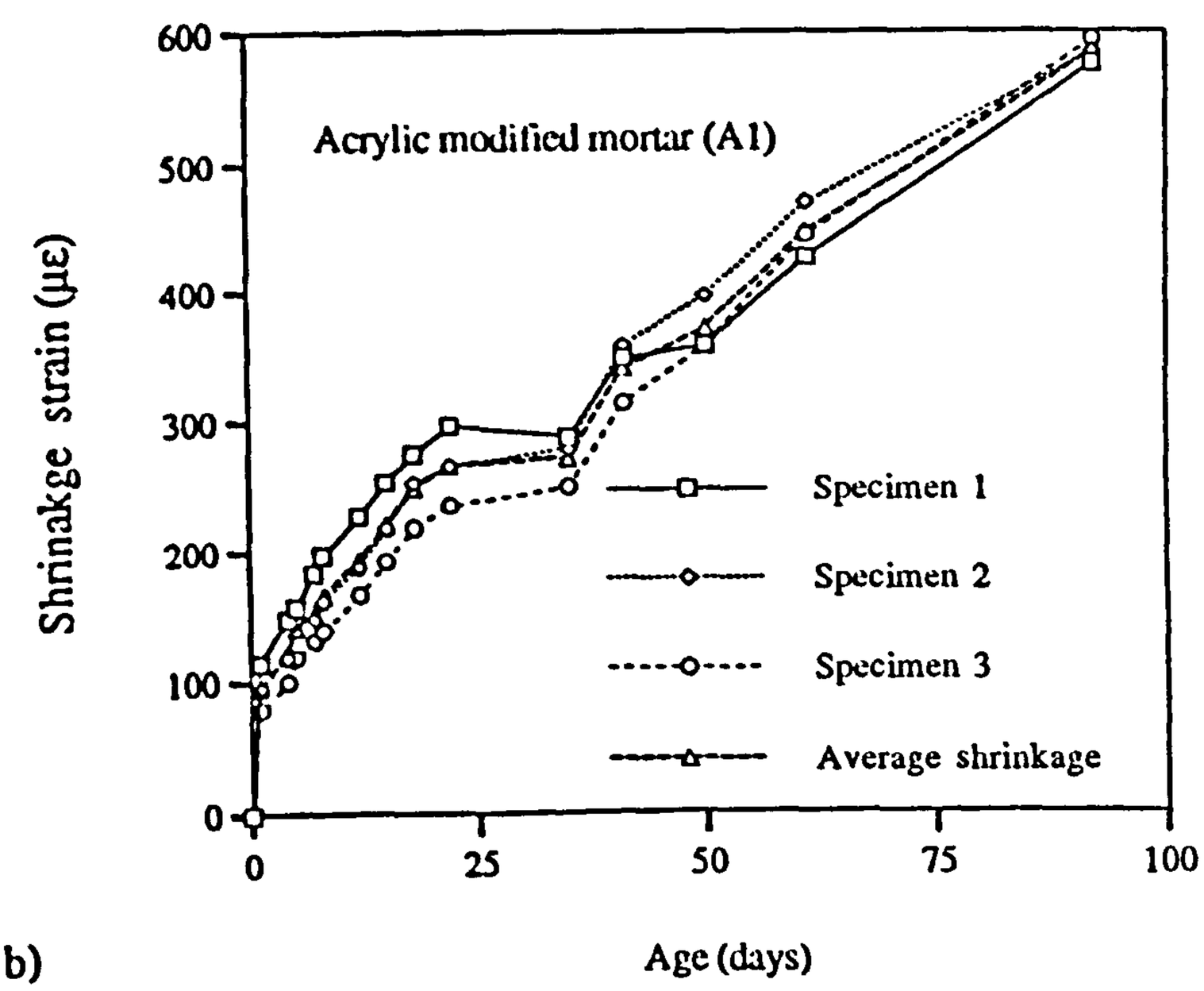

b)

Figure 7.10 Shrinkage measurement of the repair materials

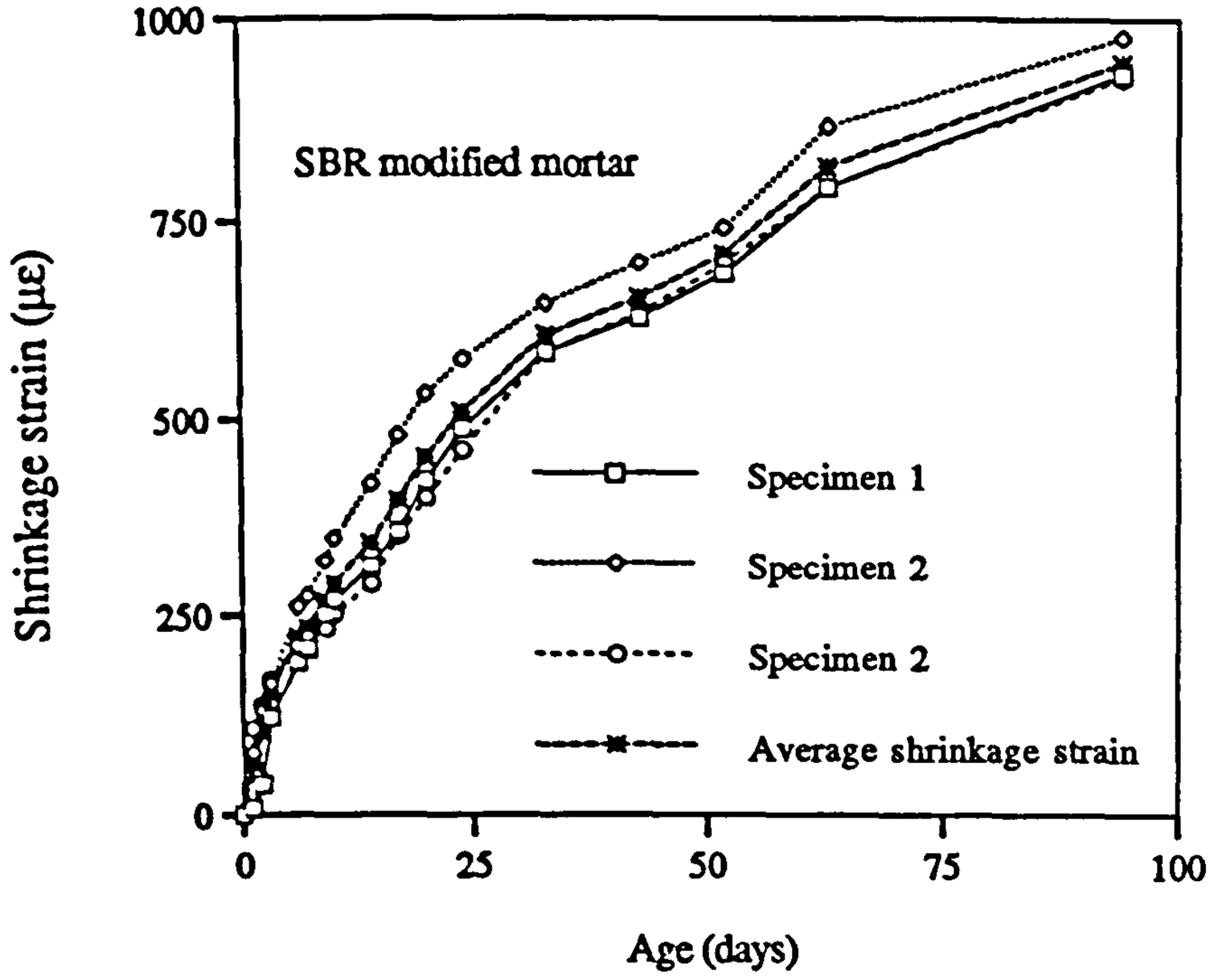

c)

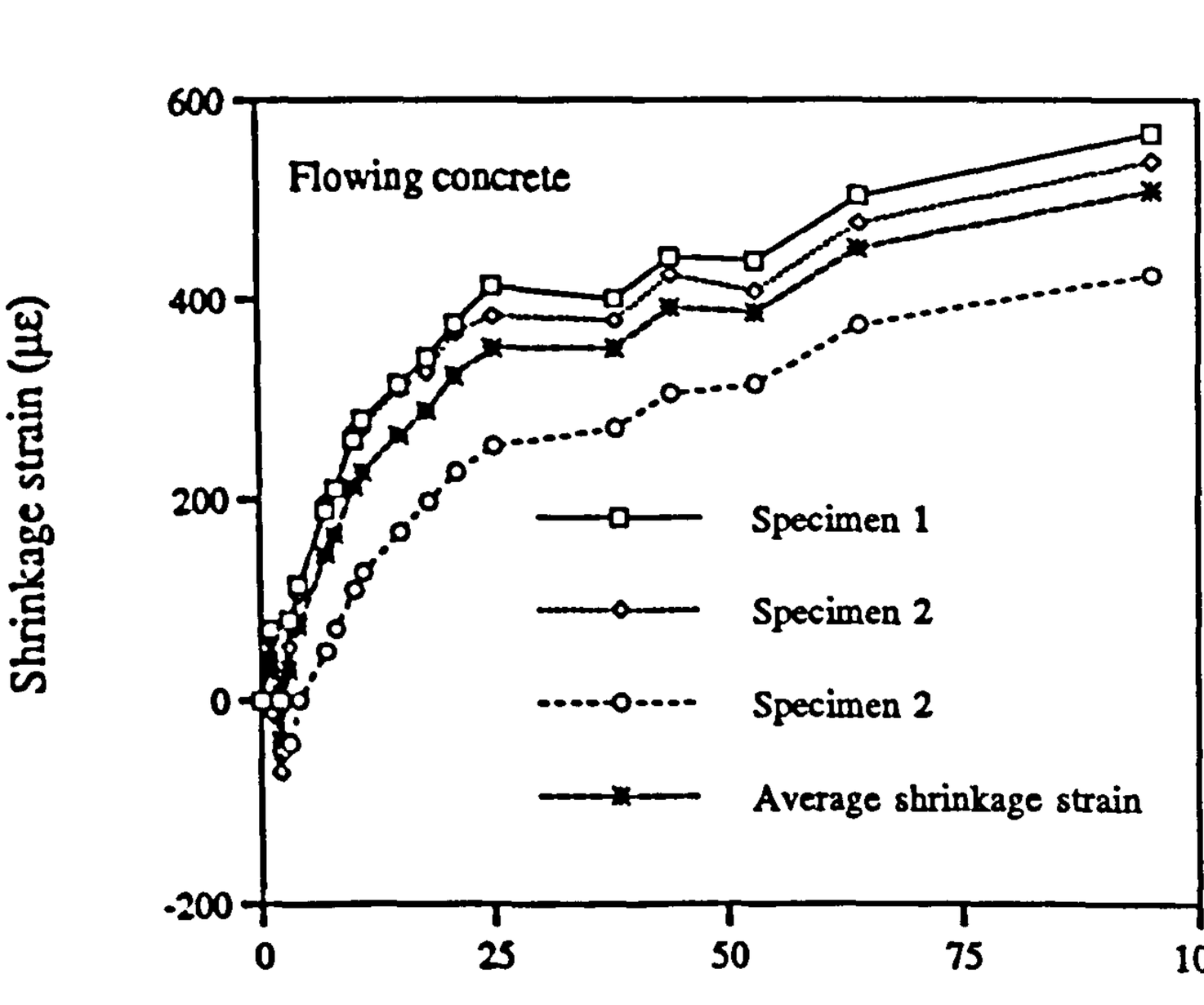

d)

Figure 7.10 Shrinkage measurement of the repair materials

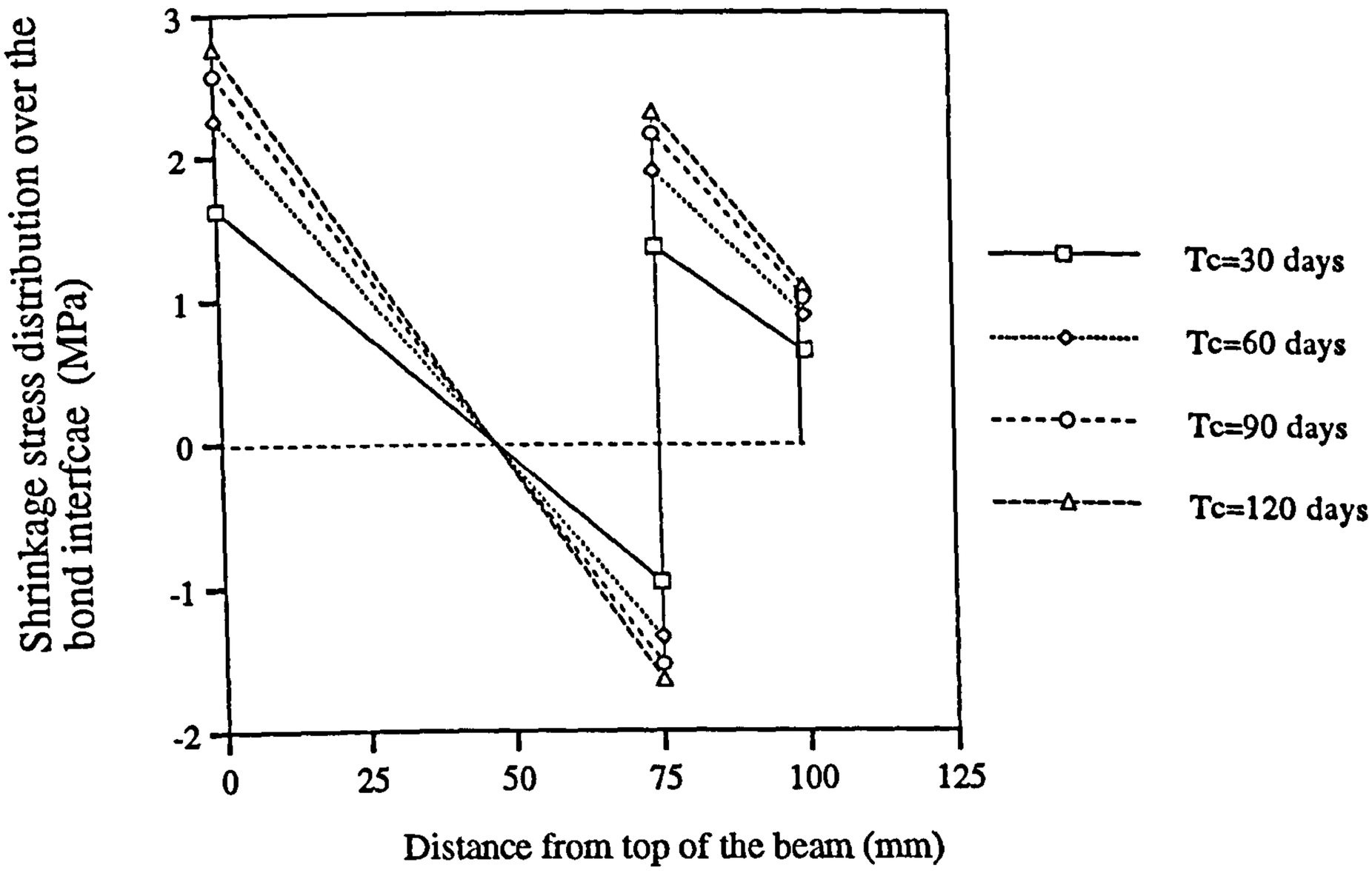

Fig.7.11 Shrinkage stress distribution in a patch flexural specimen due to differential shrinkage

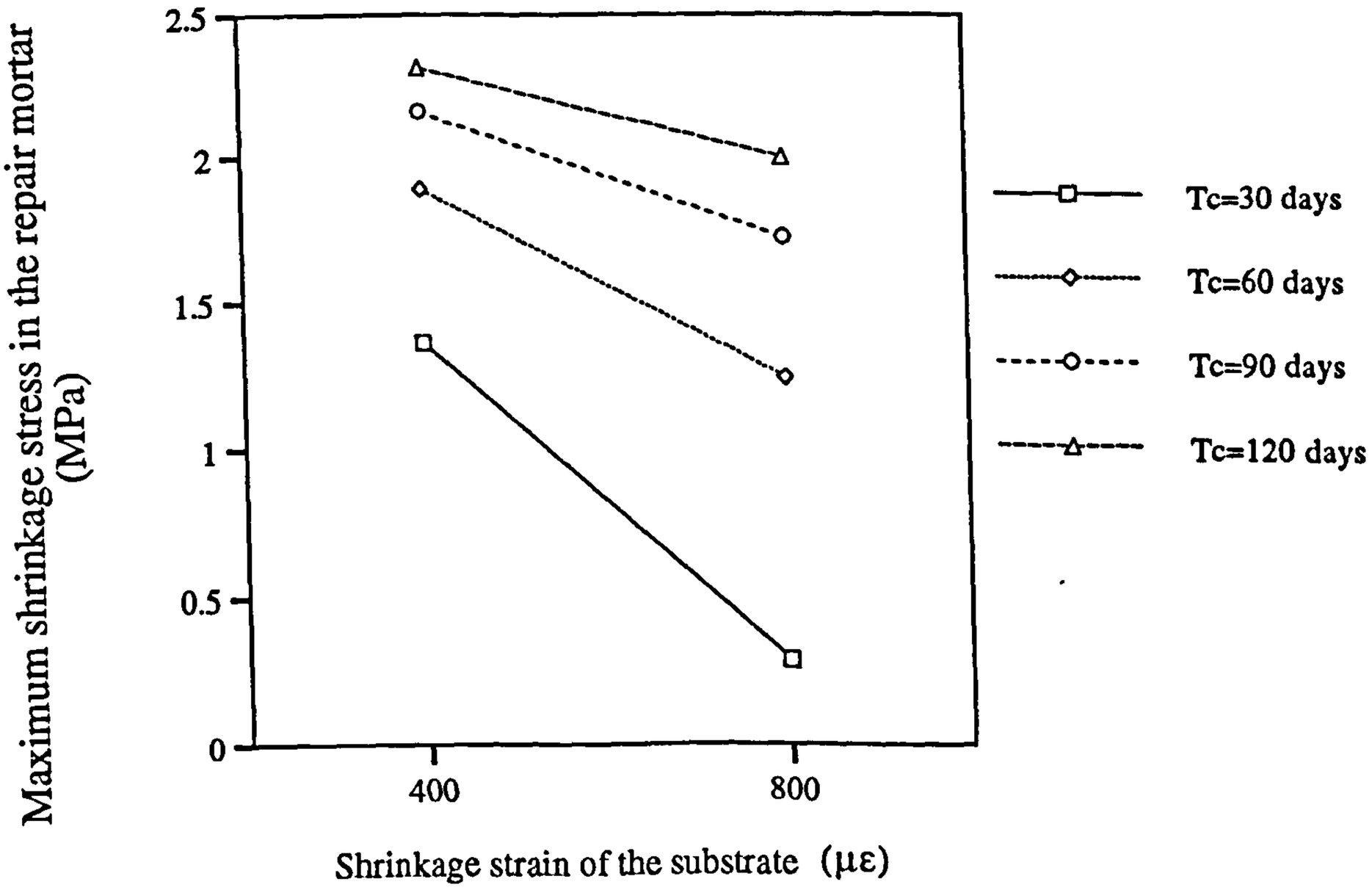

Fig.7.12 Effect of shrinkage of the substrate on the maximum shrinkage stress in the repair mortar

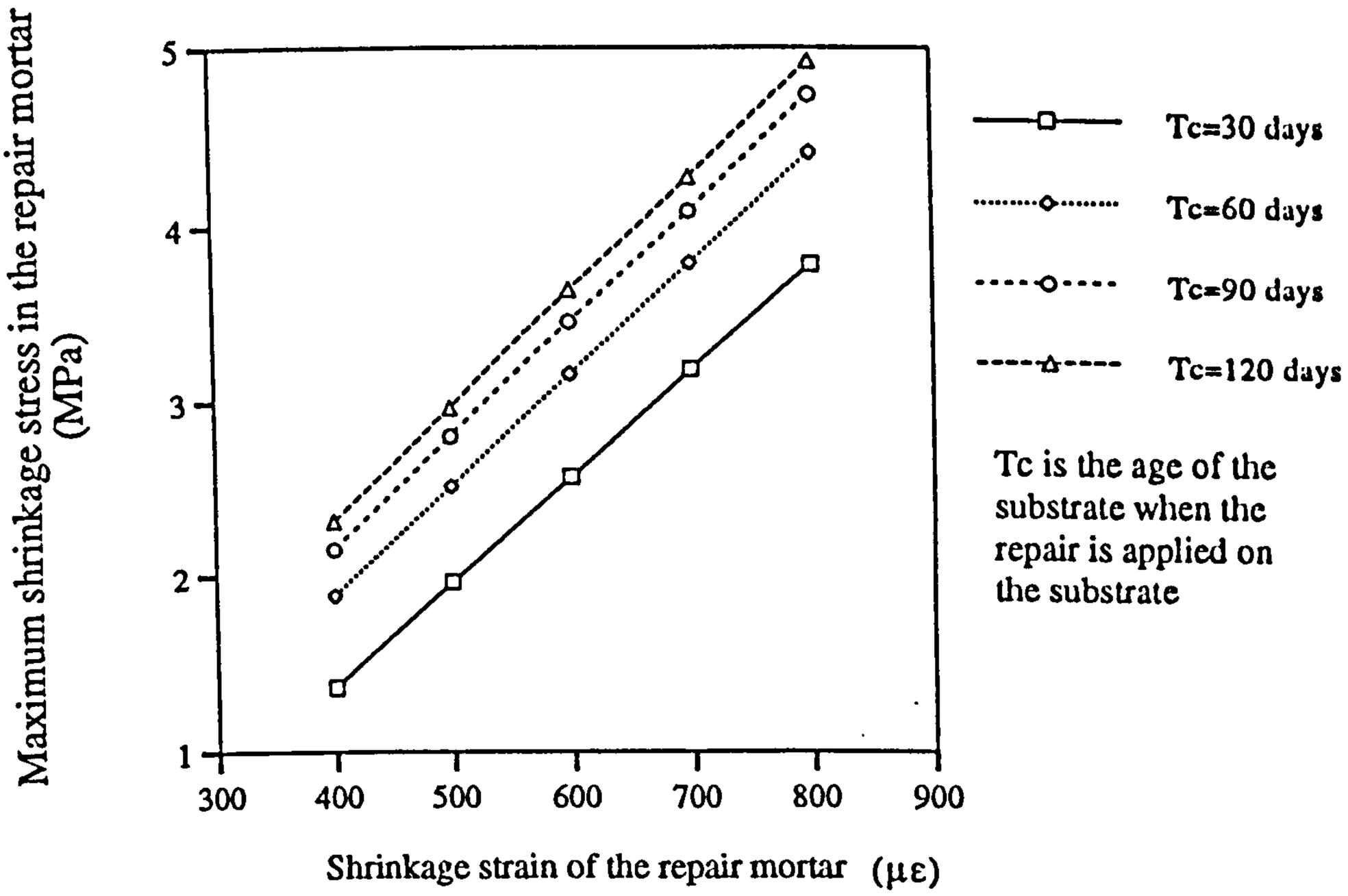

Fig.7.13 Effect of shrinkage of the repair mortar on the maximum shrinkage stress in the repair mortar

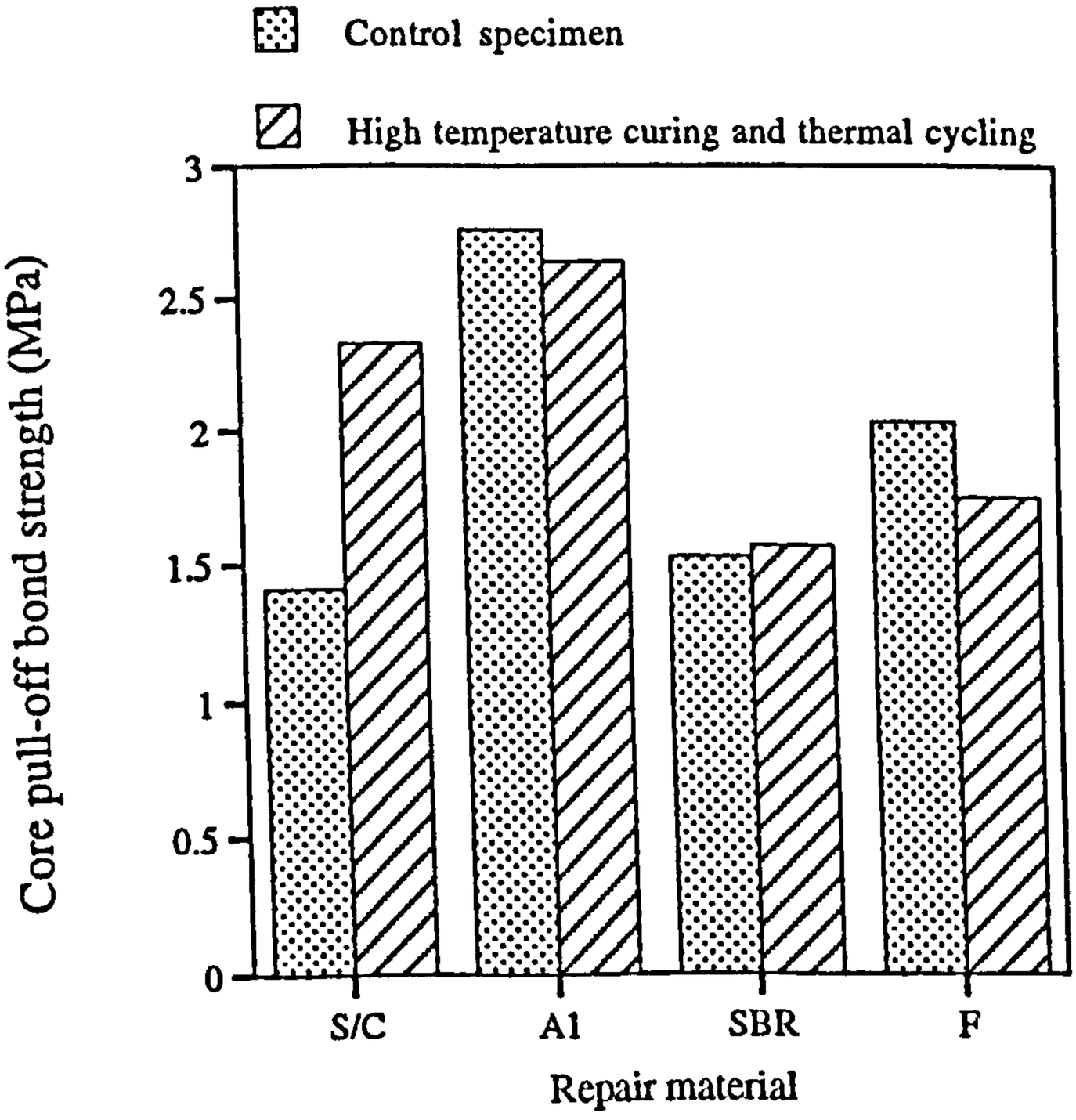

Fig.7.14 Effect of high temperature curing and thermal cycling on the core pull-off bond strength

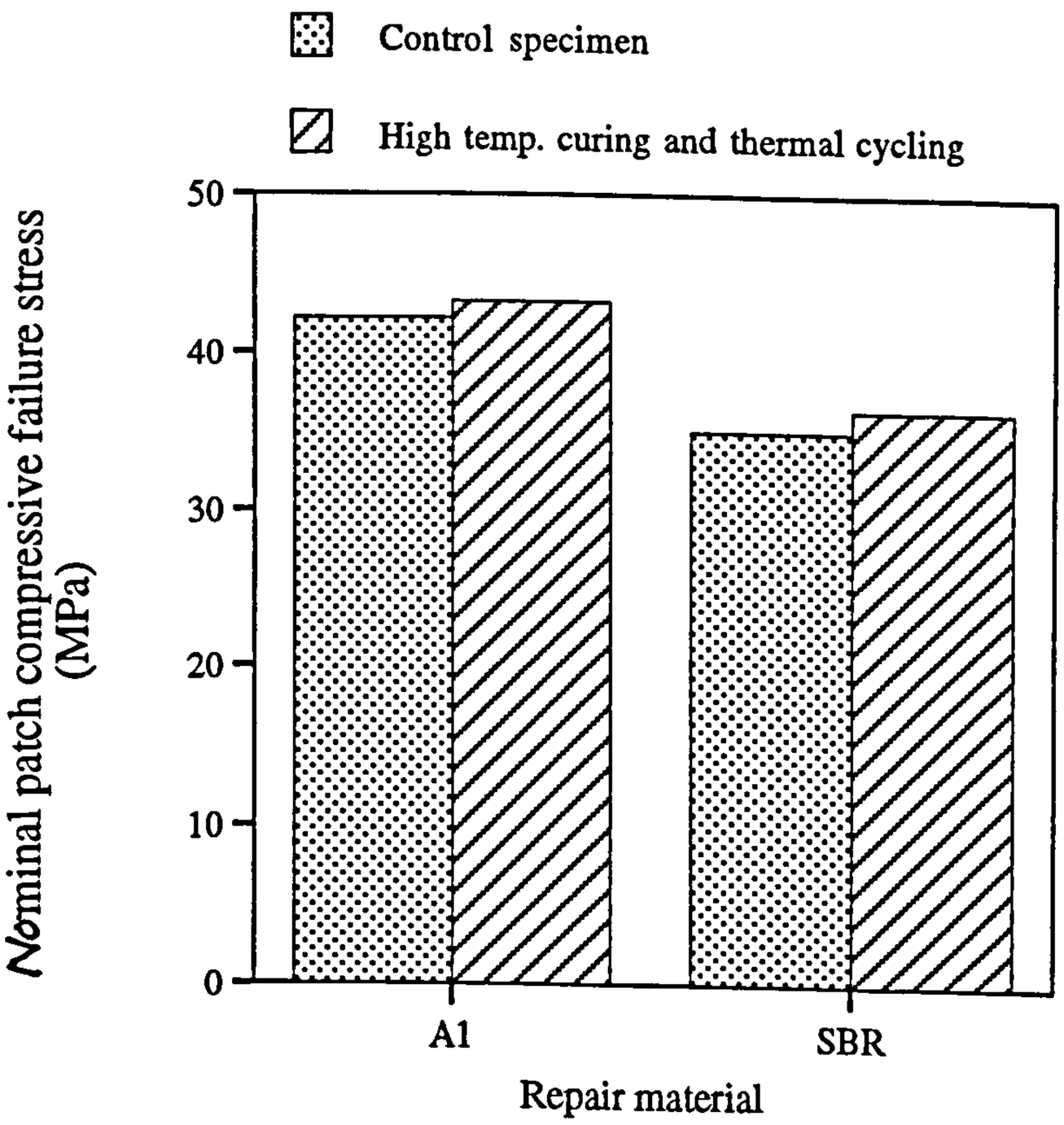

Fig.7.15 Effect of high temperature curing and thermal cycling on the nominal patch compressive failure stress

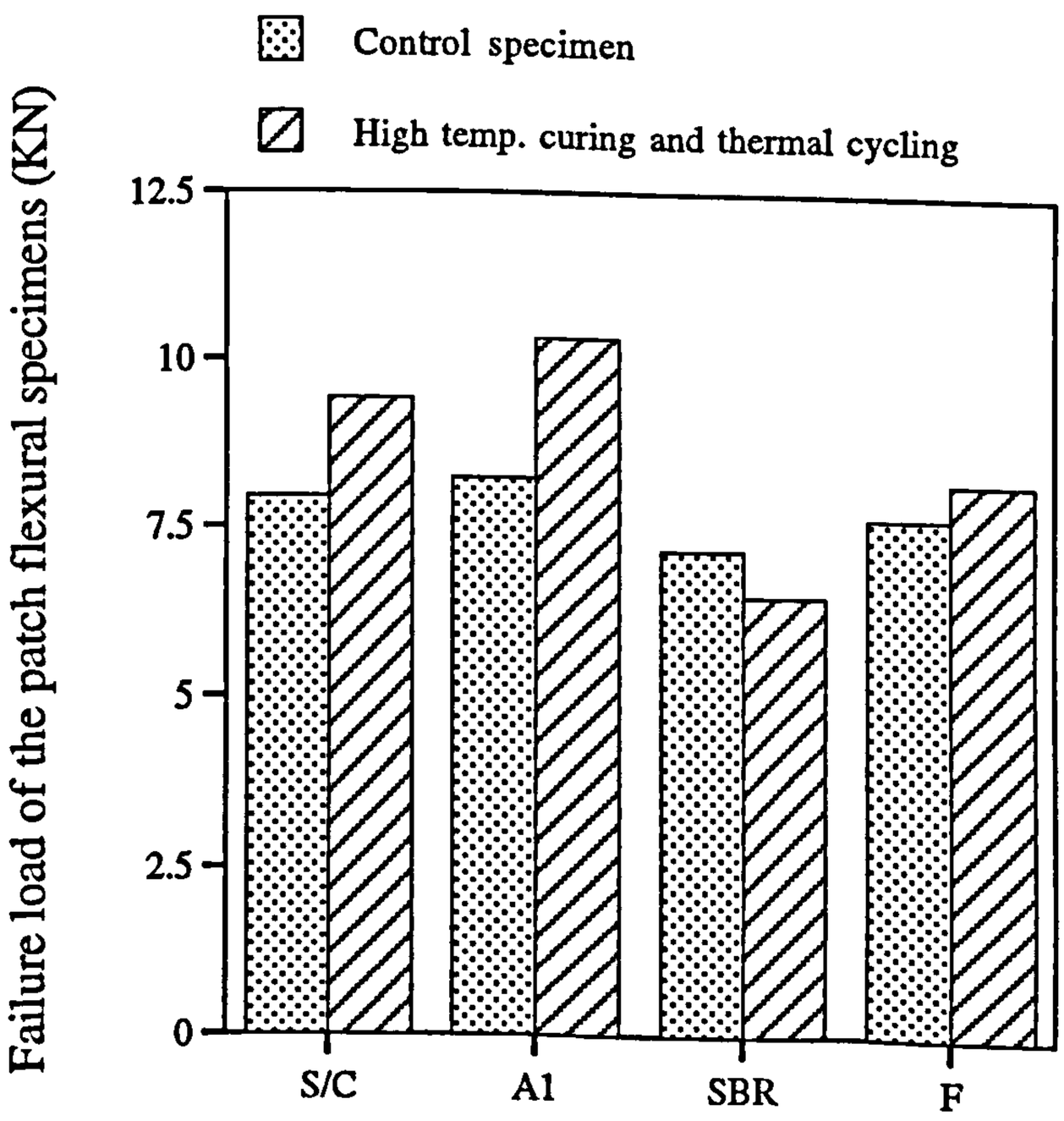

Fig.7.16 Effect of high temperature curing and thermal cycling on the failure load of patch flexural specimens

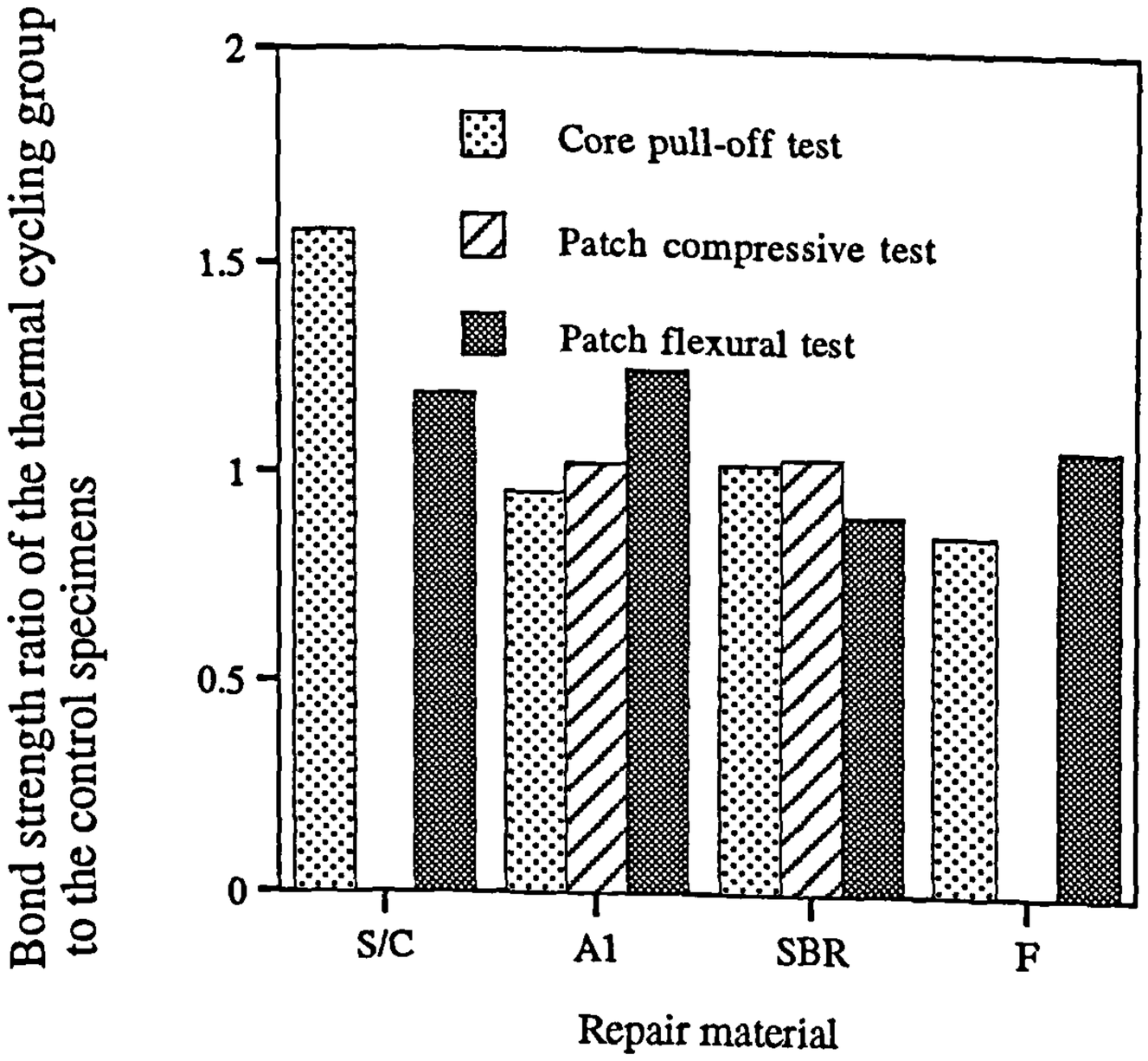

Fig.7.17 Bond strength ratio of the thermal cycling group to the control specimens with different test methods

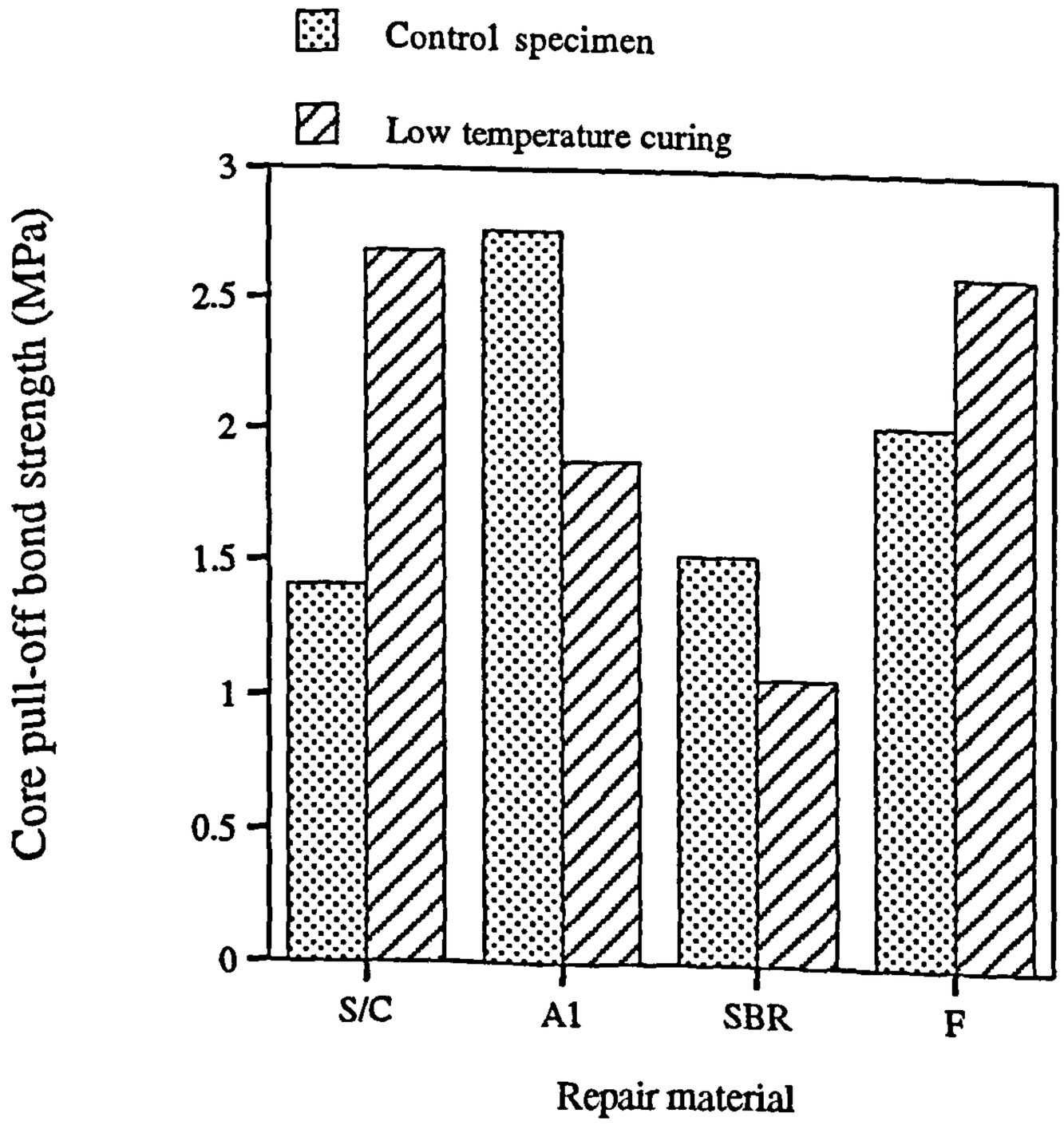

Fig.7.18 Effect of low temperature curing on the core pull-off bond strength

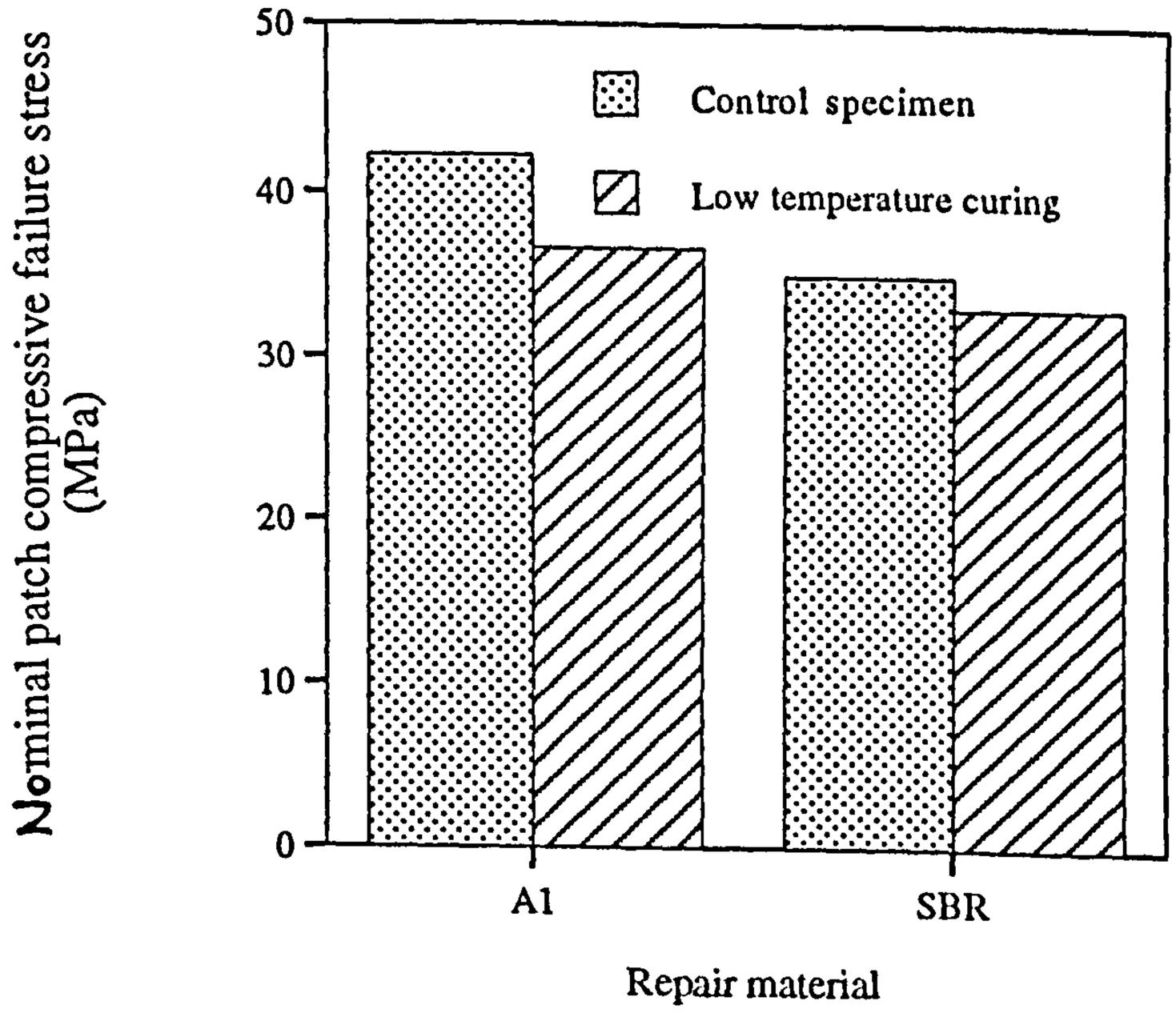

Fig.7.19 Effect of low temperature curing on the patch compressive bond strength

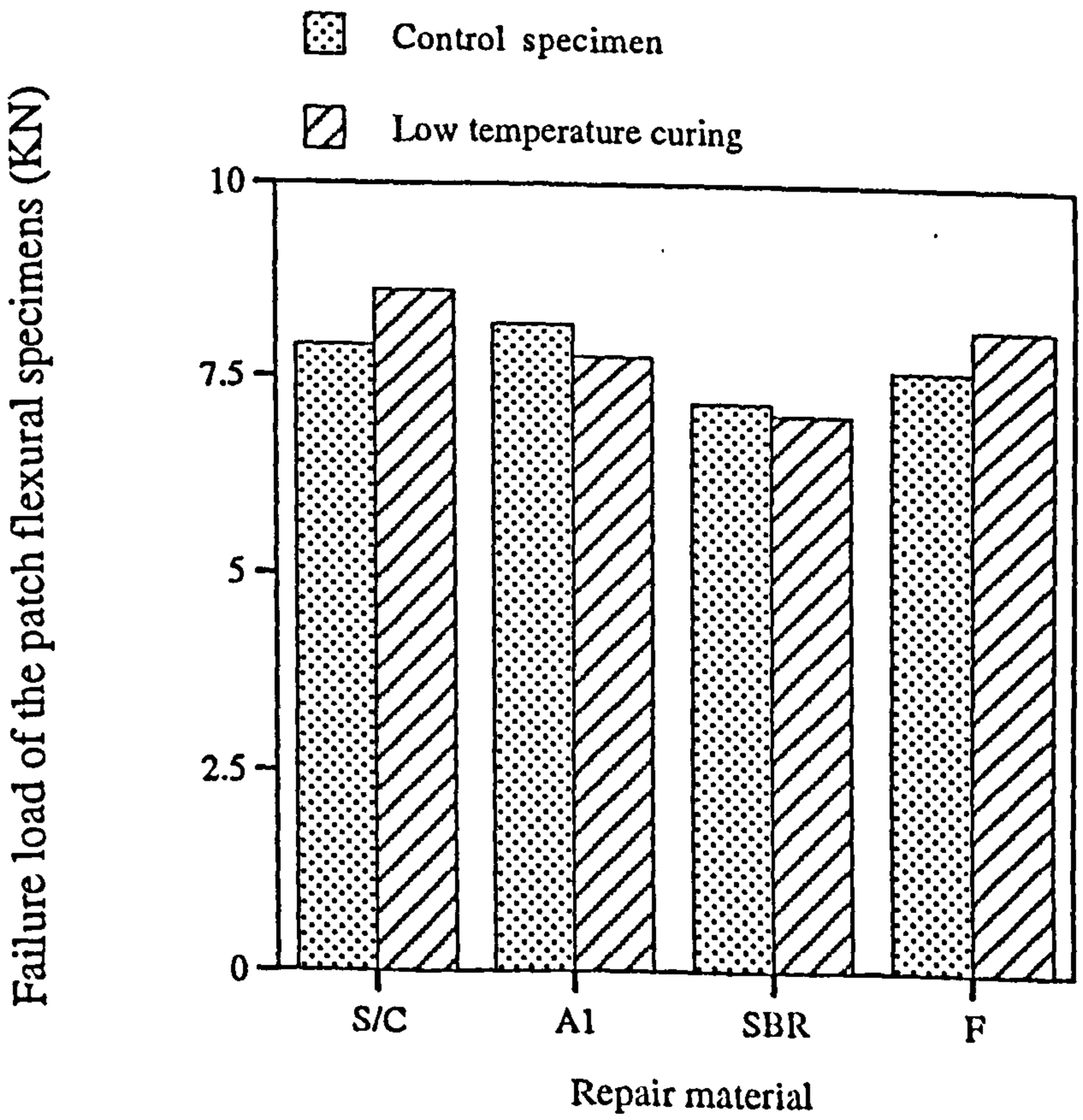

Fig.7.20 Effect of low temperature curing on failure load of the patch flexural specimens

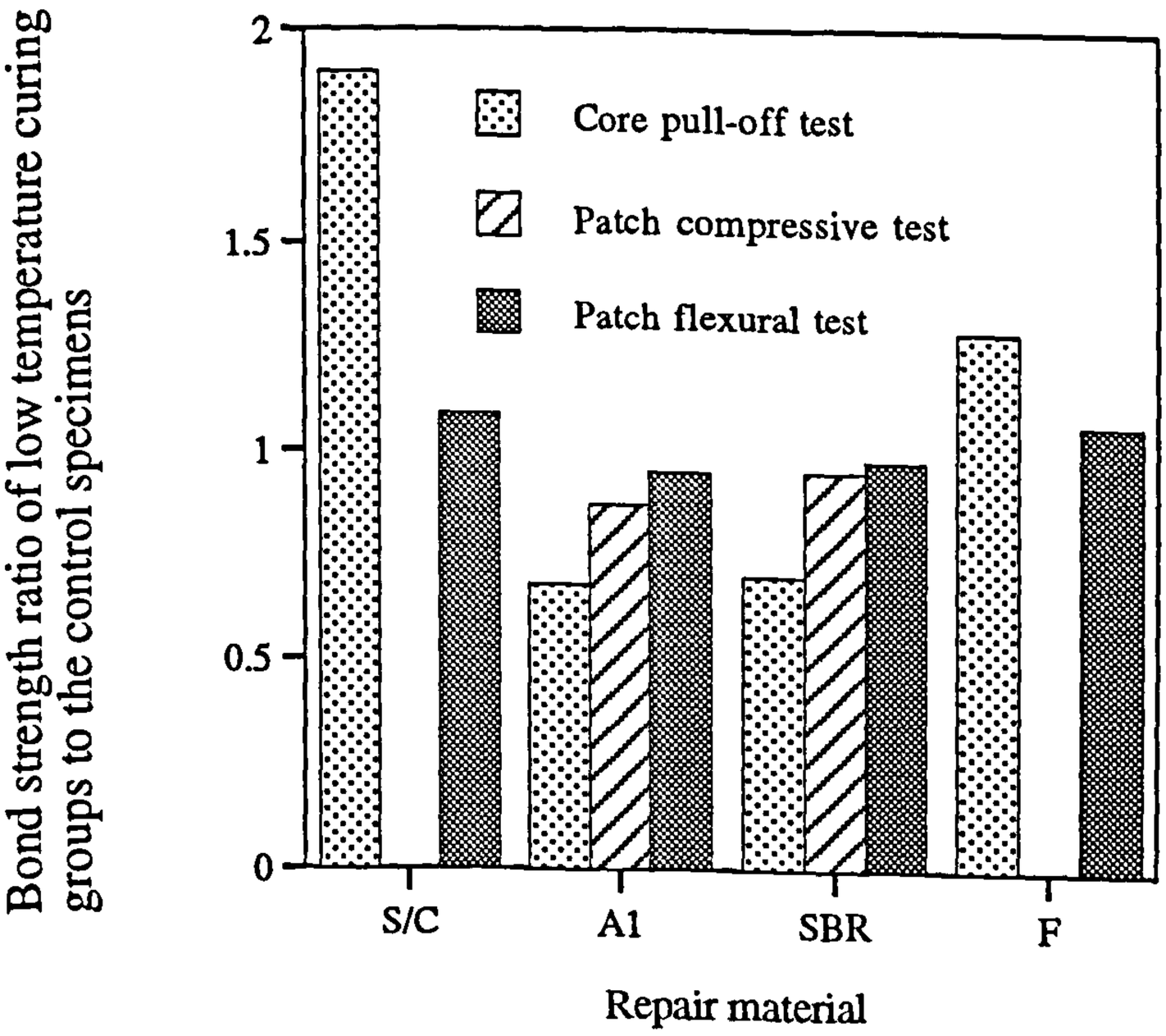

Fig.7.21 Variation in bond strength due to low temperature curing with test methods

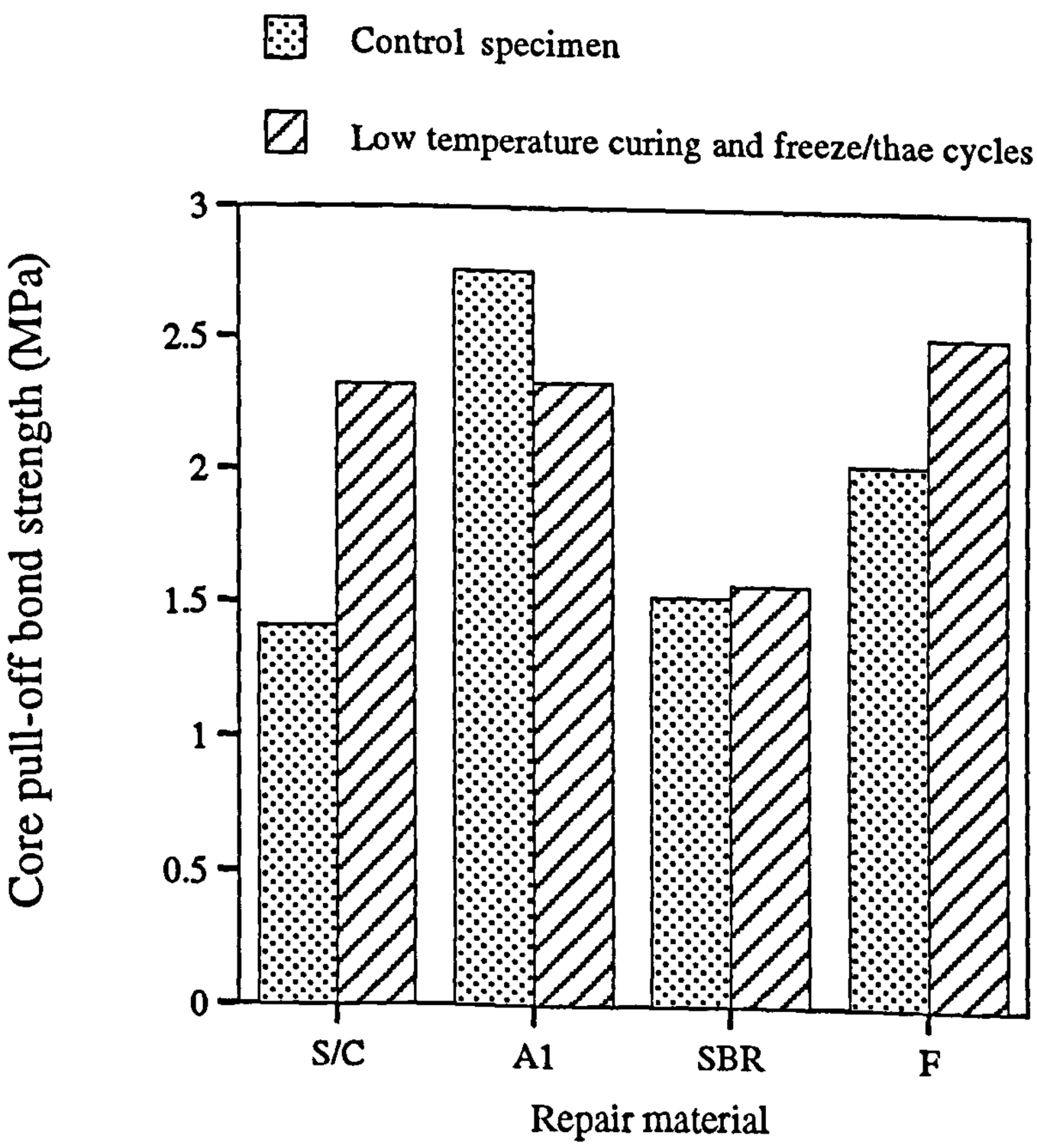

Fig.7.22 Effect of low temperature curing and freeze/thaw cycles on the core pull-off bond strength

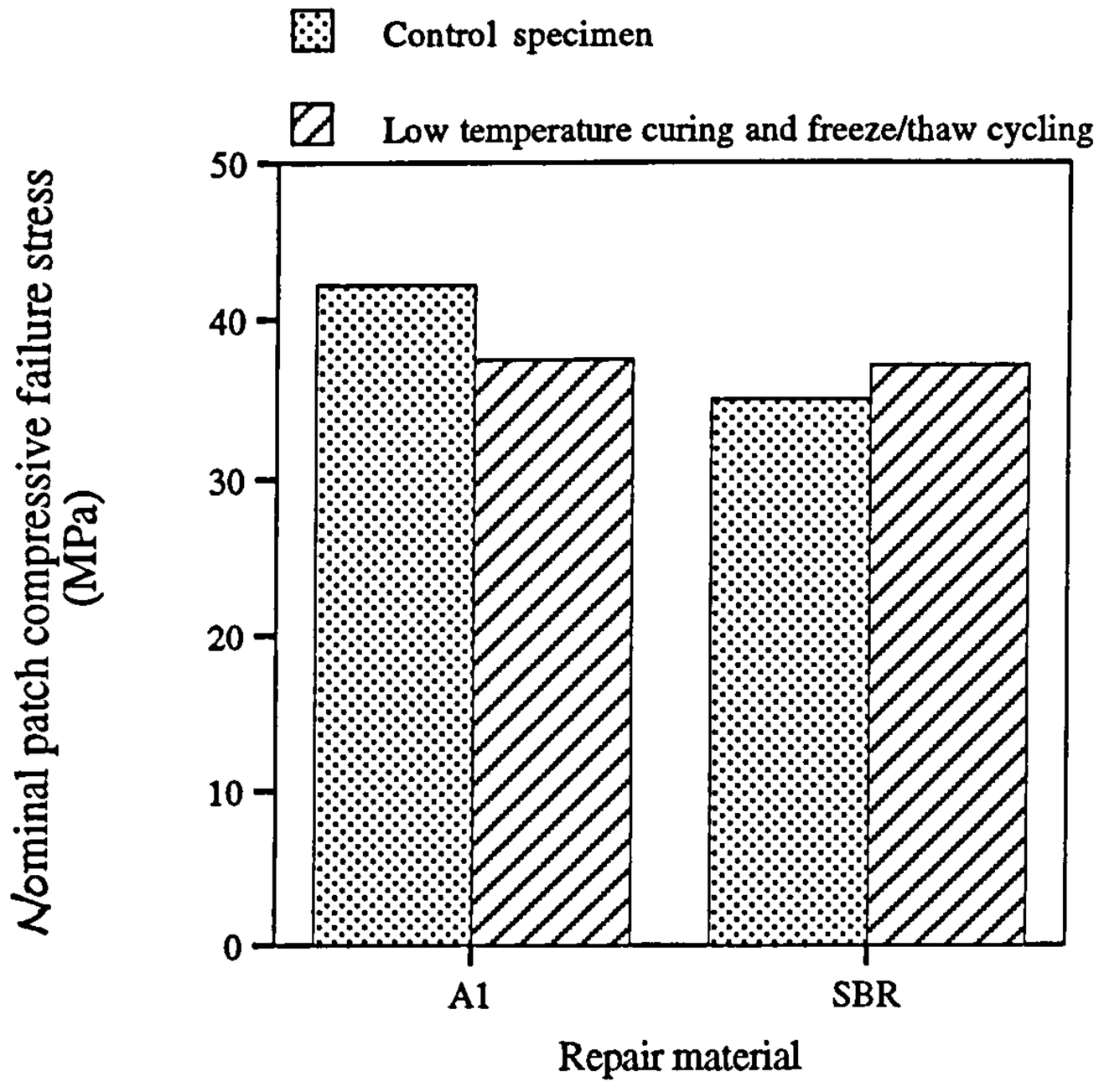

Fig.7.23 Effect of low temperature curing and freeze/thaw cycling on the nomainal patch compressive failure stress

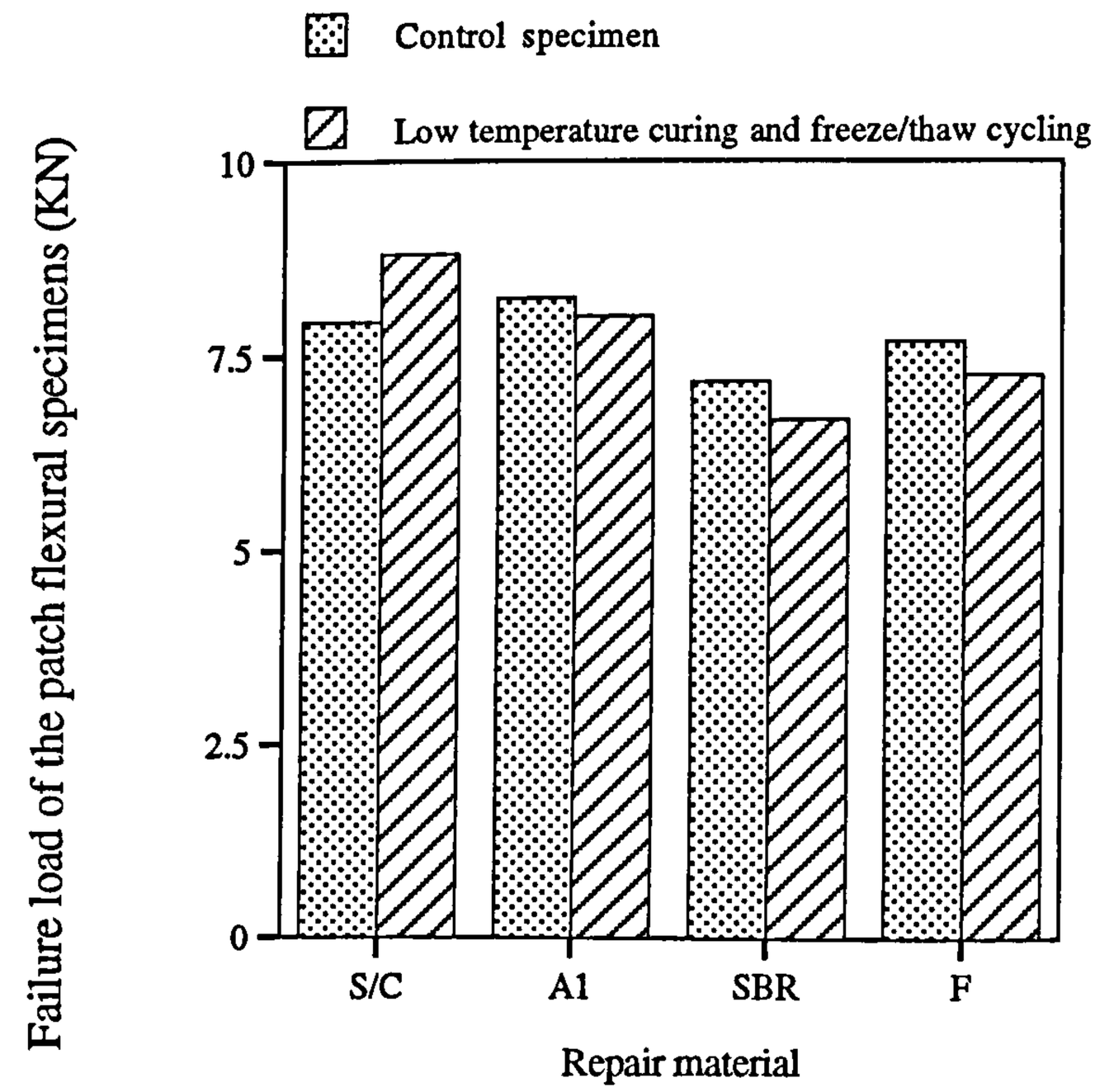

Fig.7.24 Effect of low temperature curing and freeze/thaw cycling on failure load of the patch flexural specimens

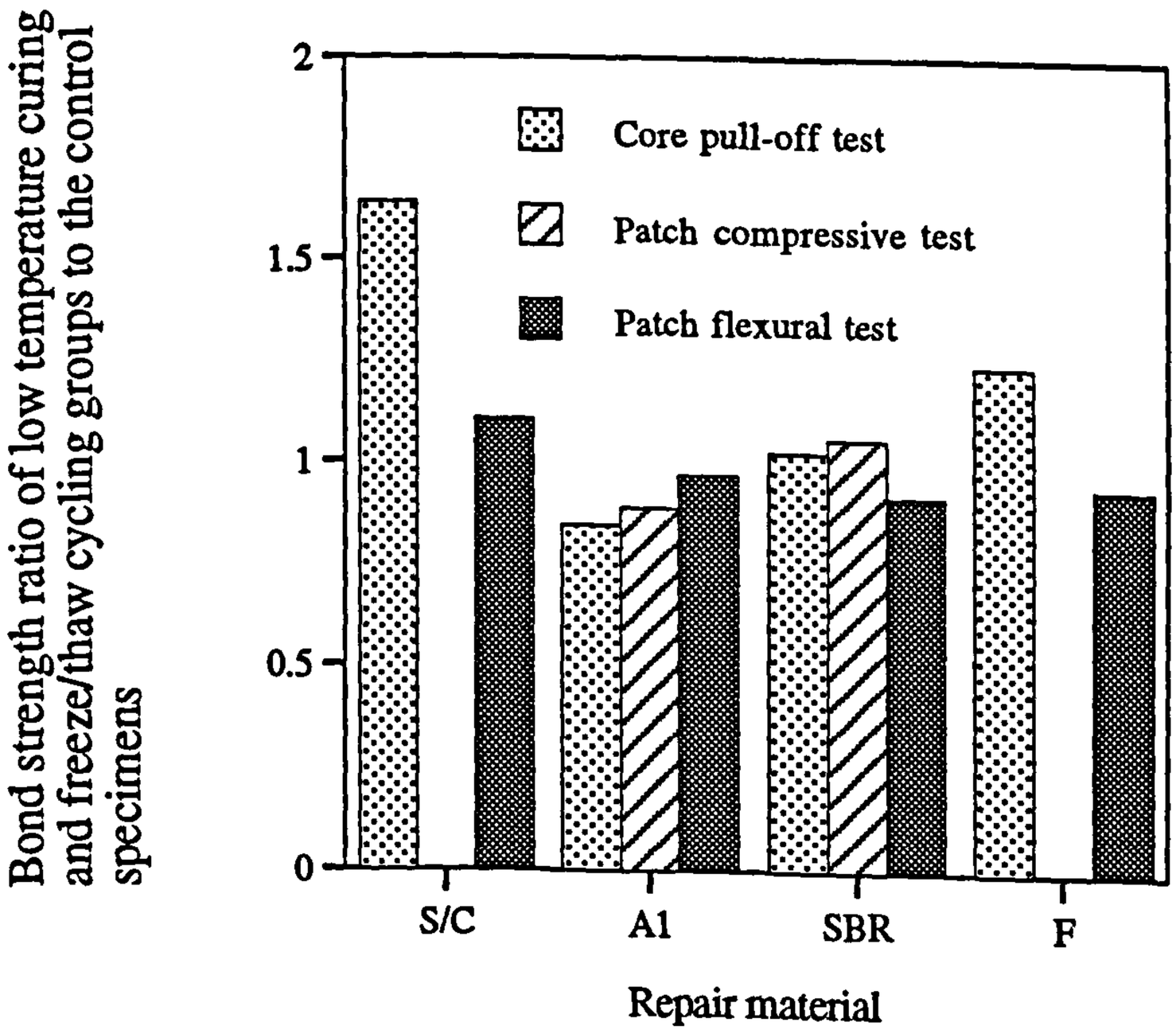

Fig.7.25 Effect of low temperature curing and freeze/thaw cycling on bond strength with each bond test method

Chapter 8

CONCLUSIONS AND SUGGESTIONS FOR FUTURE WORK

Chapter 8 Conclusions and suggestions for future work

8.1 Conclusions

This project was proceeded by some initial bond tests and followed by fully planned test programme which can be divided into three parts: evaluation of bond test methods, effect of workmanship on bond strength, and effect of environmental conditions on bond strength. In total about 800 tests have been conducted. Considering the fact that there are many factors influencing the quality of repair and no single project can cover all these parameters in detail, test results obtained by other researchers have also been used to confirm or validate the author's point of view and predictions.

Bond test methods

- There are many factors influencing measured bond strength, different test method will respond differently to those factors involved. To monitor the quality of a repair, a test method should be able to reflect the variations of crucial factors involved.
- Tensile tests are sensitive to surface defects, such as microcracks. Shear and slant shear tests are not sensitive to surface defects.
- Different test set-ups will usually produce different results. The core pull-off test has the advantage that it can be used to compare directly the quality of site-repairs and lab-repairs.
- Modulus mismatch affects the stress distribution over the bond interface, and stress concentration can be generated at the edge of bond interface. With the core pull-off test, the effect of modulus mismatch can be ignored in the interpretation of test results. Apart from stress concentration, modulus mismatch can also induce

eccentricity in a slant shear test. In the patch compressive and patch flexural tests, modulus mismatch affects how much load will be transferred from the substrate to the repair material. A low modulus repair material will share lower load.

- Variation in specimen size affects the reproducibility of test results. In a core pull-off test, it is reflected in the inclination of the core and the coring depth into the substrate. A shallow coring depth of less than 5 mm will underestimate the tensile bond strength. A coring depth of 15 mm is recommended.
- In the slant shear test, the bond direction may vary slightly depending on method used to produce the substrate. The effect of the variation of bond direction is coupled with surface roughness. If the actual bond angle diverts obviously from the critical bond direction, high variation in failure load can be expected.
- Patch tests put a repair material into a more realistic indirect stress transferring condition, but care should be taken to avoid misinterpretation of test results. A lab-repair is usually carried out to study under what situations a repair will fail, but in site-repairs, or real-repairs, all those detrimental effects should be avoided by selecting another geometry of cut-out or choosing another type of repair material.

Effect of workmanship on bond strength

- Workmanship covers many aspects, such as surface preparation, moisture condition, and curing method. To achieve a good repair every aspect has to be addressed properly.
- A rougher surface produces a higher bond strength, but the increase depends on each individual repair material. Sand/cement mortar favours a rough surface under different stress state. Polymer modified mortars are not very sensitive to surface roughness because a bond coat tends to decrease this effect.

- Bond strength depends on stress state imposed. Under a tensile stress state the surface soundness is the most important issue as surface defects will result in stress concentration which may cause premature bond failure.
- Under shear/compression stress state, the surface roughness can contribute significantly to resist bond failure. Further increase in failure load can be achieved by selecting a bond plane with a high normal/shear stress ratio.
- The effect of moisture condition at the surface layer and inside the substrate can be different. The acrylic modified cementitious mortar was the least affected with tensile bond strength varying from 2.61 to 2.85 MPa for all moisture conditions studied. The flowing concrete favours both surface dry and inside dry. Saturated and surface wet condition should be avoided.
- Bond coat improves the contact between a repair mortar and substrate. The optimum condition for a bond coat to receive a repair material varies, but a tacky condition will produce a good, though may not be the best, bond.
- Either bond coat or mortar mistiming affect the contact between the mortar and the bond coat or the substrate, which will leave some defects at the bond interface. Preventing moisture loss can partly decrease the detrimental effect of mistiming. A repair mortar should not be mixed until a few minutes before the bond coat becomes tacky, and then applied immediately after mixing.
- The requirement for a most efficient curing depends on how bond strength is gained. Bond strength developed through cement hydration favours a wet curing environment, but bond strength developed partly through formation of polymer films may prefer a slightly drier environment. Among four repair materials tested, the sand/cement mortar, flowing concrete, and the SBR modified mortar produced higher bond strength under high relative humidity environment, but the acrylic modified mortar favours a relative humidity around 70%. In view of the nature of patch repairs, covering the repair area tightly with polythene sheet is a good and practical way of curing.

Effect of environmental conditions on bond strength

- For the sand/cement mortar repaired specimens, results with all three test methods showed different degrees of increase in the bond strengths for the environmental conditions considered. The increase under different environmental conditions with the core pull-off test followed the order from high to low of: low temperature curing, low temperature curing followed by freeze/thaw cycling, high temperature curing followed by thermal cycling, and high temperature curing and drying shrinkage. The increase with the patch flexural test followed the order of the high temperature curing followed by thermal cycling, low temperature curing followed by freeze/thaw cycling, low temperature curing, and high temperature curing and drying shrinkage. The low increase with the patch flexural test suggests that in a real repair, the effect of variation in bond strength on load carrying capacity of a repaired specimen has to be considered in the light of the loading condition and geometry of cut-out. For the design or evaluation purpose, it can be assumed that the environmental condition considered had no detrimental effect on the sand/cement mortar repaired specimens.
- The acrylic modified mortar is a very good repair material with high bond strengths measured with the core pull-off test (very near the material strength), patch compressive test and patch flexural test. It can be seen that any significant increase in bond strength is difficult to measure, although high temperature curing did show an increase in bond strength. Results from the thermal cycling group showed a mixed trend, but the reduction in bond strength with the core pull-off test was very small and can be neglected. This suggests that the thermal cycling had no detrimental effect on the acrylic modified mortar. Results from both the low temperature curing and low temperature curing followed by freeze/thaw cycling showed decreases in bond strengths, with smaller effect from the second group. This suggests that initial low temperature curing is very detrimental to the polymer

system used. Either avoiding casting at winter seasons or protecting the repair from low temperature is recommended.

- The bond strengths of the SBR modified mortar are similar to plain sand/cement mortar under normal conditions. In a high temperature curing environment, the SBR modified mortar showed quite substantial increase in bond strength, but because of high shrinkage of the mortar, the contribution of high temperature curing to bond strength was impaired by thermal cycling. In low temperature curing environment, these strengths were seriously affected, which may be explained by the fact that the polymers were seriously affected. Similar detrimental effect of initial low temperature curing was observed with acrylic modified mortar. Thus, the same recommendation for the acrylic modified mortar is also suggested, i.e., low temperature curing should be avoided.
- For the flowing concrete, results from both the high temperature curing, and low temperature curing showed increases in bond strength, but tests with the thermal cycling group and the freeze/thaw cycling group showed some mixed trend. This may be related to thermal stresses generated due to differential deformation. Another factor which may influence the interpretation of test results is that the flowing concrete is not recommended for shallow patch repair. Some segregation of aggregates was observed in the slant shear test.

The study into the effects of environmental conditions was initial in scope, in that only one variable was studied in each condition. Results with all three test methods have demonstrated that they are able to show the effect of environmental conditions on a repair system. One important aspect in carrying out environmental testing is to eliminate other factors' influence by controlling the consistence of the workmanship involved. The study highlighted the importance of protecting polymer modified cementitious materials from low temperature curing.

8.2 Suggestions for future work

In chapters 5 to 7, evaluation of bond test methods, effect of workmanship on bond strength, effect of environmental conditions on bond strength have been presented. Because of the limitations on resources and time, the study of the effect of environmental conditions was limited to only one parameter in each group. This study has generated some useful information on repair materials under different environmental conditions. But an in-depth study needs to compare between one same parameter but at different levels. Other factors restraining the theoretical analysis are the material properties. Based on the work carried out in this project and similar work at other research institutions, the following work are considered needing further research.

Material properties

Properties such as long-term shrinkage measurement and creep behaviour of polymer modified cementitious repair materials have not been measured or reported frequently. Lack of this knowledge will lead people casting some doubt on long term performance and structural evaluation.

Workmanship effect

The application of polymer modified bond coat targeted at normal sand/cement mortar and concrete should be studied. Some encouraging results have been obtained using polymer modified bond coat with normal sand/cement mortar. If long term performance can be guaranteed, this can reduce cost for construction industry significantly.

Environmental conditions

Bond performance at different levels of high temperature and thermal cycling, and bond performance at different levels of low temperature and freeze/thaw cycling need to be studied. Polymers are sensitive to variations in temperature, and the possibility

that a repair being carried out in extreme climate needs to be studied. Also the performance corresponding to different cycling numbers will enable the designer or researcher to know how bond strength is affected.

Reference

1 Noel P. Mailvaganam, Repair and Protection of Concrete Structures, CRC Press, Inc. Florida 1992

2 P. R. Ainsworth, S. T. Chan, and A. S. Read, The Development of a Classification and Quality Control System for Concrete Repair Mortars, Proceedings of the Second International RILEM/CEB Symposium on Quality Control of Concrete Structures, Ghent, 12-14 June, 1991, Editor: L. Tacrwe and H. Lambotte, pp. 313-324

3 Wallace W. Sanders, Bridge repair and Rehabilitation, North American Codes of Practice, Proceedings of the Fifth International Conference on Structural Faults and repair, Edinburgh, 30 June - 2 July, 1993, Vol. 1 pp.9-12

4 Luis Calvo and Martin Mayers, Overlay Materials for Bridge Deck, Concrete International, Vol. 13 No. 7 1991 pp.46-47

5 M. K. Emberson and G. C. Mays, Significance of Property Mismatch in the Patch Repair of Structural Concrete, Part 1: Properties of Repair Systems, Magazine of Concrete Research, Vol.42 No.152, September 1990 pp.147-160

6 B. Staynes and T. Willway, The Composite Behaviour and Delamination of Thin Surface Overlays and repairs - Identification and Measurement of Controlling Parameters, Proceedings of the 5th International Congress on Polymers in Concrete, Brighton, England, 22-24 September, 1987 Ed. Barry W. Staynes pp.301-304

7 J. D. N. Shaw, Concrete Decay: Causes and Remedies, Construction Repair, Jan/Feb. 1993 Vol.7 No.1 pp. 24 - 33

8 R. T. L. Allen, S. C. Edwards, and J D N Shaw, The Repair of Concrete Structures, Glasgow Blackie Academic and Professional, 1993

9 Philip H. Perkins, Repair, Protection and Waterproofing of Concrete Structures, Elsevier Applied Science Publishers, London 1986

10 Concrete Society Technical report No.26, Repair of Concrete Damaged by Reinforcement Corrosion, Report of a Working Party, Oct. 1984

11 Concrete Society Technical Report No.38, Specification for the Patch Repair of Reinforced Concrete, 1991

12 A. F. Baker, Structural Investigations, Durability of Concrete Structures, Investigation, Repair, Protection, Ed. G. Mays, E&FN SPON 1992, pp.37-81

13 L. Knab, and C. B. Spring, Evaluation of test Methods for Measuring the Bond Strength of Portland Cement Based Repair Material to Concrete, Cement, Concrete and Aggregate, Vol. 11 No.1 Summer 1989 pp.3-14

14 Y Ohama, K. Demura, H Nagao, and T Ogi, Adhesion of Polymer-Modified Mortars to Ordinary Cement Mortar by Different Test Methods, Proceeding, RILEM Symposium on Adhesion Between Polymers and Concrete, (Aix-en-Provence, September 1986) Chapman and Hall Ltd, London 1986 pp.719-729

15 S. A. Austin and P. J. Robins, SERC Grant Final Report, The Behaviour of Concrete Patch Repairs - An Initial Study, Department of Civil Engineering, Loughborough University of Technology, March 1991

16 S. A. Austin and P. J. Robins, Development of Patch Test to Study Behaviour of Shallow Concrete Patch Repairs, Magazine of Concrete research, Vol.45 No.164 September 1993, pp.221-229

17 Johan Silfwerbrand, Improving Concrete Bond in Repaired Bridge Decks, Concrete International, Vol.12 No.9, September 1990, pp.61-66

18 D J Cleland, M Naderi, and A E Long, Bond Strength of Patch Repair Mortars for Concrete, Proceeding, RILEM Symposium on Adhesion Between Polymers and Concrete, (Aix-en-Provence, September 1986) Chapman and Hall Ltd, London 1986 pp.235-244

19 D. J. Cleland, K. M. Yeoh, and A. E. Long, The Influence of Surface Preparation methods on the Adhesion Strength of Patch repairs for Concrete, Proceedings of 3rd Int Col on Material Science and restoration, Esslingen, Germany, December 1992, Expert Verlag, pp.868-871

20 Kal R. Hindo, In-plane Bond Testing and Surface Preparation of Concrete, Concrete International, Vol.12 No.4 April 1990, pp.46-48

21 Ernest K. Schrader, Mistakes, Misconceptions, and Controversial Issues Concerning Concrete and Concrete Repairs, Concrete International, Vol.14, No.9 pp.52-56, No.10 pp.48-52, No.11 pp.54-59 1992

22 Vipulanandan, C. Paul, Performance of Epoxy and Polymer Concrete, ACI Material Journal, Vol.87, No.3, May-June 1990, pp.241-251

23 R. J. Detwiler, et al, Assessing the Durability of Concrete in Freezing and Thawing, ACI Mater. J., Vol.86 No.1, Jan-Feb 1989, pp.29-35

24 Haque, M. N. and Gopalan, M. K., Temperature and Humidity Effects on the Strength of Plain and Flyash Concrete, Proceedings, Institution of Civil Engineers (London), Vol.83 Part 2, September 1987, pp.649-657

25 Mittelalacher, M, Effect of Hot Weather on the Strength Performance of Set-retarder Field Concrete, Temperature Effects on Concrete, ASTM STP 858, T. R. Naik, Ed., American Society for testing and Materials, Philadelphia, 1985, pp.88-106

26 Nasser, K. W. and Chakraborty, M. Temperature Effects on Strength and Elasticity of Concrete Containing Admixtures, Temperature Effects on Concrete, ASTM STP 858, T. R. Naik, Ed., American Society for testing and Materials, Philadelphia, 1985, pp.118-133

27 Owens, P. L., Effect of Temperature Rise and Fall on the Strength and Permeability of Concrete Made with and without Flyash, , Temperature Effects on Concrete, ASTM STP 858, T. R. Naik, Ed., American Society for testing and Materials, Philadelphia, 1985, pp.134-149

28 C. Vipulanandan and N. Dharmarajan, Effect of Temperature on the Fracture properties of Epoxy Polymer Concrete, Cement and Concrete Research, Vol.18, No.2, 1988, pp.265-276

29 Wang, J. A., et al, Effect of Ice Formation on the Elastic Moduli of Cement Paste and Mortar, Cement and Concrete Research, Vol.18, No.6, 1988, pp.874-885

30 Brachenbury, W. R. E., et al, Flexural Strength of Polymer Modified Cement Pastes Prepared by a Novel Curing Process, Cement and Concrete research, Vol.18, No.6, 1988, pp.971-979

31 P. Balaguru, M. Ukadike, and E, Nawy, Freeze-Thaw Resistance of Polymer Modified Concrete, Proceedings of Katherine and Bryant Mather International Conference, J. M. Scanlon Ed. Atlanta, Georgia, USA, 27 April - 1 May 1987, SP-100, American Concrete Institute, pp.863-876

32 R. Subrahmonia Ayyar, Suresh N. Joshi, Effect of Temperature on the Creep Behaviour of Polymer Mortars, Proceeding, RILEM Symposium on Adhesion Between Polymers and Concrete, (Aix-en-Provence, September 1986) Chapman and Hall Ltd, London 1986 pp.75-84

33 ACI, Epoxies with Concrete, SP-21, American Concrete Institute, Detroit, Michigan, 1968

34 Kudlapur, et al, Evaluation of Cold-Weather Concrete Patching materials, ACI Mater. J., Vol.86 No.1 Jan-Feb 1989 pp.36-44

35 Rizzo, Edward, M. Selection Criteria for Concrete Repair Materials, Concrete International, Vol.11 No.9, Sep 1989 pp.46-49

36 Collins, F. G., Evaluation of Concrete Spall Repair by Pullout Test, Material and Structures, Vol.22 No.130 July 1989 pp.280-286

37 Kuhlmann, L. A., Test Method for Measuring the Bond Strength of Latex-Modified Concrete and Mortar, ACI Mater. J. Vol.87 No.4, July-Aug 1990, pp.387-394

38 Wall, J. S. and Shrive, N. G., Factors Affecting Bond Between New and Old Concrete, ACI Mater. J., Vol.85 No.2 Mar-Apr 1988, pp.117-125

39 Wall, J. S., Shrive, N. G., and Gamble, B. R., Testing of Bond Between Fresh and Hardened Concrete, Proceeding, RILEM Symposium on Adhesion Between Polymers and Concrete, (Aix-en-Provence, September 1986) Chapman and Hall Ltd, London 1986, pp.335-344

40 Judge, A. I., Cheriton, L. W., and Lambe, R. W., Bonding Systems for Concrete Repair - An Assessment of Commonly Used Materials, Proceeding, RILEM Symposium on Adhesion Between Polymers and Concrete, (Aix-en-Provence, September 1986) Chapman and Hall Ltd, London 1986 pp.661-681

41 Naderi, M., Cleland, D, and Long, A. E., In Situ Test methods for Repaired Concrete Structures, Proceeding, RILEM Symposium on Adhesion Between Polymers and Concrete, (Aix-en-Provence, September 1986) Chapman and Hall Ltd, London 1986 pp.707-718

42 Peier, W. H., Adhesion Testing of Polymer Modified Cement Mortars, Proceeding, RILEM Symposium on Adhesion Between Polymers and Concrete, (Aix-en-Provence, September 1986) Chapman and Hall Ltd, London 1986 pp.730-740

43 Dixon, J. F., and Sunley, V. K., Use of Bond Coat in Concrete Repair, Concrete (London), Vol.17 No.8 Aug 1983 pp.34-35

44 Kreigh, J. D., Arizona Slant Shear Test: A Method to Determine Epoxy Bond Strength, ACI Journal, July 1976

45 Tabor, L. J., The Evaluation of resin Systems for Concrete Repair, Magazine of Concrete research Vol.30 No.103 Dec. 1978

46 Hewlett, P. C., and Hurley, S. A., Repair materials - Selecting and testing, Structural Faults and Repair -85, 2nd International Conference, ICE, London 30 April - 2 may 1985

47 BS 6319: Part 4, Slant Shear Test Method for Evaluating Bond Strength of Epoxy Systems, 1984

48 Alexander, K. M., Wardlaw, J., and Gibert, D. J., Aggregate-Cement Bond, Cement paste Strength and the Strength of Concrete, The Structure of

Concrete, Ed. A. E. Brooks and K. Newman, Cement and Concrete Association, London, 1968 pp.59-81

49 Garron P. Anderson, S John Bernett, and K. Lawrence DeVries, Analysis and testing of Adhesive Bonds, Academic Press, London, 1977

50 Z. Su, et al, The Influence of Polymer Modification on the Adhesion of Cement Pastes to Aggregate, Cement and Concrete research, Vol.21 No.1 1991 pp.169-178

51 Chen, Zhiyuan, et al, Bond Between Marble and Cement Paste, Cement and Concrete research, Vol.17 No.4, 1987 pp.544-552

52 Atzeni, C., et al, Mechanical and Thermohydrometric Properties of Adhesion Between PCMs and Cement Supports, Cement and Concrete research, Vol.21 No 2/3, 1991 pp.251-256

53 Maultzsch, M., Properties of PCC for Repair of Concrete Structures, Proceedings of the 5th International Congress on Polymers in Concrete, Brighton, England, 22-24 September, Ed. Barry W. Staynes pp.281-285

54 Burge, T., Evaluation of Polymers for Improving Cement Mortars, Proceedings of the 5th International Congress on Polymers in Concrete, Brighton, England, 22-24 September, Ed. Barry W. Staynes pp.293-300

55 Kwasny, R., Qualification Tests on PCC Systems for the Repair of Concrete Road Bridges, Proceeding, RILEM Symposium on Adhesion Between Polymers and Concrete, (Aix-en-Provence, September 1986) Chapman and Hall Ltd, London 1986 pp.682-696

56 Perry, S. H. and Holmyard, J. M., Assessment of Materials for Repair of Damaged Concrete under Water, prepared by Imperial College for the Department of Energy, OTH90 318, 1990

57 Kwasny, R. and Schulz, R. R., What Method for Testing the Bond of Coatings to Concrete ? An appreciation of Commonly Used Thermal Cycling Test methods, Concrete Precasting Plant and Technology, Vol.52, 1986 pp.102-106 and 173-179

58 Hsu, T. T. C and Slate, F. O., Tensile Bond Strength Between Aggregate and cement paste or Mortar, ACI Journal, proceedings, Vol.60, No.4, April 1963 pp.465-485

59 Frank, L., The Dimensioning of Adhesive-Bonded Joints in Concrete Building Components, Proceeding, RILEM Symposium on Adhesion Between Polymers and Concrete, (Aix-en-Provence, September 1986) Chapman and Hall Ltd, London 1986 pp.461-473

60 Proposed European Standard, Protection and Repair of Concrete Structures, CEN/TC104/WG8/TG2 TG2/70 Draft EN YYY Part 39 October 1992

61 James A. Mandel and Samir Said, Effect of the Addition of an Acrylic Polymer on the Mechanical Properties of Mortar, ACI Mater. J., Jan-Feb 1990 pp.54-61

62 E. Burley, et al, The Performance of Different Repair Techniques and Materials under Static Loading, Proceedings, The International Conference on Structural Faults and Repair, 27-29 June 1989, London, Ed. M. C. Forde, Engineering Technics Press, Vol.1 pp.79-86

63 J. C. T. S. Climaco and P. E. Regan, Evaluation of Bond Strength between Old and New Concrete, Proceedings, The International Conference on Structural

Faults and Repair, 27-29 June 1989, London, Ed. M. C. Forde, Engineering Technics Press, Vol.1 pp.115-122

64 Warris, B., Bond between Mortar Toppings and Concrete, Proceedings, RILEM Symposium on Synthetic Resins in Building Construction (Paris, September 1967) Ed. Eyrolles, Paris pp.463-475

65 Daniel N. O'Connor, et al, Compatibility of Polyester-Styrene Polymer Concrete Overlays with Portland Cement Concrete Bridge Decks, ACI Mater J. Vol.90 No.1 Jan-Feb. 1993 pp.59-68

66 Ohama, Y., Principal of Latex Modification and some Typical properties of Latex-Modified Mortars and Concrete, ACI Mater J., Nov-Dec 1987 Vol.84. No.5

67 Chen, Zhiyuan and Wang, Jianguo, Bond between Marble and Cement Paste, Cement and Concrete Research, Vol.17 No.4 1987 pp.544-522

68 S. A. Austin and P. J. Robins, A Unified Failure Envelope from the Evaluation of Concrete Repair Bond Test, Magazine of Concrete Research, Vol. 47, No. 170, March 1995, pp.57-68

69 A. Mcleish, Standard tests for Repair Materials and Coatings for Concrete, Part 1: Pull-off Tests, CIRIA Technical Note 139, 1993

70 R. N. Shaw, R. Jones, and A. Charif, Shear Adhesion Properties of Epoxy Resin Adhesives, Proceedings, RILEM Symposium on Adhesion Between Polymers and Concrete, (Aix-en-Provence, September 1986) Chapman and Hall Ltd, London 1986 pp.741-755

71 L. A. Kuhlmann, Styrene-Butadiene Latex-Modified Concrete: The Ideal Concrete Repair Materials ? Concrete International, Vol.12 No.10 Oct 1990 pp.59-65

72 L. A. Kuhlmann, Application of Styrene-Butadiene Latex Modified Concrete, Concrete International, Vol.9, No.12 Dec 1987 pp.48-53

73 Jose A. Walters Monteiro, Evaluating Patch Repair Bond Strength, Msc thesis, Department of Civil Engineering, Loughborough University of Technology, September 1993

74 Aovad, Gason, Repair of damaged Concrete, MSc thesis, Department of Civil Engineering, Loughborough University of Technology, 1988

75 Abdellatif, O. S., Review Concrete repair Technique, MSc thesis, Department of Civil Engineering, Loughborough University of Technology, 1990

76 Dudah, I. B., Review Concrete Repair Technique, MSc thesis, Department of Civil Engineering, Loughborough University of Technology, 1990

77 A. E. Long, et al, Assessment of Concrete Strength and Durability on Site, Proceedings, International Conference on Structural Faults and Repair, 7-9 July, 1987 London, Forde Engineering Technics Press, Ed. M. C. pp.61-73

78 BS6319 : Part 7, 1985 Method for Measurement of Tensile Strength

79 S. A. Austin, P. J. Robins, and Y. Pan, Tensile Bond Testing of Concrete Repairs, Materials and Structures, Vol.28, No. 179, June 1995, pp.249-259

80 J. H. Bungey and R. Madandoust, Factors Influencing Pull-Off Tests on Concrete, Magazine of Concrete research, Vol.44 No.158 1992 pp.21-30

81 Pye, G. B. and Beaudoin, J. J., An Energy Approach to Bond Strength Determination in Cement Systems, Cement and Concrete research, Vol.22 No.4 1992 pp.551-558

82 John Cairns, Is Propping Necessary During Structural Repair of reinforced Concrete Beams, Proceedings of the Fifth International Conference on Structural faults and repair, Edinburgh, 29 June - 1 July 1993, Vol.2 pp.239-245

83 British Standard Institution, BS6350, 1982, Adhesives

84 Marko Hranilovic, Failure Criteria for Structural Joints, Proceeding, RILEM Symposium on Adhesion Between Polymers and Concrete, (Aix-en-Provence, September 1986) Chapman and Hall Ltd, London 1986 pp.650-660

85 Shiraz D Tayabji, Bridge Deck and garage Floor Scarification by Hydrojetting, Concrete International, Vol.8 No.5 May 1986 pp.43-48

86 Joseph A. Lavelle, Acrylic Latex-Modified Portland Cement, ACI Mater L. Vol.85 No.1 Jan-Feb 1988 pp.41-48

87 K. M. Yeoh, D. J. Cleland, and A. E. Long, The Effect of Environmental Conditions on Interface Adhesion Properties of Concrete Patch Repairs, Proceedings of 2nd International Conference on Inspection, Appraisal, Repair and Maintenance of Buildings and Structures, Jakarta, 1993, pp.237-244

88 B. Godart and R. Lafuente, Etude Experimentale de L'adhesion entre un beton et une resine epoxydique cors de L'assemblage par collage de voussoirs prefabriques daus les ponts en beton precontraint, Proceeding, RILEM Symposium on Adhesion Between Polymers and Concrete, (Aix-en-Provence, September 1986) Chapman and Hall Ltd, London 1986 pp.474-483

89 Al-Mandil, M. Y., Performance of Epoxy-Repaired Concrete under Thermal Cycling, Cement and Concrete Composite, Vol.12 No.1 1990 pp.47-52

90 American Concrete Institute, Guide to Cast-in-Place Architectural Concrete Practice, Chapter 9 - Treated Architectural Surfaces, ACI Committee 303 R-74

91 J. Cairns, Consequences of Bond Loss for Behaviour of Reinforced Concrete beams, Proceedings of the Fifth International Conference on Structural faults and repair, Edinburgh, 29 June - 1 July 1993, Vol.3 pp.149-154

92 G. Mays and W. Wilkinson, Polymer repairs to Concrete: Their Influence on Structural performance, Proceedings of Katharine and Bryant Mather International Conference on Concrete Durability, Ed. J. M. Scanlon, ACI SP-100, Atlanta, Georgia, USA 27 April - 1 May 1987

93 Ramirez, J. L. et al, Repair of Concrete Columns with Localized Partial Loss of Corners or Cover, Proceedings of the Fifth International Conference on Structural faults and repair, Edinburgh, 29 June - 1 July 1993, Vol.3 pp.195-203

94 M. K. Emberson and G. C. Mays, Significance of Property Mismatch in the Patch Repair of Structural Concrete, Part 2: Axially Loaded Reinforced Concrete Members, Magazine of Concrete Research, Vol.42 No.152, September 1990 pp.161-170

95 R. W. Gaul, Preparing Concrete Surfaces for Coatings, Concrete International, Vol.6 No.7 July 1984 pp.17-22

96 American Concrete Institute, , Guide for Polymer Concrete Overlays, reported by ACI Committee 548, ACI Mater J. Sept-Oct. 1993 Vol.90 No.5 pp.479-498

97 Murray, Myles A., Surface Preparation for Adhesives, Concrete International, Vol.11 No.9 Sept 1989 pp.69-71

98 Erhard G. F. Chorinsky, Repair of Concrete Floors with Polymer Modified Cement Mortars, Proceeding, RILEM Symposium on Adhesion Between Polymers and Concrete, (Aix-en-Provence, September 1986) Chapman and Hall Ltd, London 1986 pp.230-234

99 Sika Limited, Technical data sheets for Icoment 501, 504 and 508, January 1990

100 Fosroc Limited, Technical data sheets for Renderoc LA, August 1991

101 SBD Limited, Technical data sheets for Mulsifix repair mortar, December 1991

102 Felt, Earl J., Repair of Concrete Pavements, ACI Journal, Proceedings, Vol.57 No.2 August 1960 pp.139-153

103 X. Ping and J. J. Beaudoin, Effects of Transition Zone Microstructure on Bond Strength of Aggregate-Portland Cement Paste Interfaces, Cement and Concrete Research, Vol.22 No.1 1992 pp.23-26

104 R. Zimbelmann, A Method for Strengthening the Bond between Cement Stone and Aggregates, Cement and Concrete research, Vol.17 No.4 1987 pp.651-660

105 L. J. Tabor, Repair Materials and techniques, Durability of Concrete Structures, Investigation, Repair, Protection, Ed. G. Mays E & FN SPON 1992 pp.82-129

106 Exchem Mining and Construction Ltd, Technical data sheets for floorings and coatings, August 1992

107 M. Naderi, D Cleland, and A. Long, Polymer Modified Repair Materials - Strength and Durability, Proceedings of the 5th International Congress on Polymers in Concrete, Brighton, England, 22-24 September, Ed. Barry W. Staynes pp.309-313 1987

108 D. R. Plum, Polymer Modified Materials and the Curing Environment, Proceedings, International Conference on Structural Faults and Repair, 27-29 June 1989 London Ed. M. C. Forde, Engineering Technics Press, Vol.1 pp.99-101

109 M. N. Haque, Some Concrete need 7 Days Initial Curing, Concrete International, Vol.12 No.2 Feb 1990 pp.42-46

110 E. Semerad, P. Kremnitzer, W. Lacom, F. Holub and P. Sattler, Polymer Modified Mortar: Influence of Polymer Addition on Macroscopic and Microscopic Properties, Proceedings of the 5th International Congress on Polymers in Concrete, Brighton, England, 22-24 September, Ed. Barry W. Staynes pp.223-228 1987

111 N. Gowripalan, et al, Effect of Curing on Durability, Concrete International, Vol.12 No.2 Feb 1990 pp.47-54

112 P. H. Emmons and A. M. Vaysburd, Factors Affecting Durability of Concrete Repair, Proceedings of Fifth International Conference on Structural Faults and Repair, Edinburgh, 30 June - 2 July 1993 Vol.2 pp.253-267

113 Sidney Mindess and J Francis Young, Concrete, Prentice-Hall INC, Englewood Cliffs, New Jersey 1981

114 Bjegovic, D., Mikulic, D., and Ukraincik, V., Theoretical Aspect and Methods of Testing Concrete Resistance to Freezing and Deicing Chemicals, Proceedings, Katharine and Bryant Mather International Conference on

Concrete Durability, J. M. Scanlon Ed. Atlanta, Georgia, USA, 27 April - 1 May 1987, SP-100, American Concrete Institute, pp.863-876

115 K. W. Nasser and G. A. Evans, Low temperature Effects on Hardened Air-Entrained Concrete, Behaviour of Concrete under Texperature Extremes, Publication SP-39, American Concrete Institute, 1973 pp.79-90

116 Hewlett, P. C. and Hurley, S. A., The Consequences of Polymer-Concrete Mismatch, Durability and Design Life of Buildings, ICE London, 26-27 Nov. 1984 Design Life of Buildings, Thomas Telford, London 1984

117 Z. P. Bazant, et al, Statistical Extrapolation of Shrinkage Data Part 1: Regresion, ACI Mater J. Vol.84 No.1 Jan-Feb. pp.20-34, Part 2: Bayesian Updating, No.2 Mar-Apr pp.83-91

118 Robert F. Ytterberg, Shrinkage and Curing of Slabs on Grade, Concrete International, Vol.9 1987 part 1 No.4 pp.22-31, part 2 No.5 pp.54-61, part 3 No.6 pp.72-81

119 ACI Committee 209, Prediction of Creep, Shrinkage, and Temperature Effects in Concrete Structures (ACI 209R-82) American Concrete Institute, Detroit, 1982

120 CEB-FIP, Code for Concrete Structures, 3rd Edition, Paris 1978

121 Kotsira, et al, Effectiveness of Techniques for Flexural Repair and Strengthening of RC Members, Proceedings of Fifth International Conference on Structural Faults and Repair, Edinburgh, 30 June - 2 July 1993 Vol.3 pp.235-243

122 Jonasson, J. E., Analysis of Creep and Shrinkage in Concrete and Its Application to Concrete Top Layers, Cement and Concrete Research, Vol.8 No.4 July 1978 pp.441-454

123 Silfwerbrand, J., Bonding between Old and New Concrete in Structures Loaded by Static and Time-Dependent Load, Proceeding, RILEM Symposium on Adhesion Between Polymers and Concrete, (Aix-en-Provence, September 1986) Chapman and Hall Ltd, London 1986 pp.309-319

124 ASTM C666-80, Standard Test Method for Resistance of Concrete to rapid Freezing and Thawing

125 J. Sawan, Cracking due to Frost Action in Portland Cement Concrete Pavement - A Literature Survey, Proceedings of Katharine and Bryant Mather International Conference on Concrete Durability, Ed. J. M. Scanlon, ACI SP-100, Atlanta, Georgia, USA 27 April - 1 May 1987 pp.781-803

126 T. Fujiwara, Deterioration of Concrete Used in Road Bridges due to Freezing and Thawing, Proceedings of Katharine and Bryant Mather International Conference on Concrete Durability, Ed. J. M. Scanlon, ACI SP-100, Atlanta, Georgia, USA 27 April - 1 may 1987 pp.805-818

127 T. Faulkner and R. Walker, Rapid One-Cycle Test for Evaluating Aggregate Performance when Exposed to Freezing and Thawing in Concrete, Proceedings of Katherine and Bryant Mather International Conference on Concrete Durability, Ed. J. M. Scanlon, ACI SP-100, Atlanta, Georgia, USA 27 April - 1 may 1987 pp.705-722

128 Daniel Bordelean, et al, Comparative Study of Latex Modified Concrete and Normal Concretes Subjected to freezing and Thawing in the Presence of a Deicer Salt Solution, ACI Mater. J. Vol.89 No.6 Nov-Bec 1992 pp.547-553

129 P. D. Cady, R. E. Weyers and D. T. Wilson, Durability and Compatibility of Overlays and Bridge Deck Substrate Treatments, Concrete International, Vol.6 No.6 June 1984 pp.36-44
130 Bangash, M. Y. H., Concrete and Concrete Structures, Numerical Modelling and Applications, Elsevier Applied Science, 1989
131 British Standard Institution, Method for Determination of Static Modulus of Elasticity in Compression, BS1881: Part 121, 1983
132 British Standard Institution, BS4550: Method for Testing Cement, Part 3: Physical test, 1978
133 British Standard Institution, Method for Determination of Modulus of Elasticity in Compression, BS6319: Part 6, 1984
134 Gilbert, R. I., Time Effect in Concrete Structures, Elsevier, Oxford, 1988
135 RILEM Report, Fracture Mechanics of Concrete Structures, Ed. L. Elfgren, Chapman and Hall, London 1989
136 Ramirez, J. L. et al, Concrete Columns Short Repair for Total Strength Loss, Proceedings of the Fifth International Conference on Structural faults and repair, Edinburgh, 29 June - 1 July 1993, Vol.3, pp.213-220
137 Murdock, L. J., Brook, K. M., and Dewar, J. D., Concrete Materials and Practice, Sixth Edition, Edward Arnold, London, 1991
138 R. Letsch, Polymer Mortar Overlays - Measurement of Stresses, Proceedings of the 5th International Congress on Polymers in Concrete, Brighton, England, 22-24 September, Ed. Barry W. Staynes pp.119-123
139 Thanasis C. Triantafillou, et al, Strengthening of Concrete Structures with Prestressed Fibre Reinforced Plastic Sheets, ACI Structural Journal, Vol.89 No.3 May-June 1992 pp.235-244
140 C. W. Celia, An Introduction to Numerical Analysis, McGraw-Hill, London, 1969 pp.68
141 Roberts, T. M., and Haji-Kazemi, H. (1987), Theoretical Study of the hebaviour of Reinforced Concrete beams Strengthened by Externally Bonded Steel Plates, Proceedings, Institution of Civil Engineers, Part 2, March 1987, pp.39-55
142 William F. Perenchio, Irwin Kaufman, and Robert J. Krause, Concrete Repair in a Desert Environment, Concrete International, Vol.13 No.2 Feb. 1991 pp.23-26
143 David Dorsch, Repairing a Fire-Damaged Concrete Turbine Pedestal, Concrete International, Vol.13 No.6 June 1991 pp.33-38
144 Peter Mendis, A Polymer Concrete Overlay, Concrete International, Vol.9 No.12 Dec. 1987 pp.54-56
145 D F Meinheit, J F Monson, Parking Garage repaired Using Thin Polymer Concrete Overlay, Concrete International, Vol.6, No.7 July 1984 pp.7-13
146 Robert I Pearson, O'Hare Airport Departure Ramp, Concrete International, Vol.10 No.5 May 1988 pp.63-65
147 Myles A Murray, Application of Epoxy-Modified Concrete Toppings, Concrete International, Vol.9 No.12 Dec. 1987 pp.36-38
148 German Gurfinkel, Grain-Storage tank for Zaire West Africa, Concrete International, Vol.11 No.3 March 1989 pp.39-49

149 Kevin A Michols and John F. Vincent, Reinforced Overlay and Shotcrete Restore Integrity to a Multi-storey Parking Structure, Concrete International, Vol.12, No.9 Sept. 1990 pp.55-58
150 Walpole, R E and Myers R H, Probability and Statistics for Engineers and Scientists, 2nd Edition, MacMillan Publishing Co. New York, 1978 pp.580
151 Dannys Breton, et al, Contribution to the Formation mechanism of the Ytransition Zone between Rock-Cement Paste, Cement and Concrete research, Vol.23 No.2 mar. 1993 pp.335-346
152 A Carles-Gibergues, et al, New-to-old Concrete Bonding: Influence of Sulfate Type of New Concrete on Interface Microstructure, Cement and Concrete Research, Vol.23 No.2, 1993 pp.431-441
153 ACI Committee 503, Guide for the Selection of Polymer Adhesives with Concrete, ACI Material Journal, Vol.89 No.1 Jan-Feb. 1992 pp.90-105
154 Jitendra K. Bhargave, Polymer-Modified Concrete for Overlays: Strength and Deformation Characteristics, ACI SP69-14, 1982 pp.205-218
155 Klieger, P. Effect of Mixing and Curing Temperature on Concrete Strength, ACI proceedings, Vol.54 No.12 June 1958
156 Ravina, D. and Shalon, R., The Effect of Elevated temperatures on Strength of Portland Cements, Effect of Temperature on Concrete, Publication SP-25, ACI, Detroit MI 1970
157 J M Illston (ed.), Construction Materials, Their Nature and Behaviour 1994
158 Klans Altmann, Shrinkage of Concrete in Extreme Climate, Fundamental Research on Creep and Shrinkage of Concrete, Edited by F H Wittmann, Martinus Nijhoff Publishers, 1982 pp.203-212
159 ACI Committee 306, Cold Weather Concreting, ACI Material Journal Vol.85 No.4 July-Aug. 1988 pp.280-302

Appendix 1

Measurement of surface roughness index (SRI)

The surface roughness of the prepared concrete surface shall be evaluated, making use of the silica sand with a grain size of 0.05 to 0.10mm.

50g of the silica sand will be spread circularly on the concrete surface and thoroughly smoothed in order to cover the largest possible part of the concrete surface and at the same time ensure that all cavities produced by the grit blasting are filled up. The mean of the measures of three diameters (expressed in mm) taken in different positions across the circular area covered by the sand will be taken as the Surface Roughness Index (SRI) of the concrete surface (i.e., SRI = (D1 + D2 + D3)/3.0) (see Fig. A1.1).

According to the duration of the grit blasting two surface roughness can be obtained: coarse roughness and fine roughness.

Coarse roughness is the surface characteristic of a test piece with a Surface roughness Index (SRI) less than 200mm.

Fine roughness is the surface characteristic of a concrete testpiece with a Surface Roughness Index (SRI) more than 250mm

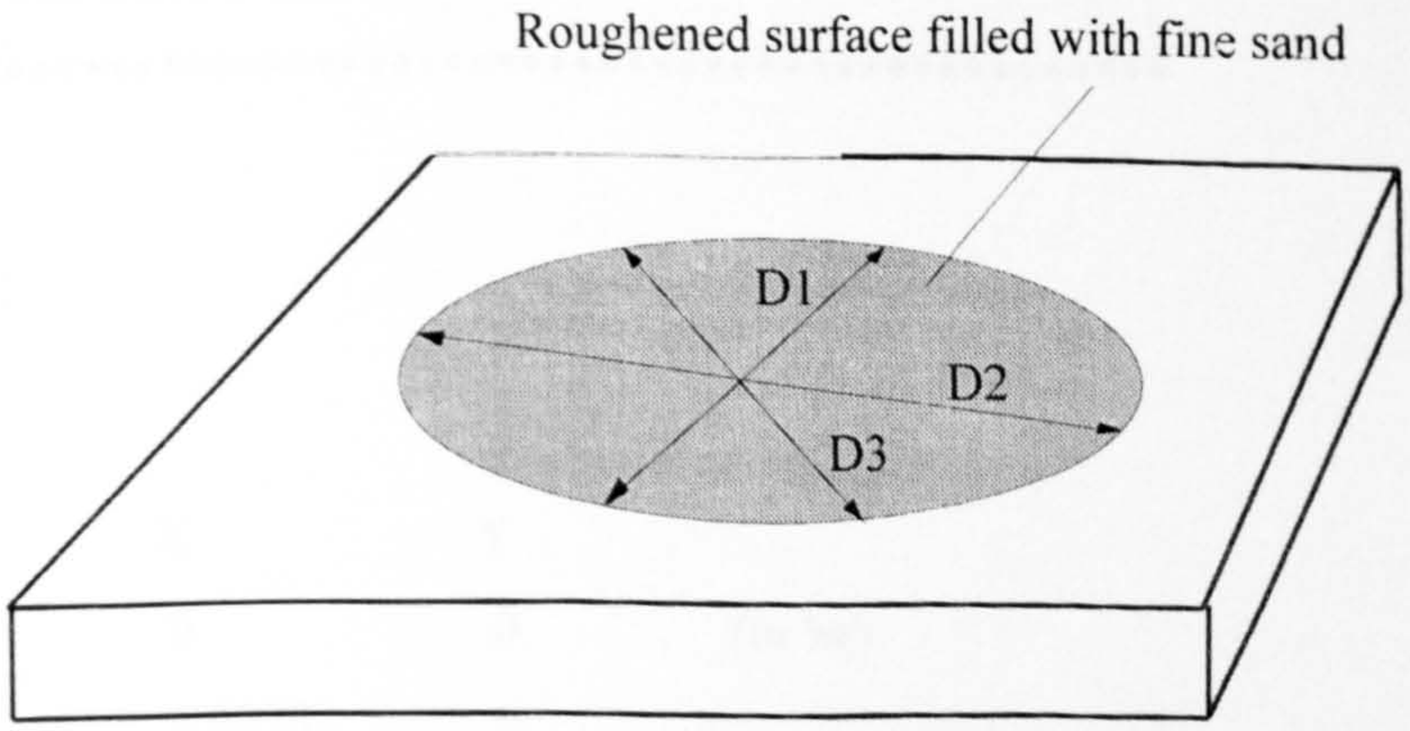

Figure A1.1 Sand patching method for measuring the surface roughness

Appendix 2

The PAFEC data files for the finite element analyses

A2.1 Introduction

The PAFEC finite element system is capable of performing a wide range of engineering calculations from static and dynamic problems to temperature, acoustic, and mode frequency analyses. The PAFEC scheme allows data to be input in a straightforward way in a modular form; the data being held in a command file constructed in a modular fashion, each module performing a particular function. A special 'control module' appears first. The output from PAFEC consists of a range of files, including several which give an account of the progress of a job covering results, graphics, restart capability.

A2.2 Data file for the case 1 (see Fig. 4.9)

```
TITLE  EFFECT OF MODULUS MISMATCH -- CASE 1
C  ************************************************************
C  *  EFFECT OF MODULUS MISMATCH ON THE STRESS        *
C  *  DISTRIBUTION OVER THE BOND INTERFACE UNDER      *
C  *  A DIRECT TENSILE STRESS                         *
C  ************************************************************

CONTROL

CONTROL.END

NODES
NODE.NUMBER      X          Y
1                0          0          (in 'm')
2                0.0275     0
3                0          0.05
4                0.0275     0.05
5                0          0.1
6                0.0275     0.1
```

7	0.0055	0.1
8	0.011	0.1
9	0.0165	0.1
10	0.01925	0.1
11	0.022	0.1
12	0.02475	0.1
13	0.026125	0.1

PAFBLOCKS

TYPE=1

ELEMENT.TYPE=36210 *(eight-noded isoparametric curvilinear quadrilaterial element)*

GROUP	PROPERTIES	N1	N2	TOPOLOGY			
1	1	1	2	1	2	3	4
2	2	1	3	3	4	5	6

MESH

REFERENCE	SPACING.LIST							
1	4	4	4	2	2	2	1	1
2	4	4	4	2	2	2	1	1
3	1	1	2	2	2	4	4	4

PLATES.AND.SHELLS

PLATE.OR.SHELL.NUMBER	MATERIAL.NUMBER
1	11
2	12

MATERIAL

MATERIAL.NUMBER	E	NU	*(modulus and Poisson's ratio, respectively)*
11	30E9	0.2	*(in N/m^2)*
12	20E9	0.13333	

(Note: E and NU can be adjusted to model different material properties)

RESTRAINTS

NODE.NUMBER	PLANE	DIRECTION
1	4	2
1	5	1

LOADS

DIRECTION=2

NODE.NUMBER	VALUE.OF.LOAD	
5	2750	*(in 'N')*

6	5500
8	5500
9	4125
10	2750
11	2750
12	2062.5
13	1375

```
6                687.5
IN.DRAW
DRAWING.NUMBER   TYPE  INFORMATION
1                  3         25
OUT.DRAW
DRAWING.NUMBER     PLOT.TYPE
1                      20
END.OF.DATA
```

A2.3 Data file for the effect of coring depth in the core pull-off test (Fig. 4.10)

```
TITLE EFFECT OF CORING DEPTH IN THE CORE PULL-OFF TEST -- CASE 2
C  ************************************************
C  *     EFFECT OF CORING DEPTH ON THE STRESS      *
C  *     DISTRIBUTION OVER THE BOND INTERFACE      *
C  *     IN THE CORE PULL-OFF TEST                 *
C  ************************************************
CONTROL
AXISYMMETRIC
PHASE=7
CLEAR.FILES
CONTROL.END
NODES   (for the coring depth of 2mm)
NODE.NUMBER      X        Y
1                0        0
2                50       0
```

3	52	0
4	100	0
5	0	27.5
6	50	27.5
7	52	27.5
8	100	27.5
9	0	30
10	50	30
11	52	30
12	100	30
13	0	50
14	50	50
15	52	50
16	100	50

For the coring depth of 10 and 15mm, change the x value of the following nodes to 60 and 65mm, respectively: Node number 3, 7, 11, 15.

PAFBLOCK

TYPE=1

ELEMENT.TYPE=36210

GROUP	PROPERTY	N1	N2	TOPOLOGY			
1	1	1	2	2	6	1	5
1	1	3	4	10	14	9	13
2	2	1	5	3	7	2	6
2	2	1	6	4	8	3	7
2	2	7	6	8	12	7	11
2	2	3	6	12	16	11	15
2	2	3	8	11	15	10	14

MESH *(This is for the coring depth of 2mm)*

REFERENCE SPACING.LIST

1	2	2	2	2	1	1	1	
2	1	1	2	2	2	4	4	4
3	1	1	2	2	2			
4	1	1	2	2	2	2		
5	1							
6	4	4	2	1	1			
7	1							
8	1							

PLATES.AND.SHELLS

PLATE	MATERIAL
1	11
2	12

MATERIAL

MATERIAL	E	NU
11	20E9	0.13333
12	30E9	0.2

RESTRAINTS

NODE	PLANE	DIRECTION
13	0	1
1	4	2

LOADS

NODE.NUMBER	DIRECTION	VALUE
1	1	-593.96
5	1	-1781.87

STRESS.ELEMENT (This is for the coring depth of 2mm)

START	FINISH
1	14
87	93

END.OF.DATA

For the coring depth of 10 and 15 mm, the MESH and STRESS.ELEMENT modules are changed to the following :

MESH (This is for the coring depth of 10mm)

REFERENCE	*SPACING.LIST*							
1	*2*	*2*	*2*	*2*	*1*	*1*	*1*	
2	*1*	*1*	*2*	*2*	*2*	*4*	*4*	*4*
3	*1*	*1*	*2*	*2*	*2*			
4	*1*	*1*	*2*	*2*	*2*	*2*		
5	*3*	*3*	*2*	*2*				
6	*4*	*2*	*2*	*1*	*1*			
7	*1*							
8	*2*							

STRESS.ELEMENT (This is for the coring depth of 10mm)

START FINISH

1 14

101 114

MESH (This is for the coring depth of 15mm)

REFERENCE SPACING.LIST

1 2 2 2 2 1 1 1

2 1 1 2 2 2 4 4 4

3 1 1 2 2 2

4 1 1 2 2 2 2

5 2 2 1 1

6 5

7 1

8 3

STRESS.ELEMENT (This is for the coring depth of 15mm)

START FINISH

1 14

101 114

A2.4 Data file for the effect of modulus mismatch in a patch compressive test (Fig. 4.11)

```
TITLE EFFECT OF MODULUS --CASE 3
C  ***************************************************
C  *    EFFECT OF MODULUS MISMATCH IN A PATCH        *
C  *    COMPRESSIVE TEST                             *
C  ***************************************************
CONTROL
PHASE=9
CONTROL.END
NODES
NODE.NUMBER    X          Y
1              0          0
2              75         0
3              77         0
4              100        0
5              77.128     30
6              79.1487    30
```

7	0	60
8	83.646	60
9	85.732	60
10	100	60
11	0	70
12	86.8604	70
13	88.98	70
14	94.5	70
15	100	70
16	0	80
17	90.634	80
18	92.7945	80
19	100	80
20	0	90
21	95	90
22	97.21	90
23	100	90
24	0	95.677
25	97.7576	95.677
26	100	95.677
27	0	100
28	100	100
29	0	200
30	100	200
31	10	200
32	20	200
33	40	200
34	60	200
35	80	200
36	90	200
37	90.488	60
38	95.244	60

ELEMENTS

GROUP	ELEMENT.TYPE	PROPERTIES	TOPOLOGY
1	36110	3	25 26 28
1	36210	3	22 26 21 25
1	36210	3	18 22 17 21
1	36210	3	13 18 12 17

1	36210	3	9	13	8	12
2	36110	2	22	23	26	
2	36110	2	18	19	22	
2	36110	2	19	23	22	
2	36110	2	13	14	18	
2	36110	2	14	19	18	
2	36110	2	14	15	19	
2	36110	2	9	36	13	
2	36110	2	36	14	13	
2	36110	2	36	37	14	
2	36110	2	37	15	14	
2	36110	2	37	10	15	

PAFBLOCKS

TYPE=1

ELEMENT.TYPE=36210

GROUP	PROPERTY	N1	N2	TOPOLOGY						
1	3	1	2	3	9	2	8	6	0	0	5
2	2	3	1	3	4	9	10	0	6	0	0
3	1	4	1	1	2	7	8	0	0	5	0
4	1	4	2	7	8	11	12				
5	1	4	2	11	12	16	17				
6	1	4	2	16	17	20	21				
7	1	4	2	20	21	24	25				
8	1	4	2	24	25	27	28				
9	1	4	5	27	28	29	30				

MESH

REFERENCE	SPACING.LIST							
1	6							
2	1							
3	3							
4	1	1	1	2	2	2	1	1
5	1	1	2	2.5	3.5			

PLATES.AND.SHELLS

PLATE.OR.SHELL.NUMBER	MATERIAL.NUMBER
1	11
2	12
3	13

MATERIAL

```
MATERIAL.NUMBER  E   NU
11                    30E9     0.2
12                    30E9     0.2
13                    30E9     0.2
RESTRAINTS
NODE.NUMBER   PLANE  DIRECTION
1                     4           2
1                     0           1
LOADS
DIRECTION==2
NODE.NUMBER      VALUE
29                    -500
30                    -500
31                   -1000
32                   -1500
33                   -2000
34                   -2000
35                   -1500
36                   -1000
END.OF.DATA
```

A2.5 Data file for the effect of modulus mismatch in the patch flexural test (Fig. 4.12)

```
TITLE  MODULUS MISMATCH IN A PATCH FLEXURAL TEST  -- CASE 4
C   ************************************************************
C   *        EFFECT OF MODULUS MISMATCH IN A PATCH              *
C   *        FLEXURAL TEST                                      *
C   ************************************************************
CONTROL
PHASE=7
PHASE=9
CONTROL.END
NODES
NODE        X          Y
1           0          0
2          28          0
```

3	135	0
4	225	0
5	0	25
6	135	25
7	225	25
8	0	100
9	135	100
10	225	100

PAFBLOCKS

TYPE=1

ELEMENT.TYPE=36210

GROUP	PROPERTY	N1	N2	TOPOLOGY			
1	1	1	2	3	4	6	7
2	2	3	2	1	3	5	6
2	2	3	4	5	6	8	9
2	2	1	4	6	7	9	10

MESH

REFERENCE	SPACING.LIST								
1	1	1	2	2	4	4	4		
2	5								
3	14	14	20	20	20	20	17	5	5
4	1	1	2	3	4	4			

PLATES.AND.SHELLS

PLATE.OR.SHELL.NUMBER	MATERIAL.NUMBER
1	11
2	12

MATERIAL

MATERIAL.NUMBER	E	NU
11	20E9	0.3
12	30E9	0.3

RESTRAINTS

NODE.NUMBER	PLANE	DIRECTION
4	5	1
2	0	2

LOADS

DIRECTION=2

NODE.NUMBER	VALUE.OF.LOAD
10	1000

END.OF.DATA

A2.6 Date file for the displacement simulated loading on eccentricity induced on unrepaired patch compressive specimens (Fig. 4.13)

```
TITLE UNREPAIRED SPECIMEN UNDER PRESCRIBED DISPLACEMENT
C       -- CASE 5
C   ***************************************************************
C   *   STRESS DISPLACEMENT OVER THE MIDDLE CROSS SECTION*
C   *   OF AN UNREPAIRED PATCH COMPRESSIVE SPECIMEN       *
C   ***************************************************************
CONTROL
PHASE=9
CONTROL.END
NODES
NODE      X       Y
1          0       0
2         75       0
3       80.966    50
4          0      100
5        100      100
6          0      200
7        100      200
8         20      200
9         40      200
10        60      200
11        80      200
PAFBLOCKS
TYPE=1
ELEMENT.TYPE=36210
GROUP=1
PROPERTY=1
N1   N2   TOPOLOGY
1    1    1  2  4  5  0  3  0  0
1    1    4  5  6  7
MESH
REFERENCE  SPACING
```

```
1                    5

PLATES.AND.SHELLS
PLATE          MATERIAL
1                    11
MATERIAL
MATERIAL         E          NU
11                   30E9         0.2
RESTRAINTS
NODE.NUMBER        PLANE      DIRECTION
1                      4                2
1                      0                1
DISPLACEMENT.PRESCRIBED
NODE.NUMBER  DIRECTION   DISPLACEMENT.VALUE
6                      2                -0.001
R5  1                  0                0
END.OF.DATA
```

A2.7 Data file for the effect of modulus mismatch in the slant shear test (Fig. 4.14)

```
TITLE  EFFECT OF MODULUS MISMATCH IN THE SLANT SHEAR TEST
C        -- CASE 6
C    ************************************************************
C    *       EFFECT OF MODULUS MISMATCH ON THE STRESS*
C    *       DISTRIBUTION IN THE SLANT SHEAR TEST          *
C    ************************************************************
CONTROL
PHASE=9
CONTROL.END

NODES
NODE       X          Y
1           0          0
2          55          0
3           0         21.37
4          55         21.37
5           0         27.37
```

6	0	33.37
7	0	39.37
8	55	116.63
9	55	122.63
10	55	128.63
11	55	134.63
12	0	134.63
13	0	156
14	55	156
15	7.5	156
16	47.5	156

LINE.NODES

LIST.OF.NODES

13	17	18	15					
15	19	20	21	22	23	24	25	16
16	26	27	14					

PAFBLOCKS

TYPE	GROUP	ELEMENT	PROPER	N1	N2	N3	TOPOLOGY			
1	1	36110	1	1	2	0	3	8	5	9
1	2	36110	3	1	2	0	5	9	6	10
1	3	36110	2	1	2	0	6	10	7	11
2	4	36110	1	1	1	1	3	4	8	
2	5	36110	2	1	1	1	7	11	12	
1	6	36210	1	1	4	0	1	2	3	4
1	7	36210	2	1	5	0	12	11	13	14

MESH

REFERENCE SPACING.LIST

1	1	1	1	2	2	2	2	2	2	2	2	1	1	1
2	1													
3	14													
4	3	2	1											
5	1	2	3											

PLATES.AND.SHELLS

PLATE	MATERIAL	THICKNESS
1	11	10
2	12	10
3	13	10

MATERIAL

```
MATERIAL      E          NU
1             30E9       0.2
2             20E9       0.2
3             20E9       0.2
RESTRAINTS
NODE   PLANE   DIRECTION
1        2        2
1        0        1
LOADS
CASE=1
DIRECTION=2
NODE          VALUE
13             -125
14             -125
17             -250
18             -250
26             -250
27             -250
15             -375
16             -375
19             -500
R6 1             0
END.OF.DATA
```

A2.8 Date file for the effect of differential deformation (Fig. 4.15)

```
TITLE EFFECT OF DIFFERENTIAL DEFORMATION -- CASE 7
C  ************************************************************
C  *     EFFECT OF DIFFERENTIAL DEFORMATION ON THE            *
C  *     STRESS DISTRIBUTION ALONG THE BOND INTERFACE         *
C  *     IN A CONCRETE OVERLAY SITUATION                      *
C  ************************************************************
CONTROL
PHASE=9
CONTROL.END
NODES
NODE     X          Y
```

```
1          0          0
2        500          0
3          0         80
4         10         80
5         20         80
6         40         80
7         60         80
8        100         80
R10  1    40          0
19         0         90
20        10         90
21        20         90
22        40         90
23        60         90
24       100         90
R10  1    40          0
35         0        100
36        10        100
37        20        100
38        40        100
39        60        100
40       100        100
R10  1    40          0
PAFBLOCKS
TYPE=1
ELEMENT.TYPE=36210
GROUP  PROPERTY   N1   N2   TOPOLOGY
1          1          1    2    1    2    3     18
2          2          1    3    3   18   35     50
MESH
REFERENCE  SPACING.LIST
1     1   1   2   2   4   4   4   4   4   4   4   4   4   4   4
2     2   2   1   1   1   1
3     2
PLATES.AND.SHELLS
PLATE        MATERIAL
1                 11
2                 12
```

MATERIAL

MATERIAL E NU ALPHA *(ALPHA : the coefficient of thermal expansion)*

11 30E9 0.2 10E-6

12 30E9 0.2 10E-6

RESTRAINTS

NODE PLANE DIRECTION

1 0 2

2 5 1

TEMPERATURE

TEMPERATURE START FINISH

-30 3 50

END.OF.DATA

Appendix 3

Effect of shrinkage in a symmetric situation

A3.1 Introduction

At any time t, the total strain in a uniaxially loaded specimen consists of a number of components, which include the instantaneous strain $\varepsilon_e(t)$, the creep strain $\varepsilon_c(t)$, the shrinkage strain $\varepsilon_{sh}(t)$, and the temperature strain $\varepsilon_t(t)$. Although not strictly correct, it is usual to assume that all four components are independent and may be calculated separately, and summed to obtain the total strain.

Ignoring the temperature effect, it can be seen from Fig. 4.17 that if shrinkage of the repair material is greater than that of the substrate concrete, tensile stress will be developed in the repair material, and compressive stress in the substrate. At any time t, the total strain developed in repair mortar can be worked out by the principle of superposition as:

$$\varepsilon_m = \varepsilon_{shm}(t, t_m) + \varepsilon_{em} + \varepsilon_{cm} \qquad \text{(A3.1)}$$

and the total strain in the substrate concrete:

$$\varepsilon_c = \varepsilon_{shc}(t, t_m) + \varepsilon_{ec} + \varepsilon_{cc} \qquad \text{(A3.2)}$$

where ε_{shm}, ε_{shc} are the shrinkage strains in the repair material and the substrate concrete, respectively;

ε_{em}, ε_{ec} are the elastic strains in the repair material and the substrate concrete, respectively;

ε_{cm}, ε_{cc} are the creep strains in the repair material and the substrate concrete, respectively; and

t_m, t_c are the age of the repair material and the substrate concrete at the time when shrinkage starts.

Equilibrium requires that the following equation be satisfied:

$$\sigma_m A_m + \sigma_c A_c = 0 \tag{A3.3}$$

Compatibility requires:

$$\varepsilon_m = \varepsilon_c \tag{A3.4}$$

It can be seen that so long as the shrinkage strains, the constitutive relationship of materials, and the creep strains, are known, shrinkage stress due to restraint provided by the substrate can be evaluated. But the determination of creep strains can be a very complicated problem.

Depending on the method used to determine the creep strain, or the creep coefficient, methods can be divided into several categories, which include the effective modulus method (EMM), age-adjusted effective modulus method (AEMM), and the rate of creep method (RCM). Each one has its advantages and disadvantages. Bearing in mind that every method is based on many assumptions and only provides approximate solution, it is better to determine the upper and lower limit of the shrinkage stresses. The actual effect of shrinkage and creep can be evaluated between these limits. It is not in the scope of this study to compare different methods. According to [134], the effective modulus method, and the rate of creep method, are adopted because they provide the lower and upper limit analyses.

A3.2 The effective modulus method (EMM)

Due to the varying stress history, the creep strains ecm, ecc are not the simple multiplying of the current elastic strains and the current creep coefficients, i.e.,

$$\varepsilon_{cm} \neq \varepsilon_{em} \cdot \phi_m \tag{A3.5}$$

$$\varepsilon_{cc} \neq \varepsilon_{ec} \cdot \phi_c \tag{A3.6}$$

In the effective modulus method, it is assumed that the creep strains are the multiplying of the current elastic strains and the current creep coefficients, i.e.,

$$\varepsilon_{cm} = \varepsilon_{em} \cdot \phi_m \tag{A3.7}$$

$$\varepsilon_{cc} = \varepsilon_{ec} \cdot \phi_c \tag{A3.8}$$

By substituting equations (A3.7) and (A3.8) into (A3.1) and (A3.2), and using the relationships (A3.3) and (A3.4), eq.(A3.9) can be worked out:

$$\varepsilon_{em} = \frac{-(\varepsilon_{shm} - \varepsilon_{shc})}{1 + \phi_m(t, t_m) + \beta\alpha + \beta\alpha\phi_c(t, t_c)} \tag{A3.9}$$

Suppose both materials are linear elastic, the stress in the repair mortar generated due to the differential shrinkage can be determined as follows:

$$\sigma_m = \varepsilon_{em} \cdot E_m = \frac{-E_m(\varepsilon_{shm} - \varepsilon_{shc})}{1 + \phi_m(t, t_m) + \beta\alpha + \beta\alpha\phi_c(t, t_c)} \tag{A3.10}$$

If the shrinkage and the creep effect of the substrate is considered very small and can be neglected, eq.(A3.10) can be simplified as:

$$\sigma_m = \frac{E_m \varepsilon_{shm}}{1 + \phi_m(t, t_m) + \beta\alpha} \tag{A3.10a}$$

A3.3 The rate of creep method

In the rate of creep method, it is assumed that the rate of creep with time is independent of the age at loading, i.e.,

$$\dot{\phi}(t, \tau_i) = \dot{\phi}(t, \tau_o) \tag{A3.11}$$

Integrating both side resulted in:

$$\phi(t, \tau_i) = \phi(t, \tau_o) + C \tag{A3.12}$$

The integrating coefficient, C, can be determined by the boundary condition:

$$\text{at } t = \tau_i, \qquad \phi(\tau_i, \tau_i) = 0$$

$$C = -\phi(\tau_i, \tau_o)$$

$$\phi(t, \tau_i) = \phi(t, \tau_o) - \phi(\tau_i, \tau_o) \tag{A3.13}$$

Suppose the elastic strain is kept constant, then

$$\varepsilon_{cc}(t_1) = \varepsilon_{ec} \cdot \phi(t_1, \tau_i)$$

$$\varepsilon_{cc}(t_2) = \varepsilon_{ec} \cdot \phi(t_2, \tau_i)$$

The difference in the creep strains can be determined as:

$$\Delta\varepsilon_{cc} = \varepsilon_{ec}[\phi(t_1, \tau_o) - \phi(t_2, \tau_o)] \tag{A3.14}$$

If a continuously varying stress history is divided into small time intervals δt, the stress $\sigma(t)$ during each interval is given by eq.(A3.14). In the limit , as δt approaches zero, the rate of change of creep depends only on the current stress and the rate of change of the creep coefficient, i.e.,

$$\dot{\varepsilon}_{cc} = \varepsilon_{ec} \cdot \dot{\phi} \tag{A3.15}$$

Changing the equilibrium condition and the compatibility requirement into the rate form, and substituting eqs.(A3.15) and (A3.3) into eq.(A3.4) will result in

$$\beta\dot{\sigma}_{shc} - \alpha\beta\dot{\sigma}_m - \alpha\beta\sigma_m\dot{\phi}_c = \dot{\sigma}_{shm} + \dot{\sigma}_m + \sigma_m\dot{\phi}_m \tag{A3.16}$$

where

$$\alpha = A_m / A_c$$

$$\beta = E_m / E_c$$

$$\dot{\sigma}_{shc} = \dot{\varepsilon}_{shc} \cdot E_c$$

$$\dot{\sigma}_{shm} = \dot{\varepsilon}_{shm} \cdot E_m$$

$$\dot{\sigma}_m(1 + \alpha\beta) + \sigma_m(\dot{\phi}_m + \alpha\beta\dot{\phi}_c) + \dot{\sigma}_{shm} - \beta\dot{\sigma}_{shc} = 0 \tag{A3.17}$$

or in another form:

$$\dot{\sigma}_m + \sigma_m F_1(t) + F_2(t) = 0 \qquad \text{(A3.18)}$$

where

$$F_1(t) = \frac{\dot{\phi}_m + \alpha\beta\dot{\phi}_c}{1+\alpha\beta}$$

$$F_2(t) = \frac{\dot{\sigma}_{shm} - \beta\dot{\sigma}_{shc}}{1+\alpha\beta}$$

The Runge-Kutta formulae was used for the numerical analysis [140]:

$$\sigma_{m+1} = \sigma_m + [K_0 + 2K_1 + 2K_2 + K_3]/6 \qquad \text{(A3.19)}$$

where

$$K_0 = \delta t \cdot f(t, \sigma_m)$$

$$K_1 = \delta t \cdot f(t + \frac{1}{2}\delta t, \sigma_m + \frac{1}{2}K_0)$$

$$K_2 = \delta t \cdot f(t + \frac{1}{2}\delta t, \sigma_m + \frac{1}{2}K_1)$$

$$K_3 = \delta t \cdot f(t + \delta t, \sigma_m + K_2)$$

$$f(t, \sigma_m) = -\sigma_m F_1(t) - F_2(t)$$

Appendix 4

Effect of shrinkage in a concrete overlay situation

In a concrete overlay situation, quite often it is the stresses at the age of the repair that cause a failure, such as delamination. It needs to determine the stress distribution over the whole bond interface, so the most vulnerable area can be highlighted and be protected accordingly. Similar work has been carried out by Roberts and Haji-Kazemi [141].

An element of a composite beam with an length of δx is shown in Fig. 4.18b. The beam is made from two materials, repair material (m) and the substrate concrete (c), joined together by a medium of assumed negligible thickness but having finite shear and normal stiffness.

Assuming that plane sections within each material remain plane, the strains can be expressed in terms of displacement u and w, relative to the local axes, respectively. For material m, the total displacement in the x-direction depth z_m, denoted by u_m, is given by:

$$u_m = u_{mo} - z_m \cdot w'_m \tag{A4.1}$$

in which the subscript m denotes repair material, and w_m' denotes the first derivative of w_m with respect to x. Similarly for material c:

$$u_c = u_{co} - z_c \cdot w'_c \tag{A4.2}$$

where u_{mo} and u_{co} are displacements along the x-direction at the central axes within the repair material and the substrate concrete, respectively.

The strains in the material m and c, denoted by ε_m and ε_c, are given by:

$$\varepsilon_m = u'_m = u'_{mo} - z_m w''_m \tag{A4.3}$$

$$\varepsilon_c = u'_c = u'_{co} - z_c w''_c \tag{A4.4}$$

Stresses can now be related to strains by moduli of materials, E_m and E_c. Only elastic behaviour was considered. If ε_{fm} and ε_{fc} define the free strains due to shrinkage and temperature, the stresses σ_m and σ_c are given by:

$$\sigma_m = \frac{E_m}{1+\phi_m}(u'_{mo} - z_m w''_m - \varepsilon_{fm}) \qquad \text{(A4.5)}$$

$$\sigma_c = \frac{E_c}{1+\phi_c}(u'_{co} - z_c w''_c - \varepsilon_{fc}) \qquad \text{(A4.6)}$$

where ϕ_m, ϕ_c are the creep coefficients of the repair material and the substrate concrete, respectively. Here the effective modulus method is used to describe the creep strain.

The axial forces t_m and t_c, and moments m_m and m_c are obtained by integrating the stresses, multiplied by an appropriate level arm in the case of moments, over the cross section area of materials m and c, denoted by A_m and A_c. Hence:

$$N_m = \int \sigma_m dA_m \qquad \text{(A4.7)}$$

$$N_c = \int \sigma_c dA_c \qquad \text{(A4.8)}$$

$$m_m = -\int \sigma_m z_m dA_m \qquad \text{(A4.9)}$$

$$m_c = -\int \sigma_c z_c dA_c \qquad \text{(A4.10)}$$

Since the strains and stresses throughout the beam have been defined in terms of four independent displacement variables, four independent equations are requires to obtain a solution. These four equations are obtained by considering the equilibrium of a small element of the beam and the compatibility at the interface between the two materials.

Resolving forces horizontally gives:

$$N_m + N_c = 0 \qquad \text{(A4.11)}$$

Resolving forces vertically and taking moments gives:

$$m_m + m_c + N_m \cdot e = 0 \qquad \text{(A4.12)}$$

The slip u_{mc} at the interface between materials m and c is the relative displacement in the x-direction of initially adjacent particles. Hence, if the shear stiffness of the joint per unit length is denoted by Ks, and z_{im} and zic are the z-co-ordinates of the interface in the two materials, then:

$$\tau = K_s \cdot u_{mc} = K_s[(u_{mo} - z_{im}W'_m) - (u_{co} - z_{ic}W'_c)] \qquad \text{(A4.13)}$$

in which τ is the shear force per unit length.

The separation at the interface between the material m and c is the relative displacement in the z-direction of adjacent particles. Hence, if the normal stiffness of the joint per unit length is denoted by Kn, then:

$$\sigma_n = K_n(w_c - w_m) \qquad \text{(A4.14)}$$

in which σ_n is the normal force per unit length. Equilibrium of an element of the material m yields the equations:

$$\tau = N'_m \qquad \text{(A4.15)}$$

$$m'_m + \tau z_{im} - f_m = 0 \qquad \text{(A4.16)}$$

$$f'_m - \sigma_n = 0 \qquad \text{(A4.17)}$$

The main equations can now be summarised as follows:

$$N_m = \int \frac{E_m}{1+\phi_m}(u'_{mo} - z_m W''_m - \varepsilon_{fm})dA_m \qquad \text{(A4.18)}$$

$$N_c = \int \frac{E_c}{1+\phi_c}(u'_{co} - z_c W''_c - \varepsilon_{fc})dA_c \qquad \text{(A4.19)}$$

$$m_m = -\int \frac{E_m}{1+\phi_m}(u'_{mo} - z_m W''_m - \varepsilon_{fm})z_m dA_m \qquad \text{(A4.20)}$$

$$m_c = -\int \frac{E_c}{1+\phi_c}(u'_{co} - z_c W''_c - \varepsilon_{fc})z_c dA_c \qquad \text{(A4.21)}$$

$$N'_m + N'_c = 0 \qquad \text{(A4.22)}$$

$$m''_m + m''_c - N_c^{\cdot} = 0 \tag{A4.23}$$

$$N_m^{\cdot} - K_s[(u_{mo} - z_{im}w'_m) - (u_{co} - z_{ic}w'_c)] = 0 \tag{A4.24}$$

$$m''_m - K_n(w_c - w_m) + N_m^{\cdot} \cdot e = 0 \tag{A4.25}$$

By integrating eqs.(A4.18) to (A4.21), the following equations can be obtained:

$$N_m = \frac{E_m A_m}{1+\phi_m}(u'_{mo} - \varepsilon_{fm}) \tag{A4.26}$$

$$N_c = \frac{E_c A_c}{1+\phi_c}(u'_{co} - \varepsilon_{fc}) \tag{A4.27}$$

$$m_m = \frac{E_m \mathrm{I_m}}{1+\phi_m} w''_m \tag{A4.28}$$

$$m_c = \frac{E_c I_c}{1+\phi_c} w''_c \tag{A4.29}$$

Substituting eqs.(A4.26) and (A4.27) into eq.(A4.22), eq.(A4.30) can be obtained:

$$\frac{E_m A_m}{1+\phi_m}(u'_{mo} - \varepsilon_{fm}) + \frac{E_c A_c}{1+\phi_c}(u'_{co} - \varepsilon_{fc}) = 0 \tag{A4.30}$$

$$u'_{co} = \varepsilon_{fc} - \frac{1+\phi_c}{1+\phi_m} \cdot \frac{E_m A_m}{E_c A_c}(u'_{mo} - \varepsilon_{fm}) \tag{A4.31}$$

Equilibrium of an element of the material in the vertical direction yields the equation:

$$f_m = m'_m + \tau \cdot z_{im} \tag{A4.32}$$

$$f'_m = \sigma_n \tag{A4.33}$$

$$\begin{aligned} \sigma_n &= m''_m + \tau' \cdot z_{im} \\ &= m_m^{\cdot} + N_m^{\cdot} \cdot z_{im} \\ &= m''_m + K_s[(u_{mo} - z_{im}w'_m) - (u_{co} - z_{ic}w'_c)] \cdot z_{im} \end{aligned} \tag{A4.34}$$

From the bending equilibrium:

$$\frac{E_m \mathrm{I_m}}{1+\phi_m} \cdot w''_m + \frac{E_c I_c}{1+\phi_c} \cdot w''_c + \frac{E_m \mathrm{I_m}}{1+\phi_m}(u'_{mo} - \varepsilon_{fm}) \cdot e = 0 \tag{A4.35}$$

$$u'_{mo} = \frac{(1+\phi_c)E_m A_m \varepsilon_{fm} e - (1+\phi_c)E_m \mathrm{I_m} w''_m - (1+\phi_m)E_c I_c w''_c}{e(1+\phi_c)E_m A_m} \qquad \text{(A4.36)}$$

$$u'''_{mo} = \frac{-(1+\phi_c)E_m \mathrm{I_m} w^{(4)}_m - (1+\phi_m)E_c I_c w^{(4)}_c}{e(1+\phi_c)E_m A_m} \qquad \text{(A4.37)}$$

Substituting eqs.(A4.36), (A4.37) and (A4.31) into the slip condition eq.(A4.24), eq.(A4.38) can be obtained:

$$\frac{(EA)_m}{\Phi_m} \cdot \frac{[-\Phi_i(EIw^{(4)})_j]}{e\Phi_c(EA)_m} - K_s[(\frac{\Phi_c N_m e - \Phi_i(EIw'')_j}{e\Phi_c(EA)_m} - z_{im}w''_m) - (\frac{\Phi_m N_c e + \Phi_i(EIw'')_j}{e\Phi_m(EA)_c} - z_{ic}w''_c)] = 0 \qquad \text{(A4.38)}$$

where

$$(EA)_m = E_m A_m$$

$$(EA)_c = E_c A_c$$

$$(EIw'')_m = E_m \mathrm{I_m} w''_m$$

$$(EIw'')_c = E_c I_c w''_c$$

$$\Phi_m = 1 + \phi_m$$

$$\Phi_c = 1 + \phi_c$$

$$N_m = E_m A_m \varepsilon_{fm}$$

$$N_c = E_c A_c \varepsilon_{fc}$$

$$\Phi_i(EIw'')_j = \Phi_m(EIw'')_c + \Phi_c(EIw'')_m$$

$$\Phi_i(EIw^{(4)})_j = \Phi_m(EIw^{(4)})_c + \Phi_c(EIw^{(4)})_m$$

or

$$\Phi_i(EIw^{(4)})_j + K_s[(\frac{\Phi_m(\Phi_c N_m e - \Phi_i(EIw'')_j}{(EA)_m} - e\Phi_m\Phi_c z_{im}w''_m) - (\frac{\Phi_c(\Phi_m N_c e - \Phi_i(EIw'')_j}{(EA)_m} - e\Phi_m\Phi_c z_{ic}w''_c)] = 0 \qquad \text{(A4.38a)}$$

If it is assumed that $w_m = w_c$, the above equation can be simplified as:

$$w^{(4)} + K_s[\frac{\Phi_m\Phi_c e(\varepsilon_{fm} - \varepsilon_{fc})}{\Phi_i(EI)_j} - (\frac{\Phi_m}{(EA)_m} + \frac{\Phi_c}{(EA)_c} + \frac{\Phi_m\Phi_c e^2}{\Phi_i(EI)_j})w''] = 0 \qquad \text{(A4.39)}$$

or

$$w^{(4)} - P^2 w'' = R \qquad \text{(A4.40)}$$

where

$$R = \frac{K_s \Phi_m \Phi_c e(\varepsilon_{fm} - \varepsilon_{fc})}{\Phi_l (EI)_j}$$

$$\Phi_l (EI)_j = \Phi_m E_c I_c + \Phi_c E_m \mathrm{I_m}$$

Eq.(A4.40) can be solved:

$$w = \alpha_1 \sinh(Px) + \alpha_2 \cosh(Px) - \frac{Rx^2}{2P^2} + \alpha_3 x + \alpha_4 \qquad \text{(A4.41)}$$

and the differentiation of the deflection w with respect to x can be obtained as follows:

$$w' = \alpha_1 P \cosh(Px) + \alpha_2 P \sinh(Px) - \frac{Rx}{P^2} + \alpha_3$$

$$w'' = \alpha_1 P^2 \sinh(Px) + \alpha_2 P^2 \cosh(Px) - \frac{R}{P^2}$$

$$w''' = \alpha_1 P^3 \cosh(Px) + \alpha_2 P^3 \sinh(Px)$$

$$w^{(4)} = \alpha_1 P^4 \sinh(Px) + \alpha_2 P^4 \cosh(Px)$$

The coefficients of α_1 to α_4 can be determined using the following boundary conditions.

(1) $w|_{x=0} = 0 \; w|_{x=0} = 0$

$$\alpha_2 + \alpha_4 = 0$$

(2) $w''|_{x=0} = 0$

$$\alpha_2 P^2 - \frac{R}{P^2} = 0$$

(3) $w|_{x=a} = 0$

$$\alpha_1 \sinh(Pa) + \alpha_2 \cosh(Pa) - \frac{Ra^2}{2P^2} + \alpha_3 a + \alpha_4 = 0$$

(4) $w''|_{x=a} = 0$

$$\alpha_1 P^2 \sinh(Pa) + \alpha_2 P^2 \cosh(Pa) - \frac{R}{P^2} = 0$$

$$\alpha_2 = \frac{R}{P^4}$$

$$\alpha_4 = -\alpha_2$$

$$\alpha_1 = \frac{\frac{R}{P^2} - \alpha_2 P^2 \cosh(Pa)}{P^2 \sinh(Pa)}$$

$$\alpha_3 = \frac{[-\alpha_1 \sinh(Pa) - \alpha_2 \cosh(Pa) + \frac{Ra^2}{2P^2} - \alpha_4}{a}$$

By integrating eq.(A4.36), eq.(A4.42) can be obtained:

$$u_{mo} = \frac{\Phi_c N_m ex - \Phi_i (EI)_j w'}{e\Phi_c (EA)_m} + \alpha_5 \qquad \text{(A4.42)}$$

The boundary condition:

$$u_{mo}\big|_{x=0} = 0$$

$$\alpha_5 = \frac{\Phi_i (EI)_j w'\big|_{x=0}}{e\Phi_c (EA)_m}$$

From eqs.(A4.15) and (A4.26), the shear stress along the bond interface can be determined:

$$\tau = N_m^{'} = \frac{E_m A_m}{1+\phi_m}(u''_{mo}) = \frac{-\Phi_i (EI)_j w'''}{e\Phi_m \Phi_c} \qquad \text{(A4.43)}$$

From eqs.(A4.34) and (A4.43), the normal stress acting on the bond interface can be determined:

$$\sigma_n = m''_m + \tau' z_{im} = \frac{E_m \mathrm{I_m}}{1+\phi_m} w^{(4)} + \frac{\Phi_i (EI)_j w^{(4)} z_{im}}{e\Phi_m \Phi_c} \qquad \text{(A4.44)}$$

The maximum and minimum tensile stresses at any cross section in the repair mortar can also be determined:

$$\sigma_m^{\max} = \frac{E_m}{1+\phi_m}(u'_{mo} - z_{im} w''_m - \varepsilon_{fm}) \qquad \text{(A4.45)}$$

$$\sigma_m^{\min} = \frac{E_m}{1+\phi_m}(u'_{mo} + z_{im} w''_m - \varepsilon_{fm}) \qquad \text{(A4.46)}$$

The maximum stress, $\sigma_m^{\max}$, occurs at the plane in contact with the substrate concrete, whilst the minimum stress, $\sigma_m^{\min}$, occurs at the free surface.

Appendix 5

Effect of shear post-peak behaviour on the ultimate failure load

In the core twist-off test, the shear stress distribution over the bond interface is not evenly distributed, with the maximum shear stress occurring at the edge of the core in the elastic stage. Because friction can develope in the bond interface if there are some shear slip, the specimen may not fail when the maximum shear stress at the edge of the core reaching the shear strength. This analysis is used for demonstrating the post-peak effect.

Assuming the shear stress -shear strain relationship follows the pattern presented in Fig.5.8a, the equilibrium condition can be formulated as following.

$$\int_0^R \tau(r) \cdot 2\pi r^2 \cdot dr = M_T \qquad \text{(A5.1)}$$

where $\tau(r)$ is the shear stress at a distance of r from the centre of the core, and

M_T is the enternally applied twist moment.

Given the maximum shear strain g, the shear stress can be determined according to Fig. 5.8a, then integrating over the cross section will result in the twist moment.

Appendix 6

Effect of the shape of a cross section on shear stress distribution

From theories in the strength of material, shear stress at a height h from the neutral axis as shown in Figure A6.1 can be determined using the following equation.

$$\tau = \frac{P}{Ib_o}\int_h^Y ybdy \qquad \text{(A6.1)}$$

where P is the total shear force acting on the cross section;
I is the moment of inertia of the cross section about the neutral axis;
bo is the width of cross section at height h above the neutral axis;
b is the width of cross section at height y above the neutral axis; and
Y is the distance from the neutral axis to the most strained fibre.

If applying this to the direct shear bond test, the shear stress distribution over the bond interface can be obtained from eq.(A6.1).

For a rectangular cross section:

$$\tau = \frac{P}{Ib}\int_h^Y ybdy = \frac{P}{2I}(Y^2 - h^2) \qquad \text{(A6.2)}$$

Because $I = \frac{bH^3}{12}$, so the shear stress can be worked out (eq. A6.3).

$$\tau = \frac{6P}{bH^3}(\frac{H^2}{4} - h^2) \qquad \text{(A6.3)}$$

The maximum shear stress and the average shear stress can be worked out :

$$\tau_{max} = \frac{6P}{bH^3}(\frac{H^2}{4} - 0) = \frac{3P}{2bH}$$

$$\tau_o = \frac{P}{bH}$$

and

$$\frac{\tau_{max}}{\tau_o} = \frac{3}{2}$$

For a circular cross section:

$$\tau = \frac{P}{Ib_o}\int_h^Y ybdy$$

$$b_o = 2\sqrt{R^2 - h^2}$$

$$b = 2\sqrt{R^2 - y^2}$$

So

$$\tau = \frac{P}{2I\sqrt{R^2 - h^2}}\int_h^R 2y\sqrt{R^2 - y^2}\,dy$$

$$= \frac{-64P}{16\pi R^4\sqrt{R^2 - h^2}}\cdot\frac{1}{2}\int_h^R \sqrt{R^2 - y^2}\,d(R^2 - y^2)$$

$$= \frac{4P}{3\pi R^4}(R^2 - h^2) \qquad \text{(A6.4)}$$

$$\tau_{max} = \frac{4P}{3\pi R^2}$$

$$\tau_o = \frac{P}{\pi R^2}$$

and

$$\frac{\tau_{max}}{\tau_o} = \frac{4}{3}$$

It demonstrates that the shear stress distribution over a circular cross section is more uniform than that over a rectangular cross section.

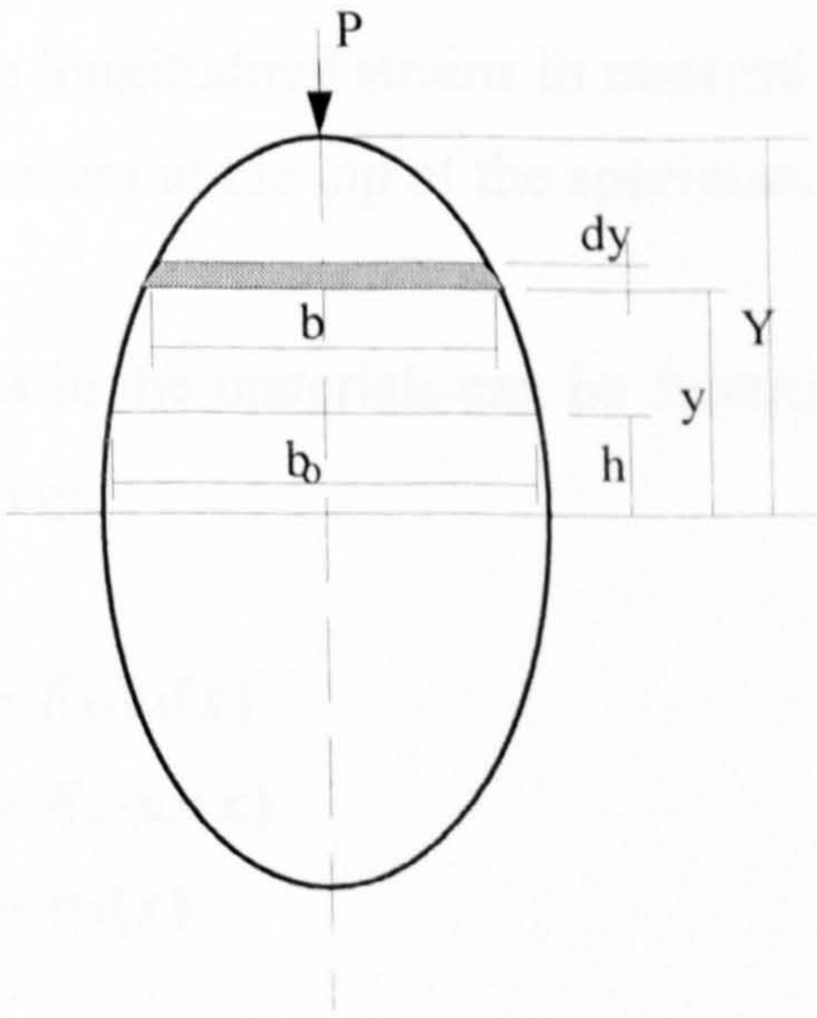

Figure A6.1 A cross section subject to shear force

Appendix 7

Effect of modulus mismatch on eccentricity induced in a slant shear test

To see the effect of modulus mismatch on eccentricity induced, an elastic analysis is presented below.

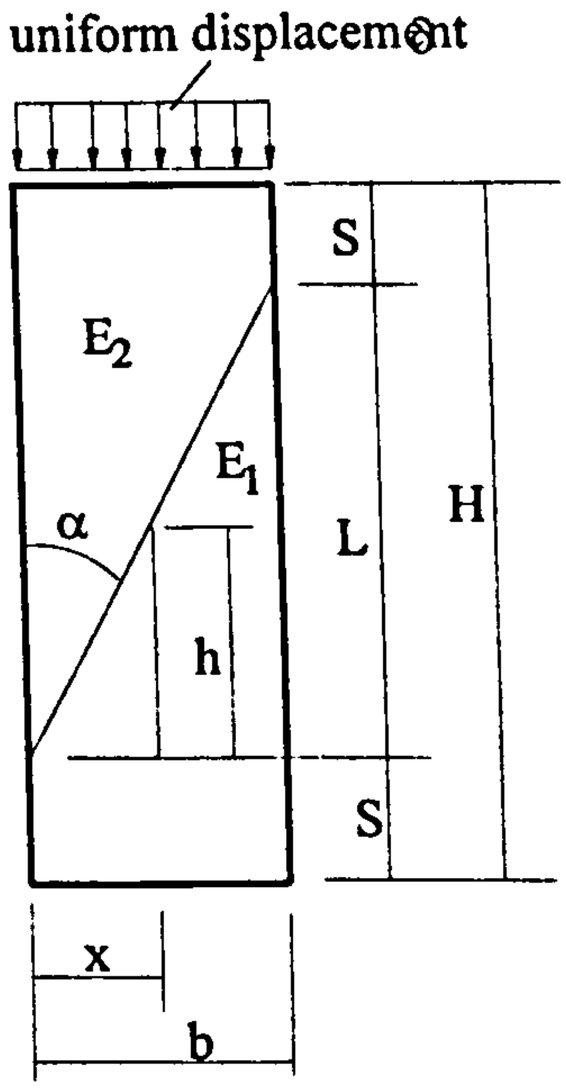

Figure A7.1 A slant shear specimen under uniform displacement

Assume that both materials are linear elastic and are stresses in the vertical direction, eq.(A7.1) can be obtained.

$$(S+h)\cdot\varepsilon_1(x)+(S+L-h)\cdot\varepsilon_2(x)=\delta \qquad \text{(A7.1)}$$

where $\varepsilon_1(x)$, $\varepsilon_2(x)$ are the longitudinal strains in material 1 and 2, respectively, δ is the applied uniform displacement at the top of the specimen.

The longitudinal stresses in the materials can be determined by relating the strains to their modulus, respectively.

$$\sigma_1(x)=E_1\cdot\varepsilon_1(x) \qquad \text{(A7.2)}$$

$$\sigma_2(x)=E_2\cdot\varepsilon_2(x) \qquad \text{(A7.3)}$$

and $$\sigma_1(x)=\sigma_2(x) \qquad \text{(A7.4)}$$

From Fig. A7.1, h=$x\cdot\cot(\alpha)$, substituting this and eqs. (A7.2) to (A7.4) into eq.(A7.1), eq.(A7.5) can be obtained.

$$\sigma = \frac{\delta \cdot E_2}{S\beta_t + x\beta_t\cot(\alpha) + S + L - x\cot(\alpha)} \tag{A7.5}$$

where β_t=E_1/E_2, is the modulus ratio.

Integrating the stresses, and multiplied bu an appropriate level are in the case of moment, over the cross section, the axial load and the bending moment can be obtained.

$$P = \int_0^b \sigma dx = \int_0^b \frac{\delta \cdot E_2}{S\beta_t + x\beta_t\cot(\alpha) + S + L - x\cot(\alpha)} dx$$
$$= \frac{\delta \cdot E_2}{K_2} \ln \frac{K_1 + K_2 b}{K_1} \tag{A7.6}$$

$$M = \int_0^b \sigma(\frac{b}{2} - x)dx = \int_0^b \frac{\delta \cdot E_2(\frac{b}{2} - x)}{S\beta_t + x\beta_t\cot(\alpha) + S + L - x\cot(\alpha)} dx$$
$$= \frac{\delta \cdot E_2}{K_2}[\frac{\frac{bK_2}{2} + K_1}{K_2} \ln \frac{K_1 + bK_2}{K_1} - b] \tag{A7.7}$$

where $K_1 = S\beta_t + S + L$

$K_2 = \beta_t\cot(\alpha) - \cot(\alpha)$ $(\beta_t \neq 1)$,

if β_t=1, M=0.

The eccentricity, e, caused due to the modulus mismatch can be obtained.

$$e = \frac{M}{P} = \frac{[\frac{\frac{bK_2}{2} + K_1}{K_2} \ln \frac{K_1 + bK_2}{K_1} - b]}{\ln \frac{K_1 + bK_2}{K_1}} \tag{A7.8}$$

when β_t=1, e=0.

Appendix 8

Statistical analysis of comparing two variables

To test a hypothesis that the difference between two population means, μ_1-μ_2, equals a specified value d_o, we proceed by the following steps:

1. Ho: μ_1-$\mu_2 = d_o$,
2. Ha: Alternatives are μ_1-$\mu_2 \neq d_o$,
3. Choose a level
4. Critical region:

   $t < -t_\alpha$ for the alternative μ_1-$\mu_2 < d_o$,

   $t > t_\alpha$ for the alternative μ_1-$\mu_2 > d_o$,

   $t < -t_{\alpha/2}$ and $t > t_{\alpha/2}$ for the alternative $\mu \neq \mu_o$,

   where t has a t distribution with $v = n_1 + n_2 - 2$ degree of freedom, provided we can assume that $\sigma_1 = \sigma_2 = \sigma_1$ and the population are approximately normally distributed.

If $\sigma_1 \neq \sigma_2$ and are unknown, then

$$v = \frac{(\frac{s_1^2}{n_1} + \frac{s_2^2}{n_2})^2}{\frac{(\frac{s_1^2}{n_1})^2}{n_1 - 1} + \frac{(\frac{s_2^2}{n_2})^2}{n_2 - 1}}$$

5. Compare $\bar{x}_1$, $\bar{x}_2$, s_1, s_2 from a random sample of size n_1 and n_2, and then compute the t test statistic

$$t = \frac{(\bar{x}_1 - \bar{x}_2) - d_o}{\sqrt{\frac{s_1^2}{n_1} + \frac{s_2^2}{n_2}}}$$

6. Decision: Reject H_0 if t falls in the critical region; otherwise not to reject H_0.

For the comparative tests, d_0 is usually set to zero because we do not know whether by changing one parameter will cause variation of test results. Hence the test adopted in this thesis was the two-tailed test, with d_0 is set to zero.